Diseño Conceptual de las Esclusas Post Panamax

TASK 2

PART A: GENERAL DESIGN CRITERIA

RevA-Pacific Actualization and Atlantic Harmonization

in association with

1 General

1.1 SCOPE

Task 2 of this conceptual design study for a triple lift lock configuration at the Pacific and Atlantic side of the Panama Canal covers the development of the design criteria. For each project feature identified in task 4 proper design criteria have to be developed.
These design criteria will be based on:

- Properly recognized standards (International)
- The terms of reference (ACP)
- The data furnished by ACP

The design criteria have to be considered as applicable for detailed design purposes. As this actual study is a concept design, which precedes all other engineering activities, the design criteria will be implemented as far as this is required on this actual concept design level.

1.2 DATA

1.2.1 TERMS OF REFERENCE (TOR)

Licitación N°. SAA-109422
Pliego de Cargas para "Diseño conceptual de las Esclusas Post Panamax" by ACP.
Licitación N°. SAA-143351
Update of Pacific Locks Conceptual Design and Harmonization of Atlantic Locks Conceptual Design.

1.2.2 DOCUMENTS FURNISHED BY ACP (TILL THE DATE OF 31-03-02)

1. ACP reports on seismic activity:
   - Report: Seismicity Evaluation Tabasara Hydel Project western Panama, ACRES Canada dec. 81
   - Report: Excerpts from the Star and Herald on the Sept. 1882 Earthquake, from Engineering & Construction Bureau, Luis Carlos Fernandez.
   - Report: El terremoto de San Blas del 7 de Septiembre 1882; E Camacho y V. Viquez, Universidad de Panama , Junio 1993
   - Technical Report 2-17: Spectral Strong Motion Attenuation in Central America, NORSAR , August 1994
   - Technical Report 2-18: Seismic Hazard for Panama, Update, NORSAR, July 1994
   - Report: Seismicity of Panama during the interval 1904-83, Seismological Dept. Upsala Sweden, A. Vergara Munoz, 1987
   - Report: El terremoto de la Vieja del 2 de Mayo 1621, un sismo intraplaca, V. Viquez y E. Camacho, Universidad de Panama, Mayo 1993
   - Report. Historical Seismicity of the North Panama Deformed Belt, E Camacho y V. Viquez, Universidad de Panama ,
   - Report: Seismicidad Historica del Extremo Occidental del Cinturon Deformado del Norte de Panama, E Camacho y V. Viquez, Universidad de Panama , Abril 1992
2. Geotechnical information
   - Plan view

- 1 set of 4 Maps en color: “Mapa geologico Republica de Panama”, scale 1/250 000 Ministerio de comercio e industrios, hojas 3, 4, 5 y 6
- Geotechnical Logs hardcopies with digital files
- Drawing with Logs showing Alignments P1 and P2:
  Alineamiento P1 y P2 Sector Pacifico, scale 1/5000 Ubicacion de sondeos, February 2002
- 3 geological longitudinal profiles
  - Profile 1 (East)
  - Profile 2 (Center)
  - Profile 3 (West)

3. Preliminary locks profile drawing
   - New Panama canal post-panamax locks profile diagram, 06/02/2002
   - 2 drawings (digital) showing 1-step and 3-step lock profiles
4. Ground Survey Information – digital topographic map in X,Y,Z coordinates
5. Moffatt & Nichol study on water saving basins Draft final Report
   Mofatt & Nichol study on water saving basins – appendices A - J
6. Harza Lock Alignment Study Report
7. Data of size & type of gates (see n° 12 and PIANC Bulletin)
8. Data on the water management (resources)
   (See questions 48 & 102 of the pre bid conference)
9. Inventory of disposal sites for excavated soil and rock, including capacity and restrictions.
10. Data on existing road access (drawing) = item n°4
11. Pacific & Gatún Lake elevations:
    a) Tidal Data (1991-1999) every 15 minutes (Temporal evolution of the ocean’s level)
    b) Gatun Elevations (1996-2000) at midnight
12. Presentation of ACP (Kick-off meeting 14/02/02)
13. Table of “Mareas Balboa”
14. Pilot Handbook
15. Real view with HARZA alignment
16. Texas A&M Report (vessel positioning systems)
17. Ship Squad Study Report
18. Emptying and filling system report:
    The third locks project of the Panama Canal, lock model tests – Design 3, August 1942
19. Data on wave propagation due to ship movement:
    Pressure Test Miraflores Locks (Pressure sensors in the chambers during the passage of boats)

20. Lighting system / Electricity feeding
Plans of Electrical distribution, Single Line Diagrams (Electrical Location Plan and Diagram) for:
    a) Pedro Miguel Locks - June 19, 1996
    b) Miraflores Locks – July 31, 1995
    c) Gatun Locks - July 14, 1998

21. Temporal Evolution of the rain and wind
"Balance hídrico superficial en la cuenca del canal de Panama", Preliminary Report, March of 2000.

22. Handbook of Lockage Procedure Locks Division

23. Coating type in use
    - Specifications for Corrosion Control Coatings
    - Plans of:
        a) Miraflores locks (10 sheets) – Corrosion Mitigation part Plan and Inspection Records - October 12, 1983
        b) All Locks (Pedro Miguel, Miraflores) – Intermediate Gates Cathodic Protection Outline of Gate Recess, UHM WHDP Hanger, Bill of Materials, and Sections. September 30, 1999
        c) All Locks – Cathodic Protection Mitre Gates, Water Compartments, 4 March 1967

24. Third locks construction effort

25. **Data missing from the Moffatt & Nichol preliminary study on water saving basins**
    - Table of figure 11.15 for one month comparison of measured versus predicted tide level in the Pacific (page 15 of main report).
    - Table is for the Pacific excedance on Appendix C
    "Finalized Percent Exceedance Distribution for Balboa Gage - Pacific Ocean Side"

26. Lock's Operation
Comments about regular operation procedures by John Wong

27. Data about talus:
"Slope criteria for conventional excavation2.dwg"

28. Description of rock
Rock Data Tables "Definic ión, Criterio de Rocas y Escala de Dureza para Aplicación de Curvas"

29. Tests of Permeability Alignment P1 & P2

30. Information on the lighting system (existing high mast) at Panama Canal Locks

31. Indice of aerial orthophotos available

32. Data about loads
    - 2 Autocad drawings showing the position of locomotives
    (typical section of either lateral and central walls),
    - 1 Autocad drawing detailing the loads of the existing locomotives on the lock wall

33. Actual lockage times for vessel movement, filling/emptying, gate operation

34. Ortho photos (Corozal Lacona, Balboa Rio Cocoli, Clayton Esclusas 1-2-3)

35. Hard copy of third locks construction effort drawings (1939)

36. Summary of results of tests on Rock formations for boring TP1 (August 2001 and TP1C (January 2001)

37a. Report "Pump Saltwater to Gatun Lake"

37b. Report "Recycling Ponds"

37c. Report "Salinity Intrusion in the Panama Canal"

38a. General drawings showing Machinery Chambers Location (6124-6125-6126

38b. Drawings of Miraflores Locks (7065-7066-7067)

39. Plans of Lighting (g1 and g2)

40. Drawings miter gates (5023, 5063, 6210,6211, 6169)

41. Partial Hydraulic Model study of FILL/SPILL Valve LHL-898

42. Comprehensive Hydraulic Model Study of E/F Valves LHL-906

43. Drawings with cut slope profiles along new canal (6)

44. Bathymetric Survey Entrado Pacifico

45. ACP max tanker

1.3 STANDARDS

The design criteria will be based on:

- ROSA 2000 Recommendations pour le calcul aux états-limites des Ouvrages en Site Aquatique (Recommendations for the design of structures in aquatic site according to the approach of the Limit States)
- PIANC Final Report of the International Commission for the study of Locks.(Bull. 55, 1986)
- CARLIER: "Memento des pertes de charge"
- "INTERNAL FLOW SYSTEM" by Miller
- "MEMENTO DES PERTES DE CHARGES" by Idel'cik

The regulations of ROSA 2000 are based on the Eurocodes and completed with specific requirements for Maritime Structures.

The Eurocodes or European Standards for the design of structures are published in 9 separate volumes :

- Eurocodes 0 and 1 contain the basics for structural design and the loads to be applied on the structures.
  At this moment they are published together as one volume “Eurocode 1”.
- In addition there are six Eurocodes for the different building materials :
  Eurocode 2: Design of Concrete Structures
  Eurocode 3: Design of Steel Structures
  Eurocode 4: Design of Composite Steel - Concrete Structures
  Eurocode 5: Design of Timber Structures
  Eurocode 6: Design of Masonry Structures
  Eurocode 9: Design of Aluminium Alloy Structures
- Finally two other Eurocodes deal with geo-technical and seismic design :
  Eurocode 7: Geo-technical Design
  Eurocode 8: Design provisions for Earthquake Resistance
- Seismic Design Guides for Port Structures – PIANC 2001

For items not included in the standards mentioned above, other suitable standards will be consulted as there are:

- BSI 6349 British Standard Code of practice for Maritime Structures
- DIN German Standards
- CUR (Dutch Recommendations)
- EAU 1996 (Recommendations of the Committee for Waterfront Structures)

1.4 DIMENSIONS

1.4.1 SHIP DIMENSIONS

The main dimensions of the ships to be taken into account are:

- length : 385.76 m (1265ft)
- width : 48.78 m (160ft)
- draft : 15.24 m (50ft)

1.4.2 Lock Dimensions

1.4.2.1 Length

The useful length of the lock chamber is fixed at **426.72** m.(1400ft). It is the distance between the downstream inner lock gate plating and the upstream vertical concrete sill.
The chambers are equipped with two gates for reasons of :

- security
- maintenance

1.4.2.2 Width

The width between the lock walls has been fixed at **55.00 m**.

1.4.2.3 Waterdepth

The **minimum** nautical waterdepth over the sills in the lock chamber is **16.76 m (55ft)**. A higher value of 18.30m has been recommended in order to obtain a minimum underkeel clearance of 3.0m inside the locks.
A minimal clearance or freeboard of 2.13 m is suggested in the T.O.R. above the maximum water level in the lock chamber. This value will be examined during the study in function of level fluctuations due to ship movement, and other requirements due to operational conditions. Minimal clearance for the lock gates will be determined separately

1.5 Main Levels

Gatun Lake	Maximum Level Minimum Level	+27.13m PLD (89ft) +24.99 m PLD (82ft)
Pacific Ocean	Maximum Level Mean Sea level Mean Low water spring Minimum Level	+3.60 m PLD +0.30 m PLD **-2.32 m PLD (design level)** –3.44 m PLD
Atlantic Ocean	Maximum Level Minimum Level	+0.41 m PLD -0.15 m PLD

1.6 OTHER REQUIREMENTS IMPOSED BY THE TOR

1.6.1 GENERAL REQUIREMENTS

- The design shall consider the future expansion of an additional lock structure (4th lane) of similar arrangement with water saving basins.
- The engineering aspects shall be developed to a level that results in a baseline cost estimate within which the project can be designed and constructed within 25% of the estimated cost.
- Maintenance is an important consideration in the design of the system and shall consider a minimum of interruption of service.
- The possible use of the gates to serve as the maintenance closure for the dry chamber maintenance of the lock shall be evaluated.
- The alignment of the access channel and the lock system has been determined by ACP.
- The locks will be operated by means of tugboat assistance, and not by locomotives.
- The lock gates will be of the rolling gate type.
- The hydraulic emptying and filling system will be a side wall integrated culvert system with lateral ports.
- The locks will be operated using 3 water saving basins connected to each lock chamber.

1.6.2 REPAIR AND MAINTENANCE

The need of dry chamber maintenance for repair and maintenance of the lock gates and the filling and emptying system has been evaluated. The dry lock chamber condition is considered as a fundamental load condition for the lock walls and the outer lock gates.

As maintenance work in a dry lock chamber causes interruption of service and leads to a higher cost of the structures, solutions will be examined to avoid this procedure.

With rolling gates it is be possible to perform maintenance in the gate recess.

The filling and emptying system is located in the lock walls, and needs no special maintenance.

CPP Consorcio Post-Panamax

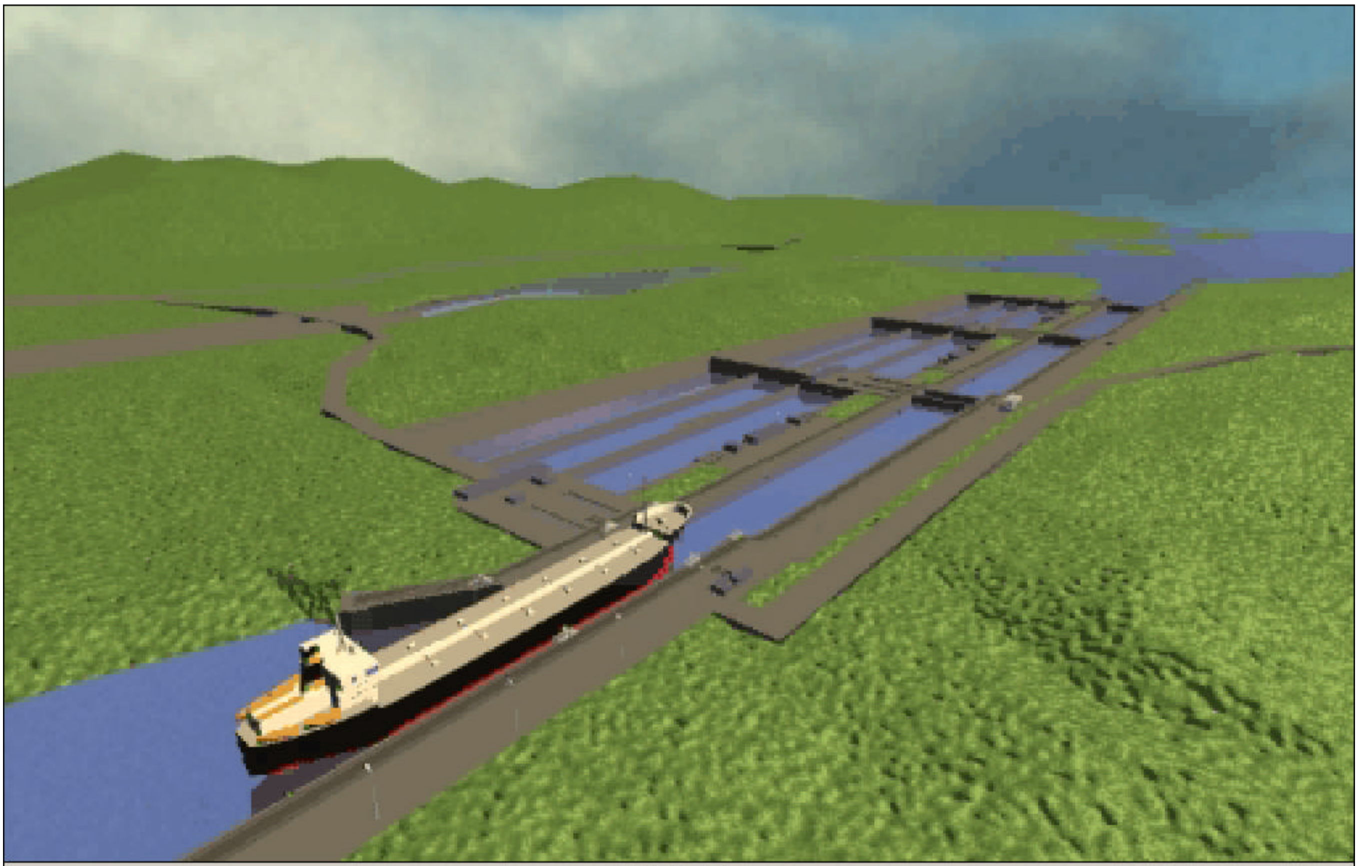

PANimatie_1.avi

Update of Pacific Locks Conceptual Design and Harmonization of Atlantic Locks Conceptual Design - Contract SAA-143351

PACIFIC LOCKS ACTUALIZATION

Task P4a – LOCK SITING

Rev 0

Tractebel Development Engineering TECHNUM COYNE ET BELLIER Compagnie Nationale du Rhône

in association with

1 Alignment

An optimized alignment has been worked out by ACP and is shown on drawing D3-0-101. The new alignment shows a curve in the section of the by-pass canal in its upstream section.
This curve has the inconvenience of not having a straight approach channel when sailing in the direction of the new lock coming from Gatun Lake. However, the curve is more than 4000m away from the upstream lock gate and can therefore not be considered as a nautical problem when compared to other sections of the existing canal. It is advised to widen the canal in the curve section according to the design rules for waterway dimensions.
In the same area the new canal is brought closer to the Pedro Miguel locks, and it will have to be verified if additional measures are required to assure side slope stability and if new dikes are to be built to separate the new canal (at Gatun Lake level) from Miraflores Lake (10m lower). Seepage might also be a problem and needs to be investigated.
The major advantage of the new curved alignment is to have considerable less excavations and as a consequence it will give more economical benefit to the project.
Another advantage is the possibility of moving the lock structure closer to the Pacific; this is explained in the next chapter.

2 Lock Siting

During the original conceptual design study, the lock siting was determined according to the optimum position along the alignment considering nautical accessibility, minimum excavation and favorable soil conditions.
As the new axis is tilted a little clockwise, the lock entrance can be shifted in the direction of the Pacific Ocean, keeping it at 5x a ship length away from the intersection with the existing canal axis in the entrance area. In doing so, the excavation volumes are further reduced.
As far as the geo-technical conditions are concerned, it has been possible to locate the downstream chamber entirely in the La Boca formation and the two upstream chambers in Basalt. Each lock head is still completely located in one single formation.
It can be concluded that the new location is optimized and to be preferred above the one from the original conceptual design; this is essentially due to the tilting of the alignment.
With this new location, closer to the Pacific entrance, the levels of the existing ground surface are lower than in the former situation. This will require additional protection for excavation work and against inundation of the construction site. This can be done by erecting dikes between the

construction site and the lower areas with excavated material, if necessary by adding sheet pile walls to reduce embankment width and to prevent seepage. As the maximum level of the Pacific Ocean is +3.60mPLD, the top level of the dikes should be situated at a level of +5.00mPLD. Drawing D3-0-101 shows a preliminary location of these additional dikes.

3 Rio Cocoli Deviation

Rio Cocoli runs into the Miraflores Lake somewhat to the north of the existing Miraflores locks. Miraflores Lake is at a +/- 10m lower level than the future by-pass canal level which will be varying between +27.13m and +24.99mPLD. During the construction of the new by-pass canal, Rio Cocoli will need to be diverted if the excavation works have to be carried out in dry circumstances, which will most probably be the case. The Rio Cocoli is however situated to the north of the new locks, and the locks excavation and construction can be realized without any diversion of the river.

A logical way of working would be to excavate the upstream by-pass canal in a first phase sufficiently distant from the actual Rio Cocoli river bed, and then deviate the river to this excavated section. At the same time the lock structure has to be built using excavated material to fill the lower parts at the north-west of the lock site and to construct protection dikes and a dam (see drawing D3-0-101).

Finally the remaining canal section has to be excavated connecting the lock with the by-pass canal. This will have to be done partly by dry excavation and by dredging.

This item needs more detailed study in order to determine the most convenient technical – economic solution. The cost estimation of these additional works is based on a rough estimation of excavations and backfilling, assuming that no additional structures have to be constructed (except embankments with local materials from excavation).

Another possibility would be to deviate the river to the south of the new locks, and connect it to the Pacific Entrance. This would require additional excavations and backfilling over a considerable length. It would probably interfere with the fourth lane construction, and therefore it is not retained in this conceptual design.

CPP Consorcio Post-Panamax

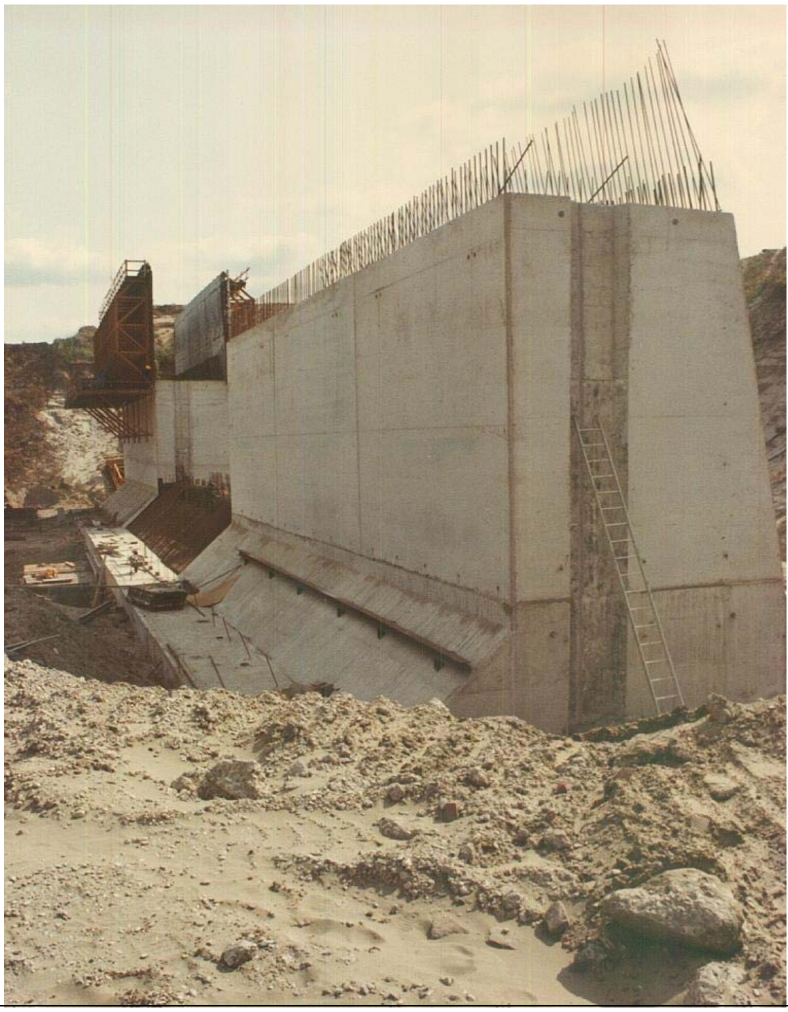

Update of Pacific Locks Conceptual Design and Harmonization of Atlantic Lock Conceptual design - Contract SAA-143351

PACIFIC LOCKS ACTUALIZATION

TASK P4b – LOCK WALLS

Rev A

in association with

1 Lock walls

1.1 DESIGN CRITERIA

Design criteria for the new lock structures have been given in the report of Task P2 - "Design Criteria" of the Pacific Locks Actualization study.

The main changes incorporated for the actualization of the Pacific locks conceptual design with respect to the previous conceptual design are as following:

- Updated width and depth of the locks due to different ship size
- Use of vessel positioning by tugboat cancels locomotive loads on lock walls
- Updated design values for earthquake analysis
- Lock siting has been optimized in relation to new alignment
- Freeboard has been reduced to 1.5 m instead of 3 m
- Culvert dimensions have been changed to 6 m high x 9 m wide.

1.2 TECHNICAL DESCRIPTION OF LOCK WALL STRUCTURE

The differences in geotechnical situation along the triple lift configuration, the dimensional requirements needing large open excavations and successful former experience, has led to the choice of a counterfort retaining wall for the conceptual design of the Pacific lock walls.

Below, a detailed description is given of the wall types adopted for the foundation in basalt rock and in the La Boca formation respectively. Reference is made to the following drawings:

- D4-B-101 Longitudinal view on the left bank lock wall
- D4-B-102 Longitudinal view on the right bank lock wall
- D4-B-103 Plan view lock chamber 1
- D4-B-104 Plan view lock chamber 2
- D4-B-105 Plan view lock chamber 3
- D4-B-106 Cross section lock walls

1.2.1 TYPE 1 – FOUNDATION IN BASALT

The retained concept for the lock wall in basalt rock is shown on drawing D4-B-106.

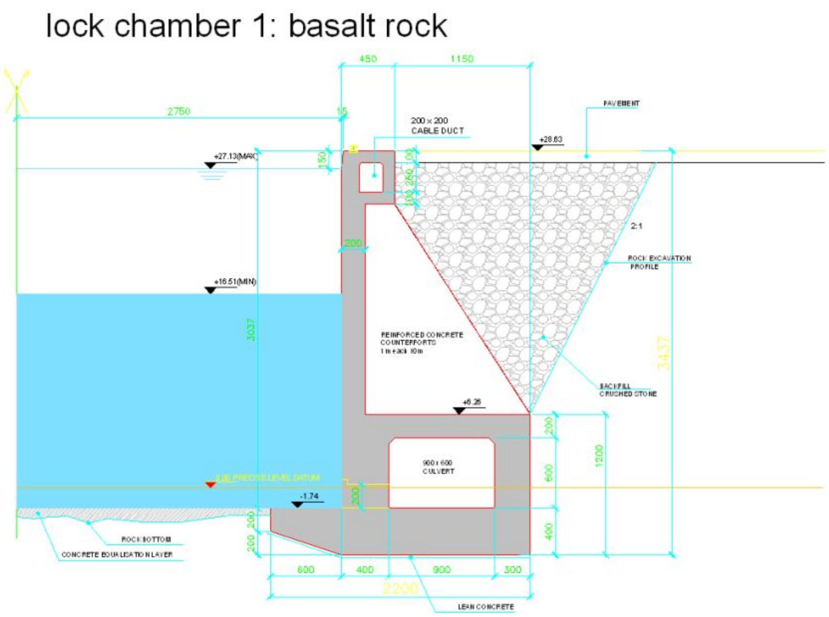

Due to the reduction in width of the top level structure, which was necessary to support the rail tracks in the original conceptual design - with the locomotive positioning system, the advantage of using RCC (roller compacted concrete) is no longer valid. On the contrary, the voluminous rock excavation enables re-use of material fragmented to the proper size, for backfilling purposes, which leads to economical benefit. Besides, the high frictional properties of the broken rock allow for reduction of the horizontal pressure, exerted by the fill on the vertical retaining wall, leading to structural optimization.

The width at the foundation level has been determined in function of required safety against overturning; sliding effects are negligible due to the embedment in solid rock.

In order to minimize excavation volumes, a heavy toe at the front side has been foreseen, instead of enlarging the footing backwards.

At the rear side a nearly vertical excavation has been considered over a limited height in order to minimize formwork and to make maximum profit of the geo-technical (rock) condition.

The culvert with dimensions 6m x 9 m (H x W), which extends over the entire length of the lock wall, is integrated in the lower part of the lock wall.

The structure is a reinforced concrete structure with reinforced concrete counterforts at regular distances.

At the top surface of the wall, additional structural concrete is required to install a cable duct and other quay side equipment, including bollards, ladders and lighting recesses.

1.2.2 TYPE 2 – FOUNDATION IN LA BOCA

Part of the new lock structure will be situated in the “La Boca” formation. Although the characteristics of this formation can be considered as fairly good corresponding to a rock mass type III – IV, with UCS-values ranging from 10-20 MPa, they are considerably lower than those of the basalt formation (RMT I-II, UCS-values 40-100 MPa).

Furthermore, it is also clear that the deformation behavior of the “La Boca” formation will be different than the one of the basalt formation under vertical loading.
(Deformation modules ranging from 2,5–6,6 GPa in La Boca, and from 8-12,5 GPa in basalt).

Also due to the different geo-technical situation, it will be necessary to excavate with flatter sloping angles thus increasing the excavation volumes, and furthermore it will also be required to use formwork for the backside of the wall over the culvert height.

Under these circumstances with less favorable rock characteristics, the lock wall structure will be larger at the footing. However, generally the same concept as for the rock foundation can be retained.

Apparently it is clear that the water content in the samples taken from the La Boca formation is relatively high in comparison with the basalt. The material is also sensitive to weathering when exposed to water, and accordingly it will be necessary to install a concrete bottom floor in the lock chamber. To avoid uplift water pressure a permeable structure will be provided (such as in the Berendrecht lock).

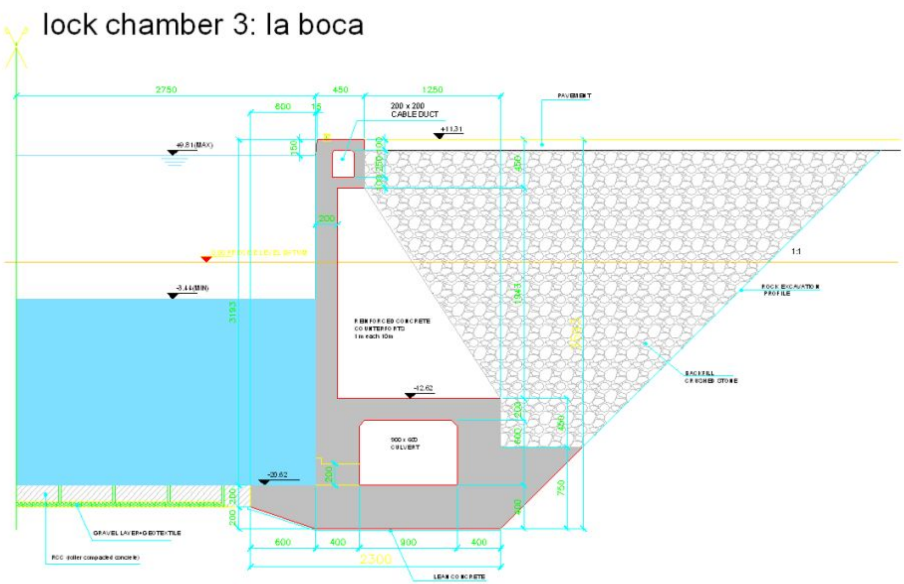

1.3 LOCK WALL ANALYSIS

1.3.1 LOADS

A. Self Weight (load case 1 = LC1)

Concrete	γ= 25.0 kN/m³
Wet backfill	γ= 20.0 kN/m³
Dry backfill	γ= 18.0 kN/m³

B. Earth Pressure (LC 2)

As the counterfort retaining walls nears geometrically to a cantilever wall type, the active lateral pressures will be calculated for a Rankine situation:

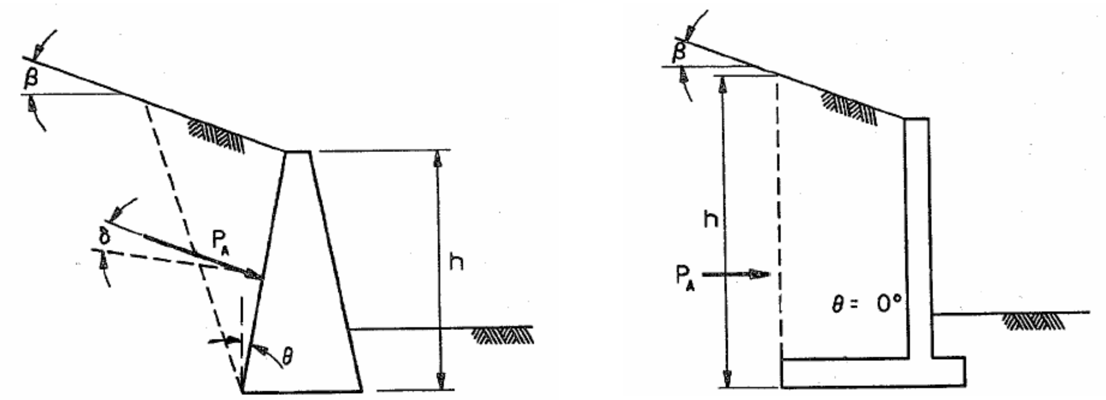

$$K_a = \frac{\cos^2(\varphi' - \theta)}{\cos^2\theta\cos(\theta+\delta)\left[1+\sqrt{\dfrac{\sin(\varphi'+\delta)\sin(\varphi'-\beta)}{\cos(\delta+\theta)\cos(\beta-\theta)}}\right]^2}$$

with δ = 0°; β = 0° and θ = 0°

The angle of friction in the filling of crushed stone is 45°

C. Water Pressure (LC 3)

Inside the lock, the minimum water level will be applied.
At the backside of the wall the maximum water level of the lock chamber will be applied.

D. Vertical live load

On the surface a vertical live load p=10 kN/m² is applied, this load case is included in normal earth pressure load case (LC2). In seismic conditions, only half of the live load is taken into account (5 kN/m²) and is included in the seismic earth pressures load case (LC6).

E. Bollards (LC 4)

The forces needed to move and hold a ship into the lock depend on:
- the water displacement of the ship;
- the velocity of entering the lock;
- the angle of the lines;
- the ratio cross section ship/lock;
- the movement of the ship during filling/emptying of the lock.

The calculation of these forces is very complicated and has been assessed during former studies (Hawser Forces Analysis by Flanders Hydraulics September 2003 / Hawser Forces Analysis by Flanders Hydraulics (CPP) March 2005). These calculations have been made for positioning systems both with locomotives and tugboats. In fact the maximum allowed hawser forces are entirely dependent on the breaking load of the hawsers and the positioning system. In the case of vessels tied up with mooring lines at fixed bollards, the breaking load could easily be higher than those determined in the above mentioned analyses. Maximum breaking loads of usual nylon mooring lines for large seagoing vessels are normally +/- 80tons (allowable working load 75%). If two lines would be used on only one bollard, this would give a maximum working load of 120tons.
For this concept design, the maximum bollard pull has consequently been set at 1500kN, a figure that corresponds very well with the recommendations of EAU1996 (page 143 – section 5.12).

As the wall is divided into segments of about 30m, the total horizontal load applied to one running meter of lock wall is 50kN/m'.

F. Seismic Loads (LC 5, 6, 7 and 8)

F.1 Earthquake level

ACP stated in its Memorandum of 20 Jan 2005 on 'Seismic Design Criteria' that an earthquake with a return period of 5000 years should be considered as Maximum Credible Earthquake (= MCE) and taken equal to the Maximum Design Earthquake (= MDE).

F.2 Performance Grade

The highest performance grade (Grade S) is applicable for
- critical structures with potential for extensive loss of human life and property
- key structures that are required to be serviceable for recovery from earthquake disaster
- critical structures that, if disrupted, devastate economic and social activities

A catastrophic failure of the locks may cause flooding in the terminal cities of the canal.

This means that the level of damages is:

- Structural: minor or no damage
- Little or no loss of serviceability

for a MCE-event.

F.3 Analysis type

As this report concerns conceptual design, a simplified analysis will be used considering equivalent static forces to apply the seismic loads on the structure.

F.4 Representative ground acceleration values

Based on the review of probabilistic seismic hazard analysis by Winter (2005), the following PGA-values can be taken as representative for the site at Miraflores:

Return period [years]	Representative PGA	Level	Load case
100	0.07		
500	0.16		
1000	**0.22**		
2500	0.32		
5000	**0.40**	MDE = MCE	LC6
10000	0.51		

The seismic coefficient k_e for use in retaining structures is defined as follows for Special Class Structures:

$$k_e = PGA/g \quad \text{for } PGA < 0.2\text{ g}$$

$$= \frac{1}{3}\left(\frac{PGA}{g}\right)^{\frac{1}{3}} \quad \text{for } PGA \geq 0.2\text{ g}$$

With according to Eurocode design (CEN 1994)

$k_{h\,(horizontal)} = k_e$
$k_{v(vertical)} = ½k_e$

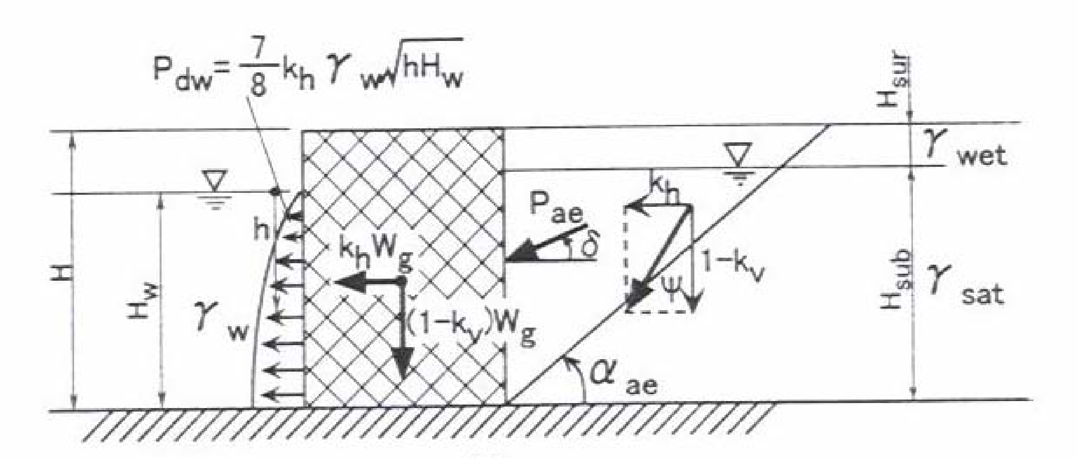

(a)

The seismic loads are calculated separately for earth pressure (LC 6), equivalent horizontal (LC 7) and vertical (LC 8) reaction forces on structural masses and water bodies (LC 5).

G. Water Pressure in Dry Lock Conditions (LC 9)

Identical to load case 3 but without water pressure at the front side (lock empty).

1.3.2 LOAD COMBINATIONS

According to ROSA 2000

A. Quasi Permanent Load Combination

QP1 1*LC1 + 1*LC2 + 1*LC3 + 1*LC4

B. Rare Load Combination

R1 1*LC1 + 1*LC2 + 1*LC9

C. Fundamental Load Combinations

F1 1.20*LC1 + 1.20*LC2 + 1*LC3 + 1.20*LC4
F2 0.90*LC1 + 1.20*LC2 + 1*LC3 + 1.20*LC4
F3 1.20*LC1 + 1.20*LC2 + 1*LC9
F4 0.90*LC1 + 1.20*LC2 + 1*LC9

D. Accidental Load Combination - MCE

MCE 1*LC1 + 1*LC3 + 0.25*LC5 + 1*LC6 + 0.25*LC7 + 0.12*LC8

1.3.3 CRITERIA

According to ROSA 2000

A. Sliding along the base

Not applicable in basalt rock.
In the La Boca formation, a concrete floor will prevent sliding

B. Turn over

Load Combination	Criterion
QP1	Compression zone A’ > 90% A
R1	Compression zone A’ > 75% A
F1 to F4	Compression zone A’ > 10% A
MCE	Compression zone A’ > 10% A

C. Load Bearing Capacity

$\gamma_d \cdot q_{ref} < q_u$
γ_d . = 1.4 for load combination F1 to F4
γ_d . = 1.0 for load combination MCE

q_u = ultimate load bearing capacity
q_{ref} = reference pressure

D. Deformations

The deformations will be checked for frequent, rare and accidental load combinations QP1, R1 and MCE.

E. Concrete Stresses

Fundamental load combinations: F1 tot F4: 1.125 x $\sigma_c < 0.85\, f_{ck}/1.5$
Accidental load combination: MCE: $\sigma_c < 0.85\, f_{ck}$

The factor 1.125 is a result of combination of the different factors in the load combinations between ROSA 2000 and Eurocode

F. Global Stability

Will be checked for the wall in La Boca formation only.

1.3.4 SOFTWARE

The calculations are made by means of “Esa-PrimaWin 3.60.381”, a finite element program. The lock wall is modeled as a 2D WALL structure, allowing forces acting in its plane.

A non-linear analysis is performed to allow for compression only supports.

1.4 TYPE 1 - FOUNDATION IN BASALT

1.4.1 INPUT DATA

A. Geometry

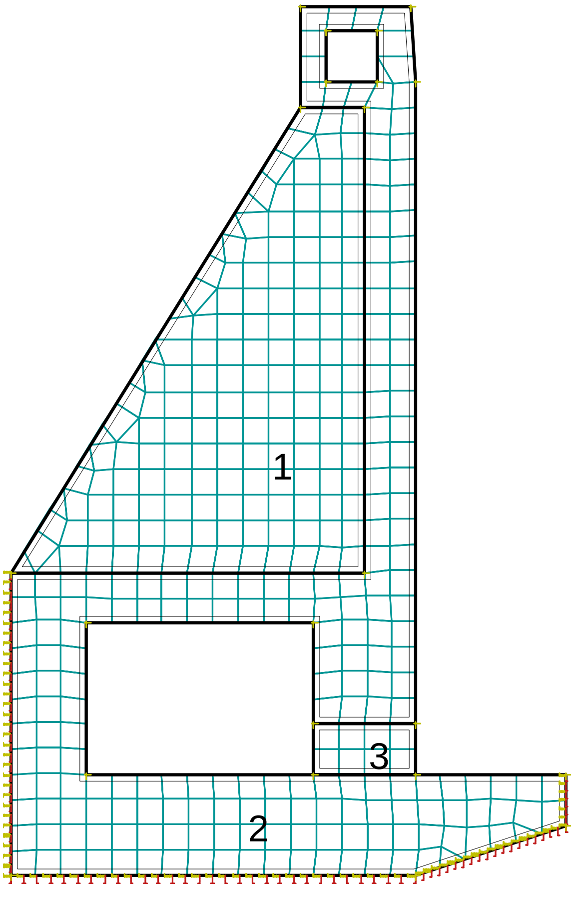

The FE model consists of the following three 2D macro structural elements :

No.	Element	Thickness
1	Reinforced concrete counterforts	0.1 m (1m each 10 m)
2	Retaining wall	1 m
3	Culvert outlet (2 m x 2 m)	0.867 m (each 15 m)

B. Materials

Name:		
C25/30-cracked		
	E modulus	20000.00 MPa
	Poisson coefficient.	0.20
	Density	2500.000 kg/m^3
	Expansion coefficient	0.01 mm/m.K

For the material corresponding to the reinforced concrete counterforts, the submerged weight of 15 kN/m^3 is taken into account, as the water pressure of LC3 are immediately applied to the main wall element.

C. Supports

The rock base is modeled by means of linear supports.

- The embedded part of the retaining wall and perpendicular to the boundary of the toe, is characterized by a linear support of, K = 1000 MN/m/m', working in compression only.
- Parallel to the base, sliding is restricted through a frictional resistance of 300 MN/m/m'.

D. Loads

D.1 Self Weight (LC1)

The total weight of the structure: 551.5 ton/m'.

D.2 Rock fill (LC2)

from	28.63		27.13	
			λav =	λah =
λa =	0.1716		0.0000	0.1716
ϕ =	45	0.79	δ =	0
θ =	0	0.00		
γ =	18			
z	p		**pv**	**ph**
28.63	10		0.000	1.716
27.13	37		0.000	6.348

from	27.13	to	24.63	
			λav =	λah =
λa =	0.1716		0.0000	0.1716
ϕ =	45	0.79	δ =	0
θ =	0	0.00		
γ =	10			
z	p		**pv**	**ph**
27.13	37		0.000	6.348
24.63	62		0.000	10.638

from	24.63	to	6.26	
			λav =	λah =
λa =	0.1716		0.0000	0.1716
ϕ =	45	0.79	δ =	0
θ =	0	0.00		
γ =	10			
z	p		**pv**	**ph**
24.63	62		0.000	10.638
6.26	245.7		0.000	42.155

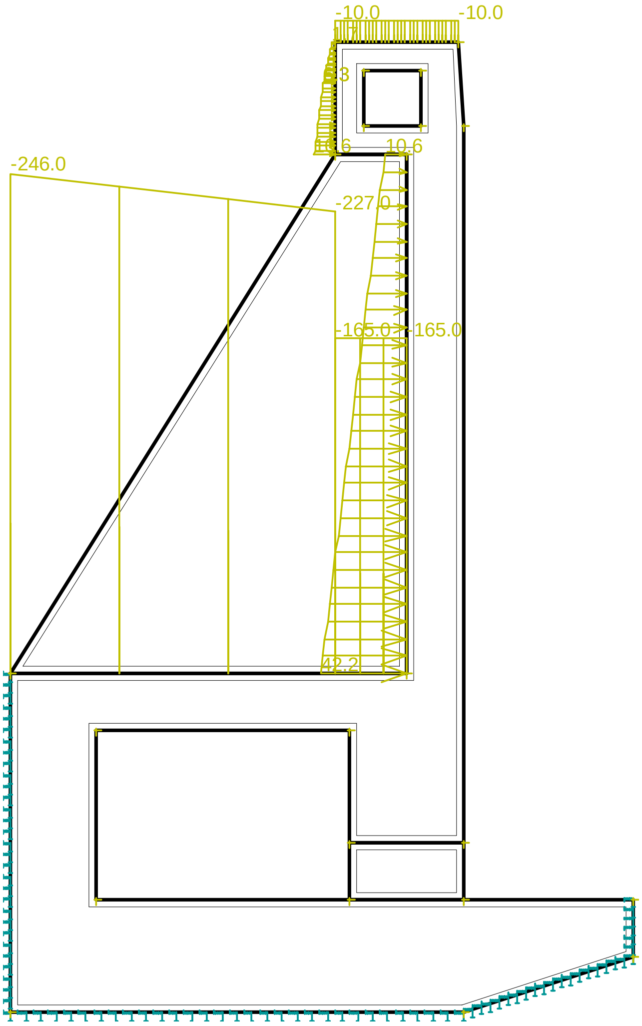

Soil weight on culvert block

X	**pv**
0	246
11.5	227
11.5	165
14	165

Remark: The active lateral pressures on the vertical through the rear edge of the retaining wall are transferred to the front wall elements for ease of implementation.

D.3 Water Pressure (LC 3)

Water level inside the lock: +16.51m
Water level outside the lock: +27.13m

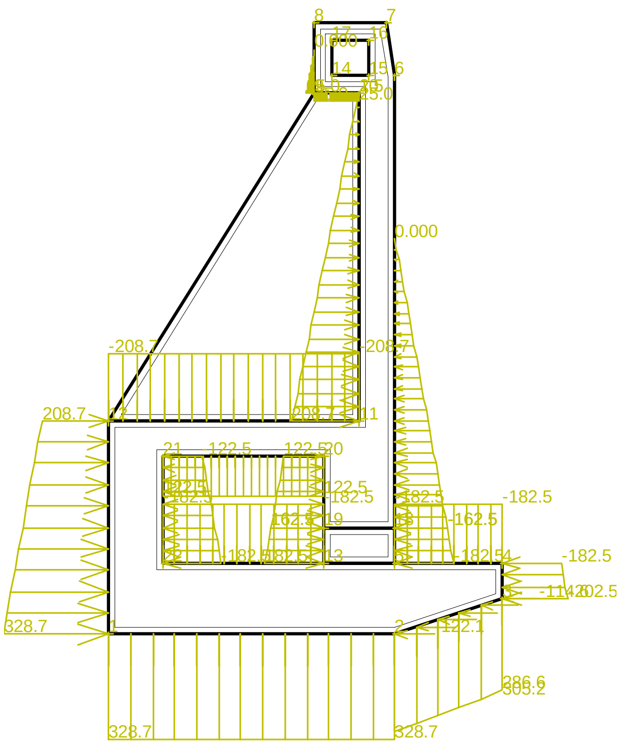

D.4 Bollard pull (LC 4)

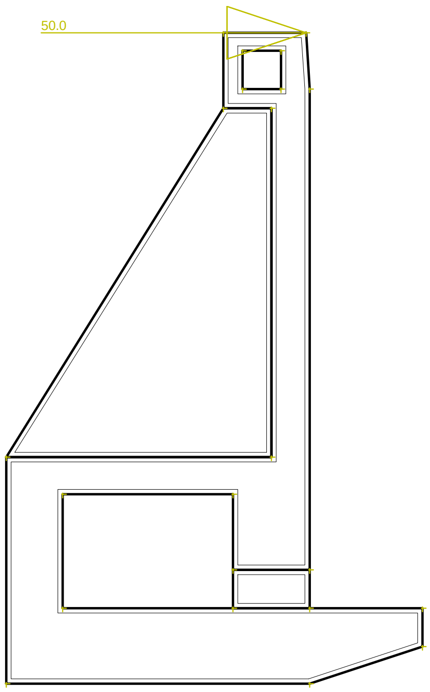

D.5 Water Pressure – Seismic loading (LC 5)

Water level inside the lock: +16.51m
Water level outside the lock: +27.13m

Additional water pressures generated by seismic action are:

Water suction forces at the outside face of the wall according to Westergaard

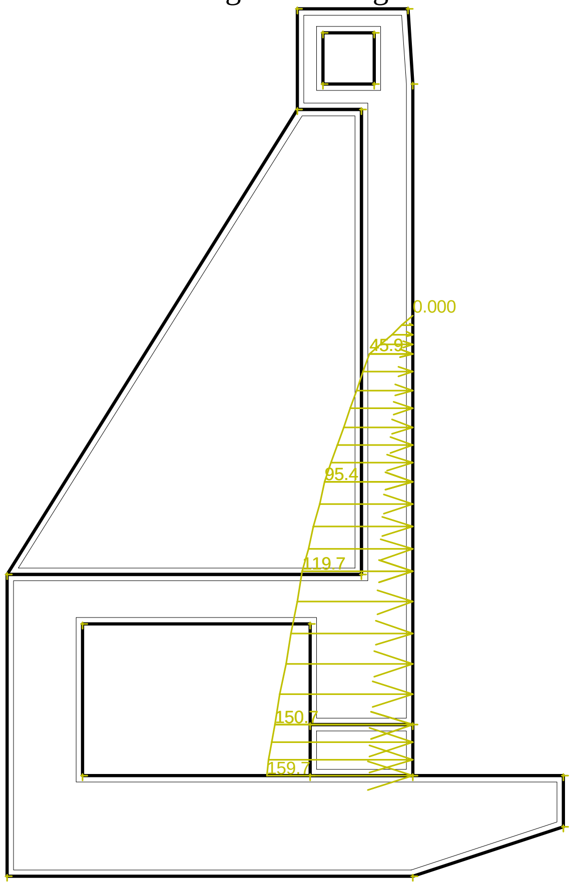

Equivalent seismic reaction forces on water body contained in culvert

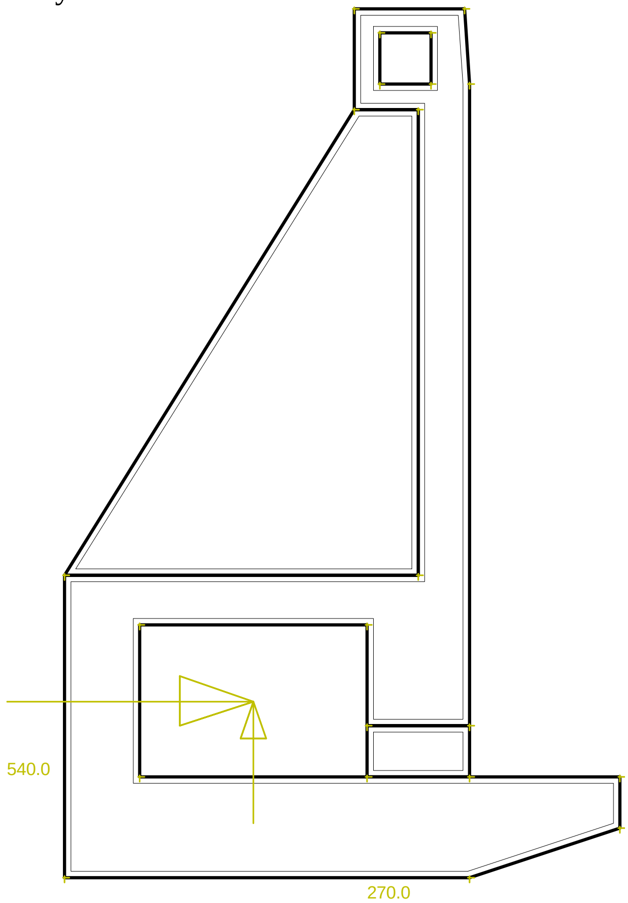

The seismic water pressure load case is valid for a unit value of k_e, and is multiplied by the respective k_e value in the corresponding load combinations.

D.6 Seismic Loads (LC 6, 7 and 8)

LC 6

The active lateral earth thrust under seismic conditions is calculated based on the Mononobe-Okabe (M-O) methodology. The M-O method is an extension of Coulomb's theory, wherein the M-O method takes into account the inertial forces acting on the soil mass during earthquake loading. It was developed to assess the stability of massive gravity walls, assuming that the retaining wall and the failure wedge act as rigid bodies.

The inertia forces are then accounted for by considering a seismic inertia angle, $\Psi = \text{atan}(k_h/(1-k_v))$, in which k_h represents the horizontal seismic coefficient or the modified horizontal seismic coefficient for dry and submerged layers respectively.

As the counterfort retaining wall under consideration is geometrically near to cantilever wall type, a Rankine situation is assumed for the calculation of the seismic active earth pressures on the vertical through the rear edge of structure. Consequently, the weight and inertia forces of the soil masses above the structure's rear base have to be taken into consideration.

Remark:

- The active lateral pressures and the horizontal inertia components of the soil masses are transferred to the front wall elements for ease of implementation.
- Half of the vertical live load is taken is accounted for in the seismic earth pressures.

LC 7 and 8

The inertia forces on the structural weight are calculated as follows:

$G_v = (1-k_v)\, G$

$G_h = k_h\, G$

With G the weight of the filling

G_v the vertical component of the weight in seismic conditions

G_h the horizontal component of weight in seismic conditions

PGA	0.4	g	k_e	0.246
k_h	0.246		k_v	0.123

CFR	0.1
Width	16

from	28.63		27.13		1.50				
			λav =	λah =		k_h'	0.246		
λa =	0.3200		0.0000	0.3200					
ϕ =	45	0.79	δ =	0	0.00	ψ	15.6	0.27	
θ =	0	0.00							
γ =	18								
z	p		pv	ph1		**Q1v**	**0.00**		
28.63	4.386		0.000	1.403		**Q1h**	**7.79**		
27.13	28.070		0.000	8.982		**Q1**	**7.79**		

Width =	11.5
b =	4.5
ph2	50.840
	ph
	52.243
	59.822

from	27.13	to	24.63		2.50			
			λav =	λah =		k_h'	0.491	
λa =	0.5638		0.0000	0.5638				
ϕ =	45	0.79	δ =	0	0.00	ψ	29.2	0.51
θ =	0	0.00						
γ =	10							
z	p		pv	ph1		**Q2v**	**0.00**	
27.13	28.070		0.000	15.826		**Q2h**	**55.02**	
24.63	50.000		0.000	28.190		**Q2**	**55.02**	

Width =	11.5
b =	4.5
ph2	56.488
	ph
	72.315
	84.679

from	24.63	to	6.26		18.37			
			λav =	λah =		k_h'	0.491	
λa =	0.5638		0.0000	0.5638				
ϕ =	45	0.79	δ =	0	0.00	ψ	29.2	0.51
θ =	0	0.00						
γ =	10							
z	p		pv	ph1		**Q2v**	**0.00**	
24.63	50.000		0.000	28.190		**Q2h**	**1352.32**	
6.26	211.142		0.000	119.041		**Q2**	**1352.32**	

Width =	14
b =	2
ph2	*61.892*
	ph
	85.907
	180.933

1415.13

Soil weight on culvert block

X	**pv**
0	211
11.5	195
11.5	145
14	145

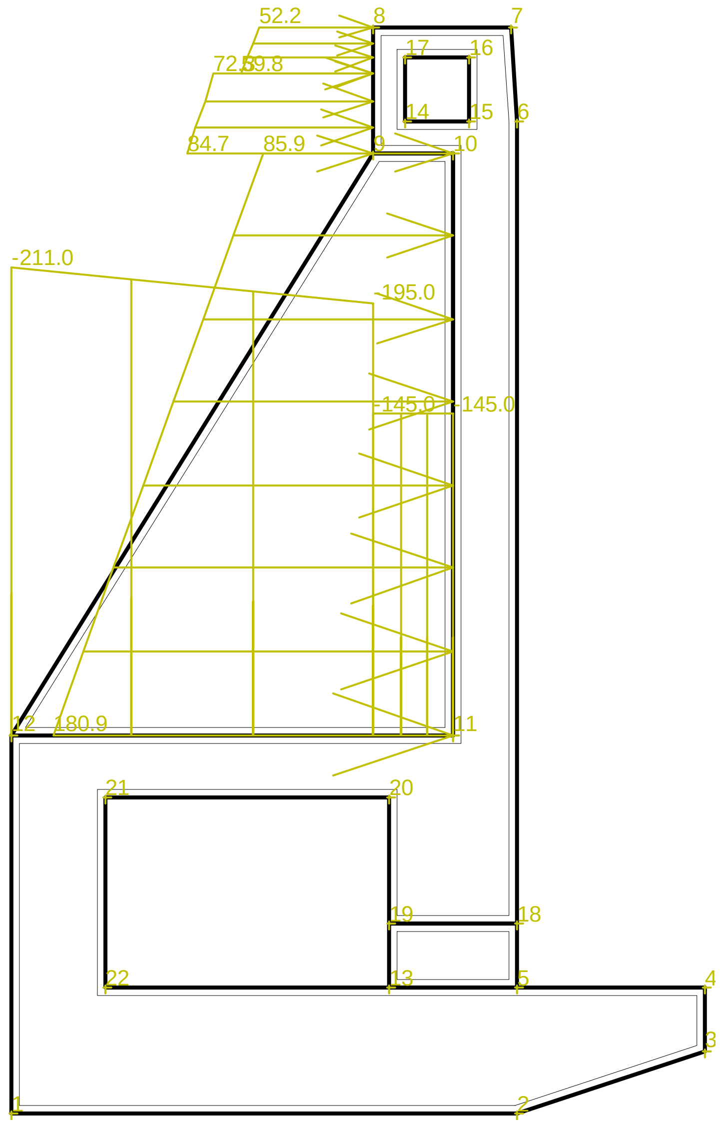

D.7 Water Pressure in Dry Lock Conditions (LC9)

Water level inside the lock: -1.74 m
Water level outside the lock: +27.13m

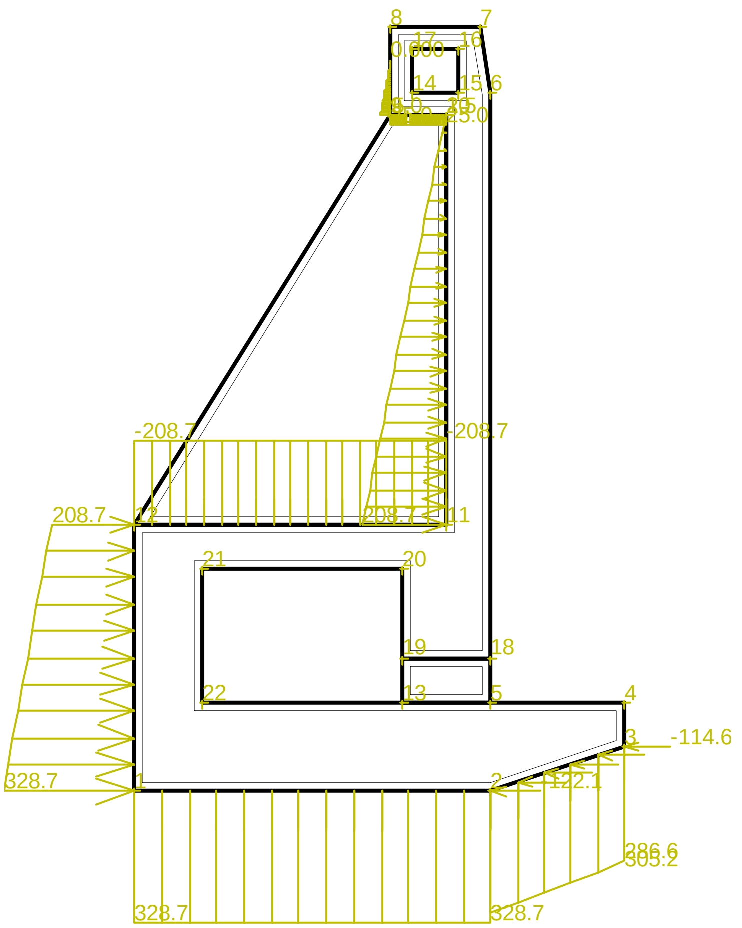

At the rear side of the wall and the bottom the same water pressure is applied as in case 3. This is a very conservative assumption as the pressure should normally be equal to zero at the front toe of the footing.

1.4.2 TURN OVER

A. Quasi Permanent Load Combination (QP1) – Lock in service

Criterion: Compression zone A' (= 91%)> 90% A

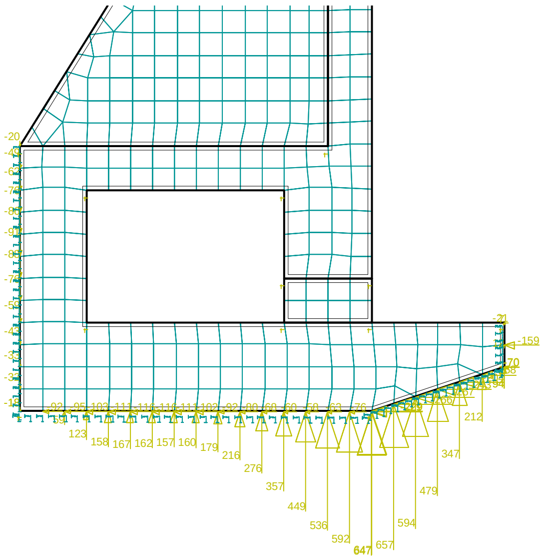

The magnitude of the vectors shown represent the support reactions in each node and not the soil pressure.

B. Rare Load Combination (R1) – Dry Lock Conditions

Criterion: Compression zone A'(= 87%) > 75% A

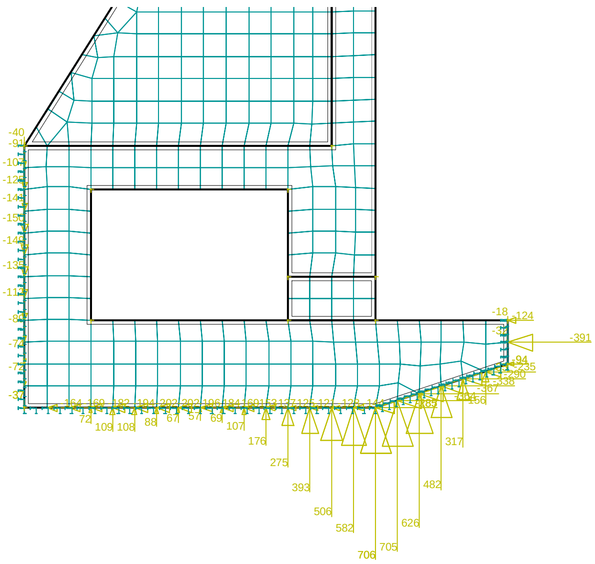

C. Fundamental Load Combinations F1 to F4

Criterion: Compression zone A’ (= 87%)> 10% A

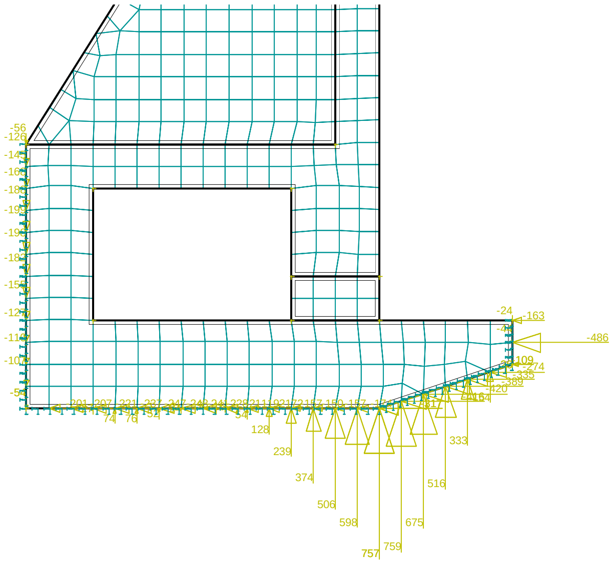

D. Accidental Load Combination – Earth Quake MCE

Criterion: Compression zone A’ (= 78%)> 10% A.

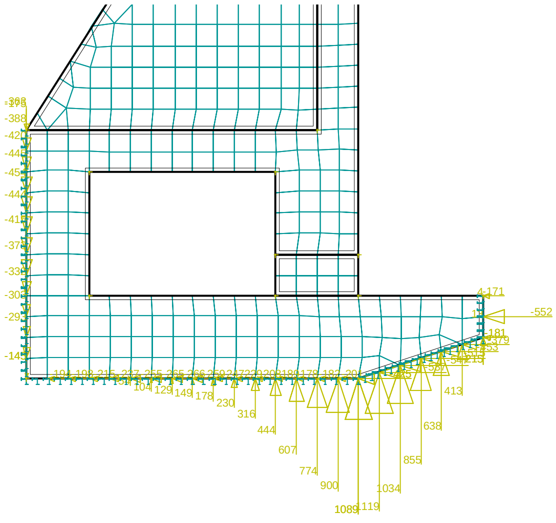

1.4.3 LOAD BEARING CAPACITY

A. Fundamental Load Combinations F1 to F4

Criterion: $\gamma_d \,.\, q_{ref} < q_u$
with $\gamma_d \,. = 1.4$

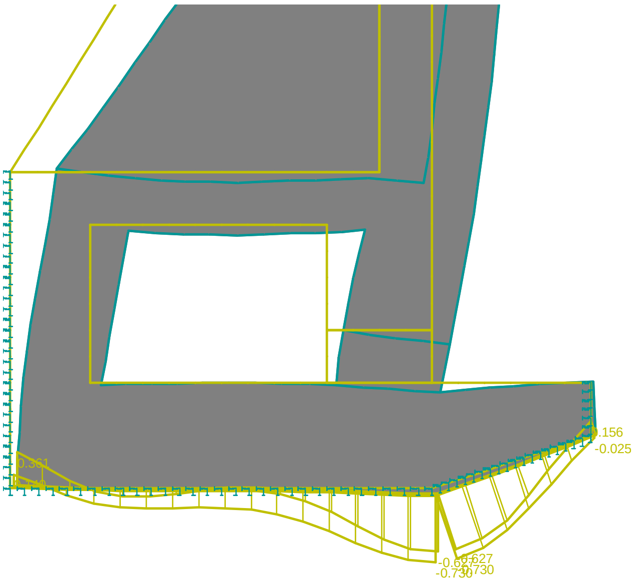

The maximum vertical displacement at the bottom of the wall is 0.730 mm, which is negligible.
This corresponds to a maximum vertical pressure of 0.000730 x 1000000 kN/m² = 730 kN/m² = 0.73 Mpa.
Consequently:

$$\gamma_d \,.\, q_{ref} = 1.4*0.730 = 1.02 < q_u = 40MPa$$

(According to report R2-A the Uni-axial Compressive Strength of the basalt rock varies from 40 to 100MPa).

B. Accidental load combination MCE

Criterion: $\gamma_d \, . \, q_{ref} < q_u$
with γ_d . = 1.0 for accidental load combinations

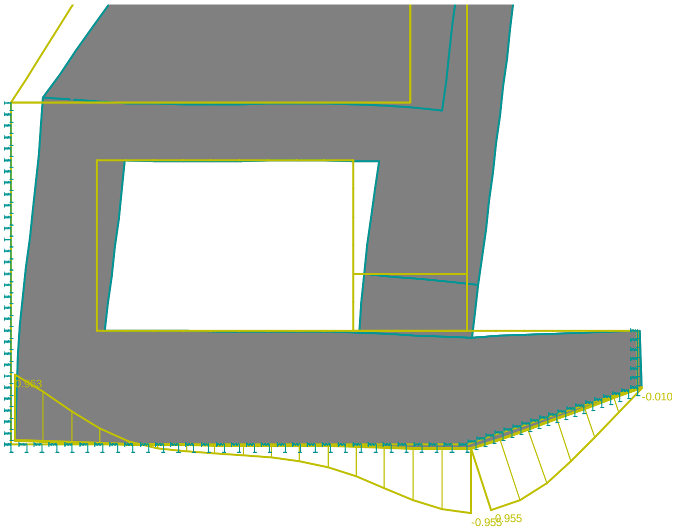

The maximal vertical displacement at the bottom of the wall is 0.955 mm
This means a vertical pressure of 0.000955 x 1000000 kN/m² = 955 kN/m² = 0.955 MPa.
Consequently:

$$\gamma_d \, . \, q_{ref} = 1.0*0.955 = 0.96 < q_u = 40\text{MPa}$$

(According report R2-A the Uni-axial Compressive Strength of the basalt rock varies from 40 to 100MPa).

1.4.4 DEFORMATIONS

A. Load Combination QP1 (Lock in Service)

Maximal horizontal displacement, $u_{x,max}$ = 9.1 mm

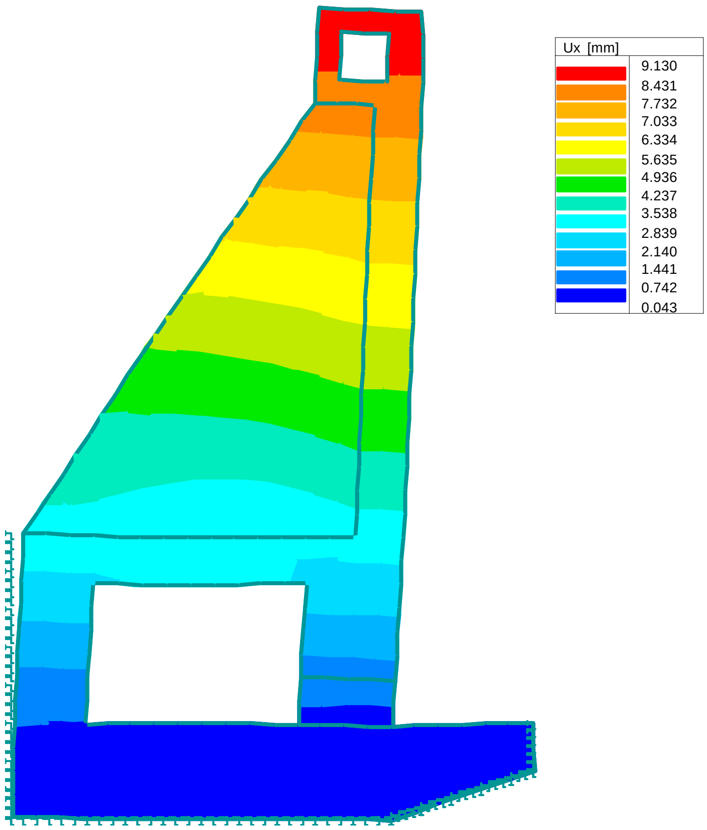

B. Load Combination R1 (Dry Lock Conditions)

Maximal horizontal displacement, $u_{x,max}$ = 9.9 mm

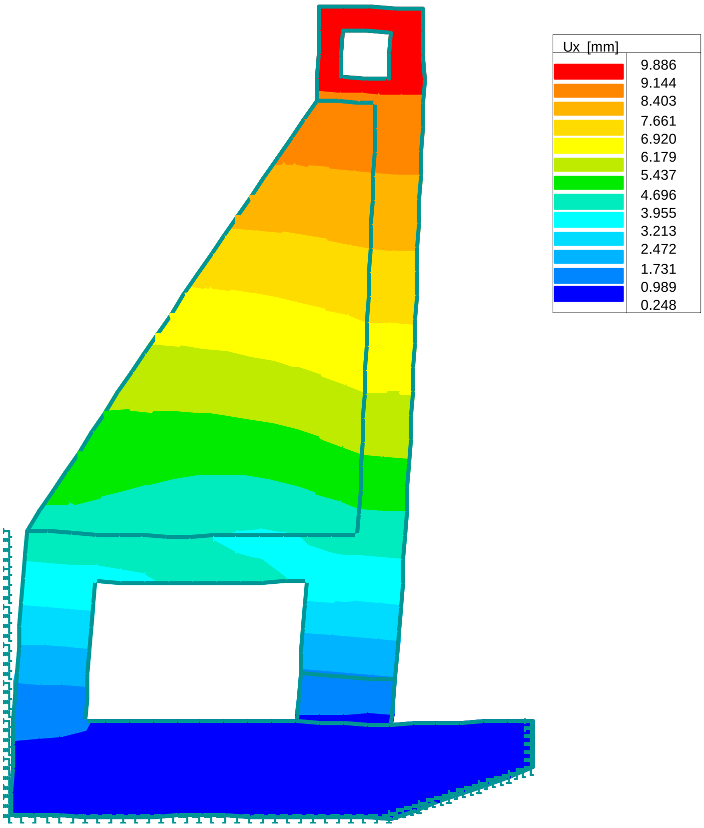

C. Load Combination MCE (Earth Quake)

Maximal horizontal displacement, $u_{x,max}$ = 24.1 mm (reference case)

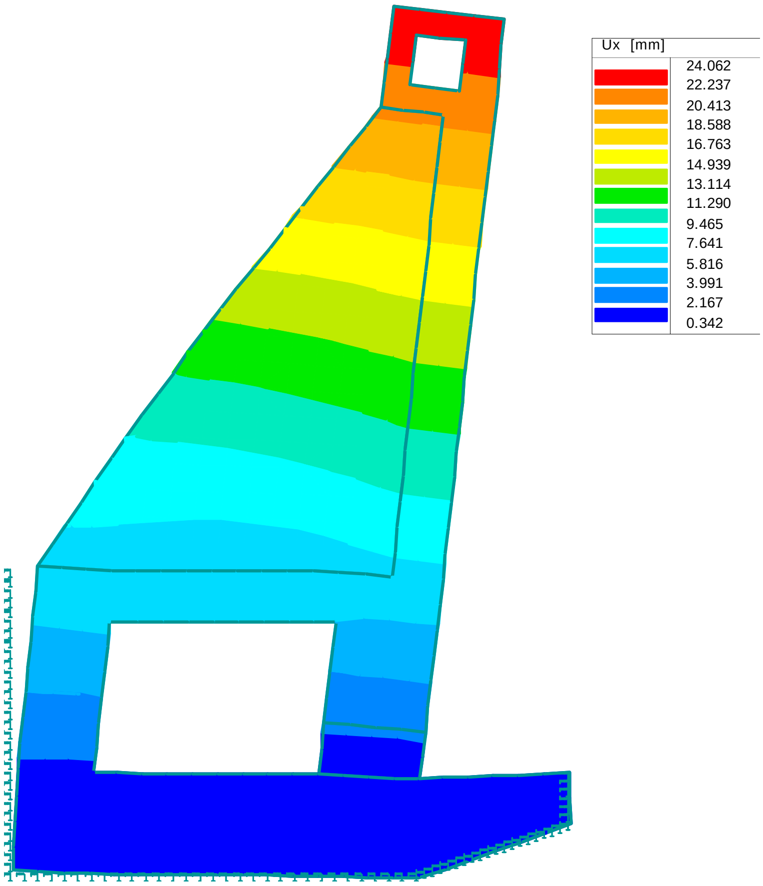

1.4.5 CONCRETE STRESSES

A. Fundamental load combinations F1 tot F4:

$1.125 \times \sigma_c < 0.85 f_{ck}/1.5$
with $f_{ck} = 25 N/mm^2$:
$\sigma_c = 13.30 N/mm^2 > 12.5 N/mm^2$
=> Local reinforcement at culvert outlet will be needed

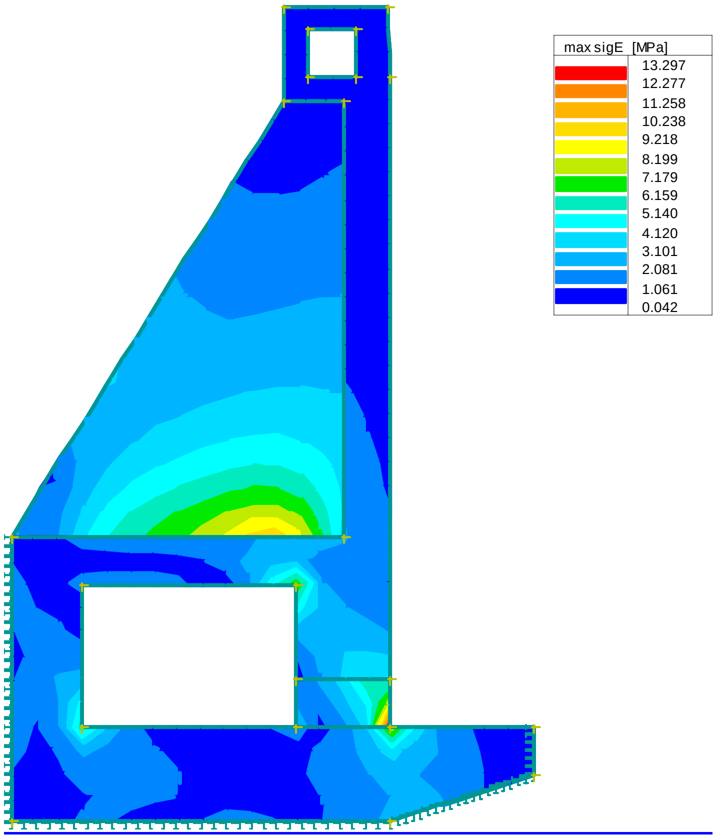

B. Accidental load combination MCE:

$\sigma_c < 0.85\ f_{ck}$
with $f_{ck} = 25 N/mm^2$:
$\sigma_c = 15.41\ N/mm^2 < 21.25\ N/mm^2$

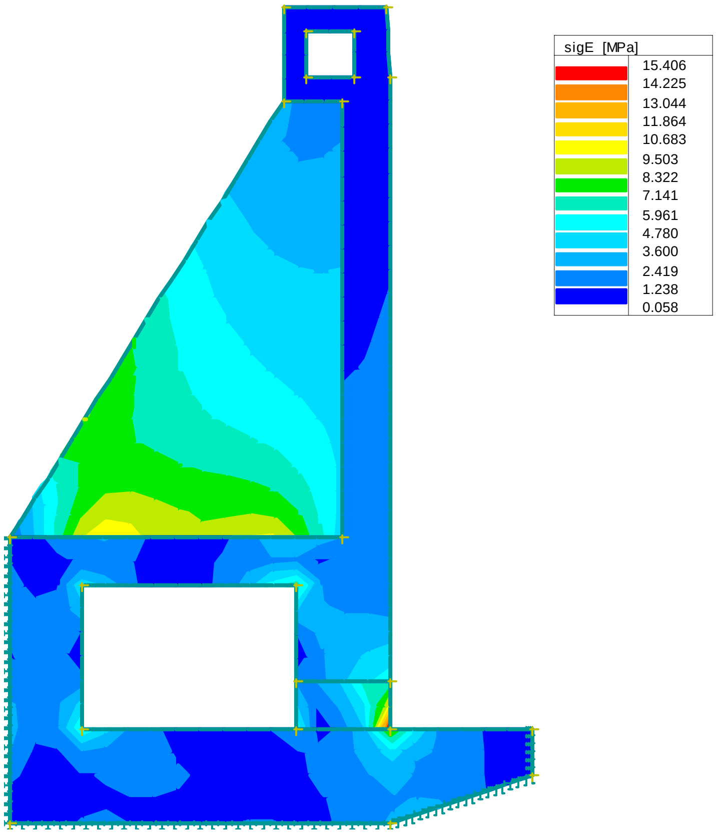

1.4.6 SUMMARY

Criterion	QP1 (Quasi Permanent Load Combination - Service)	R1 (Rare Load Combination - Dry Lock Condition)	F (Envelope of Fundamental Load Combinations)	MCE (Accidental Load Combination - MCE)
Compression zone A' > 90% A	91%	-	-	-
Compression zone A' > 75% A	-	87%	-	
Compression zone A' > 10% A	-	-	87%	78%
Load Bearing Capacity				
1.4 $q_{ref} < q_u$ (MPa)	-	-	1.02	-
$q_{ref} < q_u$ (MPa)	-	-	-	0.96
Deformations				
maximal displacement (mm)	9.1	9.9	-	24.1
Concrete stresses				
1.125 x σc < 0.85 fck/1.5	**-**	**-**	**106%**	**-**
σc < 0.85 fck	-	-	-	73%
Deep Seeted Sliding				
	-	-	-	-

1.5 TYPE 2 - FOUNDATION IN LA BOCA

1.5.1 INPUT DATA

A. Geometry

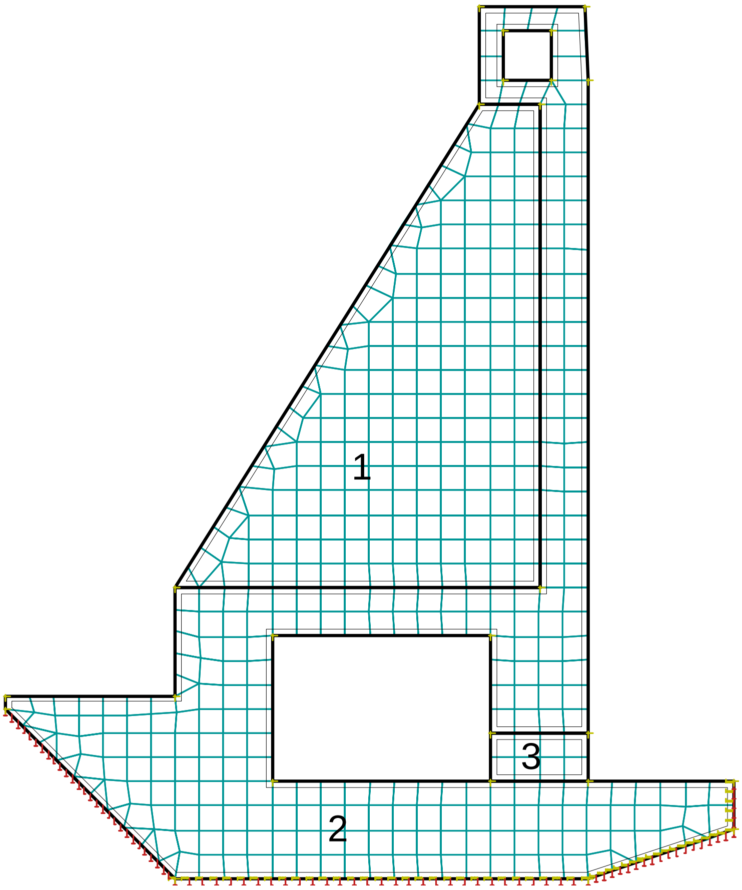

The FE model consists of the following three 2D macro structural elements:

No.	Element	Thickness
1	Reinforced concrete counterforts	0.1 m (1m each 10 m)
2	Retaining wall	1 m
3	Culvert outlet (2 m x 2 m)	0.867 m (each 15 m)

B. Materials

Name:		
C25/30-cracked		
	E modulus	20000.00 MPa
	Poisson coefficient.	0.20
	Density	2500.000 kg/m^3
	Expansion coefficient	0.01 mm/m.K

For the material corresponding to the reinforced concrete counterforts, the submerged weight of 15 kN/m^3 is taken into account, as the water pressure of LC3 are immediately applied to the main wall element.

C. Supports

The rock base is modeled by means of linear supports.

- Vertical to the base of the retaining wall and perpendicular to the boundary of the back toe, the bedding on the La Boca rock formation is characterized by a linear support of, K= 200 MN/m/m', working in compression only.
- Parallel to the base, sliding is restricted through a frictional resistance of 30% of the elasticity of the bedding.
- At the inner toe, horizontal support on the concrete floor is modeled with an elasticity of K = 1000 MN/m/m'.

D. Loads

D.1 Self Weight (LC 1)

The total weight of the structure: 665.0 ton/m’.

D.2 Rock fill Pressure (LC 2)

from	11.31		9.81	
			λav =	λah =
λa =	0.1716		0.0000	0.1716
ϕ =	45	0.79	δ =	0
θ =	0	0.00		
γ =	18			
z	p		**pv**	**ph**
11.31	10		0.000	1.716
9.81	37		0.000	6.348

from	9.81	to	7.31	
			λav =	λah =
λa =	0.1716		0.0000	0.1716
ϕ =	45	0.79	δ =	0
θ =	0	0.00		
γ =	10			
z	p		**pv**	**ph**
9.81	37		0.000	6.348
7.31	62		0.000	10.638

from	7.31	to	-12.62	
			λav =	λah =
λa =	0.1716		0.0000	0.1716
ϕ =	45	0.79	δ =	0
θ =	0	0.00		
γ =	10			
z	p		**pv**	**ph**
7.31	62		0.000	10.638
−12.62	261.3		0.000	44.832

from	-12.62	to	-17.12	
			λav =	λah =
λa =	0.1716		0.0000	0.1716
ϕ =	45	0.79	δ =	0
θ =	0	0.00		
γ =	10			
z	p		**pv**	**ph**
−12.62	261.3		0.000	44.832
−17.12	306.3		0.000	52.553

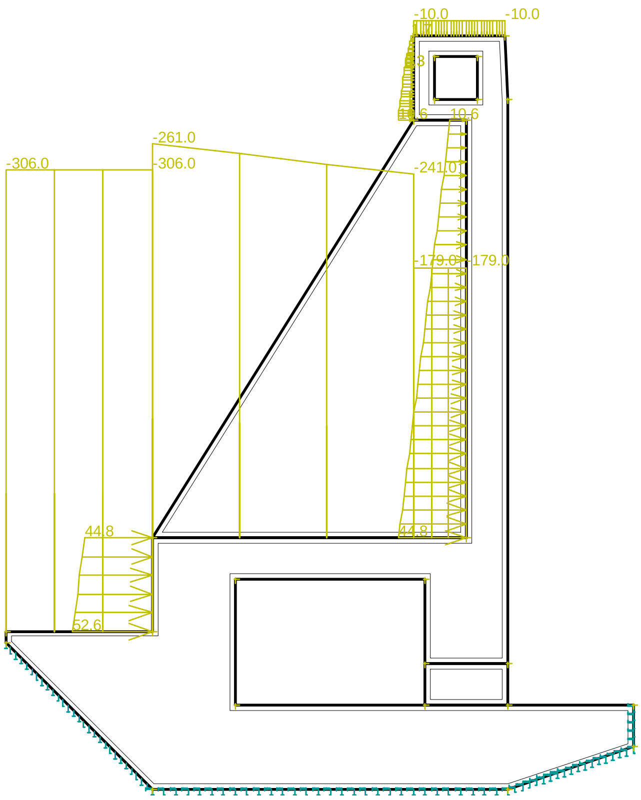

Soil weight on culvert block

X	pv
-7	306
0	306
0	261
11.5	241
11.5	179
14	179

Remark: The active lateral pressures on the vertical through the rear edge of the retaining wall are transferred to the front wall elements for ease of implementation.

D.3 Water Pressure (LC 3)

Water level inside the lock: -3.44m
Water level outside the lock: +9.81m

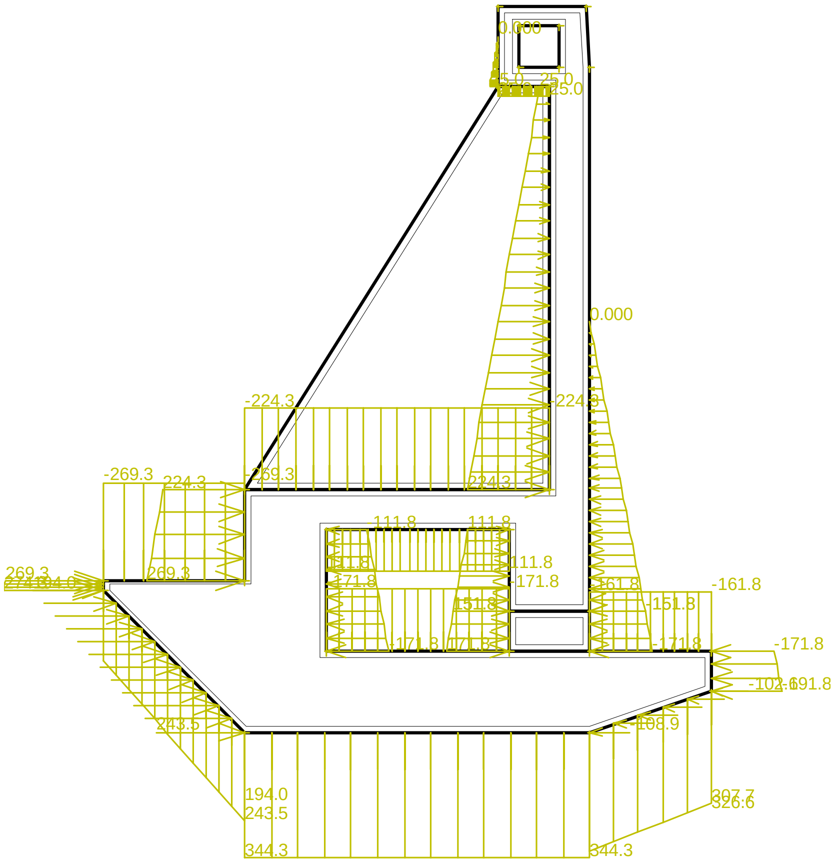

D.4 Bollard pull (LC 4)

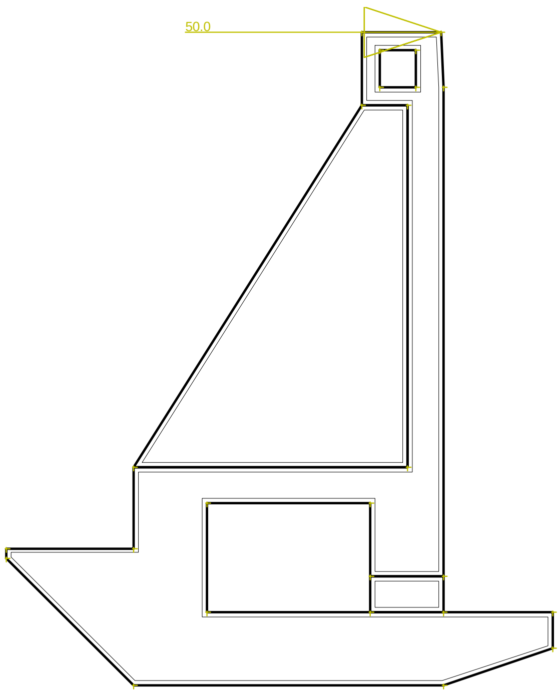

D.5 Water Pressure - Seismics (LC 5)

Water level inside the lock: -3.41 m
Water level outside the lock: +9.81 m

Additional water pressures generated by seismic action are:

Water suction forces at the outside face of the wall according to Westergaard

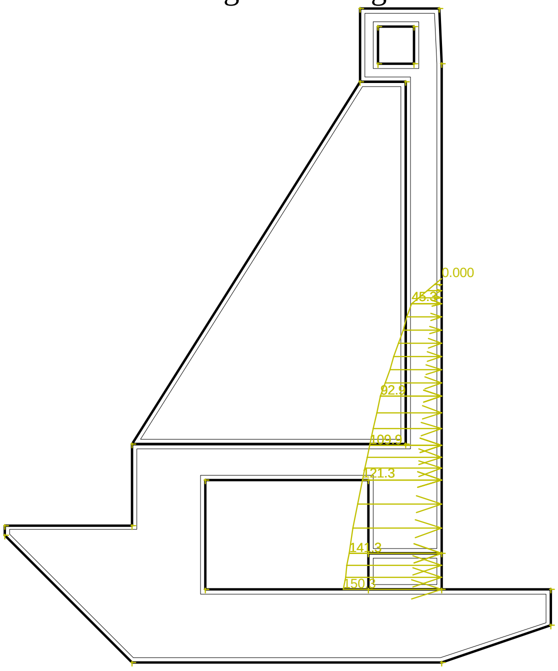

Equivalent seismic reaction forces on water body contained in culvert

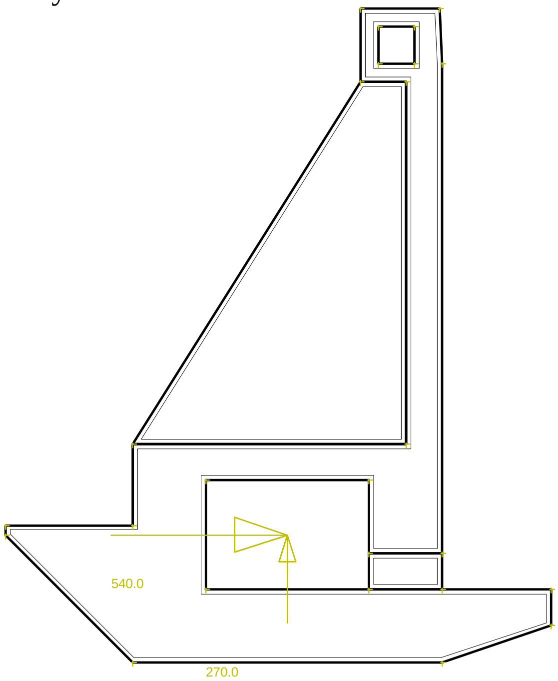

The seismic water pressure load case is valid for a unit value of k_e, and is multiplied by the respective k_e value in the corresponding load combinations.

D.6 Seismic Loads (LC 6, 7 and 8)

LC 6

The active lateral earth thrust under seismic conditions is calculated based on the Mononobe-Okabe (M-O) methodology. The M-O method is an extension of Coulomb's theory, wherein the M-O method takes into account the inertial forces acting on the soil mass during earthquake loading. It was developed to assess the stability of massive gravity walls, assuming that the retaining wall and the failure wedge act as rigid bodies.

The inertia forces are then accounted for by considering a seismic inertia angle, Ψ = atan ($k_h/(1-k_v)$), in which k_h represents the horizontal seismic coefficient or the modified horizontal seismic coefficient for dry and submerged layers respectively.

As the counterfort retaining wall under consideration is geometrically near to cantilever wall type, a Rankine situation is assumed for the calculation of the seismic active earth pressures on the vertical through the rear edge of structure. Consequently, the weight and inertia forces of the soil masses above the structure's rear base have to be taken into consideration.

Remark:

- The active lateral pressures and the horizontal inertia components of the soil masses are transferred to the front wall elements for ease of implementation.
- Half of the vertical live load is taken is accounted for in the seismic earth pressures.

LC 7 and 8

The inertia forces on the structural weight are calculated as follows:

$G_v = (1-k_v)\, G$

$G_h = k_h\, G$

With G the weight of the filling

G_v the vertical component of the weight in seismic conditions

G_h the horizontal component of weight in seismic conditions

PGA	0.4	g	k_e	0.246
k_h	0.246		k_v	0.123

CFR	0.1
Width	24

from	11.31		9.81	
			λav =	λah =
λa =	0.3200		0.0000	0.3200
φ =	45	0.79	δ =	0
θ =	0	0.00		
γ =	18			
z	p		pv	ph1
11.31	4.386		0.000	1.403
9.81	28.070		0.000	8.982

1.50			
	k_h'	0.246	
0.00	ψ	15.6	0.27

Q1v	**0.00**
Q1h	**7.79**
Q1	**7.79**

Width =	19.5
b =	4.5
ph2	86.206
	ph
	87.610
	95.189

from	9.81	to	7.31	
			λav =	λah =
λa =	0.5638		0.0000	0.5638
φ =	45	0.79	δ =	0
θ =	0	0.00		
γ =	10			
z	p		pv	ph1
9.81	28.070		0.000	15.826
7.31	50.000		0.000	28.190

2.50			
	k_h'	0.491	
0.00	ψ	29.2	0.51

Q2v	**0.00**
Q2h	**55.02**
Q2	**55.02**

Width =	19.5
b =	4.5
ph2	95.785
	ph
	111.611
	123.975

from	7.31	to	-12.62	
			λav =	λah =
λa =	0.5638		0.0000	0.5638
φ =	45	0.79	δ =	0
θ =	0	0.00		
γ =	10			
z	p		pv	ph1
7.31	50.000		0.000	28.190
−12.62	224.826		0.000	126.757

19.93			
	k_h'	0.491	
0.00	ψ	29.2	0.51

Q2v	**0.00**
Q2h	**1544.04**
Q2	**1544.04**

Width =	22
b =	2
ph2	
	ph
	125.203
	217.629

from	-12.62	to	-17.12	
			λav =	λah =
λa =	0.5638		0.0000	0.5638
φ =	45	0.79	δ =	0
θ =	0	0.00		
γ =	10			
z	p		pv	ph1
−12.62	224.826		0.000	126.757
−17.12	264.300		0.000	149.012

4.50			
	k_h'	0.491	
0.00	ψ	29.2	0.51

Q2v	**0.00**
Q2h	**620.48**
Q2	**620.48**

Width =	7
b =	17
ph2	34.384
	ph
	161.141
	183.396

2227.33

Soil weight on culvert block

X	**pv**
-7	264
0	264
0	225
11.5	207
11.5	157
14	157

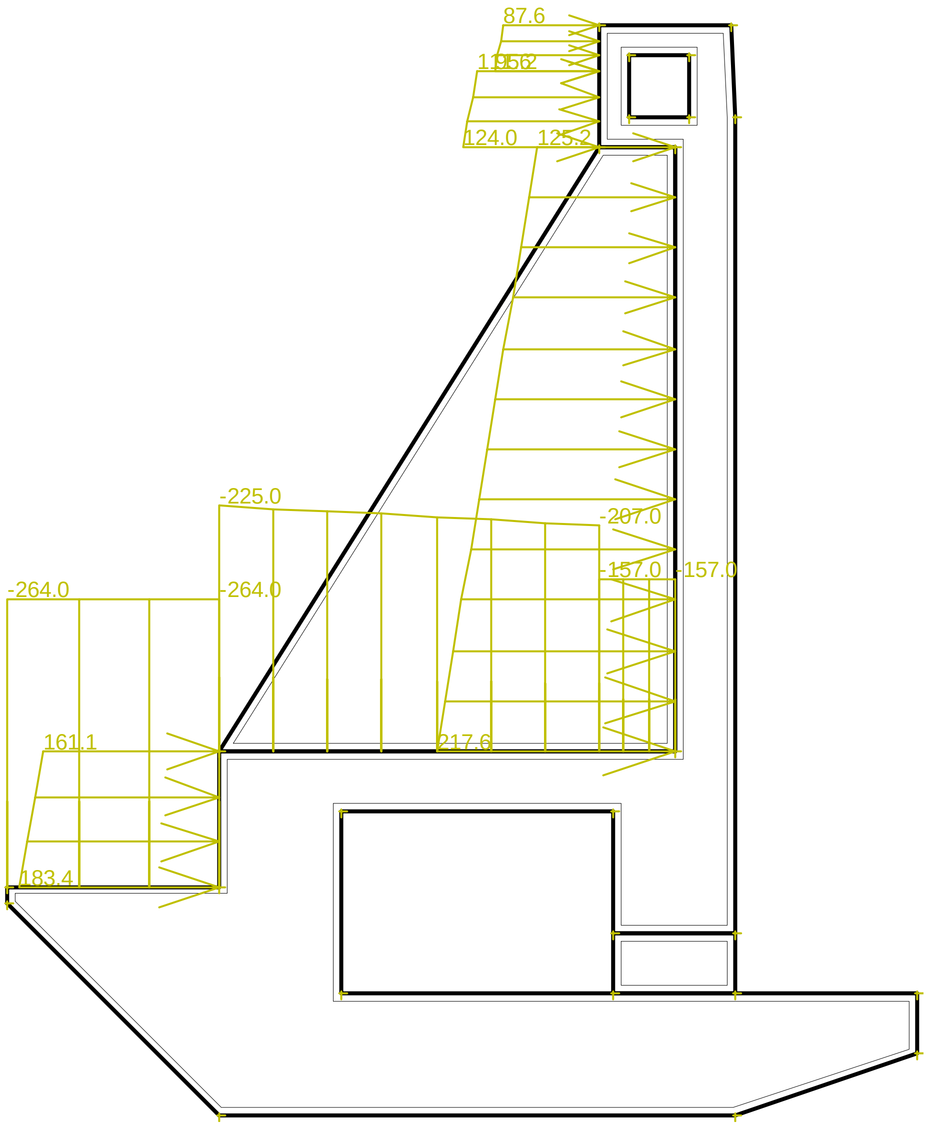

D.7 Water Pressure in Dry Lock Conditions (LC 9)

Water level inside the lock: -3.44 m
Water level outside the lock: +9.81m

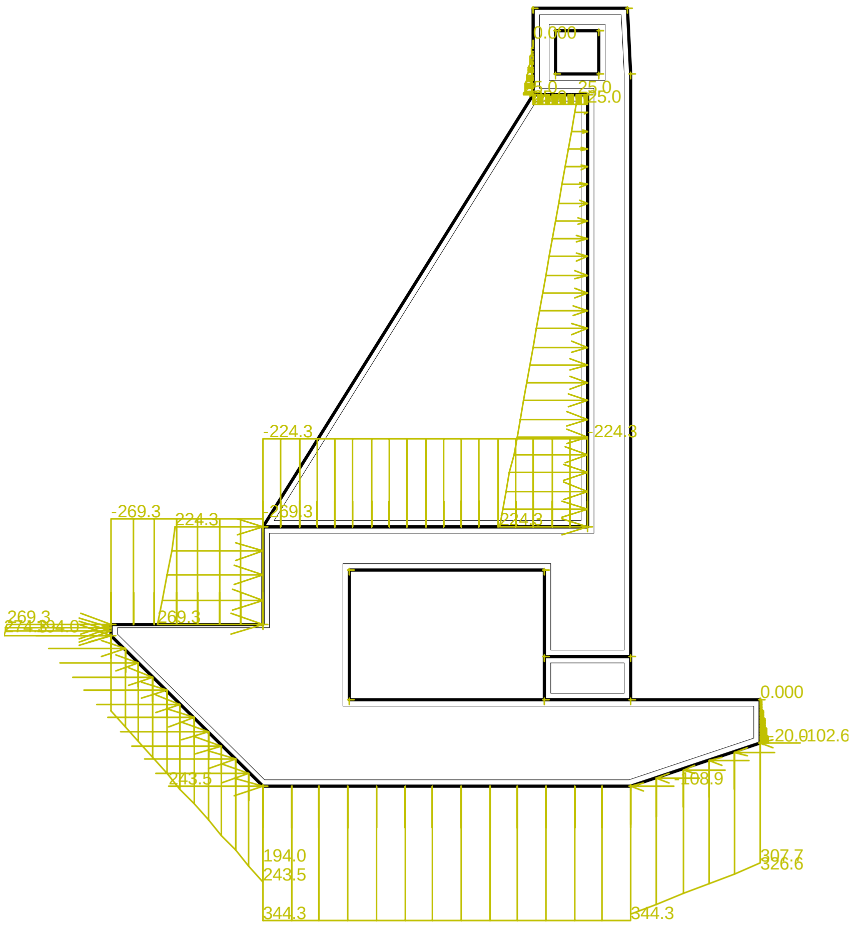

At the rear side of the wall and the bottom the same water pressure is used as in case 3. This is a very conservative assumption as the pressure should normally be equal to zero at the front of the footing.

1.5.2 TURN OVER

A. Quasi Permanent Load Combination (QP1) – Lock in service

Criterion: Compression zone A’ (= 96 %)> 90% A

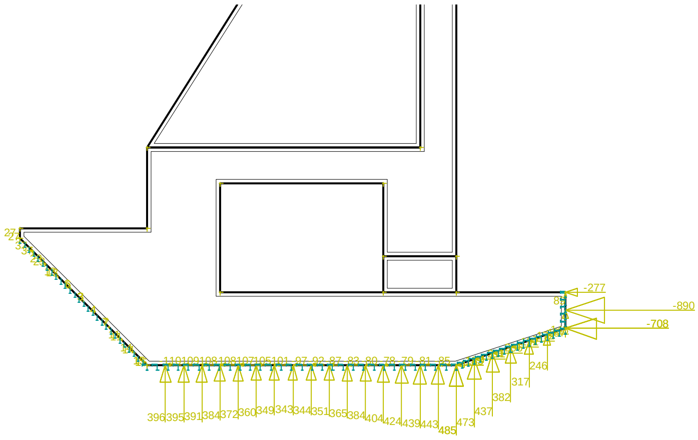

The magnitude of the vectors shown represent the support reaction in each node and not the soil pressure.

B. Rare Load Combination (R1) – Dry Lock Conditions

Criterion: Compression zone A’ (= 96 %) > 75% A

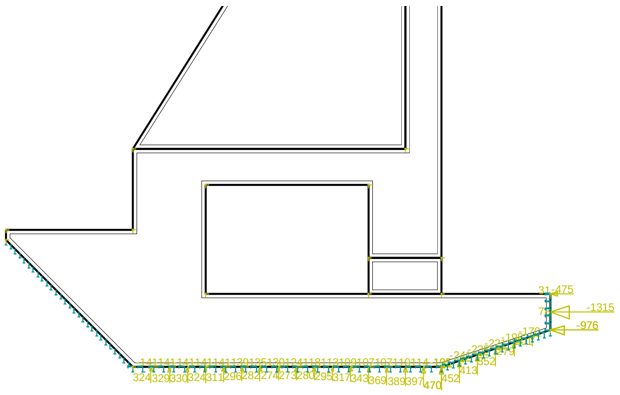

C. Fundamental Load Combinations F1 to F4

Criterion: Compression zone A’ (= 96 %) > 10% A

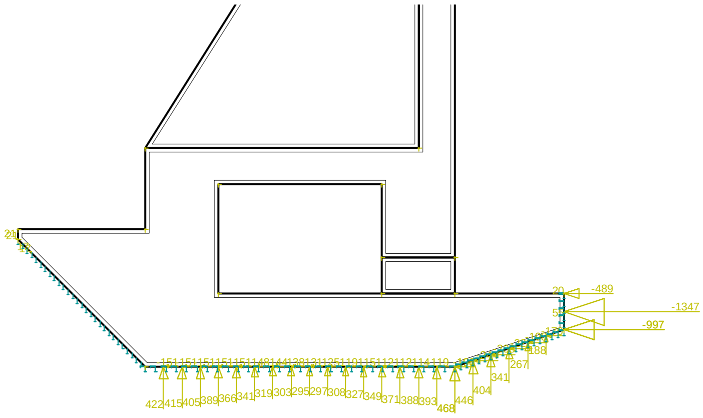

D. Accidental Load Combination – Earth Quake MCE

Criterion: Compression zone A’ (27 %) > 10% A

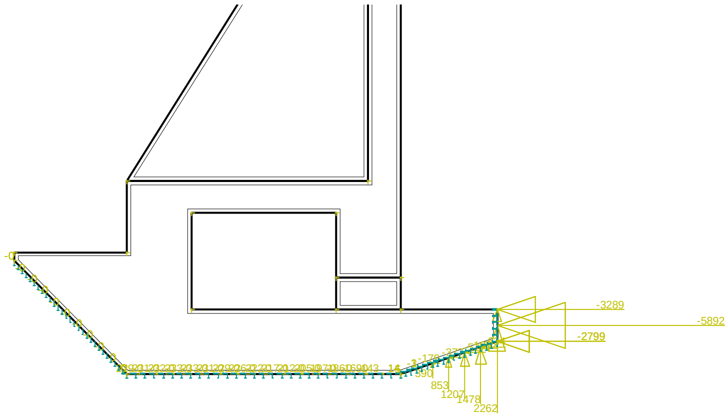

1.5.3 LOAD BEARING CAPACITY

A. Fundamental Load Combinations F1 to F4

Criterion: $\gamma_d \cdot q_{ref} < q_u$
with γ_d . = 1.4

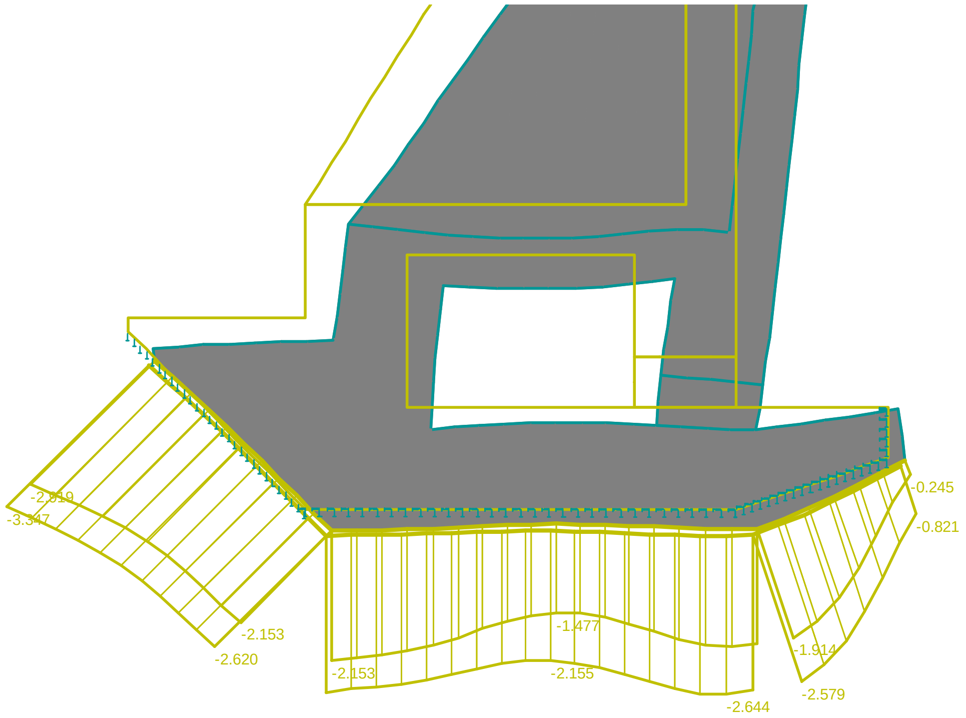

The maximum vertical displacement at the bottom of the wall is 2.644 mm, which is negligible.
This corresponds to a maximum vertical pressure of 0.0026 x 200000 kN/m² = 529 kN/m² = 0.53 Mpa.
Consequently:

$$\gamma_d \cdot q_{ref} = 1.4*0.529 = 0.74 < q_u = 10\text{MPa}$$

(According to report R2-A the Uni-axial Compressive Strength of the La Boca rock varies from 10 to 20MPa).

B. Accidental load combination MCE

Criterion: $\gamma_d \cdot q_{ref} < q_u$
with γ_d . = 1.0 for accidental load combinations

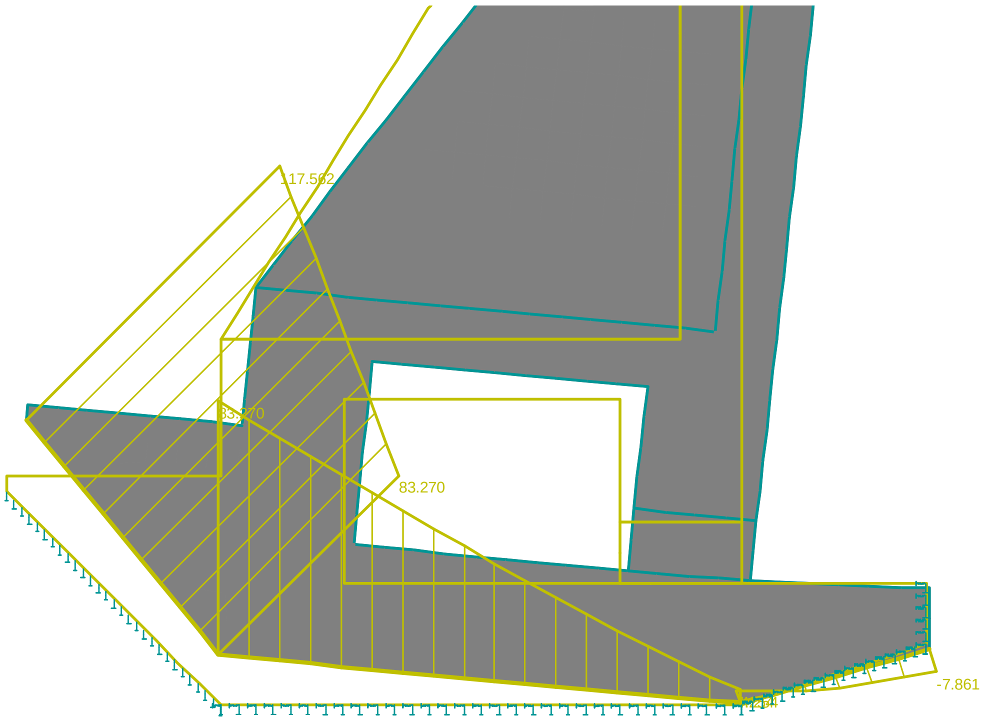

The maximal vertical displacement at the bottom of the wall is 7.861 mm
This means a vertical pressure of 0.0079 x 200000 kN/m² = 1.572 kN/m² = 1.57 MPa

According report R2-A the Uni-axial Compressive Strength of the La Boca rock varies from 10 to 20MPa.

1.5.4 DEFORMATIONS

A. Load Combination QP1 (Lock in Service)

Maximal horizontal displacement, $u_{x,max}$ = 10.3 mm

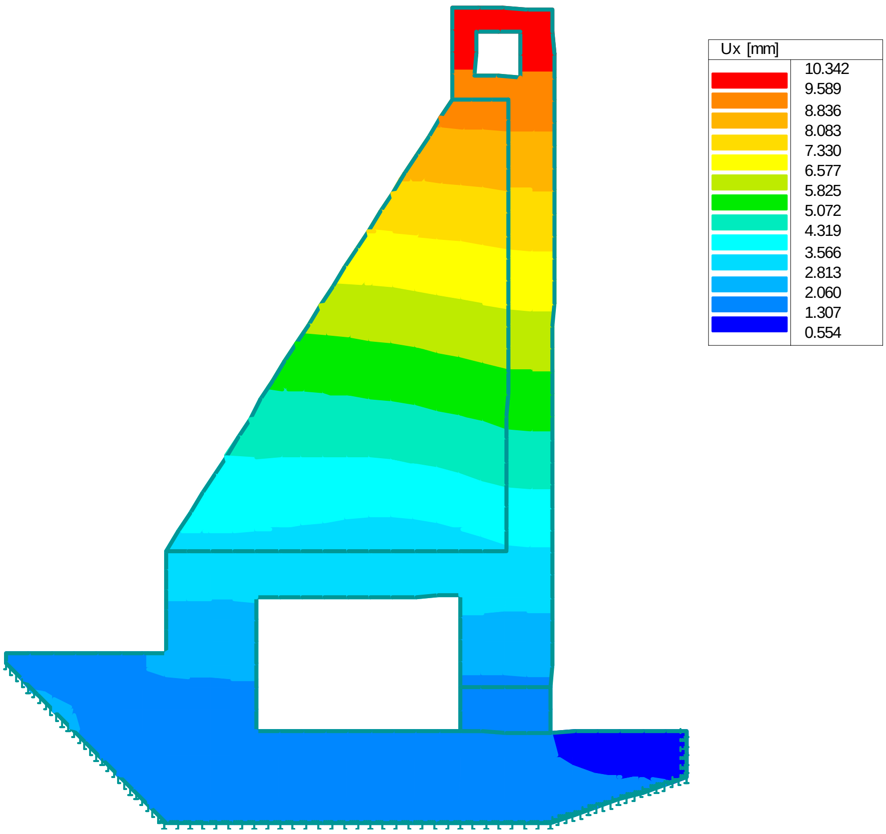

B. Load Combination R1 (Dry Lock Conditions)

Maximal horizontal displacement, $u_{x,max}$ = 10.9 mm

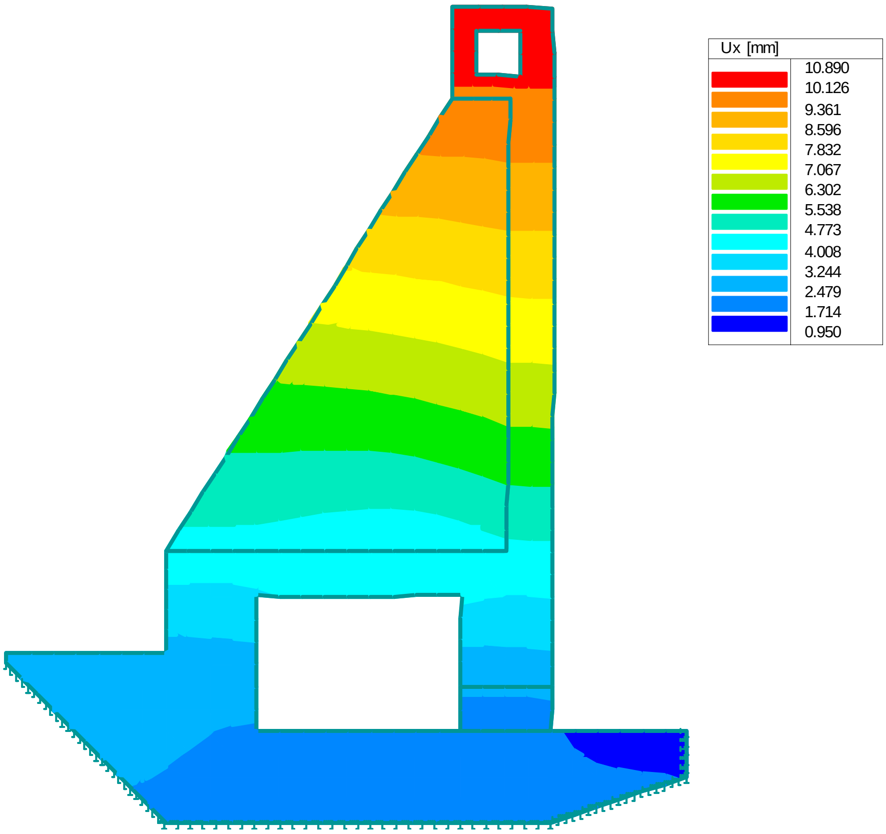

C. Load Combination MCE (Earth Quake)

Maximal horizontal displacement, $u_{x,max}$ = 191.0 mm

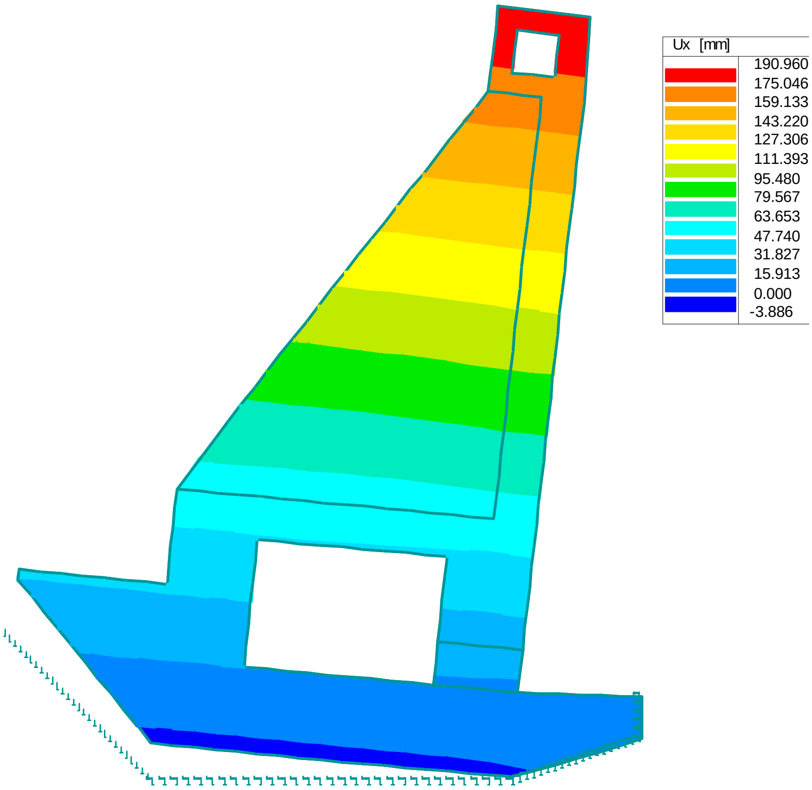

1.5.5 CONCRETE STRESSES

A. Fundamental load combinations F1 tot F4

$1.125 \times \sigma_c < 0.85\, f_{ck}/1.5$
with $f_{ck} = 25 N/mm^2$:
$\sigma_c = 11.64\ N/mm^2 < 12.5\ N/mm^2$

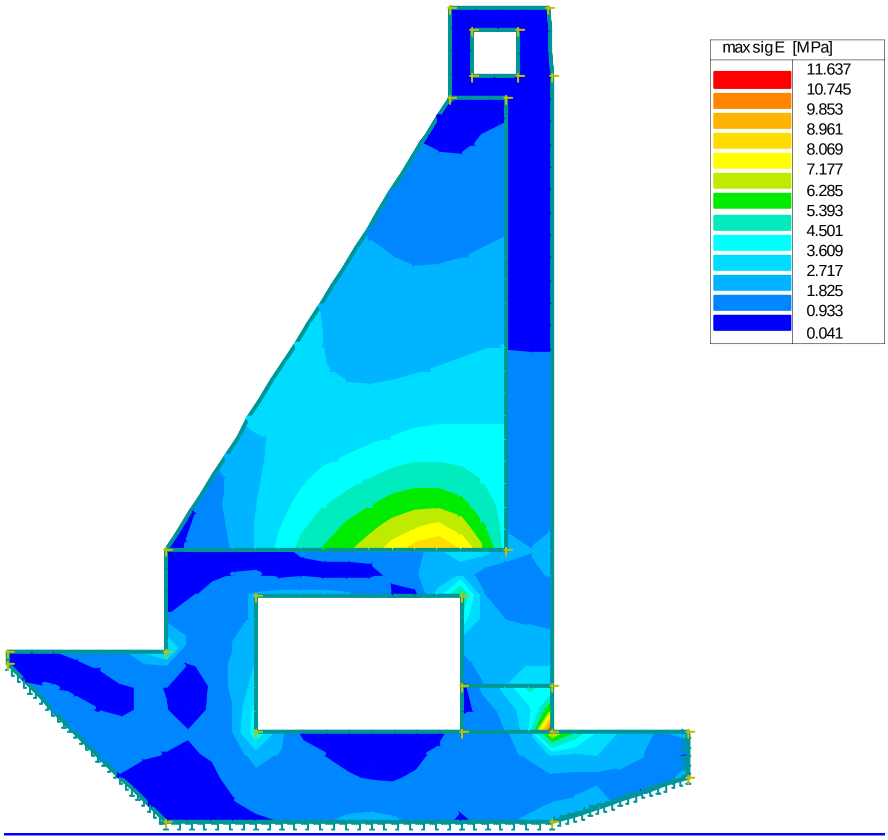

B. Accidental load combination MCE:

$\sigma_c < 0.85 \ f_{ck}$
with $f_{ck} = 25 N/mm^2$:
$\sigma_c = 39.20 \ N/mm^2 > 21.25 \ N/mm^2$
=> As concrete stresses are significantly higher, an adaptation of the geometry is recommended.

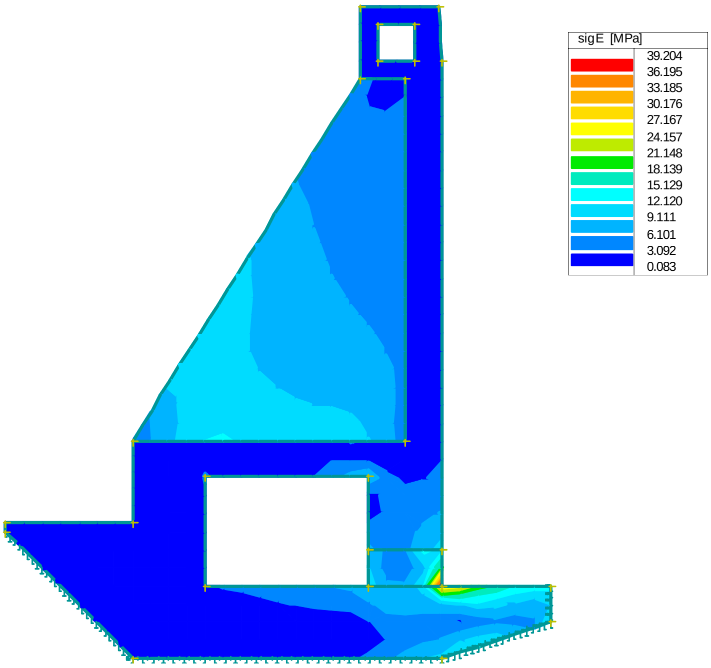

$\sigma_c = 27.43 \ N/mm^2 > 21.25 \ N/mm^2$
=> Local reinforcement will still be necessary

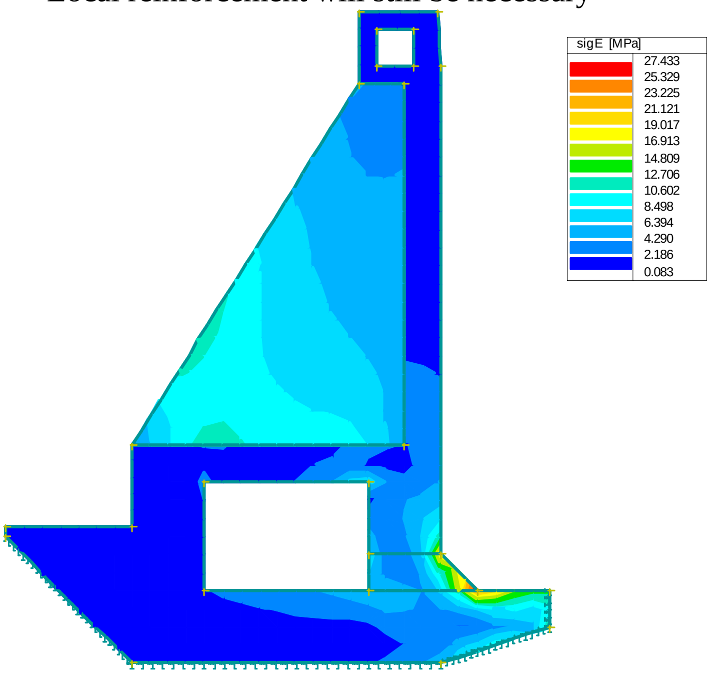

1.5.6 SUMMARY

Criterion	QP1 (Quasi Permanent Load Combination - Service)	R1 (Rare Load Combination - Dry Lock Condition)	F (Envelope of Fundamental Load Combinations)	MCE (Accidental Load Combination - MCE)
Compression zone A’ > 90% A	96%	-	-	-
Compression zone A’ > 75% A	-	96%	-	
Compression zone A’ > 10% A	-	-	96%	27%
Load Bearing Capacity				
1.4 $q_{ref} < q_u$ (MPa)	-	-	0.740	-
$q_{ref} < q_u$ (MPa)	-	-	-	1.572
Deformations				
maximal displacement (mm)	10.3	10.9	-	191
Concrete stresses				
1.125 x σc < 0.85 fck/1.5	-	-	92%	-
σc < 0.85 fck	-	-	-	**129%**
Deep Seeted Sliding				
	-	-	-	-

2 Lock heads

2.1 DESIGN CRITERIA

Design criteria for the new lock structures have been given in the report of Task P2 - "Design Criteria" of the Pacific Locks Actualization study.

The main changes incorporated for the actualization of the Pacific locks conceptual design with respect to the previous conceptual design are as following:

- Updated width and depth of the locks due to different ship sizes
- Use of vessel positioning by tugboat cancels locomotive loads on lock heads
- Updated design values for earthquake analysis
- Lock siting has been optimized in relation to new alignment
- Freeboard has been reduced to 1.5m instead of 3m

Reference is made to following drawings:

- D4-B-101 Eastern lock wall - longitudinal view
- D4-B-102 Western lock wall - longitudinal view
- D4-B-103 Plan view on lock chamber 1
- D4-B-104 Plan view on lock chamber 2
- D4-B-105 Plan view on lock chamber 3
- D4-B-106 Cross sections lock walls
- D4-B-107/109 Lock head 2
- D4-B-110/112 Lock head 1
- D4-B-113/115 Lock head 3
- D4-B-116/118 Lock head 4
- D4-B-119 Lock wall segment

2.2 TECHNICAL DESCRIPTION OF LOCK HEAD STRUCTURE

The lock head is a massive construction housing the lock gates and culvert valves.

One major condition is the geo-technical situation of the lock siting. In the 3-step configuration lock heads 1 and 2 are situated in rock (basalt) and lock heads 3 and 4 are situated in the “La Boca” formation.

As these two formations have different compressibility (Specific Design Criteria – Part A), varying from 12,5 Gpa for basalt to 2,5 Gpa for the “La Boca”, it has to be expected that differential settlements may occur. This differential settlement has to be minimized to a value that causes no problems for the behavior of the structural joints.
For further specifications about the foundation in basalt or ‘La Boca’ we refer to report R4-B-404.

In this report a section taken through the lock gate recesses is checked.

2.3 LOCK HEAD ANALYSIS

2.3.1 LOADS

A. Self Weight (case 1)

Concrete γ= 24.5 kN/m³
Wet Soil γ= 20.0 kN/m³
Dry Soil γ= 18.0 kN/m³

B. Earth Pressure (case 2)

The active earth pressure will be calculated using the formula of COULOMB-PONCELET

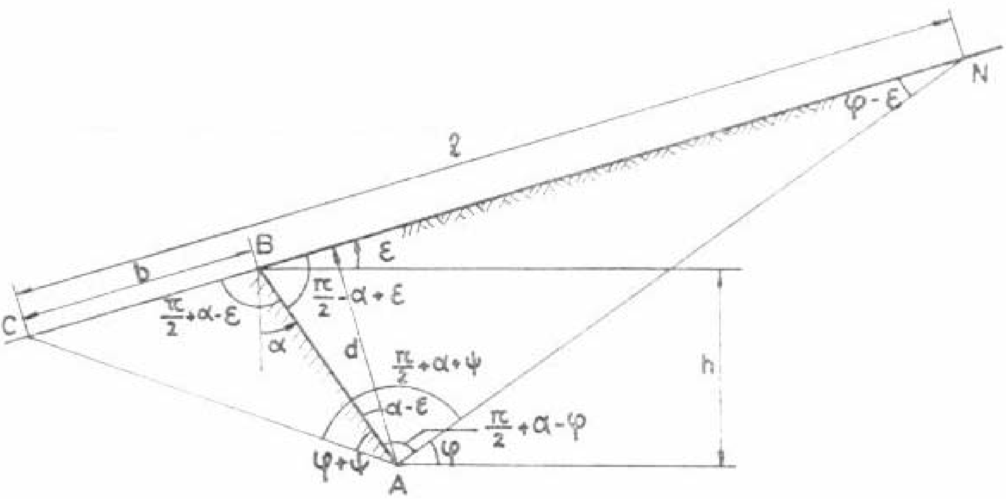

$$\lambda_a = \frac{\cos^2(\varphi - \alpha)}{\cos^2\alpha \cos(\alpha + \psi)\left(1 + \sqrt{\dfrac{\sin(\varphi + \psi)\sin(\varphi - \varepsilon)}{\cos(\alpha + \psi)\cos(\varepsilon - \alpha)}}\right)^2}$$

The angle of friction in the filling of crushed stone and sand is 45°
On the surface a load p=10 kN/m² is applied. (5 kN/m² in seismic conditions)

C. Water Pressure (case 3)

At the side of the upper chamber the maximum water level of that chamber will be applied. This level will also be applied in the recess at that side. At the side of the lower chamber the minimum water level of that chamber will be applied. This level will also be applied in the recess at that side.

D. Seismic Loads (case 4)

D.1 Earthquake level

ACP stated in its Memorandum of 20 Jan 2005 on 'Seismic Design Criteria' that an earthquake with a return period of 5000 years should be considered as Maximum Credible Earthquake (= MCE) and taken equal to the Maximum Design Earthquake (= MDE).

D.2 Performance Grade

The highest performance grade (Grade S) is applicable for

- critical structures with potential for extensive loss of human life and property
- key structures that are required to be serviceable for recovery from earthquake disaster
- critical structures that, if disrupted, devastate economic and social activities

This means that the level of damages is:

- Structural: minor or no damage
- Little or no loss of serviceability

for a MCE-event.

D.3 Analysis type

As this report concerns a conceptual design we will use the simplified analysis.

D.4 Representative ground acceleration values

Based on the review of probabilistic seismic hazard analysis by Winter (2005), and the memorandum of ACP dated January 20, 2005 the following PGA-values can be taken as representative for the site at Miraflores:

Return period [years]	**Representative PGA**	**Criterion**
100	0.07	
500	0.16	
1000	**0.22**	
2500	0.32	
5000	**0.40**	MCE=MDE
10000	0.51	

The seismic coefficient k_e for use in retaining structures is defined as follows for Special Class Structures:

$$k_e = PGA/g \quad \text{for } PGA < 0.2\ g$$

$$= \frac{1}{3}\left(\frac{PGA}{g}\right)^{\frac{1}{3}} \quad \text{for } PGA \geq 0.2\ g$$

With according to eurocode design (CEN 1994)

$k_{h\ (horizontal)} = k_e$
$k_{v(vertical)} = ½k_e$

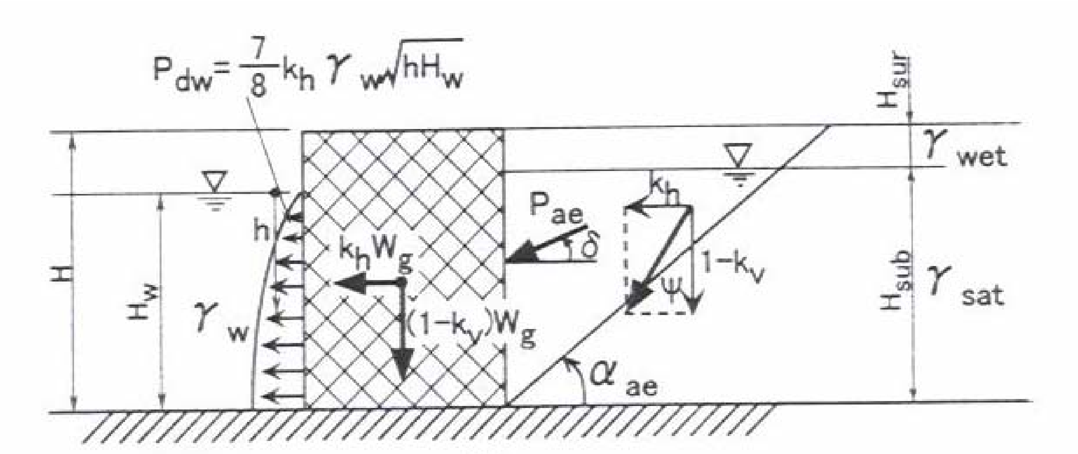

(a)

E. Water Pressure in Dry Recess Conditions (case 5 & 6)

In case 5 the one recess on the side of the upper chamber is put in dry conditions. In case 6 both recesses at put in dry conditions.

F. Upper Wagon (case 7)

The reaction forces of the upper wagon are taken form the report R4-D-403.

2.3.2 LOAD COMBINATIONS

According to ROSA 2000

A. Quasi Permanent Load Combination

CASE 101	= 1.00 x	[1]	+ 1.00 x	[2]	+ 1.00 x	[3]	+ 1.00 x	[7]

B. Accidental Load Combination – MCE (=MDE)

CASE 102	= 1.00 x	[1]	+ 1.00 x	[3]	+ 1.00 x	[4]

C. Rare Load Combination

CASE 103	= 1.00 x	[1]	+ 1.00 x	[2]	+ 1.00 x	[5]
CASE 104	= 1.00 x	[1]	+ 1.00 x	[2]	+ 1.00 x	[6]

D. Fundamental Load Combinations

CASE 105	= 1.20 x	[1]	+ 1.20 x	[2]	+ 1.00 x	[3]	+ 1.20 x	[7]
CASE 106	= 0.90 x	[1]	+ 1.20 x	[2]	+ 1.00 x	[3]	+ 1.20 x	[7]
CASE 107	= 1.20 x	[1]	+ 1.20 x	[2]	+ 1.00 x	[5]		
CASE 108	= 0.90 x	[1]	+ 1.20 x	[2]	+ 1.00 x	[5]		
CASE 109	= 1.20 x	[1]	+ 1.20 x	[2]	+ 1.00 x	[6]		
CASE 110	= 0.90 x	[1]	+ 1.20 x	[2]	+ 1.00 x	[6]		

2.3.3 CRITERIA

According to ROSA 2000

A. Sliding along the base

Due to the ground pressure at both sides of the lock head, sliding will not occur.

B. Turn over

The lock head can not turn over, due to dimensions and the ground pressure at both sides of the head.

C. Load Bearing Capacity

$\gamma_d \cdot q_{ref} < q_u$
γ_d . = 1.4 for load combination 105 to 110
γ_d . = 1.0 for load combination 102 (MCE)

qu = ultimate load bearing capacity
qref = reference pressure

D. Deformations

The deformations will be checked for frequent and rare load combinations 101, 102 (MCE), 103 and 104.

E. Concrete Stresses

Fundamental load combinations: 105 tot 110: 1.125 x σc < 0.85 fck/1.5
Accidental load combination: 102 (MCE): σc < 0.85 fck

The factor 1.125 is caused by the different factors in the load combinations between ROSA 2000 and EuroCode.

F. Global Stability

Global stability will not be a problem, when the items in part C, D and E are checked.

2.3.4 SOFTWARE

The calculations are made by means of "Esa Prima win", a finite element program. The model we will use is a 2D-model.

2.4 TYPE 1 - FOUNDATION IN BASALT

2.4.1 INPUT DATA

A. Geometry

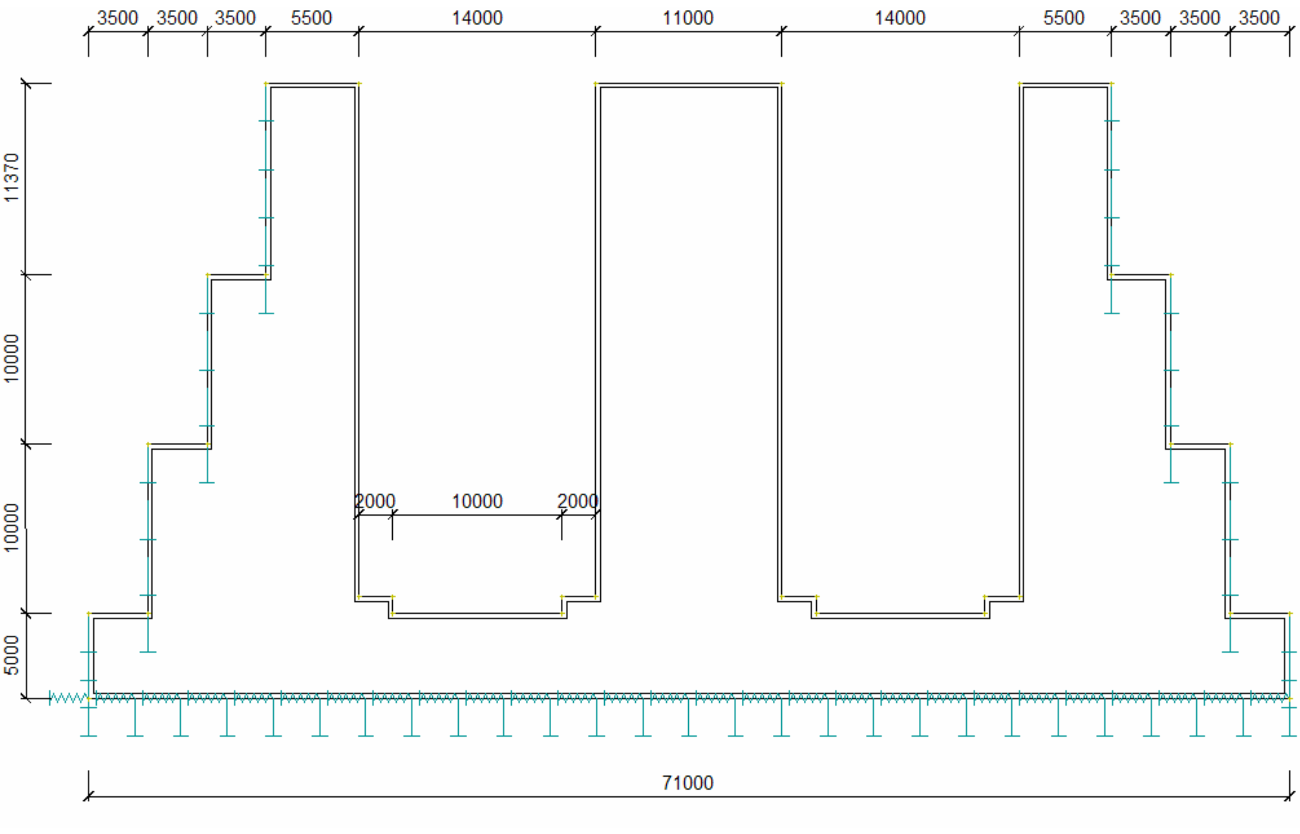

B. Materials

Material	E kN/m²	Nu	W/V kN/m3	Alpha
CONCRETE	19620000.000	0.100	24.525	0.0000100

C. Supports

The rock base is modeled by means of a linear support.

Vertical lock head elements:
Linear support with K= 200.000 kN/m² is introduced.
This support only works when compressed.

Horizontal rock base:
Linear support with K= 1.000.000 kN/m² is introduced.
This support only works when compressed. A small horizontal support is given to the rock base, to avoid trivial results of the calculation.

The K-values are estimated values.

D. Loads

D.1 Self Weight (case 1)

D.2 Earth Pressure (case 2)

We assume that the rock does not perform any pressure on the wall.

side upper chamber			
		lambda ah	lambda av
lambda a	0,1620	0,1403	0,0810
depth (m)	pressure (kN/m²)	ph (kN/m²)	pv (kN/m²)
0	10	1	1
1,5	37	5	3
11,37	146	20	12
21,37	246	34	20
31,37	346	48	28
36,37	396	56	32
side lower chamber			
		lambda ah	lambda av
lambda a	0,1620	0,1403	0,0810
depth (m)	pressure (kN/m²)	ph (kN/m²)	pv (kN/m²)
0	10	1	1
11,37	215	30	17
20,97	387	54	31
21,37	401	56	33
31,37	501	70	41
36,37	551	77	45

Horizontal component:

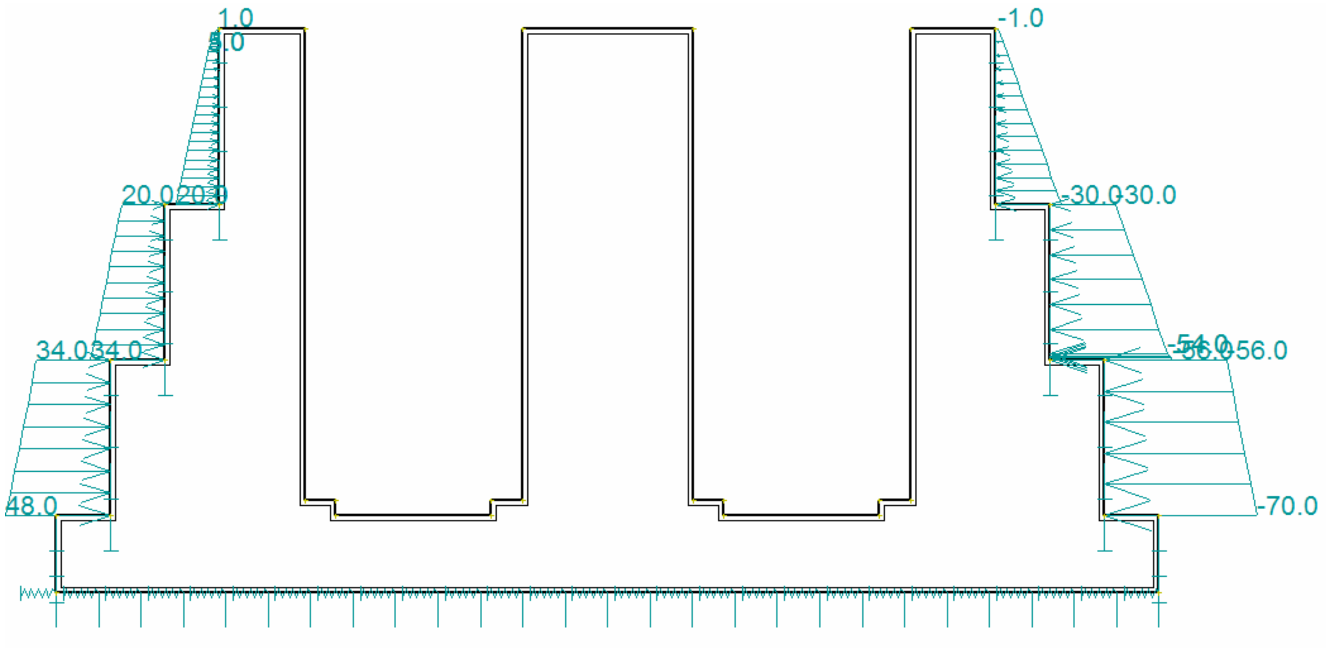

Vertical component:

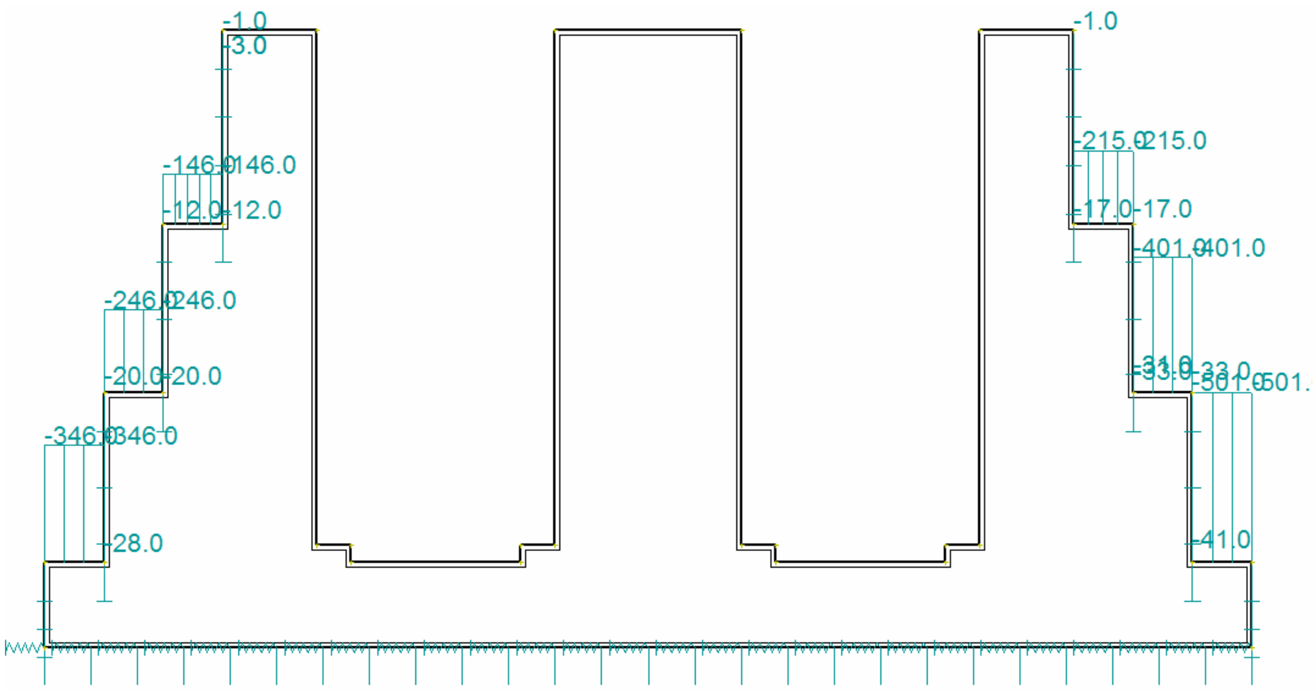

D.3

Water Pressure (case 3)

Water level side upper chamber (maximum): + 27.13 m
Water level side lower chamber (minimum): + 7.66 m

Water pressure onto the sides and bottom of the lock head

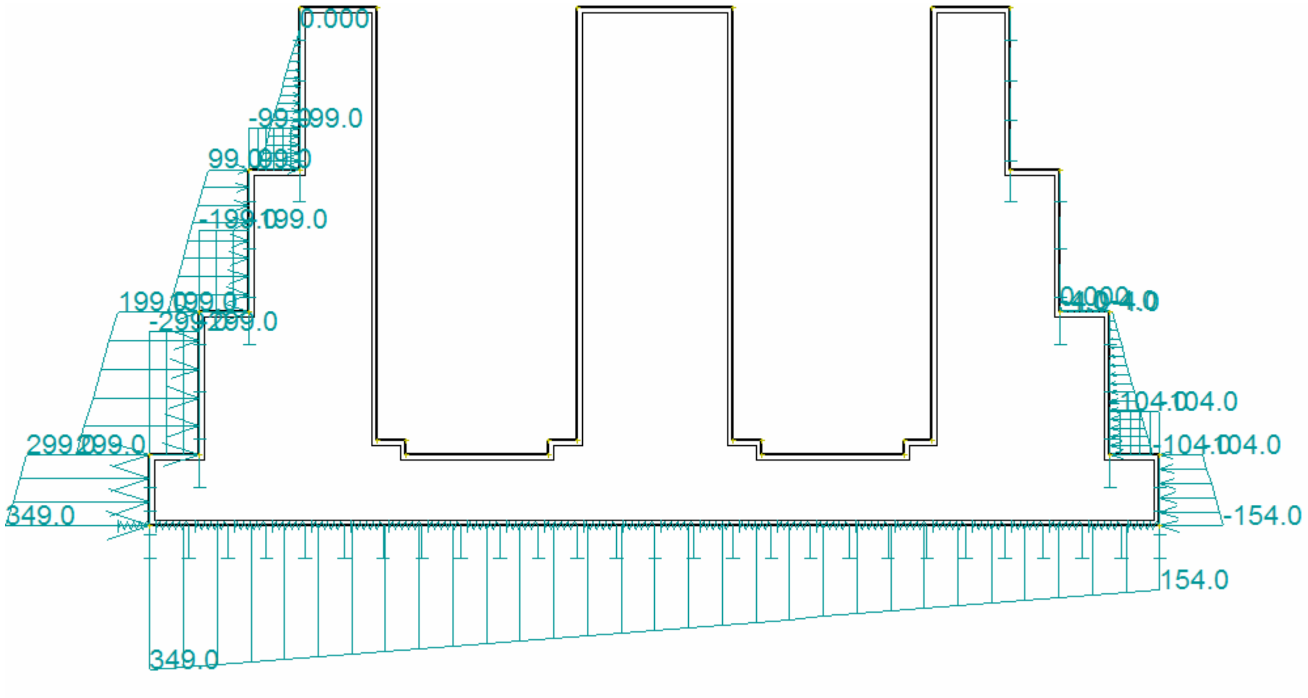

Water pressure inside the lock head

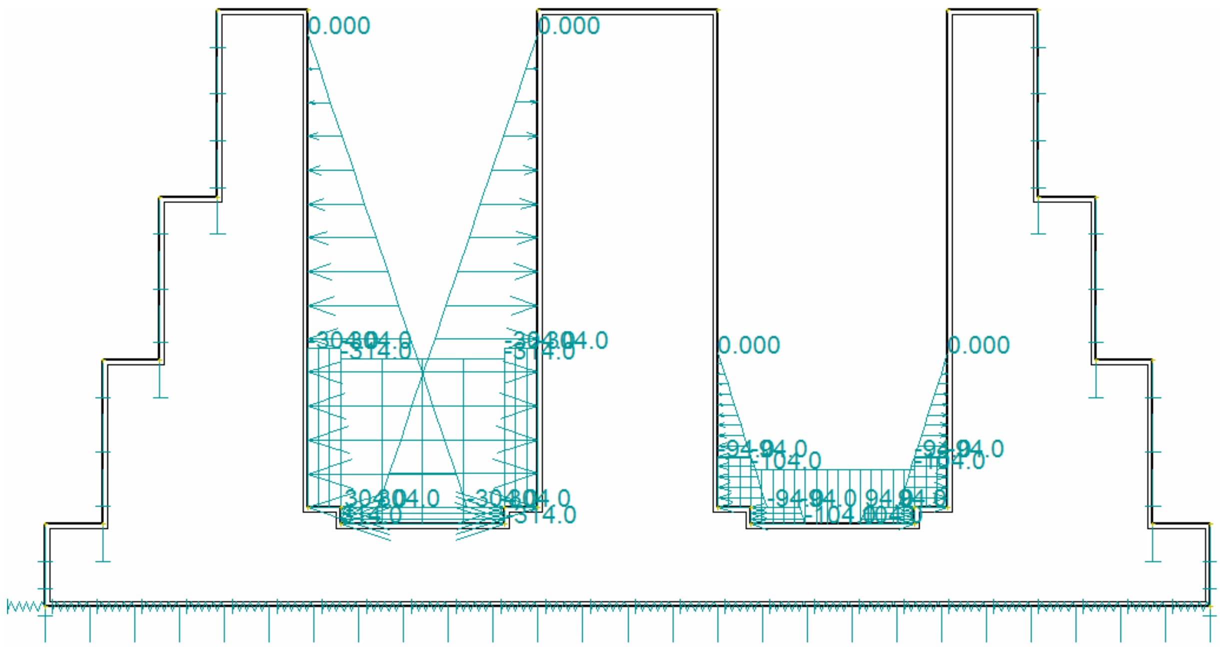

Seismic Loads (case 4)

The inertia forces on the structural weight are calculated as follows:

$G_v = (1-k_v)\ G$

$G_h = k_h\ G$

With G the weight of the structure including the backfill above the heel or toe of the structure and any water within the backfill

G_v the vertical component of the weight in seismic conditions

G_h the horizontal component of weight in seismic conditions

According to the PIANC regulations for Seismic design of Port Structures, the earth pressures due to seismic action are calculated using the Mononobe-Okabe equation. The inertia forces are then accounted for by considering a seismic inertia angle, Ψ = atan ($k_h/(1-k_v)$), in which k_h represents the horizontal seismic coefficient or the modified horizontal seismic coefficient for dry and submerged layers respectively.

Additional water pressures generated by seismic action are taken into account according to Westergaard formula. The seismic water pressure load case is valid for a unit value of k_e, and is multiplied by the respective k_e value in the corresponding load combinations.

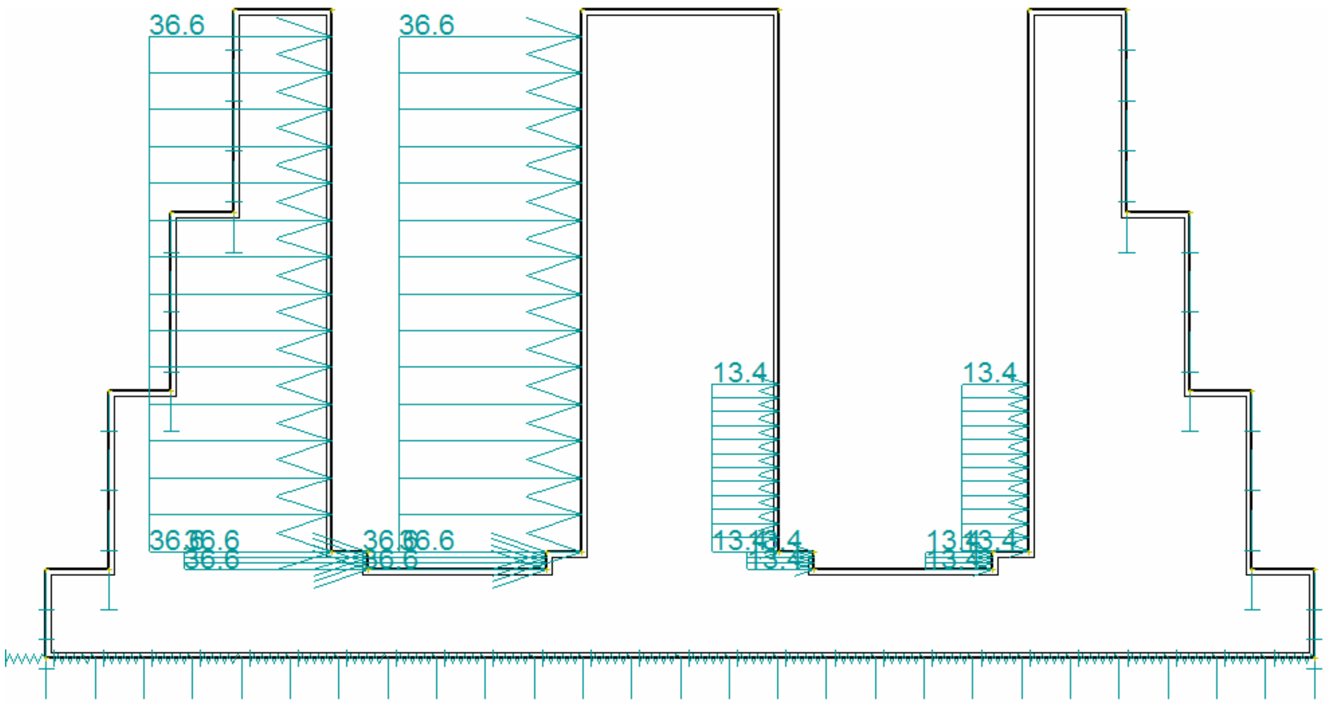

D.5 Water Pressure in Dry Lock Conditions (case 5 - 6)

In case 5 the one recess on the side of the upper chamber is put in dry conditions. In case 6 both recesses at put in dry conditions.

Case 6: normal water pressure without water pressure inside the lock head

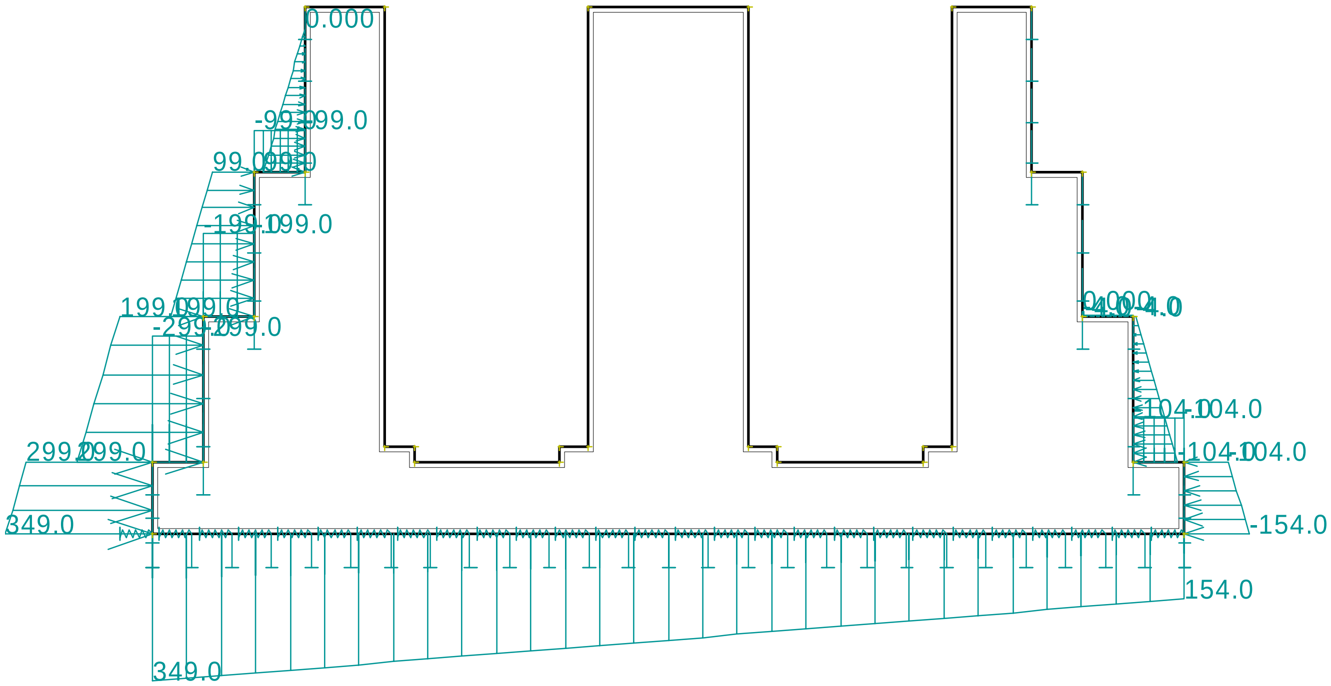

Case 5: normal water pressure combined with a maximum water level in the gate recess near the lowest chamber

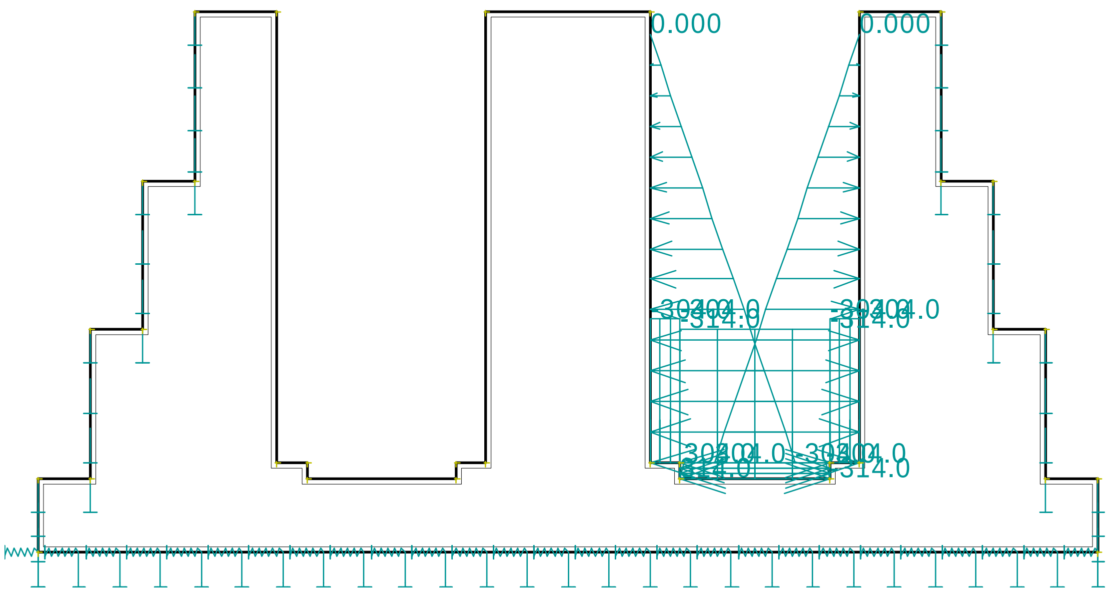

D.6

Upper wagon (case 7)

Loads due to the upper wagon are taken from report R4-D-403.

Gates 2,3		Side of flooded zone	Other side	Total vert. reaction
Base case: H = 11 m	Upper wagon	1500 kN	800 kN	2300 kN
	Lower wagon	1900 kN	1200 kN	3100 kN

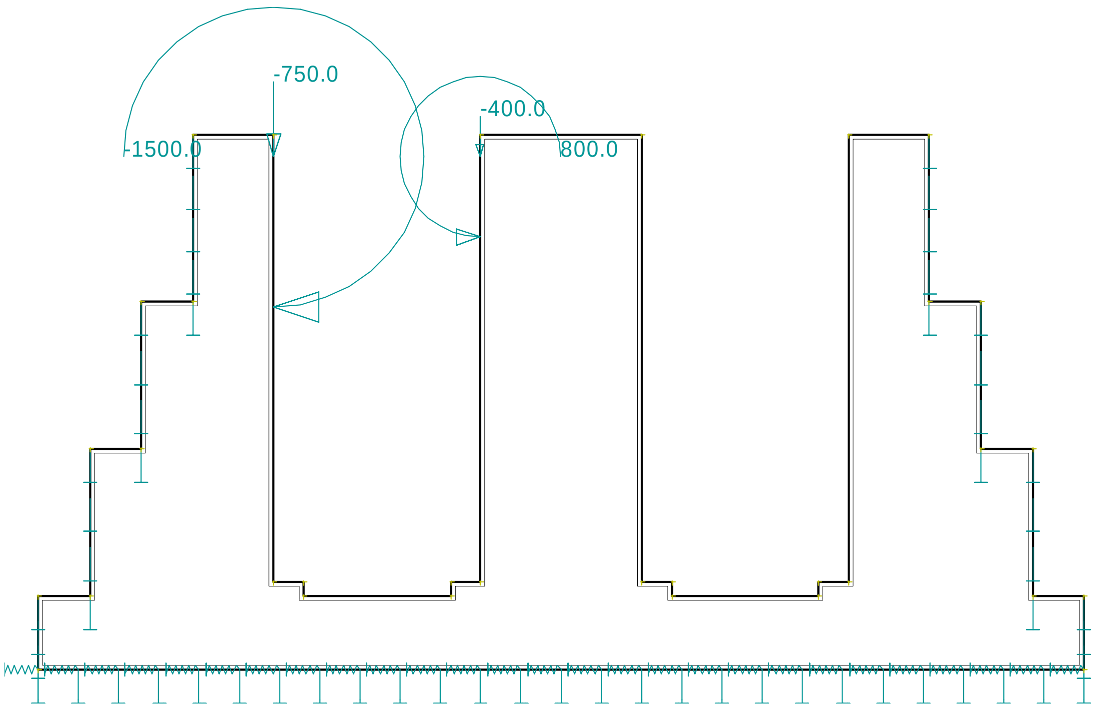

2.4.2 Load Bearing Capacity

A. Fundamental Load Combinations 105 to 110

Criterion: $\gamma_d \,.\, q_{ref} < q_u$
with γ_d . = 1.4

The maximal vertical displacement at the bottom of the wall is 0.9 mm
This means a vertical pressure of 0.0009 x 1000000 kN/m² = 900 kN/m² = 0.9 MPa

(According to report R2-A the Uni-axial Compressive Strength of the basalt rock varies from 40 to 100MPa).

Vertical movement

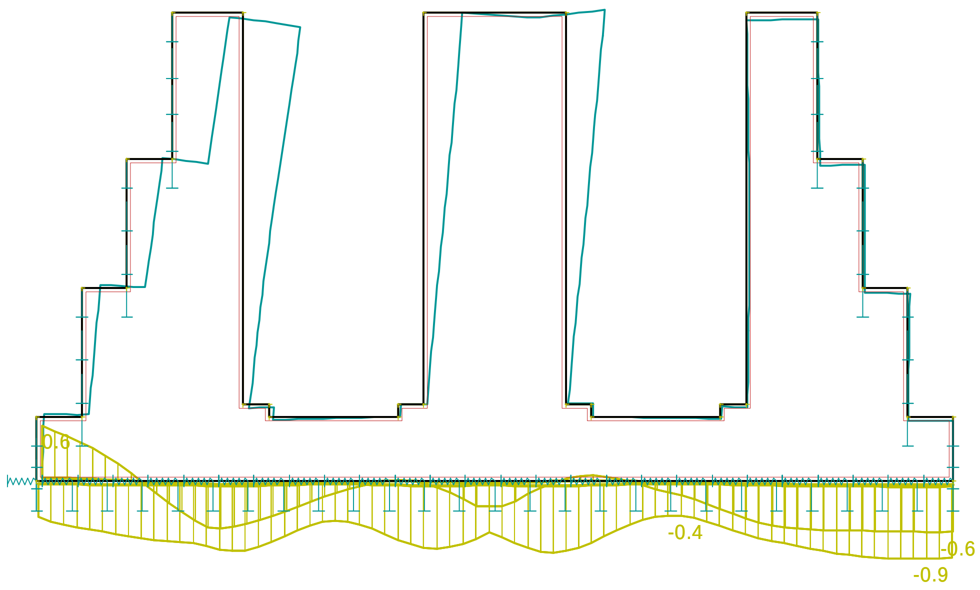

B. Accidental load combination 102 (MCE)

Criterion: $\gamma_d \cdot q_{ref} < q_u$
with γ_d . = 1.0 for load combination 102

The maximal vertical displacement at the bottom of the wall is 1.3 mm
This means a vertical pressure of 0.0013 x 1000000 kN/m² = 1300 kN/m² = 1.3 MPa

(According to report R2-A the Uni-axial Compressive Strength of the basalt rock varies from 40 to 100MPa).

Vertical movement

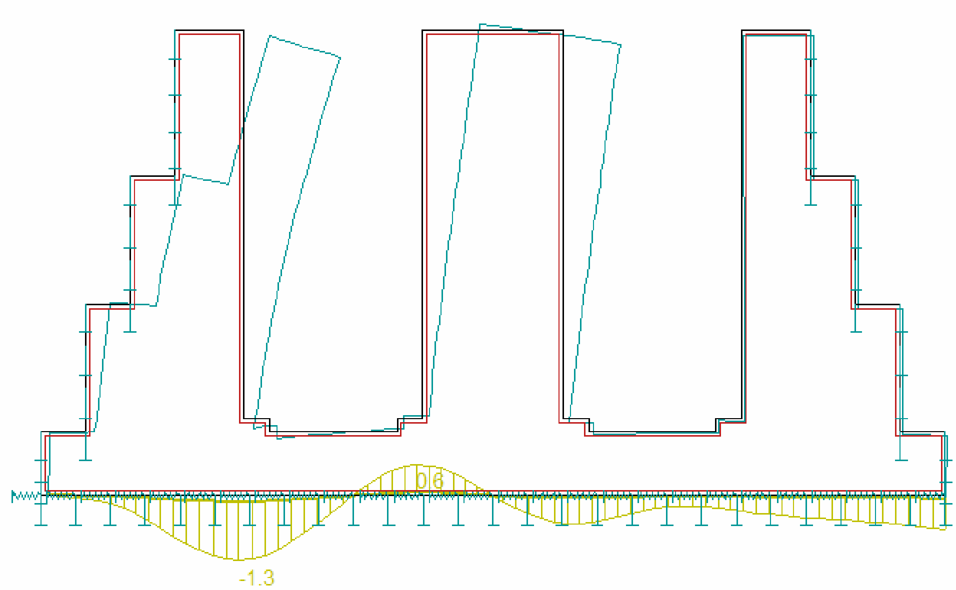

2.4.3 DEFORMATIONS

A. Load Combination 101 (Lock in Service)

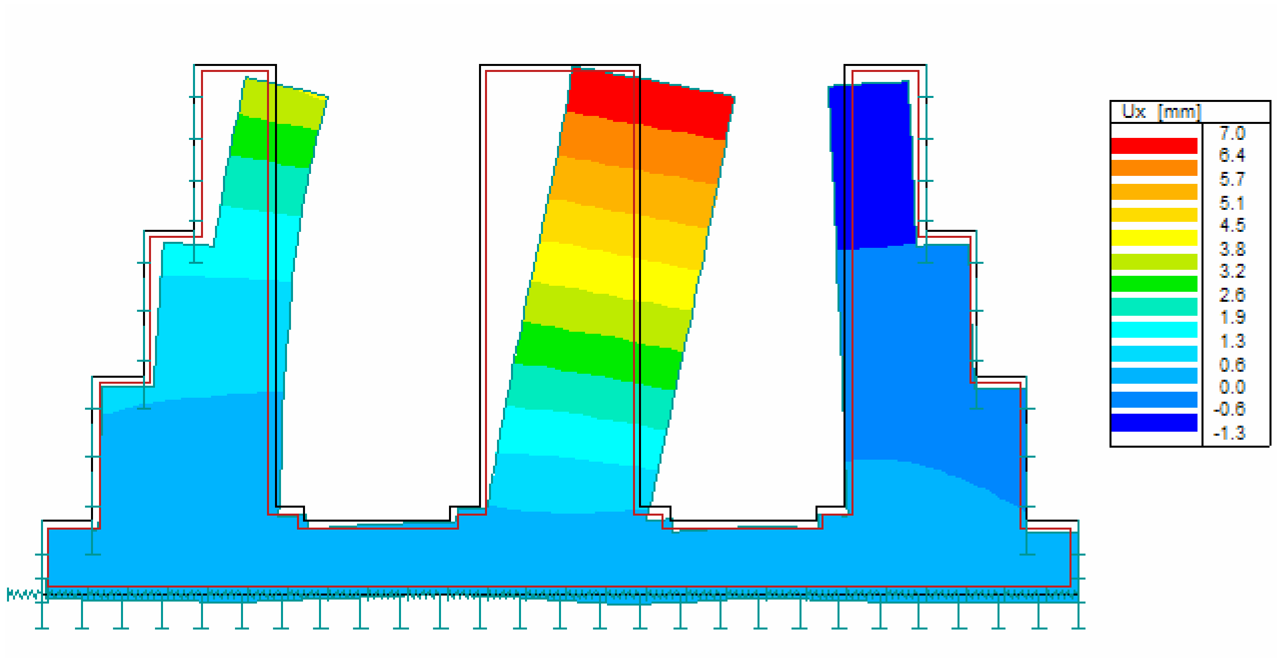

B. Load Combination 102 (MCE)

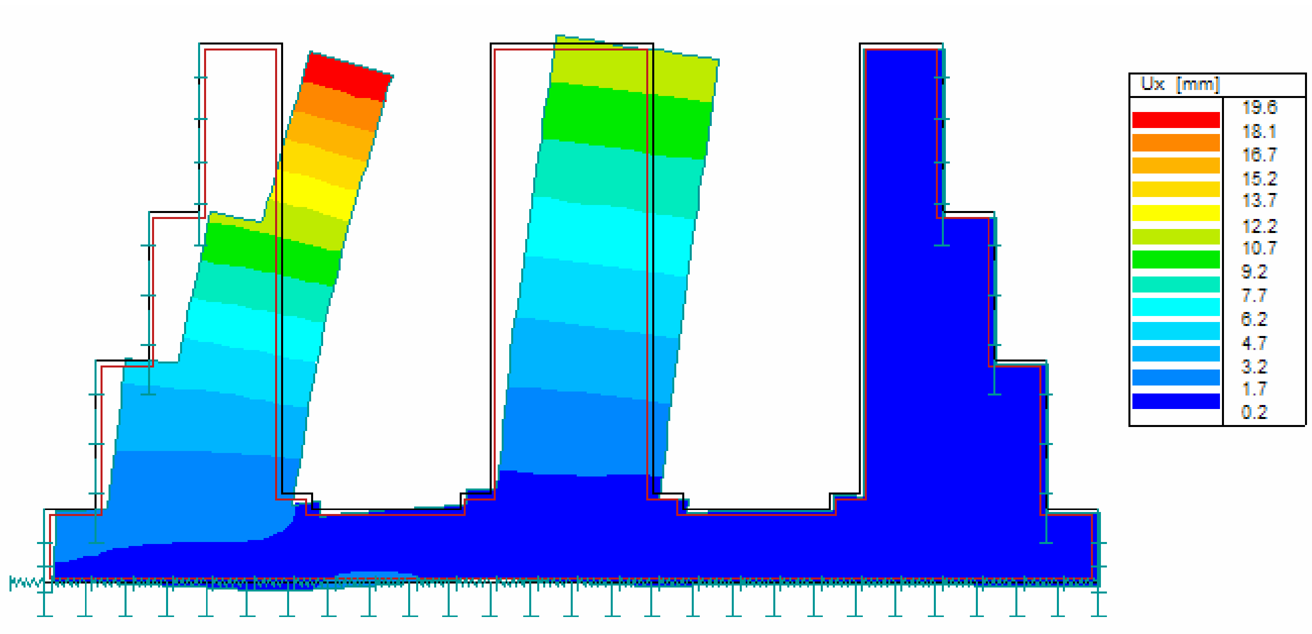

C. Load Combination 103 (1 gate recess in dry conditions)

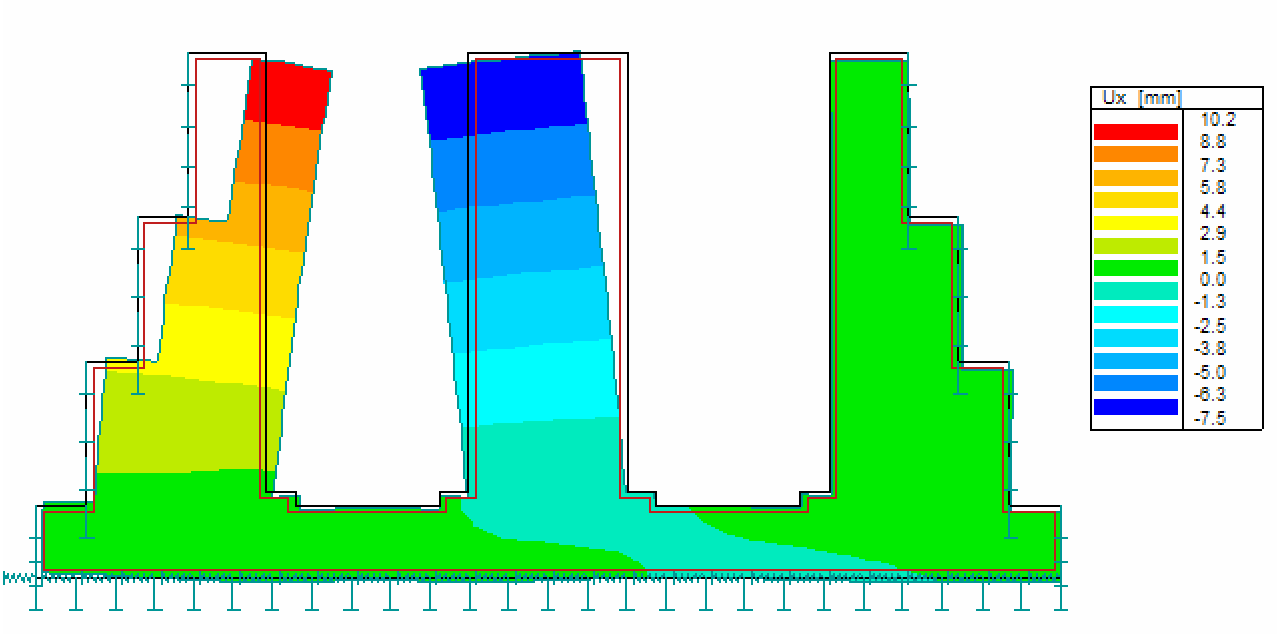

D. Load Combination 104 (2 gate recesses in dry conditions)

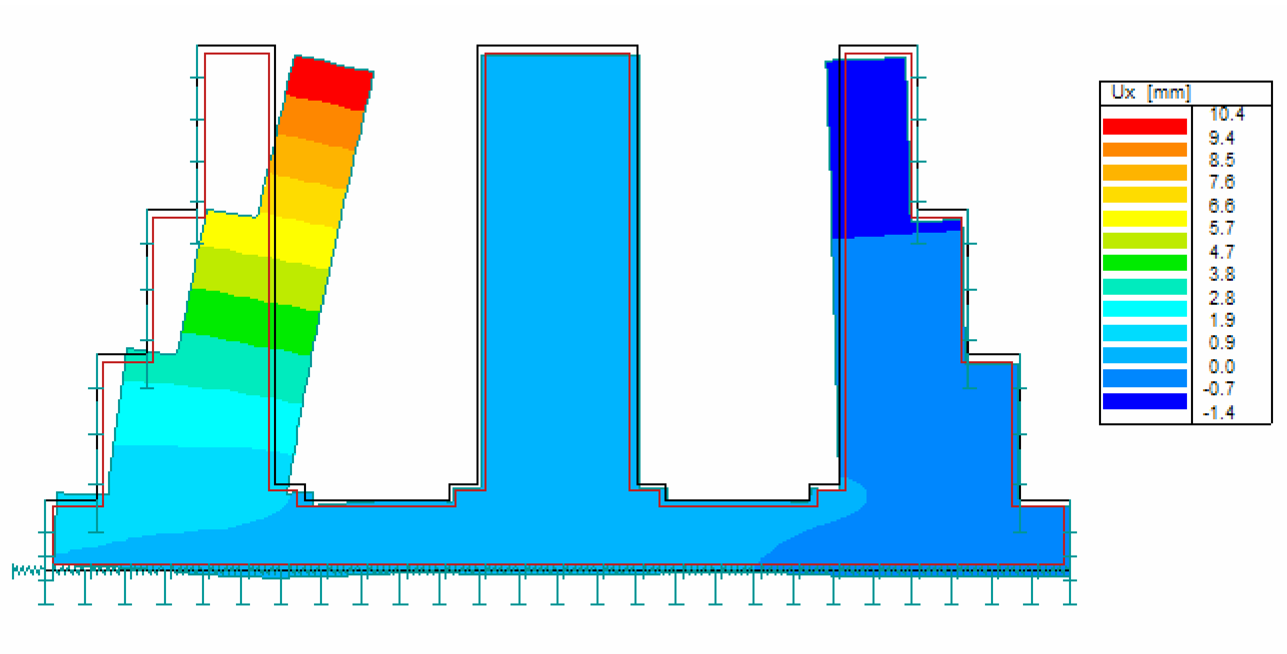

2.4.4 CONCRETE STRESSES

A. Fundamental load combinations 105 tot 110:

1.125 x σc < 0.85 fck/1.5
This means σc < 12.5 N/mm²

The results are satisfying for this conceptual design. Details have to be studied by means of a 3D-model.

Stresses in the horizontal direction – maximum compression = 2.9 N/mm²

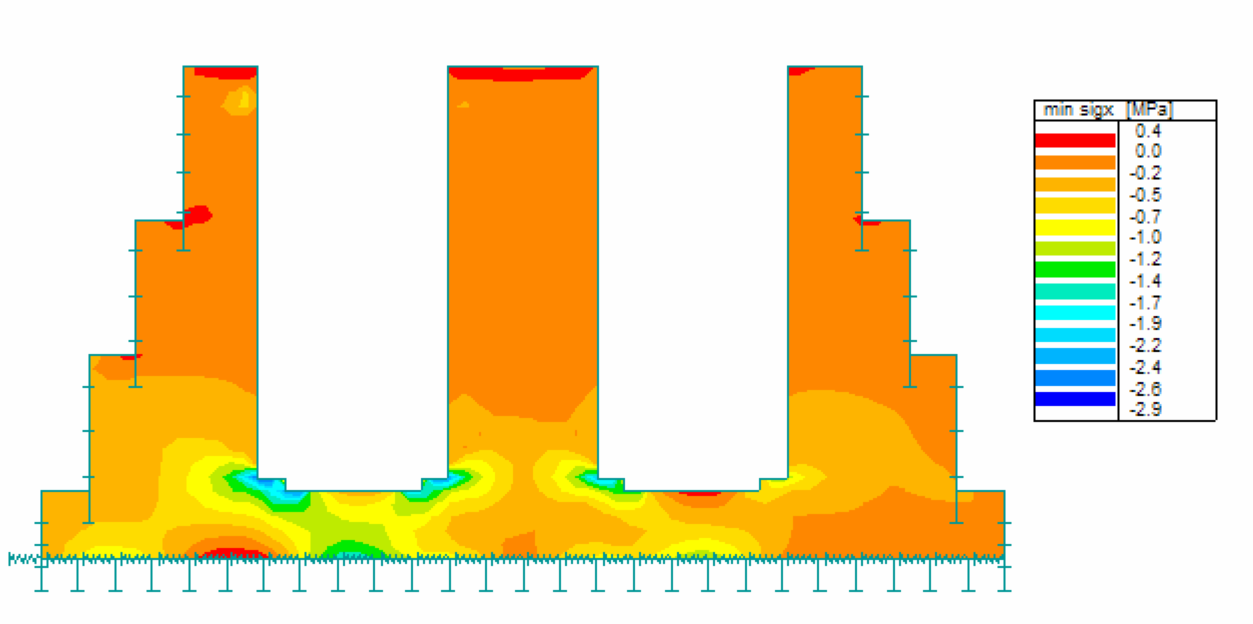

Stresses in the vertical direction – maximum compression = 7.5 N/mm²

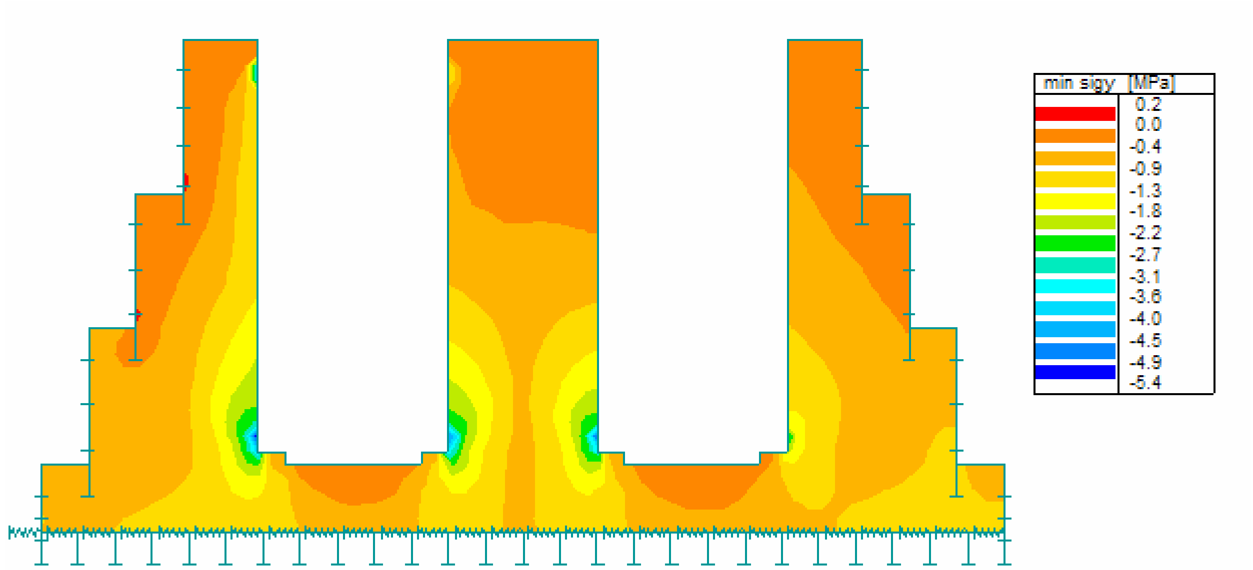

B. Accidental load combination 102 - MCE

$\sigma c < 0.85$ fck
This means $\sigma c < 21.25$ N/mm²

Stresses in horizontal direction – maximum compression = 4.5 N/mm²

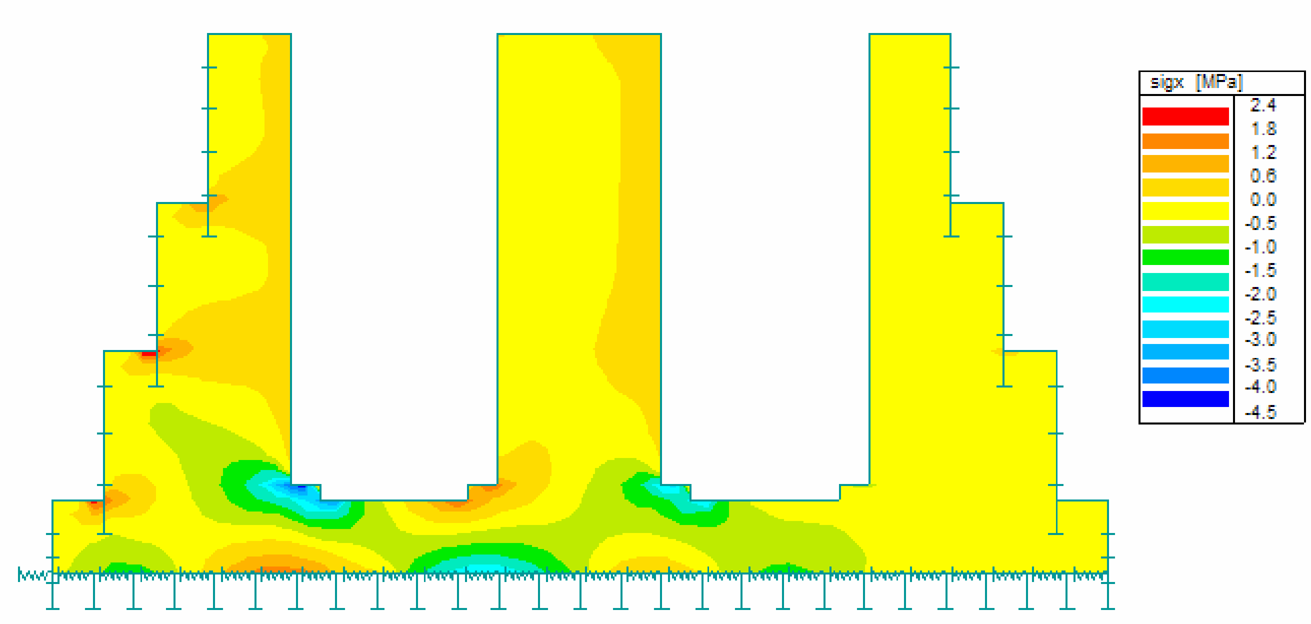

Stresses in vertical direction – maximum compression = 8.6 N/mm²

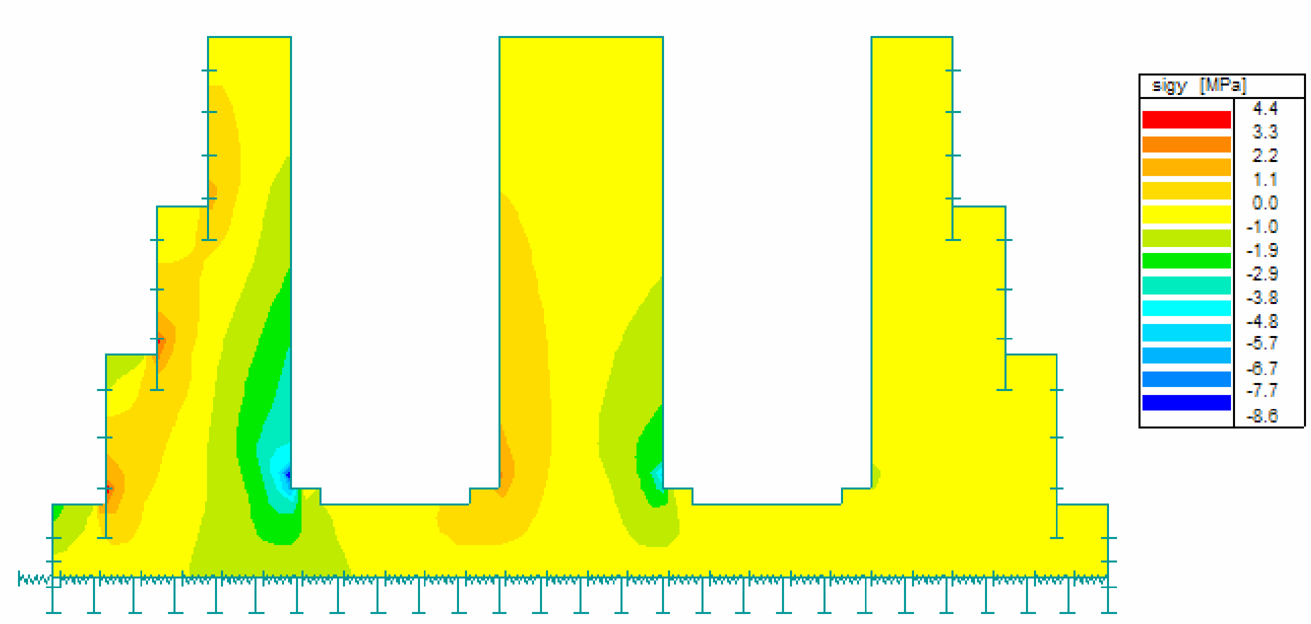

2.4.5 SUMMARY

	quasi permanent load combination - service	accidental load combination - MCE	rare load combination - dry gate recess	rare load combination - dry gate recess	Fundamental load combination	Fundamental load combination	Fundamental load combination	Fundamental load combination	Fundamental load combination	Fundamental load combination
	101	**102**	**103**	**104**	**105**	**106**	**107**	**108**	**109**	**110**
Load Bearing Capacity										
$1.4\ q_{ref} < q_u$	-	-	-	-	OK	OK	OK	OK	OK	OK
$q_{ref} < q_u$	-	OK	-	-	-	-	-	-	-	-
Deformations										
Max horizontal displacement (cm)	0.70	1.96	1.02	1.04	-	-	-	-	-	-
Concrete stresses										
$1.125 \times \sigma_c < 0.85$ fck/1.5	-	-	-	-	OK	OK	OK	OK	OK	OK
$\sigma_c < 0.85$ fck	-	OK	-	-	-	-	-	-	-	-

2.5 TYPE 2 - FOUNDATION IN LA BOCA

2.5.1 INPUT DATA

A. Geometry

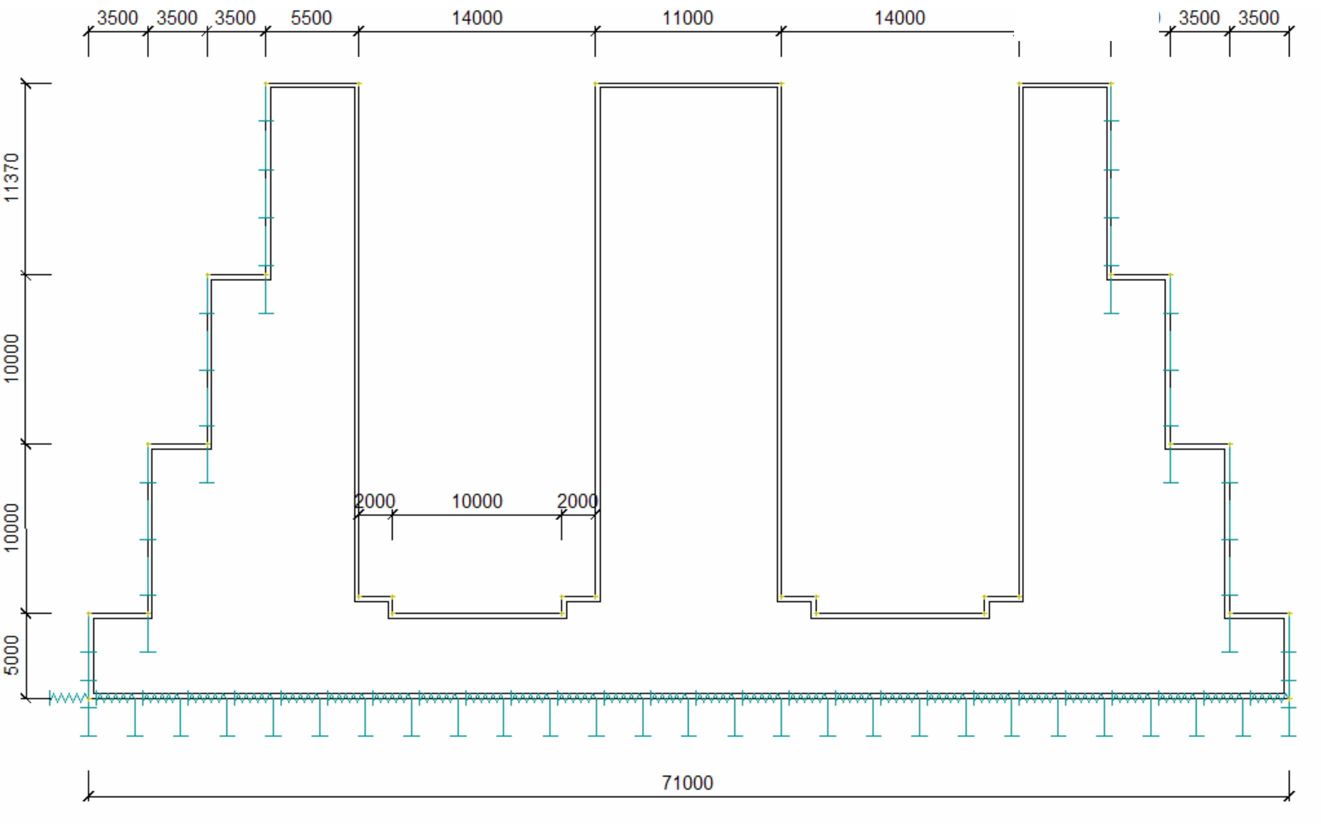

B. Materials

Material	E kN/m²	Nu	W/V kN/m3	Alpha
CONCRETE	19620000.000	0.100	24.525	0.0000100

C. Supports

The 'la boca' base is modeled by means of a linear support.

Vertical lock head elements:
Linear support with K= 200.000 kN/m² is introduced.
This support only works when compressed.

Horizontal rock base:
Linear support with K= 200.000 kN/m² is introduced.
This support only works when compressed. A small horizontal support is given to the rock base, to avoid trivial results of the calculation.

The K-values are estimated values.

D. Loads

D.1 Self Weight (case 1)

D.2 Earth Pressure (case 2)

side upper chamber

		lambda ah	lambda av
lambda a	0,1620	0,1403	0,0810
depth (m)	pressure (kN/m²)	ph (kN/m²)	pv (kN/m²)
0	10	1	1
1,5	37	5	3
11,37	146	20	12
21,37	246	34	20
31,37	346	48	28
36,37	396	56	32

side lower chamber

		lambda ah	lambda av
lambda a	0,1620	0,1403	0,0810
depth (m)	pressure (kN/m²)	ph (kN/m²)	pv (kN/m²)
0	10	1	1
11,37	215	30	17
20,97	387	54	31
21,37	401	56	33
31,37	501	70	41
36,37	551	77	45

Horizontal component

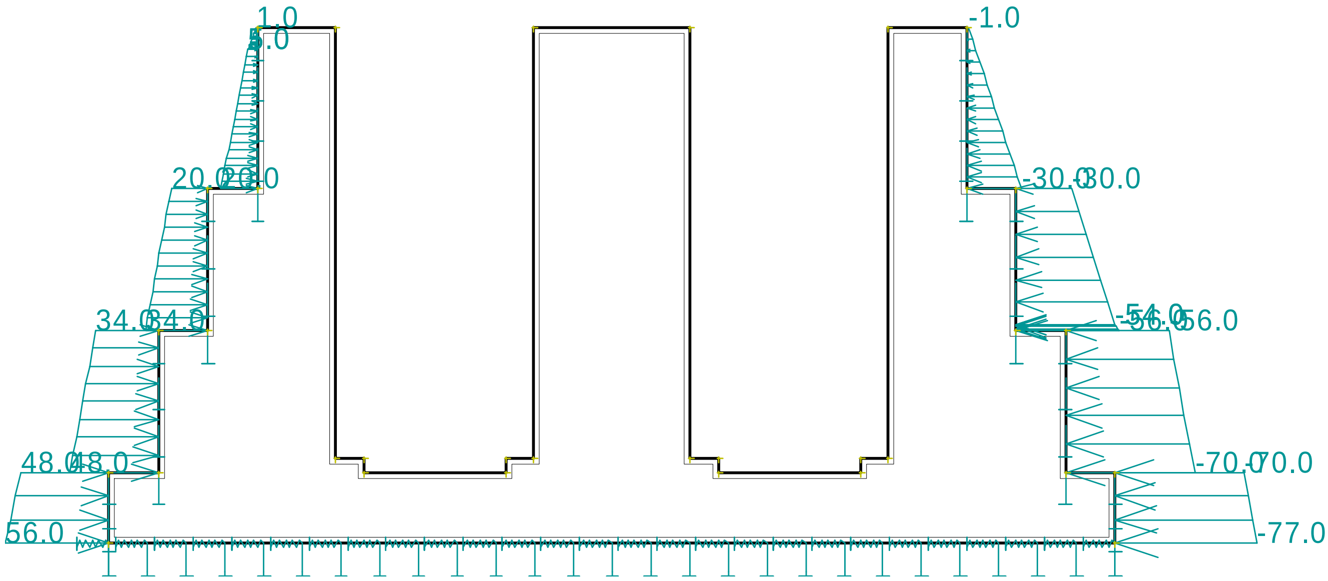

Vertical component

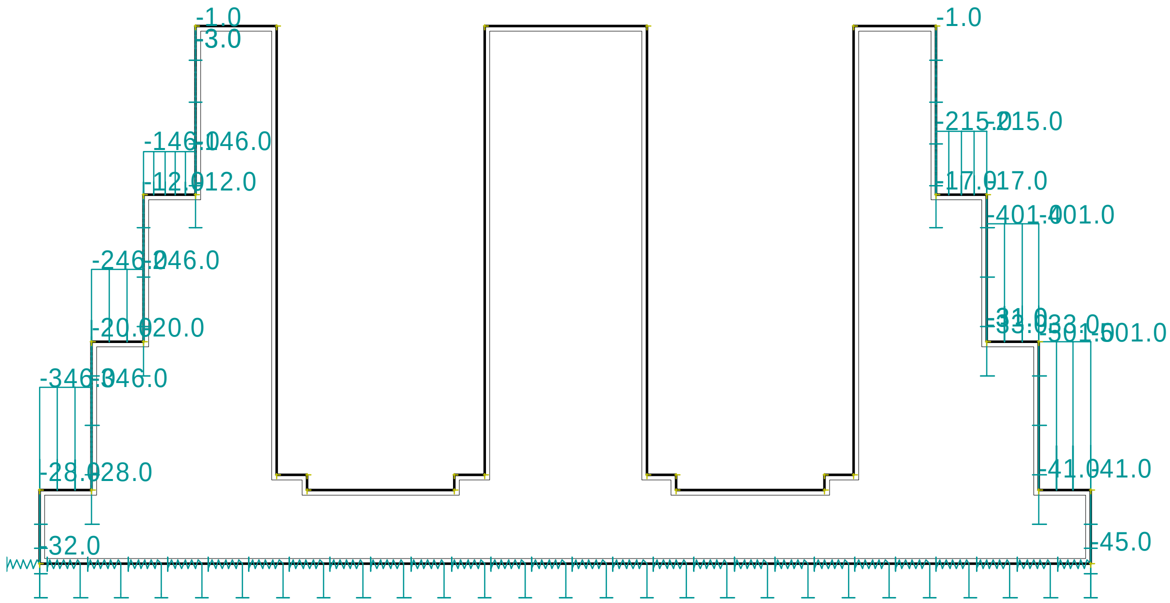

D.3 Water Pressure (case 3)

Water level side upper chamber (maximum): + 27.13 m
Water level side lower chamber (minimum): + 7.66 m

Water pressure onto the sides and bottom of the lock head

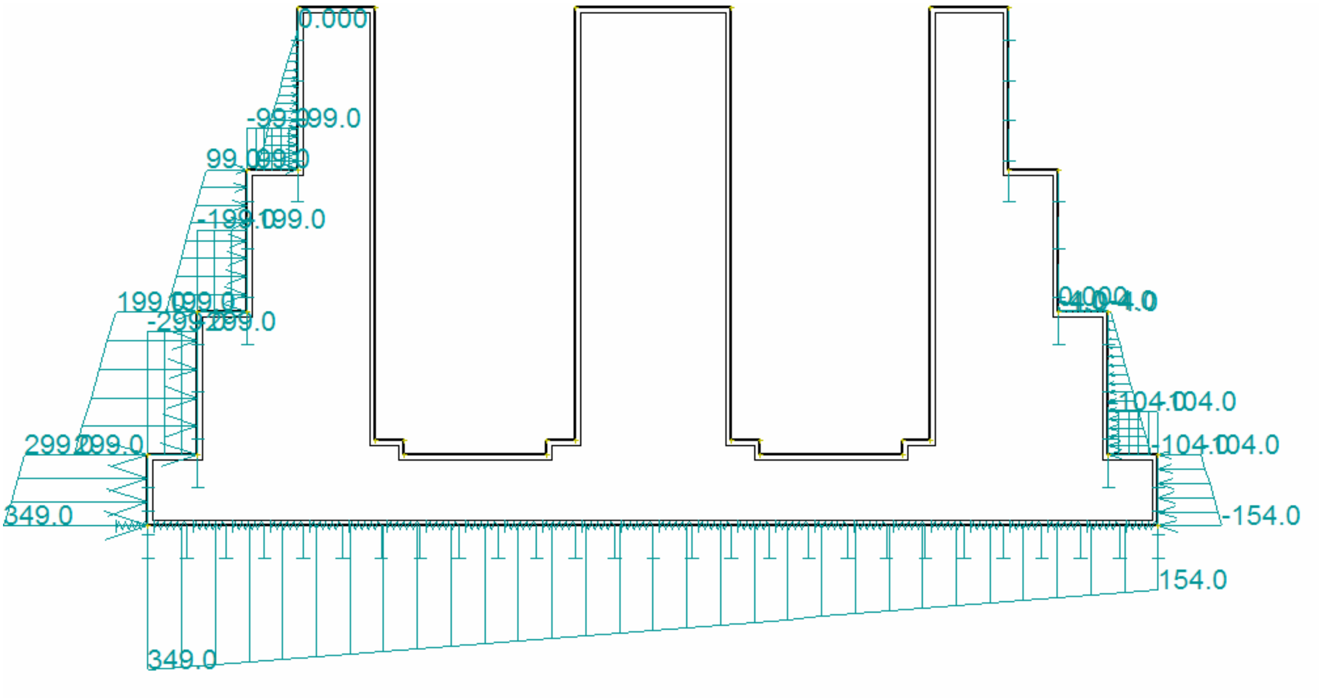

Water pressure inside the lock head

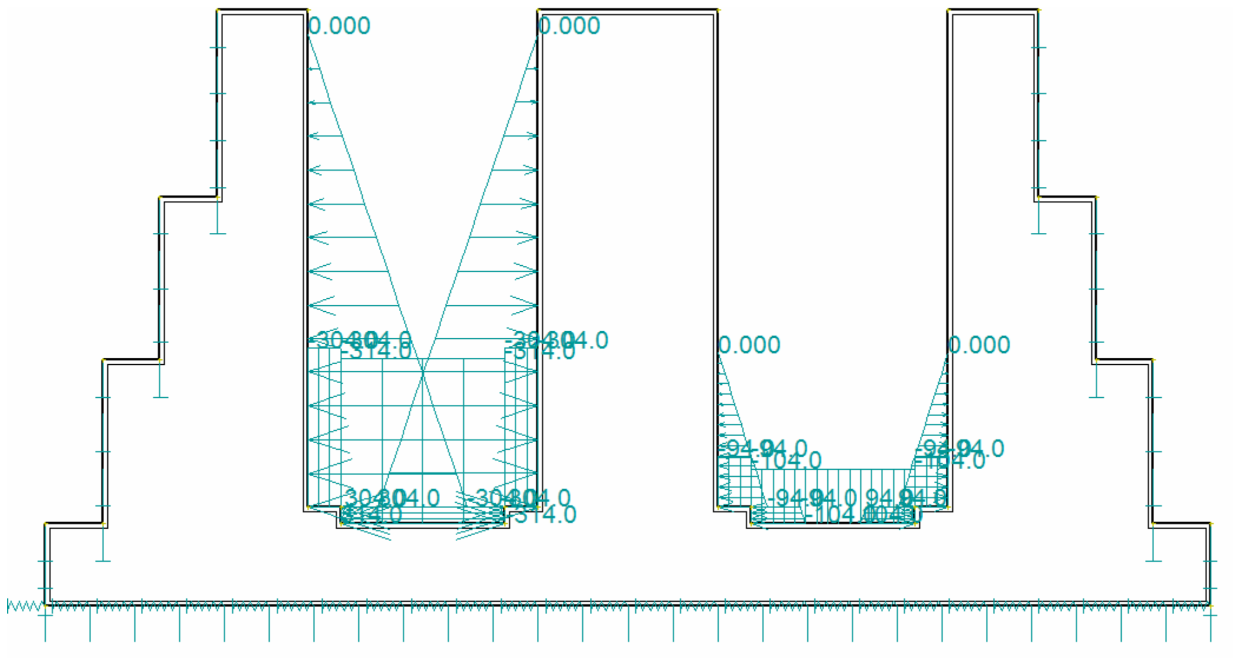

D.4 Seismic Loads (case 4)

The inertia forces on the structural weight are calculated as follows:

$G_v = (1-k_v)\ G$

$G_h = k_h\ G$

With G the weight of the structure including the backfill above the heel or toe of the structure and any water within the backfill

G_v the vertical component of the weight in seismic conditions

G_h the horizontal component of weight in seismic conditions

According to the PIANC regulations for Seismic design of Port Structures, the earth pressures due to seismic action are calculated using the Mononobe-Okabe equation. The inertia forces are then accounted for by considering a seismic inertia angle, $\Psi = \text{atan}\ (k_h/(1-k_v))$, in which k_h represents the horizontal seismic coefficient or the modified horizontal seismic coefficient for dry and submerged layers respectively.

Additional water pressures generated by seismic action are taken into account according to Westergaard formula. The seismic water pressure load case is valid for a unit value of k_e, and is multiplied by the respective k_e value in the corresponding load combinations.

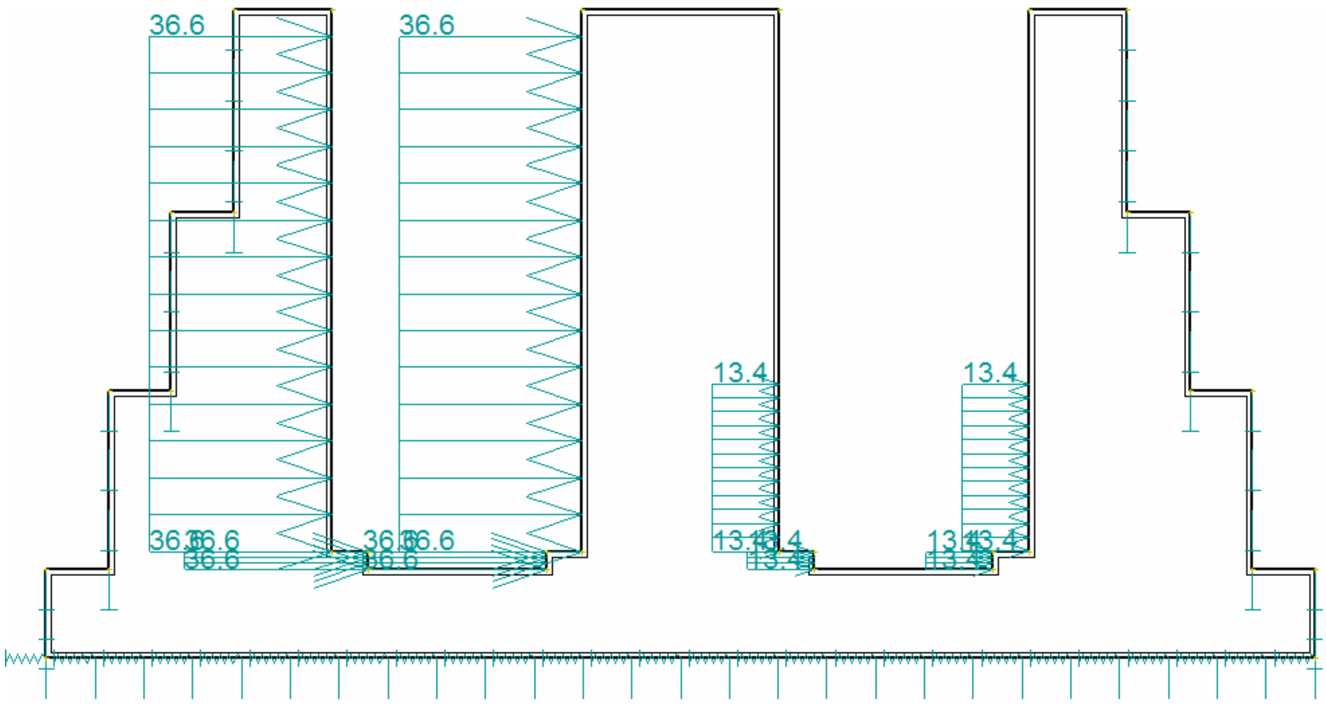

D.5 Water Pressure in Dry Lock Conditions (case 5-6)

In case 5 the one recess on the side of the upper chamber is put in dry conditions. In case 6 both recesses at put in dry conditions.

Case 6: normal water pressure without water pressure inside the lock head

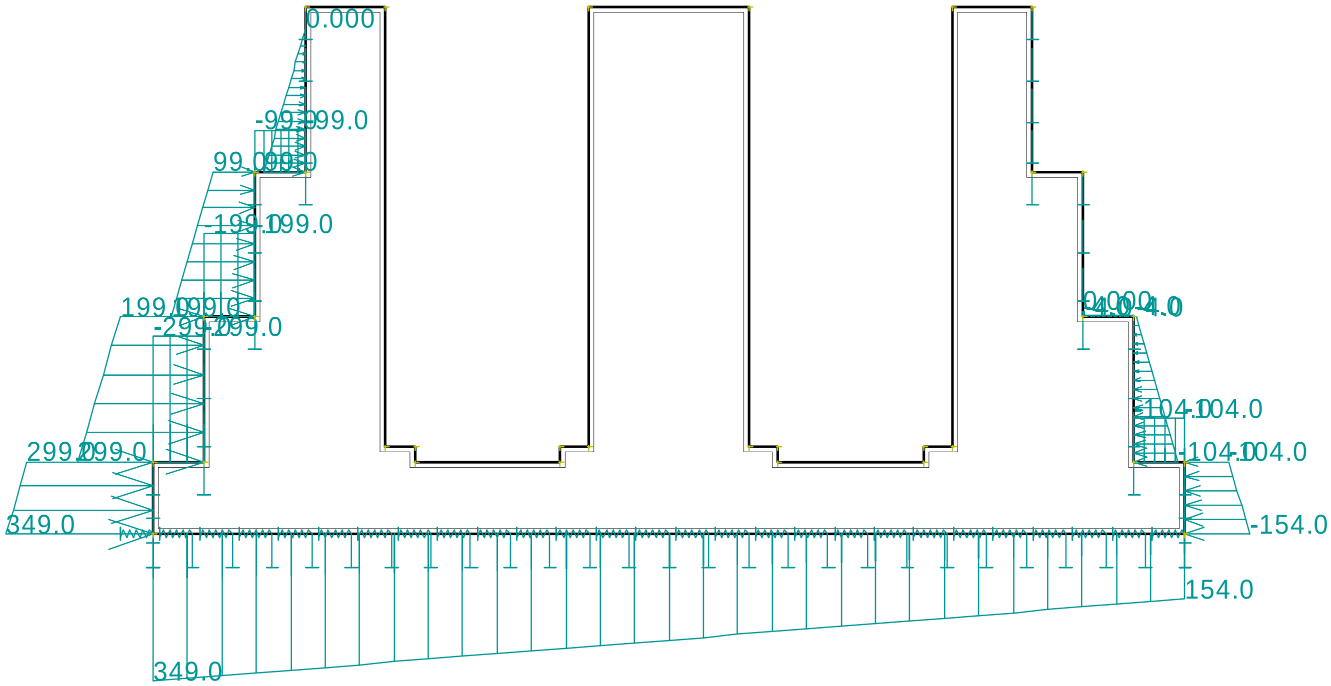

Case 5: normal water pressure combined with a maximum water level in the gate recess near the lowest chamber

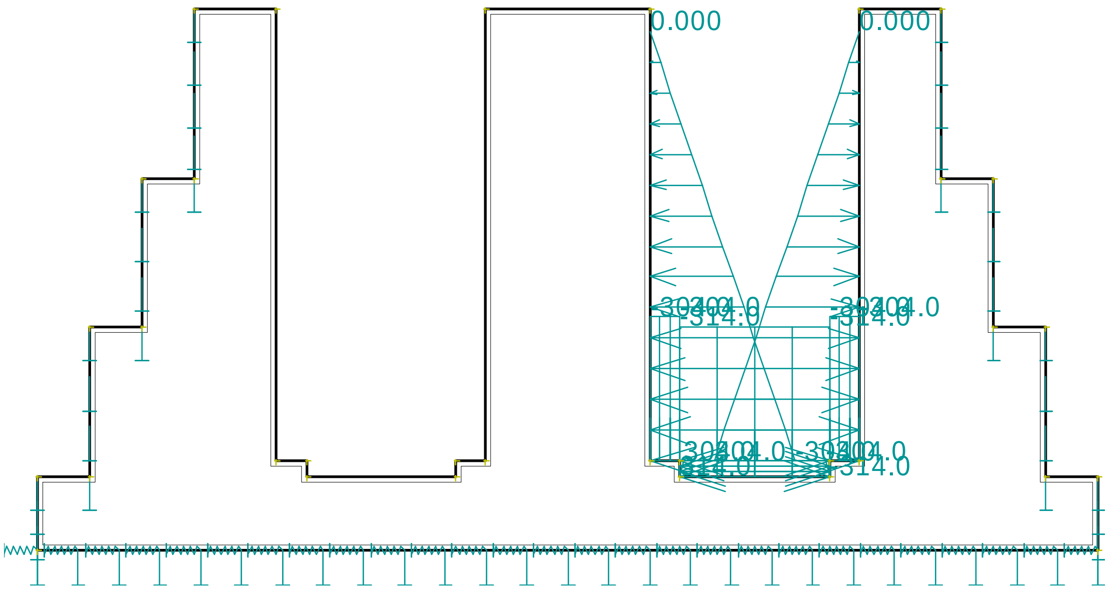

D.6 Upper wagon (case 7)

Loads due to the upper wagon are taken from report R4-D-403.

Gates 2,3		Side of flooded zone	Other side	Total vert. reaction
Base case: H = 11 m	Upper wagon	1500 kN	800 kN	2300 kN
	Lower wagon	1900 kN	1200 kN	3100 kN

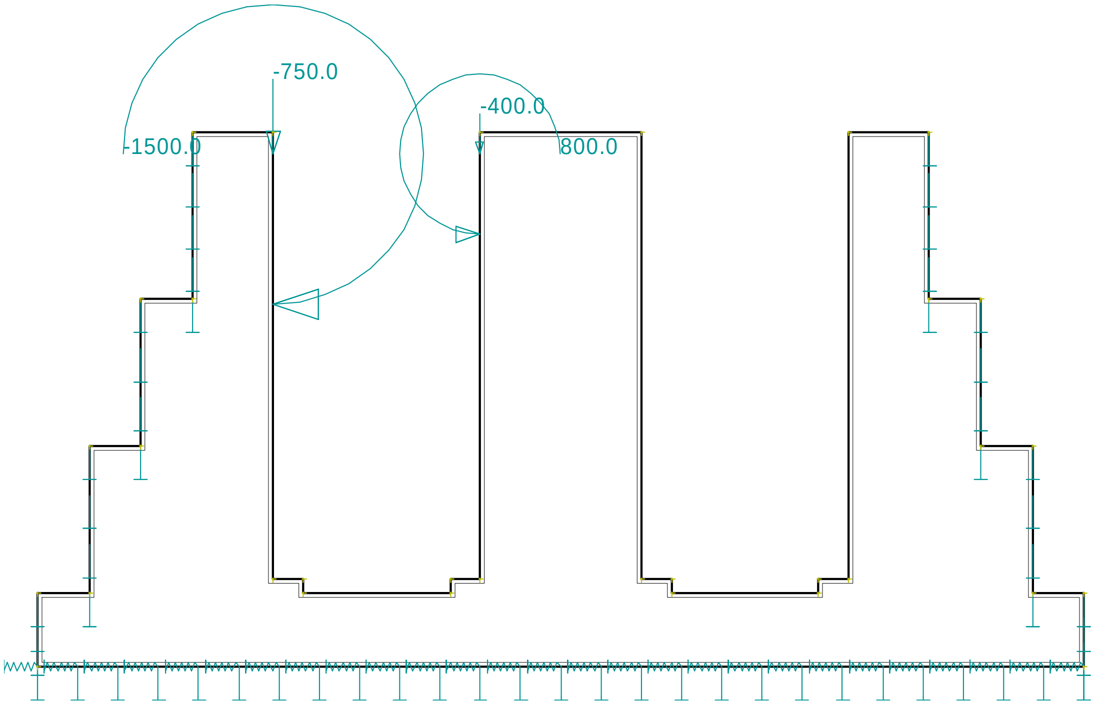

2.5.2 LOAD BEARING CAPACITY

A. Fundamental Load Combinations 105 to 110

Criterion: $\gamma_d \cdot q_{ref} < q_u$
with γ_d . = 1.4

The maximal vertical displacement at the bottom of the wall is 4.2 mm
This means a vertical pressure of 0.0042 x 200000 kN/m² = 840 kN/m² = 0.84 Mpa

Vertical displacement

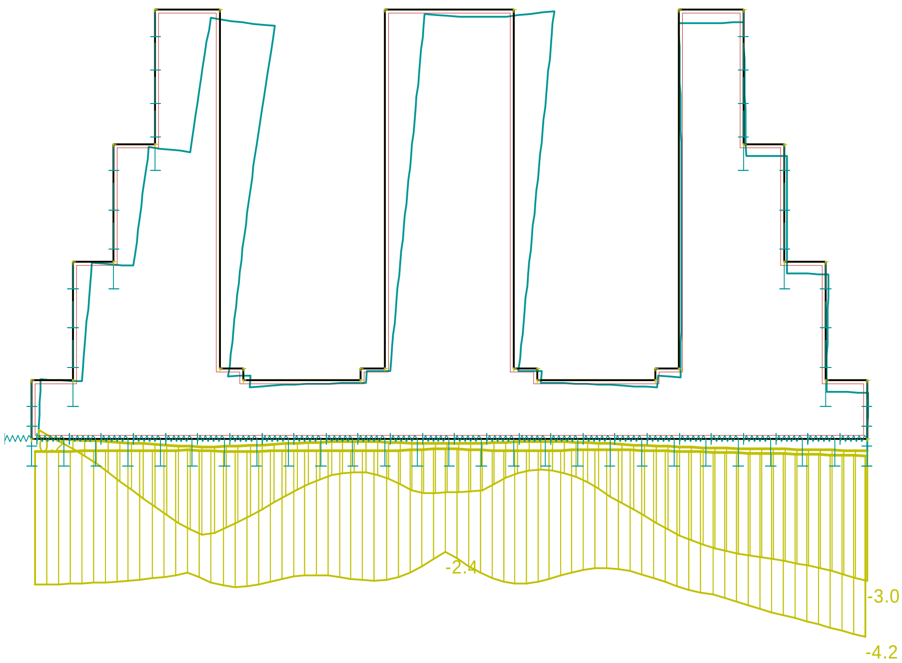

B. Accidental load combination 102 - MCE

Criterion: $\gamma_d \cdot q_{ref} < q_u$
with γ_d . = 1.0

The maximal vertical displacement at the bottom of the wall is 4.1 mm
This means a vertical pressure of 0.0041 x 200000 kN/m² = 820 kN/m² = 0.82 MPa

Vertical displacement

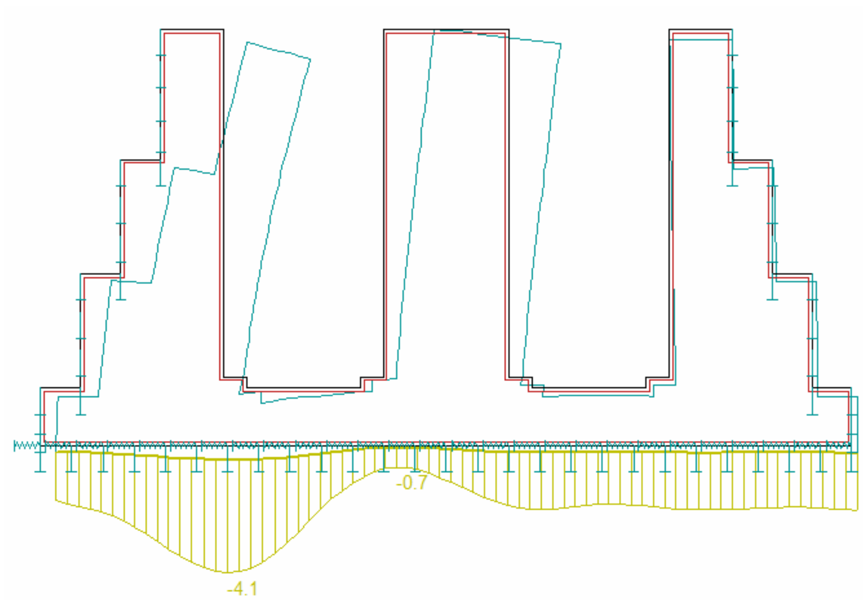

2.5.3 DEFORMATIONS

A. Load Combination 101 (Lock in Service)

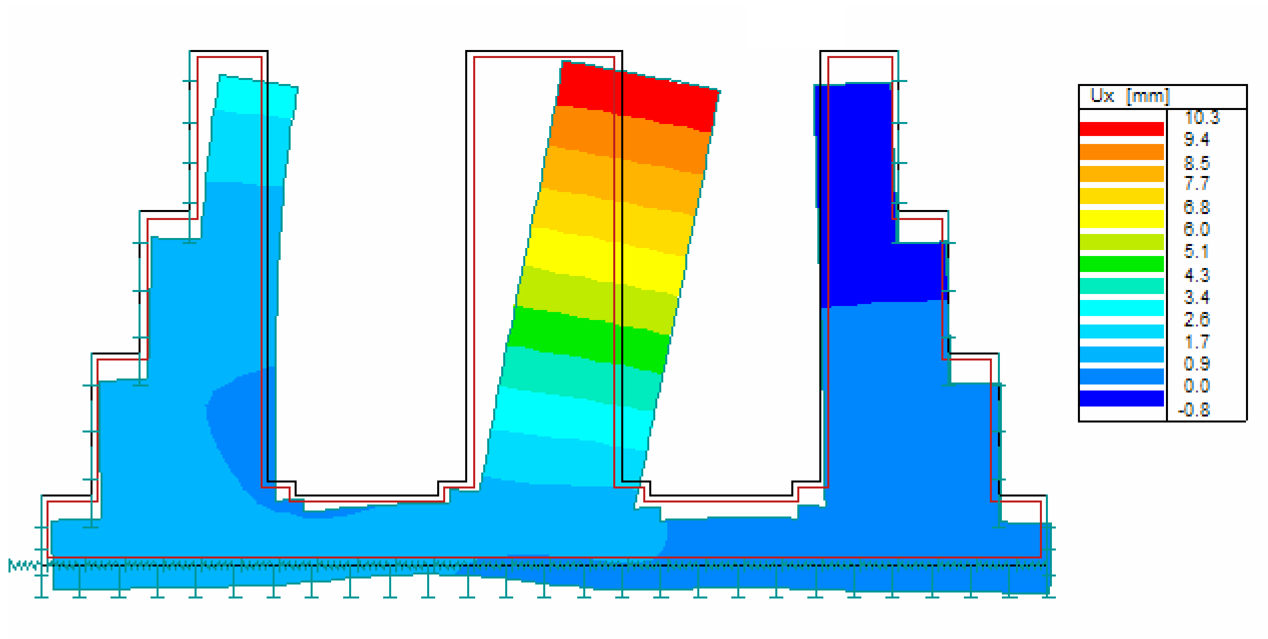

B. Load Combination 102 (MCE)

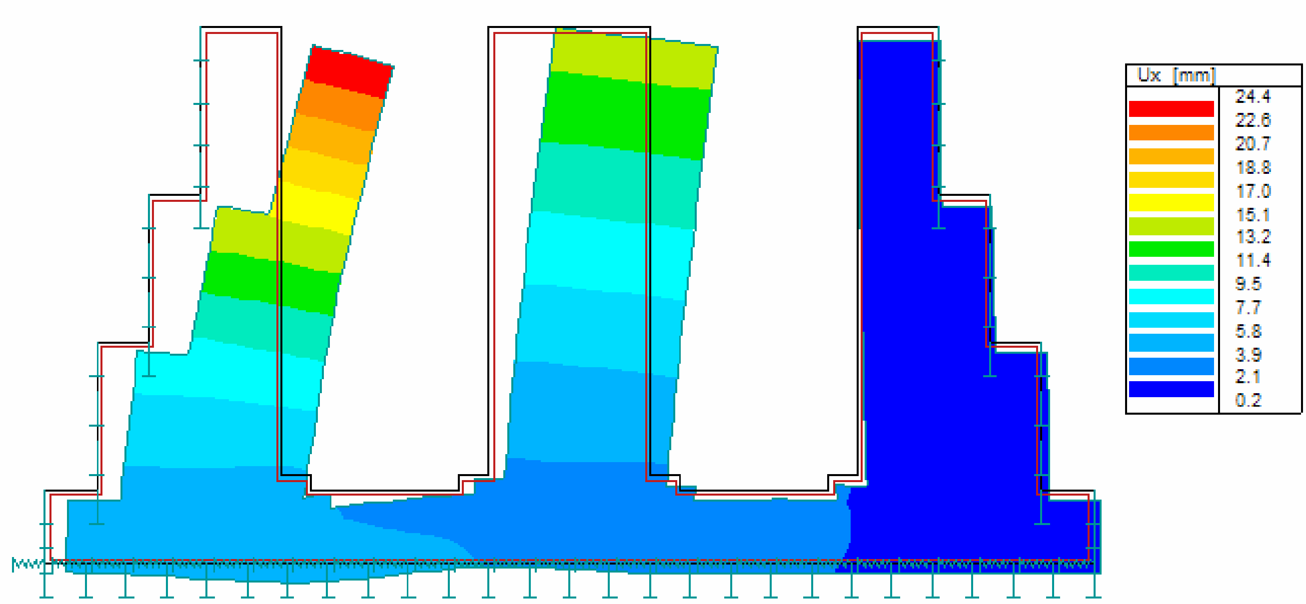

C. Load Combination 103 (1 gate recess in dry conditions)

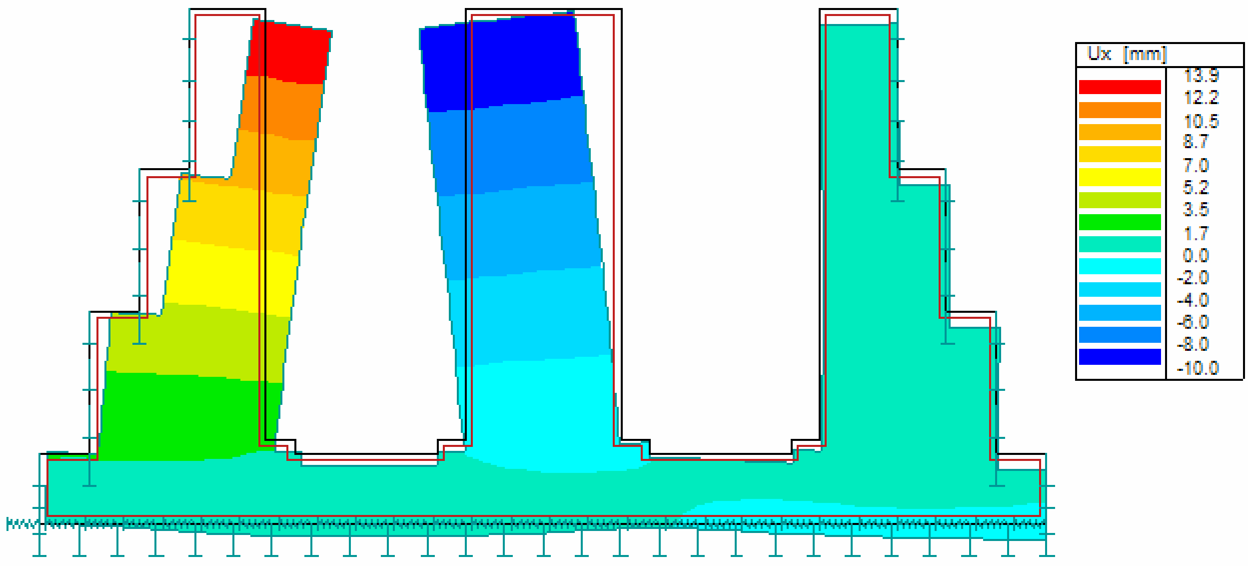

D. Load Combination 104 (2 gate recesses in dry conditions)

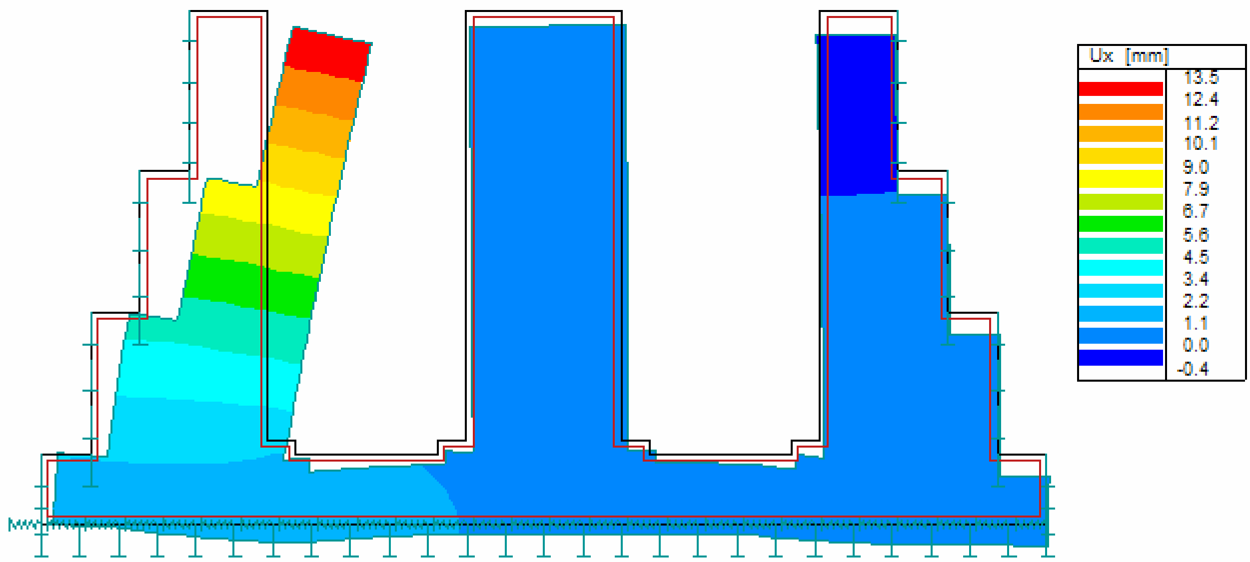

2.5.4 CONCRETE STRESSES

A. Fundamental load combinations 105 tot 110:

Criterion: $1.125 \times \sigma c < 0.85\ fck/1.5$

This means $\sigma c < 12.5$ N/mm²

Stresses in horizontal direction – maximum compression = 3.9 N/mm²

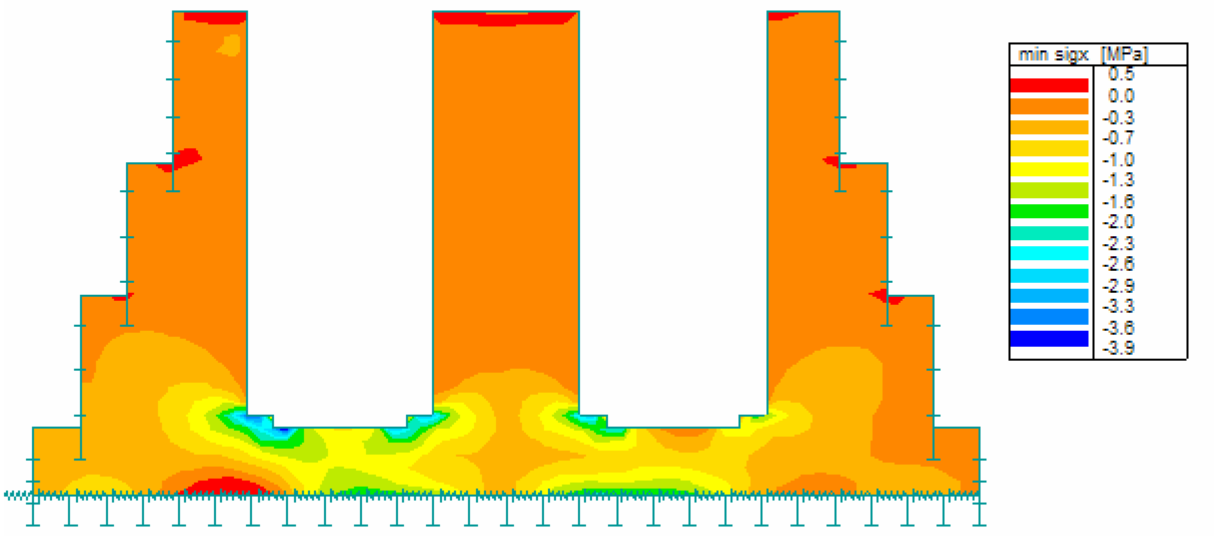

Stresses in vertical direction – maximum compression = 5.9 N/mm²

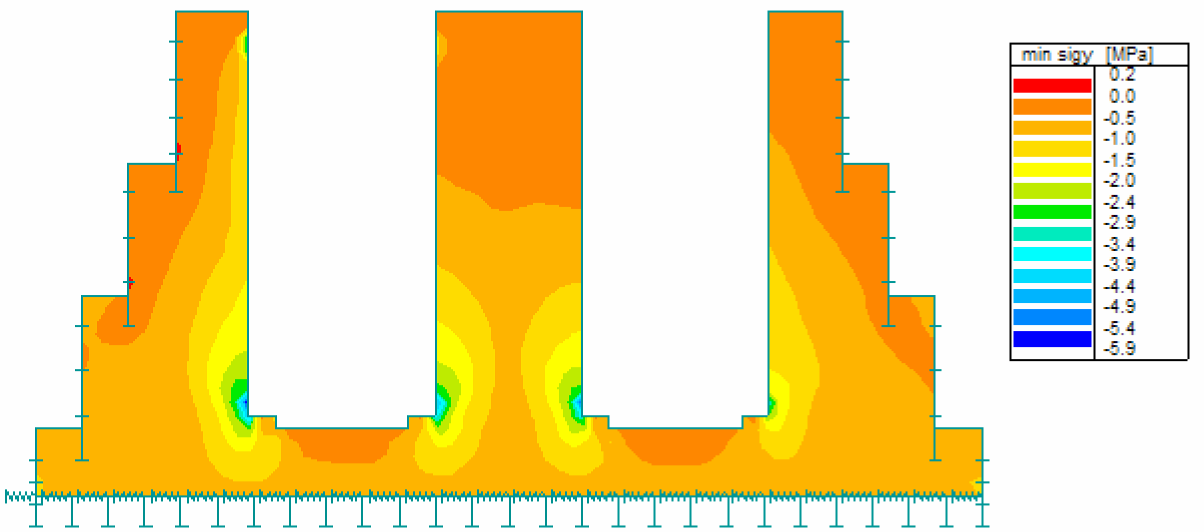

Accidental load combination 102 - MCE

Criterion: σc < 0.85 fck
This means σc < 21.25 N/mm²

Stresses in horizontal direction – maximum compression = 6.6 N/mm²

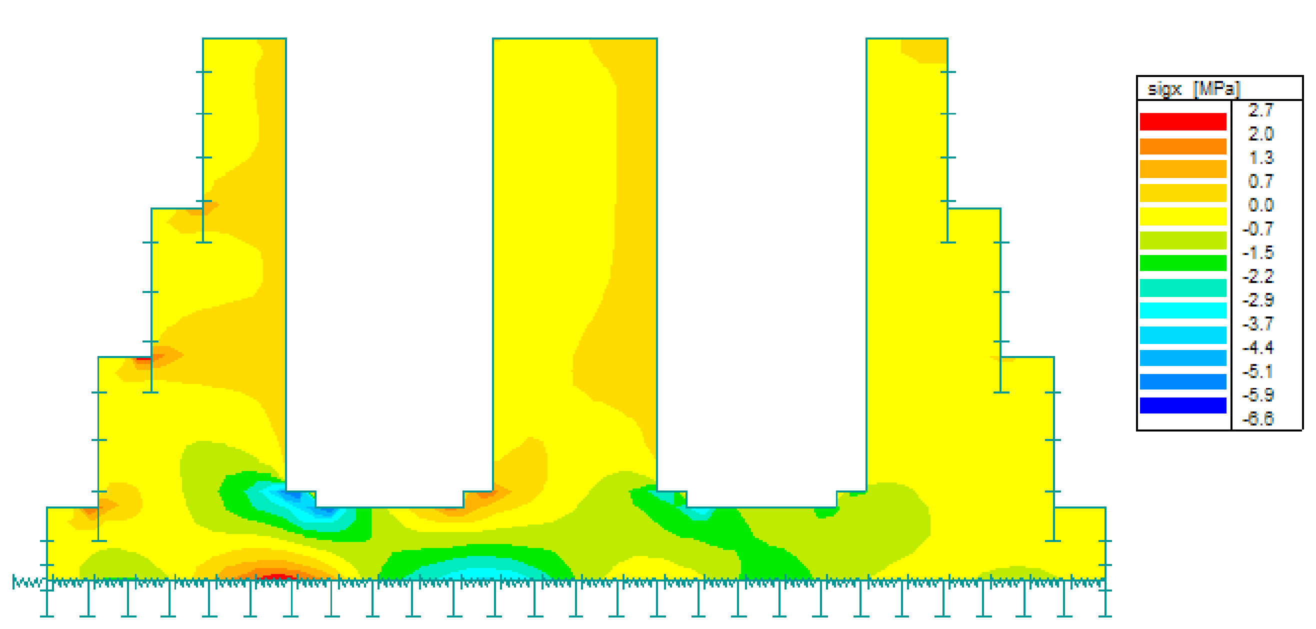

Stresses in vertical direction – maximum compression = 9.4 N/mm²

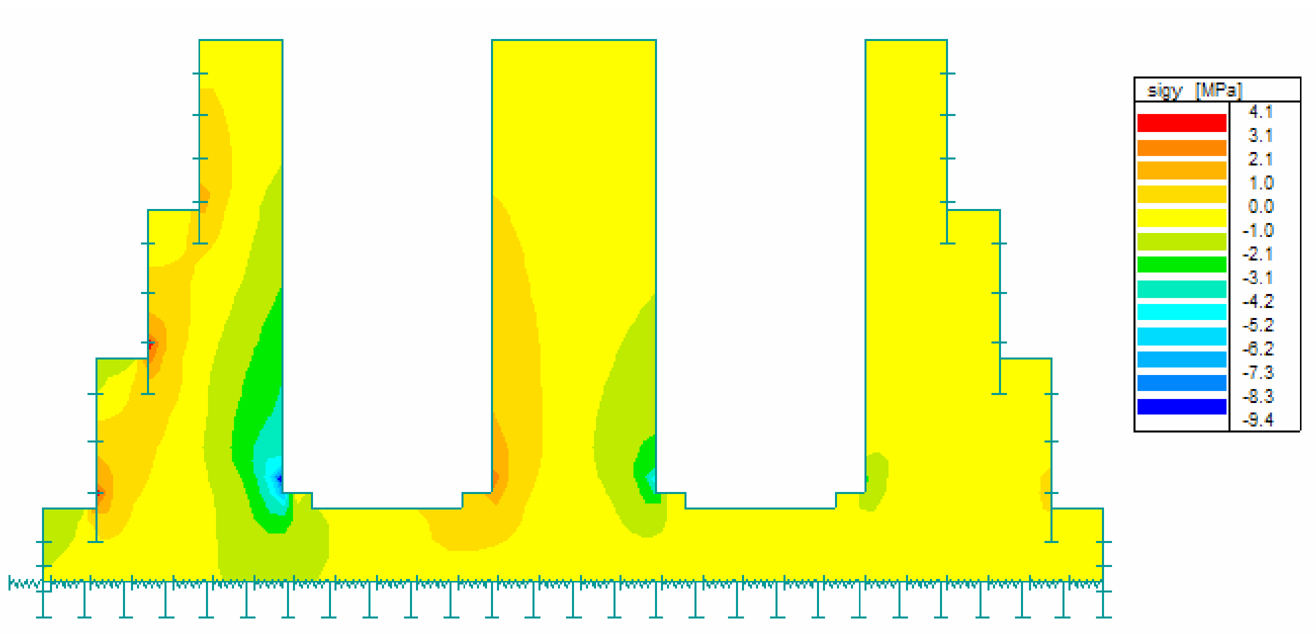

2.5.5 SUMMARY

	quasi permanent load combination - service	accidental load combination - MCE	rare load combination - dry gate recess	rare load combination - dry gate recess	Fundamental load combination	Fundamental load combination	Fundamental load combination	Fundamental load combination	Fundamental load combination	Fundamental load combination
	101	**102**	**103**	**104**	**105**	**106**	**107**	**108**	**109**	**110**
Load Bearing Capacity										
$1.4\ q_{ref} < q_u$	-	-	-	-	OK	OK	OK	OK	OK	OK
$q_{ref} < q_u$	-	OK	-	-	-	-	-	-	-	-
Deformations										
Max. hor. displacement (cm)	1.03	2.44	1.39	1.35	-	-	-	-	-	-
Concrete stresses										
$1.125 \times \sigma_c < 0.85$ fck/1.5	-	-	-	-	OK	OK	OK	OK	OK	OK
$\sigma_c < 0.85$ fck	-	OK	-	-	-	-	-	-	-	-

2.6 CONTACT STRESSES

2.6.1 BOTTOM SEAL

A. Forces onto the bottom seal

Maximum horizontal reaction forces at the sill bearing occur during retaining of the (maximum) water level difference. They result directly from the 2D-beam grid model computations presented in appendix A of the report 'lay out of rolling gates' after an optimization of the stiffness of the cantilevering bottom ends of the vertical frames. Doing so uplift from the sill bearing of the skin plating at the gate bottom edges is avoided.
To derive the maximum contact stress, the minimum spreading length (along the azobé wooden beams of 500 mm width) is indicated in the tables below.

The results mentioned in the report of the lay-out of the rolling gates are the following:

	Reaction force at frame (3.15 m length)	Max. contact stress (min. 540 mm)
Gate PA1	7500 kN (ULS)	28 N/mm² (ULS)

	Reaction force at frame (3.18 m length)	Max. contact stress (min. 540 mm)
Gate PA2-3	11400 kN (ULS)	42 N/mm² (ULS)
Gate PA4	10400 kN (ULS)	39 N/mm² (ULS)

B. Calculation of the contact stresses

The bottom seal is made of two basalt (or a similar material) elements: one for the direct contact with the gate and one making the placement of a habitat possible.

Because of the gap in the second stone we can not spread the force vertically. We use in our calculation a contact height of 35 cm.

Horizontally the force can be spread over an angle of 45 degrees. A contact width of (200 cm + 54 cm + 200 cm) = 454 cm is obtained.

Thus the contact stresses onto the concrete can be derived:

11400 kN / (35 cm x 454 cm) = 7.17 N/mm²

The maximum tensile stresses within the seal caused by the contact stress can be estimated by formulas in literature.

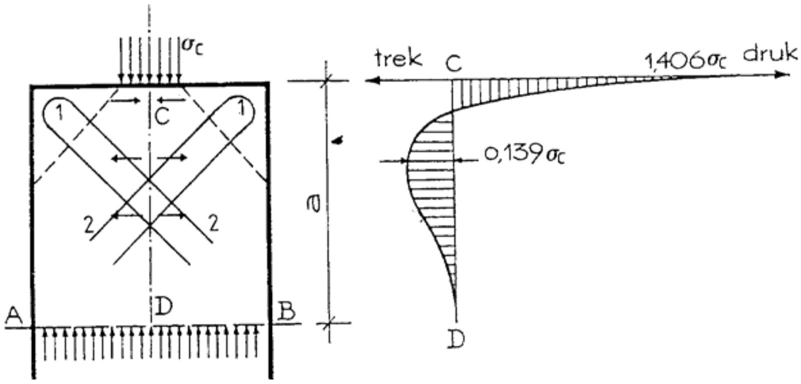

$\sigma_t = 0.139 \times \sigma_c$
$\sigma_t = 0.139 \times 42$ N/mm² = 5.84 N/mm² < 6.67 N/mm² = 10 N/mm²/1.5

The tensile strength is kept below the admissible tensile strength of the material, which is mentioned in the design criteria. No additional safety factor is used for the contact stresses because the dry lock condition is considered as a rare load combination (safety factor = 1).

2.6.2 LATERAL BEARINGS

A. Forces onto the lateral bearings

Maximum horizontal reaction forces at the lateral bearings (on the lock walls) occur during retaining of the (maximum) water level difference. From the 2D-beam grid model computations presented in appendix A of the report ‘lay-out of rolling gates’, the reaction forces at the horizontal frames are obtained (corresponding to the same optimized stiffness distribution). Subsequently the part of the vertical frame structure at the contact with the lock walls is modeled as a continuously elastically supported beam, which is loaded by these reaction forces. The maximum contact stresses are listed below.

The results mentioned in the report of the lay-out of the rolling gates are listed below.

Gate 1	Max. contact stress (at R1)
	35 N/mm² (*)

Gates 2,3,4	Max. contact stress at R1	Max. contact stress at R3
	45 N/mm²	52 N/mm² (*)

(*) Based on our experience with 3D-modelling of the recently designed new rolling gates for the Van Cauwelaert lock (port of Antwerp) we expect that the contact stresses at R4 are overestimated at least by 10 N/mm² due to the underestimation of the beam stiffness at the air chamber. Therefore the contact stress at R1 should be considered as determinative, like in the case of Gate PA1.

B. Calculation of the contact stresses

The vertical seal is made of a basalt (or a similar material) element. The sealing at the side with the gate recesses is different from the one on the other side, because it has to work as seal for the bulkhead.

The maximum contact stresses that are given remain constant along several meters in height. Therefore we cannot spread the force in the vertical direction.

Horizontally the force can be spread over the width of the sealing stone. A contact width of 160 cm has been obtained.

Thus the contact stresses onto the concrete can be derived:

$$52 \text{ N/mm}^2 \times 500\text{mm}/1600\text{mm} = 16.25 \text{ N/mm}^2$$

The maximum tensile stresses within the seal caused by the contact stress can be estimated by formulas in literature.

$$\sigma_t = 0.139 \times \sigma_c$$
$$\sigma_t = 0.139 \times 45 \text{ N/mm}^2 = 6.26 \text{ N/mm}^2 < 6.67 \text{ N/mm}^2 = 10 \text{ N/mm}^2/1.5$$

The tensile strength is kept below the admissible tensile strength of the material, which is mentioned in the design criteria. No additional safety factor is used for the contact stresses because the dry lock is considered as a rare load combination (safety factor = 1).

3 Literature

ACP (2005). Memorando. ACP Seismic Design Criteria.

CAMERON W.I. & GREEN R.A. Development of engineering procedure for evaluating lateral earth pressures for seismic design of cantilever retaining walls.

http://www.scia-online.com/esawin/index.html

PIANC (2001). Seismic design guidelines for port structures. WG No. 34 of the Maritime Navigation Commission. International Navigation Association. A.A. Balkema Publishers

ROSA (2000). Recommendations for the design in limit states of structures in aquatic environments.

TRACTEBEL, TECHNUM, COYNE ET BELLIER & CNR (2002). Diseño Conceptual de las Esclusas Post Panamax. Triple Lift Lock System. Task 2 & 3

TRACTEBEL, TECHNUM, COYNE ET BELLIER & CNR (2002). Diseño Conceptual de las Esclusas Post Panamax. Triple Lift Lock System. Task 4

WINTER T. (2005). Review of the probabilistic seismic hazard analysis for Miraflores and Gatun locks carried out by USGS. Orléans.

CPP Consorcio Post-Panamax

Update of Pacific Locks Conceptual Design and Harmonization of Atlantic Locks Conceptual Design-Contract SAA-143351

PACIFIC LOCKS ACTUALIZATION

TASK P4C – Emptying and Filling System

Rev D

in association with

List of annexes

Annex 13-3:	Filling middle chamber with max fall of 8.10 m – Levels inside the gates, the recesses and between the two gates
Annex 14-1:	Emptying the WSB in a lock with max fall of 8.40m. Impact of the ports size reduction on the balancing of the flow. Ports 1 to 5.
Annex 14-2:	Emptying the WSB in a lock with max fall of 8.40m. Impact of the ports size reduction on the balancing of the flow. Ports 6 to 10.
Annex 14-3:	Emptying the WSB in a lock with max fall of 8.40m. Impact of the ports size reduction on the balancing of the flow. Ports 11 to 15.
Annex 14-4:	Emptying the WSB in a lock with max fall of 8.40m. Impact of the ports size reduction on the balancing of the flow. Ports 16 to 20.
Annex 14-5:	Filling the WSB from a lock with max fall of 5.00m. Impact of the ports size reduction on the balancing of the flow. Ports 1 to 5.
Annex 14-6:	Filling the WSB from a lock with max fall of 5.00m. Impact of the ports size reduction on the balancing of the flow. Ports 6 to 10.
Annex 14-7:	Filling the WSB from a lock with max fall of 5.00m. Impact of the ports size reduction on the balancing of the flow. Ports 11 to 15.
Annex 14-8:	Filling the WSB from a lock with max fall of 5.00m. Impact of the ports size reduction on the balancing of the flow. Ports 16 to 20.
Annex 15-1:	Flushing of the brackish water. Lock to lock operation without using the WSB. Filling with max head of 21.10 m. Discharges in the ports
Annex 15-2:	Flushing of the brackish water. Lock to lock operation without using the WSB. Filling with max head of 21.10 m. Velocities in the ports
Annex 15-3:	Flushing of the brackish water. Lock to lock operation without using the WSB. Filling with max head of 21.10 m. Discharge difference between ports 1 and 20
Annex 16-1:	Flushing of the brackish water. Lock to lock operation without using the WSB. Emptying with max head of 21.10 m. Discharges in the ports
Annex 16-2:	Flushing of the brackish water. Lock to lock operation without using the WSB. Emptying with max head of 21.10 m. Velocities in the ports
Annex 16-3:	Flushing of the brackish water. Lock to lock operation without using the WSB. Emptying with max head of 21.10 m. Discharge difference between ports 1 and 20
Annex 17	More refined dynamic analysis of ship motion and vessel positioning system

0 Executive summary

The present report deals with the conceptual design of the filling and emptying system of the Post-Panamax Third lane of Locks. The design has already been made on the Pacific side for the following configurations of:

- a triple-lift lock structure, equipped with 3 water saving basins each,
- a single-lift lock structure, equipped with 6 water saving basins,
- a double-lift lock structure, equipped with 2 water saving basins each

This report deals with the **actualization of the triple-lift lock study, Pacific side**, object of a new contract between ACP and the Consortium CPP.

The actualization was requested by the modifications brought to the project by ACP, after the first conceptual design studies. The main modification concerns the width of the locks.

All the assumptions and design criteria are given in the final report on Design Criteria.

The lock system consists of three lock chambers with 3 water saving basins each, on the east bank of the second lane that will allow **to save nearly 87 %** [1] **of the total water required to lock 1 ship** (semi convoy mode). Besides, the west bank remains free for the future fourth lane construction.

The chamber and water saving basin levels have been set up using the same software as for the other studies. This software gives the minimum and maximum water levels reached in the chambers and the 3 basins and provides the water usage and the water saving rate for each lockage as well as the daily number of up- or down lockages.

[1] *The three-step lock system saves 2/3 of the volume of a* ***single lock*** *chamber.*

Moreover, the water saving basins save: $e = \frac{n}{n+2}$ *= 60 % of the 1/3 remained (with the same area for WSB and lock chamber : m= wsb area / lock area = 1), where n is the number of water saving basins per lock*

So, the total water saving rate is e':

$$e' = \frac{2}{3} + \frac{1}{3}e = \frac{3n+4}{3n+6}$$

For n=3, e' = 0.87, i.e. 87 %

Based on the results of the former configurations, the scope of work of this configuration identifies **a side-wall culvert and ports filling and emptying system to be studied.**

The system has been modeled and pre designed with the hydraulic software Flowmaster ™.- as far as the hydraulic circuits of the conduits, longitudinal culverts and ports as well as the valves are concerned – and a 2D/3D model for the water flow in the lock chamber (based upon state-of-the-art Delft3D software) – as far as the analysis of the hawser forces is concerned.

During the simulations, the same values of the following parameters as for the first configuration of three locks have been tested by default:

- Culverts, conduits and ports size,
- Number of ports,
- Schedule of the valve control

leading to a feasible but not yet completely optimized configuration.

The calculated filling and emptying times fit in with the times required by the design values and/or the guidelines. The velocities reached in culverts and ports are acceptable, taking into account that the maximum velocities could be reduced by providing adapted shapes to the ‘’circuits’’ components (especially ports) on one hand and opening and closing rates of the valves on the other hand.

The system provides quite a uniform flow distribution and an upstream-downstream and east-west balanced filling. The remaining dissymmetry, that could be responsible for strengths on the hawsers exceeding the acceptable level, has been examined. Thus, it has been shown that the maximum hawser forces- associated with the selected F/E system and some limited hydraulic optimizations- are already within a range of guideline values based upon literature and own calculations.

Solutions to reduce it have been tested on the 2D/3D Delft mathematical model at a conceptual level of design. It has been shown that these solutions have potential for further reduction of the maximum hawser forces towards the lower end of the range of he guidelines values.

This report also provides, at a conceptual level of design, a study of the possible risks concerning the cavitation phenomenon.

The next stage, which is the preliminary design of the filling and emptying system, should mainly allow to:

- Optimize the culvert & conduits dimensions and shape, and port number,
- Optimize the valve schedule,
- Define the port distribution along the lock chamber, their position and orientation,
- Evaluate accurately the expected strengths on the hawsers, by means of the 2D/3D Delft mathematical model

This stage will require more advanced numerical modeling, prior to and in parallel with a physical scale model study. The results achieved on this model are required before starting the final design, and in any case before the tender procedure.

This conceptual design is made for locks using water saving basins, according to the TOR. If the water saving basins are not used, the E/F times may have to be largely increased in case of exceptional operation mode, or the E/F system may need to be adapted/modified in case of normal operation mode, as the head would be much larger in most operating scenarios.

1 Foreword

1.1 CONTRACT

This report is performed within the scope of the contract n° SAA-143351 awarded on November 24, 2004 to the Consortium named CPP (Consorcio Post Panamax) by the client ACP (Autoridad del Canal de Panama).

This report concerns the first part of the contract : new Panama Canal lock system conceptual design actualization study, Pacific side.

This contract follows a previous one, awarded to the same Consortium, in January 2002, and concerns the same lock system, with different configurations: one, two and three steps.

This new contract was awarded to update the previous studies by integrating some technical modifications (lock dimensions, ship handling system...)

1.2 SCOPE OF WORK

This report deals with the actualization of the triple lift lock study on the Pacific side of the Panama Canal.

The actualization is performed on the basis of the former studies realized by CCP and takes into consideration the choices made by ACP:

- Using a 3 lift lock system, each lock chamber being equipped with 3 water saving basins;
- Using tug boats instead of locomotives as positioning system;
- Operation of the locks with rolling gates;
- Using a filling and emptying hydraulic system with longitudinal side wall culverts and ports;
- Reduction of the lock width from 61.00 to 55.00 m.

The scope of work of the actualization study mainly consists in:

- Setting the levels of the chambers and the water saving basins, using the new data: Gatun lake levels, double sinusoid for the Pacific levels;
- Calculate the heads between the different pools (Gatun lake, chambers, water saving basins, Pacific Ocean);
- Calculate the water usage and the water saving rate;
- Optimizing the F/E system using Flowmaster ™ for the hydraulic circuits, in combination with a two-dimensional model for the flow in the lock chamber (2D/3D Delft) in order to analyze the hawser forces,
- Designing the hydraulic system at a conceptual level according to the solution described above;,
- Determining approximately the number of ships passing through the locks in the semi convoy mode

2 Introduction

2.1 BACKGROUND

The actual locks of the Panama Canal are going to be saturated in less than ten years. In addition, the new Post Panamax vessels cannot pass through the locks.

The "Autoridad del Canal de Panama" is conducting a study to evaluate the feasibility of a third lane of locks for bigger vessels. However, there is a lack of water at the present time to operate the new locks, that's why new solutions have to be found.

None of these kinds of locks have yet been designed. The engineering work starts with a conceptual design study. The purpose of this study is not to design the locks in detail, but to allow ACP to choose the best solution according to the following subjects: hydraulic filling and emptying systems, water saving basins, type of gates, civil works, electro–mechanical equipment,…

2.2 BRIEF DESCRIPTION

The Panama Canal is mainly composed of the Gatun Lake, and two sets of locks, one on the Atlantic side and one on the Pacific side of the Canal.

The Pacific side locks are composed of two distinct blocks, which frame the lake Miraflores:

- A set of two lines of two step locks, on the Pacific side, the Miraflores locks, for nearly two third of the head;
- A set of two lines of single step locks, on the Gatun lake side, the Pedro Miguel locks, for the remaining head.

Each lock has the following dimensions:

- Useful length : 305 m
- Useful width : 33.50 m
- Maximum vessel draft : 12 m (39.5 ft) in tropical fresh water

The maximum tidal range on the Pacific coast is nearly 7 m; the level of the Gatun Lake can be lowered by a little less than 2 m during the dry season (from 26.67 m PLD to 24.84 m PLD). ACP intends to raise the Gatun lake maximum level, in order to improve the channel transit capacity.

All the locks are able to handle 65 000 dwt ships, called Panamax ships, in semi-convoy mode, i.e. the ships sail 12 hours in one way and the next 12 hours in the other way.

The present locks will be saturated in a few years. In addition they are not able to pass the larger ships: 105 000 dwt container vessel, 140.000 dwt bulk carrier and further up to 200 000 dwt ships, called Post Panamax. The ACP (Autoridad del Canal de Panama) has then decided to investigate possibilities to construct new and larger locks.

The main issue from a hydraulic point of view is the lack of water to operate these new locks. Existing locks are already consuming nearly all the available water of the watershed. During the dry season, the resource is lower than the consumption and leads to lowering of the Gatun lake level. In addition, some other needs (municipal and industrial), increase continuously, competing with the water demand required to operate the locks.

The present hydraulic project has two main purposes:

- Design an efficient hydraulic system for filling and emptying operations, and for limited hawser forces
- Propose water saving systems (in addition to new resources)

The present project on the Pacific side consists in the stepping of the head at one single place, by means of a triple lift lock system, equipped with 3 water saving basins for each lock chamber, to the West of the present alignment. These new locks need also a new channel. (See annexes 1.1 and 1.2 of the previous report on the 3 lift locks system R4-C-402)

3 Terms of reference

3.1 LEVELS

Note: PLD (Precise Level Datum) is the reference system for the Panama Canal. All levels in this report refer to that reference

3.1.1 GATUN LAKE

Maximum level: +27.13 m PLD (89 ‘)
Minimum level: +24.99 m PLD (82 ‘)

3.1.2 PACIFIC OCEAN

Ranging from – 3.44 m to +3.60 m PLD

It has been decided to design the bottom levels of the chambers (sills) with the Mean Low Water Spring (MLWS) level, i.e. a tidal range from –2.32 m to +2.40 m PLD

3.2 SIZES - DIMENSIONS

- Useful length of the locks : 426.72 m (1 400 ‘)
- Useful width of the locks : 55.00 m (180 ‘)
- Water depth (**minimum** water over the sills) : 16.76 m (55 ‘)
- Freeboard : 2.13 m (to be verified)

3.3 WATER SAVING RATE

The three-step lock with 3 water saving basins per lock chamber shall save 60 % per lock chamber and 87 % * of the total water required to lock a ship.

** see footnote in section C/0-1*

3.4 OPERATING TIME

It is desired to keep the filling or emptying time in an 8-10 min lap time without using the water saving basins for a single lift of the triple lift lock system. This time is given rather as a guideline than as a TOR, as the TOR are set up for locks operating with water saving basins.

The time needed for a lockage using the water saving basins is not specified, nevertheless it must not increase too much the filling /emptying times without using water saving basins. The guidelines of the times are given in Chapter 5.1.

3.5 NUMBER OF SOLUTIONS TO BE STUDIED

Only one solution for the filling and emptying system has to be studied in this actualization study. It is the system with side wall culverts and ports.

3.6 COST AND MAINTENANCE OF THE SYSTEM

Special attention will be paid to these points:

- A compromise has to be reached between the level of efficiency of the system and the corresponding costs.

- The redundancy of the system is very important to obtain a high level of reliability, minimizing traffic interruptions.

4 Design criteria and assumptions

4.1 DESIGN CRITERIA

Reference is made to the reports:

- R2 – A : Part A General Design Criteria
- R2 – B : Part B Specific Design Criteria
- R4 – C : Filling and emptying system

4.2 ASSUMPTIONS

- Saving 87 % of the lockage water implies the use of 3 water saving basins per step or 9 for the global triple lift system (see 3.3); no additional recycling system has been retained by ACP
- The water saving basins will be built only on one side of the locks
- Only side-by-side water saving basins will be studied
- Considering the operating times, and to be in accordance with the results of the first study of the triple lift configuration, the target time for filling and emptying of the chamber using the water saving basins is approximately 51 minutes. This will lead to a reduction of the dimensions of the culverts and valves of the F/E system.
- The surface of the lock that has been taken into consideration for the filling / emptying simulations is 27 500 m². It includes the surface between the adjacent gates, the surface of the gate recesses and part of the gate surface (95 %) as shown on the sketch below:

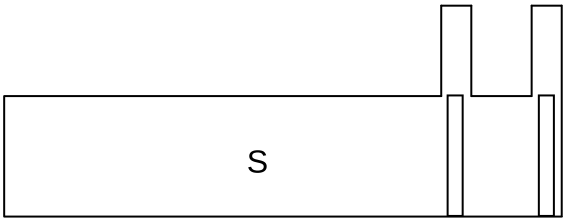

Figure 4.2-a

- The valves will be of the vertical plane valve type, rectangular, with rollers.
- Each valve will be surrounded by slots in order to insert stoplogs for maintenance or repair works. According to ACP's request, these slots will have the same size as the main valve slots so that they can be equipped with auxiliary valves if required. Access shafts for material and personnel will be provided on both sides of the main valves.
- The scheduling in semi convoy mode, which is the present way to lock ships, will be retained for the 3rd lane of locks in that configuration.
- The design of the filling system will take into consideration the possibility for smaller ships to pass through the new locks in tandem or multiple lock transit. This will affect in particular the admissible rate of turbulence in the chamber.

5 Levels of the chambers and water saving basins

All elevations are referred to precise level datum (P.L.D)

5.1 PRESENTATION OF THE METHOD AND INPUT DATA

This study consists in the calculation of the water surface elevation, both in chambers and water saving basins (WSB), anytime during a lockage and taking into accounts the tidal variation of the ocean. It allows to determine the chamber and WSB main dimensions (bottom and top elevation, gate height…).

All the calculations are performed with software developed by the Consultant as already presented in the previous studies.

All the data entered in the program are detailed hereafter:

➢ **The Pacific Ocean levels**

The tides of the Pacific Ocean have been taken into account, considering both daily and monthly variations of the tide:

- Daily variations are represented by a 12.47 hours period. This value was determined with the 1991 year data (resolution with Statgraphics software)
- Monthly variations are represented by a 14.4 days period.

As it has been specified in the TOR, two tidal ranges have been considered:

- Maximum range from -3.44 m to +3.60 m PLD
- Mean Low Water Spring range from -2.32 m to +2.40 m PLD

The resulting equations which were entered in the software are shown below:

$$Z_{ocean}(t) = a + \sin\left(\frac{2\pi t}{12.47*60}\right)*\left(b + 0.6*\sin\left(\frac{2\pi t}{14.4*24*60}\right)\right)$$

with t in minutes
a = 0.08 b = 2.92 for the maximum range
and a = 0.04 b = 1.76 for the MLWS range

The graphs resulting from this equation are given in annex 1.1.

➢ **The Gatun lake levels**

According to the TOR, the maximum and minimum values are:

Maximum level: .... +27.13 m PLD (89 ‘)
Minimum level: .... +24.99 m PLD (82 ‘)

The maximum level is resulting from another study (‘’Raising Gatun Lake”). The minimum level results from an examination of the variations of the lake levels over 18 years (period 1980 – 1997), see annex 1.2.

➢ **Freeboard and minimum water depth**

Freeboards and minimum water depths taken into account for the design of the structures are the following:

	Water depth (m)	Freeboard (m)
Chamber	18.30	1.50
Water saving basins	1.00	0.80

Table 5.1-a

The minimum water depth of 18.30m in the lock chambers is higher than specified in the terms of reference. This is due to the fact that it was shown that the corresponding UKC of 1.50m affects too much the hawser forces.

The freeboard of 1.5 m is confirmed both in the PIANC report on locks and in Dutch literature on lock design (Ontwerp van Schutsluizen – RWS 2000). In Berendrecht the maximum water level is +7.50 m above the sea level and the lock heads are at +9.00 m the above sea level.

Freeboard depends on the water oscillation amplitudes in the chamber during lockage. A scale model is required to get precise values of these oscillations; and the same remarks are to be taken into account for the water saving basins freeboard.

As far as the water saving basins are concerned, the minimum water depth of 1 meter will be confirmed in this actual study.

NB: Adopted values do not affect the results of calculation.

- **Scheduling**

The simulations are undertaken with the ‘’semi-convoy mode’’ scheduling.

- **Characteristic operating times**

Operating times in the simulations are the following:

	duration time (mn)
Gate opening or closing	5
Chamber filling or emptying time (using WSB)	5
Water saving basin filling or emptying	4
Inner cycle ship displacement	12
Mean value for entry of 1st ship and exit of last ship	20
Re-initialization of water levels at the turn around	30

Table 5.1-b

Note: the purpose of the software is to set the levels of the chambers and the water saving basins; the indicated times do not affect these levels when modified.

Nevertheless, it gives information about the mean daily water usage and the number of ship transits through the locks in both directions.

- **Generic names for locks and water saving basins**

The 3 lock chambers are identified as : upper, middle and lower

Water saving basins are identified as : top, intermediate and bottom

So, when the upper-bottom wsb is addressed, it would mean the bottom water saving basin of the upper lock chamber.

5.2 WATER LEVELS CALCULATION

A specific software has been developed to calculate the water levels in the chambers and the water saving basins during the different stages of a lockage in the case of **a triple lift lock system with three water saving basins per lock chamber**.

The software allows simulating cycles scheduled in convoy mode:

- From Gatun lake to Pacific Ocean during 12 hours
- From Pacific Ocean to Gatun lake during 12 hours

The software also gives the water saving rate and the water usage during lockage and calculates the heads of each filling or emptying operation.

The equations used in the software are based on the equalization of water levels between the chamber and the water saving basins (see the explanation below).

5.2.1 DESCRIPTION OF THE CALCULATION METHOD

➢ **Equalization of the levels between a chamber and a WSB**

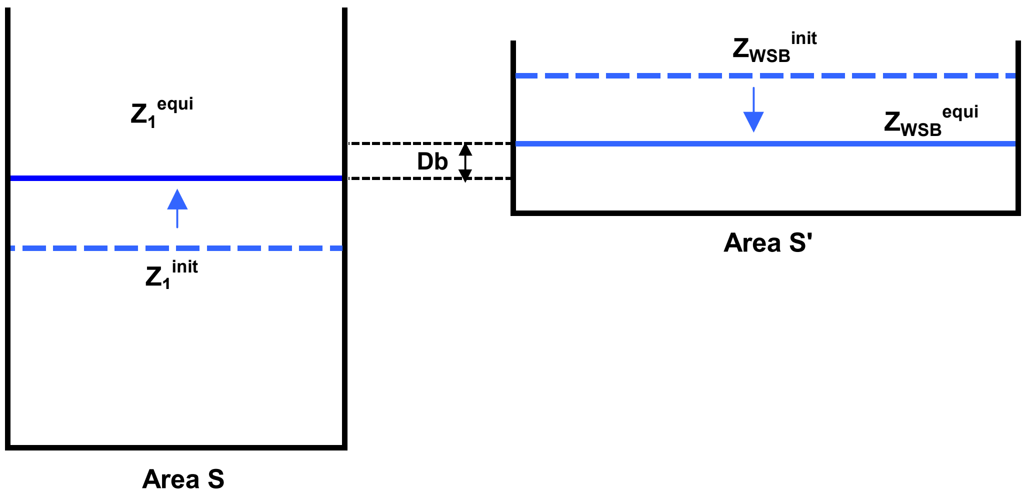

Figure 5.2.1-a

Equation system

$$\begin{cases} \left[Z_{WSB}^{init} - Z_{WSB}^{equi}\right]S' = \left[Z_1^{equi} - Z_1^{init}\right]S \\ Z_{WSB}^{equi} = Z_1^{equi} + Db \end{cases}$$

System solution

$$Z_1^{equi} = \frac{Z_1^{init} * S + Z_{WSB}^{init} * S' - Db * S'}{S + S'} = \frac{Z_1^{init} + m * \left(Z_{WSB}^{init} - Db\right)}{1 + m} \quad \text{with} \quad m = \frac{S'}{S}$$

$$Z_{WSB}^{equi} = \frac{Z_1^{init} + m * Z_{WSB}^{init} + Db}{1 + m}$$

Remark: Db (residual filling depth) is usually about 10 to 20 cm.

This residual filling depth was adopted in coordination with the electro-mechanical experts, in order to save time (the last 10 to 20 cm would need too much time to be filled or emptied). The valves are closed before equalization. In this case the water saved is not exactly 60%, as it was shown during the first presentations in 2002 (e.g. for Db = 0.1 and m = 1, water saving rate = 58.7 %). The right value of 60% may be reached by increasing the area of the wsb, which is reflected in the civil drawings. Anticipated valve closure is taken into account by Flowmaster™ software

- **Equalization of the levels between two chambers**

1- First stage, for example : filling of lower chamber from middle chamber

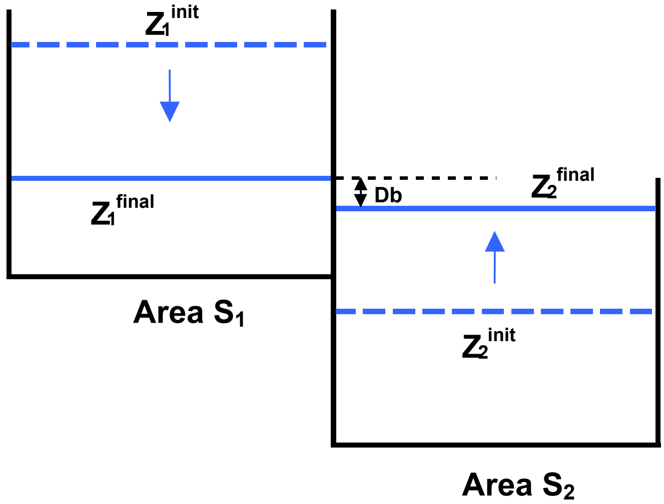

Figure 5.2.1-b

Equation system

$$\begin{cases} \left[Z_1^{init} - Z_1^{final}\right]S_1 = \left[Z_2^{final} - Z_2^{init}\right]S_2 \\ Z_1^{final} = Z_2^{final} + D \end{cases}$$

System solution

Before the opening of the gate, the levels are:

$$Z_2^{final} = \frac{Z_1^{init} * S_1 + Z_2^{init} * S_2 - D * S_1}{S_1 + S_2}$$

$$Z_1^{final} = \frac{Z_1^{init} * S_1 + Z_2^{init} * S_2 + D * S_2}{S_1 + S_2}$$

Remark: in the case of rolling gate, D is equal to zero, , i.e. .$Z_2^{final} = Z_1^{final}$.
In the PIANC report on locks, part 6 : gates and valve § 2.4 : rolling gates it is indicated that the gates are usually operated with equalization of levels but are so heavy constructed that it is possible to move them before equalization A device to detect the breaking of the gate seals at equalization will be installed, allowing to start opening of the gates.

2- Second stage: opening of the gate

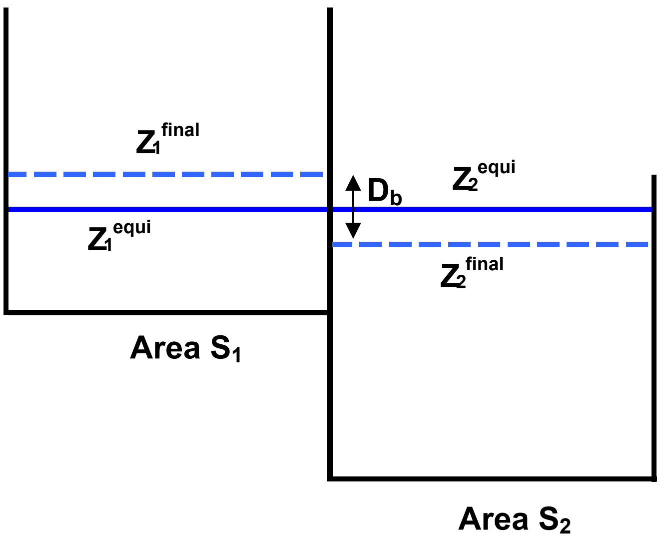

Drawing 5.2.1-c

$$Z_1^{equi} = Z_2^{equi} = \frac{Z_1^{final} * S_1 + Z_2^{final} * S_2}{S_1 + S_2}$$

5.2.2 INITIALIZATION OF WATER SURFACE ELEVATION IN THE CHAMBER AND WATER SAVING BASINS

At the beginning of a simulation, the initialization of the water surface elevation in the chambers and water saving basins depends on the head between Gatun Lake and Pacific Ocean level and on the direction of the lockage.

The figures below illustrate the way of initializing the water surface elevations (drawings made for *m* = 1)

- Lockage from Lake to Ocean

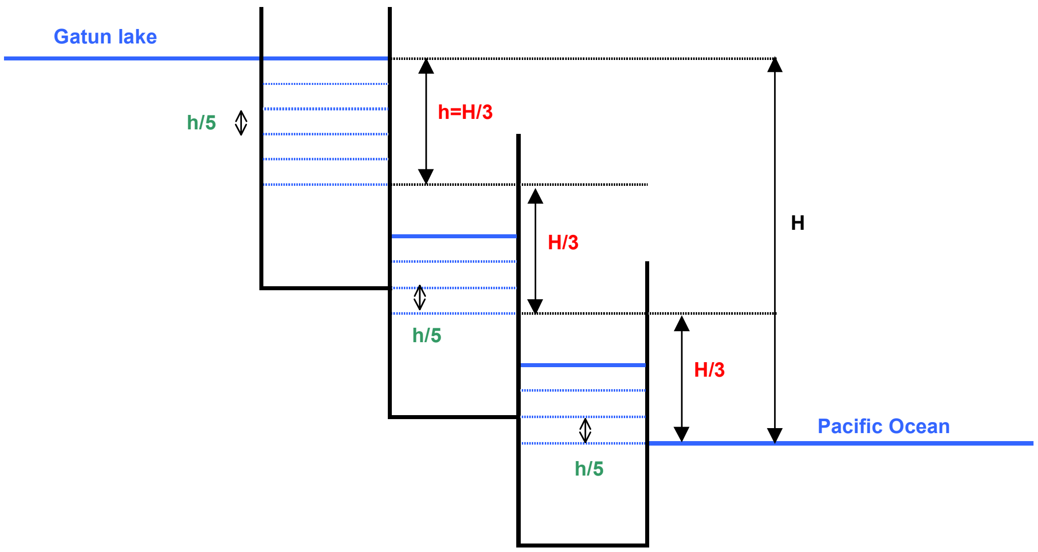

Figure 5.2.2-a

When the simulation starts, the water surface elevations are initialized as below:

- Upper chamber : .... Z_{lake}
  Upper-top WSB : .... $3h/5 + 2H/3 + Z_{mean\ ocean}$
  Upper-intermediate WSB : $2h/5 + 2H/3 + Z_{mean\ ocean}$
  Upper-bottom WSB : ... $h/5 + 2H/3 + Z_{mean\ ocean}$

- Middle chamber : .... $3h/5 + H/3 + Z_{mean\ ocean}$
  Middle-top WSB : ..... $3h/5 + H/3 + Z_{mean\ ocean}$
  Middle-intermediate WSB : $2h/5 + H/3 + Z_{mean\ ocean}$
  Middle-bottom WSB : .. $h/5 + H/3 + Z_{mean\ ocean}$

- Lower chamber :........... $3h/5 + Z_{mean\ ocean}$
  Lower-top WSB : ...... $3h/5 + Z_{mean\ ocean}$
  Lower-intermediate WSB : $2h/5 + Z_{mean\ ocean}$
  Lower-bottom WSB : ... $h/5 + Z_{mean\ ocean}$

With $Z_{mean\ ocean}$ = 0.30 m PLD

- Lockage from Ocean to Lake

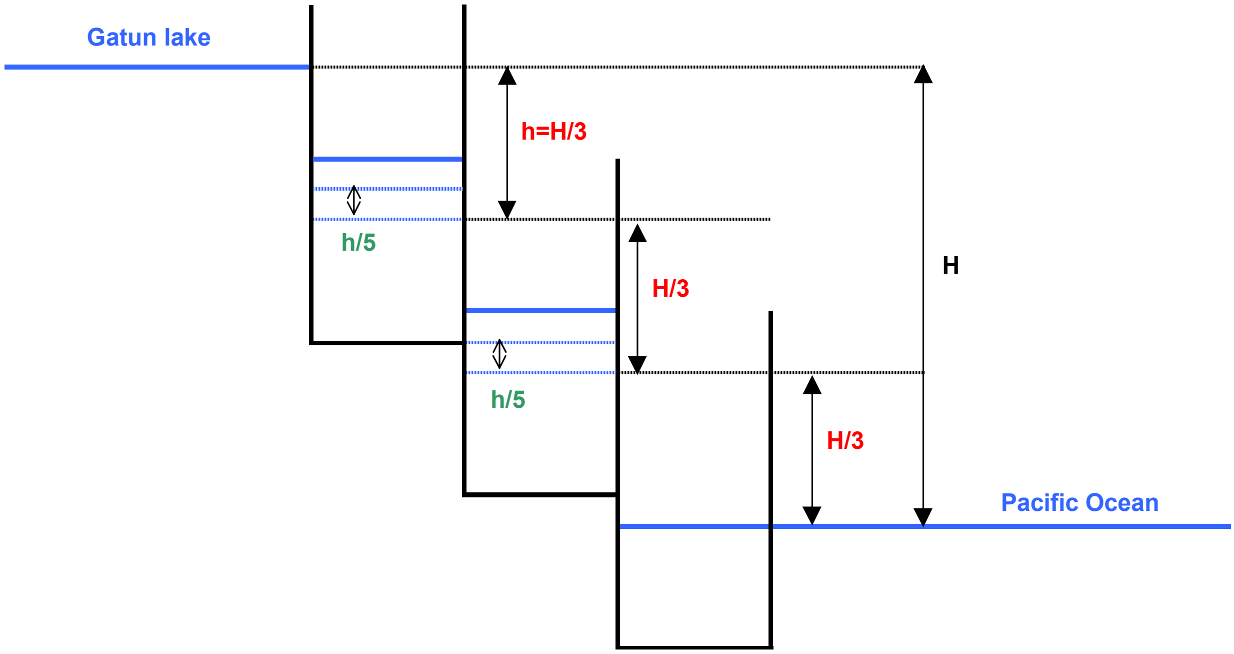

Figure 5.2.2-b

When the simulation starts, the water surface elevations are initialized as below:

- Upper chamber : .... $2h/5 + 2H/3 + Z_{mean\ ocean}$
  Upper-top WSB : .... $4h/5 + 2H/3 + Z_{mean\ ocean}$
  Upper-intermediate WSB : $3h/5 + 2H/3 + Z_{mean\ ocean}$
  Upper-bottom WSB : . $2h/5 + 2H/3 + Z_{mean\ ocean}$

- Middle chamber : .... $2h/5 + H/3 + Z_{mean\ ocean}$
  Middle-top WSB : ..... $4h/5 + H/3 + Z_{mean\ ocean}$
  Middle-intermediate WSB : $3h/5 + H/3 + Z_{mean\ ocean}$
  Middle-bottom WSB : $2h/5 + H/3 + Z_{mean\ ocean}$

- Lower chamber : .... $Z_{ocean}(t_0)$
  Lower-top WSB : ...... $4h/5 + Z_{mean\ ocean}$
  Lower-intermediate WSB : $3h/5 + Z_{mean\ ocean}$
  Lower-bottom WSB : $2h/5 + Z_{mean\ ocean}$

With $Z_{mean\ ocean}$ = 0.30 m PLD
And $Z_{ocean}(t_0)$ level Pacific Ocean at the beginning of the cycle

More details concerning levels initialization are given in annex 1.4

5.3 DEFINITION OF THE BOTTOM SETTING SCENARIOS

The levels of the chambers and the water saving basins given below have been set according to the two simulations defined hereafter:

- The levels of the bottom floor and top of the chambers have been set with the combination of the following values :

  - Gatun Lake : + 27.13 m PLD ; + 24.99 m PLD
  - Pacific Ocean : ranging from +2.40 m PLD to – 2.32 m PLD

- The levels of the bottom floors and tops of the water saving basins have been set with the combinations of the following values :

  - Gatun Lake : + 27.13 m PLD ; + 24.99 m PLD
  - Pacific Ocean : ranging from + 3.60 m PLD to – 3.44 m PLD

  Originally, all levels were set up with extreme tides. In order not to penalize too much the design (cost savings), ACP decided to calculate the lock sills with the MLWS level (Mean Low Water Spring level). Indeed, when very low tides occur (rare events), it is possible to postpone the transit of huge draft vessels and to lock other ones in priority.
  Eventually, it could be decided also to set the WSB levels with the MLWS levels. This will need to be considered during further design optimization.

- **For this actualization study**, the water saving basins and lock chamber have the same area ($m = 1$),

- **For this actualization study**, the residual filling depth was set to Db = 0.0 m

The scenarios have been tested over a 160 cycles period (1 cycle corresponds to 12 hours of down-lockage or up-lockage), i.e. the total duration time of the simulation represents nearly 80 days (see explanation below).

Several simulations have been run to assess the sensitivity of the results to the parameter “Number of 12 hours cycles”, i.e. the duration of the simulation (see annex 1.5).

The tables 5.3-a and 5.3-b below present the results for the minimum and maximum levels, in function of the duration of the simulations (see also annex 1.5):

	Minimum level in m PLD											
Simulation duration in days	Upper chamber	Top WSB	Inter. WSB	Bottom WSB	Middle chamber	Top WSB	Inter. WSB	Bottom WSB	Lower chamber	Top WSB	Inter. WSB	Bottom WSB
10	17.68	23.09	21.29	19.49	8.45	14.06	12.21	10.34	-3.44	4.60	2.35	-0.19
20	17.68	23.09	21.29	19.49	8.45	14.06	12.21	10.34	-3.44	4.50	2.30	-0.29
40	17.65	23.08	21.28	19.47	8.34	14.01	12.16	10.29	-3.44	4.45	2.24	-0.32
60	17.64	23.08	21.27	19.46	8.30	14.00	12.13	10.23	-3.44	4.36	2.19	-0.32
80	17.63	23.07	21.27	19.45	8.22	13.98	12.11	10.19	-3.44	4.29	2.03	-0.42
100	17.63	23.07	21.27	19.45	8.22	13.98	12.10	10.19	-3.44	4.27	2.03	-0.44
110	17.63	23.07	21.27	19.45	8.22	13.98	12.10	10.19	-3.44	4.27	2.03	-0.44

Table 5.3-a

	Maximum levels in m PLD											
Simulation duration in days	Upper chamber	Top WSB	Inter. WSB	Bottom WSB	Middle chamber	Top WSB	Inter. WSB	Bottom WSB	Lower chamber	Top WSB	Inter. WSB	Bottom WSB
10	26.67	24.93	23.19	21.45	17.99	16.27	14.58	12.90	9.65	8.09	6.62	5.37
20	26.67	24.93	23.19	21.45	17.99	16.27	14.58	12.90	9.65	8.09	6.62	5.37
40	26.67	24.93	23.19	21.45	17.99	16.27	14.58	12.90	9.66	8.09	6.62	5.38
60	26.67	24.93	23.19	21.45	17.99	16.27	14.58	12.90	9.66	8.09	6.62	5.38
80	26.67	24.93	23.19	21.45	17.99	16.27	14.58	12.91	9.66	8.09	6.62	5.38
100	26.67	24.93	23.19	21.45	17.99	16.27	14.58	12.91	9.66	8.09	6.62	5.38
110	26.67	24.93	23.19	21.45	17.99	16.27	14.58	12.91	9.66	8.09	6.62	5.38

Table 5.3-b

It can be seen that after 80 days of simulation, the minimum and maximum level values have been achieved.

See annex 1.5 for graphics results.

5.4 RESULTS

The results obtained according to the scenarios defined above for the levels of the upper, middle and lower chamber, as well as the levels in the water saving basins are given in the following tables:

- **Lock chambers**

Mean Low Water Spring levels are used to set up the locks sills, for cost savings

Limit conditions		Water level in m PLD			
Gatun lake level in m PLD	Ocean tide amplitude in m PLD		Upper chamber	Middle chamber	Lower chamber
27.13	[-2.32 ; +2.40]	maxi	27.13	18.23	9.55
24.99	[-2.32 ; +2.40]	mini	16.56	7.88	-2.32

Table 5.4-a

- **Water saving basins**

Limit conditions		Water level in m PLD									
Gatun lake level in m PLD	Ocean tide amplitude in m PLD		Upper-top WSB	Upper-intermediate WSB	Upper-bottom WSB	Middle-top WSB	Middle-intermediate WSB	Middle-bottom WSB	Lower-top WSB	Lower-intermediate WSB	Lower-bottom WSB
27.13	[-3.44 ; +3.60]	maxi	25.36	23.59	21.82	16.55	14.82	13.12	8.21	6.71	5.43
24.99	[-3.44 ; +3.60]	mini	21.61	19.92	18.22	13.08	11.32	9.52	3.96	1.81	-0.53

Table 5.4-b

6 Water saving rate

The triple lift lock system equipped with 9 water saving basins allows a very good water saving rate (real value of 85.75 % instead of theoretical one of 86.67 %). This difference is due to the reset of the levels at noon when changing the sailing direction for the ships (semi convoy mode).

6.1 CALCULATION BY THE SOFTWARE

The total head between the Gatun Lake and the Pacific Ocean varies in relation to the Pacific Ocean tides and Gatun Lake level. Specific calculations are made with the software to assess the water consumption (volume of water taken from the Gatun Lake) and the water saving rate for each lockage.

- Water usage

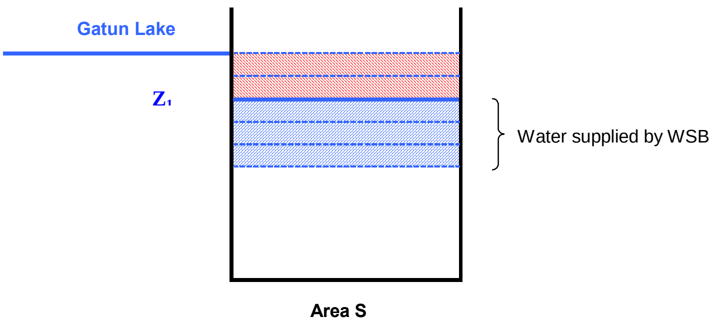

Figure 6.1-a

Let Z_1 be the water level in the upper lock at the end of the WSB-to-lock chamber operations. The software calculates the volume taken from the lake by:

$$V_{lake} = (Z_{lake} - Z_1) * S$$

This volume is calculated for each filling operation of the lock.

- Water saving rate

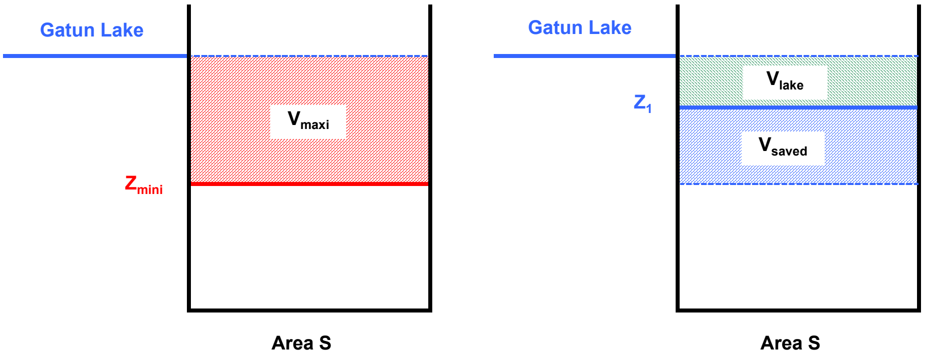

Figure 6.1-b

Let Z_{mini} be the water level in the upper lock at the beginning of the filling operation. Without any water saving basin, the volume of water required to fill the lock chamber would be equal to:

$$V_{\max i} = \left(Z_{lake} - Z_{\min i}\right) * S$$

The water saving basins allow saving a volume equal to:

$$V_{saved} = \left(Z_1 - Z_{\min i}\right) * S$$

The water saving rate is then calculated for each cycle by the relation:

$$e = \frac{V_{saved}}{V_{\max i}}$$

The water saving rate is calculated for every filling operation of the lock and at the end of the simulation. The final water saving rate is calculated by:

$$E = \frac{\sum V_{saved}}{\sum V_{\max i}}$$

The results achieved with the software are coherent with the theoretical ones.

6.2 RECOMMENDATIONS

The initial chamber and water saving basins floors and wall elevations, the number of possible transits, and the water usage calculations are established with the present hypothesis and data introduced in the software developed by the Consortium CPP.
These results are still applicable and are not affected by the final filling and emptying times resulting from the Flowmaster™ hydraulic analysis and the final design operating times.

7 Filling and emptying systems

General criteria

Based on the results of the former studies concerning the triple lift lock, the single lift lock and the double lift lock, the terms of reference for the three step-lock study assumed that the best solution to study is the following:

- A filling / emptying system with lateral culverts and ports. The side wall culverts extend over the whole length of the lock.
- A system of 3 side-by-side water saving basins per lock chamber, connected to the lateral culverts by means of conduits.

This system has been retained for the present actualization study.

8 Hydraulic design of the filling / emptying system

In accordance with the previous chapter, the system to be studied includes a lateral alimentation with culverts and ports incorporated in the lock walls.

The modifications of the F/E system proposed hereafter take into account the initial design of the triple lift lock system and the optimizations proposed through the studies of the single and double lift lock systems.

8.1 SOFTWARE AND METHODS USED IN THE STUDY

The emptying/filling system has been studied with the software FLOWMASTER 2. Software Flowmaster 2 is a Community Trade Mark of Flowmaster Holding BV. A description of this tool has been given in the report of the first configuration.

8.2 CALIBRATION OF THE SOFTWARE

The calibration of the software was based on the physical model study of the Panama Canal locks performed in 1942. (see annex 3.4 of the first configuration report).

The Flowmaster model gave acceptable results, since the flow rate difference was found to be less than 10 %. All documents concerning this test and two other ones are given in annex 3.4 of the first configuration report.

8.3 HYDRAULIC DESIGN

The filling/emptying system presented hereafter consists of lateral culverts and ports. The longitudinal culverts are used for the filling and emptying of the lock. It has been demonstrated for the first configuration that this system was to be preferred because:

- Of its ability to provide a good distribution of the flow;
- Of its reliability (redundancy in case of a valve default);
- Construction of an expensive concrete bottom floor can be avoided.

8.3.1 DESCRIPTION

The hydraulic system is based on two lateral culverts (one in each side of the lock walls) each one connected to the lock chamber by means of ports. The connection with the water saving basins is made by 4 conduits per basin.

The figure hereafter gives an overview of the modeled system:

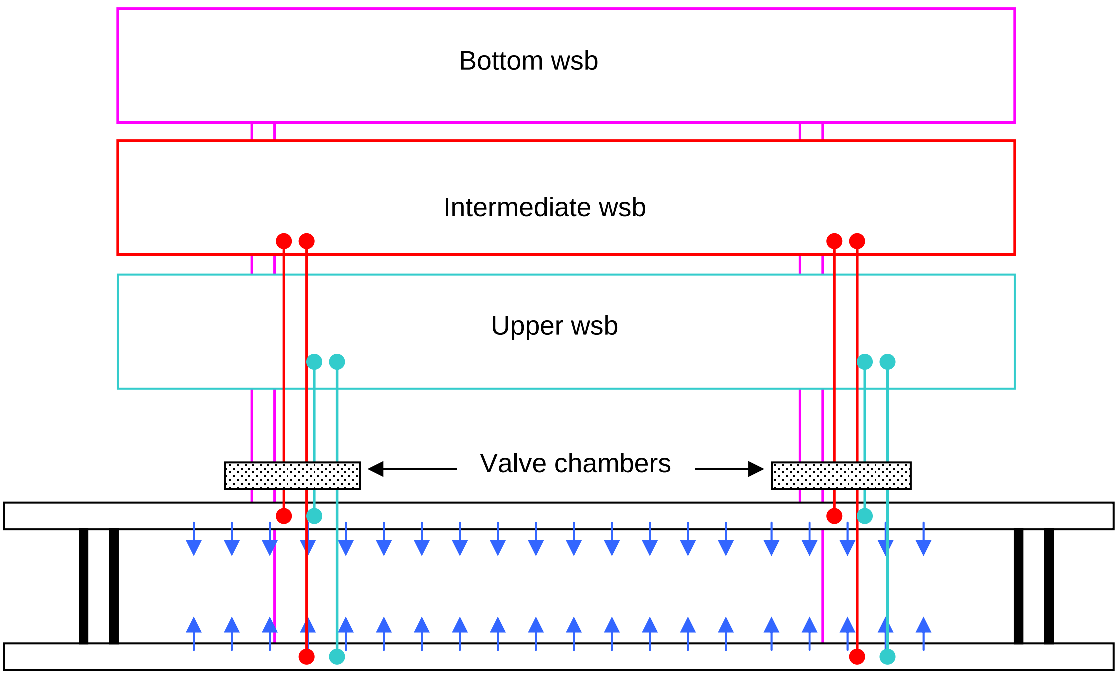

Figure 8.3.1-a : filling & emptying system – plan view

A homogeneous filling of the chamber is obtained by spreading the discharge over a sufficiently long distance through a sufficient number of ports. In the present case, there are 20 ports on both sides of the lock chamber, equally divided over part of the lock chamber length. The ports are uniformly spaced c/c 15 m. Consequently, the ports are distributed over half of the total length, which complies with the general recommendations of this type of F/E system.

Due to head losses, the head decreases along the culvert, leading to higher discharges in the upstream ports and less discharges in the downstream ports, thus resulting in a non - uniform distribution. To anticipate, the culvert size must be large enough in order to reduce head losses and obtain a head which is more or less constant over the culvert ports.

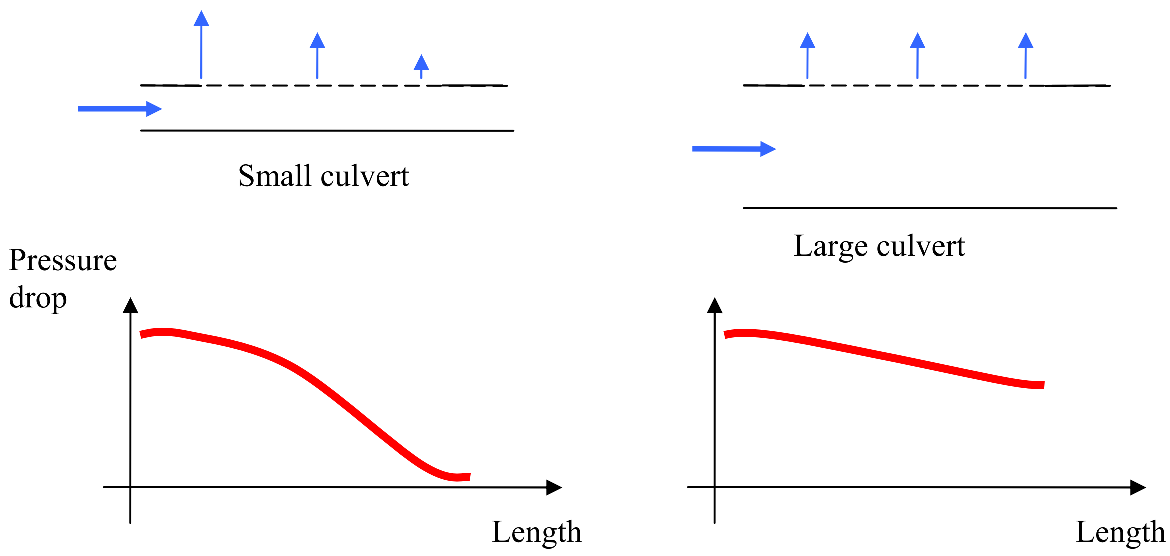

Figures and graphs 8.3.1-b

NB: the water can partially flow backward through the filling/emptying system when a ship enters the chamber. Consequently, the piston effect resulting from the ship entrance in the lock chamber can be reduced.

Connection water saving basins – lock chamber

The same ports of the emptying / filling system are used. Each basin is connected to both lateral culverts in two points (see on sketch above). Consequently, using the water saving basins leads to upstream-downstream symmetry and quite an acceptable left-right side symmetry (slightly different head losses).

There is a total of 12 conduits connecting the water saving basins to the chamber (4 conduits per water saving basin).

8.3.2 SIZE OF CULVERTS, CONDUITS AND PORTS

The most important difference with the former studies concerns the reduction of the lock width, from 61.00 m to 55.00 m. The volume being consequently reduced, while keeping almost the same filling and emptying times, it was possible to reduce the culverts and valves dimensions.

The hydraulic design leads to the following sizes:

	Shape	Size (WxH)	Section (m²)	Quantity	Total section (m²)
Side-wall culverts	rectangular	9 m x 6 m	54	2	108
Valves	rectangular	4.5 m x 6 m	27		27
WSB-to-lock conduit	rectangular	4.5 m x 6.0 m	27	4 per basin	108
Ports	rectangular	2 m x 2 m	4	40, 20 per lock side	160

Table 8.3.2-a

As far as the water saving basins are concerned, the number of conduits, the section and the total section of the conduits and ports is to be considered for each of the three saving basins.

Compared to the first solution, the size of the culverts has been reduced by 20%.

8.3.3 FLOWMASTER MODEL PARAMETERS

The same model parameters as in the first solution have been retained. The main characteristics of the most important components are as following:

- **Culvert**: the culvert size is given above; the absolute roughness of the inner surface is 0.025 mm, which corresponds to the absolute roughness of a smooth concrete pipe (cf. Internal Flow System from D.S. Miller).

- **Valve**: the valves used in the model are valve gates with a section equal to the pipe section.

- **Discrete loss**: in order to take into account the kinetic energy dissipation in every chamber (or component assimilated to a chamber), discrete losses have been introduced downstream the ports with a loss coefficient of 1. The reverse flow coefficient is taken equal to 0.5.

- **T-junctions**: T-junctions are used to model the ports. Loss coefficients in T-junctions are automatically set depending on the two branch flow and area ratios. The calibration of those components demonstrated that they are suitable to model the ports.

8.4 FILLING AND EMPTYING TIMES

8.4.1 ELEMENTARY OPERATIONS

About 70 simulations have been run with Flowmaster in order to estimate the filling and emptying times, the flow rate, and the maximum velocities reached in the culverts. The simulations take into account the variations of Gatun Lake and Pacific Ocean levels.

According to the terms of reference, the simulations have been performed for lockages using water saving basins.

The table below gives an overview of the filling and emptying times for a lockage with water saving basins. This table takes into account the levels calculated with CPP's software: minimum and maximum heads that can be reached between the Lake or Ocean and the lock chambers or between a water saving basin and a lock chamber either during filling or emptying phases.

The filling and emptying times have been determined for a minimum valve opening time of 2 min (either for Lake or Ocean-to-lock chamber or water saving basins-to-lock chamber operations), This time was raised from 1 min in the first study to 2 min in this actualization study, considering more precise characteristics of the valves lifting systems, in coordination with the electro-mechanical design team

The maximum global time has to be calculated by considering the worst case: highest head between the downstream lock and the Ocean. The heads between the water saving basins and the locks are then given by CPP's software.

Operation	Head in m	Opening time of the valves (sec)	F/E time (sec)	Highest average velocity (m/s)	
				Culvert	Ports
Upper lock filling	3.70 max head	120 (2 mn)	280 (4 mn 40 s)	4.8	4.8
	3.30 min head	120 (2 mn)	270 (4 mn 30 s)	4.5	4.5
Lock-to-lock equalization	8.10 max head	120 (2 mn)	270 (4 mn 30 s)	5.5	6.6
	5.70 min head	120 (2 mn)	230 (3 mn 50 s)	4.4	5.3
Emptying lower lock	8.30 max head	420 (7 mn)	530 (8 mn 50 s)	5.8	6.9
	0.00 min head	/	/	/	/
Filling the lower lock's WSB	5.00 max head	120 (2 mn)	185 (3 mn 5 s)	5.0	3.6
	0.00 min head	/	/	/	/

Operation	Head in m	Opening time of the valves (sec)	F/E time (sec)	Highest average velocity (m/s)	
				Culvert	Ports
Emptying the lower lock's WSB	8.40 max head	120 (2 mn)	245 (4 mn 5 s)	6.5	4.9
	0.00 min head	/	/	/	/

Table 8.4.1-a

For all those simulations, the velocities in culverts and ports do not exceed 7 m/s; there is consequently no risk of an accelerated erosion of the culverts and ports. As Flowmaster only gives average velocities in any section, it will be necessary to verify on the scale model that this velocity is not exceeded too much in some critical flowing sections.

To reach that criterion in the particular case of emptying the lower lock chamber into the Ocean while having the maximum head of 8.30 m, the valve opening diagram was modified: the opening time of 7 minutes gives a filling time of 8’50”.

8.4.2 CONSIDERATION OF FREQUENCIES OF THE HEADS

Considering this unitary operation, the guideline of 5’ is exceeded. However, by analyzing the classified levels curve hereafter (lake Gatun at maximum 27.13 m PLD, and Ocean level at -3.32 m PLD), we can consider that the frequency of that maximum head is very low: the head between the lower lock chamber and the Ocean is 95% of the time inferior to 6.30 m; in that case, the corresponding filling time decreases from 8’50” to 6’35” with a valve opening time of 4’ instead of 7’ (max velocity in the culvert of 7.0 m/s).

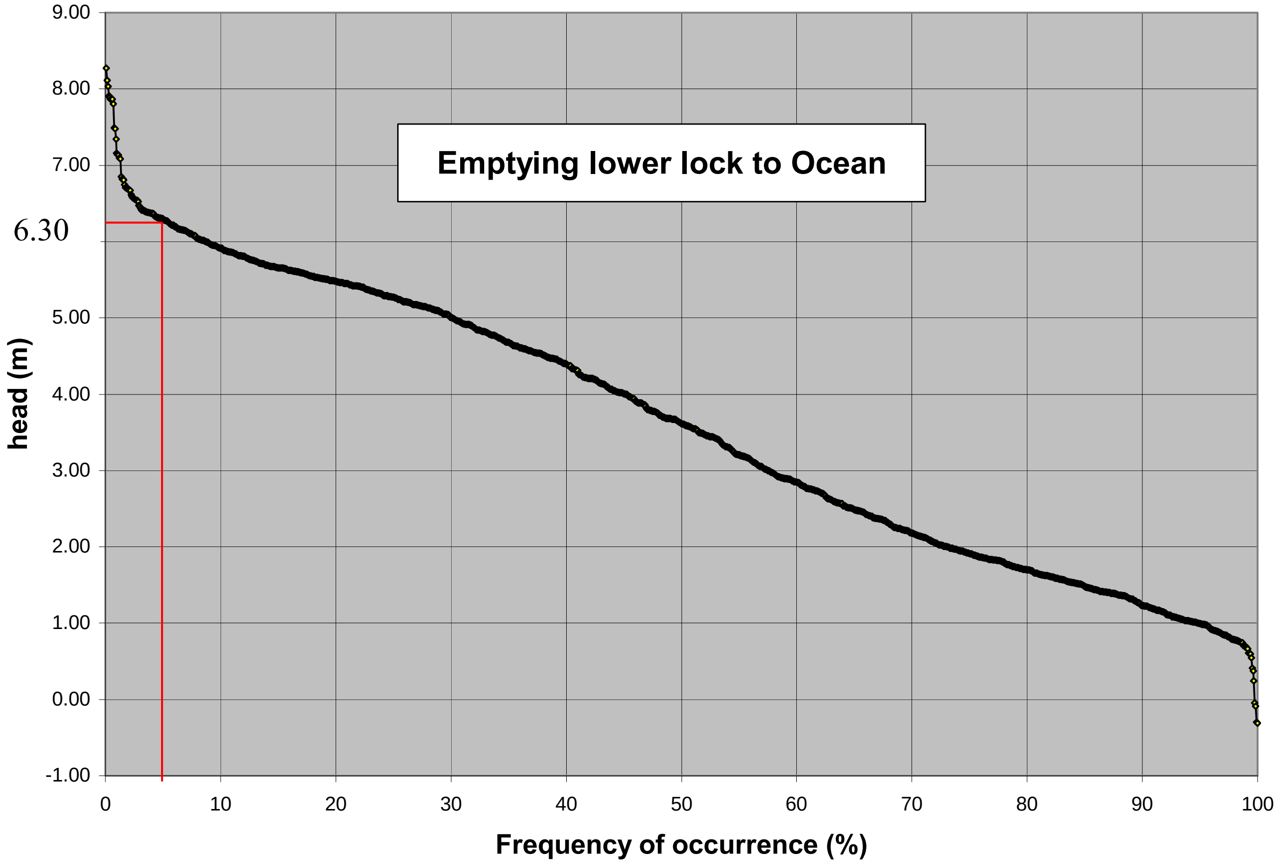

Graph 8.4.2-a

Considering the series of operations for the lower lock in the particular case of the highest head, the total time requested is about 16'35" (8'50" + 3 x 2'35'', see table 8.4.2-b hereafter), which remains inferior to the guideline of 17' (3 x 4' + 1 x 5').

	Lock				WSB			
Step	Initial level	Final level	Head	Filling time	Initial level	Final level	Head	Filling time
Filling lower top WSB	9.17	7.83			6.49	7.83	**1.34**	**2'35**
Filling lower intermediate WSB	7.83	6.42			5.01	6.42	**1.41**	**2'35**
Filling lower bottom WSB	6.42	4.95			3.49	4.95	**1.47**	**2'35**
Emptying lower lock to the Ocean	4.95	- 3.32	**8.30**	8'50				

Table 8.4.2-b

8.4.3 ANTICIPATED VALVE CLOSURE

In the particular case of dealing with heads in each water saving basin being about 1.40 m, which is a low value and corresponds to the maximum emptying head of the table 8.4.2-b, the valve needs to be partly opened during 2’45” approximately. The valve closure is anticipated in order not to get an over-filling of the WSB.

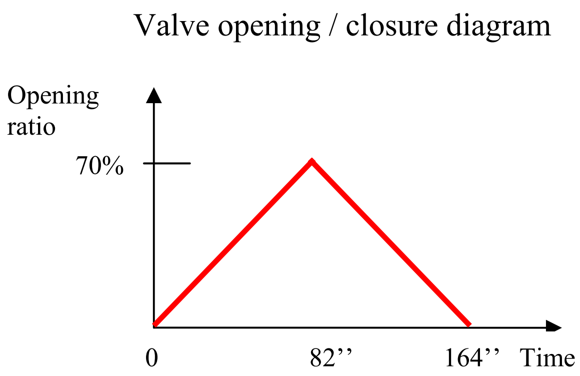

Figure 8.4.3-a

Considering that the closure time of the valve is anticipated, an additional time has to be considered to reach the equalization of the levels in the worst configuration (emptying the lower lock into the Ocean). For the majority of the elementary operations, the global additional time is about 10”.

As a result, the global operating time for the **worst configuration** (lower lock, highest head) remains close to the target time of the guidelines (16’35” + 3x 10” = 17’05” instead of 17’).

Consequently, most of the time, the operating times will be inferior to the target time.

8.4.4 GLOBAL HYDRAULIC TIME OF A WHOLE LOCKAGE OPERATION BETWEEN THE GATUN LAKE AND THE PACIFIC OCEAN

In order to test the global performance of the system, the total hydraulic time has been calculated for the set of operations corresponding to the lockage of a ship between Gatun Lake and the Pacific.

The operations pointed out in the following table correspond to the **longest** elementary operations that occur simultaneously to the **regular** elementary operations that logically follow each other. For instance, the operation “Middle bottom WSB to Middle Lock” is longer than “Upper lock to Upper top WSB” which is the first operation once the ship has entered the upper lock. The hydraulic time of that operation is consequently retained for the calculation.

When requested to comply with the velocity criteria, the valve opening time has been increased.

The case below refers to the maximum head lower lock / Pacific Ocean

From	To	Head	Time (s)	Opening valve	Anticipate closure	Ports
Bottom WSB	Middle lock	3.68	1’48		+10”	+5”
Upper lock	Inter WSB	3.61	2’10		+10”	+5”
Upper lock	Bottom WSB	3.61	2’10		+10”	+5”
Lower lock	**Ocean**	**8.28**	8’50	+2’	+10”	+5”
Bottom WSB	Lower lock	8.38	4’05		+10”	+5”
Inter WSB	Lower lock	5.66	2’40		+10”	+5”
Top WSB	Lower lock	4.24	2’00		+10”	+5”
Middle lock	Lower lock	7.08	3’55	+2’	+10”	+5”
Upper lock	Top	3.6	2’10		+10”	+5”
Lower lock	Inter WSB	3.89	2’20		+10”	+5”
Lower lock	Bottom WSB	4.77	2’50		+10”	+5”
Lower lock	Ocean	6.31	6’42	+1’	+10”	+5”

Table 8.4.4-a

The total hydraulic duration is then 41’40”, which is considerably lower than the guideline of 3 x 17’ = 51’. This will be beneficial to reduce the strengths on the hawsers (see chapter 10).

Considering the additional time due to anticipated valve closure, the global time is 49’40”.

The annexes 1.6 and 1.7 show in more detail the sequence of operations. It can be seen that when several operations appear simultaneously, the maximum head, i.e. time, is retained, which confirms the performance of the system.

This is an example retained for the worst case. In the next phase of studies, all durations of cycles will have to be calculated.

8.4.5 DETAILED RESULTS

Note : port n°1 is the most upstream one; port n° 20 is the most downstream one

The graphs representing the flow rate and the water surface elevation in the lock chamber are given in annexes 2 to 6. The graphs are mainly of 3 types:

Type 1 (see graph 8.4.5-a below): the graph shows the discharge in the ports when filling or emptying the WSB, in function of time. Each graph has been given a different color corresponding with the specific port. The graphs show a good distribution over the ports, due to the symmetric connections of the conduits linking the WSB to the main longitudinal culverts. The dispersion is due to the ratio of the total ports area to the culvert area (see chapter 10).

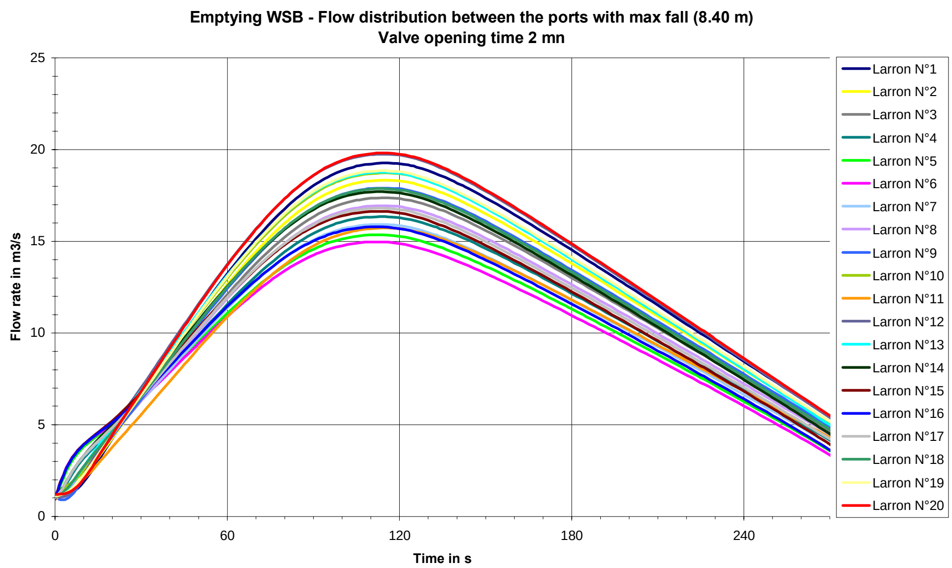

Graph 8.4.5-a

Type 2 (graph 8.4.5-b below): discharge in the ports when emptying a lock (lock to lock equalization). The graphs show an unbalanced distribution in the ports, due to the fact that the flow starts at the downstream extremity of the longitudinal culvert. Two stages appear on the graph:

- First stage: discharge through the ports starts earlier downstream than upstream.
- Second stage: once the flow has started through every port, some differences in the flow rate remain. The flow rate through the downstream ports is higher.

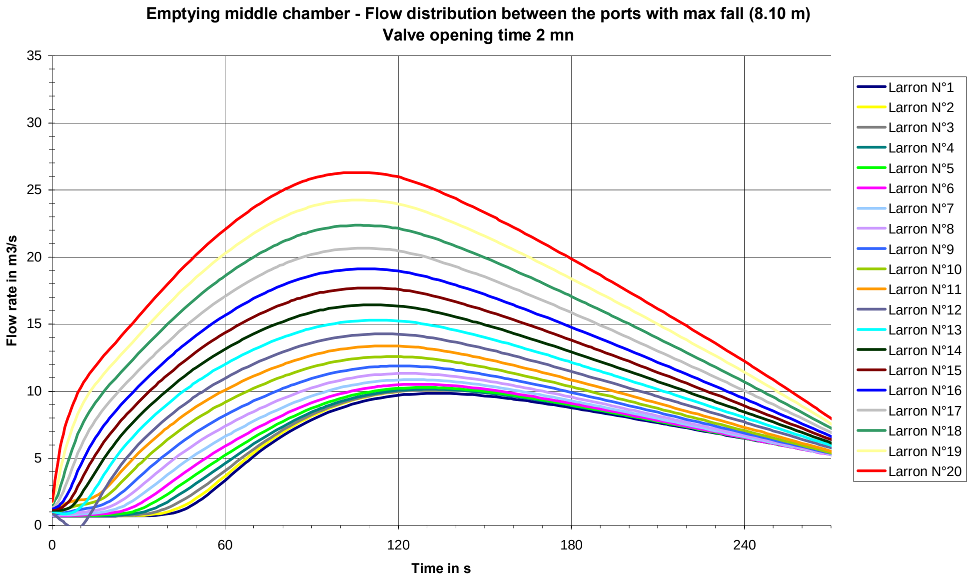

Graph 8.4.5-b

Type 3 (graph 8.4.5-c below): discharge in the ports when filling a lock (lock to lock equalization). The graphs show an unbalanced distribution in the ports, due to the fact that the flow starts at the upstream extremity of the longitudinal culvert. Two stages appear on the graph:

- First stage: discharge through the ports starts earlier upstream than downstream
- Second stage: once every port has started to discharge, some differences in the flow rate remain. The downstream ports still show a higher flow rate.

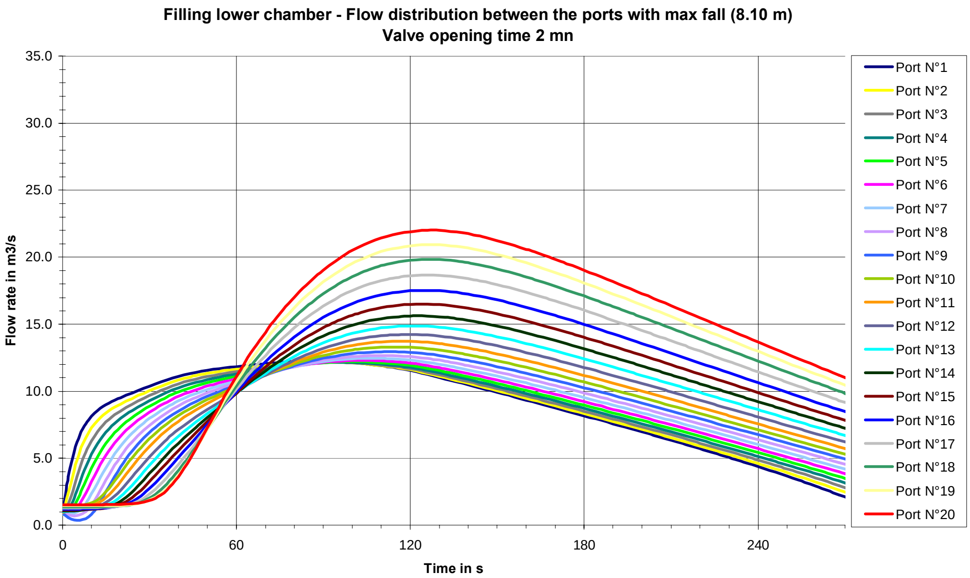

Graph 8.4.5-c

9 Cavitation and air demand

9.1 General principle

The figure below shows a schematic connection between two chambers (or water saving basin)

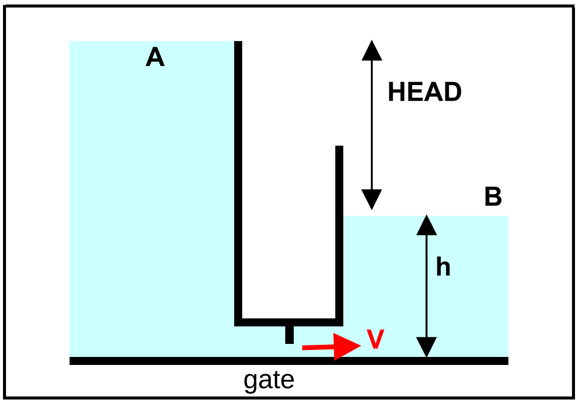

Figure 9.1-a

At the downstream side of the valve, the high velocity jet has a capacity of carrying away the water located just above it. The pressure of the water decreases according to the kinetic energy $V^2/2g$ of the jet. So the static pressure 'h' downstream the valve can be reduced accordingly.

If the pressure becomes lower than the water vapor pressure, h_v, water begins to boil at room temperature and cavitation appears with production of vapor bubbles. Cavitation produces noise and vibration, and implosion of bubbles can damage the structures and especially the valves.

The following non-dimensional number gives the condition of cavitation:

$$\sigma = \frac{P - P_v}{1/2\rho V^2} = \frac{h - h_v}{V^2/2g}$$

Pv = 0.02 bar hv = 20 cm vapor pressure (at 20 °C)
Cavitation can appear if $\sigma < \sigma_v$; σ_v given by the literature ($\sigma_v \approx 1$)

Remarks

According to the Bernoulli equation and neglecting head losses, the kinetic energy $V^2/2g$ of the jet is equal to the head between the chambers giving:

$$\sigma = \frac{h-0.2}{head} \approx \frac{h}{head}$$

So, if the head is less than the water height above the jet, cavitation can not appear.

<u>Head < h $\Leftrightarrow$ no cavitation</u>

In case of a head greater than h, more precise calculations of head losses must be done. Flowmaster is able to run simulations making allowance for the cavitation phenomenon.

A solution to avoid cavitation on the valves is to lower their sills (adopted in the Niffer lock case in France). Yet cavitation depends a lot on the valve cutting edge shape

9.2 APPLICATION TO THE TRIPLE LIFT LOCK

Cavitation spreading is examined in the regular operating mode (i.e. with the water saving basins), according to the TOR.

- *Lock to lock*

As the head between two chambers or between the Gatun Lake and the first lock is always smaller than 8.10 m and the minimum water height in the chamber is 18.3 m (Head < h), cavitation cannot appear.

The annex 7 shows the evolution of the valve pressure during the emptying of the middle chamber. Due to the large water depth of the valves relatively to the water levels in the pools, the pressure on the valve remains much higher than the vapor pressure, which guaranties that cavitation cannot appear, except maybe in the very first seconds (the Flowmaster calculation isn't sufficiently accurate to confirm the total absence of cavitation in such a short time span).

The physical scale model, by giving the pressures downstream the valve at a great sampling frequency, will give access to the pressure values right at the valve opening

- *Water saving basins to lock*

As the head between the water saving basins and the chamber is always smaller than 8.40 m and the minimum water height in the chamber is 18.3 m (Head < h), cavitation cannot appear.

- *Ocean to lock*

As the head between the lower lock chamber and the Ocean is always smaller than 8.30 m and the minimum water height in the chamber is 18.3 m (Head < h), cavitation cannot appear.

10 Hawser forces analysis

10.1 THEORETICAL ASPECTS

The examination of the origin of the hawser forces has been done in the first report of the triple lift lock system. A similar methodology will be applied to determine the hawser forces in the worst situation of the actualization.

In general terms, one can say that hawser forces arise in the lines of a vessel-positioning system (e.g. mooring lines) as a response to the motion of a ship, which in turn is a response to the forces exerted by the water flow in the lock chamber onto the ship.

The forces on the ship's hull can be of various natures (hydrostatic forces due to translatory waves, skin friction, form drag, effect of concentrated water jets, effect of water density gradients). In the conceptual design phase, it is common to take only the main force component into consideration, i.e. hydrostatic forces. The effect of the other forces is to be accounted for in the design phase, based upon empirical formulae, physical scale modeling and advanced numerical modeling.

During emptying and filling operations, oscillating waves and mass movements of water occur in the chamber. These unsteady phenomena are the result of valve operations in the system, which create surges (translatory waves) propagating in the chamber and reflecting against the walls, the gates and the ship.

The celerity C of the wave is $\sqrt{gh}$, so the period of oscillation T = 2L/C (L = chamber length) is decreasing during the filling. (Remark: These formulae are valid for a lock chamber in which no ship is present. The presence of a ship creates also oscillations with smaller wave lengths and periods.)

As a consequence, the water surface in the chamber oscillates around an average level, generally sloping from the upstream to the downstream end of the lock.

The more the inflow injection is concentrated at one end of the lock, the steeper the average water surface slope becomes and the higher the force on the ship will be.

The main hydrostatic force component acting on the ship results from this slope and can be calculated by the expression:

$$F_x = P * S$$

Where P is the displacement weight of the vessel,
S is the average slope in the chamber (oscillating).
F_x is the longitudinal component of the hydrostatic force (i.e. along the longitudinal axis of the lock chamber).

In fact, S should represent the pitch angle of the ship. It is common, however, in the conceptual design phase to define the pitch angle by means of the instantaneous water level difference at bow and stern of the ship.

Remark: More detailed analyses in literature - which are more appropriate in the later design phase – take a dynamic equation for the pitch angle into account, including inertia effects of the ship's mass and the added mass, damping, forces in mooring lines etc. In a similar way, extra dynamic equations for other degrees of freedom of the ship (e.g. heave or surge) are sometimes taken into account as well. In Annex 17 to this report, an even more complete dynamic analysis is illustrated, accounting for all degrees of freedom of the ship.

In the remainder of this chapter, the following topics will be discussed:

- In section 10.2, the origin of the unbalanced discharges through the ports in the lock chamber walls, which are the main cause of the translatory waves (hence water surface slopes and hydrostatic forces), is clarified,
- In section 10.3, the methodology for calculating the hawser forces in the conceptual design phase is presented,
- In section 10.4, the methodology for evaluating hawser forces is sketched, i.e. hawser force criteria are specified,
- In section 10.5, calculated hawser forces in the case of the basic hydraulic design (i.e. for the culverts, ports and valve operation presented in chapter 8) are presented
- In section 10.6, it is explained how the hawser forces can still be reduced by means of some first optimizations of the hydraulic design (i.e. modifying the valve opening diagram and the ports dimensions)
- In section 10.7, the resulting hawser forces are presented for the optimized hydraulic design
- In section 10.8, conclusions are drawn with respect to the hawser force analysis in this conceptual design phase, and recommendations for further studies in the design phase are given

10.2 ORIGIN OF THE UNBALANCED FLOWS

10.2.1 GENERAL

Two different phenomena explain the unbalanced discharges observed in the former graphs (discharges in the ports against time).

The first phenomenon concerns the transitory period during which the ports start to flow out one after another. The first port is the closest to the valve. This means that considering the filling operation of a lock chamber from the lake or from another lock chamber, the first port that will flow is the upstream one.

The discharge curves have the following shape:

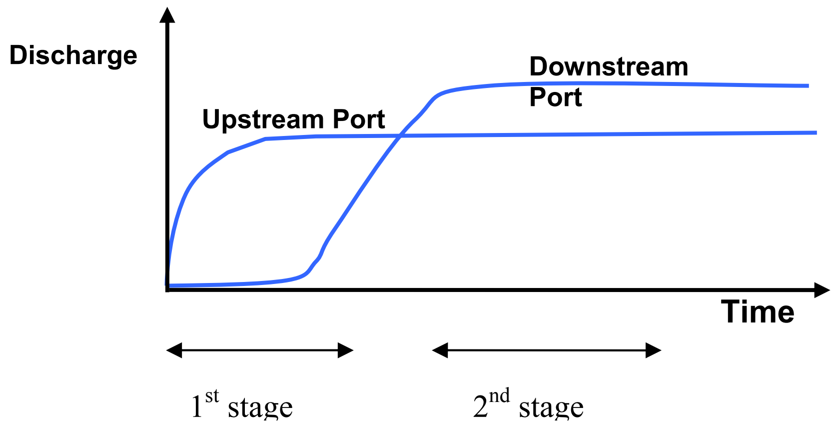

Figure 10.2.1-a

The figure above shows the time series of the discharges of the upstream port and the downstream one.

Considering the emptying of a chamber, the first port to flow will be the downstream one.
During the first stage, it was observed on real locks fed by a longitudinal system that a port starts discharging only when the upstream port has reached a high percentage of its maximum discharge; this phenomenon can be mathematically explained through the dynamic equation of the unsteady flow.

The second stage corresponds to the quasi-steady period, which is the period during which all the ports have began to discharge. The differences between the discharges come from the pressure distribution along the culvert; this distribution is a function of the area ratio between the ports and the culvert and of the elementary head losses of each port. Because of the decreasing velocity in the culvert from upstream to downstream, the efficient area of the ports as the inclination of their flows into the chamber vary, which is responsible for the head loss variation.

The different configurations of the discharge distribution, according to the area ratios, are as follows:

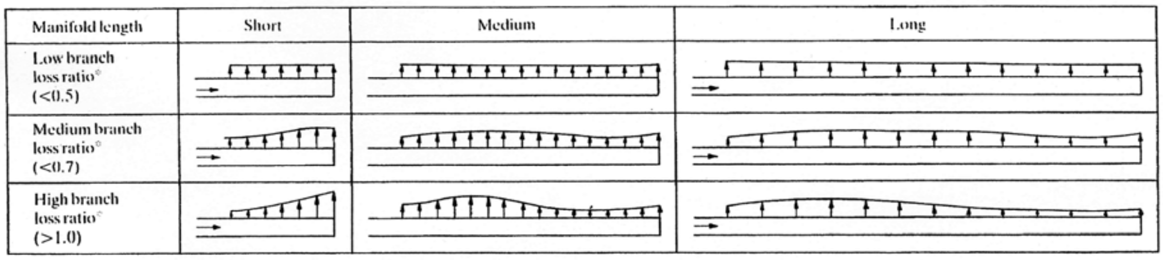

Flow distribution in the filling operation

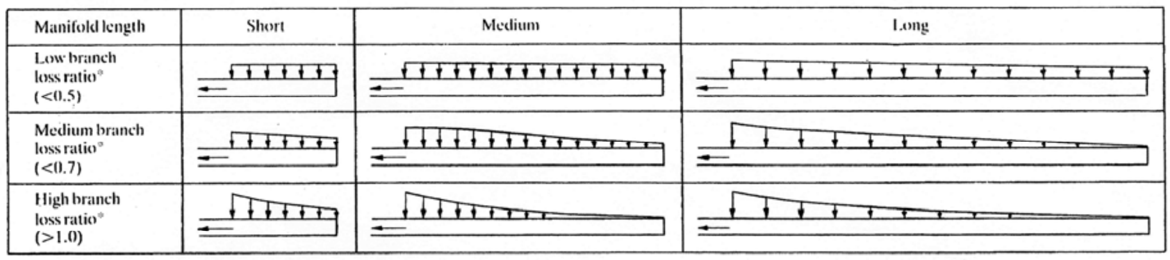

Flow distribution in the emptying operation

Loss ratio = f (total ports area / culvert area)

Figure 10.2.1-b – Source: DS Miller

10.2.2 THE TWO STAGES IN A LOCKAGE

Two stages take place during any lockage:

1. The first stage corresponds to the filling of the lock from the WSB or to the emptying of the lock chamber into the WSB.
2. The second stage corresponds to the complement to the filling of the lock from the upper lock chamber (or from the lake) or to the emptying of the lock chamber into the lower lock chamber (or into the Ocean)

10.2.2.1 1st stage

Due to the way the WSB are connected to the main culverts (see annex 17); the first stage gives a symmetrical filling or emptying of the lock chamber. Differences between the ports discharges are observed among each group of 5 ports but don't affect the general symmetry of the filling.

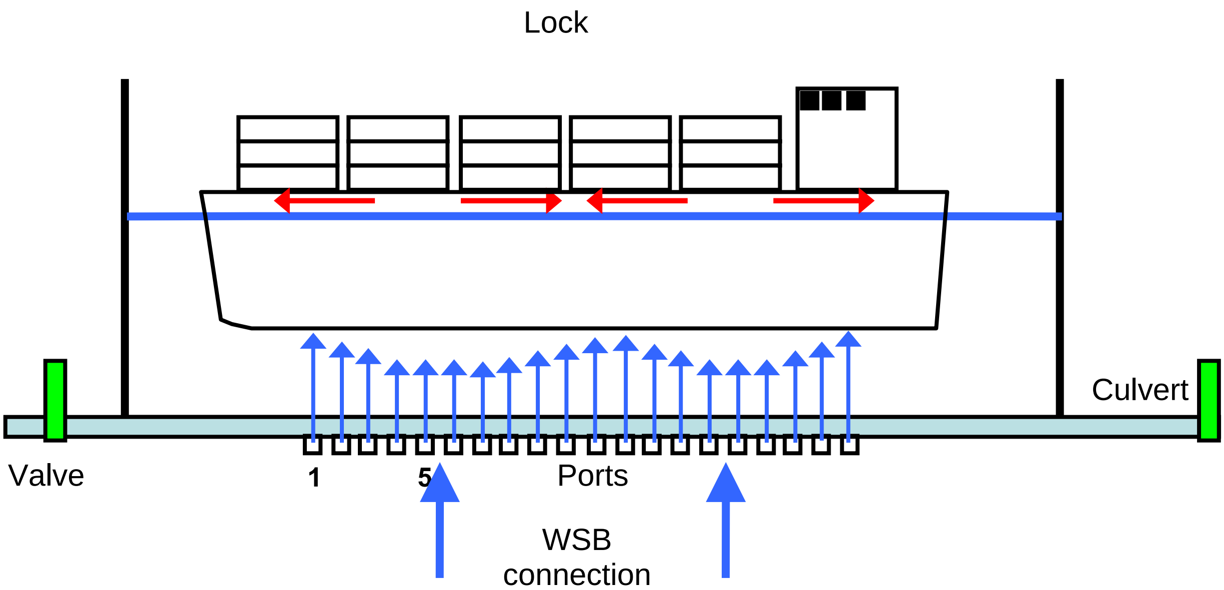

Drawing n°10.2.2-a

10.2.2.2 2nd stage

During the second stage, the filling / emptying is done by the main longitudinal culvert and thus leads to dissymmetrical discharges in time (unsteady flow) and in space (quasi-steady flow).

Filling

This stage comes after filling a great volume of the lock chamber through the WSB, which means that the dissymmetry will blur inside the volume of water, thus attenuating the forces in the hawsers.

Emptying

This stage is the last one of the lockage. The main dissymmetry appears at the beginning of the operation (transient stage), which means that the water volume surrounding the ship in the lock is still important; the efforts on the hawsers will be reduced thanks to the possibility for the water to flow in that volume. Getting closer to the equilibrium level with the downstream chamber or with the Ocean, the remaining dissymmetry will be due to the unbalanced discharges between the ports in the quasi-steady regime.

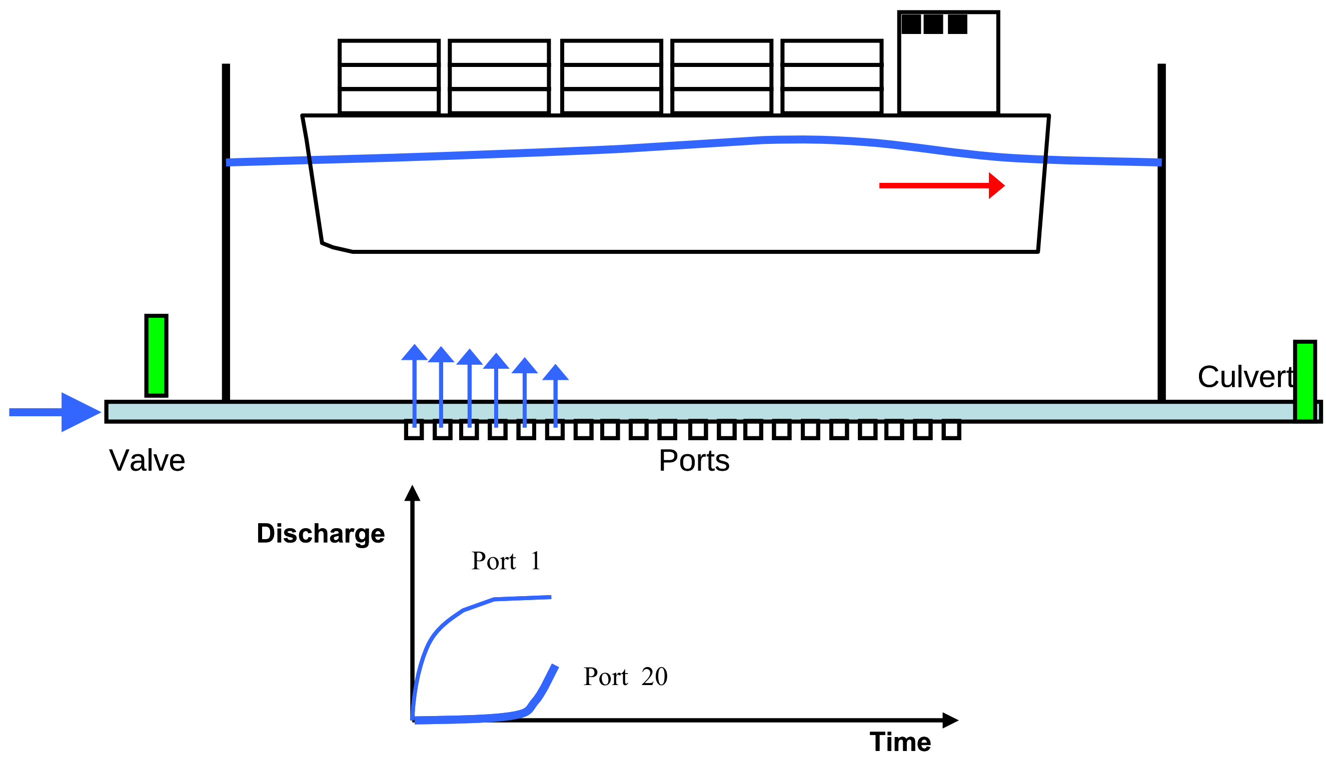

Drawing n°10.2.2-b

The drawing n°10.3.1-b represents the discharges of the ports at the beginning of the filling operation. The curves schematize the discharge of the first port and the port that is just beginning to flow.

This phenomenon is currently observed on the existing locks.

Beginning the filling or emptying operation from one side generates a longitudinal wave (drawing) that will be responsible for hawser forces. This wave is modeled in the 2D/3D Delft mathematical model and will also be modeled in the physical model on a proper scale.

The graphs in annexes 8 to 10 for the different configurations show the differences of flows between the upstream and the downstream port. This parameter gives a first evaluation of the hawser forces. The flow rate difference between extreme ports has not to be directly linked to the hawser forces because in reality any dissymmetry tends to be smoothened by the flow that it generates in the lock, around and beyond the ship.

Case 1: filling the lock chamber with the WSB. We assume that the distribution is symmetrical and does not generate hawser forces on a ship centered on the F/E system. The discharge difference between the extreme ports of a group of 5 does not exceed 2 m^3/s in the unsteady flow and 4 m^3/s in the quasi-steady flow on an average of 17 m^3/s, which is less than 25 %.

Case 2: emptying the middle chamber (max head of 8.10 m), the difference between the extreme ports (n°1 and n°20) reaches 17 m^3/s at the end of the unsteady stage, which is about 100% of the average discharge. During the second stage, the difference decreases to 16 m^3/s.

Case 3: filling the lower chamber with max fall of 8.10 m, the difference reaches 8 m^3/s in the first stage and 12 m^3/s in the second on an average value of 16 m^3/s.

Case 4: Emptying lower lock – max fall of 8.30 m. The difference reaches 17 m^3/s on an average value of 17m^3/s.

Case 5: Filling the WSB from the lock. The head being lower, and the distance between the extreme ports (in a group of 5) being far shorter, the difference between the discharges is only about 2 m^3/s.

These results show that with the valve opening time of 2’ and a uniform distribution of the ports along the main culvert, the discharges are not sufficiently balanced. Consequently, this system will need further optimization in a second phase of combined physical model testing and numerical analysis.

However, different possibilities to reduce the efforts have already been explored in the scope of this conceptual design study and are highlighted in the next chapter.

10.3 METHODOLOGY TO CALCULATE HAWSER FORCES

In the conceptual design phase, the hawser forces analysis boils down to the calculation of the longitudinal component, F_x, of the hydrostatic force on the ship’s hull. It is common to make F_x, non-dimensional by taking the ratio of the force and the displacement weight of the design ship.

As explained in section 10.1, to calculate the variation of F_x in time, one needs the variation in time of the water level difference at bow and stern of the design ship. In order to calculate the evolution in time of those water levels, a 2D numerical model for the water flow in the lock chamber has been set-up.

The model has been set-up by Flanders Hydraulics Research based upon an accepted, state-of-the-art, commercial, software package for shallow water flow (Delft3D software). The assumption of shallow water flow is acceptable because the horizontal dimensions are much larger than the vertical ones (hence vertical acceleration terms in the equations can be neglected.). No salinity variations are taken into account. It has been verified that running in a 3D mode (i.e. using several layers to represent variations over the vertical dimension) brings no extra information to the results of a 2D simulation. Since the latter runs much faster, the simulations in this conceptual design phase are all based upon 2D simulations.

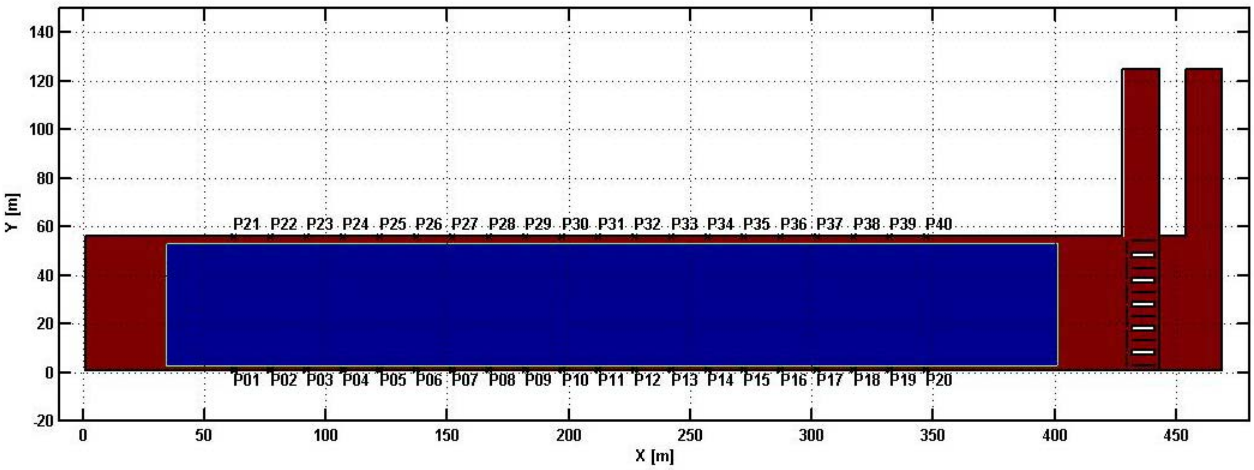

Figure 10.3-a : Computational grid for 2D simulation of water flow in lock chamber

The computational grid is shown in Figure 10.3-a, and consists of square cells with size 1 meter. The presence of the design ship is taken into account by defining a fictitious ‘atmospheric pressure field’ on top of the water surface. That pressure field causes a box-shaped ‘trough’ in the water surface to mimic the underwater part of the ship’s hull, see Figure 10.3-b. The dimensions of the box are the length, the beam and the draft of the ship. Notice that by doing so, no block coefficient for the design ship is taken into account and the blockage effect of the ship in the numerical model will be exaggerated in comparison to reality. This means that the numerically calculated hawser forces will err to the conservative side. For reasons of consistency, the numerically calculated hawser forces will be dimensionless as a 1/1000 fraction of the displacement weight of the ship as it is present in the numerical model (i.e. no block coefficient), rather than by the displacement weight of realistic design ships (i.e. accounting for realistic block coefficients).

Remark: in later design studies, one could modify the atmospheric pressure field to have a more realistic representation of the underwater part of the ship’s hull.

At the position of the ports (see 10.3-a) the discharge timeseries, which have to be previously calculated by means of the Flowmaster 2 software, are applied as boundary conditions to the 2D model.

After running the 2D model, in each point of the computational grid times series of the water levels (as well as timeseries of the two components of the depth-averaged water velocity) are available. From these water level times series, the hydrostatic forces upon the ship’s hull, and in particular the longitudinal component F_x, can be calculated.

Remark: In Annex 17 to this report, all 3 hydrostatic force components and 3 hydrostatic moments are required as an input to a more complete dynamic model of the ship’s motion and vessel positioning.

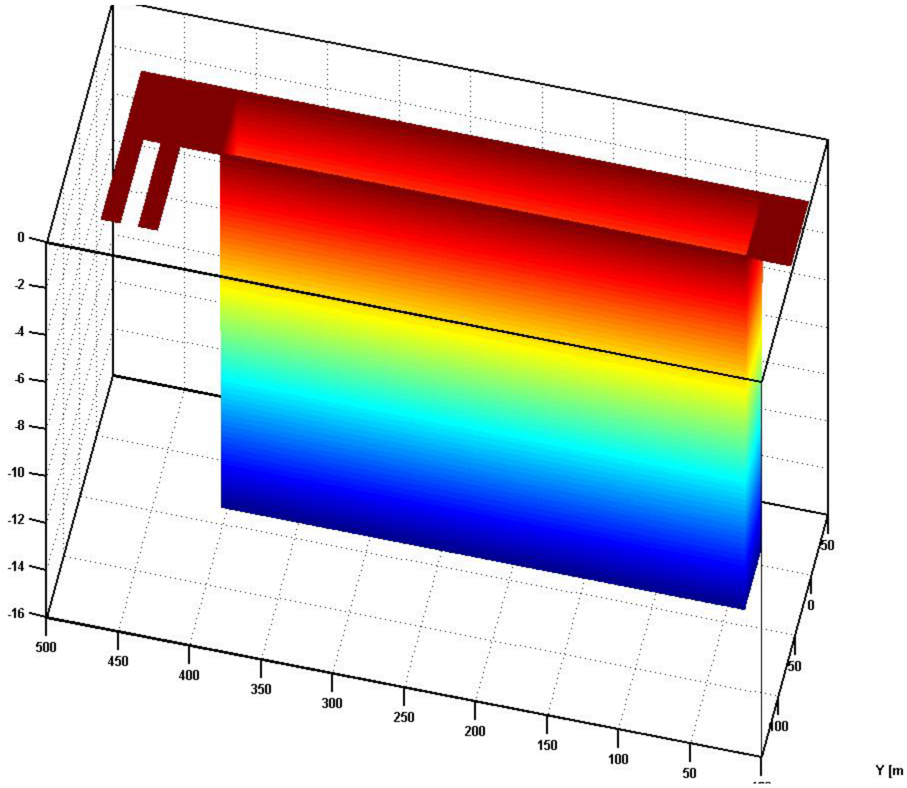

Figure 10.3-b : Effect of applying fictitious atmospheric pressure field in order to simulate the presence of the ship's hull in the lock chamber

10.4 HAWSER FORCES CRITERIA

This chapter describes the continuous process linking the 1st study where locomotives were used and this actualization study, where tugboats are expected to handle the ships.

After having calculated hawser forces, the question arises which values are acceptable and which are not. In principle, hawser forces are acceptable if both the lines in the vessel-positioning system (e.g. tugs, locomotives, bollards,…) don't break <u>and</u> the motion of the ship remains within acceptable limits (which are a function of the geometry of the lock chamber and the ship). To verify these conditions, one should model the full dynamics of the ship motion as well as the vessel-positioning system. Traditionally, one preferred to avoid this effort, since this required considerable extra computational resources, as well as the need to specify all kinds of geometrical and elastic characteristics of the different components of the system.

Therefore, several 'shortcut' practices have been put forward as hawser force criteria. A couple of decades ago, one even circumvented the calculation of hawser forces by only considering the rate of change of the average water level in the lock chamber. If this rate of change was lower than certain threshold values (e.g. Dutch and Belgian guidelines: 1 to 3 m/min, depending on lift and type of bollards; see also PIANC guidelines) the hawser forces were believed to be acceptable. Actually, this kind of criterion sets a limit to the maximum discharge through (the longitudinal culvert and) the ports.

Later on, it became common practice as far as hawser force criteria are concerned, to calculate (see section 10.3 or rather one-dimensional equivalents there off) the longitudinal component of the hydrostatic force F_x and require it to drop below certain threshold values F_x^{max}. For inland navigation, threshold values of the order of 1 ‰, were common in Belgium and in the Netherlands (see PIANC guidelines for comparable practices in other countries). Later on, one became aware that the threshold values should somewhat depend upon the way of mooring the ship (e.g. the number of lines, their geometric characteristics with respect to the ship's axes, their material and elastic characteristics, type of winches to (pre)tension the lines, etc.) and upon the displacement weight of the ship.

The latter remark is especially valid for ocean-going vessels, where the capacity of the mooring system is relatively weak in comparison to inland navigation. Research commissioned by the Dutch Ministry of Transport and Public Works revealed in 1974 that (for a particular mooring system with 4 mooring lines rigidly fixing the ship against one lock chamber wall: i.e. head and stern line plus fore and aft spring) the threshold values were in the range of 0.14 to 0.26 ‰ for a ship size of 40.000 dwt, whereas for a ship of 120.000 dwt the range was 0.11 tot 0.21 ‰. The variation within each range, is due to the different choice of material (steel or nylon) as well as the different choices of pre-tension in the lines. Of course, the question arises whether evolutions in material characteristics (lines) and technology (e.g. winches) since the early seventies would not lead to higher acceptable threshold values nowadays. This investigation is out of the scope in the conceptual design phase, but should be addressed in later design stages.

The foregoing paragraph shows that:

- Threshold values for ocean-going vessel are smaller than for inland navigation
- It is shortsighted to believe that 'universal' threshold values exist, valid for whatever kind of vessel-positioning system ; at most an order of magnitude can be learnt from research on other kinds of mooring systems

Therefore, in this conceptual phase, a rough estimate will be made to derive an approximate threshold level value taking into account some realistic mooring systems for the Panama locks.

Let's first consider the 'traditional' mooring system with 8 locomotives, of which the configuration is shown in Figure 10.4-a.

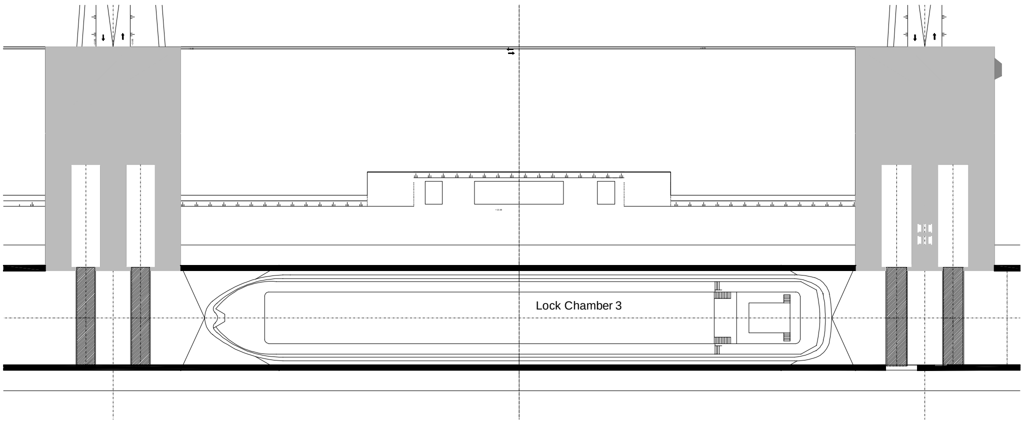

Figure 10.4-a : Configuration for calculating hawser forces with usage of locomotives

Let's take the following assumptions (which are for the new 3rd lane locks all open to discussion with ACP responsables, pilots, tugmaster etc.):

- The ship lies in the middle of the lock chamber.
- The locomotives attached to the hawsers at the bow and stern are positioned at the upper limit of the lock chamber.
- The angle between the amidships hawser and the wall of the lock chamber is 30° (in the horizontal plane, see ϑ in Figure 10.4-b).
- The rising of the water level in the lock is 10 m at maximum.
- The minimum freeboard between water level and ground level is 1.5 meter.
- The hawser is connected to the ship at a point that is situated 3 m above the water level for bulk carriers and 12 m for container ships.
- The hawsers have a maximum reaction force of R=35 ton

Based on the foregoing assumptions, one can estimate the minimum and maximum hawser angles in the vertical plane (see Φ in Figure 10.4-b). An auxiliary sketch is given in Figure 10.4-c, representing a vertical cross section through the lock chamber and the ship.

At the left of Figure 10.4-c, one notices the left lock chamber wall to which the hawsers (in red: full line=amidships hawsers, traced line=hawsers at bow or stern) are attached (locomotives not drawn). At the right of Figure 10.4-c is similarly indicated the right lock chamber wall. In the lock chamber itself is the ship drawn (black rectangle) both in the lowest (lower rectangle) and the highest position (upper rectangle).

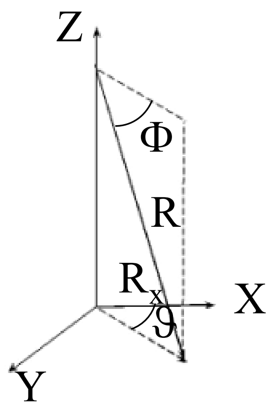

Figure 10.4-b : Definition of angles ϑ and Φ

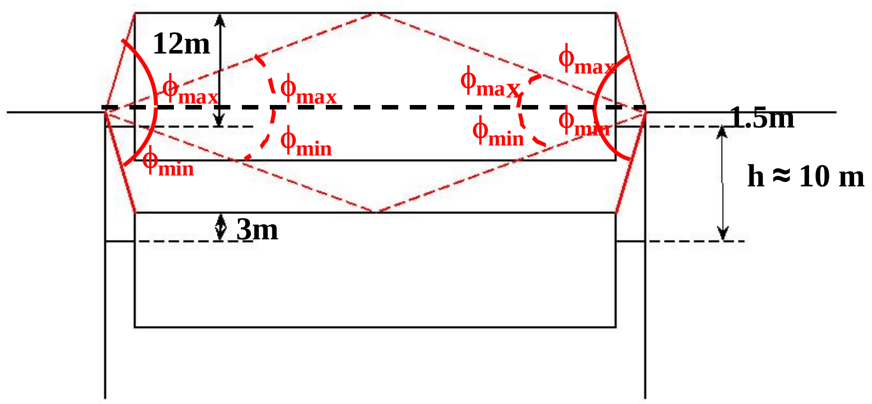

Figure 10.4-c : Configuration for the computation of the vertical angles Φ

After some elementary geometrical calculations, one can prove that:

- hawsers at bow and stern:

$\vartheta = 42.5°$

$\Phi_{min} = \Phi_{max} = 21°$

- amidships hawsers:

$\vartheta = 30°$

$\Phi_{min} = \Phi_{min} = 74°$

The threshold value for the longitudinal force on the ship that corresponds to the system above, is given by the following expression:

$$F_x^{\max} = \frac{f\left\{2.\left[R.\cos(\vartheta).\cos(\Phi)\right]_{bow/stern} + 2.\left[R.\cos(\vartheta).\cos(\Phi)\right]_{amidships}\right\}}{\Delta}$$

In the numerator of the foregoing expression, the factor f represents the ratio between the reaction force (R) in the cable to the external force (F) acting on the cable. The exact value for f depends on the characteristics of the mass-spring-system (=ship-line-system) as well as on the way the external force is applied in time.

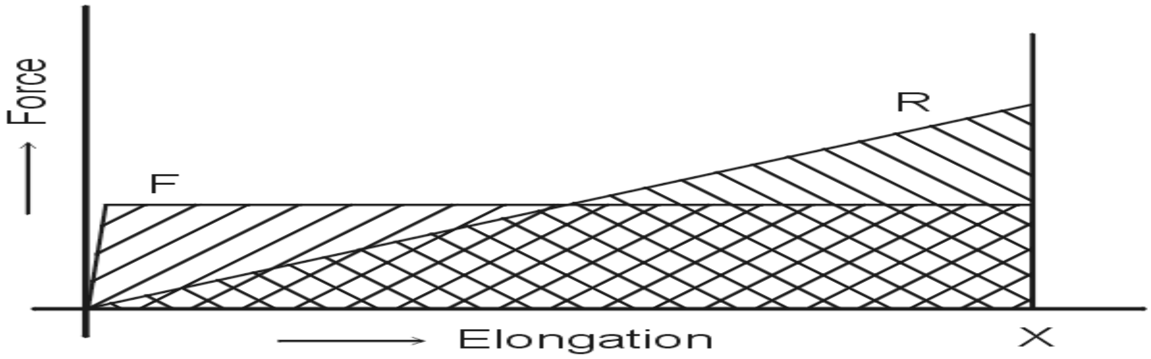

Figure 10.4-d : Mass-spring system (force vs. elongation) for a ship fixed with one single cable

For a linear spring characteristic (k=spring stiffness) and a step function (=suddenly imposed) for the external force F, one can take the energy balance into consideration:

$$F\ x = 0.5.R.x = 0.5\ k\ x^2$$

yielding:

$$f = R/F = 2.$$

In reality, the mass-spring system modelling of the behaviour of the moored ship and its cables will be much more complex than illustrated above. For instance, on the one hand non-linear behaviour of the lines results in higher values of f. On the other hand, pretension in the cables (which is assumed to be the case for the Panama locks) counteracts this negative effect (i.e. leads to a reduction of f). Therefore, in the conceptual design phase, f = 2 is believed to be a reasonable value.

Remark: In more detailed studies, see e.g. in the Annex 17 to this report, one could not only take nonlinear spring characteristics and pretension of the hawsers into account, but one could also account for the real time history of the external force instead of the assumption of the step function in time which was assumed in the foregoing reasoning. This will lead to more refined estimates of the factor f.

In the denominator of the expression for F_x^{max}, Δ represents the displacement weight of the design ship. For the design ship, only the dimensions are given in the TOR (L= 385.60m, B=48.77m, T=15.24m) and no block coefficient C_B is specified. Reasonable values are:

- C_B =0.60 for a container carrier
- C_B =0.82 for a tanker or bulkcarrier.
-

Consequently, the displacement weight Δ is:

- Δ= 171 940 ton for a container carrier design ship
- Δ= 234 985 for a tanker or bulkcarrier design ship.

Finally, inserting all the quantitative estimates derived above into the expression for F_x^{max}, valid for a vessel-positioning system based upon locomotives, yields:

- F_x^{max} = 0.19 ‰ for a container carrier design ship
- F_x^{max} = 0.14 ‰ for a tanker or bulkcarrier design ship.

Remark: higher values for F_x^{max} would be obtained if the displacement were not based upon L_{oa}=385.60m, but on lower and more realistic values like e.g. L_{bp}.

Notice that these values were based upon all kinds of assumptions, which are believed to be reasonable (yet sometimes deliberately taken to the conservative side) for the conceptual design phase. In later studies however, it is clear that the assumptions will certainly benefit from in depth discussions with responsables from ACP, including e.g. pilots and tugmasters.

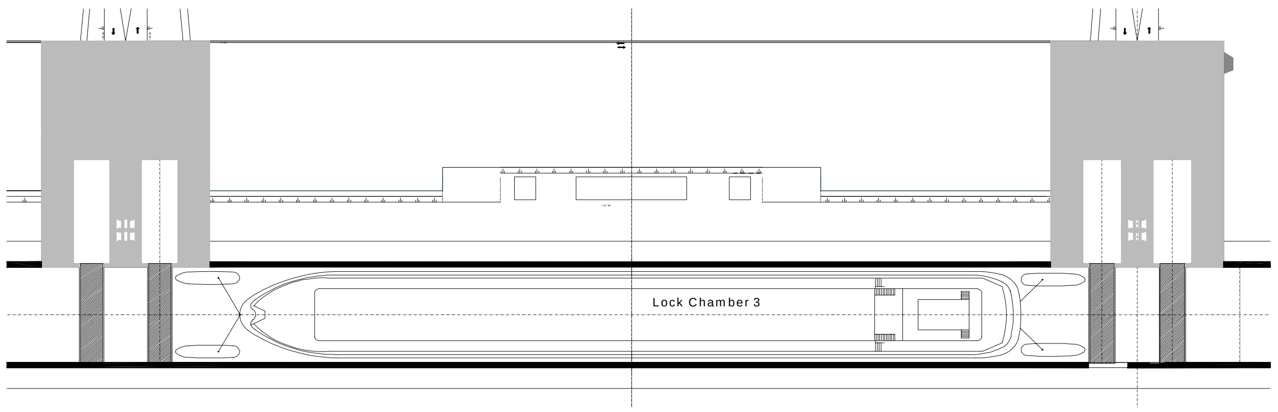

Figure 10.4-e : Sketch of design ship and tugboats in the lock chamber

The latter remark is even more valid if considering tug boat assistance (instead of locomotives) as a vessel-positioning system. Indeed, when considering tug boat assistance, one could attempt to derive similar threshold values for F_x^{max}, in a similar way as was carried out above for a 'traditional' vessel-positioning system consisting of locomotives. Again one would have to make all kinds of assumptions about number, type and size of tugs, maximum bollard pull, number of lines, type and spring characteristics of lines, location of tugs with respect to ship, geometrical angles of hawsers in horizontal and vertical plane,…). Some rough estimates with 4 tugs of bollard pull 60 ton, each trying to keep its position (i.e. constantly applying its maximum bollard pull, independently of the motion of the ship), yields values of F_x^{max} in the same order as indicated above for the vessel-positioning system based upon locomotives.

Two remarks should be added for the sake of completeness:

- The combination of the dimensions of the new locks as well as the dimensions of the design ship are such that not much place is left for tugs to assist the ship ; consequently, in later design studies experienced tugmasters and pilots of ACP should be involved in the elaboration of the vessel-positioning system based upon tugs, in order to put forward a solution which is both realistic and as effective as possible.
- The use of tugs in the abovementioned way is probably not the best one. It is indeed questionable whether constantly applying the maximum bollard pull is effective. A more 'dynamically controlled' mooring system is conceivable in which the force applied by the tugs is a function of the motion of the ship, such that the ship's motion is counteracted. E.g. in case of a ship moving ahead, the two tugs aft generate their (partial or full, depending on the speed of the ship) bollard pull; if the ship moves astern, the two tugs fore act similarly. In the Annex 17 to this report, it is shown that such a vessel-positioning system manages to keep the vessel motion under control with 4 tugs of 60 ton, even though the nondimensionalized hawser force F_x reached values up to 0.53 ‰.

Summarizing all the information mentioned above, it should be clear that no 'universal' hawser force criteria exist and that the specific situation of geometry of lock, ship and the characteristics of the vessel-positioning system determine the acceptable threshold values for the hawser forces.

Therefore, in the conceptual design phase, one will use the threshold level F_x^{max} in the range of 0.14 ‰ up to ca. 0.50 ‰ merely as a guideline, in order to have a goal for optimizating the hydraulic circuits (i.e. longitudinal culverts, ports, valves). It should not be considered as a sharp and absolute value for F_x above which the F/E-system should be considered as totally unacceptable and below which the F/E-system would be called ideal.

In a later design phase, further discussion with ACP personnel (e.g. pilots and tugmasters) will lead to a more concrete definition of a practically feasible, efficient and effective vessel-positioning system, enabling to define more refined hawser force criteria, which will be respected thanks to further optimization possibilities of the hydraulic design (longitudinal culverts, ports, valves).

10.5 RESULTING HAWSER FORCES FOR BASIC HYDRAULIC DESIGN

In Figure 10.5-a (filling) and Figure 10.5-c (emptying), the discharge series through the ports, which are provided by the Flowmaster 2 simulations in the case of the so-called basic hydraulic design (i.e. prior to any attempts to optimize the hydraulic design, see chapter 8), are presented. These data are imposed as boundary conditions to the 2D simulation of the water flow in the lock chamber.

The 2D simulation leads (among other things) to two timeseries of the waterlevel at bow and stern of the ship, see green and red curves in Figure 10.5-b (right vertical axis). The timeseries of the water level difference at bow and stern of the ship allows us to calculate the timeseries of the longitudinal component of the hydrostatic force F_x (nondimensionalized by the displacement weight of the ship), see the blue curve in Figure 10.5-b (left vertical axis).

Different cases are considered (filling vs. emptying, outer door closed). The results are graphically shown in Figure 10.5-b and Figure 10.5-d. The corresponding maximum values for F_x are summarized in Table 10.5-e.

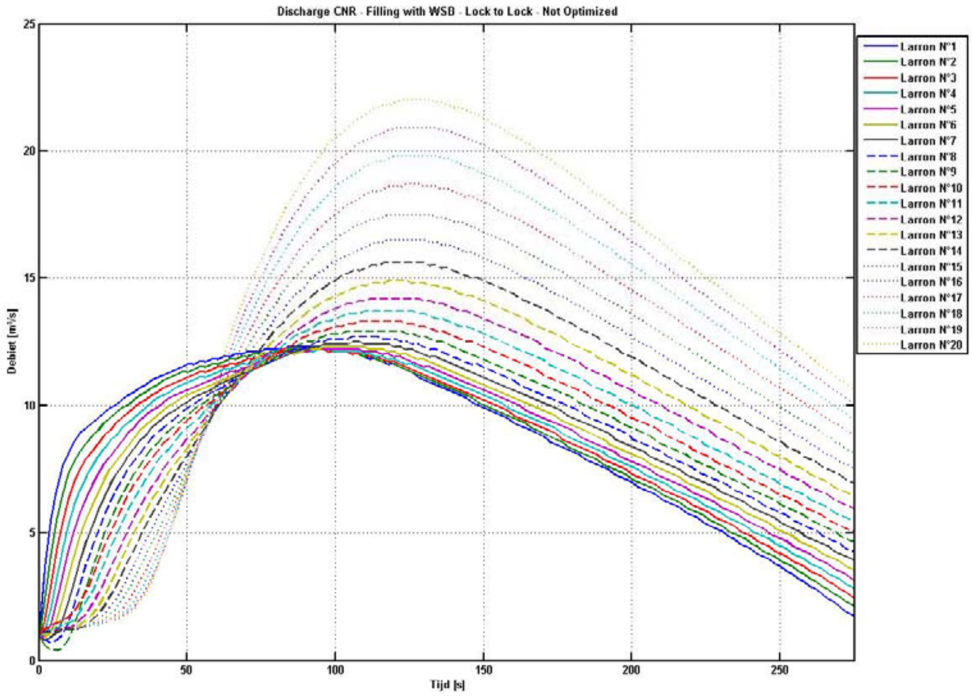

Figure 10.5-a : Discharge time series - Filling - lock to lock phase – basic design

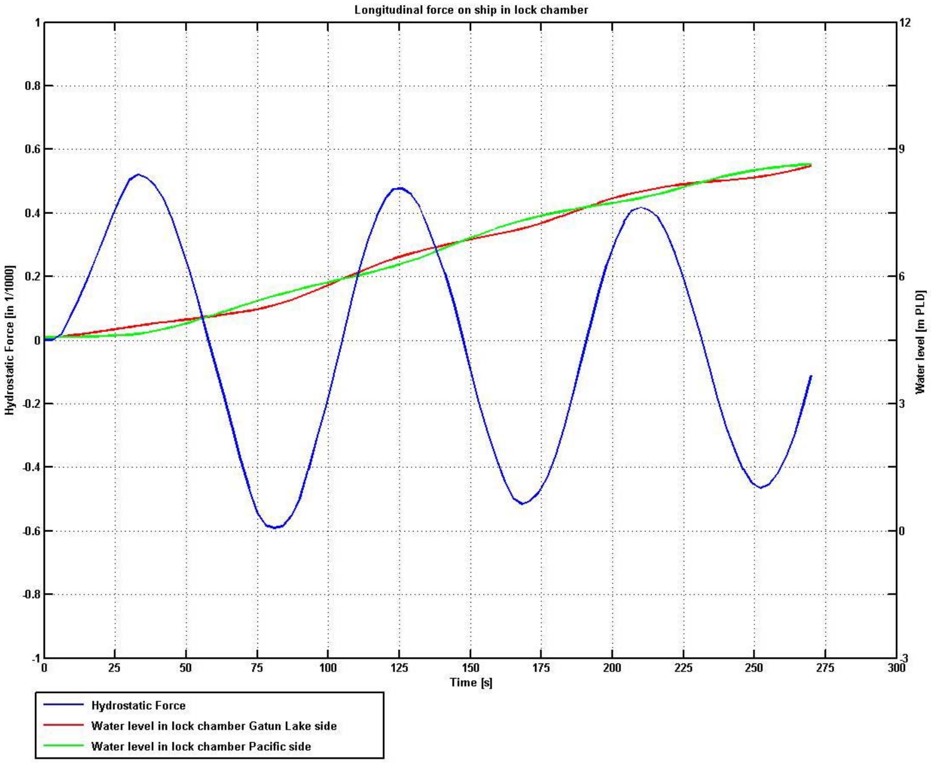

Figure 10.5-b : Filling - Lock to Lock phase - configuration outer gate closed – basic design

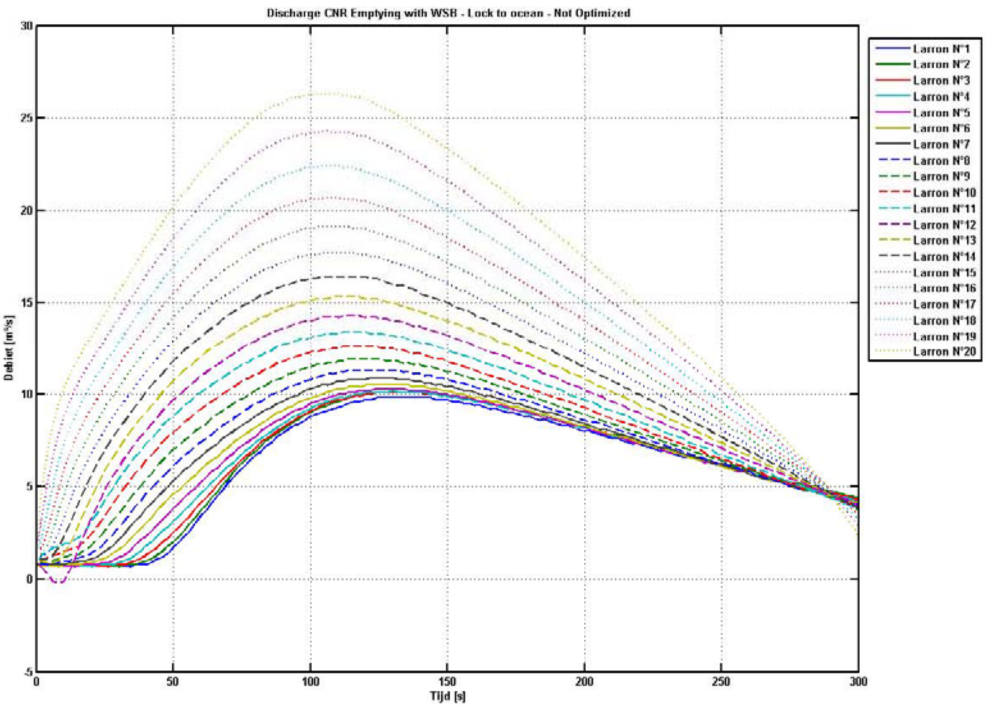

Figure 10.5-c : Discharge time series - Emptying - lock to lock phase – basic design

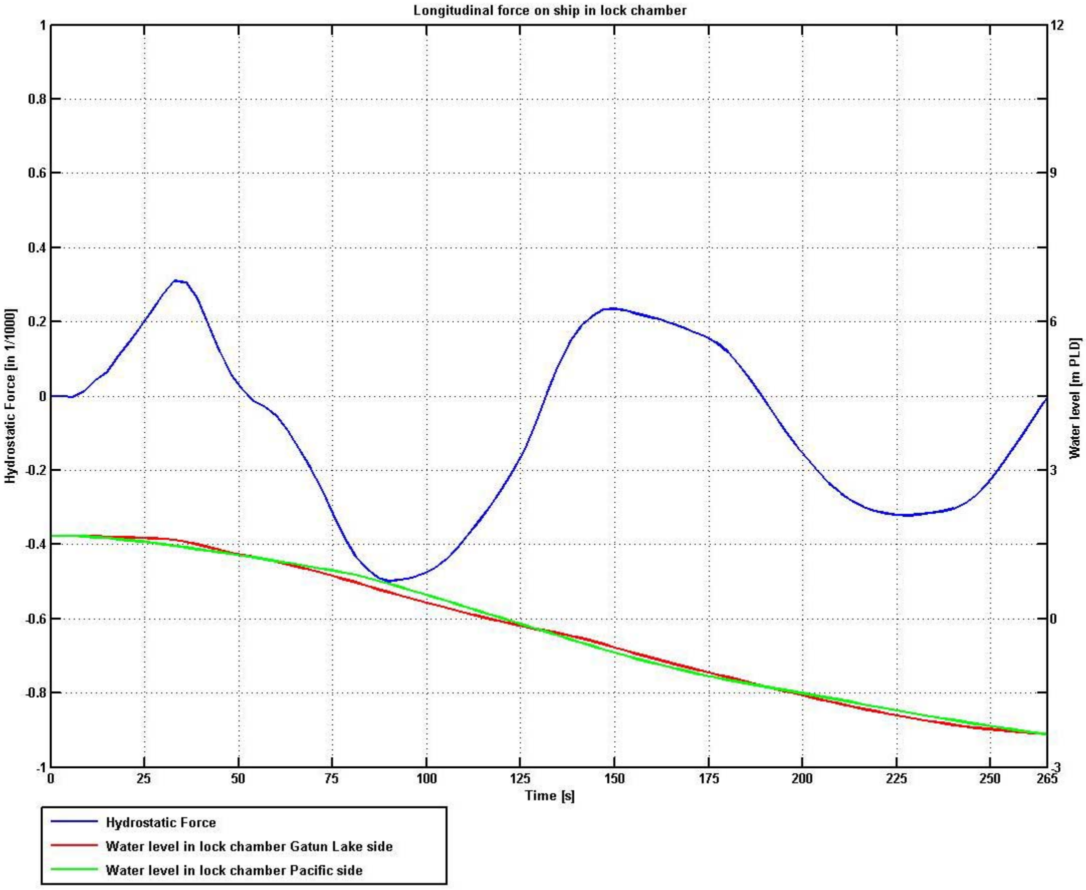

Figure 10.5-d : Emptying - Lock to Lock phase - configuration outer gate closed – basic design

		basic case
filling	**outer gate closed**	0.59
emptying	**outer gate closed**	0.50

Table 10.5-e : Overview of maximum hawser forcesF_x [‰] during filling and emptying of the lock

Notice that the maximum hawser forces (i.e. the peak values for F_x, though they don't last long in time) are above the range (0.14 ‰ up to ca. 0.50 ‰) indicated as a guideline for the conceptual design in section 10.4. This shows that the basic hydraulic design needs further optimization in order to reduce the hawser forces.

10.6 WAYS TO REDUCE THE HAWSER FORCES

The elementary ways to reduce the hawser forces that happen during the operations from lock to lock, by reducing the differences of discharges between the ports, are:

- Unsteady stage: by modifying the opening diagram of the valve. Opening the valve slower makes it possible for each port to get some discharge quicker, as the upstream ones reach their cruising speed earlier.
- Quasi-steady stage: by reducing the efficient area of the ports that have the higher discharge, the distribution can be better balanced.
- Concentrating the ports closer to the "gravity center" of the lock chamber: it has already been shown by means of physical model testing that this leads to a reduction of the hawser forces. In addition, this was confirmed by numerical simulations of Flanders Hydraulics Research with different dispositions of ports.
- Increasing the number of ports and modify their size and spacing : this way has not been yet explored
- Modify the F/E system (central secondary culvert as suggested in the return on experience of 1915 – paper of R.H. Whitehead - and similar to many Rhône locks)

10.6.1 MODIFYING THE VALVE DIAGRAM

The normal valve opening time is 2'. It was chosen in relation with the electro-mechanical team, in relation to the valve dimension.

In order to reduce the gap between the ports in the unsteady stage, opening times of 4 and 6 minutes have been tested.

The corresponding filling times are:

Operation	Head in m	Valve opening in s.	Filling time in s.	Highest average velocity in m/s	
				Culvert	Port
F/E of the lock chamber	8.10 max	120 (2 mn)	270 (4 mn 30 s)	5.5	6.6
		240 (4 mn)	315 (5 mn 15 s)	4.6	5.5
		360 (6 mn)	365 (6 mn 5 s)	3.9	4.7

Operation	Head in m	Valve opening in s.	Delta Q ($Q_{PortN°20}$-$Q_{PortN°1}$) in m³/s	
			Delta Q min	Delta Q max
Filling the lock chamber	8.10 max head	120 (2 mn)	-8.5	11.3
		240 (4 mn)	-5.7	9.5
		360 (6 mn)	-4.5	8.4
Emptying the lock chamber	8.10 max head	120 (2 mn)	/	18.7
		240 (4 mn)	/	14.2
		360 (6 mn)	/	12.1

Table 10.4.1-a

This modification allows to reduce by 30 % the discharge difference during an emptying or a filling operation, with an opening time of 6'. At the same time , the filling time increases but the gap reduces: 4'30" are necessary with an opening time of 2' while only 6'05" are necessary with the opening time of 6'.

The efforts in the hawsers will be reduced in the same direction, the proportion having to be calculated by the 2D/3D Delft mathematical model.

The graphs in annexes 8 and 9 show the curves of the filling stage, on which appears the shift in time associated with the reduction of the discharges difference.

10.6.2 MODIFYING THE PORT DIMENSIONS

In order to reduce the flow rate of the downstream ports, the following reduction of the ports size was tested:

Port nb	1	2	3	4	5	6	7	8	9	10
Height m	2	2	2	2	2	2	2	2	1.9	1.8
Width m	2	2	2	2	2	2	2	2	2	2
Area m²	4	4	4	4	4	4	4	4	3.8	3.6
Equiv. diameter	2.26	2.26	2.26	2.26	2.26	2.26	2.26	2.26	2.20	2.14
$A_{port}/A_{culvert}$	0.07	0.07	0.07	0.07	0.07	0.07	0.07	0.07	0.07	0.07

Port nb	11	12	13	14	15	16	17	18	19	20
Height m	1.7	1.6	1.5	1.45	1.4	1.35	1.3	1.25	1.2	1.15
Width m	2	2	2	2	2	2	2	2	2	2
Area m²	3.4	3.2	3	2.9	2.8	2.7	2.6	2.5	2.4	2.3
Equiv. diameter	2.08	2.02	1.95	1.92	1.89	1.85	1.82	1.78	1.75	1.71
$A_{port}/A_{culvert}$	0.06	0.06	0.06	0.05	0.05	0.05	0.05	0.05	0.04	0.04

Table 10.4.2-a

NB : the equivalent diameter is the diameter of a pipe having the same section, it is an input for Flowmaster

Port n°1 is the most upstream one; port n° 20 is the most downstream one

The impact of that modification appears in the following board:

Operation	Head in m	Dimensions of the ports in m	Time en s (mn s)	Highest average velocity in m/s	
				Culvert	Port
F/E of the lock chamber	8.10 max head	Without reduction of the ports dimensions	270 (4 mn 30 s)	5.5	6.6
		Reduction of the ports	280 (4 mn 40 s)	5.3	8.6

Operation	Head in m	Valve aperture in s	Delta Q ($Q_{PortN°20}$-$Q_{PortN°1}$) in m^3/s	
			Delta Q min	Delta Q max
Filling lock chamber	8.10 max head	Without reduction of the ports dimensions	-8.5	11.3
		Reduction of the ports	-8.8	4.1
Emptying lock chamber	8.10 max head	Without reduction of the ports dimensions	/	18.7
		Reduction of the ports	/	12.7

Table 10.4.2-b

Reducing the ports area increases the filling time by only 10 seconds, which is very low, reduces the difference in flows between the ports by 2/3 for the filling operation, which is more critical, and by 1/3 for the emptying operation.

The graphs in annex 10 illustrate the optimization.

The impact is very good for the filling operation; the dimensions of the last ports can be chosen in order to reach almost the same discharge for the extreme ports during the quasi-steady stage.

On the other hand, the retained configuration is less but still efficient during the emptying operation, because the downstream ports, being close to the control valve, keep on discharging more. The head loss coefficients are calculated by Flowmaster considering the discharges and the ratio between ports and culverts areas, for each step of calculation.

10.6.3 COMBINING THE TWO METHODS

Combining the two optimization methods (increasing the valve opening time and the size reduction of the downstream ports) allows to improve the flow distribution in each stage.

<table>
<tr><th rowspan="2">Operation</th><th rowspan="2">Head in m</th><th rowspan="2">Valve opening in s.</th><th rowspan="2">Dimensions Of the ports in m</th><th rowspan="2">Filling time in s</th><th colspan="2">Highest average velocity in m/s</th></tr>
<tr><th>Culvert</th><th>Ports</th></tr>
<tr><td rowspan="6">F/E of the lock chamber</td><td rowspan="6">8.10 m max head</td><td rowspan="2">120 (2 mn)</td><td>Without reduction of the ports dimensions</td><td>270 (4 mn 30 s)</td><td>5.5</td><td>6.6</td></tr>
<tr><td>Reduction of the ports</td><td>280 (4 mn 40 s)</td><td>5.3</td><td>8.6</td></tr>
<tr><td rowspan="2">240 (4 mn)</td><td>Without reduction of the ports dimensions</td><td>315 (5 mn 15 s)</td><td>4.6</td><td>5.5</td></tr>
<tr><td>Reduction of the ports</td><td>325 (5 mn 25 s)</td><td>4.4</td><td>7.2</td></tr>
<tr><td rowspan="2">360 (6 mn)</td><td>Without reduction of the ports dimensions</td><td>365 (6 mn 5 s)</td><td>3.9</td><td>4.7</td></tr>
<tr><td>Reduction of the ports</td><td>375 (6 mn 15 s)</td><td>3.8</td><td>6.2</td></tr>
</table>

Table 10.4.3-a

Combining the two methods would lead to filling or emptying times that exceed the guidelines in a minority of cases and for a single operation in a cycle (a filling or emptying cycle combines lock operations and wsb operations), as the maximum head of 8.10 m has a low frequency of appearance (see graph 8.4.2-a).

Besides, it was also demonstrated that the global time for the whole operation of the downstream lock chamber doesn't exceed the target time of 17': one can imagine for example that an emptying cycle cannot combine in the same cycle high heads both for lock operation and water saving basins operations. If the head is high for the lock operation, it is on the contrary low in wsb operations: the time lost in lock operation is saved on wsb operations (see also 8.4.2-b).

This can be demonstrated with the in house CPP software: some routines will be added to calculate for each stage the real operating time (time vs head)

The graphs in annexes 11 illustrate the effect of the combined methods for the filling of the lower chamber.

The graphs in annexes 12 illustrate the effect of the combined methods for the emptying of the middle chamber.

As it was indicated formerly, these results shall not be considered as the final design of the F/E system. The calculations have been done to demonstrate that it is perfectly possible to optimize the F/E system, which will however need more detailed analysis.

These more detailed analyses will both combine Flowmaster™ simulations and 2D/3D Delft mathematical model simulations, prior to the construction of a physical model. Finally, the physical model, by measuring of the hawser forces, will allow to completely check the F/E system. Numerical simulations are very useful to obtain a first estimation of the forces, but are not sufficiently accurate for final design.

Note : one can however mention that Flowmaster™ input data were calibrated on the physical model study of the Panama Canal locks performed in 1942 (refer to 1st configuration report)

10.6.4 IMPACT ON THE OPERATIONS BETWEEN THE WSB AND THE LOCKS

As it has been explained before, the filling or emptying by means of the WSB provide a well balanced flow. Consequently, reducing the size of the ports, as it has been proposed before, in order to improve the lock-to-lock operations will have an adverse but limited impact on the WSB-to-lock operations.

The calculations have been performed with the ports size reduction of chapter 10.4.2. The graphs in annex 14 show the differences of behavior between the 4 groups of 5 ports each, with and without size reduction.

The results show that the impact of the ports size reduction is quite limited. The most important port size reduction concerns the downstream ports. In that area, the ports reduction generates a more balanced flow. In the other groups of 5 ports, the impact is limited. The reduction increases the discharge of some ports and reduces the discharge of some others, but the order of magnitude remains the same.

To conclude, the impact of the size reduction in these operations is limited in the WSB operations, but this is not as important as for the lock to lock operations (see above), because the operations with wsb produce well balanced flow distributions. It interferes with the well balanced filling or emptying operations realized by the WSB but will not increase too much the hawser forces: it was demonstrated by numerical model that hawser forces during wsb operations are far below the ones during lock to lock operations. This will have to be once again verified on the 2D/3D Delft mathematical model and finally validated on the scale model.

10.7 RESULTING HAWSER FORCES AFTER 1ST OPTIMIZATION OF HYDRAULIC DESIGN

In **Figure 10** (filling) and Figure 10.7-c (emptying), the discharge series through the ports, which are provided by the Flowmaster 2 simulations in the case of the so-called first hydraulic optimizations (i.e. combination of increasing valve opening time and reduction of the downstream ports sections, see section 10.6.3), are presented. These data are imposed as boundary conditions to the 2D simulation of the water flow in the lock chamber.

The 2D simulation leads (among other things) to two time series of the water level at bow and stern of the ship, see green and red curves in Figure 10.7-b (right vertical axis). The timeseries of the water level difference at bow and stern of the ship allows us to calculate the timeseries of the longitudinal component of the hydrostatic force F_x (non-dimensionalized by the displacement weight of the ship), see the blue curve in Figure 10.7-b (left vertical axis).

Different cases are considered (filling vs. emptying, outer door closed). The results are graphically shown in Figure 10.7-b and Figure 10.7-dc. The corresponding maximum values for F_x are summarized in Table 10.7-e.

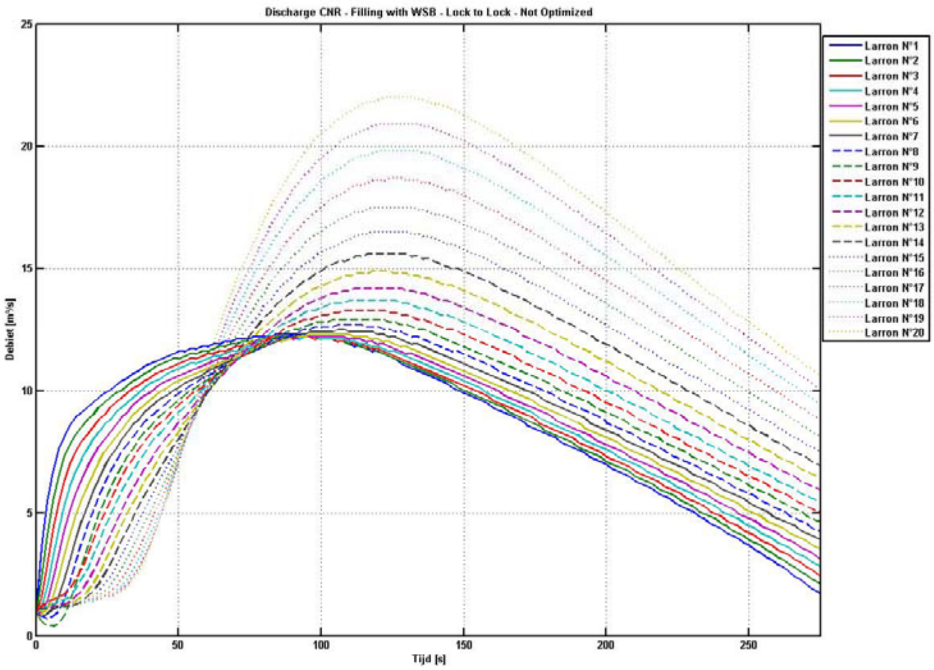

Figure 10.7-a : Discharge time series - Filling - lock to lock phase - first hydraulic optimizations

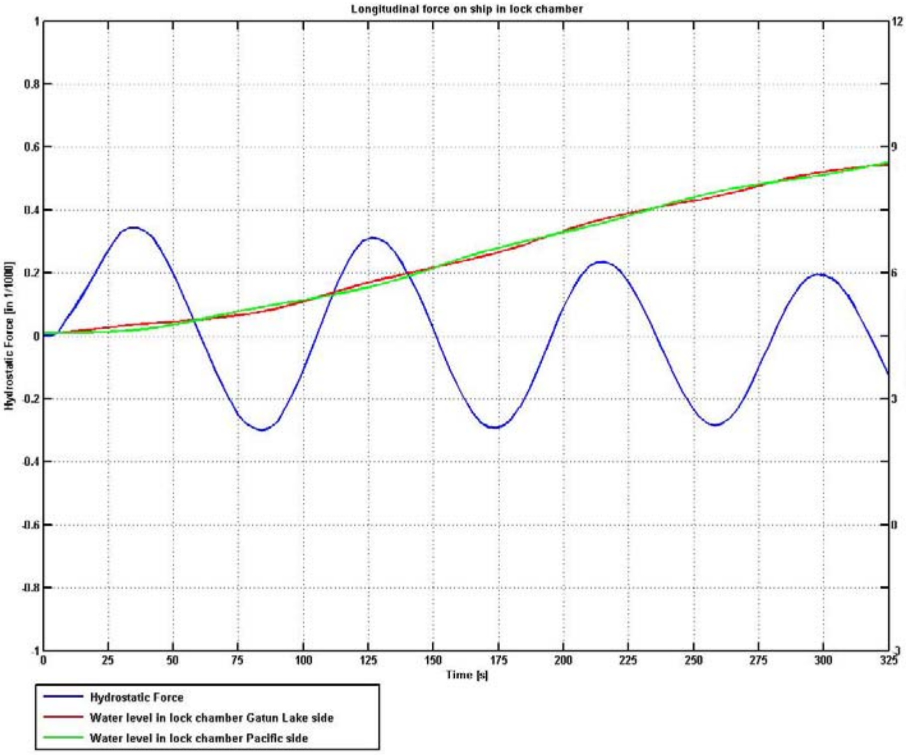

Figure 10.7-b : Filling - Lock to Lock phase - configuration outer gate closed – first hydraulic optimizations

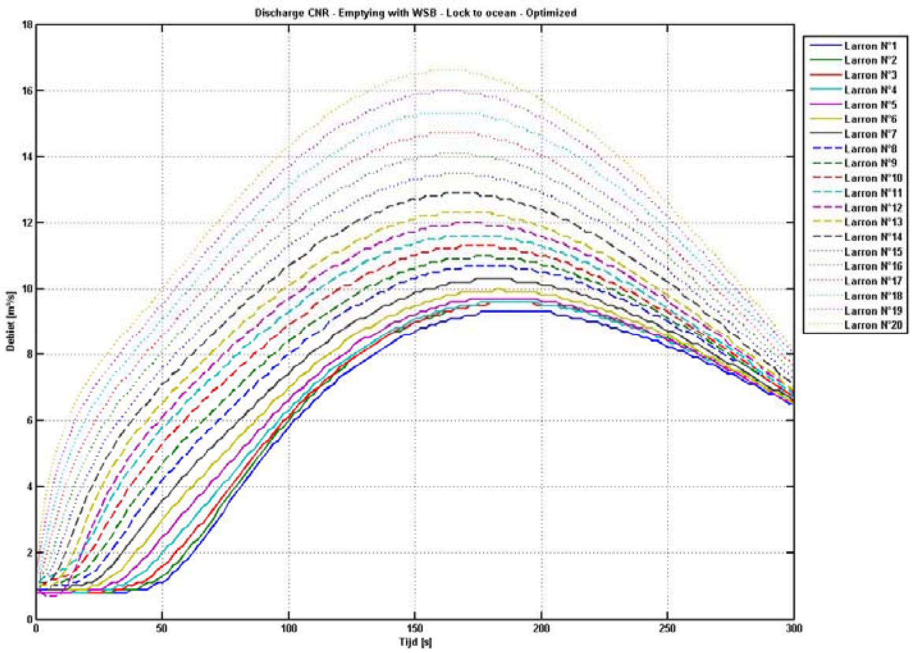

Figure 10.7-c : Discharge time series - Emptying - lock to lock phase - first hydraulic optimizations

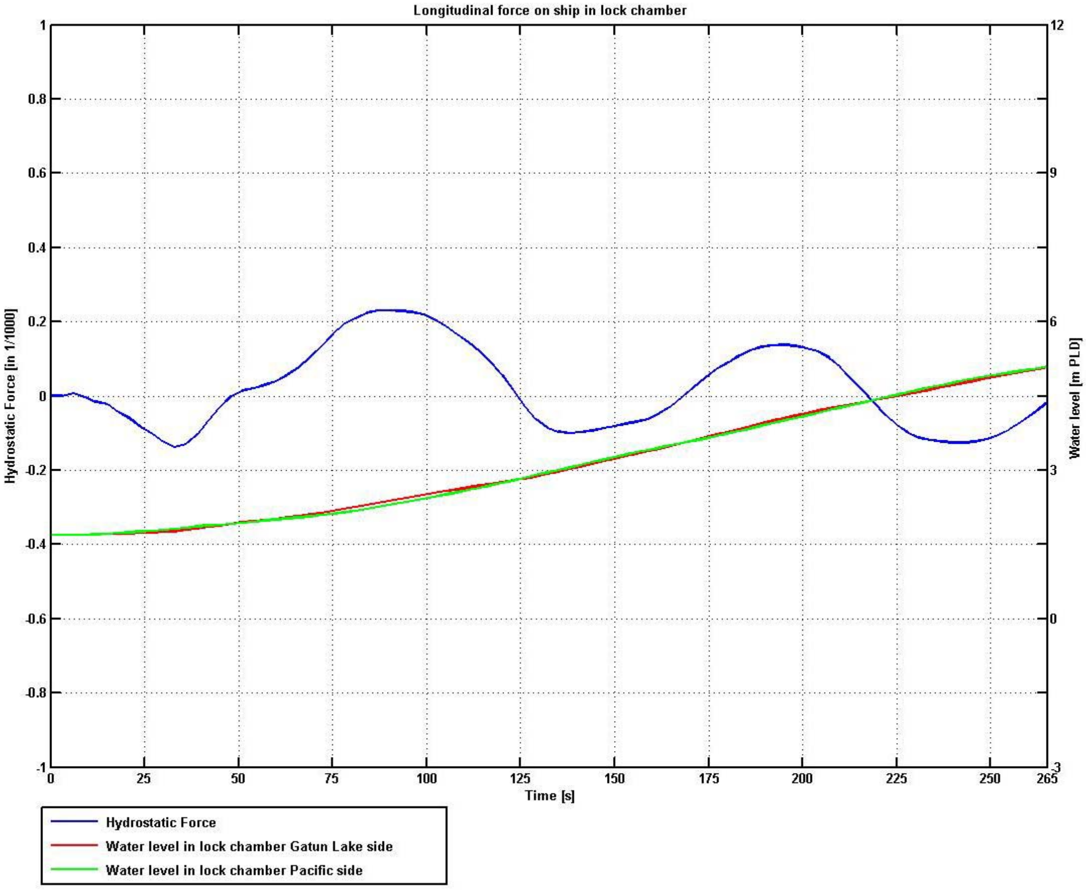

Figure 10.7-d : Emptying - Lock to Lock phase - configuration outer gate closed – first hydraulic optimizations

		configuration	
		basic case	**optimized**
filling	**outer gate closed**	0.59	0.34
emptying	**outer gate closed**	0.50	0.21

Table 10.7-e : Overview of maximum hawser forces F_x [‰] during filling and emptying of the lock

Notice that the maximum hawser forces in the case of the first hydraulic optimizations, have been reduced with (roughly speaking) a factor 2 as compared to the case of the basic hydraulic design. Moreover, the values attained are now in the range of guideline values for the conceptual design (0.14 up to ca. 0.50 ‰, see section 10.4).

By further optimizations of the hydraulic design in the later design stages, one could attempt to reach even lower values of the maximum hawser forces (i.e. much closer to the lower end of the range of guideline values indicated in section 10.4). Several means for further hydraulic optimizations exist:

- Optimization of the ports (number, size, positions)
- Optimization of the valve opening diagram
- Optimization of the local head losses
- Dynamically controlled mooring (see the Annex 17 to this report).

An illustration of further optimization potential, based upon modifying the valve opening diagram is given in Table 10.7-f. The original diagram refers to the one applied in section 10.7, which consists of a linear opening in 4 minutes time. Diagram 1 and 2 are two alternatives in which the opening takes in two linear parts (each with its own opening speed, the first part being the slowest).

	First part	Second part	Total opening time	Increase of filling time
Original diagram	**100% in 4'**	**0% in 0'**	**4'**	**0''**
Diagram 1	**10% in 1'**	**90% in 2'**	**3'**	**30''**
Diagram 2	**25% in 2'**	**75% in 1'30**	**3'30**	**0''**

Table 10.7-f : Modifications to the valve opening diagram

		Original diagram	Diagram 1	Diagram 2
filling	**outer gate closed**	0.34	0.27	0.25
	inner gate closed	0.32	0.19	0.3

Table 10.7-g : Overview of maximum hawser forces F_x [‰] during filling of the lock

The associated maximum hawser forces are indicated in Table 10.7-g. Notice that diagram 1 leads to reduced forces as compared to the case of the original diagram. For Diagram 2, however, the indicated figures in Table 10.7-g are somewhat misleading. The optimization effected by diagram 2 takes place in the first stage of filling (the so-called transient stage). Combining diagram 2 with another optimization (e.g. optimizing ports) which does affect the second stage of filling, therefore seems to be worth further investigations in the later design phase.

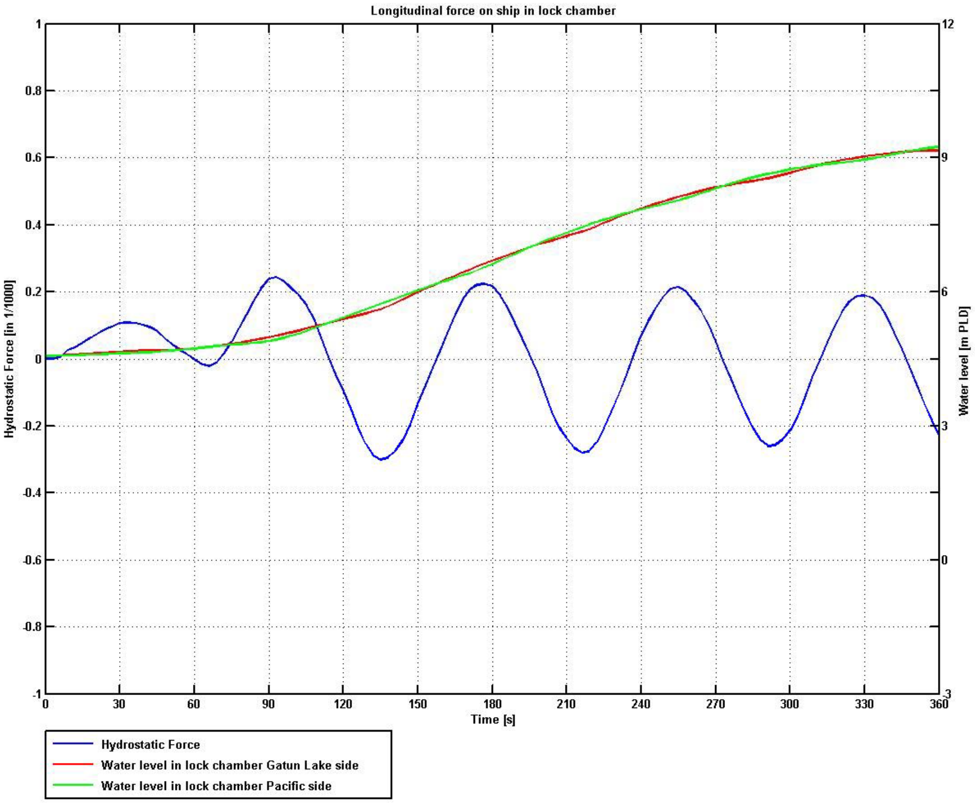

Figure 10.7-h : Filling – inner gate closed - Valve opening diagram 2

10.8 CONCLUSION

Because of the complexity of the hydraulic phenomena involved and because the vessel positioning system is not yet specified in all its details, it is impossible to determine at a conceptual design level the hawser forces with absolute accuracy. For doing so in later design studies, another stage of study is needed, i.e. combining Flowmaster™ simulations and more detailed numerical modeling of hawser forces with the 2D/3D Delft model, both prior to and in parallel with physical modeling. These investigations, however, should be proceeded by in depth discussions with ACP personnel (e.g. pilots, tugmasters,…) in order to come up with a vessel positioning system which is both practically feasible and as efficient as possible.

In this conceptual design phase, however, it has been shown that the maximum hawser forces - associated with the selected F/E-system (i.e. side wall filling/emptying through longitudinal culverts and ports) and some limited hydraulic optimization - are already within a range of guideline values based upon literature and preliminary calculations and numerical modeling.

Moreover, several means of hydraulic optimization (e.g. valve opening diagram, design of ports, local head losses, and dynamically controlled mooring forces), have clearly indicated that there is potential for further reduction of the maximum hawser forces towards the lower end of the range of guideline values. Such optimization efforts, however, are out of the scope of the present conceptual hydraulic design study and will have to be analysed during further design phases.

11 Flows between the gates

The Panama triple lift lock system will use double gates between two chambers, in order to improve security. Consequently, the volume between two adjacent gates has to be filled or emptied in parallel of the chamber itself.

To this volume has to be added the volume of water of the gates itself and the volume of the gate recesses.

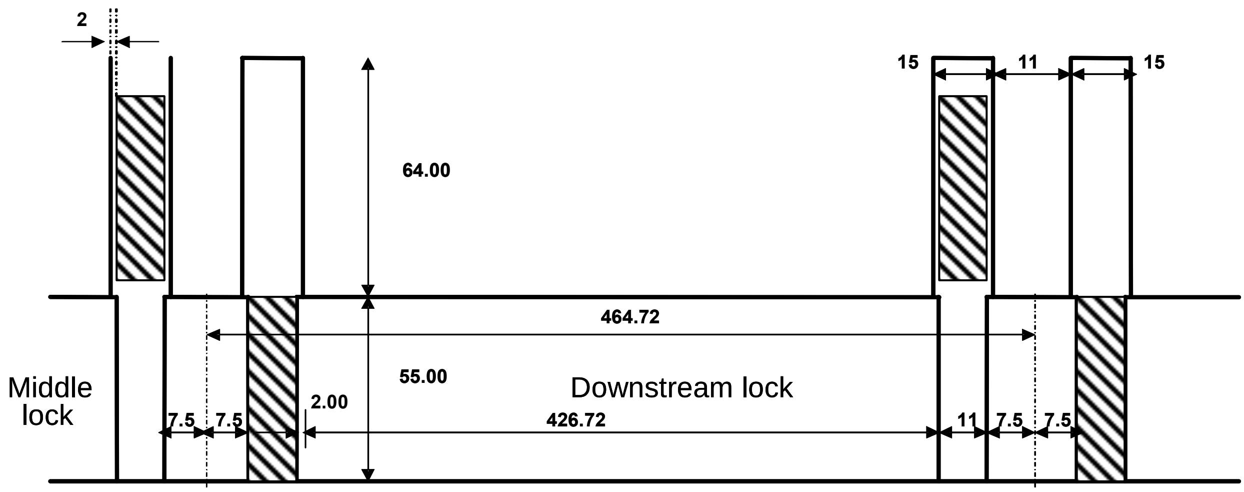

Figure 11-a

A = (2.00 + 426.72 + 11.00 x 95% + 7.50 + 7.50 + 11.00 x 95%) x 55.00 + 2 x 15.00 x 64.00 = 27 414 m2
A eq = 27 500 m2

The widths of the gates are respectively: 2 * 7.00 m ; 2 * 10.00 m ; 2 * 10.00 m ; 2 * 11.00 m

The surface of the volume comprised in each gate and its recess is about:

$$15 \times 64 + 0.95 \times 55 \times 11 = 1\,535 \text{ m}^2$$

The surface of the volume comprised between the two gates is about: 15 x 55 = 825 m^2

In the former calculations, the equivalent global surface of the lock chamber was used. In order to make a first dimensioning of the systems needed to fill and empty these secondary volumes, the Flowmaster™ model has been modified to represent 4 chambers.

To allow the filling and emptying of the gates, their upstream face will be equipped with circular openings totalizing an area of about 18 m².

To realize the communication between the upstream chamber (or the Gatun lake) and the volume between two gates, two valves of a total area of 24 m² are required. Those valves will be installed inside a conduit integrated in the gate structure. They will normally remain opened. In case of maintenance on the downstream gate, the valves will be shut down by entering the gate in its recess and connecting the valve to its hydraulic command system.

The locations of these openings and valves will have to be determined during detailed gate design. The areas were determined in order to get small additional times (see further), and a global head lower than 1.00 m (see annexes .

This kind of system (valves) exists at the Zeebruges lock, in Belgium.

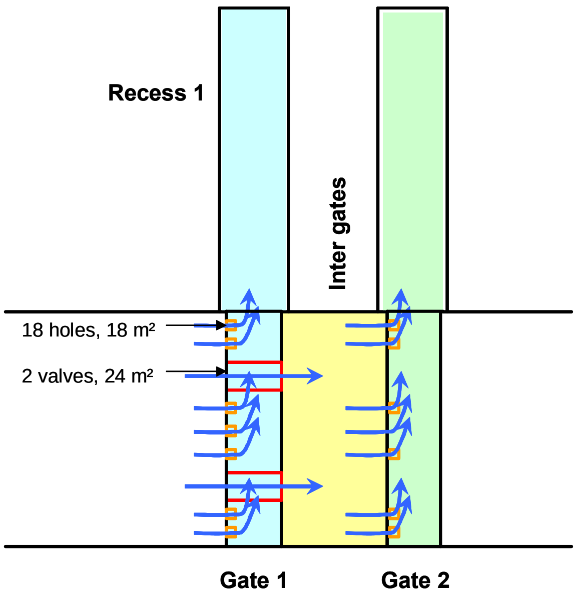

Figure 11-b

The calculations have been run in three cases:

- Emptying the lower chamber into the Ocean
- Filling the upper chamber from the Gatun lake
- Filling the middle chamber

Emptying the lower chamber

The graphs in annex 13-1 show the maximum level differences between:

- the lock chamber and the and the first gate: 0.4 m

- the first gate and the volume between the two gates: 0.2 m
- the volume between the two gates and the second gate: 0.4 m

The maximum level difference between the chamber lock and the second gate is about 1m.

The requested additional time necessary to reach the complete equalization of the levels between the lock chamber and the downstream gate is about 30 seconds.

The dynamic overfilling effect that will help break the seal is the same in all configurations (inner or outer gate closed, or both)

Filling the upper chamber

The calculation was made with the required time of 7' for the valve opening, in order not to exceed the maximum velocity.

The graphs in annex 13-2 show the maximum level differences between:

- the lock chamber and the and the first gate: 0.25 m
- the first gate and the volume between the two gates: 0.1 m
- the volume between the two gates and the second gate: 0.2 m

The maximum level difference between the chamber lock and the second gate is about 0.6 m.

The required additional time necessary to reach the complete equalization of the levels between the lock chamber and the downstream gate is about 25 seconds.

The dynamic overfilling effect that will help break the seal is the same in all configurations (inner or outer gate closed, or both)

Filling the middle chamber

The calculation was undertaken to make the comparison with the former case: here the opening time of the valve is only 2' to respect the velocity criteria.

The graphs in annex 13-3 show the maximum level differences between:

- the lock chamber and the first gate: 0.40 m
- the first gate and the volume between the two gates: 0.1 m
- the volume between the two gates and the second gate: 0.3 m

The maximum level difference between the chamber lock and the second gate is about 0.8 m.

The required additional time necessary to reach the complete equalization of the levels between the lock chamber and the downstream gate is about 25 seconds.

The dynamic overfilling effect that will help break the seal is the same in all configurations (inner or outer gate closed, or both)

To conclude, the results are not far different from the former case.

This dimensioning has been done at a conceptual level. However it proves, provided that the total areas of the ports in the gates and of the valves inside the upstream gate are sufficient, the filling or emptying of the secondary volumes needs only additional times of 25’’ to 30 ‘’ at maximum (with double gate operating).

Note : these added times may be reduced in case of F/E operations with only outer gates closed after stopping of the ships in the chambers (inner gates in their recesses).

12 Connection of the WSB to the main culverts

In order to decrease the head losses in the connection between the main culverts and the conduits, it is proposed to modify its initial shape by softening the angles. It will be compulsory to pay special attention to those connections to prevent high head losses during filling or emptying the WSB: only one conduit will flow at a time, which is favorable for secondary currents to develop and to slow down the flow.

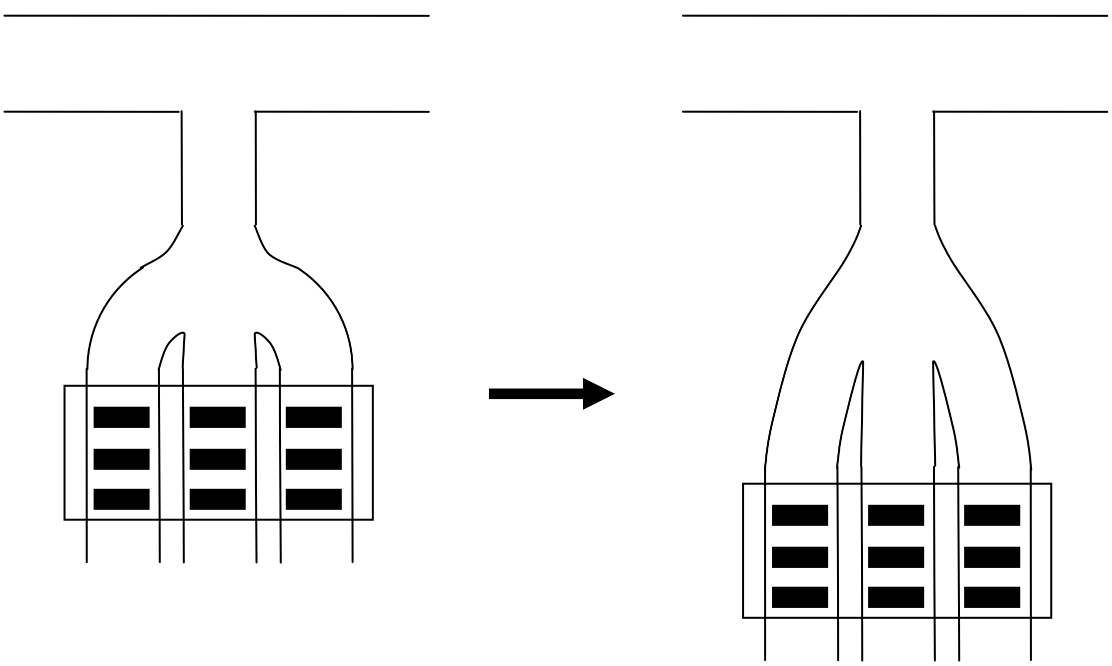

Figure 12-a

The final design will be made according to the hydraulics rule book and finally validated on a specific physical scale model.

13 Flushing

In order to reduce the salt intrusion levels in the locks, ACP intends to perform some flushing when necessary. This operation would be done without any ship in the locks and without using the WSB; the fresh water from the Gatun Lake would allow to push away the salt water.

Some calculations have been performed in order to give the order of magnitude of the required times for those operations.

	Lockages without WSB				
Operation	Head (m)	Valve aperture (s)	F/E time in s	highest average velocity (m/s)	
				Culvert	Port
Filling of the upper lock	10.10 max head	360 (6 mn)	560 (9 mn 20 s)	6.9	7.0
	7.20 min head	360 (6 mn)	490 (8 mn 10 s)	5.5	5.5
Filling / Emptying of locks	21.10 max head	540 (9 mn)	590 (9 mn 50 s)	6.5	7.7
	13.90 min head	360 (6 mn)	440 (7 mn 20 s)	5.7	6.8
Emptying the lower lock	11.70 max head	540 (9 mn)	650 (10 mn 50 s)	6.7	7.9
	6.30 min head	/	/	/	/

Table 13-a

They show (see annexes 15 and 16) that the flow rate differences between the extreme ports are superior to those obtained while using the WSB. The valves must be opened slower than in the above simulations, in order not to exceed the Design Criteria. In the filling operation, the velocity of the downstream ports (nb 19 and 20) exceeds the Design Criteria: the valve shouldn't be opened entirely, which would increase again the filling time. These operations are however expected to be relatively rare.

In addition the risk of cavitation increases.

The global estimated hydraulic time is about 30 minutes, in order to respect the velocity criteria.

This operating time must not be compared to the operating time while using the WSB, in particular if the intention would be not to use them, for example in the wet season to lock ships. This operating time is realistic only without any ship in the locks. Lockage of ships without using the water saving basins as a regular operation mode needs further studies, and probably some modifications in the F/E system.

14 Conclusion

The actualization study has shown that the filling and emptying system that has been designed, provided some geometrical modifications, is adapted to the new configuration. It allows to comply with the design criteria and the guidelines for a triple lift lock system equipped with 3 water saving basins per lock chamber.

Compared to the first study, this one is more than an actualization study as the design has also been optimized:

- Calculation of heads and operating times (first calculations of real cycle durations),
- Improvement in valve opening diagrams and first optimizations of the culvert/port network,
- More accurate calculation of hawser forces,
- Filling of the downstream parts of the locks in between the doublegates,
- Flushing of water to prevent salt water intrusion.

In addition, the size of the culverts has been reduced by 20%, and the water usage has been reduced by nearly 10%

In the subsequent studies (preliminary design), the explored tracks will have to be optimized, especially as far as the vessel positioning system and the associated analysis of the hawser forces are concerned.

This will be done by means of more detailed numerical modeling (based upon the Flowmaster™ software in combination with the 2D simulation of the water flow in the lock chamber and more refined numerical modeling of forces and dynamics of ship and vessel positioning system), both prior to and in parallel with the realization of the physical scale model.

On the physical scale model, a precise measurement of the hawser forces will allow to give an important feedback on the F/E system. The numerical modeling should rather be seen as an efficient optimization tool for the hydraulic design (both in gaining quality of the F/E-system as well as in minimizing the total research time), whereas the physical model will be used to confirm the acceptability of the final design of the optimized F/E-system.

Annex 1-1.doc

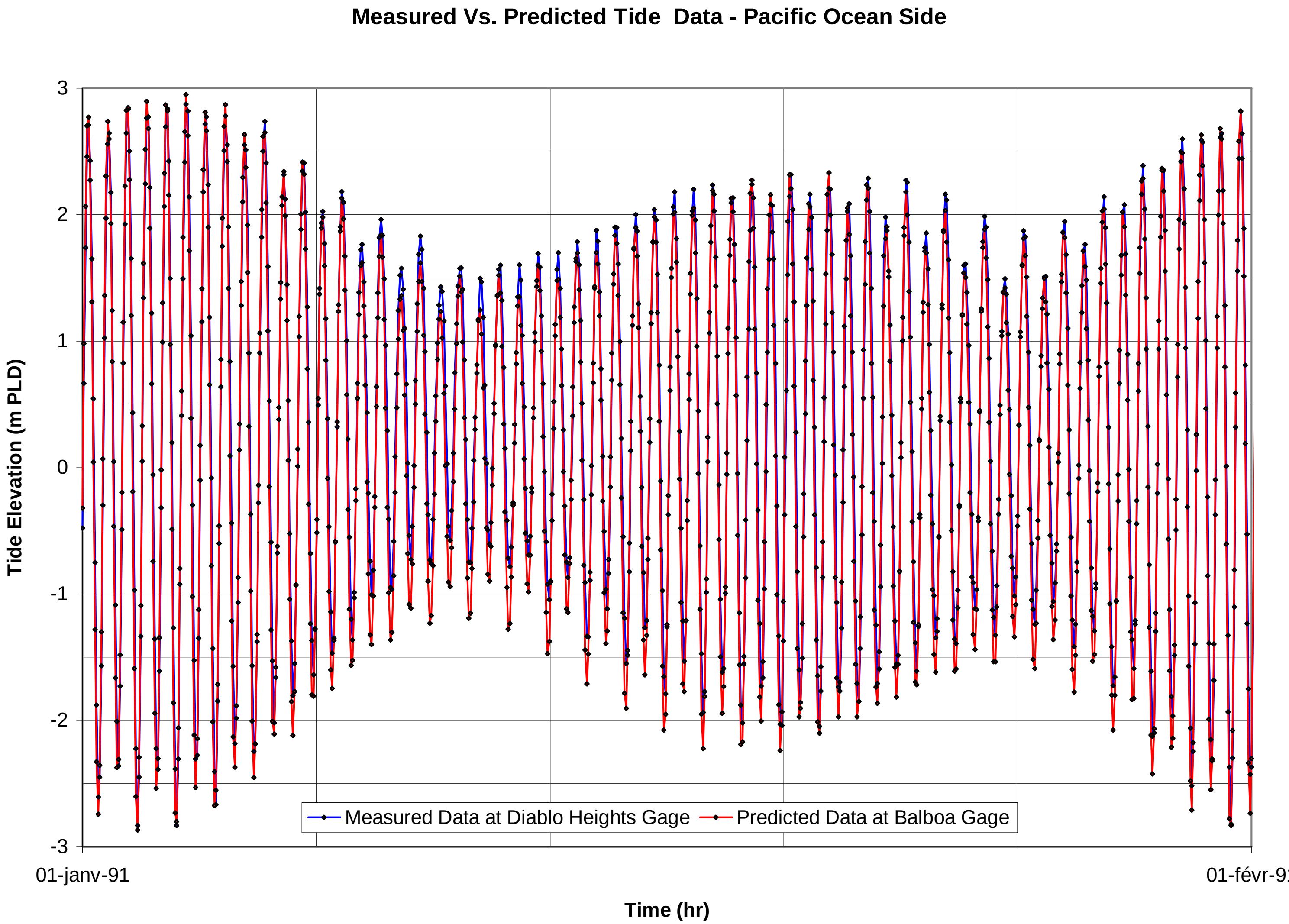
Measured Vs. Predicted Tide Data - Pacific Ocean Side
Tide Elevation (m PLD)
3
2
1
0
-1
-2
-3
01-janv-91
01-févr-91
Time (hr)
Measured Data at Diablo Heights Gage
Predicted Data at Balboa Gage

Annex 1-1.doc

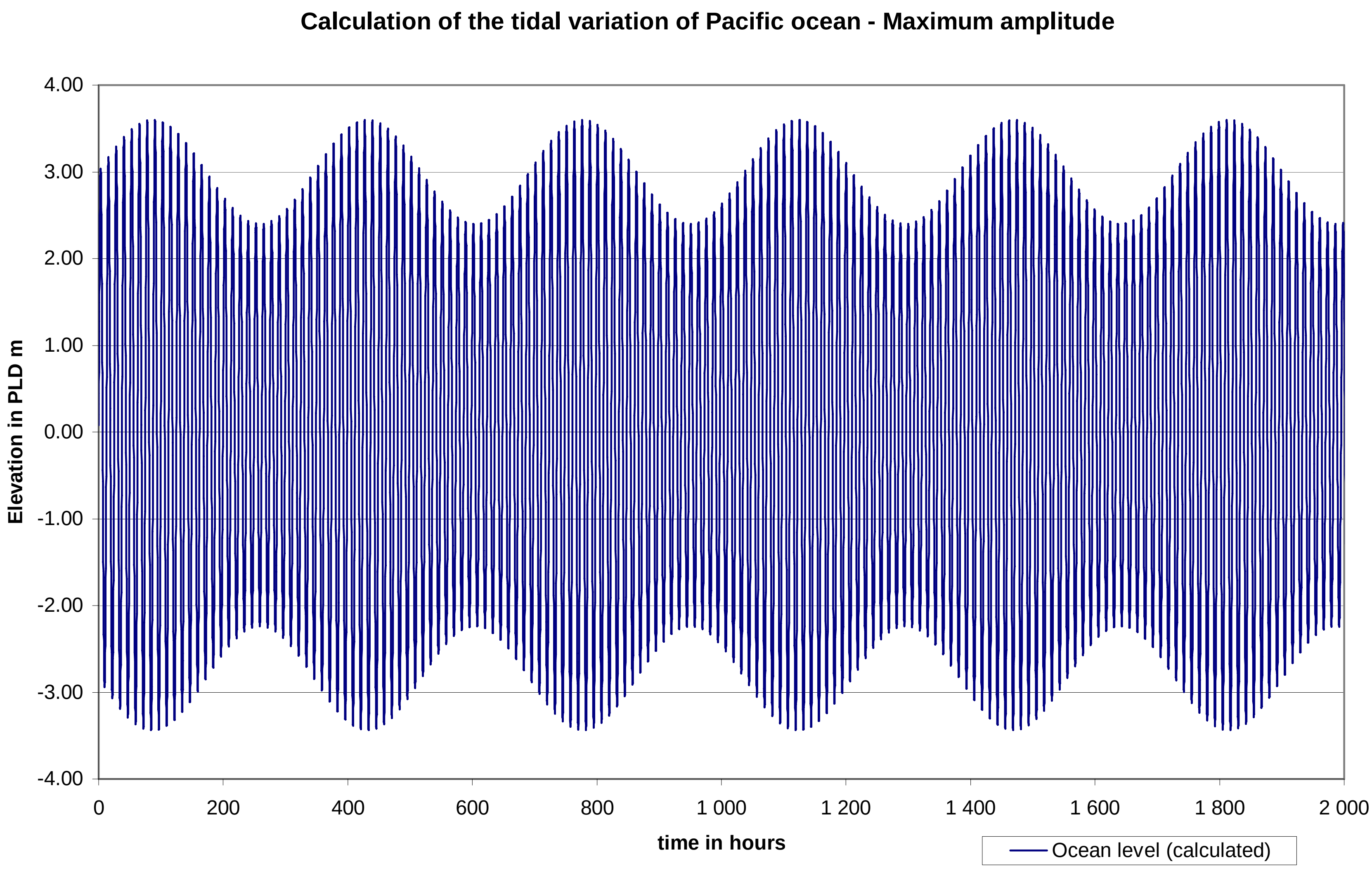

Calculation of the tidal variation of Pacific ocean - Maximum amplitude
4.00
3.00
2.00
1.00
0.00
-1.00
-2.00
-3.00
-4.00
Elevation in PLD m
0
200
400
600
800
1 000
1 200
1 400
1 600
1 800
2 000
time in hours
Ocean level (calculated)

Annex 1-1.doc

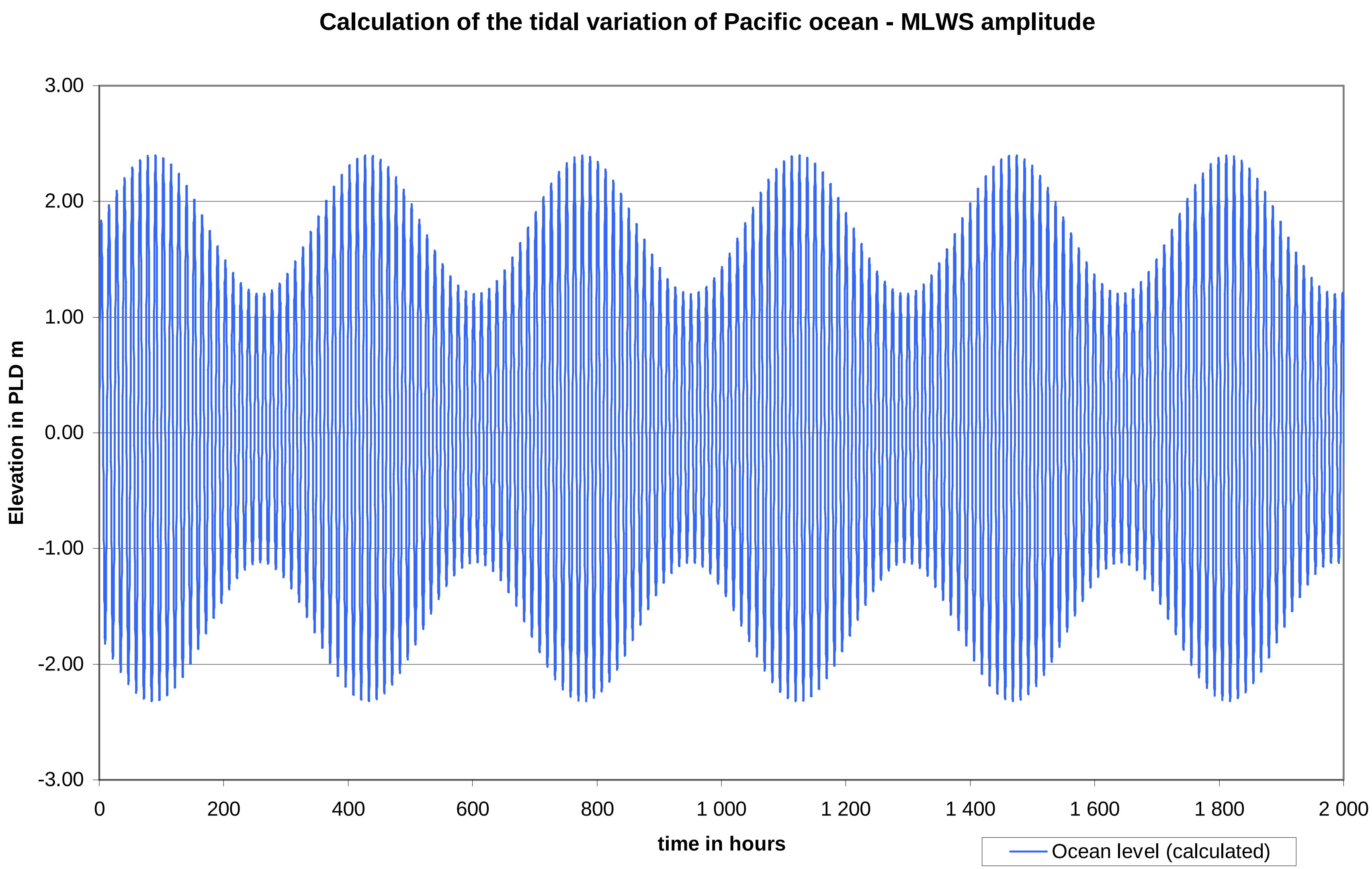

Calculation of the tidal variation of Pacific ocean - MLWS amplitude
Elevation in PLD m
3.00
2.00
1.00
0.00
-1.00
-2.00
-3.00
0
200
400
600
800
1 000
1 200
1 400
1 600
1 800
2 000
time in hours
Ocean level (calculated)

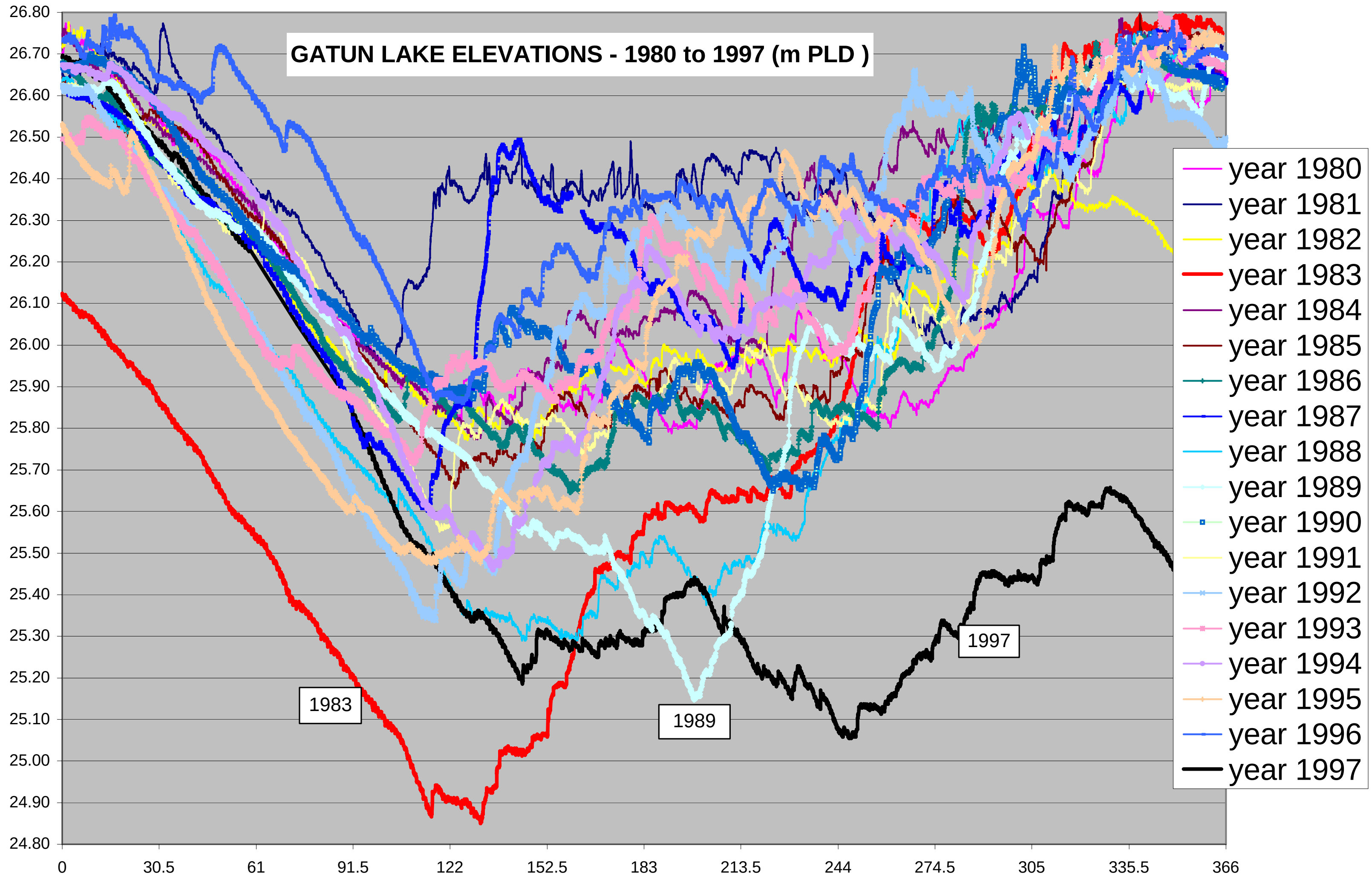
GATUN LAKE ELEVATIONS - 1980 to 1997 (m PLD)
26.80
26.70
26.60
26.50
26.40
26.30
26.20
26.10
26.00
25.90
25.80
25.70
25.60
25.50
25.40
25.30
25.20
25.10
25.00
24.90
24.80
0
30.5
61
91.5
122
152.5
183
213.5
244
274.5
305
335.5
366
1983
1989
1997
year 1980
year 1981
year 1982
year 1983
year 1984
year 1985
year 1986
year 1987
year 1988
year 1989
year 1990
year 1991
year 1992
year 1993
year 1994
year 1995
year 1996
year 1997

Annex 1-3.doc

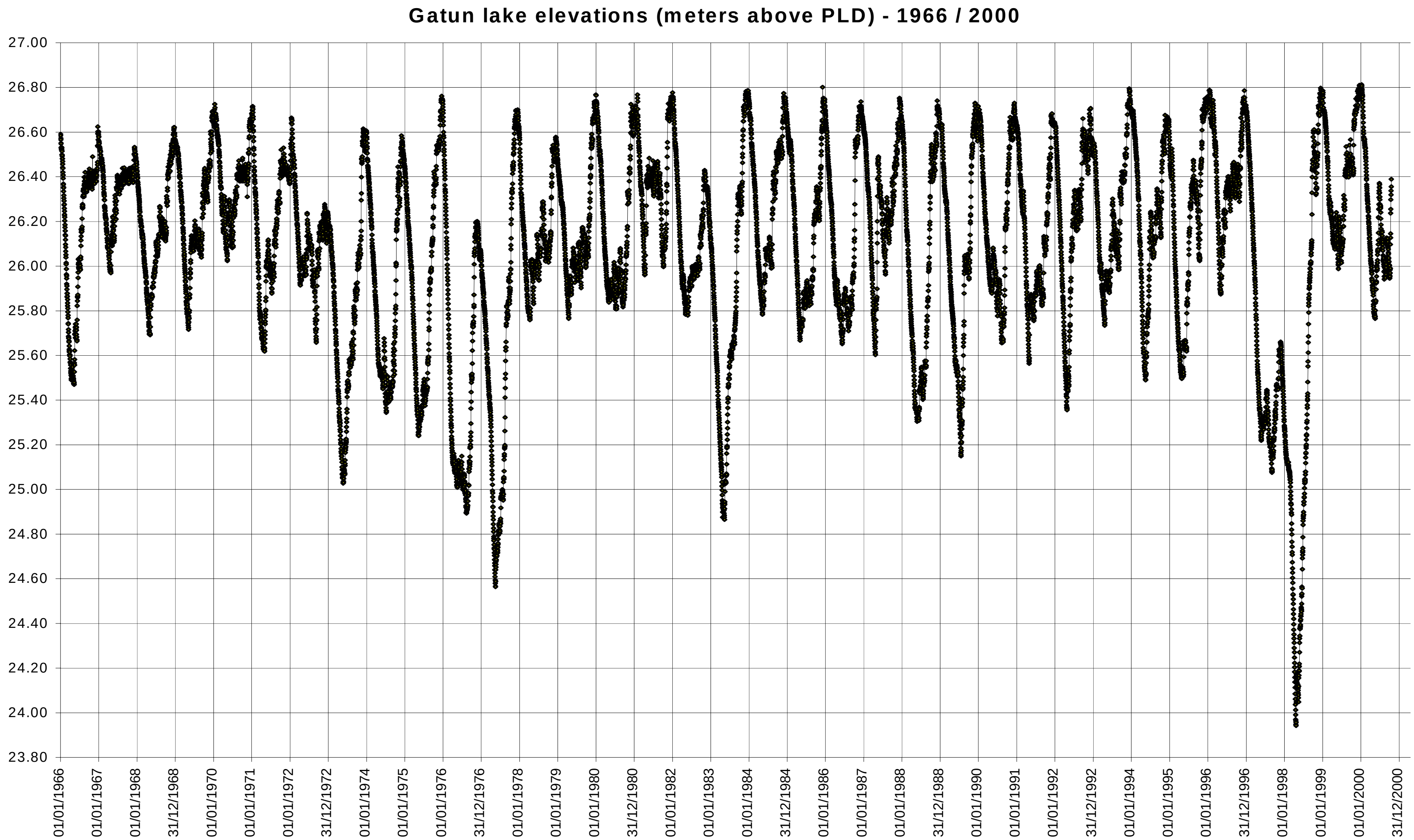

Gatun lake elevations (meters above PLD) - 1966 / 2000
27.00
26.80
26.60
26.40
26.20
26.00
25.80
25.60
25.40
25.20
25.00
24.80
24.60
24.40
24.20
24.00
23.80
01/01/1966
01/01/1967
01/01/1968
31/12/1968
01/01/1970
01/01/1971
01/01/1972
31/12/1972
01/01/1974
01/01/1975
01/01/1976
31/12/1976
01/01/1978
01/01/1979
01/01/1980
31/12/1980
01/01/1982
01/01/1983
01/01/1984
31/12/1984
01/01/1986
01/01/1987
01/01/1988
31/12/1988
01/01/1990
01/01/1991
01/01/1992
31/12/1992
01/01/1994
01/01/1995
01/01/1996
31/12/1996
01/01/1998
01/01/1999
01/01/2000
31/12/2000

Annex 1-4.doc

This annex presents additionnal simulations run in order to show that extreme water levels reached in chamber and WSB depend on initialization conditions at the beginning.

We first made a simulation given the following conditions:

- Gatun lake level : 27.13 PLD m
- Pacific ocean level at time 0 : +3.60 PLD m
- Starting levels in chamber and WSB for the first 12h cycle calculated with a total head of 23.53 m (27.13 – 3.60), see H/3 and h/5 value on annex 1.
- Reset levels in chamber and WSB for all 12h cycles (excepted the first one) calculated with a total head of 26.82 m (27.13 - 0.3048), see H/3 and h/5 value on annex 1.

NB: 0.3048 PLD m corresponds to the mean ocean level.
The results are shown on graphs 1 (see hereafter).

We made the same simulation with Pacific Ocean level starting at -3.44 PLD m at time 0:

- Gatun lake level : 27.13 PLD m
- Pacific ocean level at time 0 : -3.44 PLD m
- Starting levels in chamber and WSB for the first 12h cycle calculated with a total head of 30.57 m (27.13 – (-3.44)), see H/3 and h/5 value on annex 1.
- Reset levels in chamber and WSB for all the 12h cycle (excepted the first one) calculated with a total head of 26.82 m (27.13 - 0.3048), see H/3 and h/5 value on annex 1.

The results are shown on graphs 2 (see hereafter).

It can be seen that the initial levels conditions in lock chamber and WSB lead to a water level shift at the beginning of the first 12h cycle. Then, the water levels reach quickly a mean value and oscillate around it until the end of the simulation. Those levels are the ones indicated on the drawing n° D2-0-106.

The graph 2 shows the results of other simulations given the following conditions:

- Gatun lake level : 27.13 PLD m
- Pacific ocean level at time 0 : +3.60 and -3.44 PLD m

Annex 1-4.doc

- Starting levels in chamber and WSB for all the 12h cycle calculated with a total head of 26.82 m (27.13 - 0.3048), see H/3 and h/5 value on annex 1.

The graphic 3 does not show any water level shift whatever the initial Pacific Ocean level.

To conclude, it appears that the best way to operate the locks is to initialize water levels in lock chamber and WSB taking into account the mean Ocean level (0.3048 PLD m). Any other initialization leads :

- to shift the water level in lock chamber by almost 1 m (1.03 m) in the worst case and to oversize the lock chamber height.

- to lower the level of sills of the chambers by nearly 2 m value (1.80 m)

- both

Annex 1-4.doc
Graph 1

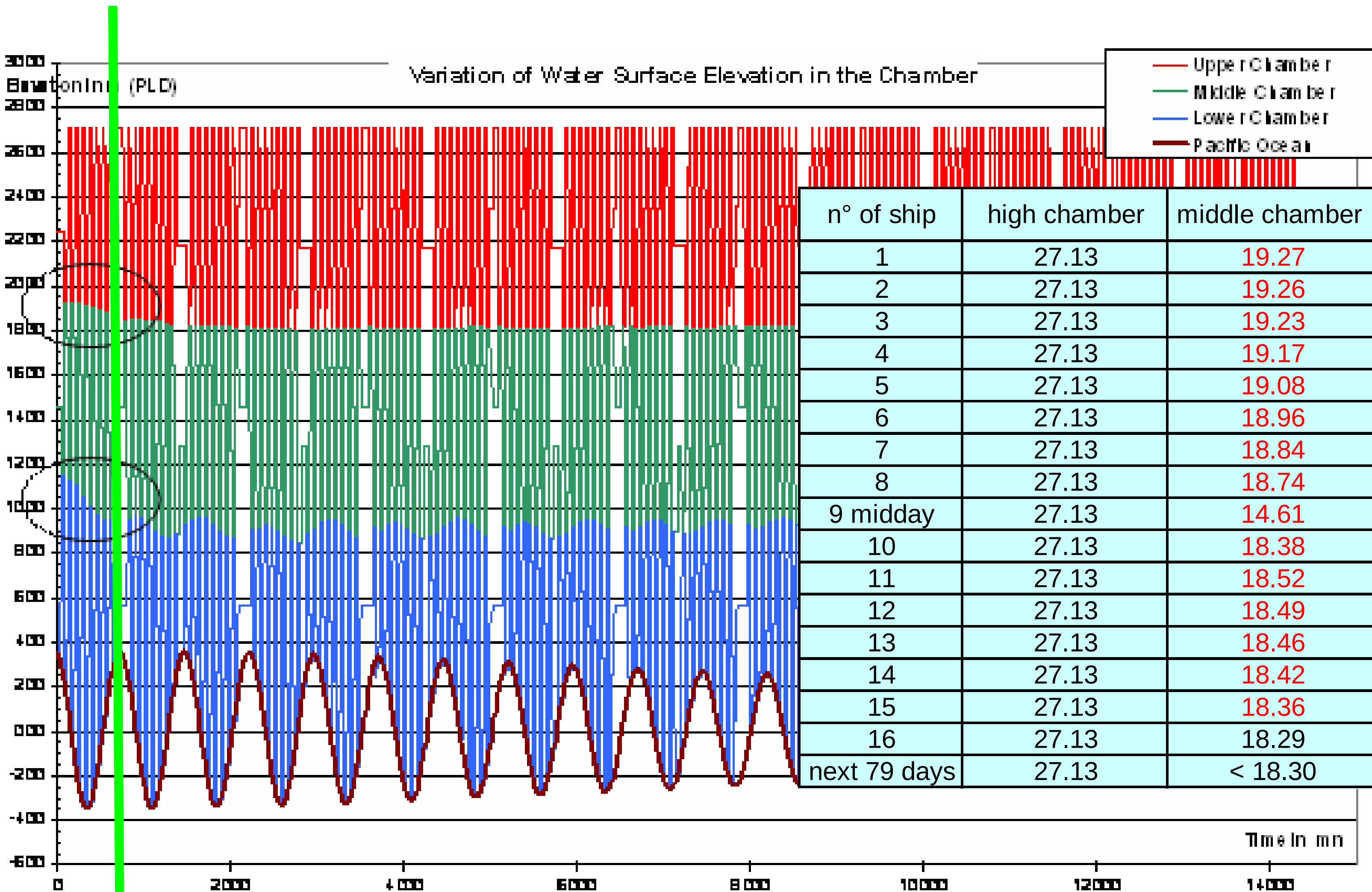

n° of ship	high chamber	middle chamber	low chamber
1	27.13	19.27	11.41
2	27.13	19.26	11.29
3	27.13	19.23	11.00
4	27.13	19.17	10.55
5	27.13	19.08	10.10
6	27.13	18.96	9.70
7	27.13	18.84	< 9.81
8	27.13	18.74	"
9 midday	27.13	14.61	"
10	27.13	18.38	"
11	27.13	18.52	"
12	27.13	18.49	"
13	27.13	18.46	"
14	27.13	18.42	"
15	27.13	18.36	"
16	27.13	18.29	"
next 79 days	27.13	< 18.30	< 9.81

Limit of the first 12h cycle

Annex 1-4.doc
Graph 2

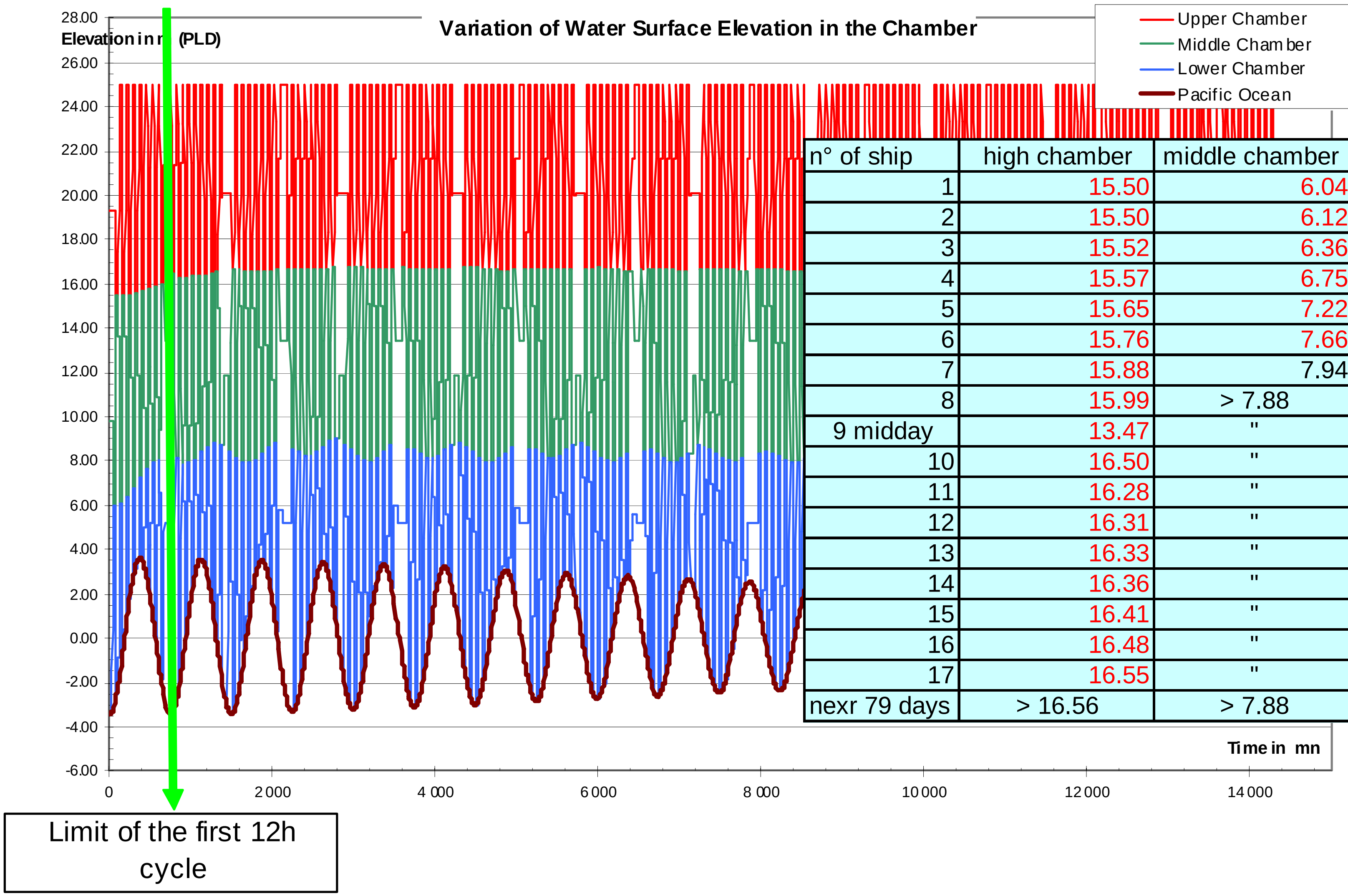

n° of ship	high chamber	middle chamber	low chamber
1	15.50	6.04	ocean level
2	15.50	6.12	"
3	15.52	6.36	"
4	15.57	6.75	"
5	15.65	7.22	"
6	15.76	7.66	"
7	15.88	7.94	"
8	15.99	> 7.88	"
9 midday	13.47	"	"
10	16.50	"	"
11	16.28	"	"
12	16.31	"	"
13	16.33	"	"
14	16.36	"	"
15	16.41	"	"
16	16.48	"	"
17	16.55	"	"
nexr 79 days	> 16.56	> 7.88	

Annex 1-4.doc
Graph 3

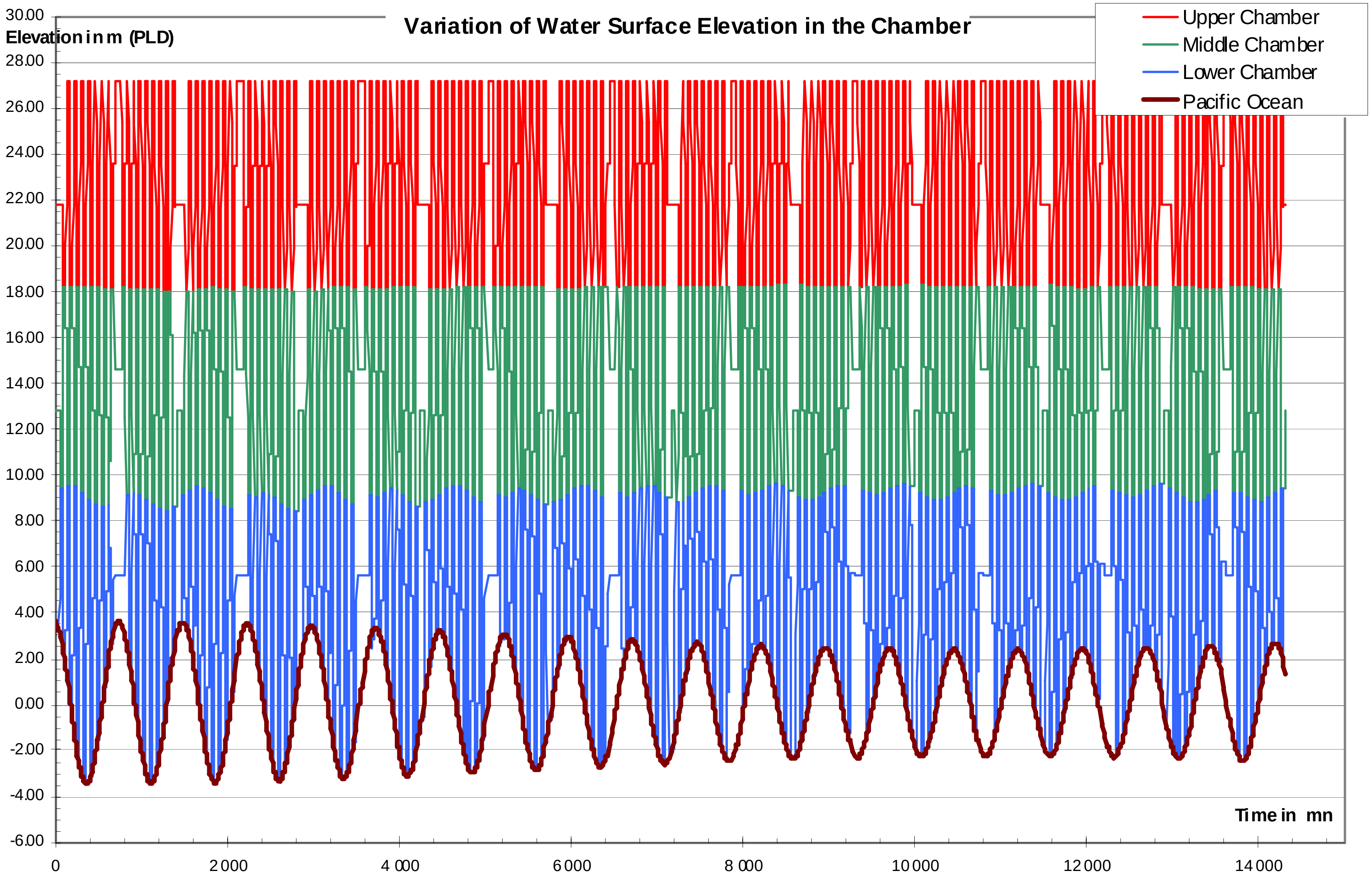

Annex 1-5.doc

	Minimum level in m PLD											
Simulation duration in days	Upper chamber	Up. WSB	Inter. WSB	Low. WSB	Middle chamber	Up. WSB	Inter. WSB	Low. WSB	Lower chamber	Up. WSB	Inter. WSB	Low. WSB
10	17.68	23.09	21.29	19.49	8.45	14.06	12.21	10.34	-3.44	4.60	2.35	-0.19
20	17.68	23.09	21.29	19.49	8.45	14.06	12.21	10.34	-3.44	4.50	2.30	-0.29
40	17.65	23.08	21.28	19.47	8.34	14.01	12.16	10.29	-3.44	4.45	2.24	-0.32
60	17.64	23.08	21.27	19.46	8.30	14.00	12.13	10.23	-3.44	4.36	2.19	-0.32
80	17.63	23.07	21.27	19.45	8.22	13.98	12.11	10.19	-3.44	4.29	2.03	-0.42
100	17.63	23.07	21.27	19.45	8.22	13.98	12.10	10.19	-3.44	4.27	2.03	-0.44
110	17.63	23.07	21.27	19.45	8.22	13.98	12.10	10.19	-3.44	4.27	2.03	-0.44

	Maximum levels in m PLD											
Simulation duration in days	Upper chamber	Up. WSB	Inter. WSB	Low. WSB	Middle chamber	Up. WSB	Inter. WSB	Low. WSB	Lower chamber	Up. WSB	Inter. WSB	Low. WSB
10	26.67	24.93	23.19	21.45	17.99	16.27	14.58	12.90	9.65	8.09	6.62	5.37
20	26.67	24.93	23.19	21.45	17.99	16.27	14.58	12.90	9.65	8.09	6.62	5.37
40	26.67	24.93	23.19	21.45	17.99	16.27	14.58	12.90	9.66	8.09	6.62	5.38
60	26.67	24.93	23.19	21.45	17.99	16.27	14.58	12.90	9.66	8.09	6.62	5.38
80	26.67	24.93	23.19	21.45	17.99	16.27	14.58	12.91	9.66	8.09	6.62	5.38
100	26.67	24.93	23.19	21.45	17.99	16.27	14.58	12.91	9.66	8.09	6.62	5.38
110	26.67	24.93	23.19	21.45	17.99	16.27	14.58	12.91	9.66	8.09	6.62	5.38

Annex 1-5.doc

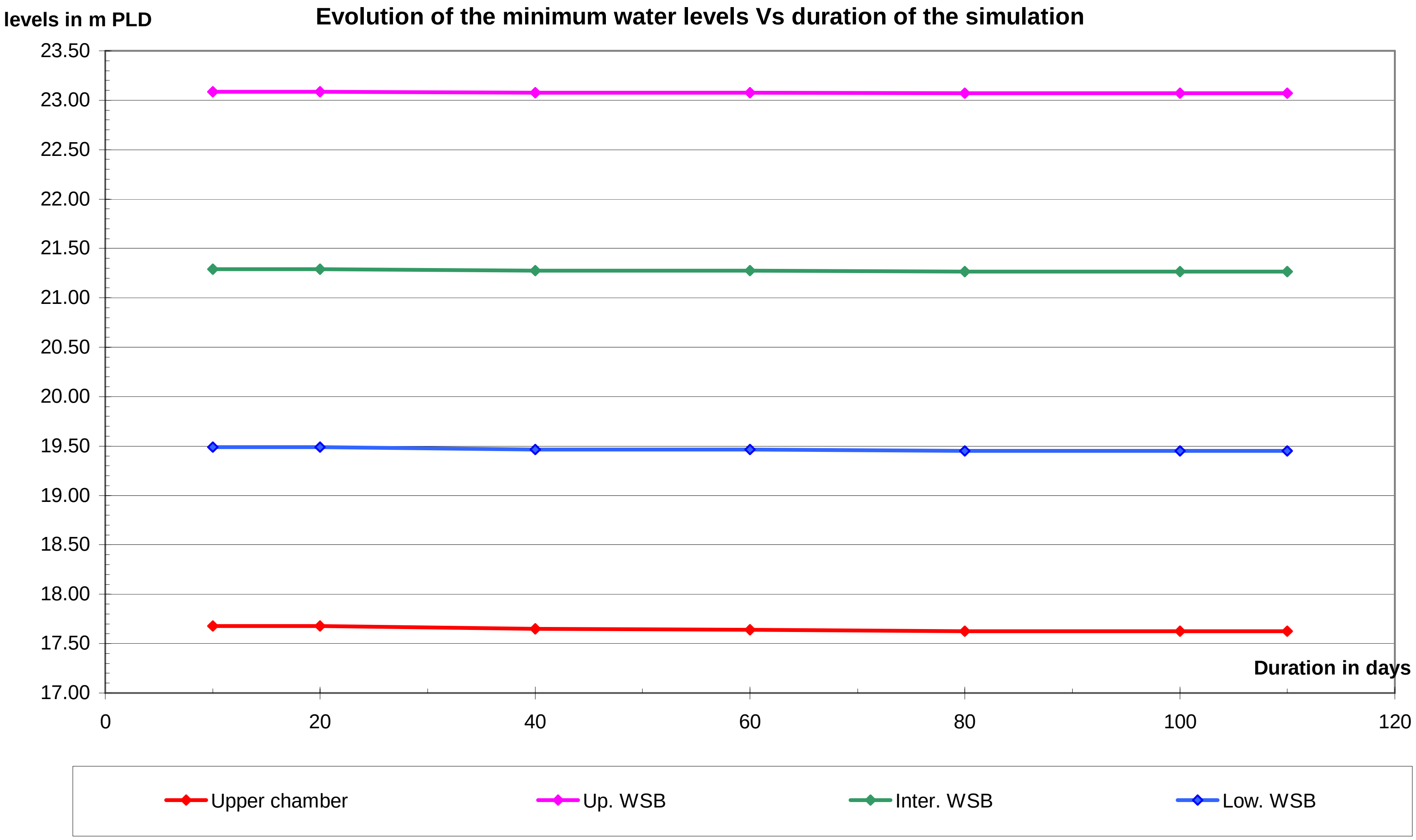

Evolution of the minimum water levels Vs duration of the simulation
levels in m PLD
23.50
23.00
22.50
22.00
21.50
21.00
20.50
20.00
19.50
19.00
18.50
18.00
17.50
17.00
0
20
40
60
80
100
120
Duration in days
Upper chamber
Up. WSB
Inter. WSB
Low. WSB

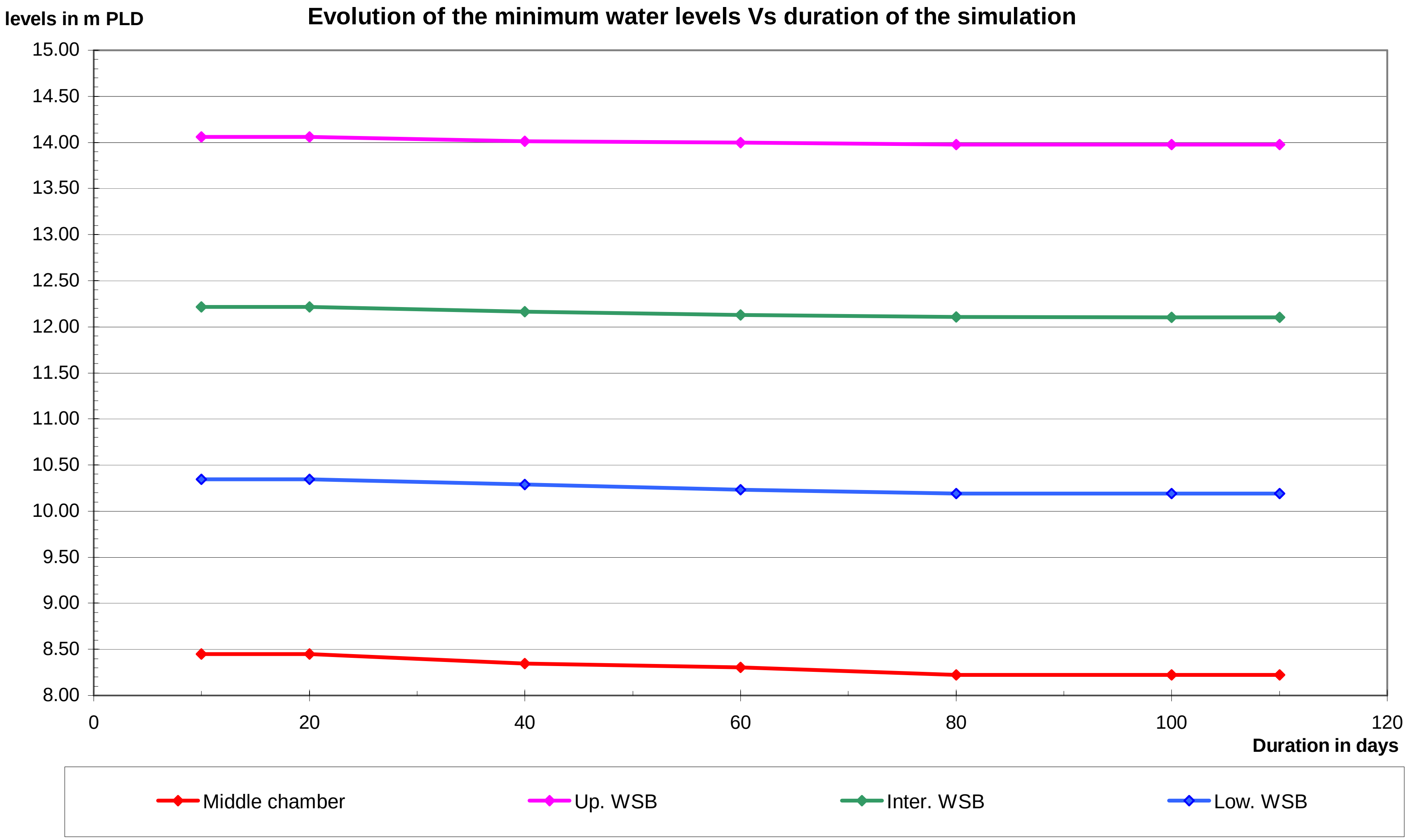
levels in m PLD
Evolution of the minimum water levels Vs duration of the simulation
15.00
14.50
14.00
13.50
13.00
12.50
12.00
11.50
11.00
10.50
10.00
9.50
9.00
8.50
8.00
0
20
40
60
80
100
120
Duration in days
Middle chamber
Up. WSB
Inter. WSB
Low. WSB

Annex 1-5.doc

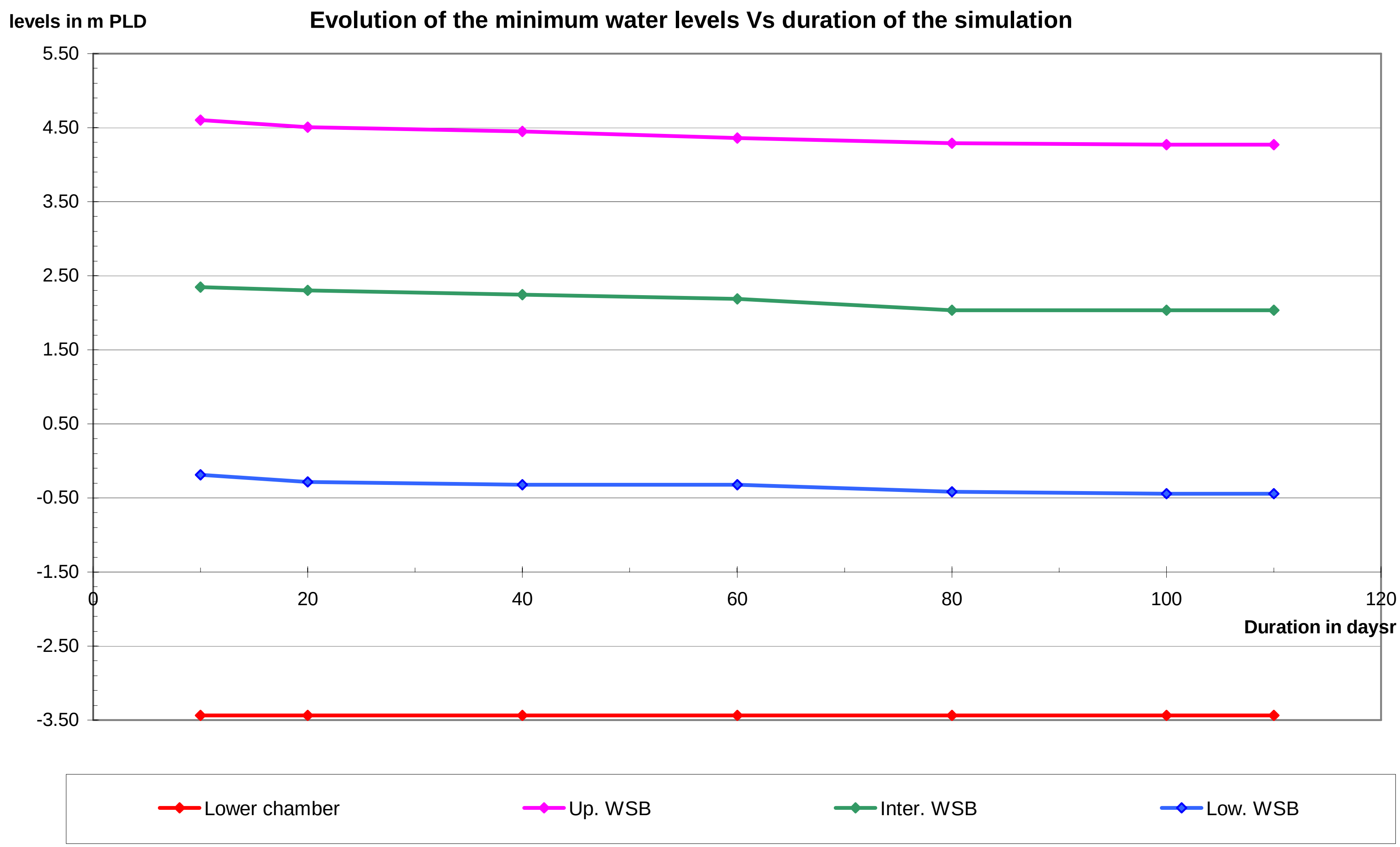
levels in m PLD
Evolution of the minimum water levels Vs duration of the simulation
5.50
4.50
3.50
2.50
1.50
0.50
-0.50
-1.50
-2.50
-3.50
0
20
40
60
80
100
120
Duration in daysr
Lower chamber
Up. WSB
Inter. WSB
Low. WSB

Annex 1-6.doc

Lift Lac/Upper lock	Lift Upper lock/Top WSB	Lift Upper lock/Inter. WSB	Lift Upper lock/bottom WSB	Lift Upper lock/Middle lock	Lift Middle lock/Top WSB	Lift Middle lock/Inter. WSB	Lift Middle lock/bottom WSB	Lift Middle lock/Lower lock	Lift Lower lock/Top WSB	Lift Lower lock/Inter. WSB	Lift Lower lock/Bottom WSB	Lift Lower lock/Ocean
	3.61						**-3.68**		2.68			
sb		**3.61**				-3.56				2.82		
			3.61		-3.54						2.93	
				7.16								**8.28**
			-3.58		3.58						**-8.38**	
		-3.59				3.56				**-5.66**		
	-3.6						3.56		**-4.24**			
3.60								**7.08**				
	3.60						-3.54		3.54			
sb		3.60				-3.55				**3.89**		
			3.60		-3.56						**4.77**	
				7.16								**6.31**
‹												

Annex 1-7.doc

1	entry of 1st ship into upper lock
2	closing of upstream gates upper lock
3	closing upstream gates lower lock
4	filling upper top wsb
5	filling middle lock by middle bottom wsb
6	filling lower top wsb
7	filling upper intermediate wsb
8	filling middle lock from middle intermediate w
9	filling lower intermediate wsb
10	filling upper bottom wsb
11	filling middle lock from middle top wsb
12	filling lower bottom wsb
13	F/E upper lock / middle lock
14	E lower lock into Ocean
15	opening downstream gates lower lock
16	opening upstream gates middle lock
17	displacement 1st ship upper lock / middle loc
18	closing downstream gates lower lock
19	closing upstream gates middle lock
20	filling upstream lock from upper bottom wsb
21	filling middle top wsb
22	filling lower lock from lower bottom wsb
23	filling upper lock from upper intermediate wsb
24	filling middle intermediate wsb
25	filling lower lock from lower intermediate wsb
26	filling upper lock from upper top wsb
27	filling middle bottom wsb
28	filling lower lock from lower top wsb
29	F/E middle lock / lower lock
30	filling upper lock from Gatun lake
31	opening upstream gates upper lock
32	opening downstream gates middle lock
33	displacement 1st ship middle lock / lower lock
34	entry of 2nd ship into upper lock
35	closing upstream gates upper lock
36	closing upstream gates lower lock

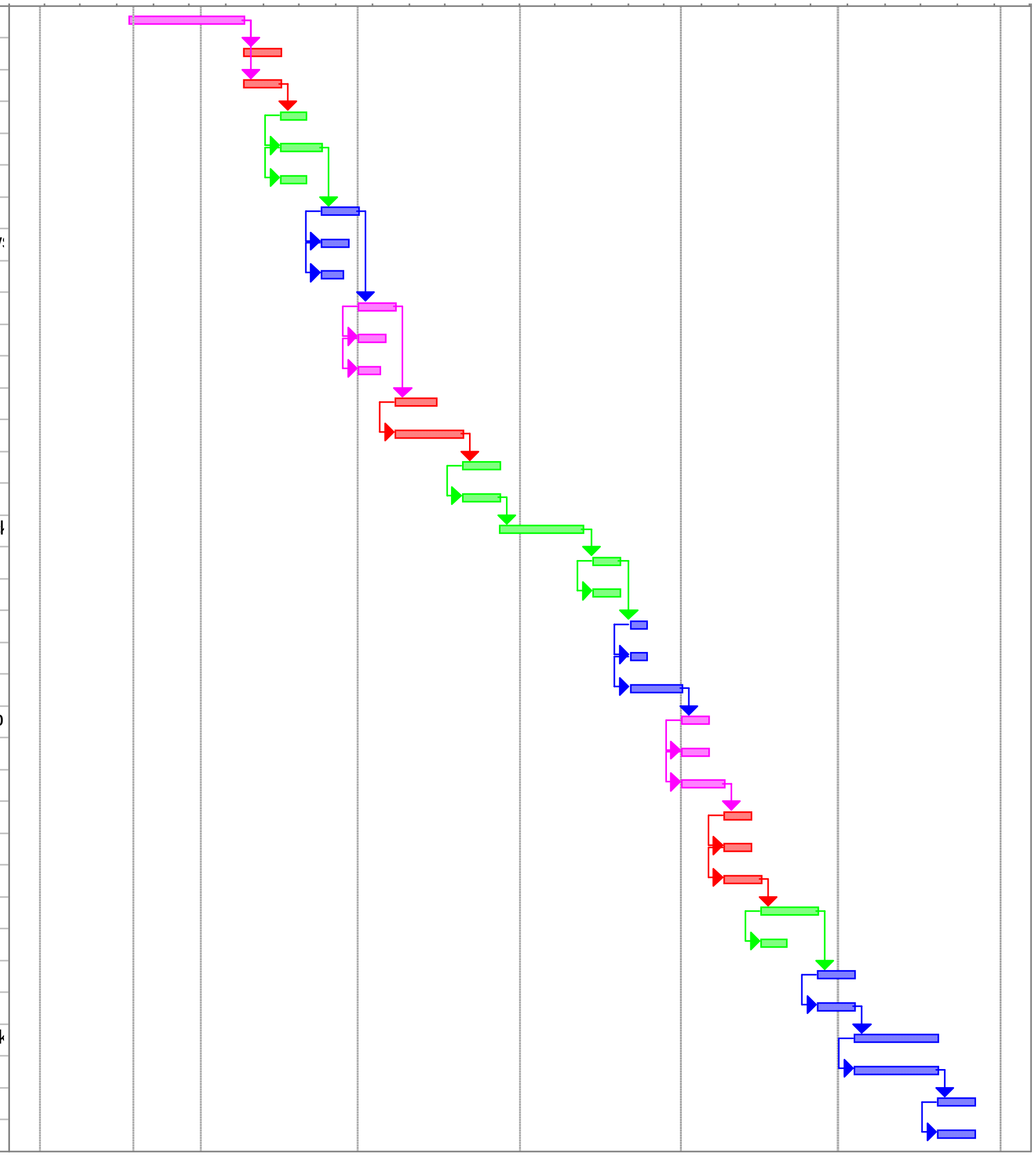

Annex 2-1.doc

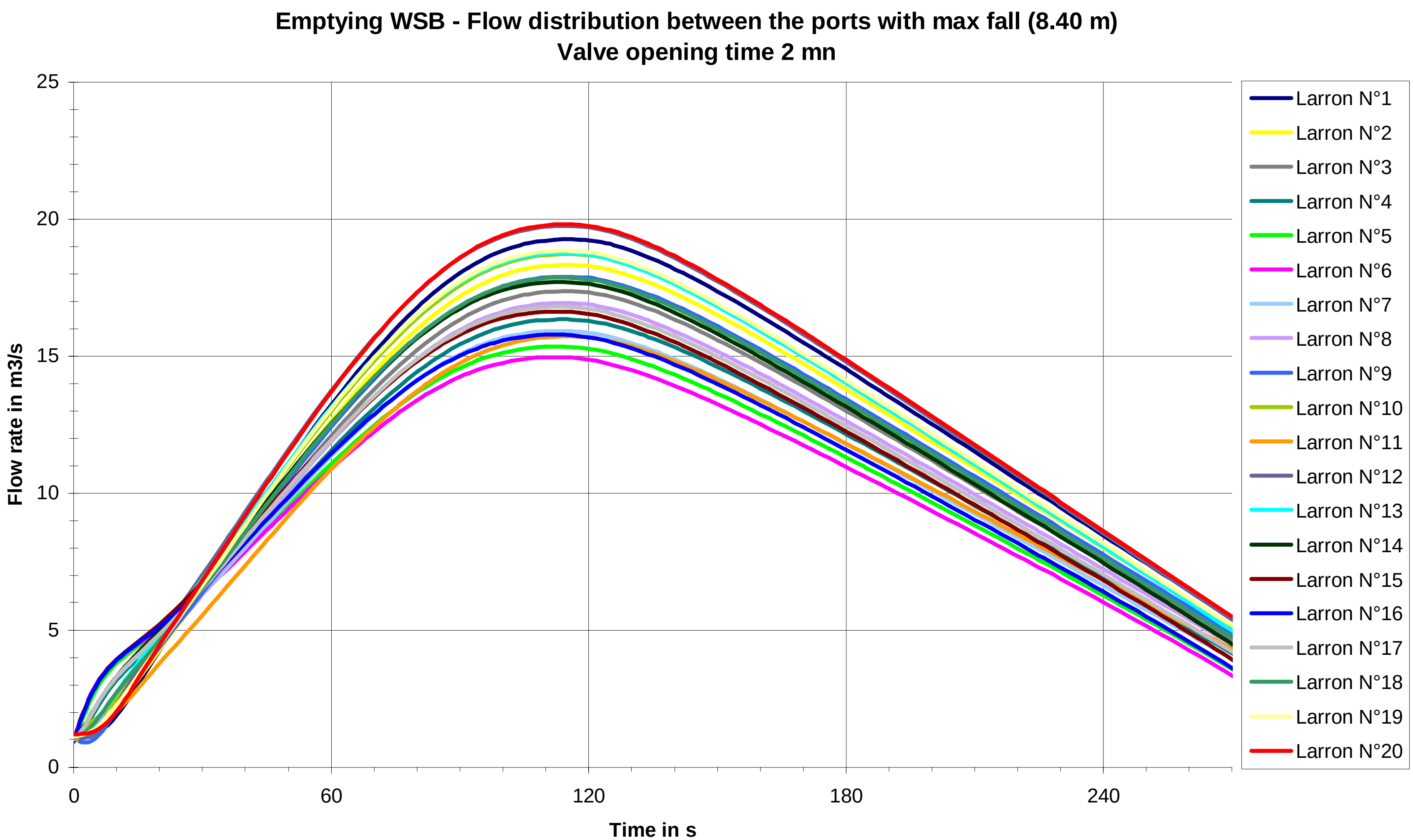
Emptying WSB - Flow distribution between the ports with max fall (8.40 m)
Valve opening time 2 mn
Flow rate in m3/s
25
20
15
10
5
0
0
60
120
180
240
Time in s
Larron N°1
Larron N°2
Larron N°3
Larron N°4
Larron N°5
Larron N°6
Larron N°7
Larron N°8
Larron N°9
Larron N°10
Larron N°11
Larron N°12
Larron N°13
Larron N°14
Larron N°15
Larron N°16
Larron N°17
Larron N°18
Larron N°19
Larron N°20

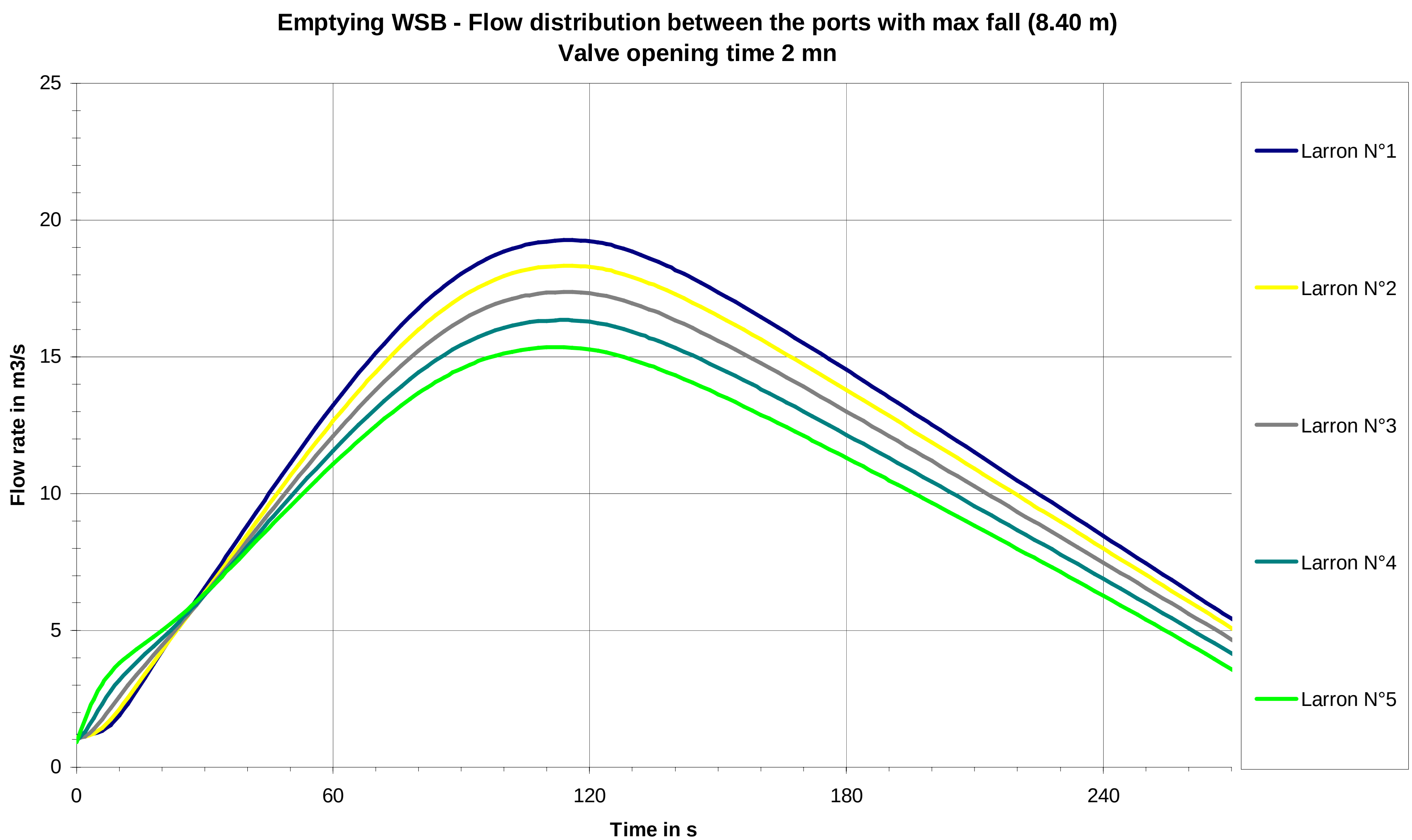
Emptying WSB - Flow distribution between the ports with max fall (8.40 m)
Valve opening time 2 mn
Flow rate in m3/s
Time in s
0
5
10
15
20
25
0
60
120
180
240
Larron N°1
Larron N°2
Larron N°3
Larron N°4
Larron N°5

Annex 2-3.doc

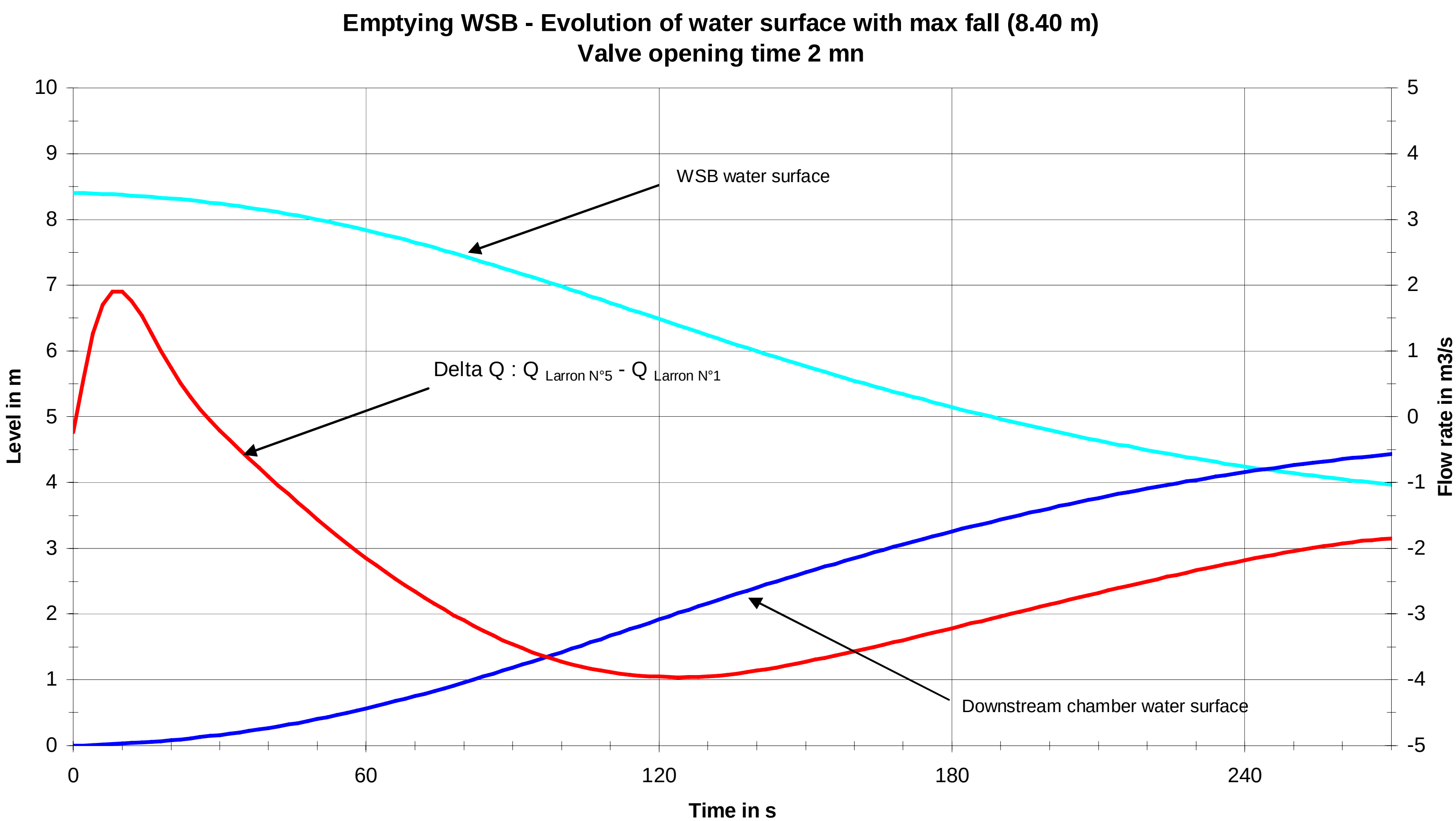

Emptying WSB - Evolution of water surface with max fall (8.40 m)
Valve opening time 2 mn
WSB water surface
Delta Q : Q Larron N°5 - Q Larron N°1
Downstream chamber water surface
Level in m
Flow rate in m3/s
Time in s
0
60
120
180
240
10
9
8
7
6
5
4
3
2
1
0
5
4
3
2
1
0
-1
-2
-3
-4
-5

Annex 3-1.doc

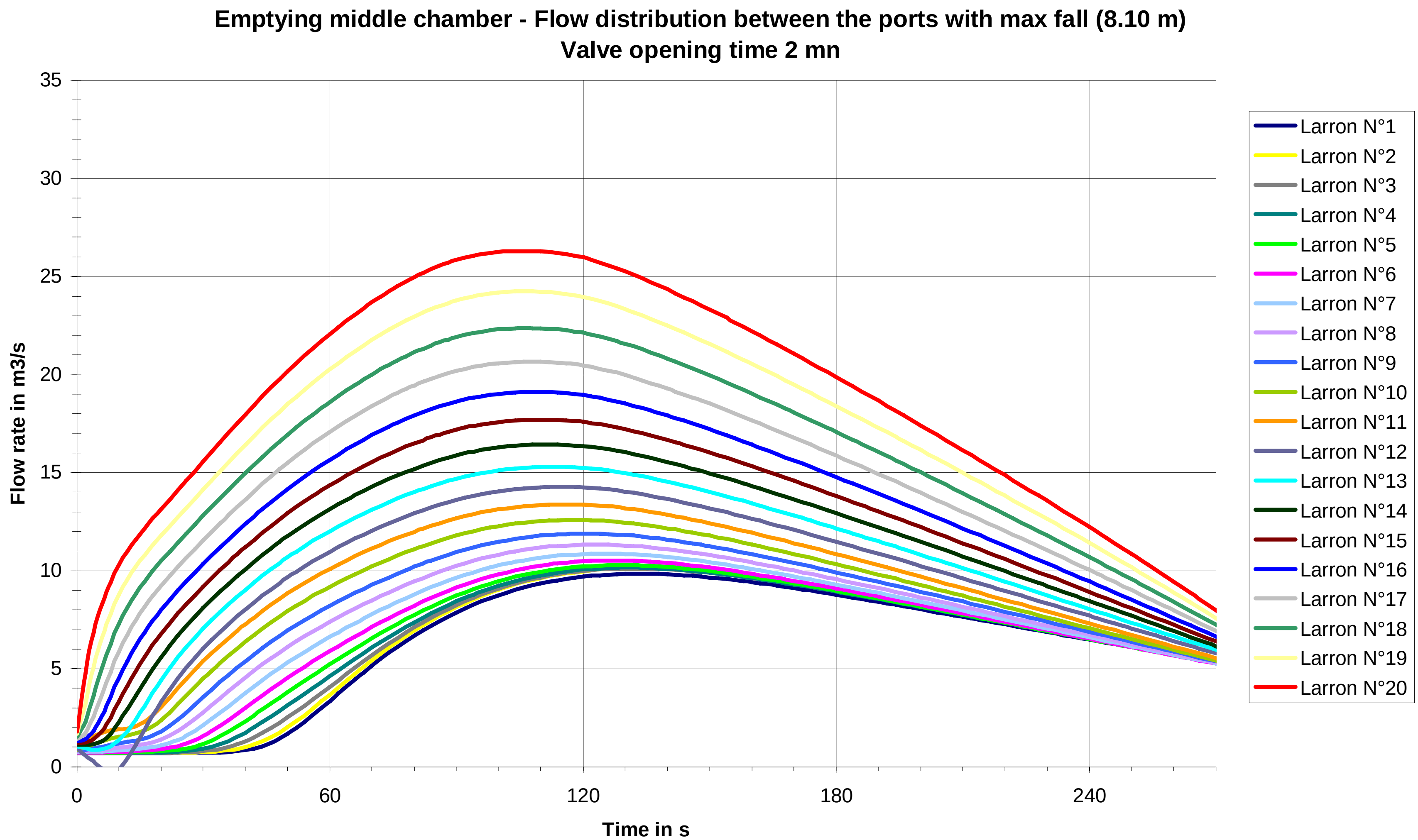

Emptying middle chamber - Flow distribution between the ports with max fall (8.10 m)
Valve opening time 2 mn
Flow rate in m3/s
Time in s
0
5
10
15
20
25
30
35
0
60
120
180
240
Larron N°1
Larron N°2
Larron N°3
Larron N°4
Larron N°5
Larron N°6
Larron N°7
Larron N°8
Larron N°9
Larron N°10
Larron N°11
Larron N°12
Larron N°13
Larron N°14
Larron N°15
Larron N°16
Larron N°17
Larron N°18
Larron N°19
Larron N°20

Annex 3-2.doc

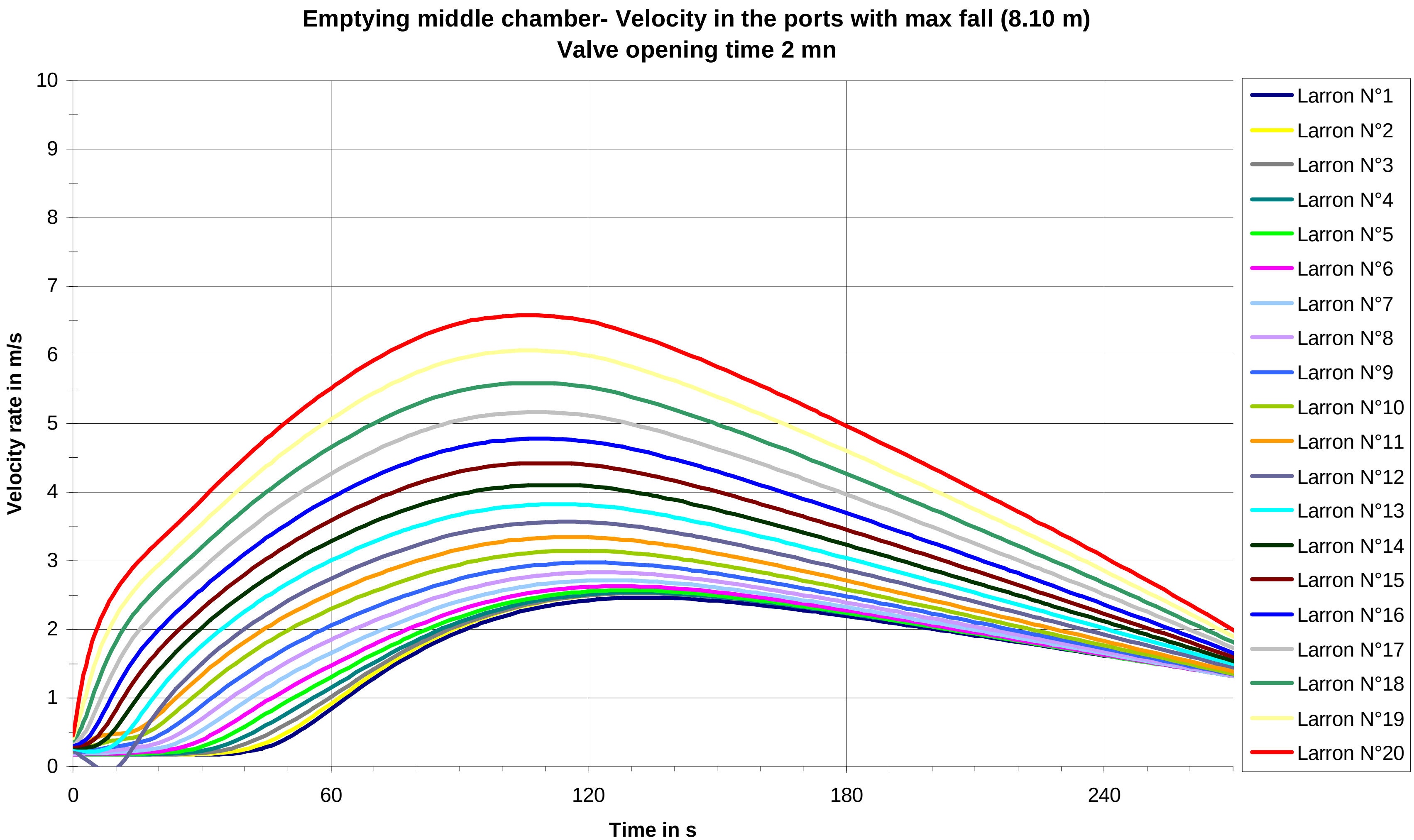
Emptying middle chamber- Velocity in the ports with max fall (8.10 m)
Valve opening time 2 mn
Velocity rate in m/s
Time in s
0
1
2
3
4
5
6
7
8
9
10
60
120
180
240
Larron N°1
Larron N°2
Larron N°3
Larron N°4
Larron N°5
Larron N°6
Larron N°7
Larron N°8
Larron N°9
Larron N°10
Larron N°11
Larron N°12
Larron N°13
Larron N°14
Larron N°15
Larron N°16
Larron N°17
Larron N°18
Larron N°19
Larron N°20

Annex 3-3.doc

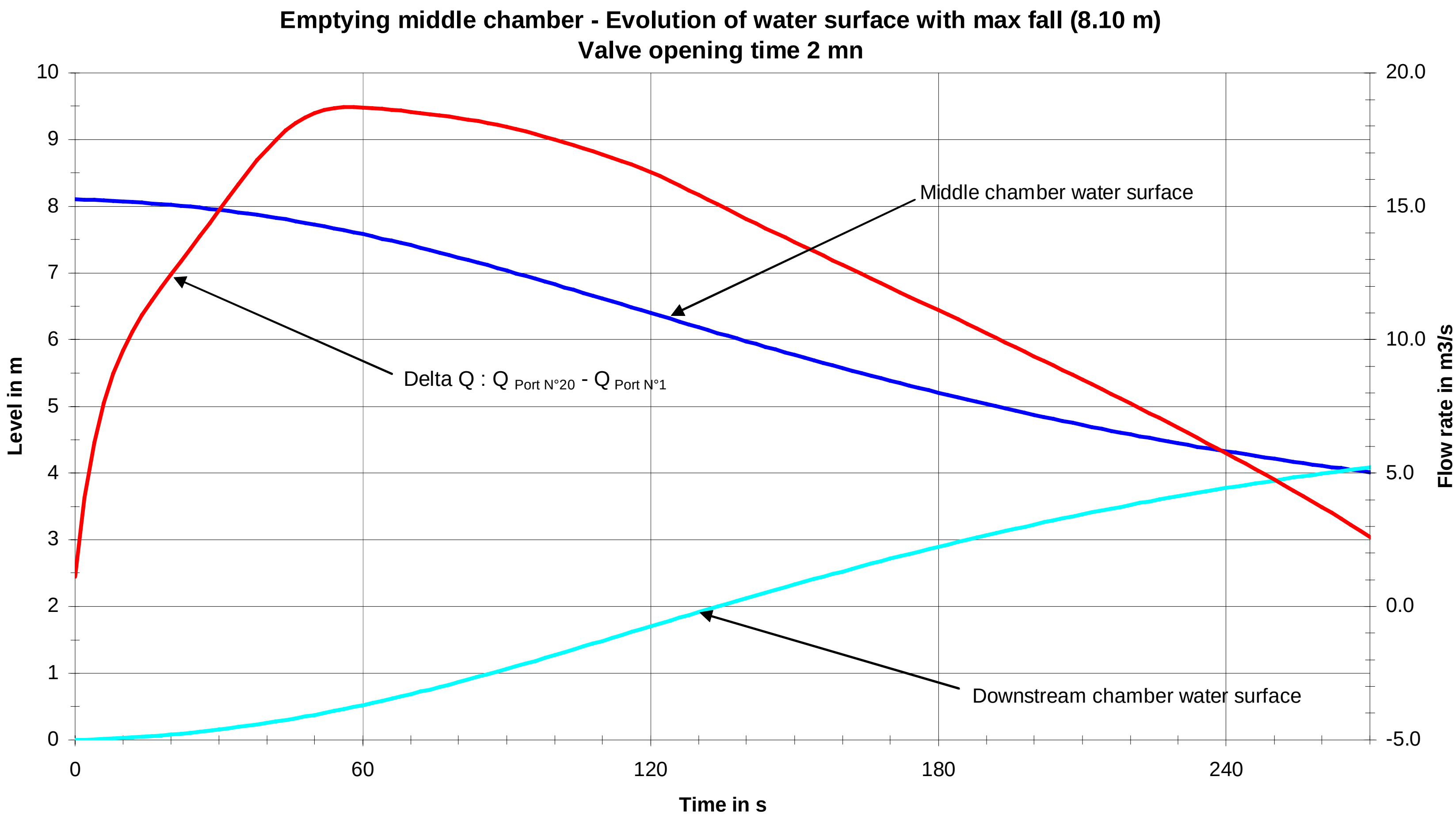

Emptying middle chamber - Evolution of water surface with max fall (8.10 m)
Valve opening time 2 mn
Level in m
Flow rate in m3/s
Time in s
0
1
2
3
4
5
6
7
8
9
10
-5.0
0.0
5.0
10.0
15.0
20.0
0
60
120
180
240
Middle chamber water surface
Delta Q : Q Port N°20 - Q Port N°1
Downstream chamber water surface

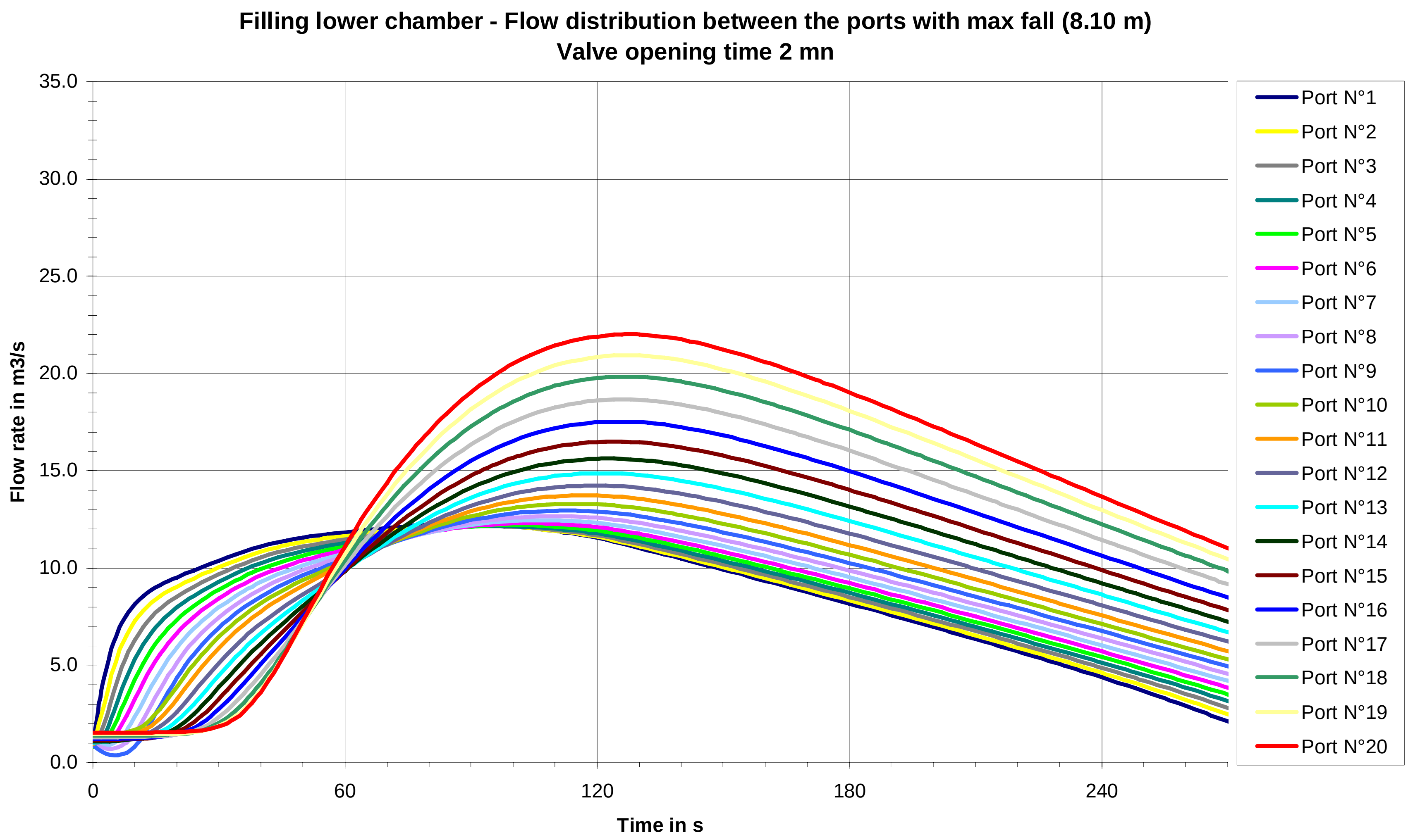
Filling lower chamber - Flow distribution between the ports with max fall (8.10 m)
Valve opening time 2 mn
Flow rate in m3/s
Time in s
35.0
30.0
25.0
20.0
15.0
10.0
5.0
0.0
0
60
120
180
240
Port N°1
Port N°2
Port N°3
Port N°4
Port N°5
Port N°6
Port N°7
Port N°8
Port N°9
Port N°10
Port N°11
Port N°12
Port N°13
Port N°14
Port N°15
Port N°16
Port N°17
Port N°18
Port N°19
Port N°20

Annex 4-2.doc

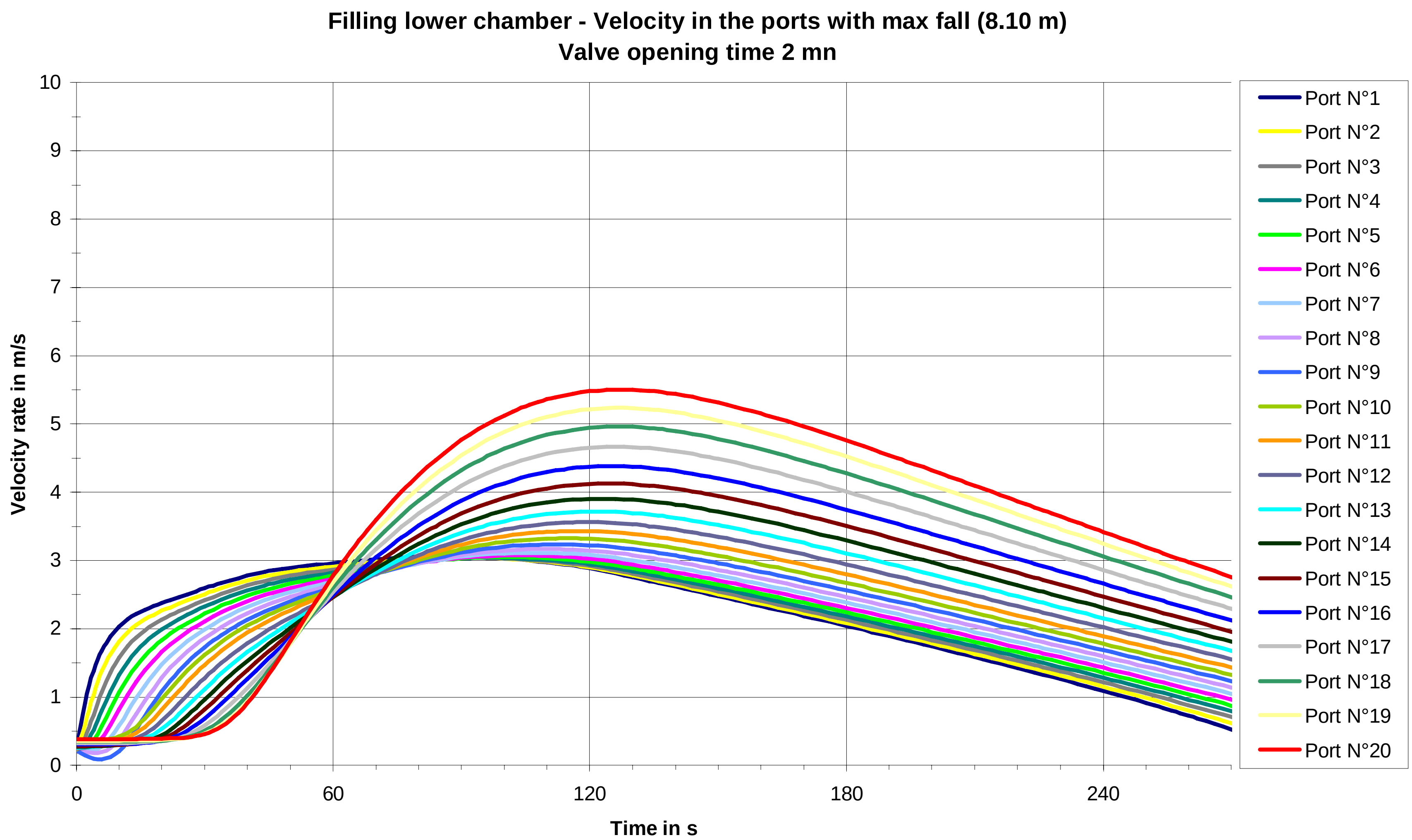

Filling lower chamber - Velocity in the ports with max fall (8.10 m)
Valve opening time 2 mn
Velocity rate in m/s
Time in s
0
1
2
3
4
5
6
7
8
9
10
0
60
120
180
240
Port N°1
Port N°2
Port N°3
Port N°4
Port N°5
Port N°6
Port N°7
Port N°8
Port N°9
Port N°10
Port N°11
Port N°12
Port N°13
Port N°14
Port N°15
Port N°16
Port N°17
Port N°18
Port N°19
Port N°20

Annex 4-3.doc

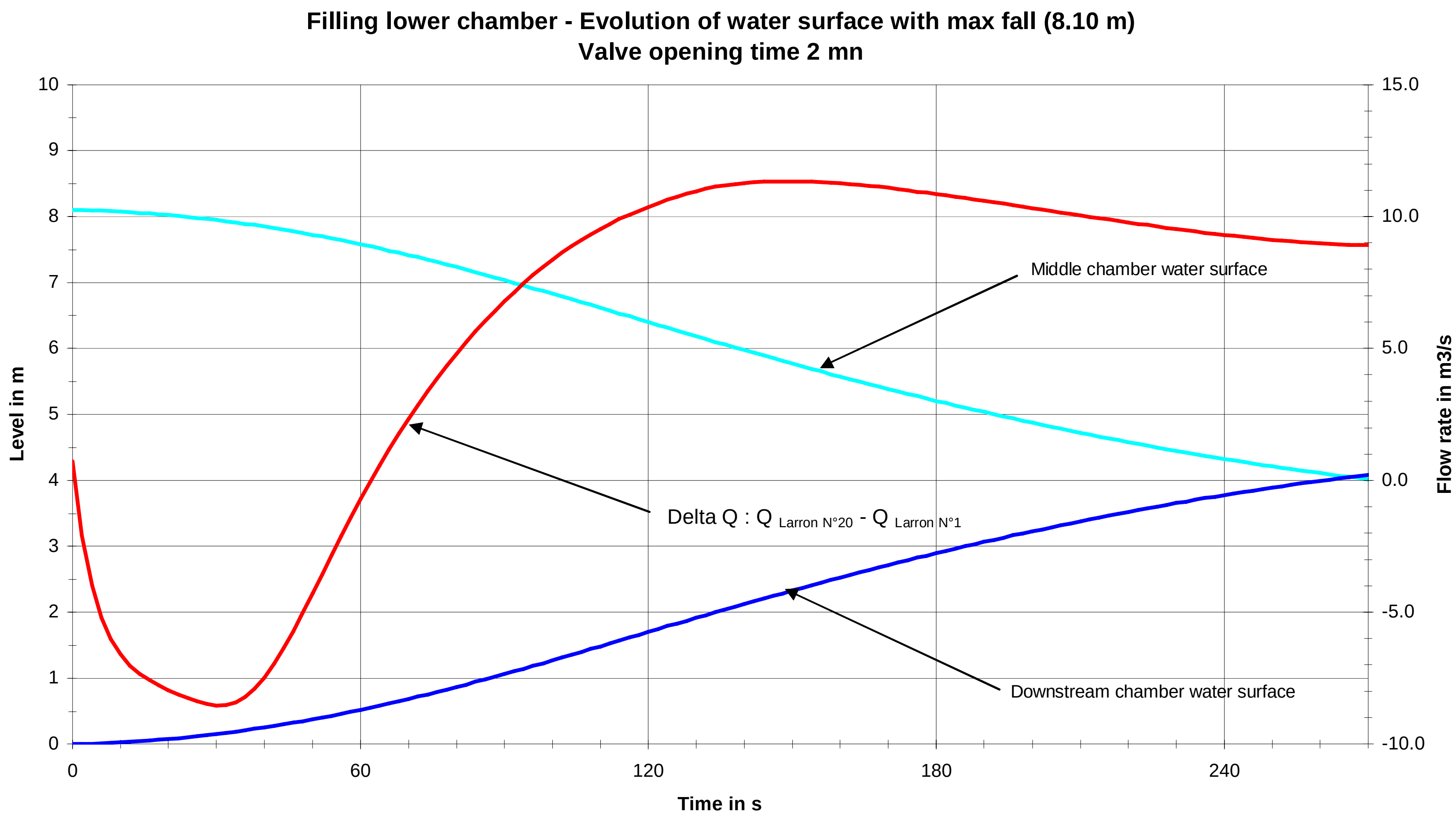

Filling lower chamber - Evolution of water surface with max fall (8.10 m)
Valve opening time 2 mn
Level in m
Flow rate in m3/s
Time in s
Middle chamber water surface
Delta Q : Q Larron N°20 - Q Larron N°1
Downstream chamber water surface
0
1
2
3
4
5
6
7
8
9
10
15.0
10.0
5.0
0.0
-5.0
-10.0
0
60
120
180
240

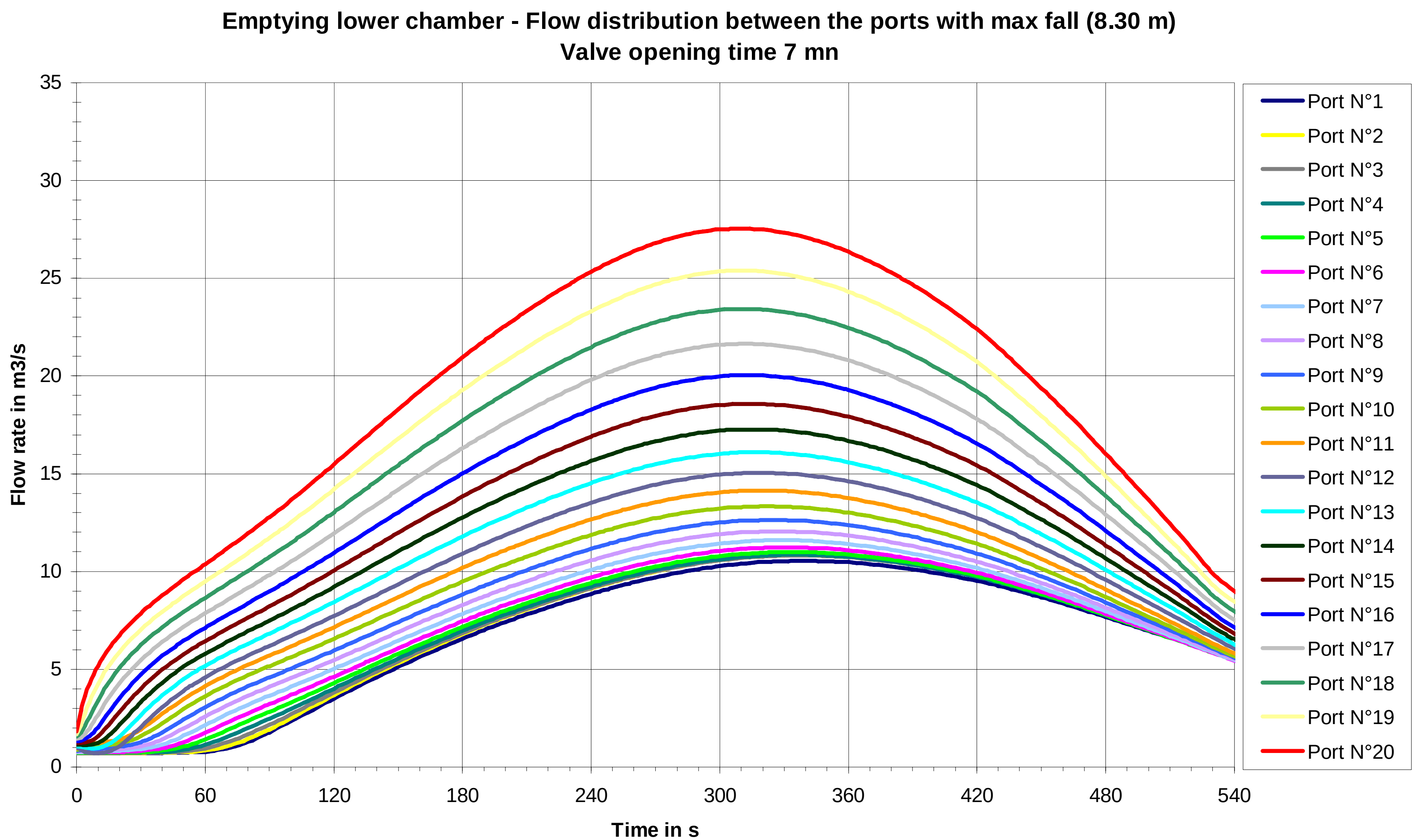
Emptying lower chamber - Flow distribution between the ports with max fall (8.30 m)
Valve opening time 7 mn
Flow rate in m3/s
Time in s
0
5
10
15
20
25
30
35
0
60
120
180
240
300
360
420
480
540
Port N°1
Port N°2
Port N°3
Port N°4
Port N°5
Port N°6
Port N°7
Port N°8
Port N°9
Port N°10
Port N°11
Port N°12
Port N°13
Port N°14
Port N°15
Port N°16
Port N°17
Port N°18
Port N°19
Port N°20

Annex 5-2.doc

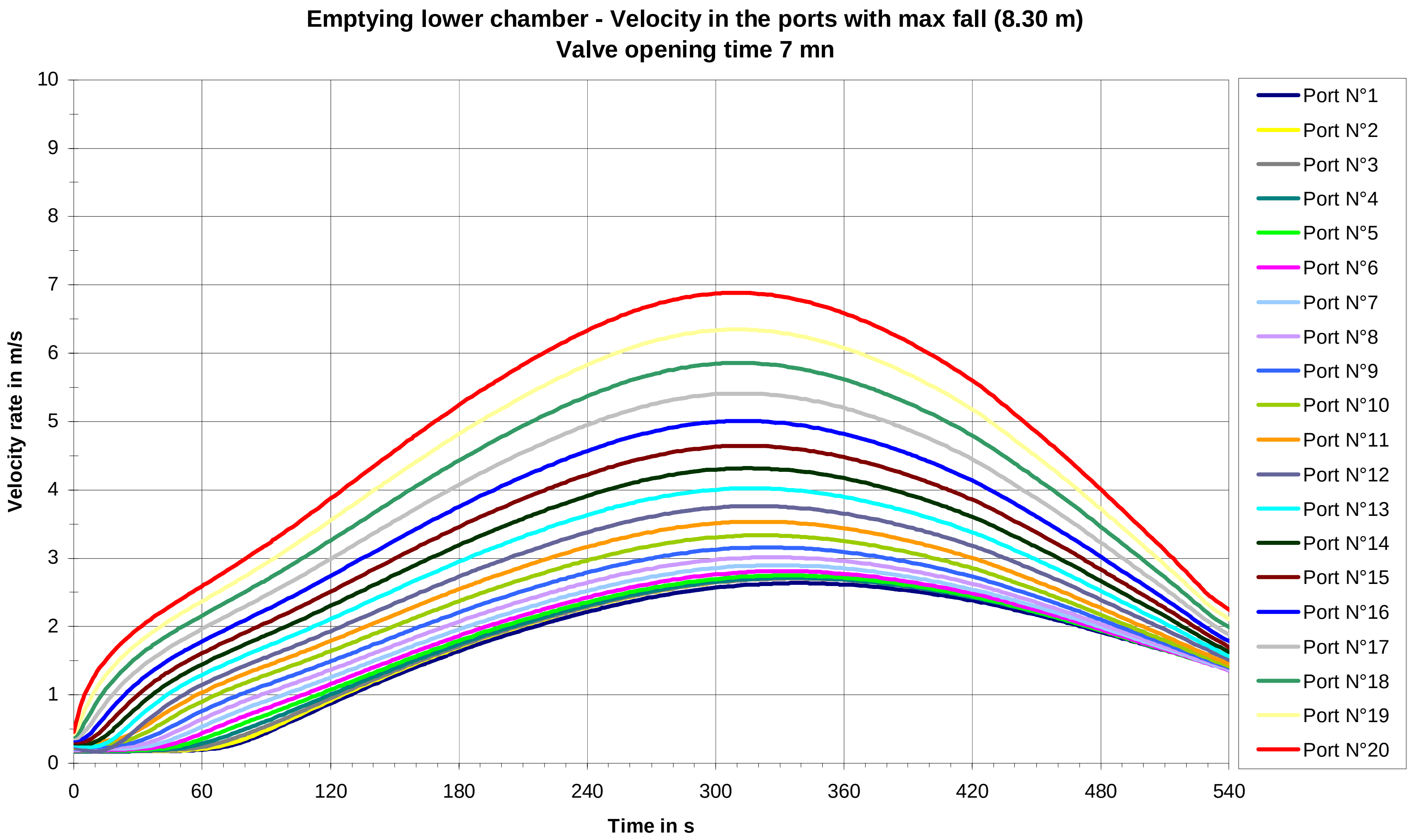

Emptying lower chamber - Velocity in the ports with max fall (8.30 m)
Valve opening time 7 mn
Velocity rate in m/s
Time in s
0
1
2
3
4
5
6
7
8
9
10
0
60
120
180
240
300
360
420
480
540
Port N°1
Port N°2
Port N°3
Port N°4
Port N°5
Port N°6
Port N°7
Port N°8
Port N°9
Port N°10
Port N°11
Port N°12
Port N°13
Port N°14
Port N°15
Port N°16
Port N°17
Port N°18
Port N°19
Port N°20

Annex 5-3.doc

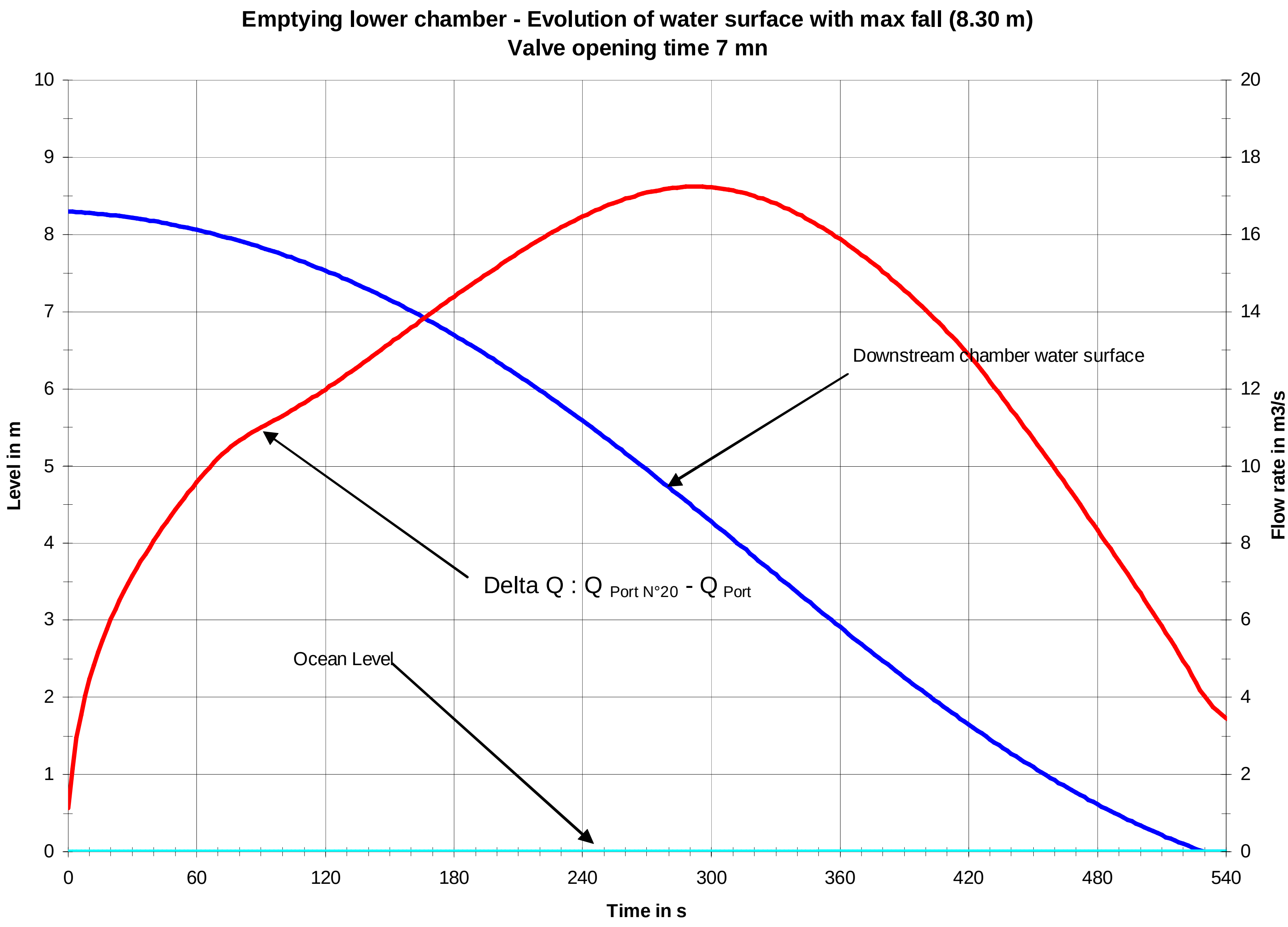

Emptying lower chamber - Evolution of water surface with max fall (8.30 m)
Valve opening time 7 mn
Level in m
Flow rate in m3/s
Time in s
10
9
8
7
6
5
4
3
2
1
0
20
18
16
14
12
10
8
6
4
2
0
0
60
120
180
240
300
360
420
480
540
Downstream chamber water surface
Delta Q : Q Port N°20 - Q Port
Ocean Level

Annex 6-1.doc

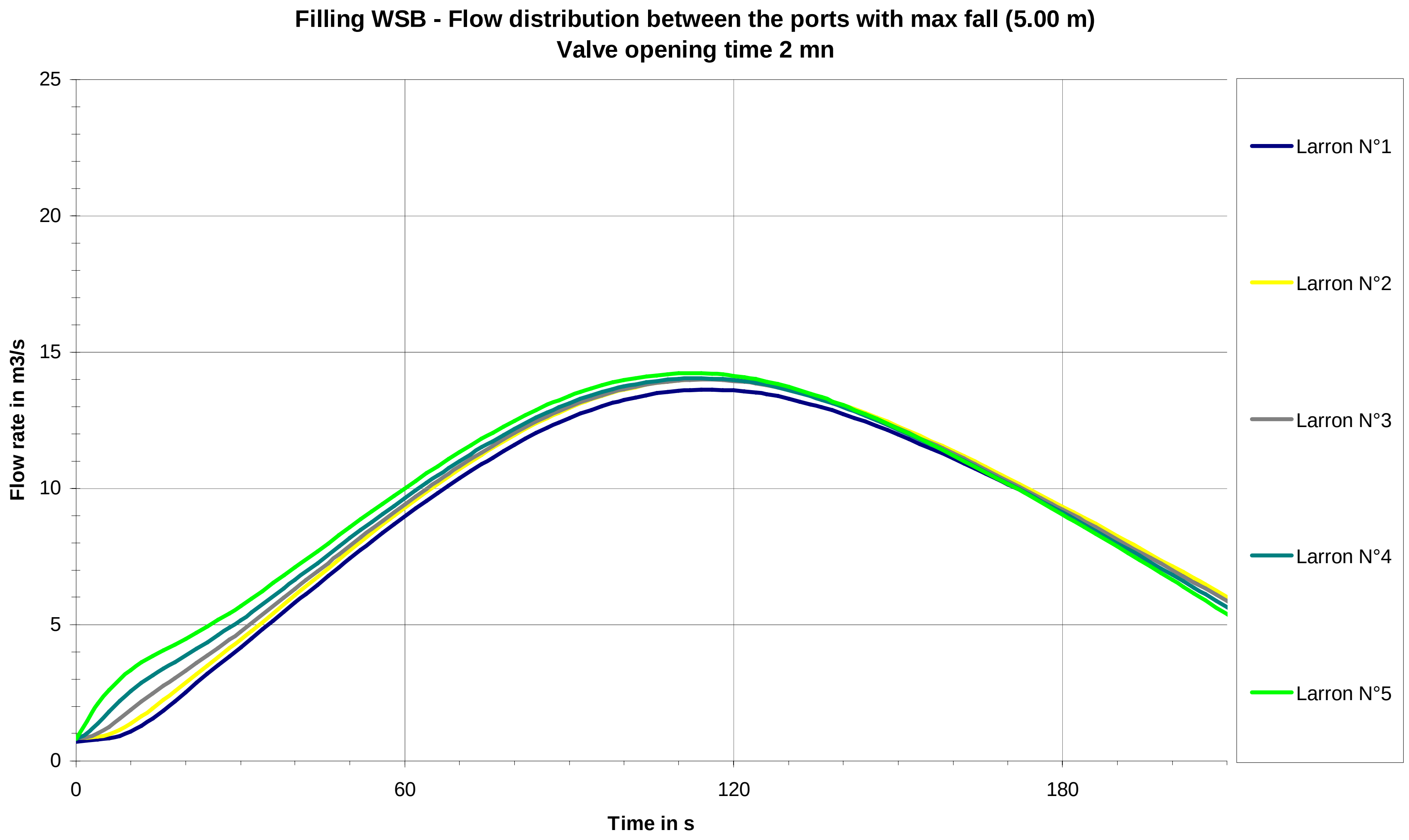

Filling WSB - Flow distribution between the ports with max fall (5.00 m)
Valve opening time 2 mn
Flow rate in m3/s
25
20
15
10
5
0
0
60
120
180
Time in s
Larron N°1
Larron N°2
Larron N°3
Larron N°4
Larron N°5

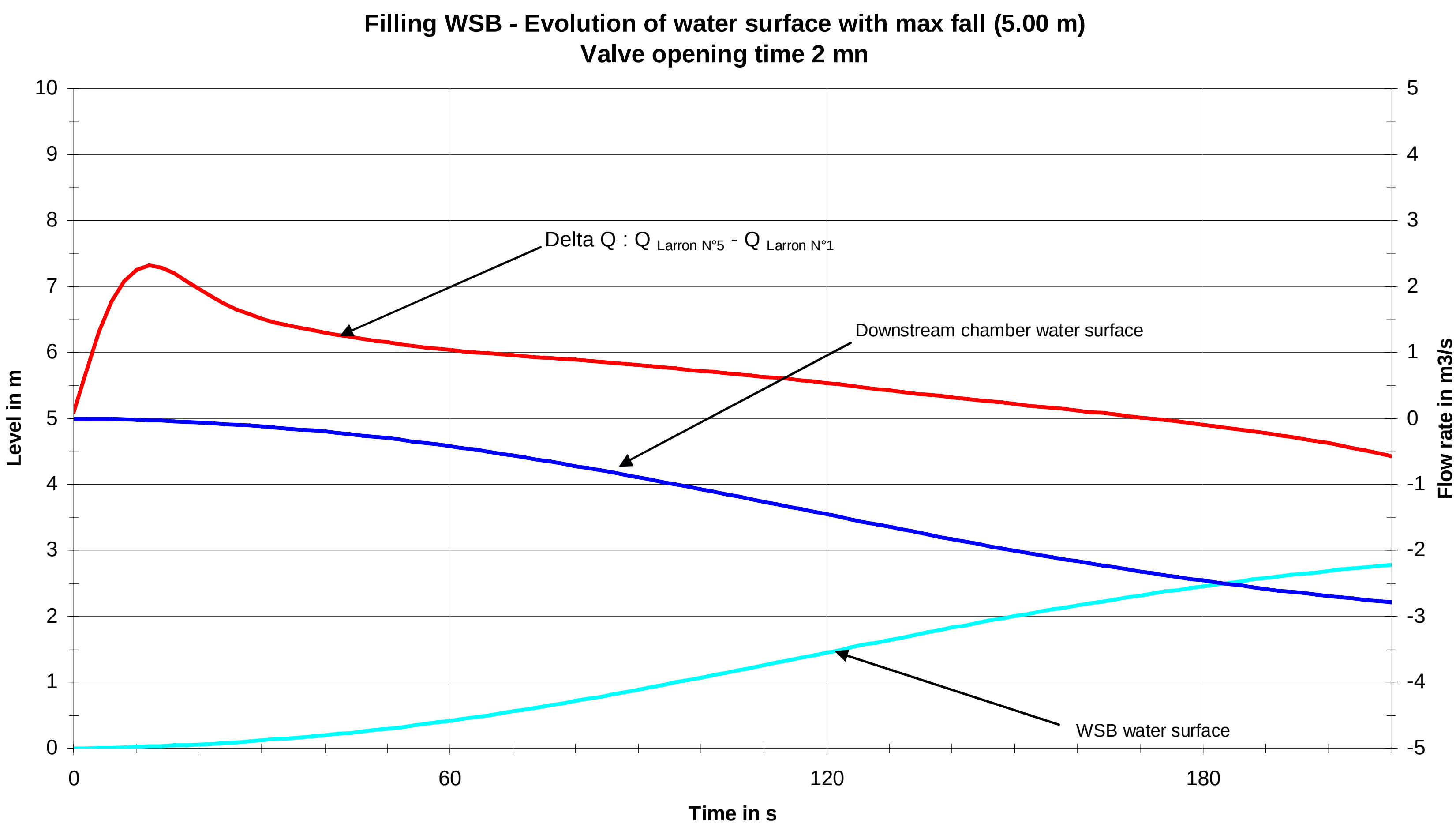
Filling WSB - Evolution of water surface with max fall (5.00 m)
Valve opening time 2 mn
Level in m
Flow rate in m3/s
Time in s
Delta Q : Q Larron N°5 - Q Larron N°1
Downstream chamber water surface
WSB water surface
0
1
2
3
4
5
6
7
8
9
10
-5
-4
-3
-2
-1
0
1
2
3
4
5
0
60
120
180

Annex 7.doc

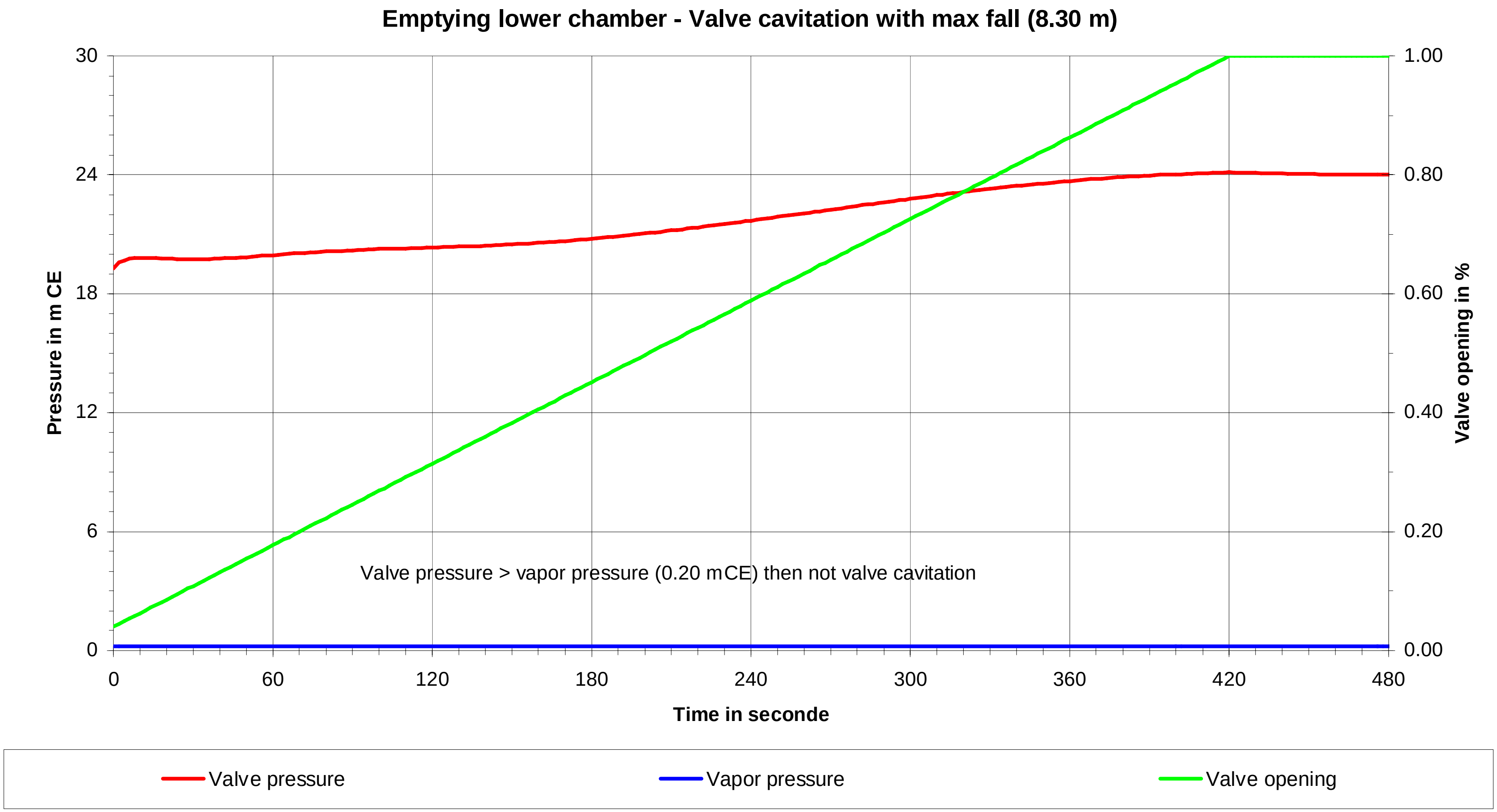

Emptying lower chamber - Valve cavitation with max fall (8.30 m)
Pressure in m CE
Valve opening in %
Time in seconde
30
24
18
12
6
0
1.00
0.80
0.60
0.40
0.20
0.00
0
60
120
180
240
300
360
420
480
Valve pressure > vapor pressure (0.20 mCE) then not valve cavitation
Valve pressure
Vapor pressure
Valve opening

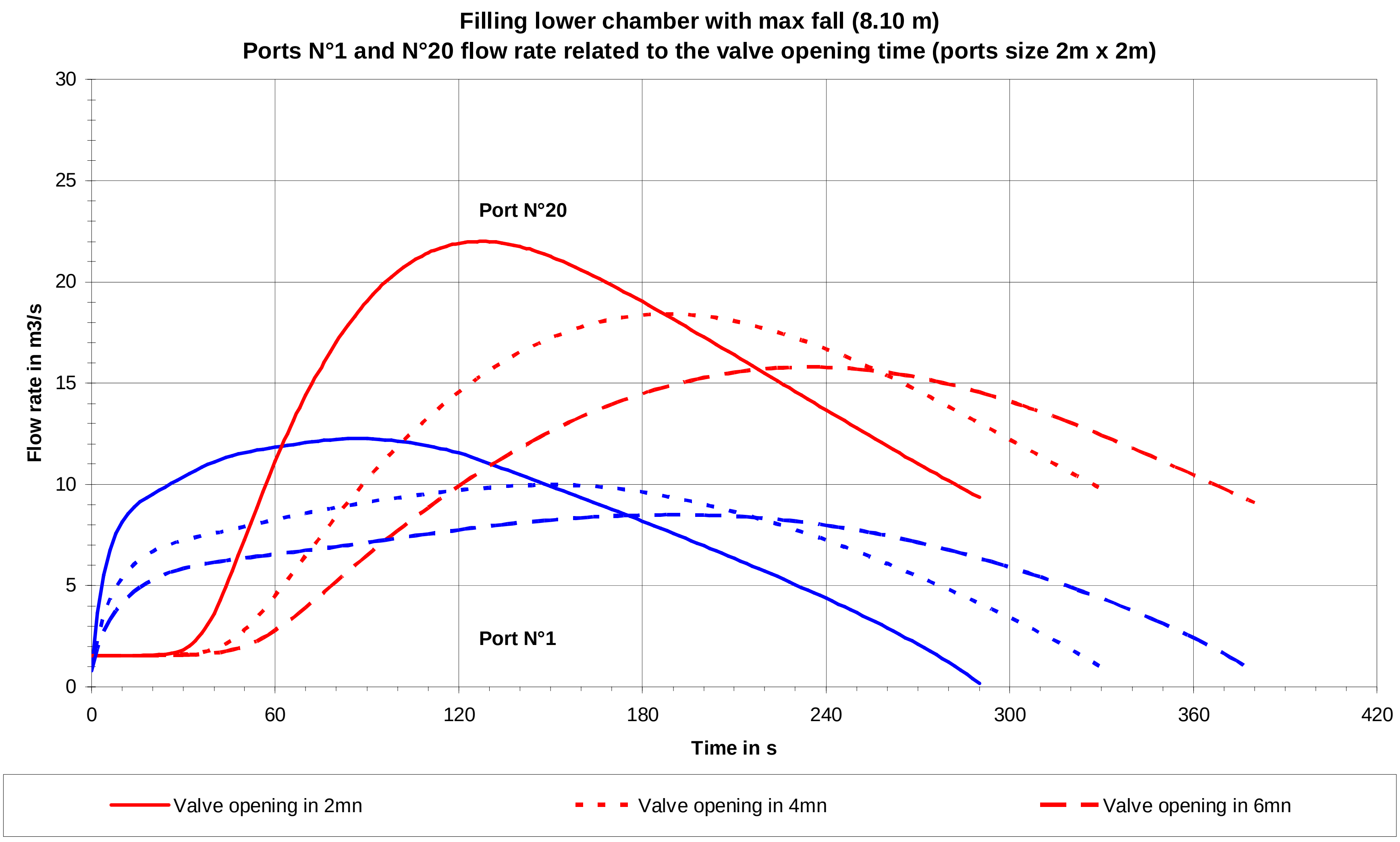
Filling lower chamber with max fall (8.10 m)
Ports N°1 and N°20 flow rate related to the valve opening time (ports size 2m x 2m)
Flow rate in m3/s
Time in s
Port N°20
Port N°1
0
5
10
15
20
25
30
0
60
120
180
240
300
360
420
Valve opening in 2mn
Valve opening in 4mn
Valve opening in 6mn

Annex 8-2.doc

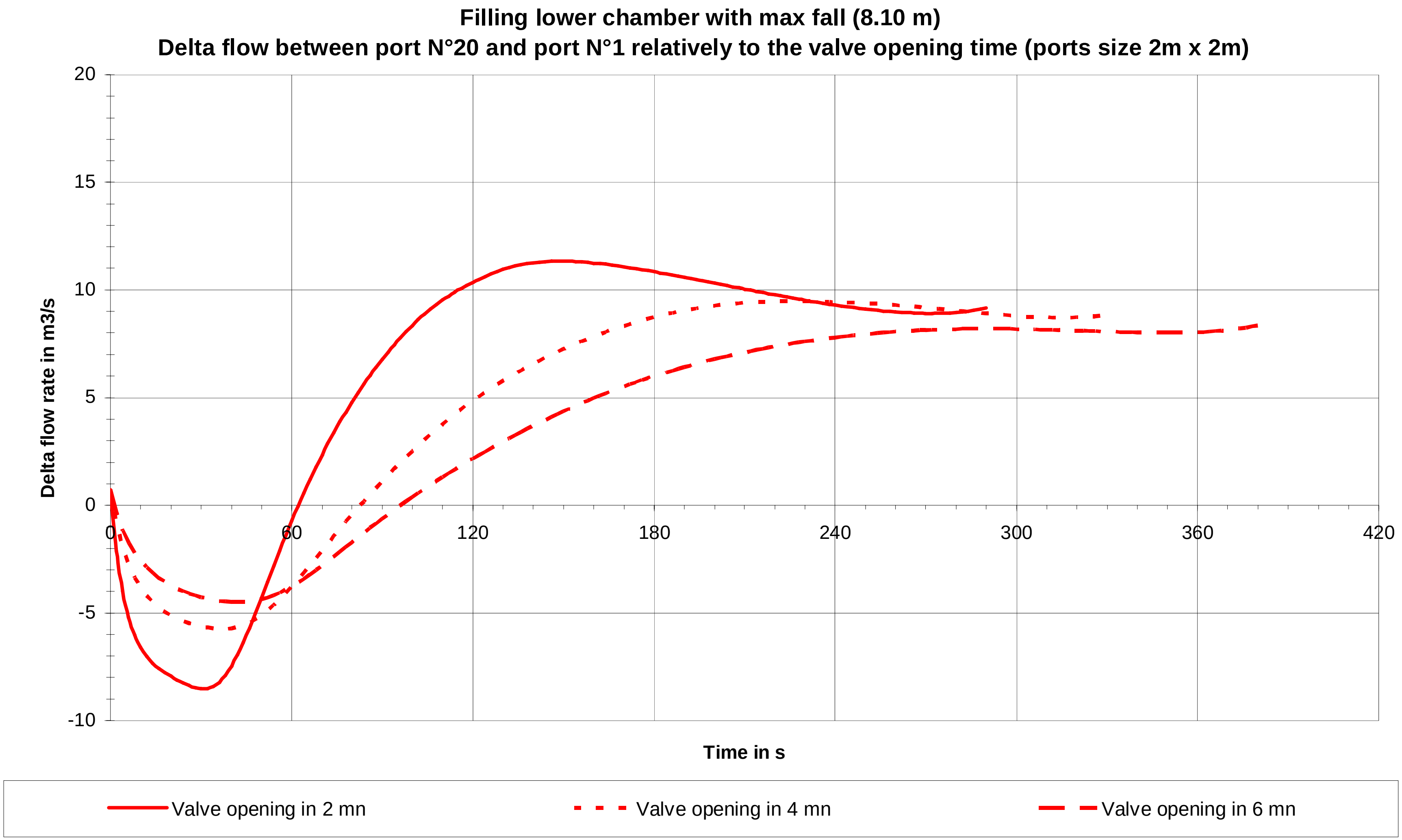

Filling lower chamber with max fall (8.10 m)
Delta flow between port N°20 and port N°1 relatively to the valve opening time (ports size 2m x 2m)
Delta flow rate in m3/s
20
15
10
5
0
-5
-10
0
60
120
180
240
300
360
420
Time in s
Valve opening in 2 mn
Valve opening in 4 mn
Valve opening in 6 mn

Annex 9-1.doc

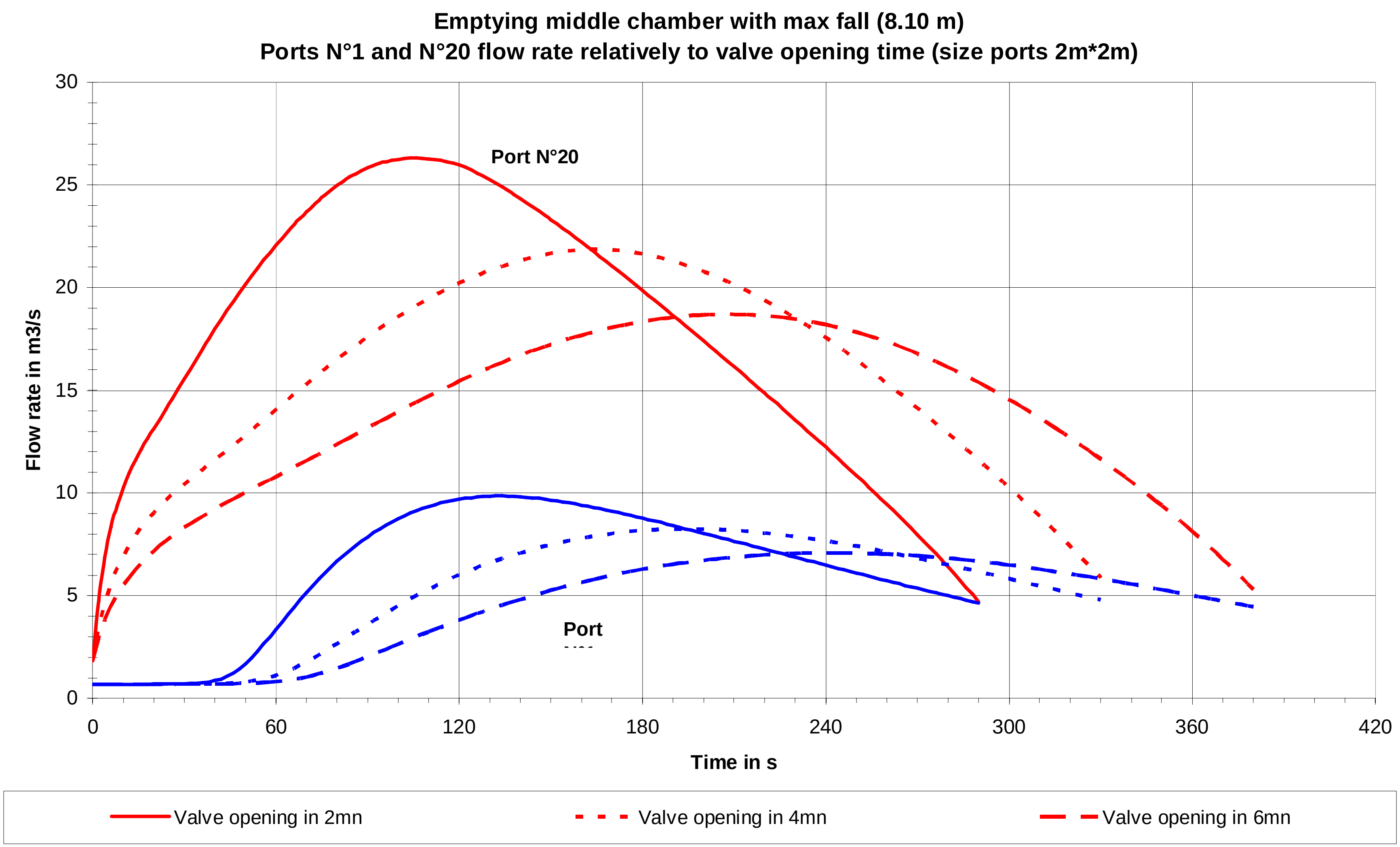

Emptying middle chamber with max fall (8.10 m)
Ports N°1 and N°20 flow rate relatively to valve opening time (size ports 2m*2m)
Flow rate in m3/s
30
25
20
15
10
5
0
0
60
120
180
240
300
360
420
Time in s
Port N°20
Port
Valve opening in 2mn
Valve opening in 4mn
Valve opening in 6mn

Annex 9-2.doc

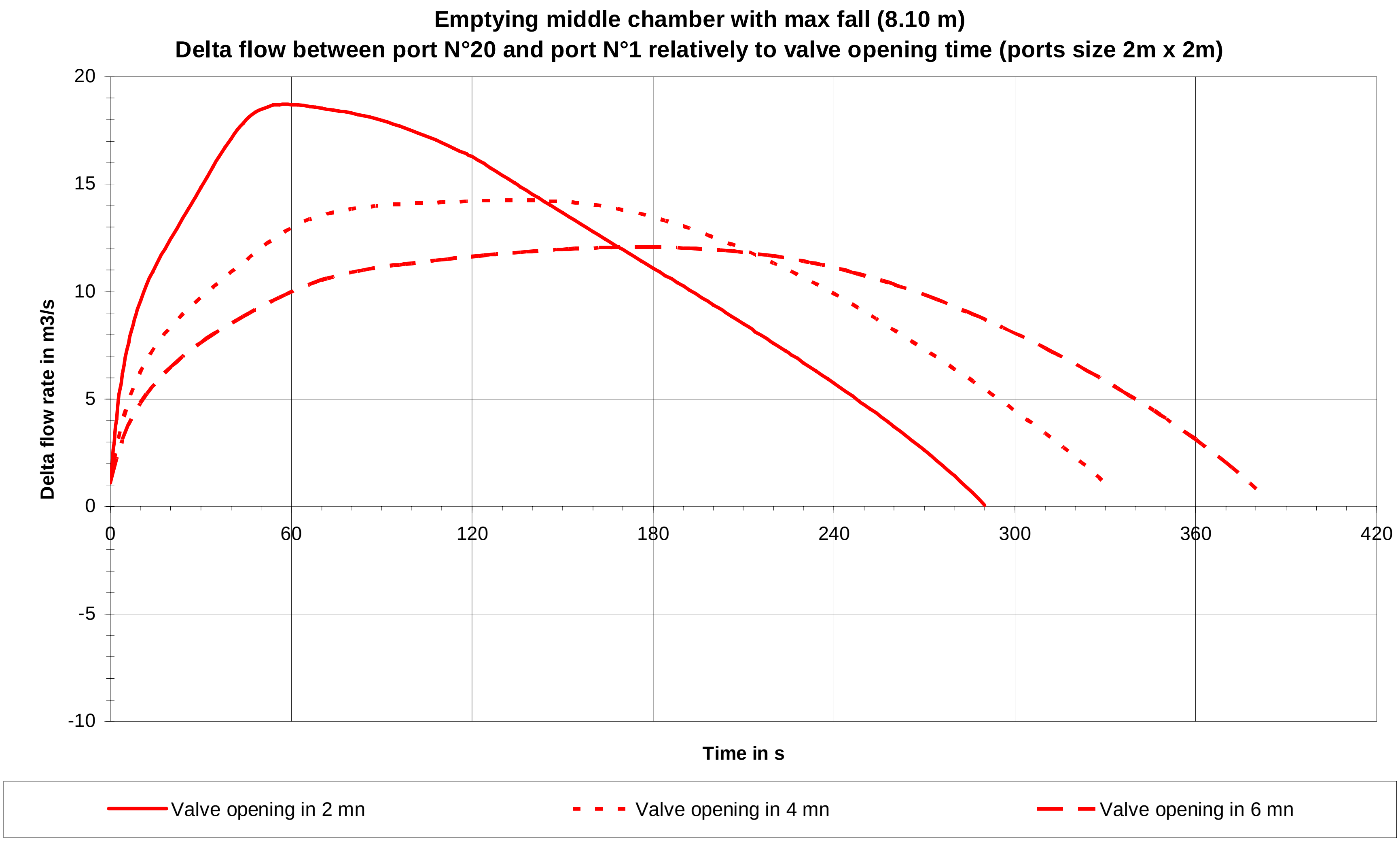

Emptying middle chamber with max fall (8.10 m)
Delta flow between port N°20 and port N°1 relatively to valve opening time (ports size 2m x 2m)
20
15
10
5
0
-5
-10
Delta flow rate in m3/s
0
60
120
180
240
300
360
420
Time in s
Valve opening in 2 mn
Valve opening in 4 mn
Valve opening in 6 mn

Annex 10-1.doc

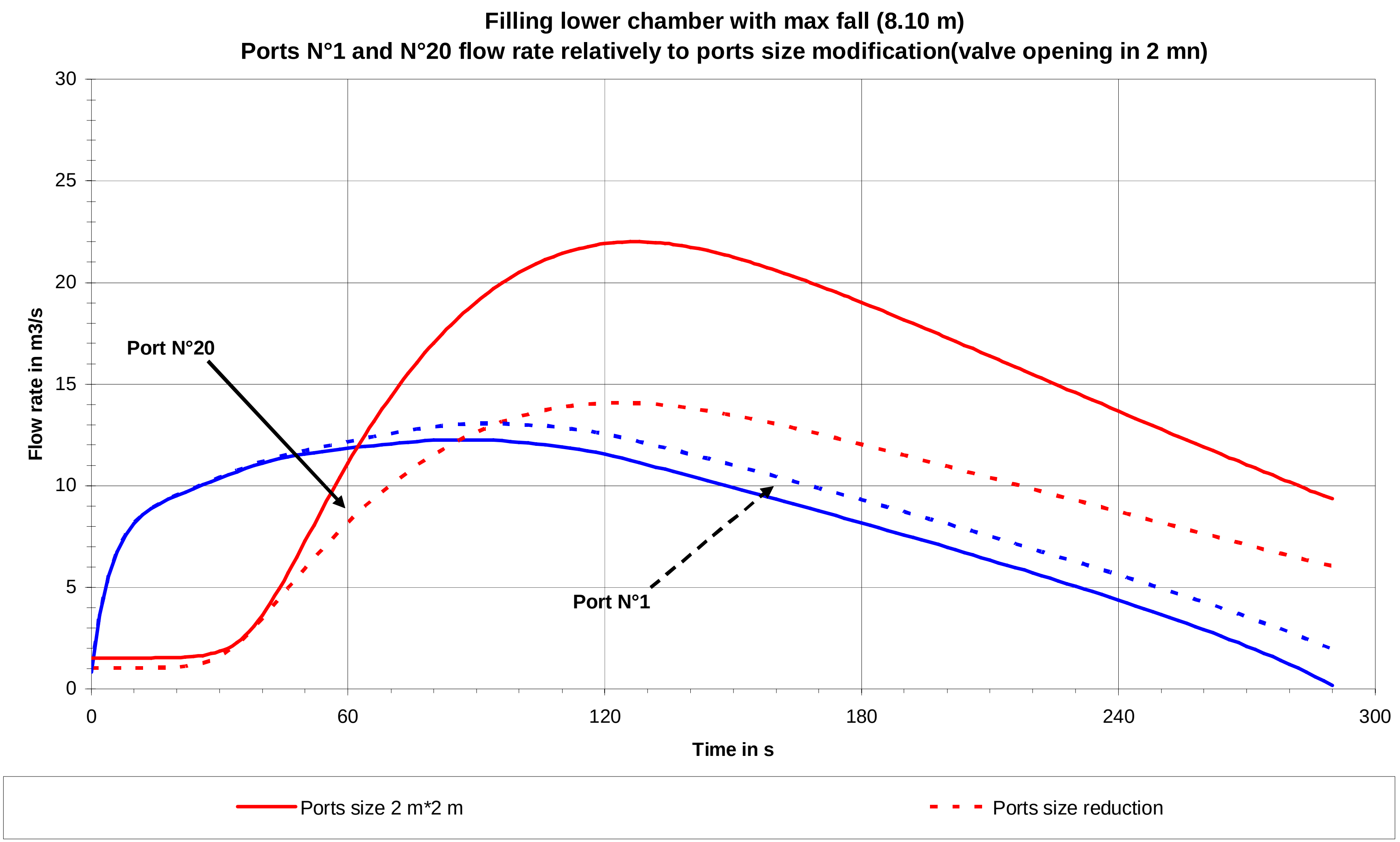

Annex 10-2.doc

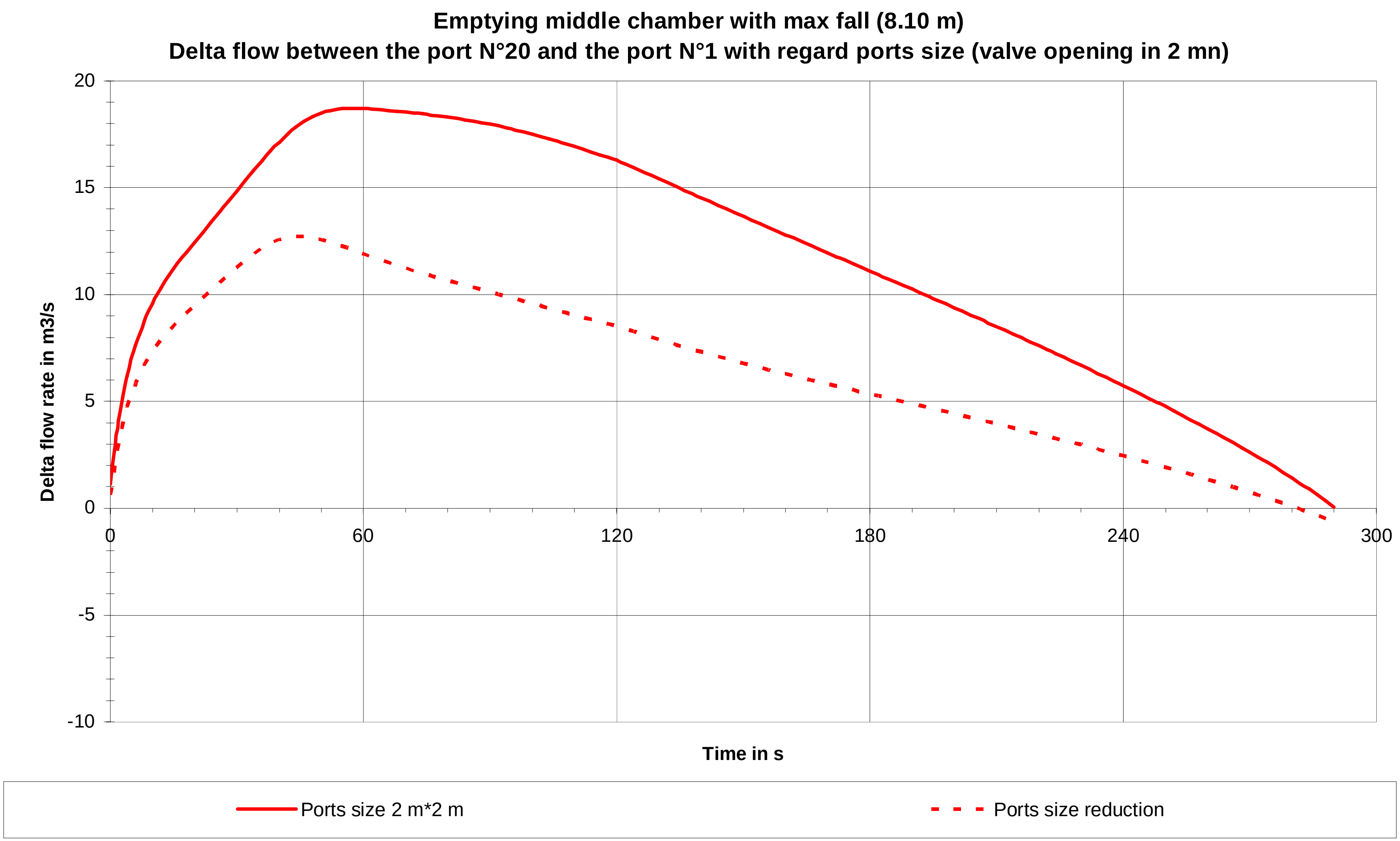

Annex 11-1.doc

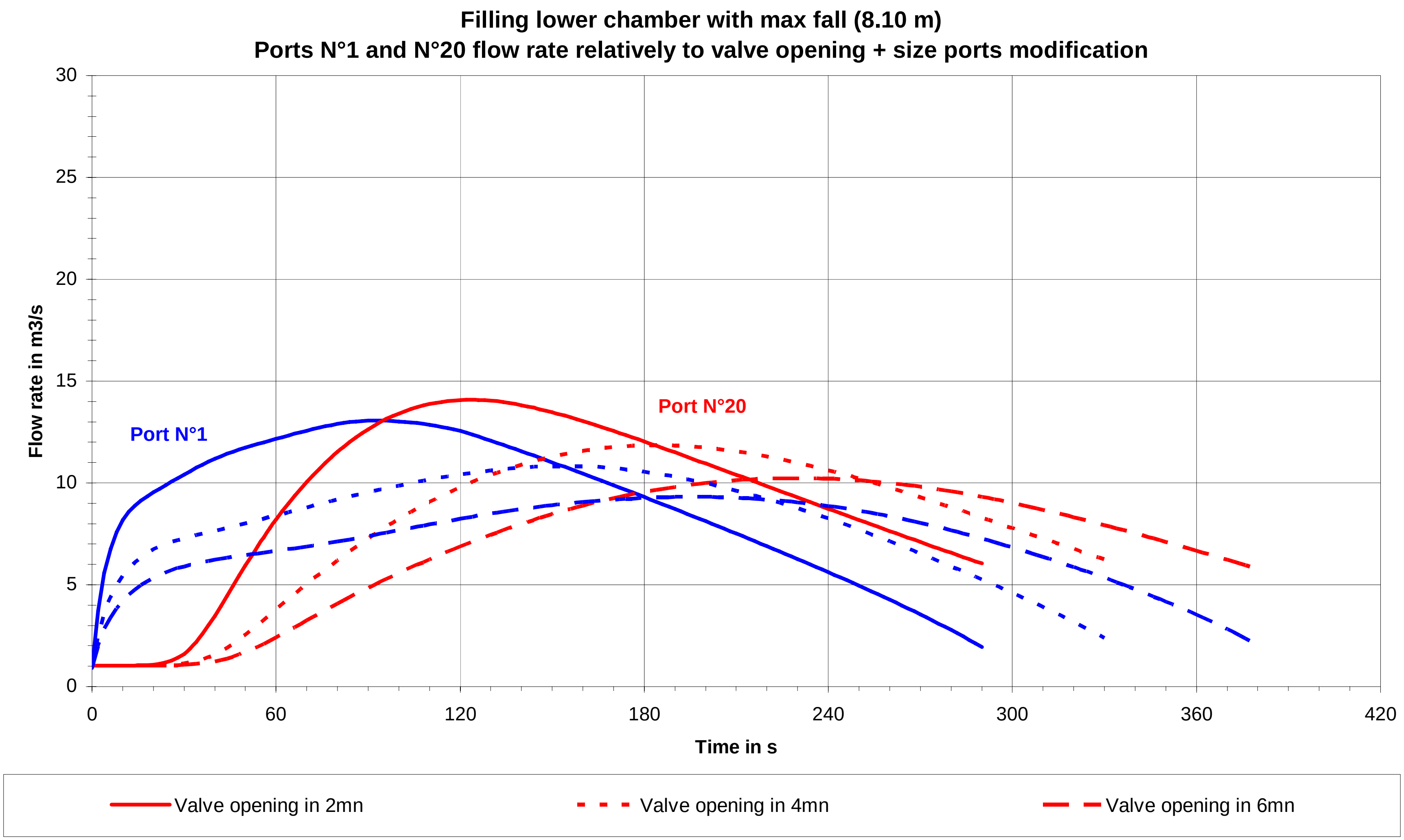

Annex 11-2.doc

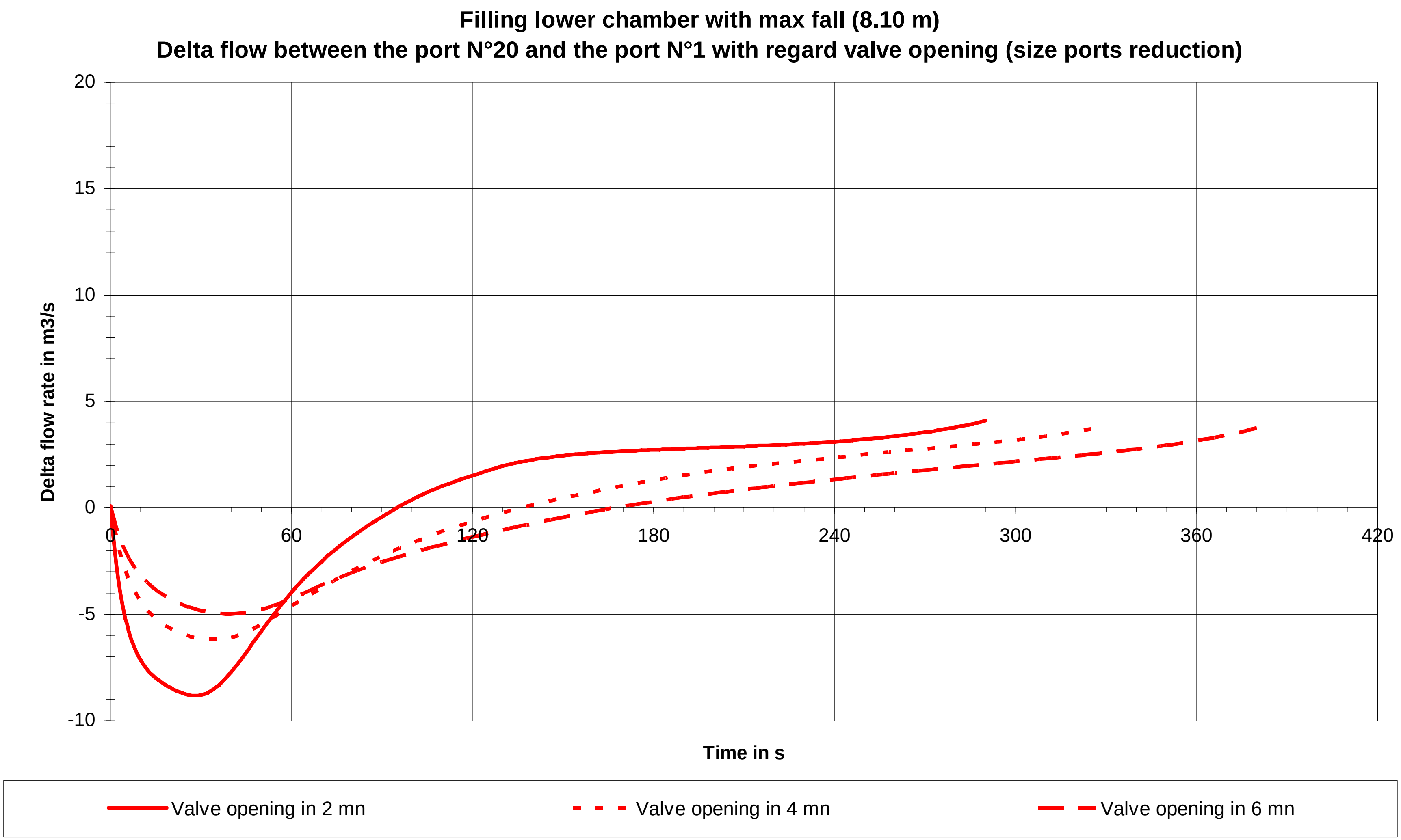

Annex 12-1.doc

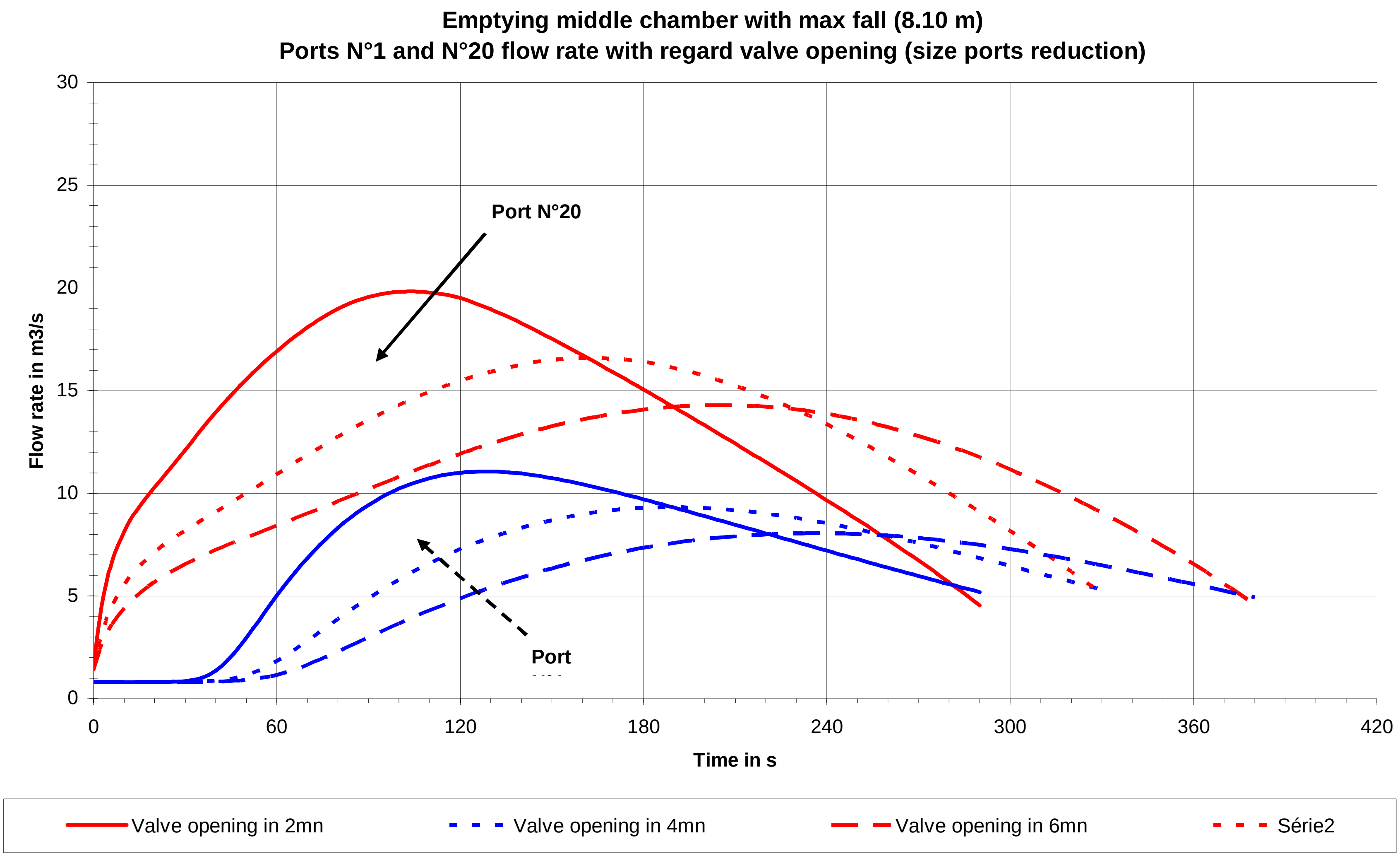

Annex 12-2.doc

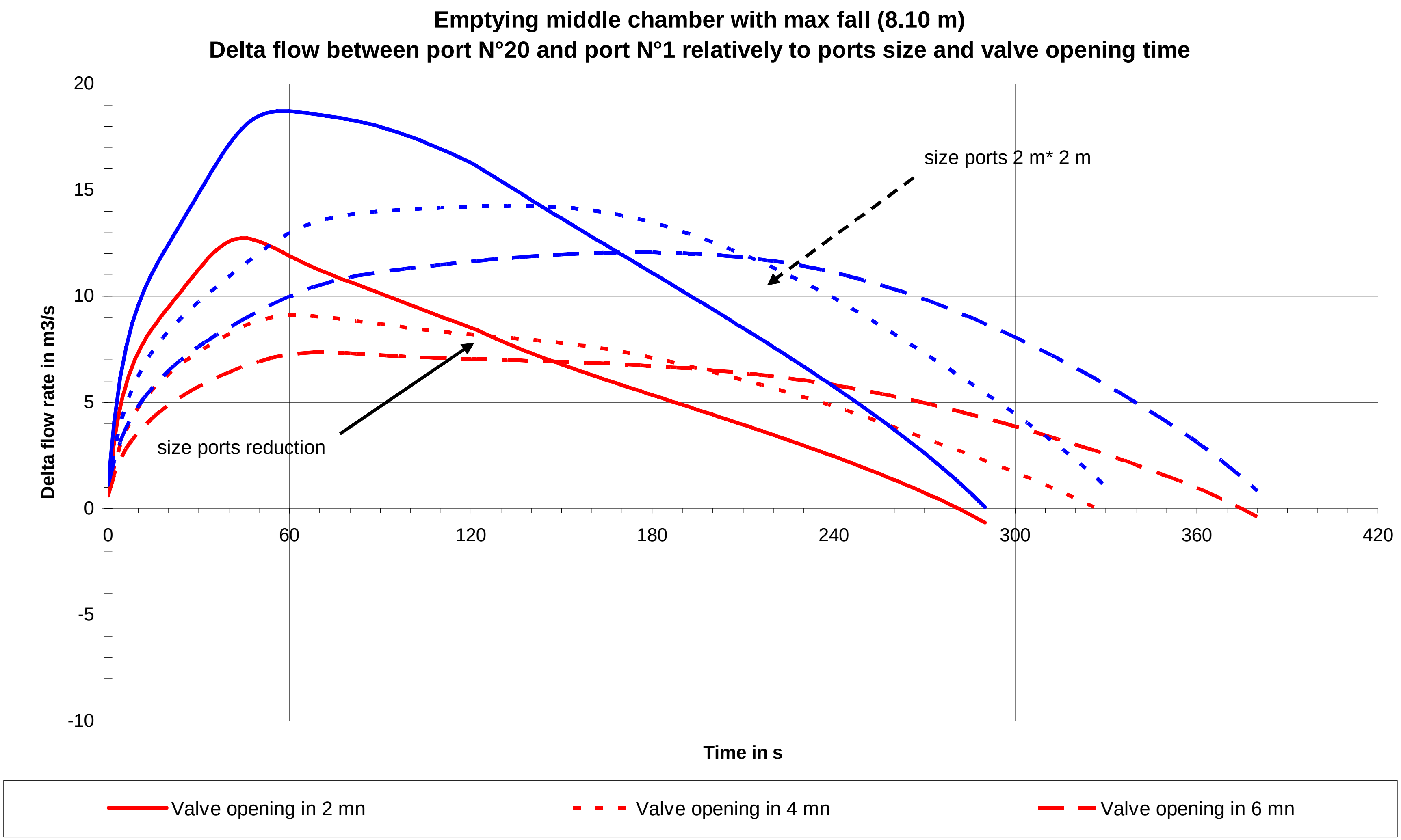

Annex 13-1.doc

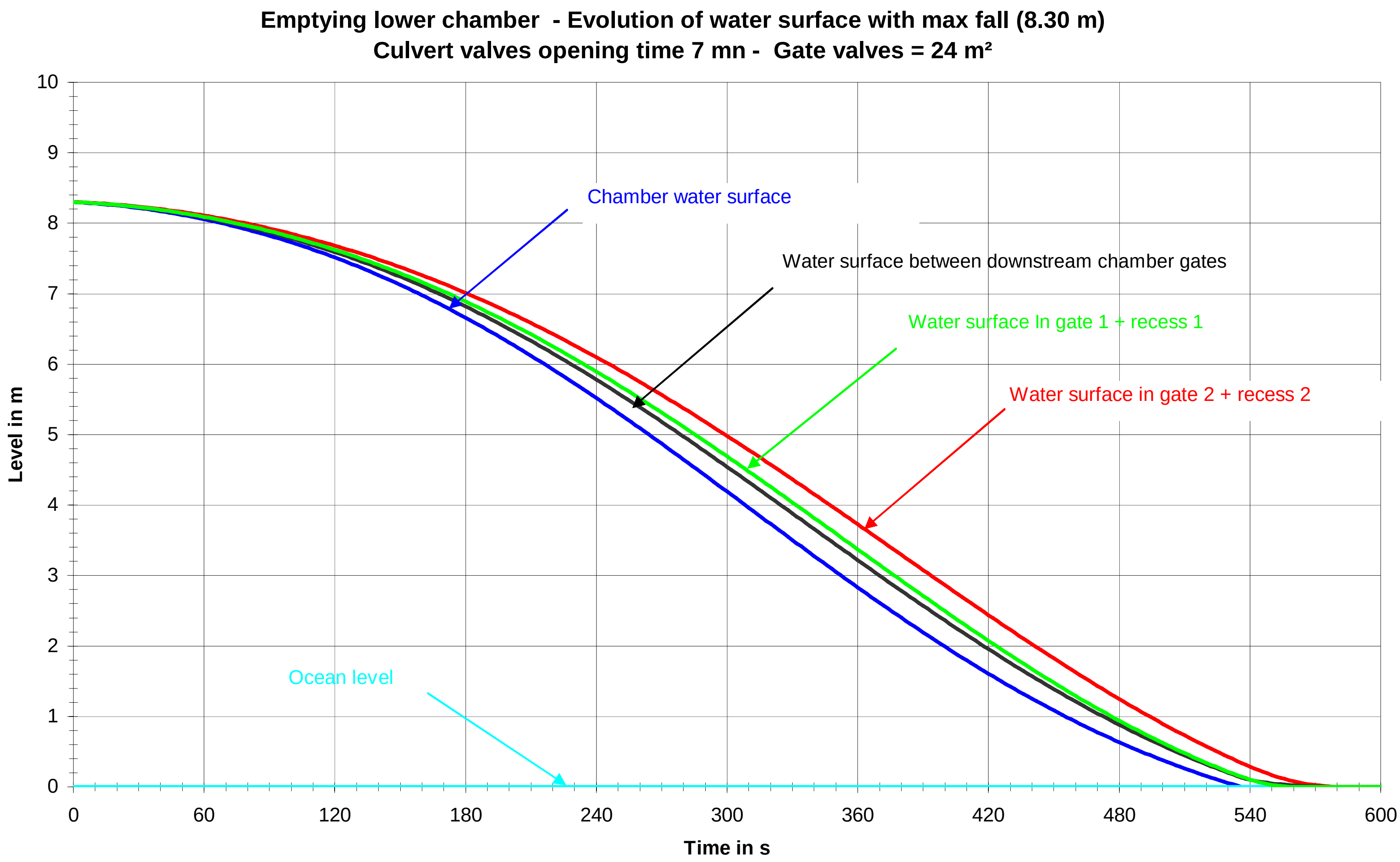

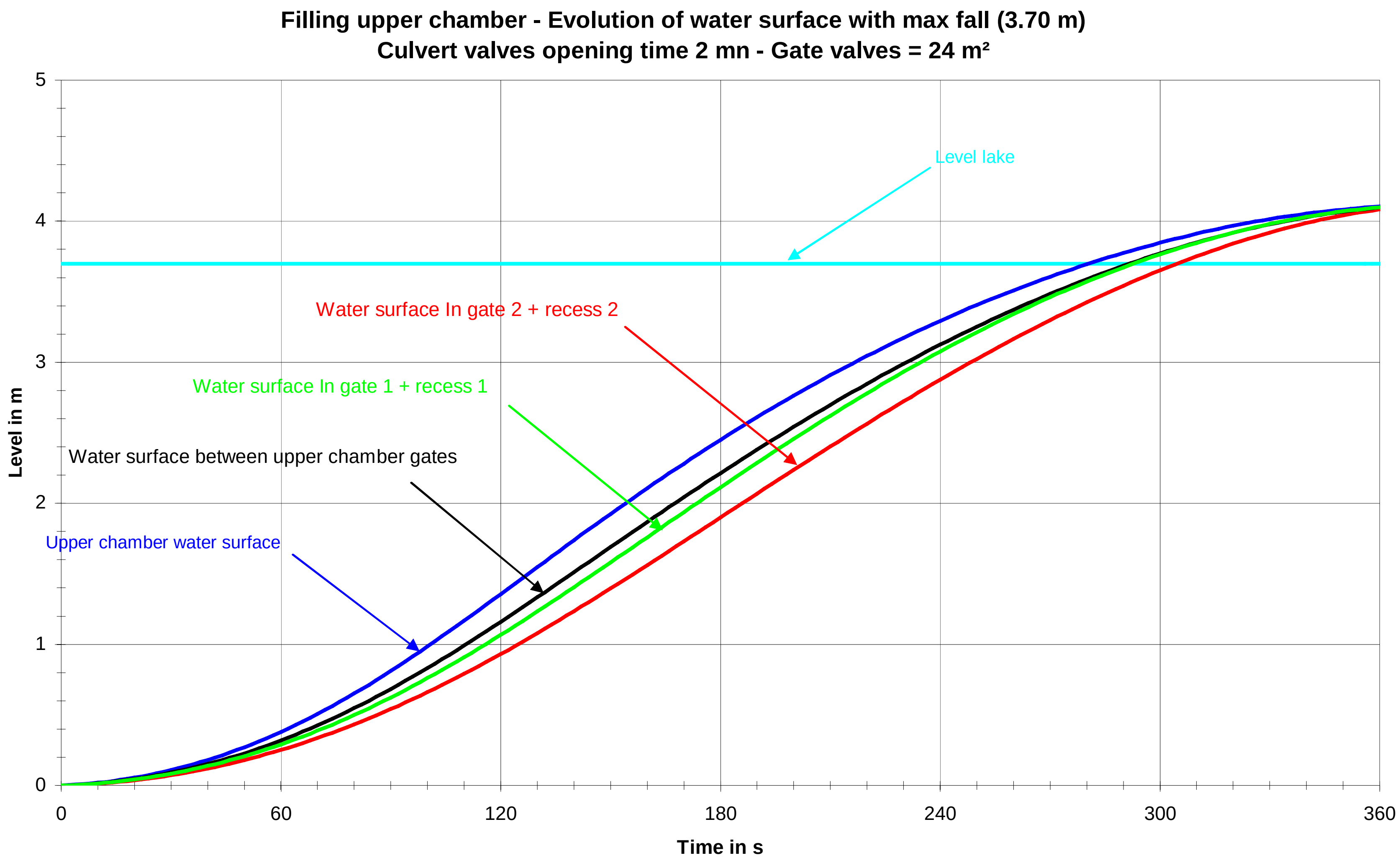
Filling upper chamber - Evolution of water surface with max fall (3.70 m)
Culvert valves opening time 2 mn - Gate valves = 24 m²
Level in m
Time in s
Level lake
Water surface In gate 2 + recess 2
Water surface In gate 1 + recess 1
Water surface between upper chamber gates
Upper chamber water surface
0
1
2
3
4
5
0
60
120
180
240
300
360

Annex 13-3.doc

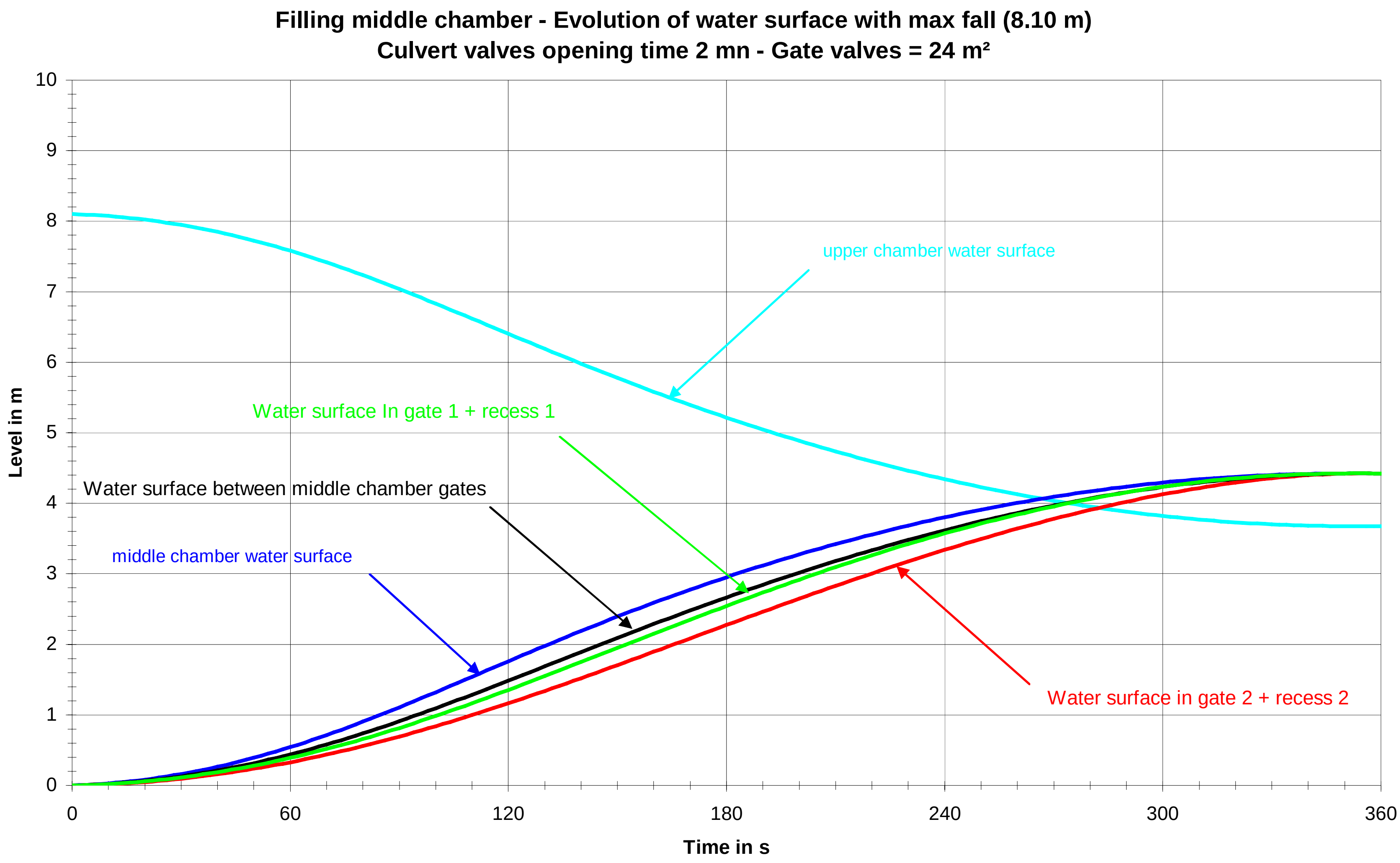

Annex 14-1.doc

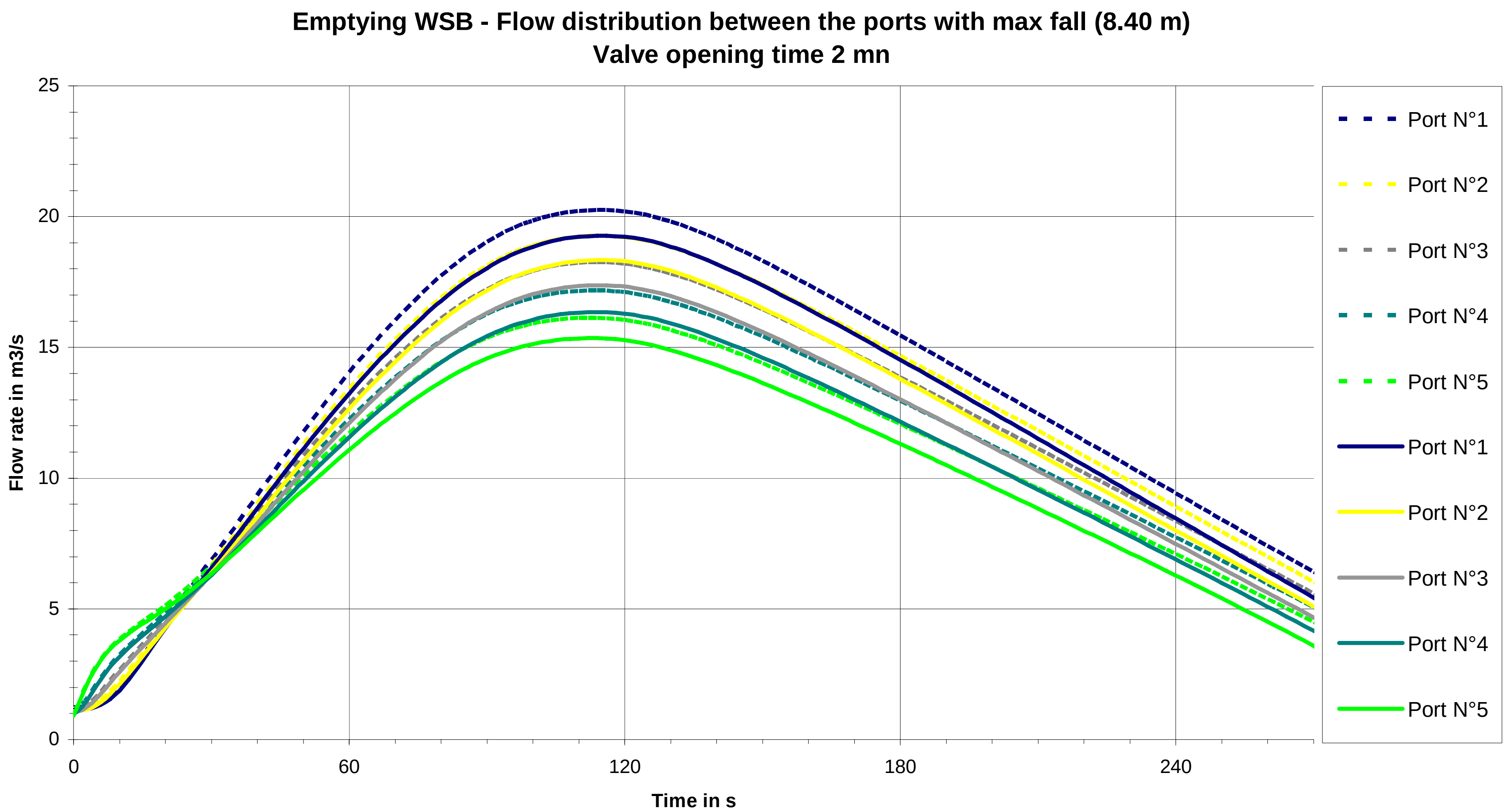

Port without size reduction

Port with size reduction

Annex 14-2.doc

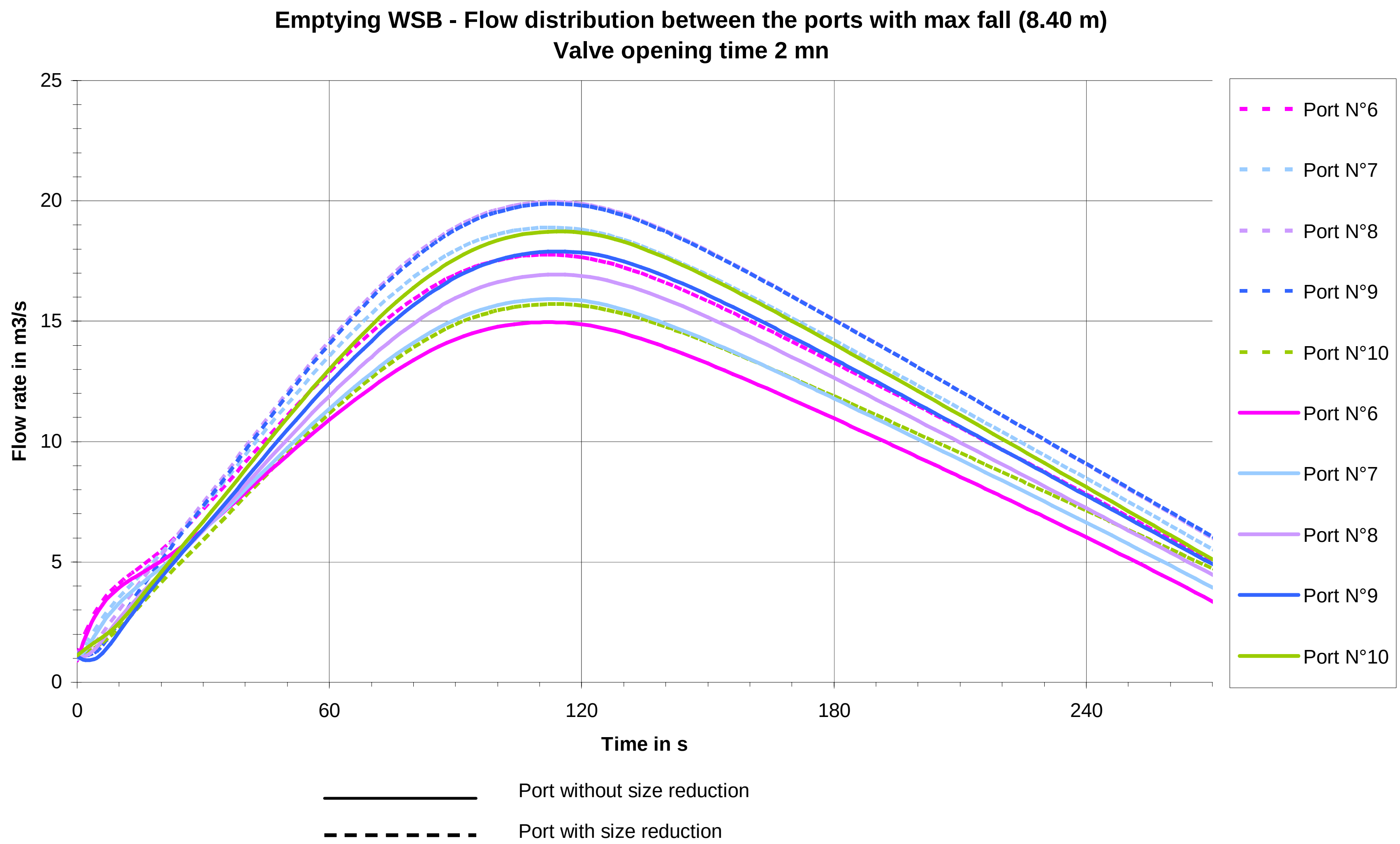

Annex 14-3.doc

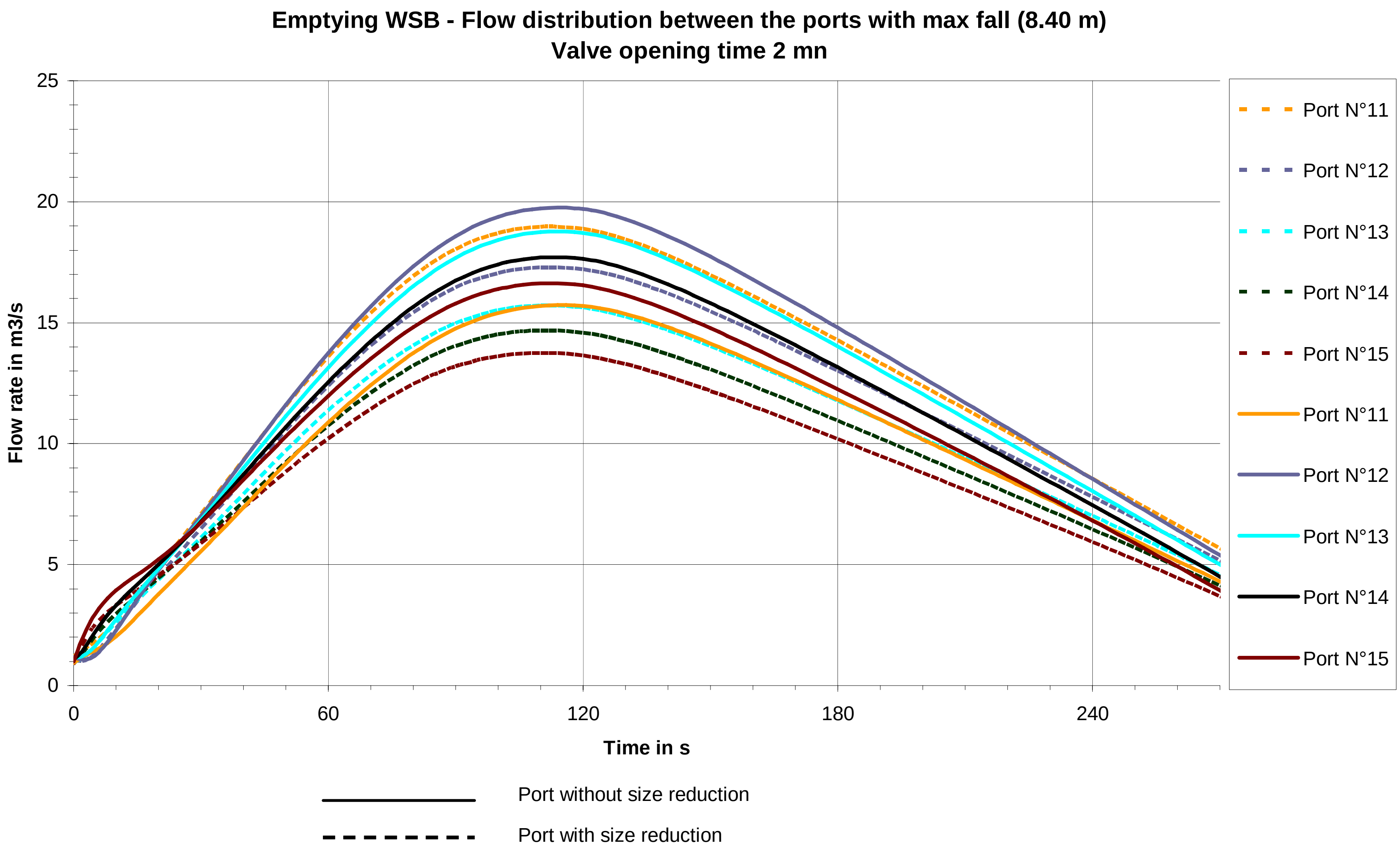

Annex 14-4.doc

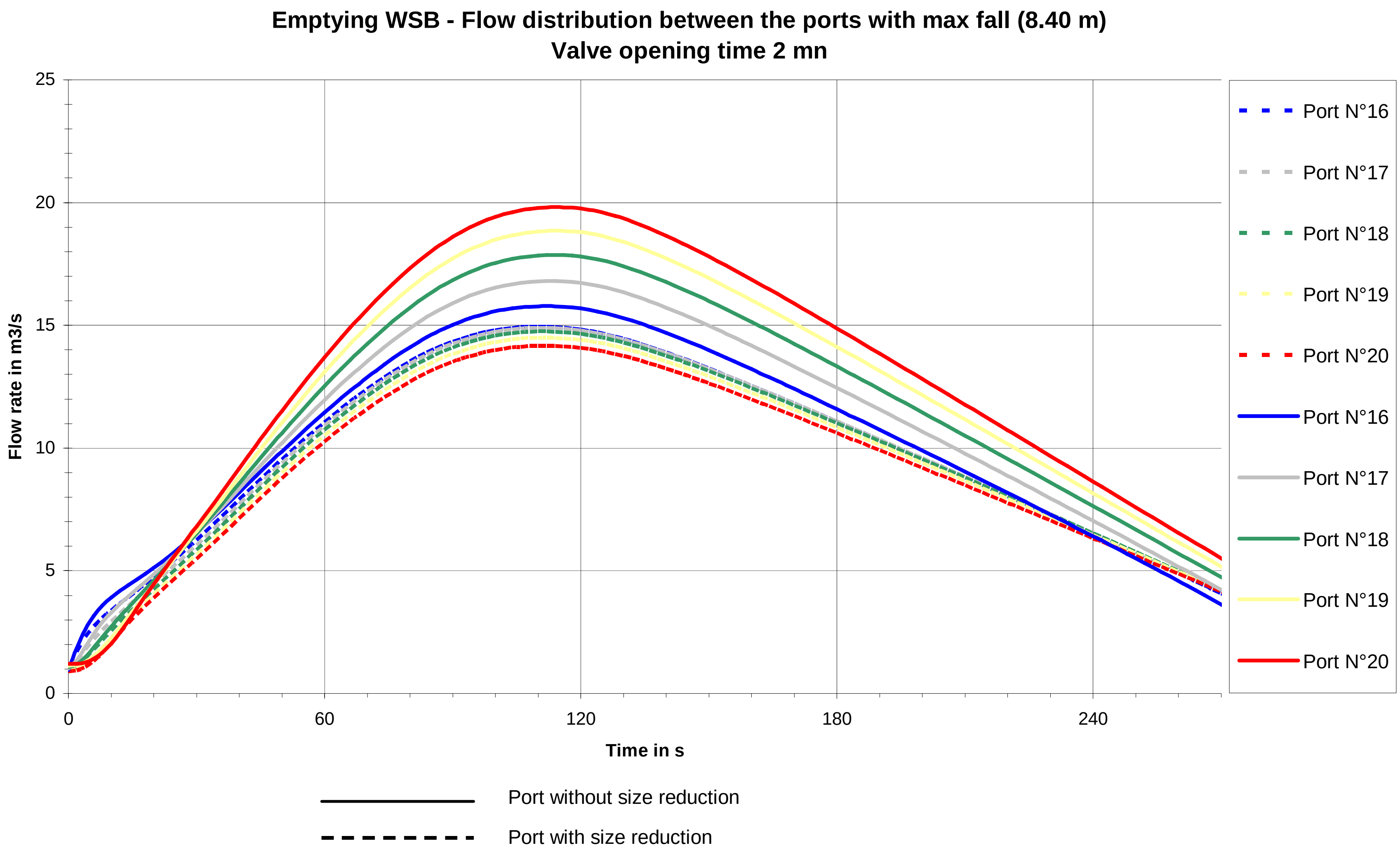

Annex 14-5.doc

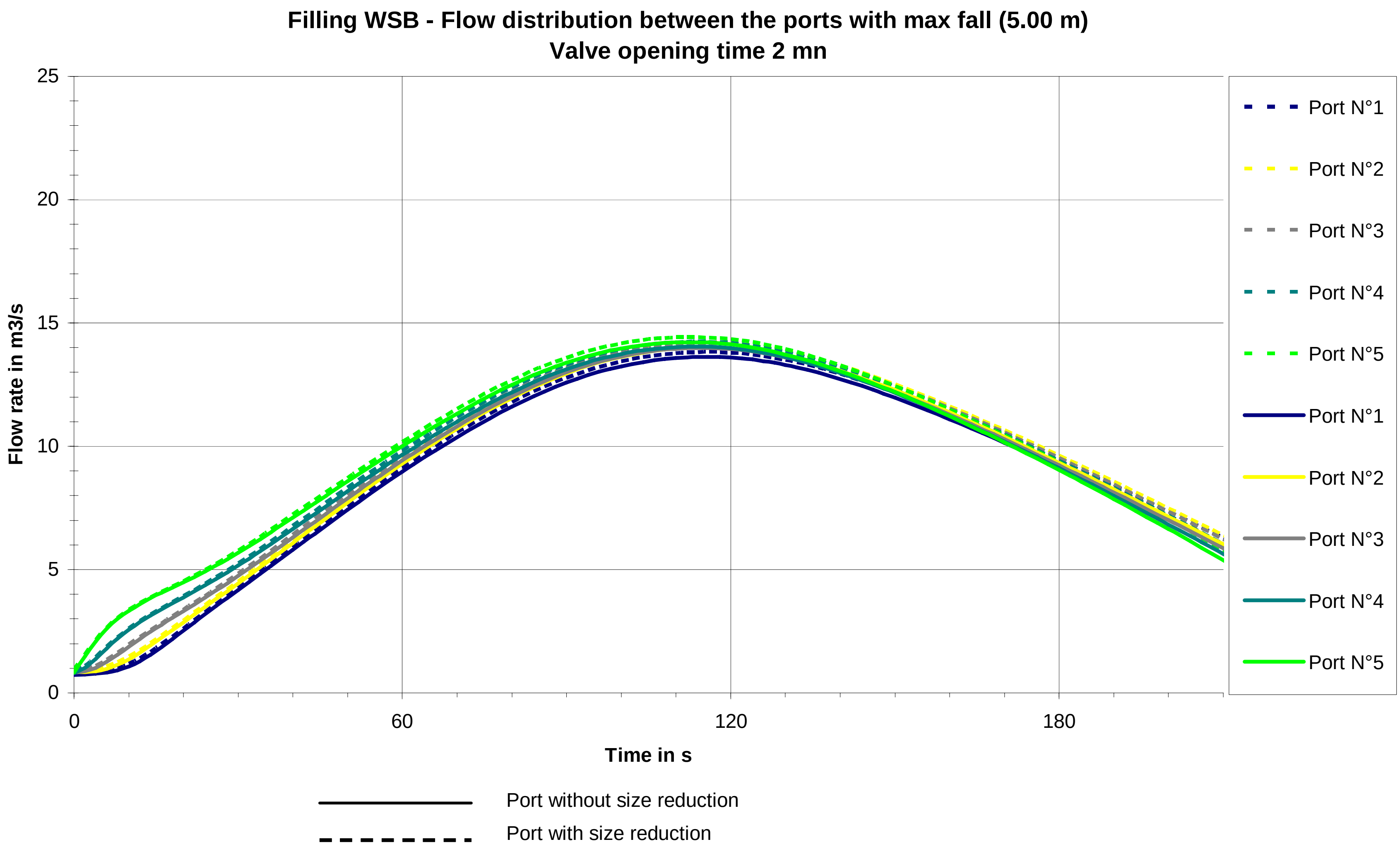

Annex 14-6.doc

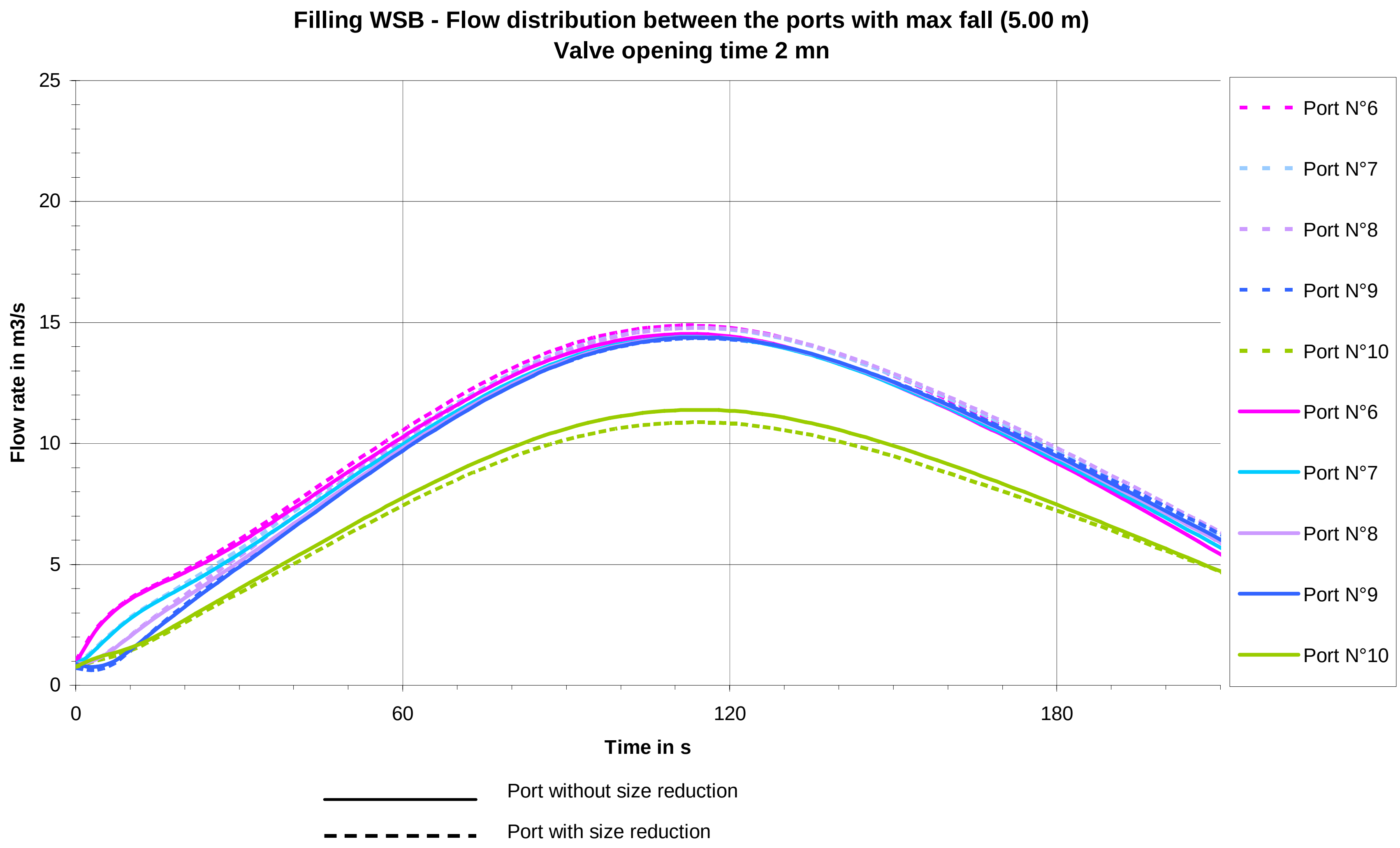

Annex 14-7.doc

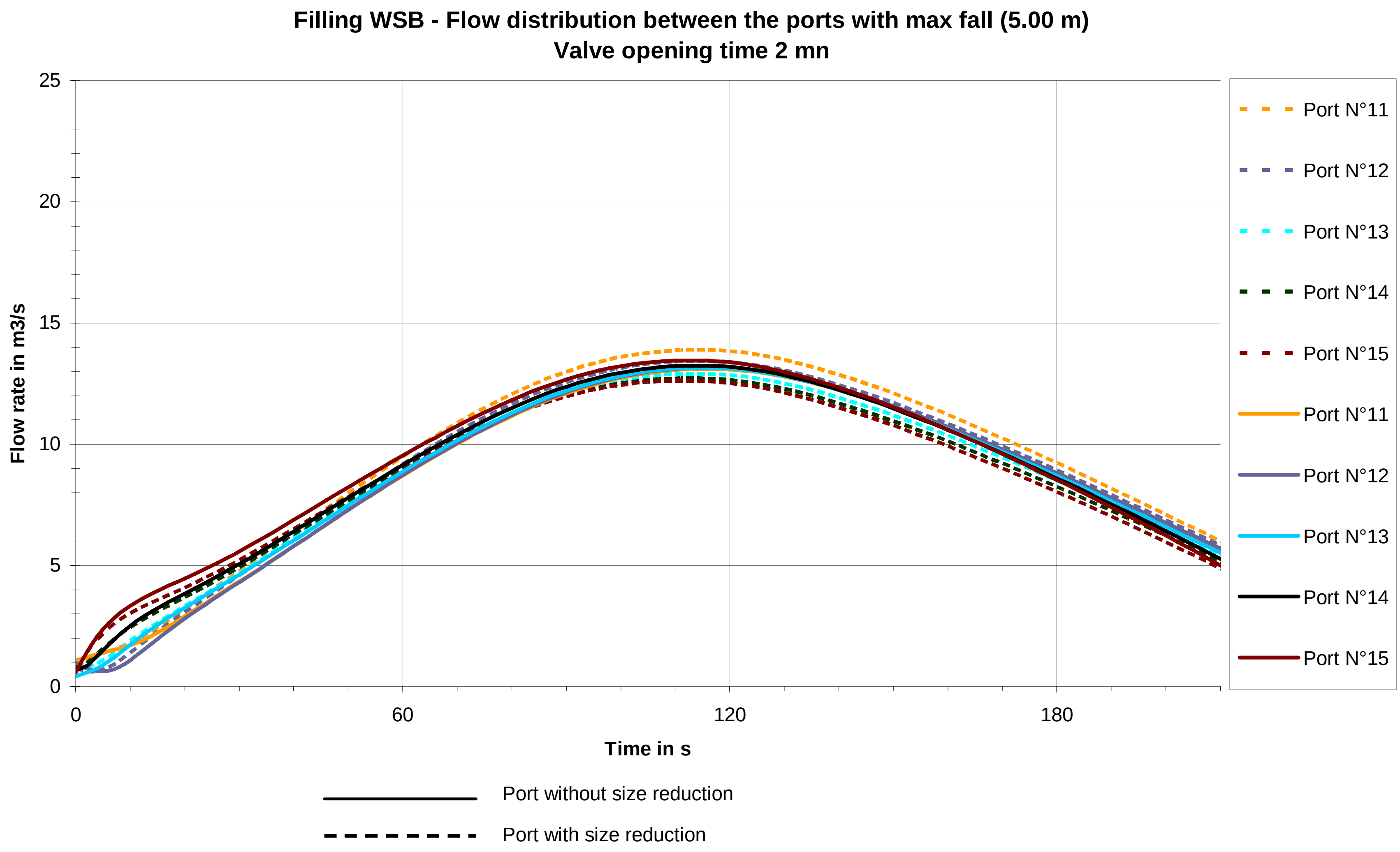

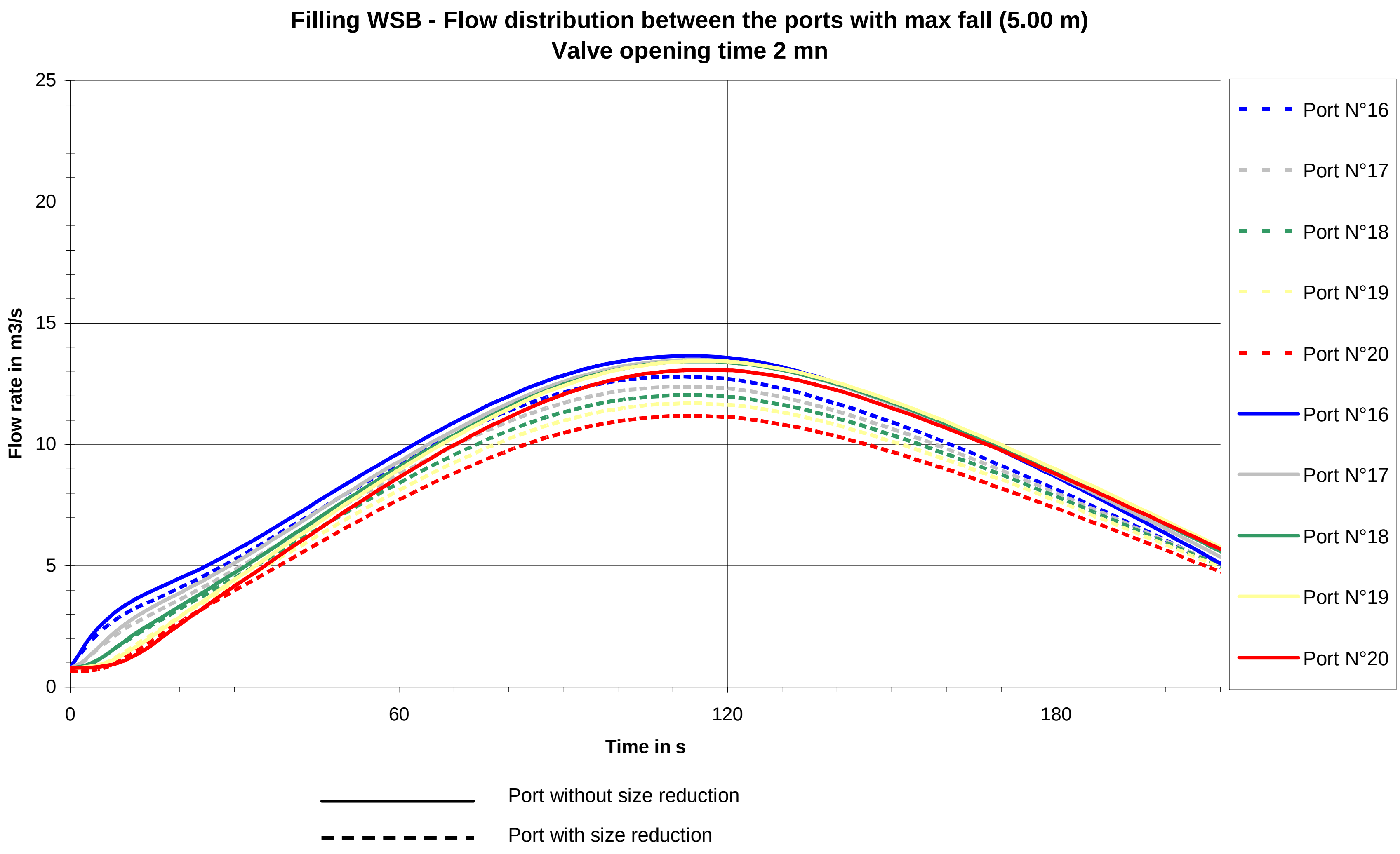
Filling WSB - Flow distribution between the ports with max fall (5.00 m)
Valve opening time 2 mn
Flow rate in m3/s
Time in s
0
5
10
15
20
25
0
60
120
180
Port N°16
Port N°17
Port N°18
Port N°19
Port N°20
Port N°16
Port N°17
Port N°18
Port N°19
Port N°20
Port without size reduction
Port with size reduction

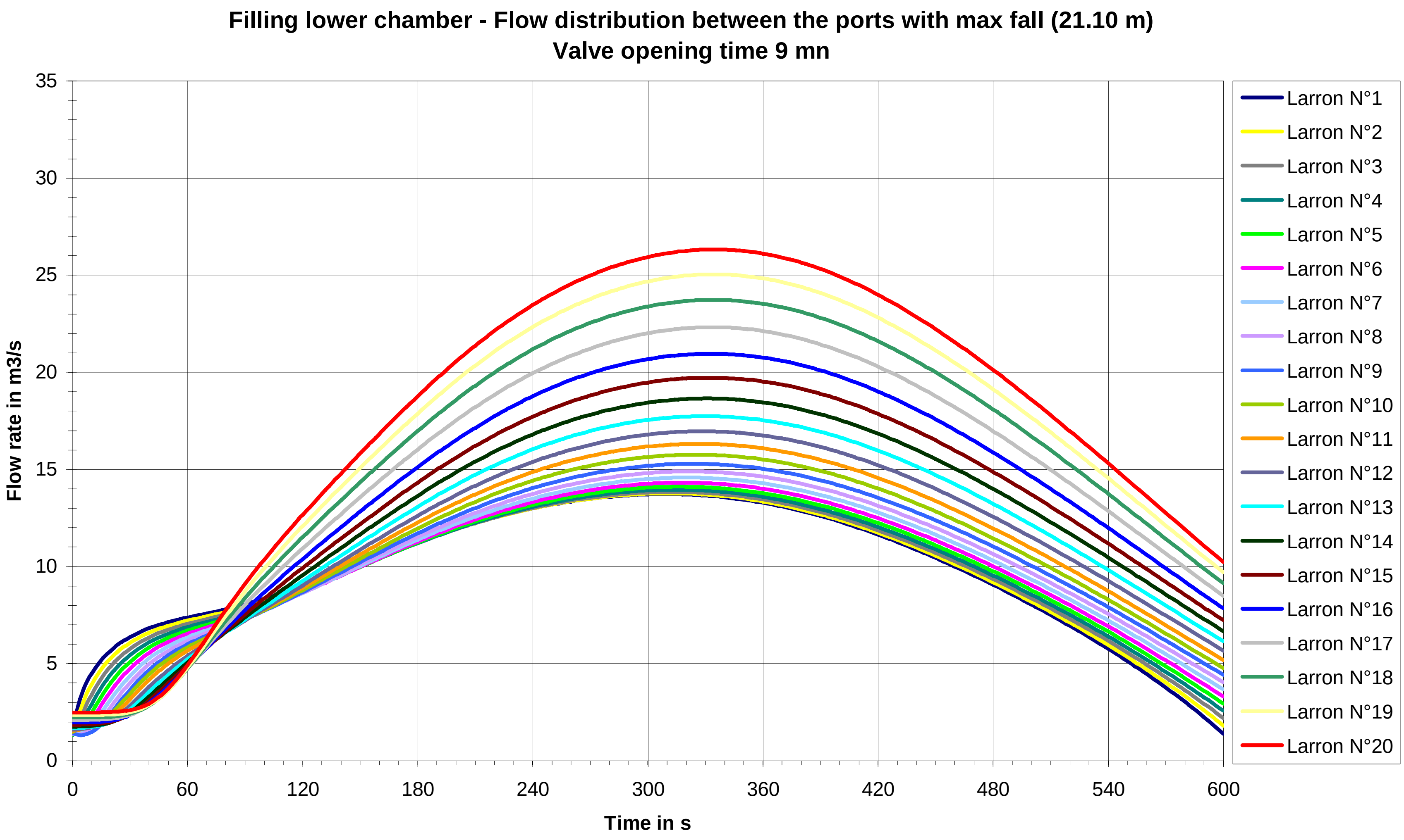
Filling lower chamber - Flow distribution between the ports with max fall (21.10 m)
Valve opening time 9 mn
Flow rate in m3/s
Time in s
0
5
10
15
20
25
30
35
0
60
120
180
240
300
360
420
480
540
600
Larron N°1
Larron N°2
Larron N°3
Larron N°4
Larron N°5
Larron N°6
Larron N°7
Larron N°8
Larron N°9
Larron N°10
Larron N°11
Larron N°12
Larron N°13
Larron N°14
Larron N°15
Larron N°16
Larron N°17
Larron N°18
Larron N°19
Larron N°20

Annex 15-2.doc

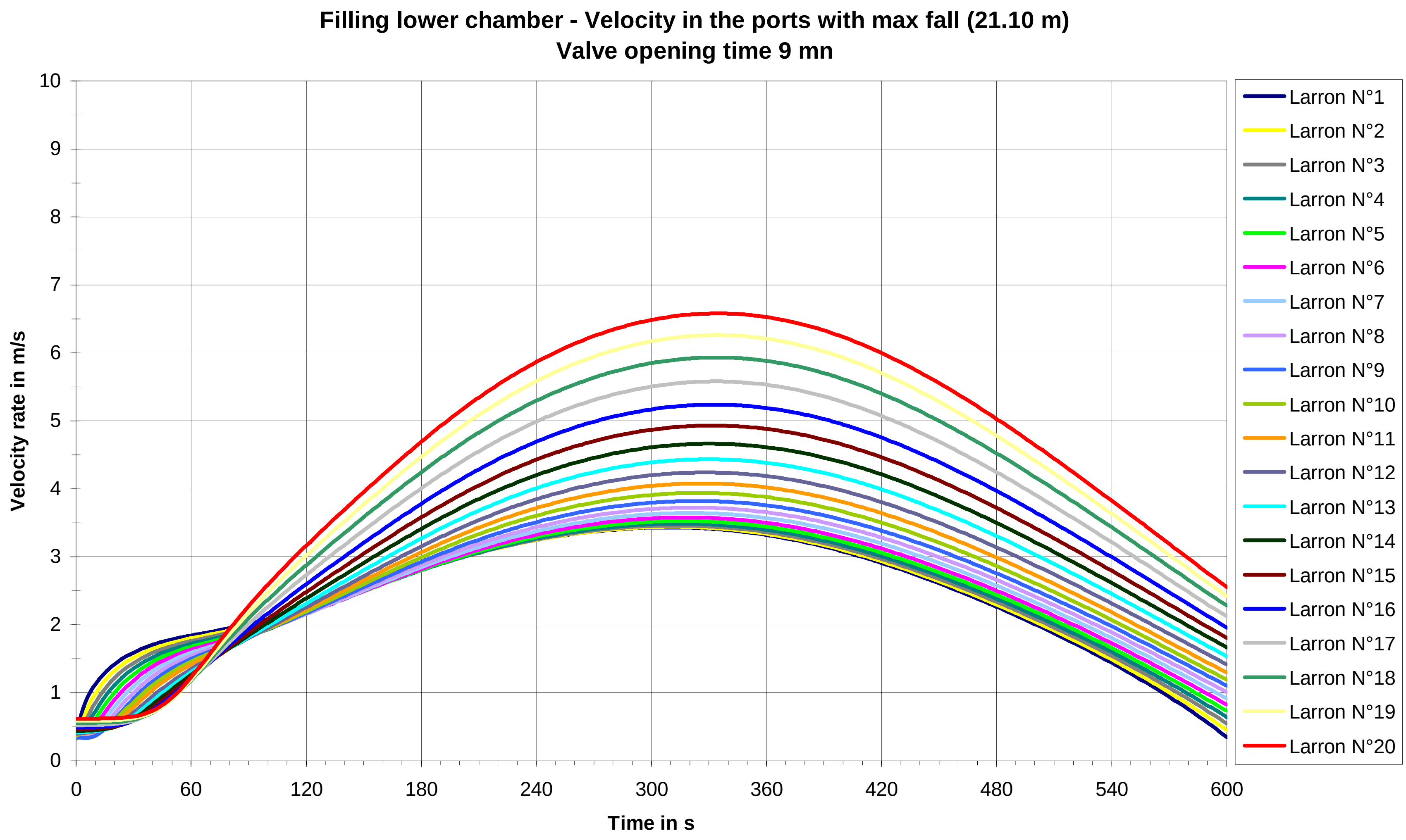

Annex 15-3.doc

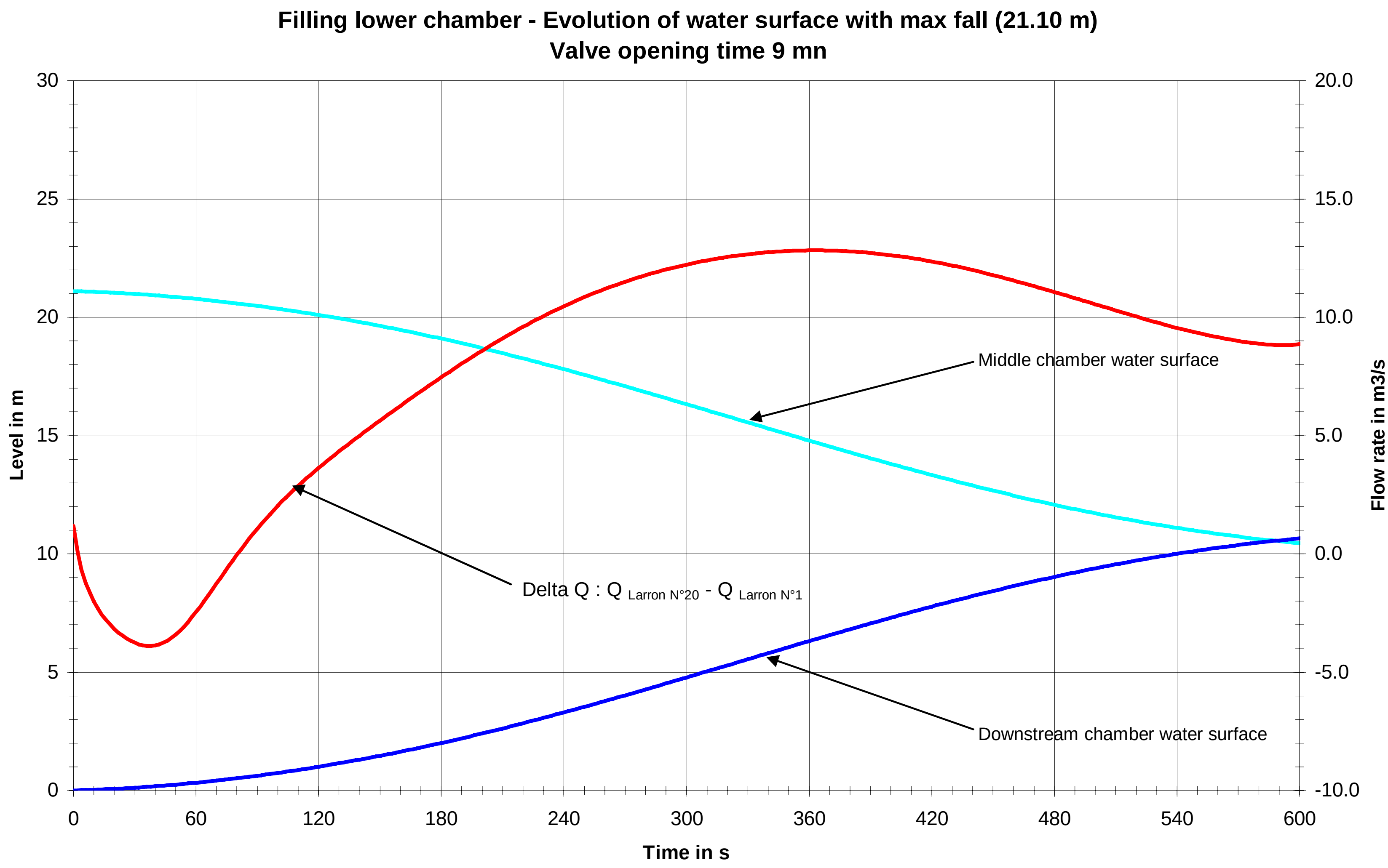

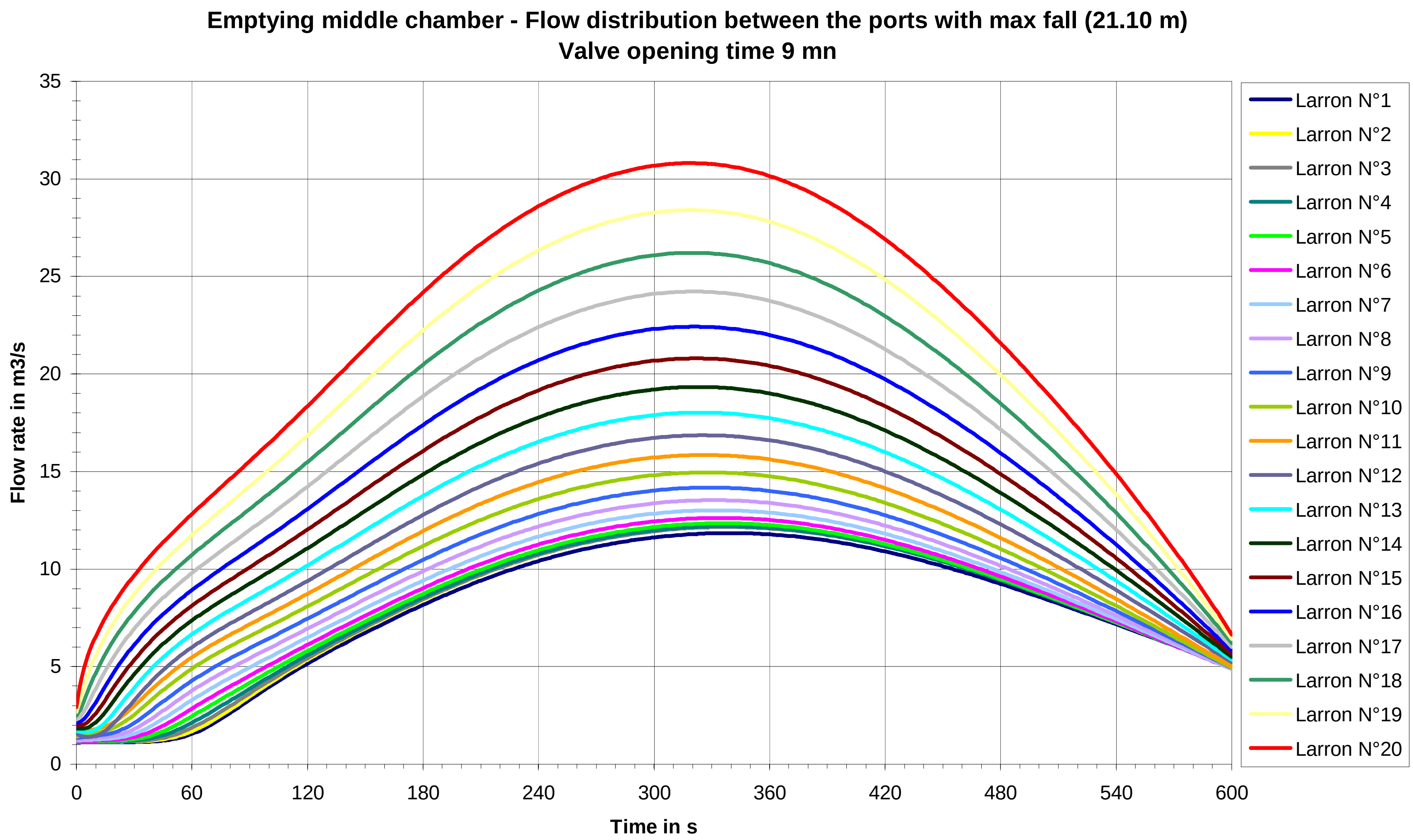
Emptying middle chamber - Flow distribution between the ports with max fall (21.10 m)
Valve opening time 9 mn
Flow rate in m3/s
Time in s
0
5
10
15
20
25
30
35
0
60
120
180
240
300
360
420
480
540
600
Larron N°1
Larron N°2
Larron N°3
Larron N°4
Larron N°5
Larron N°6
Larron N°7
Larron N°8
Larron N°9
Larron N°10
Larron N°11
Larron N°12
Larron N°13
Larron N°14
Larron N°15
Larron N°16
Larron N°17
Larron N°18
Larron N°19
Larron N°20

Annex 16-2.doc

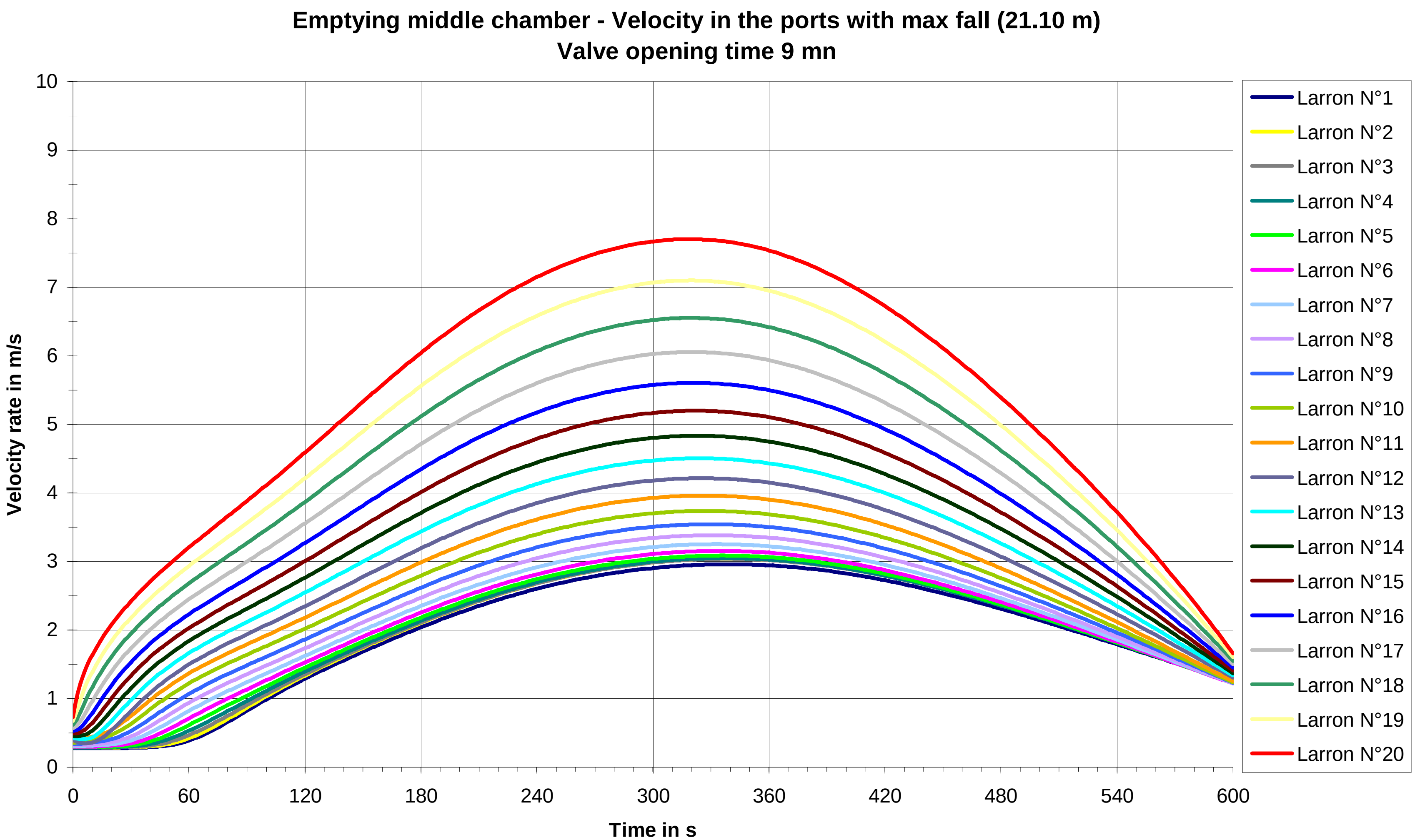

Annex 16-3.doc

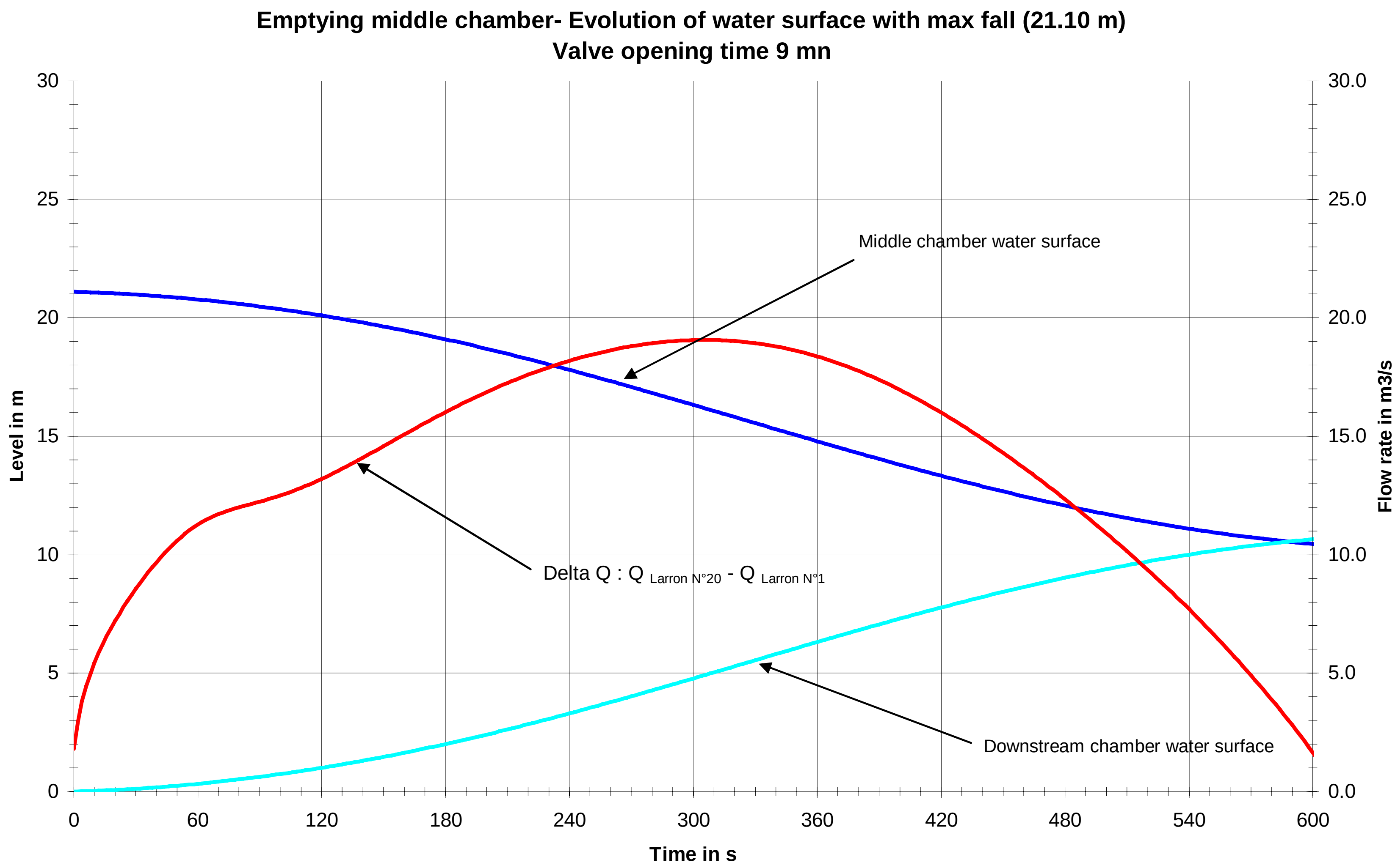

Annex 17

More refined dynamic analysis of ship motion and vessel positioning system

As mentioned in sections 10.3 and 10.4, a more refined dynamic analysis of the hawser forces (though not common in the conceptual hydraulic design phase) has been undertaken by Flanders Hydraulic Research in close collaboration with prof.dr.ir. Marc Vantorre of the Maritime Technology Division of Ghent University.

The purpose of this advanced analysis was twofold:

- illustrate the potential of the methodology for further optimizations of both the hydraulic design as well as the vessel positioning system for later design stages
- get some first idea about hawser force criteria related to tug boat assistance as a vessel positioning system

The methodology is similar to the one described in section 10.3, as far as the calculation of the discharge time series (Flowmaster 2 simulations) and the 2D simulations of the flow in the lock chamber are concerned.

In the more refined approach, however, not only the longitudinal component of the hydrostatic force will be calculated based upon the predicted water level time series of the 2D model, but also the other two components of the hydrostatic force as well as the three components of the hydrostatic moments acting on the ship's hull. In Figure Annex-17.1, the results are shown for the basic hydraulic design case (filling with WSB – configuration outer gate closed, see section 10.5), i.e. the design which has not been optimized at all and for which the (nondimensionalized) longitudinal force component F_x reaches a maximum of about 0.53 ‰.

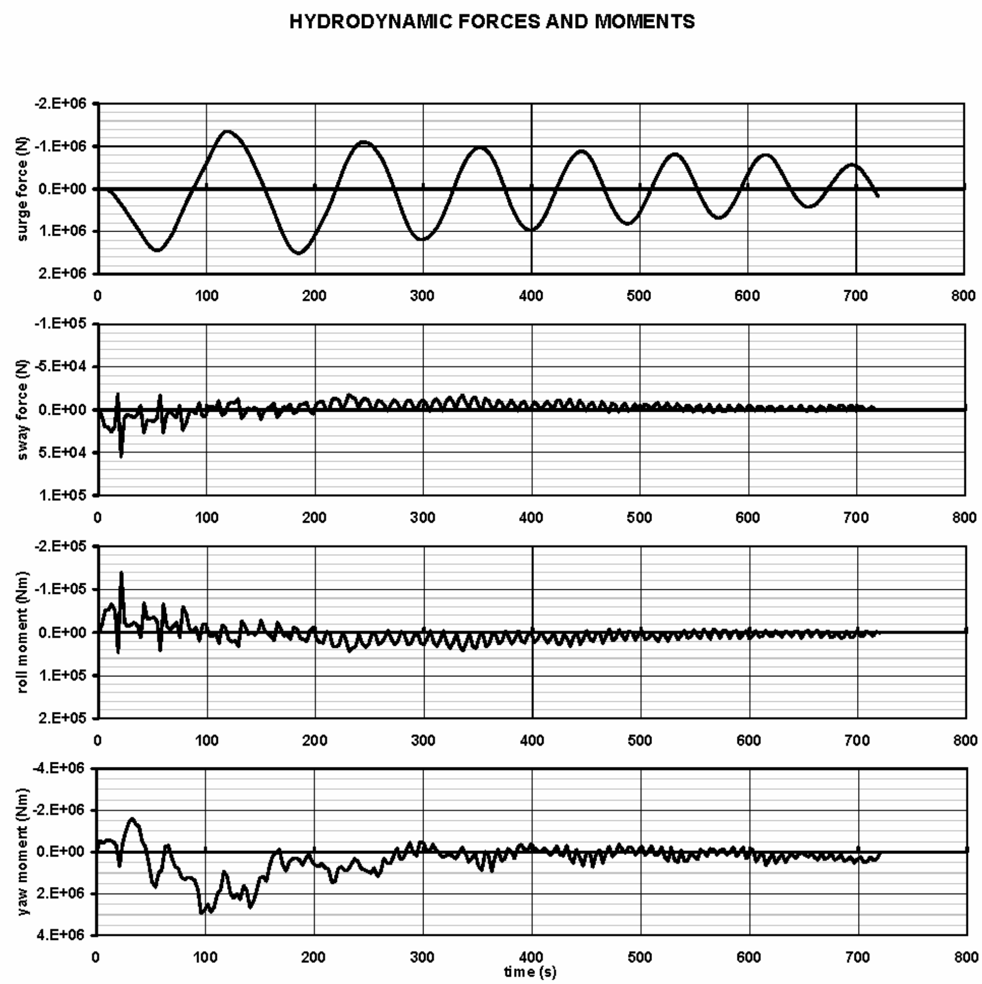

Figure Annex-17.1 : time series of hydrodynamic forces and moments

The six time series of hydrodynamic forces and moments will be fed into a dynamical model for the ship (i.e. six degrees of freedom are considered by means of a simplified set of motion equations) and the vessel positioning system (i.e. certain spring characteristics of the lines are assumed) developed by prof. Vantorre.

A design ship with following dimensions is considered:

Length	365.76	m
Beam	48.77	m
Draft	15.24	m
Block coefficient	0.60	

Preliminary calculations have been carried out with two types of vessel positioning systems:

- "Mooring lines": the lines act as linear springs, with limitation of forces;
- "Tugs": forces in the lines are generated so that the ship's longitudinal motion is counteracted.

The first system can be realised by mooring points fixed to the shore (e.g. bollards, locomotives), or by tugs keeping their positions. The second system requires dynamic control that can typically be realised by tugs, although it may also be implemented on a locomotive system.

In order to make comparison easier, it is assumed that the initial position of the lines are equal for both systems:

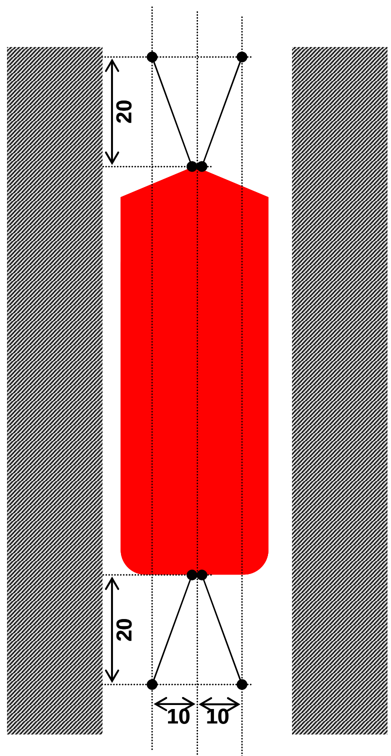

A vertical distance of 10 m is chosen between the connection points of the lines.

For the "mooring lines" system, a breaking strength of the wires of 1500 kN is selected, with an elongation of 2% at breaking force. The line force is assumed to be proportional to the relative elongation. The force in the moorings is limited to 600, 800, 1000, 1200 and 1500 kN, respectively.

The "tug assistance" system is assumed to generate a force dependent on the longitudinal velocity of the ship. In case of a velocity ahead, the two tugs aft generate their full bollard pull as soon as the velocity exceeds 0.01 m/s; for lower speeds, the line force is reduced proportionally. If the ship moves astern, the two tugs fore act similarly. The maximum line force is limited to 300, 400, 500 and 600 kN, respectively.

The dynamic behaviour of the ship subject to hydrodynamic forces and moments (calculated by means of the Delft 3D of Flanders Hydraulics Research) is simulated in six degrees of freedom by means of a simplified set of motion equations.

The following may be concluded:

- A dynamically controlled system requires line forces that are significantly smaller than a static mooring system.

- Further calculations reveal that, in the case of static mooring, a less stiff mooring system leads to instable motions.

- Even with rather limited control forces (e.g. 4 tugs * 300 kN, see Figure Annex-17.2 and Figure Annex-17.3), the surge motion of the ship is limited to 10 m, if the forces are controlled dynamically. This range can be reduced to about 2.5 m if the control forces are doubled (see Figure Annex-17.4 and Figure Annex-17.5).

- If the longitudinal motions are under control, lateral motions do not appear to cause any problems.

Important remark: One should not forget that these conclusions are drawn based upon a non-optimized, basis hydraulic design. The question arises whether these conclusions should be amended (most likely in the favourable sense) when taking benefit of the first hydraulic optimizations in the conceptual design (leading to a reduction of the longitudinal force component with about a factor 2, see section 10.7). It is advocated to investigate this in later design phases, where even further hydraulic optimizations can be explored.

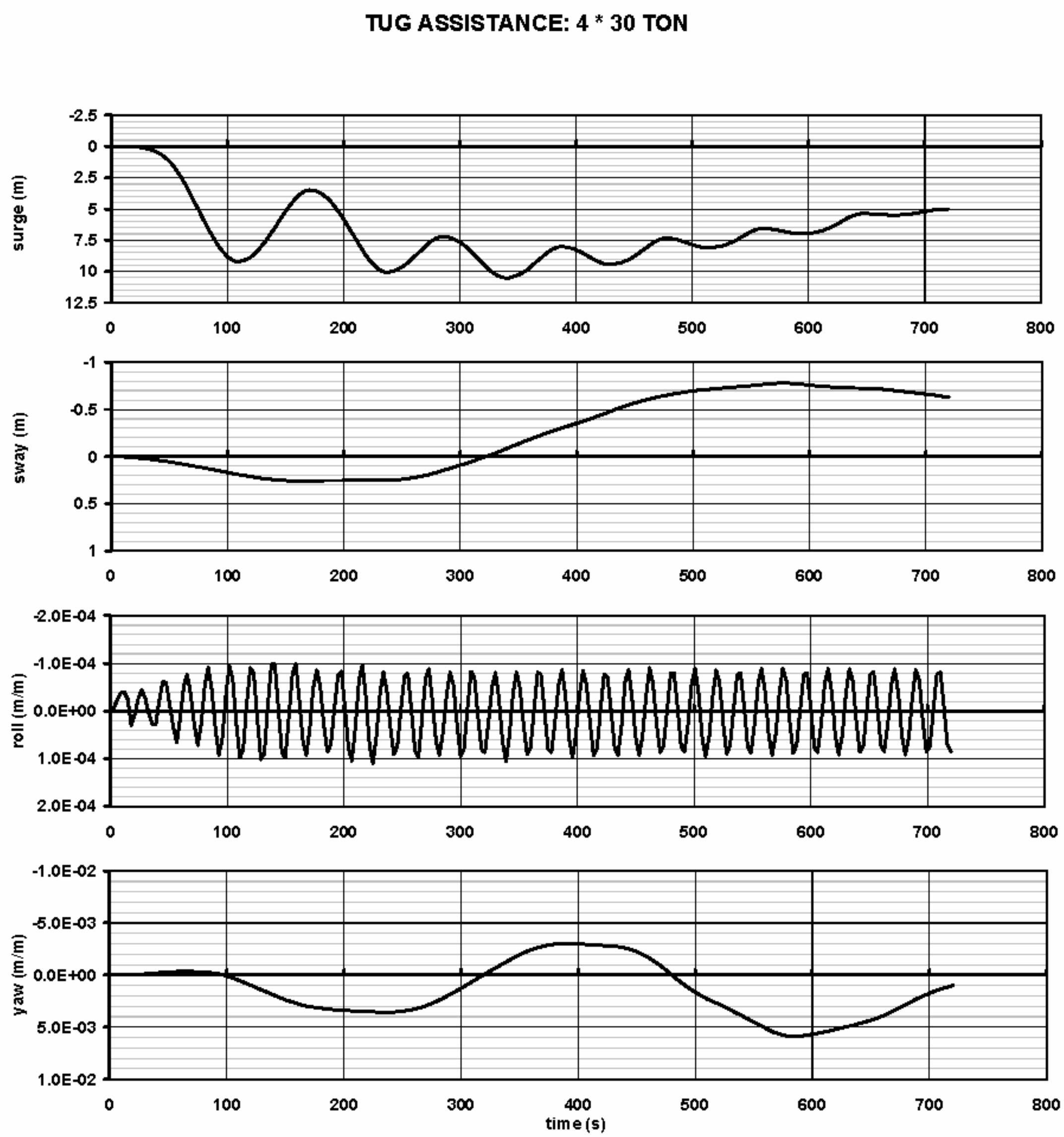

Figure Annex-17.2 : Ship motion in case of dynamic mooring with 4 tugs * 30 ton

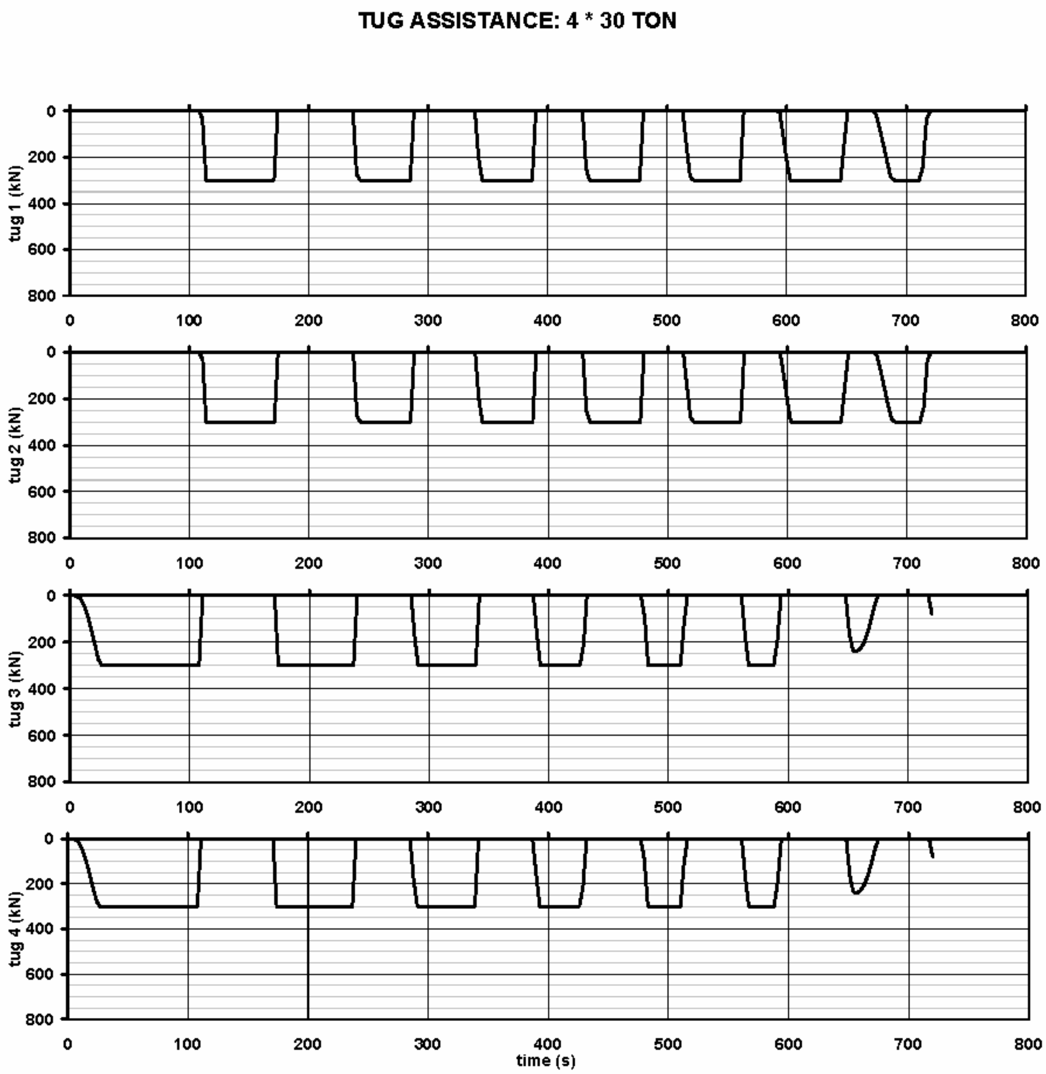

Figure Annex-17.3 : Hawser forces in case of dynamic mooring with 4 tugs * 30 ton

TUG ASSISTANCE: 4 * 60 TON

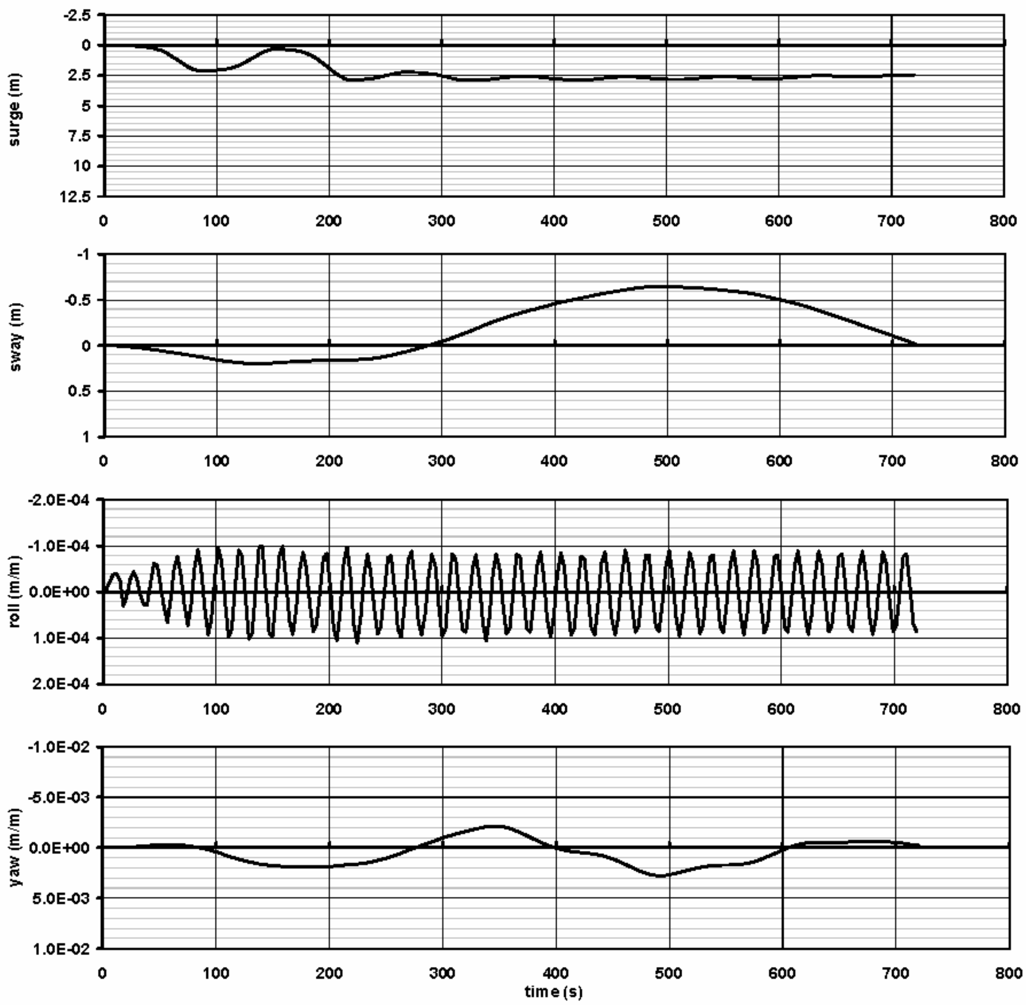

Figure Annex-17.4 : Ship motion in case of dynamic mooring with 4 tugs * 60 ton

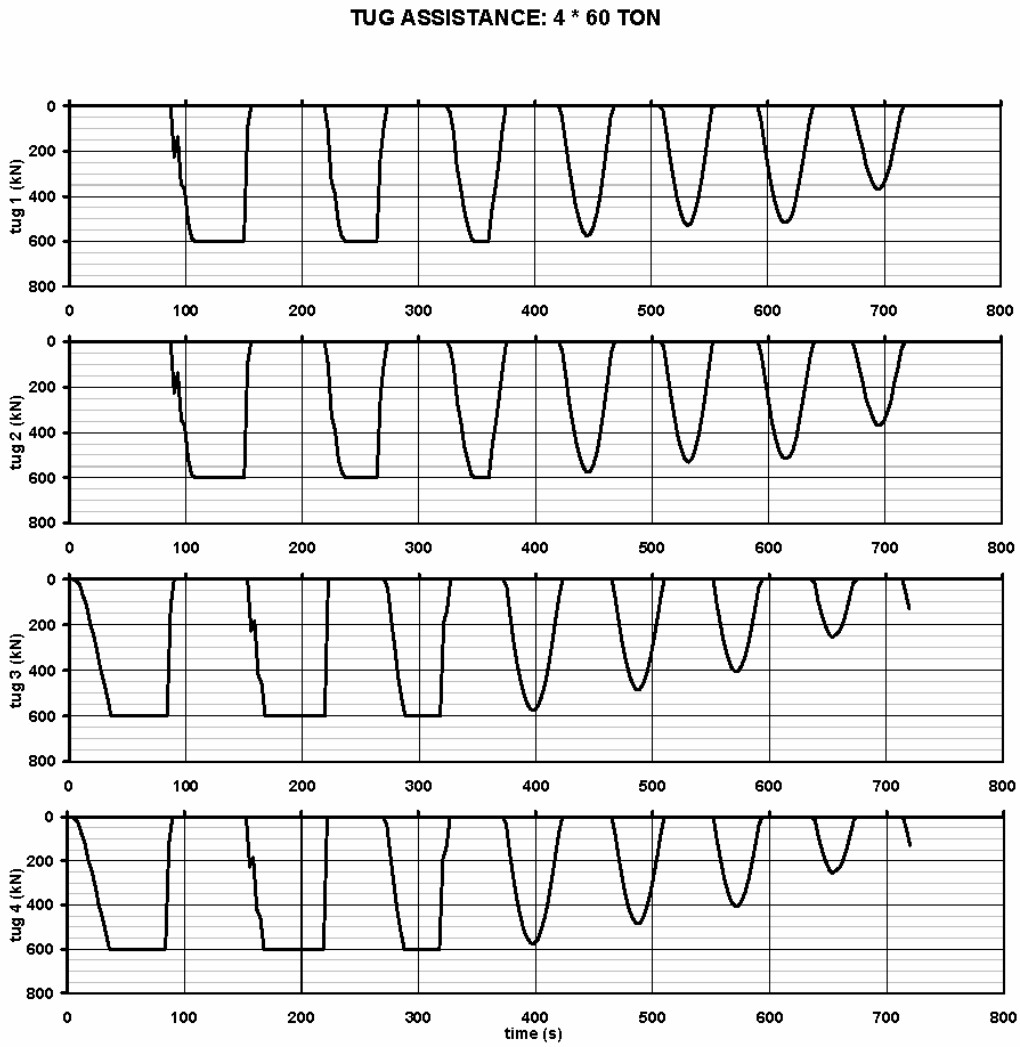

Figure Annex-17.5 : Hawser forces in case of dynamic mooring with 4 tugs * 60 tons

CPP Consórcio Post-Panamax

Update of Pacific Locks Conceptual Design and Harmonization of Atlantic Lock Conceptual design - Contract SAA-143351

PACIFIC LOCKS ACTUALIZATION

TASK P4d – LOCK GATES – Lay out of rolling gates

Tractebel Development Engineering — TECHNUM — COYNE ET BELLIER — Compagnie Nationale du Rhône

in association with

SBE — Port of Antwerp — FITA — AOSO

Lay out of rolling gates

1 BASIC DATA

1.1 WATER AND BOTTOM LEVELS

Following water levels and corresponding bottom levels of the different lock chambers are taken in account for the concept design of the gates structures and lay out. All level data are in m and refer to PLD. Note that (only) for lock head PA1 a minimum sill depth of 16.76 m (55 ft) is proposed.

	Gate PA1	Gate PA2	Gate PA3	Gate PA4
Max. water level upstream	+ 27.13	+ 27.13	+ 18.30	+ 9.81
Min. water level open/close gates	+ 24.99 (*)	+ 16.51	+ 7.66	- 3.44
Min. water level downstream	+ 16.51	+ 7.66	- 2.32 (**)	- 2.32 (**)
Sill level (downstream)	+ 8.23	- 1.74	- 10.42	- 20.62

(*) For maintenance operations in the gate recesses a safety allowance is considered: the minimum water level for floating operations of the gates is taken +23.00 m PLD (see 2.3)
(**) A minimum downstream water level of -3.44 m is considered in an ultimate loading case.

1.2 GEOMETRY

The axis to axis distance between the vertical bearings of the gates at the lock walls is taken 57.24 m (i.e.: the width of the lock chamber plus an excess length of 2.24 m).
The center of the horizontal bearing at the bottom of the gates is positioned 0.40 m below the level of the sill. The axis level of the horizontal bottom frame will be situated 1.27 m above this level in order to facilitate access under the gates during maintenance and repair operations, in particular to replace the lower support wagon.

No specific optimum shaping is considered: at the relatively low operating speeds of gates the hydrodynamic forces are relatively small compared with the inertia forces acting simultaneously on the heavy lock gate structures and the large moving water masses which are exchanged between the gate recesses and the lock chamber during operations.

To achieve a smooth filling and emptying (F/E) of the lock chamber, with a minimum delay of the water level evolution in the space between a pair of lock gates in each lock head, openings may be introduced in the lower upstream skin plating panels. Consequently the lay out of the stiffening of these panels (in compression!) has to be adapted accordingly.
Possibly even valves are to be built in the gates for a fast water level equalization throughout.

Upstream gates PA1
The skin plating extends over an additional 0.45 m (horizontal) and 0.25 m (vertical) from the above defined bearing axes. Thus the total horizontal length of the gate skin plating is 58.14 m.

Intermediate and downstream gates PA2 - PA3 resp. PA4
For gates PA2, PA3 and PA4 the axis to axis distance between the vertical bearings of the gates at the lock walls is taken 57.24 m like for gates PA1. Added to the width of the lock chamber (55 m), gates PA2, PA3 and PA4 also have an excess length of 2.24 m. At this conceptual design stage there is no evidence that additional excess length at the rear end would be required considering the accommodation in the lock head for the slot bulkhead (see 3.8) at the gate recesses.
The skin plating extends over an additional 0.45 m (horizontal) and 0.25 m (vertical) from the above defined bearing axes. Thus the total horizontal length of the gate skin plating is 58.14 m.

1.3 STANDARDIZATION

Based on the basic data listed above, the following assumptions on standardization are made for the concept design of the gates structures and lay out.

1. The intermediate gates PA2 and PA3 have an identical structural lay out. As a consequence, gates PA3 have an increased height of 0.15 m compared to the "tailor made" situation of 1 m freeboard above the local maximum water level. Conversely gates PA2 have a level of air chamber which is 0.17 m lower than the level which normally would have been chosen. The said deviations from the "tailor made" structures are found practically negligible.
   It has been verified that these gate structures are suitable for the Atlantic locks complex as well. In that case the deviations from the "tailor made" structures are somewhat larger; the additional cost of these are commented in the report on the harmonization study of the Atlantic locks.
   An important advantage of such standardization is a certain flexibility during the construction phase of the two lock structures: according to the progress of both works, a call can be made on the steel constructor to deliver these "standardized" gates on either site.
2. The center of the horizontal bearing at the bottom of all gates remains positioned 0.40 m below the level of the sill at all lock heads; no deepening of the lock heads below the gates is proposed to minimize the risk of objects getting stuck between the seals of the gates. As a consequence, gates PA3 have an increased freeboard (1.15 m) above the local maximum water level.

3. All relative measures of support rolling wagons and cantilevering branch remain identical among standardized gates, in order to keep all mechanical connection parts identical. As a consequence, support rolling wagons and their rails for gates PA3 have an increased level above the local maximum water level, causing a build up with increased height above the lock platform at the lock head PA3.
4. Lower support rolling wagons will be standardized as much as possible (as a - preferably common - spare one is proposed); upper support rolling wagons may be "tailor made" (as no spares are proposed, considering its relative ease of maintenance thanks to its position above the water level).
5. The thickness of the skin plating and the type of stiffener profile may be differentiated for each panel in the cross section only. No differentiation is considered in the longitudinal direction of the gates, yielding a maximum economy of scale (e.g.: automatic welding) during construction and a minimum risk of human error during assembly.
6. The number of different plate thicknesses and type of stiffener profiles are kept to a minimum.

1.4 LOAD CASES ASSUMPTIONS

The following assumptions on load cases are made for the concept design of the gates structures and lay out.

1. Traffic load is considered to be of a moderate level for which normal bridge deck designs apply.
2. The gates resist the water pressures due to the possible differences between the water levels listed in the table sub 1.1. An ultimate limit loading case with an increased maximum upstream water level by 1 m is considered (in combination with an extreme low downstream water level at gates PA3 and PA4). Gates PA1 and PA4 (reversed - see 3.9) are verified to be able to retain the water in case of a lock chamber dewatering.

   As an accidental load case the gates are able to additionally resist the water pressures induced by “maximum credible” earthquakes (MCE) with a peak ground acceleration (PGA) up to 0.4 g. In this concept design the quasi-static “Westergaard” procedure is adopted to estimate these excess pressures. The horizontal seismic coefficient (kh) is taken according to the PIANC seismic design guidelines for port structures (see design criteria).

   A reduction factor according to Housner is applied for the case of water pressures generated in bodies of water with finite length (relative to the total waterdepth), i.c.: between the two skin platings of the lock gates and between two adjacent lock gates.

   More sophisticated (dynamic) analysis procedures may reveal more precise (less conservative) conclusions. These may be considered in a more detailed phase of the design.
3. The gates are not subject to back pressures from the downstream side: locking procedures will be designed such that the water level at the downstream side of each gate never exceeds the water level at the upstream side.
4. The stability against rolling over of a floating gate is not considered as a determinative design criterion; however the metacentric height will be checked afterwards to assess the possible need for auxiliary equipment and provisions during floating operations.
5. Floating of the gates stabilized in upright position is still possible after complete flooding of three watertight zones (of each two compartments of the air chamber - length = 2 * 3.18 m = 6.36 m), e.g. due to local damage after a ship collision. It is assumed that a bulb of a huge ship can damage at the same time two adjacent transversal walls between watertight zones.

2 GATE STRUCTURE DESIGN

2.1 GENERAL

In what follows the concept design of the structure and lay out is presented for rolling gates of the “wheelbarrow” type, i.e. with a submerged lower support wagon running on rails at the bottom of the lock chamber and an upper support wagon on rails above the water.

For all gates a symmetrical structure with double skin plating is proposed in order to achieve a maximum of safety against global collapse in the event of accidental ship collisions. Weight reduction through the use of compact compression members instead of compressed plating is marginal. Through an appropriate choice of the width of the gates (enabling to float them in a stable manner), material stress levels are kept sufficiently limited to guarantee safety against buckling risk, which is determinative in this case.

Note on buckling design standards: compressed plating is designed against buckling according to the Belgian standard NBN B 51-002 (August 1988), based on the linear elastic buckling theory (similar to for example DIN 4114) in combination with the safety concept adopted in the present Eurocode 3. The appropriate effective stiffeners are designed according to the technical notes of the CECM.

Observing these options, the same design procedure is followed as described in the methodology of the earlier CPP concept design study.
Note on fatigue: the gate structures (and most of the load bearing parts fixed to it) are subjected to cyclic loading and unloading, going along with the locking operations. The number of cycles over a 100 years life time design period is set at N = 25 cycles/day x 36525 days = 9.125×10^5 (see section 3.10 of the specific design criteria).

Based on our experience with common material stress levels (below the limit value for fatigue) for the proposed steel grade S355J2G3 and with common overall lay outs of the structural framework of rolling gates, an a priori estimate is made of the total width and weight of the gates and the spacing between the vertical frames.
Thus the necessary height of the air chamber is estimated and a local analysis yields the necessary “equivalent” thickness of the plating (i.e.: taking in account the material consumption for the necessary longitudinal stiffeners – see 2.2). The position of the top and bottom of the air chamber is fixed observing the minimum water level at closing and opening operations (see 2.3) and an appropriate upper deck is designed for the traffic loads to be considered (2.4). Based on the assumption of an equivalent plate thickness of the intermediate horizontal frames, an overall cross section analysis yields an estimate of the torsion stiffness distribution over the horizontal frames, taking in account their contingence.
Then a 2D-beam grid model of the gate structure (integrated over the width) is drawn up. Subsequently the assumed material tension levels are verified, in particular for the design of the compressed parts against buckling and the (local) design of the longitudinal stiffeners. Both elements may have a

considerable impact on the final weight distribution of the gate structure, allowing to verify the height of the air chamber, the reaction forces at the support wagons and the floating stability.

Hereafter the concept design of some particular parts of the lock gates is discussed. It will be indicated how a more detailed level of design may lead to optimization of the obtained results.

Finally the main characteristics are listed (2.5) for which convergence occurs with the design procedure mentioned above.
Gates PA2 and gates PA3 have an identical structure (occasionally denoted as PA2-3). Moreover it appears that gates PA2-3 and PA4 require almost the same width. Therefore an identical width is proposed for the three lower support wagons. Thus it is possible to limit the number of different spare parts, which are interchangeable for these three types of gates.
From the attached cross section drawings of the proposed concepts it can be seen that the proposed intermediate water levels do not allow an identical gate structure for gates PA2-3 and PA4.

2.2 SKIN PLATING AND STIFFENERS

The skin plating is divided in different panels between the horizontal structural frames considered. Each panel is designed separately to retain the water pressure (p) that acts upon it. The choice of the thickness (e) of the plating is based on experience, such to limit the material tension for a chosen width of the gates. It is to be confirmed and possibly optimized in a more detailed level of design.

If B denotes the height of a panel, the number n of longitudinal stiffeners is determined such that their spacing l = B/(n+1) satisfies the following:

$$\frac{pl^2}{12} \leq \sigma_{max} \cdot \frac{e^2}{6} \tag{2.1}$$

If L denotes the horizontal length of a panel between two vertical structural frames, the required stiffener profile (minimum moment of inertia I and bending module W, in combination with an effective strip of plating) results from:

$$\frac{(pl)L^2}{24} \leq \sigma_{max} \cdot W \tag{2.2a}$$

$$\frac{(pl)L^3}{384\,E\,I} \leq \left(f/L \right)_{max} \tag{2.2b}$$

where σ_{max} and $(f/L)_{max}$ are respectively the maximum allowed material stress level (for local load transfer) and (local) displacement of the stiffener profile in combination with an effective strip of plating (taking in account the shear lag effect), which are chosen based on experience with similar structures and taking in account the (global) material stresses derived from the 2D-beam grid model.

Note that the adopted design value of the (local) bending moment (2.2a) holds halfway between two vertical frames. The doubled value locally occurring at the connection with the vertical frames is resisted by additional triangular stiffener plates, which also transfer the corresponding (local) shear forces to the frames. In order to arrive at moderate material stress levels in plating and connecting welds (fatigue!) the σ_{max}-value is chosen appropriately for each panel and each stiffener according to the occurrence frequency (probability) of the loading case considered (accidental, ultimate or service limit state).

From a catalogue of commercially available standardized steel profiles, the necessary cross sectional area A is derived such that the "equivalent" plate thickness (e_{eq}) for the 2D-beam grid characteristics and the weight estimation of the considered panel becomes:

$$e_{eq} = e + \frac{n \cdot A}{B} \qquad (2.3)$$

2.3 POSITION OF TOP AIR CHAMBER

In general the top level of the air chamber is to be chosen such that (if possible) the air chamber remains entirely submerged during opening and closing of the gates, thus avoiding excessive loading on the support wagons.

In this case the top level of the air chamber is taken 0.50 m below the lowest water level at which opening and closing of the gates will take place (see basic data sub 1.1), allowing for possible water level fluctuations in the lock chambers.

For gate PA1 an additional safety margin below the estimated lowest lake Gatun level is considered, with a head allowance to keep the slot bulkhead pressed against the bearings of the gate recess. Thus it is possible in all circumstances to create a sufficient free working space under the floating gates in the gate recess. This consideration does not apply to the other gates, as the water level in their gate recess may be adjusted (elevated) if necessary. The thus lowered position of the air chamber of gate PA1 does not significantly affect its floating stability, as it has a relatively low level of center of gravity (compared to the other gates) and the air chamber remains in a relatively elevated position.

2.4 ROAD BRIDGE DECK

For this concept design, the road bridge deck lay out is taken similar to the one of the Berendrecht lock gates, which has more or less similar horizontal dimensions of deck panels between the structural frames and the edges. Furthermore two movable deck panels at the extremities are proposed to bridge the height difference from the top level of the gates to the ground level of the surrounding concrete structure by a ramp of 10% inclination angle. This would be applied for gates PA1 only.
These lay outs are subject to further investigation in a more detailed level of design.

2.5 CONCLUSIONS: MAIN DIMENSIONS AND CHARACTERISTICS

The general cross sectional lay out of the different gates for the Pacific locks complex is shown on the attached drawings. A lateral and aerial view and a section over half of the gate length is shown as well.

The proposed inner diameter of the vertical access tubes is 1.0 m and the outer diameter of the horizontal access tube in the air chamber is 2.3 m. The air chamber has one longitudinal separation wall, constituting two adjacent watertight compartments in each cross section.

Although a slight difference occurs in the height and in the freeboard above the minimum operating water level, it is found that an identical structure for gate PA2 and gate PA3 is appropriate. Gate PA3 will have a slightly increased freeboard allowance of 1.15 m above the maximum water level in the corresponding upstream lock chambers, compared with the 1 m assumed for the other gates.

Below some dimensions and characteristics are listed for the proposed concepts of the gates. Note that these figures are to be confirmed and subject to revision in a more detailed level of design.
E.g.: additional longitudinal separation walls in the air chamber will increase the stability against rolling over of a floating gate, but will complicate the separate accesses of the watertight compartments from the central horizontal access tube. Moreover the weight of the gates will increase substantially and the entire lay out of the gates (below the top level of the air chamber) is subject to revision.

Axis levels (m PLD) of horizontal frames	Gate PA1	Gate PA2	Gate PA3	Gate PA4
R1: top of upper frame = bridge deck	+ 28.13	+ 28.13	+ 19.45	+ 10.81
R2: intermediate frame above air chamber	not present	not present (optimized gate structure)		
R3: intermediate frame above air chamber	+ 24.94 (*)	+ 21.98[5] (*)	+ 13.30[5] (*)	+ 3.43[5] (*)
R4: top of air chamber	+ 21.75	+ 15.84	+ 7.16	- 3.94
R5: bottom of air chamber	+ 15.95	+ 9.34	+ 0.66	- 10.24
R6: intermediate frame below air chamber	+ 12.52[5] (*)	+ 4.23[5] (*)	- 4.44[5] (*)	- 14.99[5] (*)
R7: bottom frame	+ 9.10	- 0.87	- 9.55	- 19.75
R8: bottom bearing at the sill	+ 7.83	- 2.14	- 10.82	- 21.02
R9: bottom edge of skin plating	+ 7.58	- 2.39	- 11.07	- 21.27

(*) no horizontal connecting framework nor plating present

	Gate PA1	Gate PA2	Gate PA3	Gate PA4
Width (outside plating)	7 m	10 m	10 m	11 m
Spacing between vertical frames	3.18 m	3.18 m	3.18 m	3.18 m
Weight per lateral area (height x length)	1300 kg/m²	1500 kg/m²	1500 kg/m²	1500 kg/m²
Weight of gate structure	1550 tons	2600 tons	2600 tons	2700 tons

In general the figures above for gates PA1 are considered to be reasonable and very well in line with existing rolling gates. Gates PA2-3 and PA4 are of an extraordinary size, excluding any possible comparison. In general it is concluded that the proposed solution with rolling gates is well feasible as even the large gates PA2-3 and PA4 may be operated and handled in a safe and durable way, meeting all the practical criteria set out in the terms of reference.

Additional design computations are performed to investigate the possibility of reducing the width of gate PA4 from 11m (as proposed – see table above) to 10 m to obtain a uniform width of all "large" gates (all but PA1). This gate structure is referred to as gate PA4-10. The table below shows a comparison of the main characteristics taking approximately in account (the weight and the position of) all auxiliaries and equipment to be fixed to the various designed gate structures.

	Gate PA4-10	Gate PA4 (proposed)
Width (outside plating)	10 m	11 m
Spacing between vertical frames	3.18 m	3.18 m
Weight per lateral area (height x length)	1450 kg/m²	1500 kg/m²
Weight of gate structure	2600 tons	2700 tons
Max. righting moment (rm) (*)	30%	100%
GM (metacentric height) at max rm	60%	100%
Angle of inclination at max. rm	55%	100%

(*) Upper support rolling wagon considered fixed to the floating gate structure

Reducing the width of the gate requires heavier skin plating and/or stiffener profiles, especially in the upper zone of the gate structure, to resist the loading on the gate. This is particularly disadvantageous for the resistance of the gate against capsizing and the dynamic (rolling) behavior during floating operations. The table above gives a relative indication of the significant drop in (maximum) righting moment, metacentric height GM and angle of inclination at maximum righting moment for the gate structure PA4-10 compared to the proposed 11 m wide gate structure PA4. Still the (maximum) righting moment remains positive and thus in principle no auxiliary floating equipment and/or crane assistance is required for maneuvering gate structure PA4-10 in situations with sufficiently limited heeling moments (mainly due to wind and waves). From a more detailed analysis resulting absolute values of the righting moment may be compared to the actually occurring heeling moments to evaluate the floating stability. At this conceptual stage a gate width of 11 m is recommended as a minimum. Still the lower support wagons for 10 m wide gates may be used for these gates as well (see drawings).
In principle improvements of the mentioned characteristics are possible by dismounting the upper support rolling wagon prior to each floating maneuver. However this is a costly and time consuming operation requiring crane assistance and the dismounting of all connection trusses (both horizontal and vertical – see section 3.5) and therefore this is not recommended (loss of flexibility in emergency conditions!).

Gates PA1 and PA4 are suitable for dewatering the lock chamber. For gates PA1 this doesn't cause additional costs since the gates almost completely run dry at their downstream side already during normal locking operations when the water level in the upstream lock chamber equalizes with the water level in the downstream lock chamber (normal loading case).
In principle gates PA4 (double plated but like gates PA1 with seals only on the downstream side) might be reversed for this purpose and maneuvered to an appropriately shaped separate bearing. Subsequently the dewatering of the lock constitutes a less severe loading case than the service loading case during normal locking operations (see section 3.9). Considering the relatively moderate maximum downstream water level at the Pacific side (+3.60 m PLD) to retain at the downstream lock head in case of dewatering, an additional smaller type of gate, similar to PA1, would be an optimum solution. Doing so the dimensions of the additional bearing details may be kept to a minimum as well. In a more detailed phase of design, the necessity of bolted connections (possibility of dismounting) for the cantilevering branch (see section 3.5) can be investigated versus the possibility of (preferably) fixed (pre-fabricated) welded connections to the gate structure. The latter option possibly requires an adaptation of the lock wall structure at the top of the additional bearings.

3 LAY OUT OF DETAILS

3.1 GENERAL

In this section the conceptual lay outs of some operational features and details of the proposed rolling lock gates are presented. As stated in the methodology of the earlier CPP concept design study, similar lay outs of corresponding details of the rolling gates in operation at the large locks in the port of Antwerp (Belgium) are proposed.
Relevant excerpts from archive drawings of the Berendrecht lock gates are included in this report.
The appropriateness of the use of these details or those of the recently designed new rolling gates for the Van Cauwelaert lock (port of Antwerp) in the actual gates in the Panama case is evaluated where necessary, also considering the computations presented in section 5.

3.2 SEALS AND FENDERS

Both vertical (at the lock walls) as horizontal (at the bottom near the sill) seals are proposed to be massive beams. They have a rectangular cross section of 500 mm width and 250 mm thickness. The beams may be of azobé wood (considered in the computations) or a high performance composite material. The beams will be fixed on the skin plating on the downstream side of the gates between plate stiffeners of 150 mm width and 15 mm thickness.
These beams also constitute the supports of the gates against the bearings of the surrounding lock chamber structure (lock walls and sill). In section 5 it will be shown that the pressure levels in the beams require sufficient high strength materials, excluding currently available elastomeric materials.

3.3 FIXED SUPPORTS

At the sill level the gates have cantilevering extensions of their vertical frames. At the bottom end of these extensions fixed supports are designed such that the gate can rest on the bottom of the lock chamber or a gate recess when the lower support wagon (see 3.4) is absent (e.g.: due to maintenance)

On the extensions at the downstream side of the gate a steel reinforced elastomeric block is fixed to support a flexible cantilevering extension of the skin plating (see illustration). This system allows to adjust to a certain degree the reaction forces which will be exerted on the gates at the sill. This may be necessary to avoid uplift from the sill bearing of the skin plating at the gate bottom edges due to an inappropriate distribution of stiffness over the gate structure.

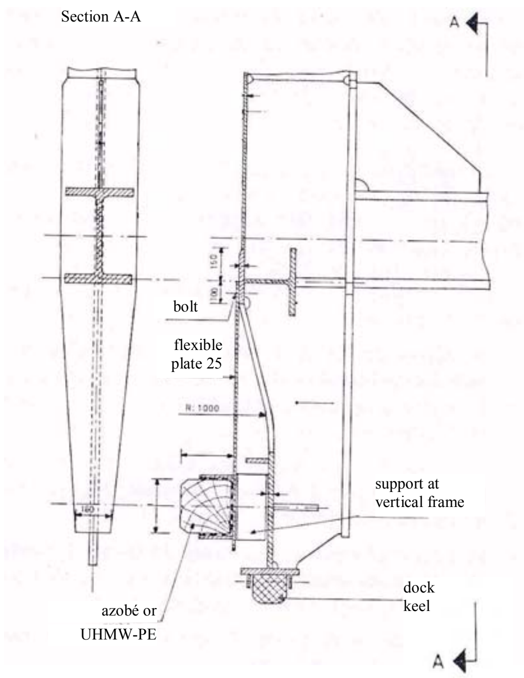

Seals and bottom support

3.4 LOWER SUPPORT WAGON UPSTREAM GATES PA1

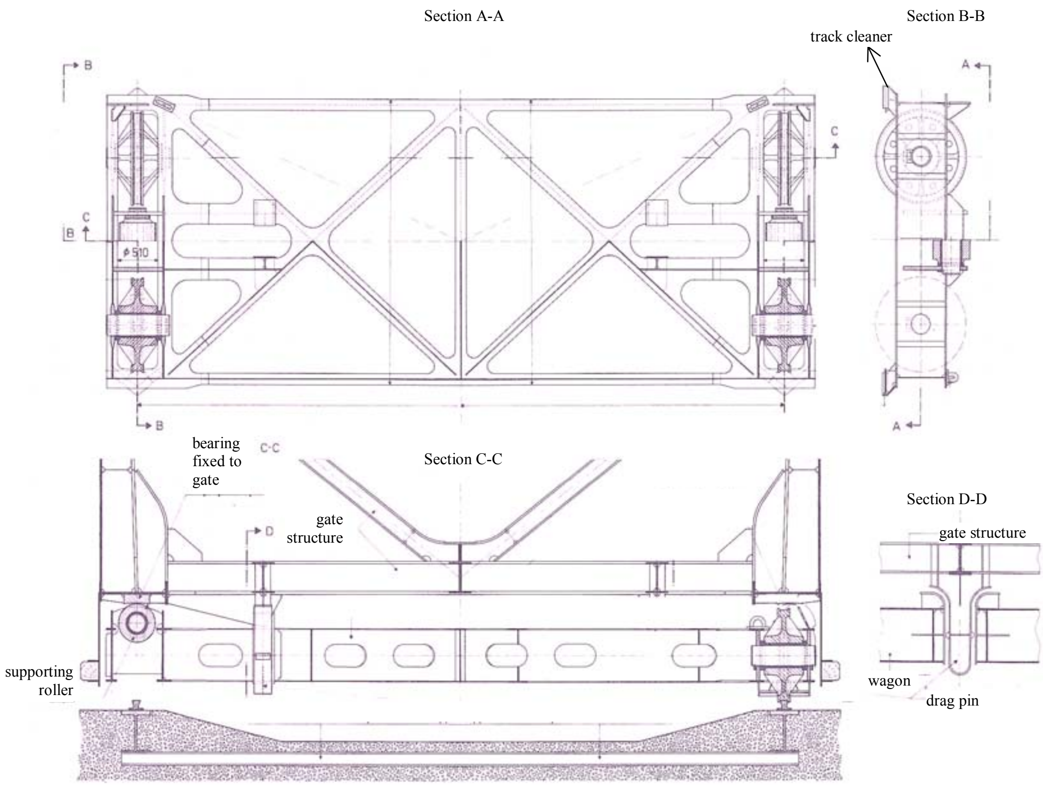

Lower support wagon

3.5 UPPER SUPPORT WAGON

From the assessment of the maximum vertical reaction forces over the range of operating conditions (see 5.2) it is concluded that a design similar to the upper support wagon of the Berendrecht lock is appropriate. A more extended framework design of I-shaped beams is proposed, similar to the recently designed new rolling gates for the Van Cauwelaert lock (port of Antwerp), as shown on the attached drawings. The flanges of the beams directly connect to a pair of longitudinal stiffeners of the skin plating of the gates. A lateral guidance wheel is built in at each side of the cantilevering supports.

3.5.1 General view

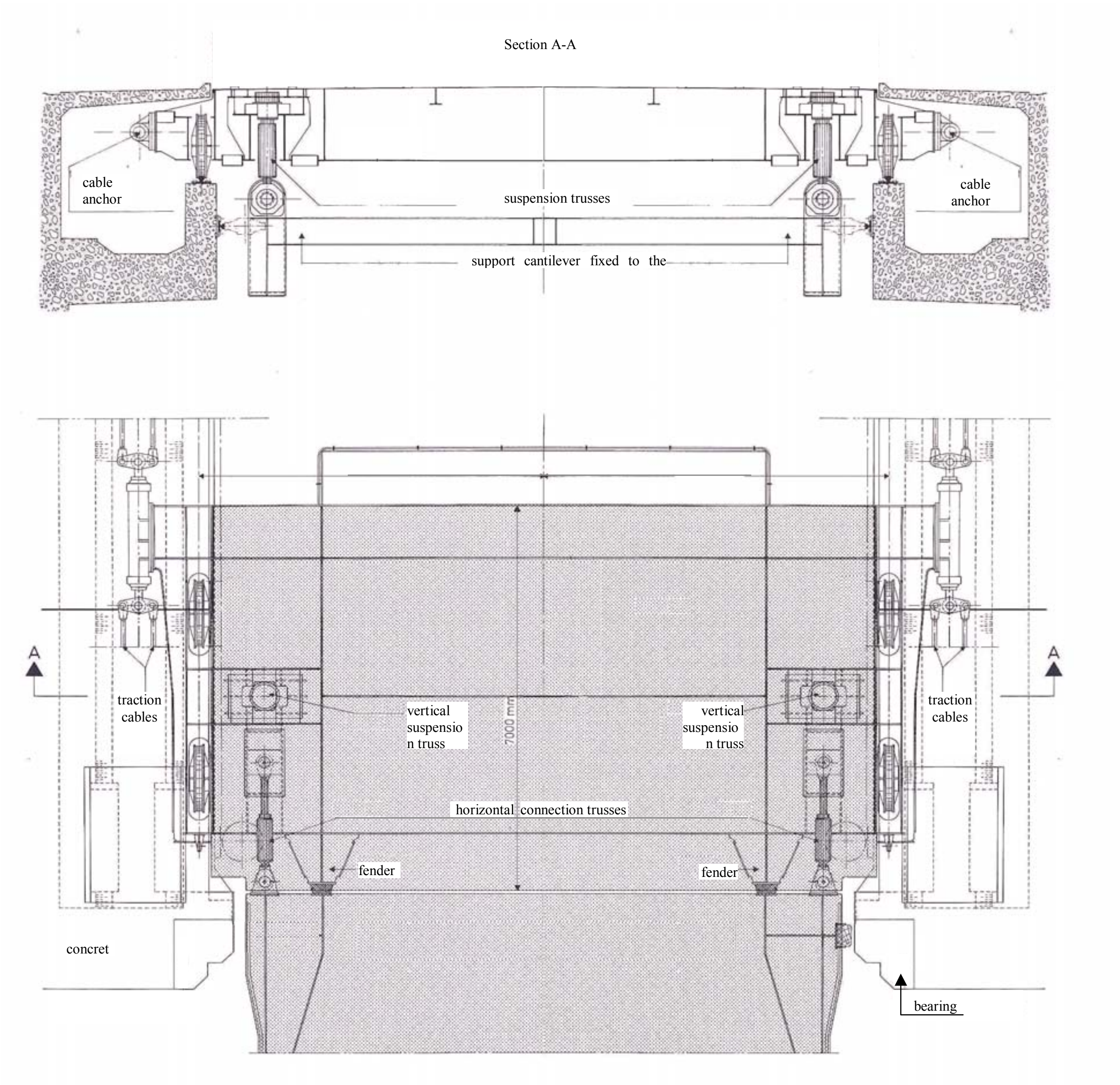

Upper support wagon

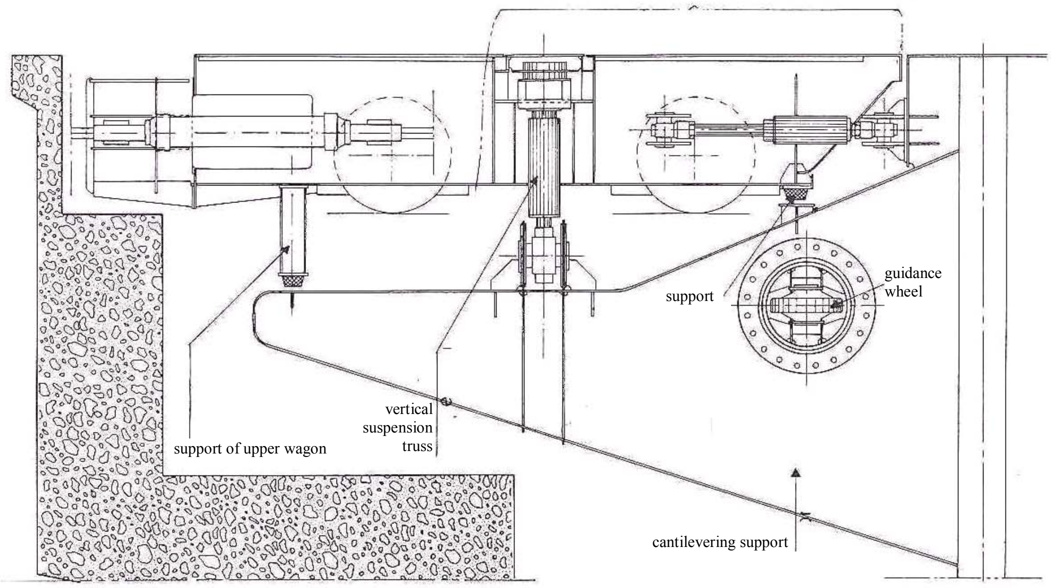

Lateral view of upper support wagon with cantilevering support

3.5.2 Details

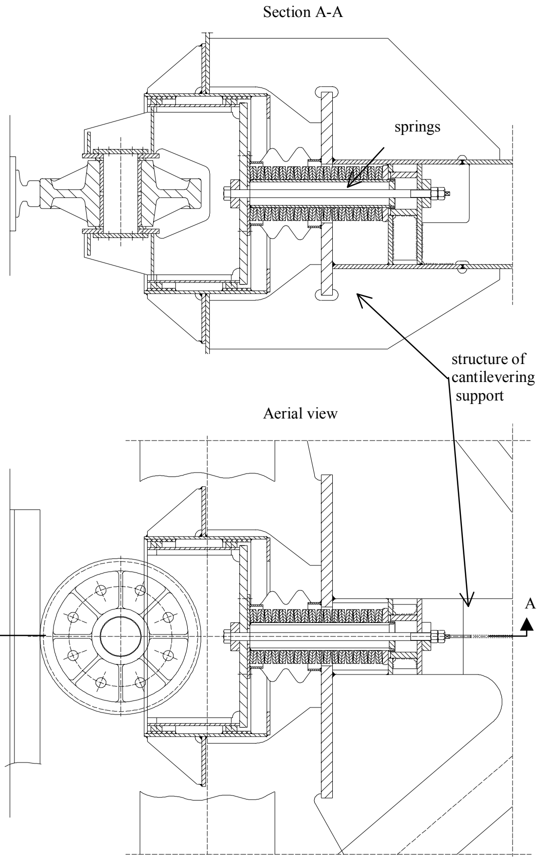

Guidance wheel

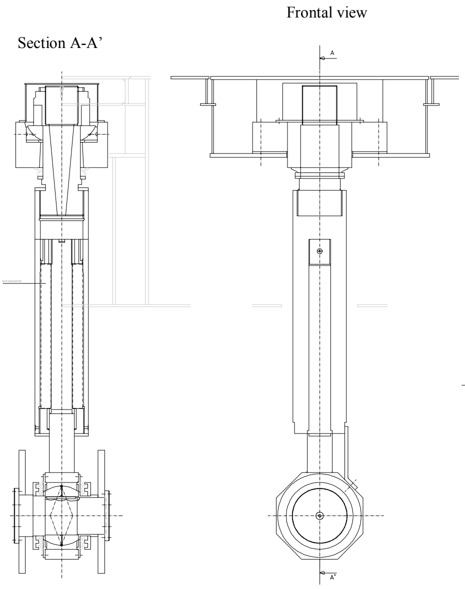

Vertical suspension truss

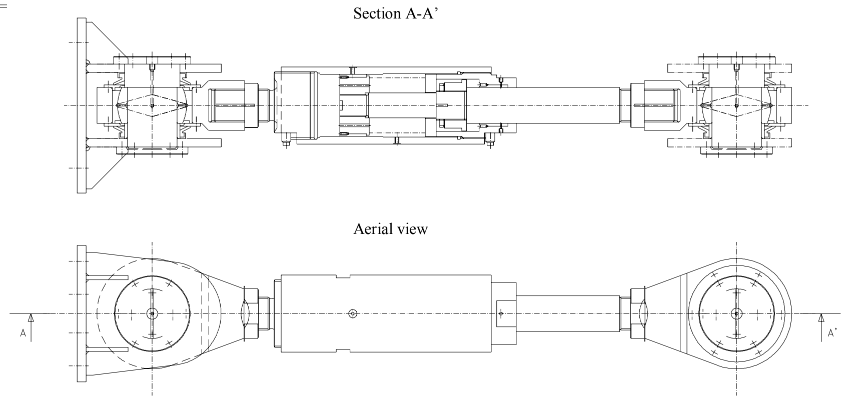

Horizontal connection truss

3.6 LOWER SUPPORT WAGON INTERMEDIATE AND DOWNSTREAM GATES

From the assessment of the maximum vertical reaction forces over the range of operating conditions (see 5.2) it is concluded that for the lower support wagons a design similar to the rolling gates of the Berendrecht lock (port of Antwerp) is appropriate. The necessary wheel bearing capacity does not exceed 1250 kN (see section 5.2), which also holds for the recently designed new rolling gates for the Van Cauwelaert lock (port of Antwerp).

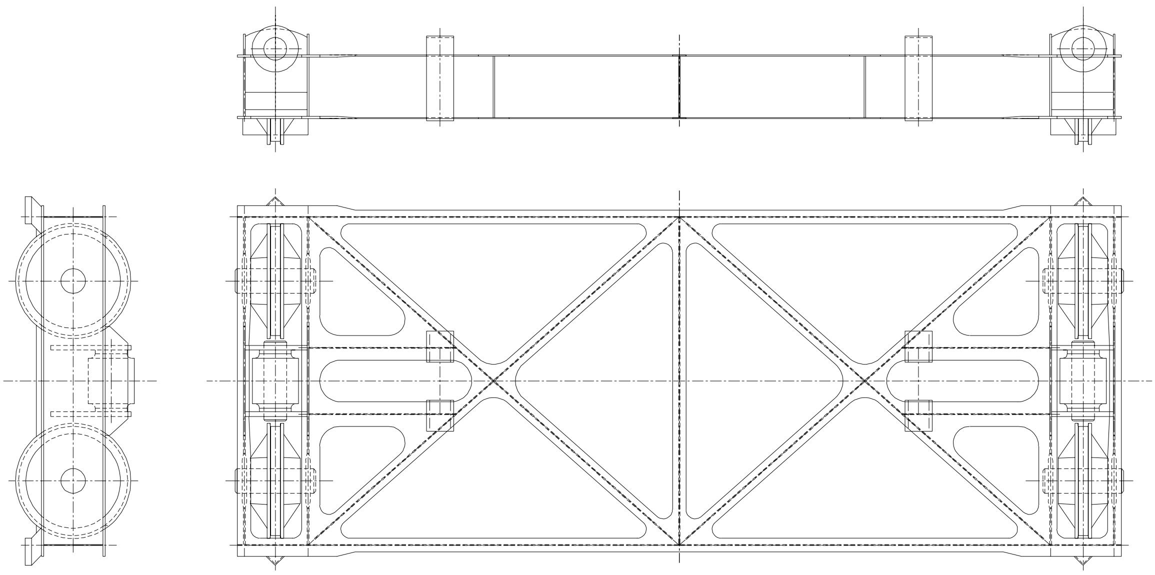

Lower support wagon PA2, PA3, PA4

3.6.1 Support maintenance wagon

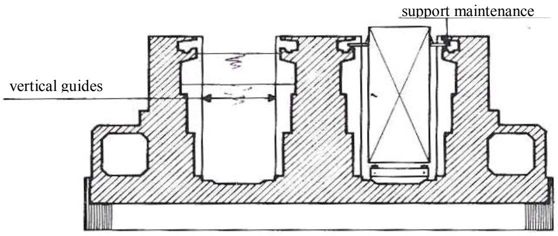

Gate in suspended position

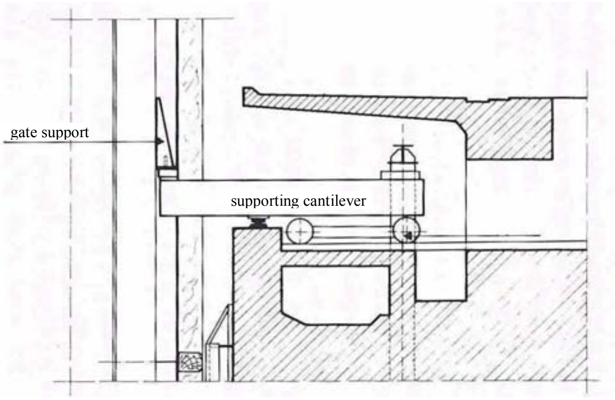

Support maintenance wagon : position in lock structure

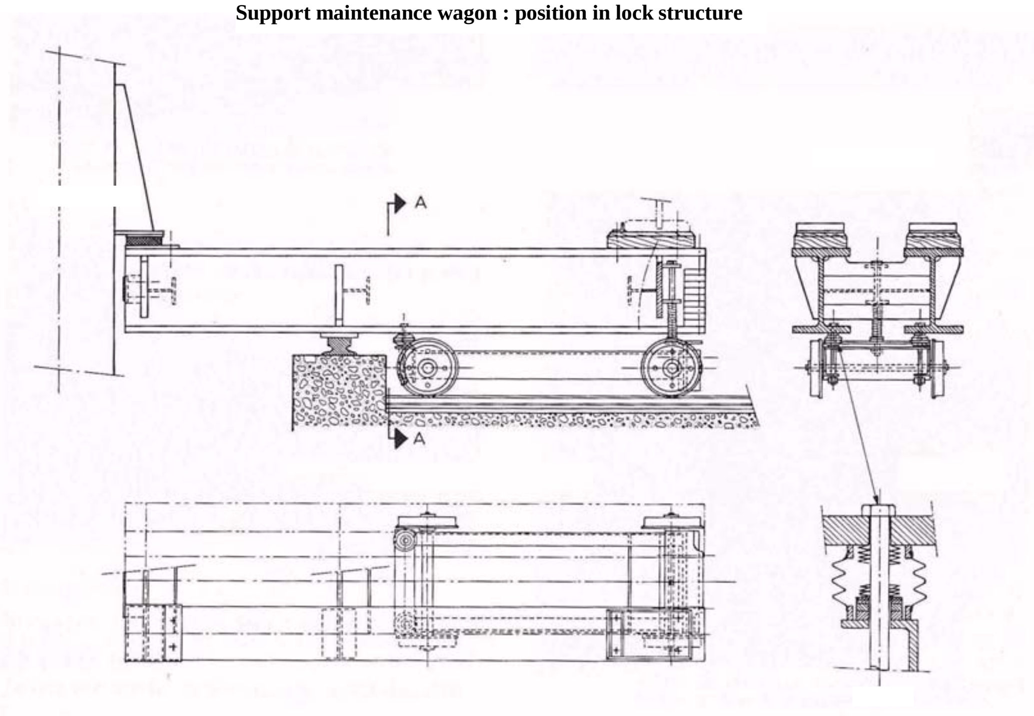

3.6.2 Slot bulkhead

The width of the proposed rolling gate structures is comparable to the width of the Berendrecht lock gates. Consequently a design similar to the slot bulkhead of the Berendrecht lock is appropriate (see illustration).

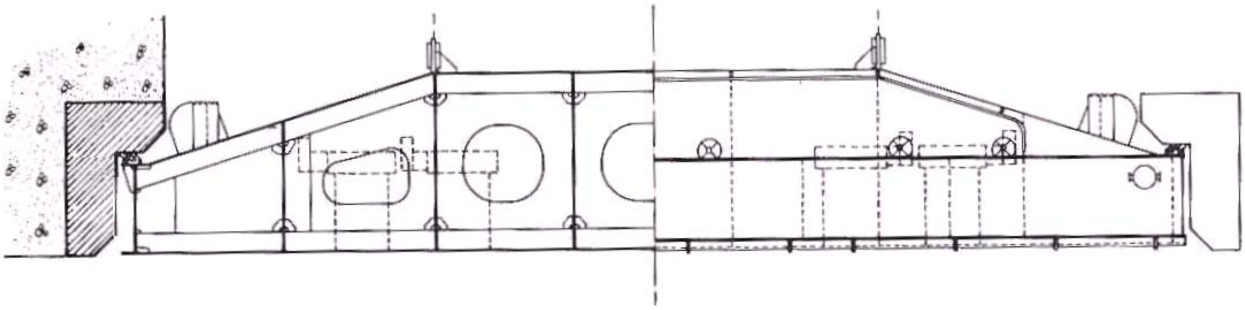

Slot bulkhead

3.7 NOTE ON LOCK DEWATERING PROCEDURE

At the *upstream* lock head the upstream side will be equipped with an additional shaping (among others including an additional sill) to provide an additional bearing. A gate PA1 is maneuvered from its gate recess and relocated to constitute a water retaining closure plate against this additional bearing.

At the *downstream* lock head the downstream side will be equipped with an additional shaping (among others including an additional sill) to provide an "inverse" bearing. Against this inverse bearing preferably an appropriate PA1-like gate is maneuvered (although in principle a gate PA4 might be used for this purpose as well) to constitute a water retaining closure plate. Gates PA4 have on only one side (downstream) seals, which have to be positioned relatively close to the bearings. On the other (upstream) side sufficient spacing between the gate and the wall of its gate recess will be provided for maneuvering such that the cumbersome dismounting and remounting of fender beams (at the bottom) is avoided. Lateral guidance of the operating gates PA2-3 and PA4 at the upstream side will be performed by appropriate wheel fenders, which are fixed to the (upstream) wall of the gate recess. These fenders may be dismounted and remounted relatively easy to provide the necessary lateral space for the gate maneuvers. Gates PA1 have lateral guidance wheels built in their cantilevering supports at both the upstream and the downstream side (see 3.5).

Working at the rails of the lower support wagon of all gates PA1, PA2, PA3 and PA4 will be performed inside a habitat tunnel, which is accessed through the slot bulkhead (section 3.8) from the dewatered corresponding gate recess. Thus it is not necessary to achieve (dry) lock chamber conditions for these maintenance operations and maneuvering of the gates from and back to their gate recesses is avoided.

4 SAMPLE COMPUTATIONS FOR GATE PA1

4.1 GENERAL

In this section sample computations are presented for the case of gate PA1. The applied formulae and the corresponding results will be demonstrated as adopted for the concept design of the proposed rolling lock gates. In appendix A the main results are listed for gate PA1.
It should be noted that more thorough procedures can be followed in an advanced level of design and optimization. Some results of preliminary 3D-FEM computations are discussed as well. They are listed in more detail in appendix B.

4.2 LIST OF SYMBOLS

The following symbols will be used (in order of appearance):

H:	"width" of the gates, i.e.: distance between outsides of plating (m)
L:	spacing between two adjacent vertical structural frames (m)
B:	height of a plating panel between two adjacent horizontal structural frames (m)
$e_{(eq)}$:	(equivalent) thickness of a plating panel (m)
$p_{w.c}$:	characteristic value of the water pressure on a plating panel (N/m²)
n:	number of longitudinal stiffeners over the height B (-)
n_e:	number of effective stiffeners against buckling (-)
l:	spacing between longitudinal stiffeners (m)
b:	spacing between effective stiffeners against buckling (m)
b_e:	effective width, allowing for shear lag effect (-)
A:	cross section area (m²)
I:	(geometric) moment of inertia (m^4)
W:	bending module (I/v) (m³)
R:	subscript referring to (longitudinal) stiffener, in combination with effective plating strip (-)
α:	shape factor of plating panel = L/B or L/b or B/L (-)
β:	relative width of a plating panel = b/e (-)
δ:	relative cross section = A/(B.e) (-)
γ^*:	critical relative stiffening factor against buckling (-)
m	= 4 for open sections of stiffeners; = 2.5 for closed (e.g.: omega) stiffener profiles
γ^{**}	= m . γ^*
υ:	Poisson's coefficient = 0.3 for structural steel; $12.(1-\nu^2) = 10.92$
σ:	(subscript referring to) normal stress (both tension, compression) (N/m²)

τ: (subscript referring to) shear stress (N/m²)
x: (subscript referring to) longitudinal spatial co-ordinate (m)
y: (subscript referring to) transversal spatial co-ordinate (m)
ψ: ratio between minimum and maximum value of longitudinal normal stress at plate edges (-)
ρ: ratio between corrected values of shear stress and longitudinal normal stress (-)
c: correction coefficient (inverse of safety factor) (-)
c*: maximum critical value of correction coefficient c (-)
w: subscript referring to the web of an I-shaped beam (corresponding to a frame) (-)
ac: subscript referring to parts belonging to the air chamber (-)

4.3 2D-BEAM GRID MODEL

Both vertical and horizontal structural frames are modeled as I-shaped beams. The skin plating is assigned as flanges to the beams to which it is nearest. The longitudinal compression members of the upstream skin framework of the gates (instead of the plating) also constitute a flange for their corresponding beam. For the webs of the beams corresponding to the intermediate horizontal frames, an assumption is made on the equivalent plate thickness of the horizontal transversal connections.

An overall cross section analysis yields an estimate of the torsion stiffness distribution over the horizontal frames, taking in account their contingence.
Finally the stiffness of the flexible plates at the bottom is tuned to avoid uplift of the bottom corner edges of the skin plating of the gates.

With these geometric characteristics of each beam a 2D-beam grid of the gate structure (integrated over the width) is drawn up.
Doing so the distribution of the section forces and displacements is derived with the (in Europe widely used) ESA-primaWin structural engineering software. Subsequently the material tension levels at the extremities (flanges) of the cross section are computed, in particular for the design of the compressed parts against buckling.

An output document generated by the applied structural engineering software is attached as Appendix A, showing input and output (reaction forces (kN), section forces (kN, kNm), material stresses, deformations (mm)) for the 2D-beam grid model.

Note that the listed reaction forces shown at page 8 can be found as follows:

$$R_{normal} = 1000\,\frac{kg}{m^3}\cdot 10\frac{m}{s^2}\cdot\frac{(10.62\ m)^2}{2}\cdot 57.24\ m + 1000\,\frac{kg}{m^3}\cdot 10\frac{m}{s^2}\cdot 10.62\ m\cdot 57.24\ m\cdot 8.68m = 85040\,kN$$

$$R_{ultimate} = 1000\,\frac{kg}{m^3}\cdot 10\frac{m}{s^2}\cdot\frac{(11.62\ m)^2}{2}\cdot 57.24\ m + 1000\,\frac{kg}{m^3}\cdot 10\frac{m}{s^2}\cdot 11.62\ m\cdot 57.24\ m\cdot 8.68m = 96380kN$$

The resulting material stresses are shown for each frame in appendix A page 10-12 (load case "ULS": self weight + dewatered chamber + MCE). The corresponding results for the normal service load case "SLS" are not shown.

4.4 DOWNSTREAM AIR CHAMBER PLATING

The plate thickness is chosen corresponding to the tension level derived from the 2D-beam grid model. The longitudinal stiffeners are chosen according to the procedure described in section 2.2. For the lowest zone of the downstream air chamber plating (panel R4-R5) of gate PA1 holds:

L = 3.18 m
B = 5.50 m
e = 16 mm
$p_{w.c}$ = 115 kN/m² (11.5 m water column) + 46 kN/m² (MCE, Westergaard) = 161 kN/m²

yielding:

n = 7 longitudinal stiffeners type 1/2IPE360
l = 0.688 m (= B/8)
b_e = 42.2 cm
I = 5993 cm^4
W = 434.9 cm³ (at flange edge of stiffener)
W = 1030 cm³ (at outside plating edge)
e_{eq} = 1.6 cm + 7 x 36.36 cm² / 550 cm = 2.06 cm

For these characteristics the relations (2.1), (2.2a) and (2.2b) of section 2.2 hold with σ_{max} = ca. 0.75 * 355/1.1 = 242 N/mm², leaving sufficient resistance for the characteristic global stress of 151 N/mm² (see appendix A p. 10). In the accidental load case (incl. MCE) considered, there is no need to arrive at a sufficiently moderate total stress to account for fatigue.

A similar procedure is followed for the other plating panels, yielding e_{eq}-values that are used to derive characteristics for (the flanges of) the I-shaped members of the 2D-beam grid model (see below).

Gate PA1 : Plating panel characteristics					
Double skin plating	downstream side (tension in base case)				
Panel	B	e	profile	n	e_{eq}
R1_top-R3_intermed	319	1.6	1/2 IPN300	3	1.92
R3_intermed-R4_top ac	319	1.6	1/2 IPN300	3	1.92
R4_top ac-R5_bottom_ac	550	1.6	1/2 IPE360	7	2.06
R5_bottom_ac-R6_intermed	357.5	1.6	1/2 IPE400	4	2.07
R6_intermed-R7_bottom	357.5	1.6	1/2 IPE400	4	2.07
Flexible plate	127	3.0	none	0	3.00
	upstream side (compression in base case)				
R4_top ac-R5_bottom_ac	550	1.6	1/2 IPE750-147	7	2.79

4.5 UPSTREAM AIR CHAMBER PLATING (COMPRESSED)

In order to obtain an appropriately stiffened plating panel to safely resist the longitudinal compression loading, the longitudinal stiffeners are chosen such that the buckling risk of stiffeners doesn't exceed the buckling risk of the separate plating strips between the stiffeners. This is obtained by choosing I_R above a critical value as follows:

$$I_R \geq \gamma^{**} \frac{Be^3}{12\,(1-\upsilon^2)} \tag{4.1}$$

where $$\gamma^{**} = m \cdot MAX\left[\gamma^*_{\sigma_x} ; \gamma^*_{\sigma_y} ; \gamma^*_{\tau}\right] \tag{4.2}$$

The critical relative stiffening factors γ* for each simple loading case mainly depend on the shape parameter α of each panel. When the number of stiffeners increases, the shear force case is determinative. For three cases a closed formula is published in the technical notes of CECM (n_e = 1, 2 and infinite respectively):

$$\gamma^*_{\tau(1)} = \frac{5.4}{\alpha}\left(\frac{2}{\alpha} + \frac{2.5}{\alpha^2} - \frac{1}{\alpha^3} - 1\right) \tag{4.3.1}$$

$$\gamma^*_{\tau(2)} = \frac{12.1}{\alpha}\left(\frac{4.4}{\alpha} - 1\right) \tag{4.3.2}$$

$$\gamma^*_{\tau(\infty)} = \frac{28}{\alpha} - 20\,\alpha \tag{4.3.3}$$

For other n_e-values (> 2) an interpolation formula is used.

For the upper half upstream air chamber plating (panel R4-R5) of gate PA1, considering again (like the downstream panel, see 4.4) e = 16 mm and n_e = 7 effective stiffeners against buckling, holds:

b = B/8 = 0.688 m
$\gamma^*_{\tau(1)}$ = 31.21, $\gamma^*_{\tau(2)}$ = 23.77, $\gamma^*_{\tau(\infty)}$ = 72.36
$\gamma^*_{\tau(7)}$ = 31.21 (interpolation in case of anomaly $\gamma^*_{\tau(1)} > \gamma^*_{\tau(2)}$)
γ^{**} = 124.84
$I_{R\text{-}min}$ = 16360 cm^4

Choosing profiles 1/2IPE750-147 yields (with b_e = b and n = 7 stiffeners as obtained in 4.4):

I_R = 52569 cm^4
e_{eq} = 1.6 cm + 7 x 93.75 cm² / 550 cm = 2.79 cm

Consequently the compressed plating panel safely resists buckling if the separate panels between the (effective) stiffeners have a sufficient safety against buckling. This is evaluated as follows.

The critical resistances against buckling for simple loading cases are respectively:

$$\sigma^o_{x,cr} = k_{\sigma_x}\,\sigma_E \tag{4.4.1}$$

$$\sigma^o_{y,cr} = k_{\sigma_y}\,\sigma_E \tag{4.4.2}$$

$$\tau^o_{cr} = k_{\tau}\,\sigma_E \tag{4.4.3}$$

wherein the Euler stress is defined as: $\sigma_E = \dfrac{\pi^2 \; E}{12\,\beta^2 \; (1-\nu^2)} = \dfrac{189800 \cdot N/mm^2}{\beta^2}$ (4.5.0)

with β = b/e the relative width of the plating panel

The k-factors follow from linear elastic buckling theory.
For ψ = 1 we have the following formulas:

$$k_{\sigma_x} = \left(MIN[\alpha;1] + \frac{1}{MIN[\alpha;1]} \right)^2 \tag{4.5.1}$$

$$k_{\sigma_y} = \frac{\left(MIN[\alpha;1] + \dfrac{1}{MIN[\alpha;1]} \right)^2}{\alpha^2} \tag{4.5.2}$$

$$k_\tau = \frac{5.34}{(MIN[\alpha;1])^2} + \frac{4}{(MAX[\alpha;1])^2} \tag{4.5.3}$$

Assuming proportionality between the critical resistances for the combined loading case and the actual stresses σ_x, σ_y and τ, the non-reduced ("ideal") combined critical comparison stress level is given by:

$$\sigma^{id}_{c,cr} = \frac{\sigma_c}{\dfrac{4-\rho}{4} \cdot \dfrac{\sigma_y}{\sigma^o_{y,cr}} + \sqrt{\left[\dfrac{\rho}{4}\dfrac{\sigma_y}{\sigma^o_{y,cr}}\right]^2 + \left[\dfrac{\sigma_x}{\sigma^o_{x,cr}}\right]^2}} \quad \text{for } \rho \le 1 \tag{4.6.1}$$

$$\sigma^{id}_{c,cr} = \frac{\sigma_c}{\dfrac{1+2\,\rho}{4\,\rho} \cdot \dfrac{\sigma_y}{\sigma^o_{y,cr}} + \sqrt{\left[\dfrac{2\,\rho - 1}{4\,\rho}\dfrac{\sigma_y}{\sigma^o_{y,cr}}\right]^2 + \left[\dfrac{\tau}{\tau^o_{cr}}\right]^2}} \quad \text{for } \rho \ge 1 \tag{4.6.2}$$

wherein $\rho = \dfrac{\tau \cdot k_{\sigma x}}{\sigma_x \cdot k_\tau}$ (4.7)

which is reduced if $\sigma^{id}_{c,cr} > 0.8 \cdot f_y$ as follows:

$$\sigma^{red}_{c,cr} = y \cdot f_y \quad \text{with } y = \frac{0.8 + 0.2 \cdot \sqrt{1 - \dfrac{0.6}{x^2}}}{1 + \dfrac{0.04}{x^2}} \quad \text{and } x = \frac{\sigma^{id}_{c,cr}}{f_y} > 0.8 \tag{4.8.1}$$

otherwise:

$$\sigma^{red}_{c,cr} = \sigma^{id}_{c,cr} \tag{4.8.2}$$

Finally the actual Von Mises comparison stress σ_c in the compressed plating panel

$$\sigma_c = \sqrt{\sigma_x^{\ 2} + \sigma_y^{\ 2} - \sigma_x\sigma_y + 3\,\tau^2} \tag{4.9}$$

is compared with the reduced combined critical comparison stress through a correction factor c defined as:

$$c = \frac{\sigma_c}{\sigma^{red}_{c,cr}} \tag{4.10}$$

Safety against buckling of the plating is guaranteed if this value does not exceed the critical limit value c* = 0.83 which holds for the determinative zone in the middle of the span (case with relatively small shear stress and almost pure compression ψ = 1). In general c* equals a weighted average of the squares of the simple load case critical values:

$$c^* = \sqrt{\frac{\left[\frac{\sigma_x \cdot c_x^*}{\sigma^o_{x,cr}}\right]^2 + \left[\frac{\sigma_y \cdot c_y^*}{\sigma^o_{y,cr}}\right]^2 + \left[\frac{\tau \cdot c_\tau^*}{\tau^o_{cr}}\right]^2}{\left[\frac{\sigma_x}{\sigma^o_{x,cr}}\right]^2 + \left[\frac{\sigma_y}{\sigma^o_{y,cr}}\right]^2 + \left[\frac{\tau}{\tau^o_{cr}}\right]^2}} \tag{4.11}$$

wherein c^*_x ranges from 0.83 (pure compression) to 1.05 (pure bending), c^*_y = 0.83 and c^*_τ = 1.05

The 2D-beam grid model yields the actual design values σ_x = 151 N/mm², σ_y = 39 N/mm² and τ = 8 N/mm² (see appendix A p. 10-12) in the middle of the span of the air chamber. The critical resistance values for the simple load cases are respectively: 411.2 N/mm², 112.6 N/mm² and 561.7 N/mm² based on the respective k-factors: 4.00, 1.10 and 5.53.

Using the equations above yields c = 0.72 < 0.83 = c* showing sufficient safety against plate buckling.

4.6 CONCLUSION: CHARACTERISTICS OF I-SHAPED BEAMS FOR 2D-BEAM GRID MODEL

Following the procedure described above, the characteristics of the I-shaped beams corresponding to the horizontal frames are obtained as listed in the table below (all units in cm).

Gate PA1 : Horizontal frame characteristics									
Hor. Frame	A_{comp}	$A_{tension}$	$A_{flanges}$	A_{web}	I_t	I_y	I_z	Wel_y	Wel_z
R1 top	356	307	663	931	4,40E+08	1,18E+08	6,51E+05	326 889	8 162
R3	712	614	1326	700	2,70E+08	1,89E+08	5,21E+06	515 208	32 647
R4-top ac	1124	874	1998	1473	3,10E+08	3,00E+08	3,14E+07	799 997	144 718
R5-bottom ac	1189	938	2126	1473	3,10E+08	3,16E+08	3,65E+07	843 288	160 797
R6	841	741	1582	700	2,90E+08	2,20E+08	7,89E+06	602 533	44 146
R7 bottom	624	751	1375	700	4,70E+08	1,94E+08	5,85E+06	523 535	38 293

The 2-D beam grid model with these characteristics was used to derive the material stresses used in the computations illustrated above. This shows that convergence has been reached. Thus it may be concluded that the proposed structure fulfils the stability rules.

4.7 NOTE ON ACCURACY AND MORE DETAILED LEVEL OF DESIGN

The above mentioned results based on the design procedure described in the methodology of the earlier CPP concept design study eventually should be subject to a verification analysis by means of a full 3D Finite Element modeling including plates and frameworks. Thus the spatial contingence of the frames can be assessed more accurately and the design of the beams of the vertical and horizontal frameworks can be optimized.
Based on our experience with such 3D-modeling verification exercises, e.g. with the recently designed new rolling gates for the Van Cauwelaert lock (port of Antwerp), we can state that the accuracy of the above described procedure certainly allows a cost estimate within the limit imposed by the terms of reference.
For the gate PA1 structure a preliminary 3D-FEM analysis was carried out, indicating that the model assumptions adopted for this concept design are sufficiently accurate as stated. More details on the model set up and some computational results are listed in appendix B. Note that only a HALF gate is represented, taking in account the symmetry in structural geometry, loads and boundary conditions.

5 REACTION FORCES

5.1 GENERAL

Proceeding according to the methodology of the earlier CPP concept design study, as illustrated in section 4 of this report, the distribution of horizontal reaction forces on the water retaining gates is determined. Horizontal reaction forces occur both at the extremities of the gates (vertical lateral bearings on the lock walls) and at the bearing at the sill. Vertical forces occur at the upper and lower support wagons during opening and closing of the gates.

5.2 VERTICAL SUPPORTS - ROLLING WAGONS

Maximum vertical forces at the support wagons will occur during operations (closing, opening) of the gates. It is assumed that the wheels of both the support wagons should remain pressed with a minimum vertical reaction force (ca. 600 kN) on the rails to guarantee a proper functioning of the connections in operational circumstances. The vertical reaction forces increase when the water level decreases, causing the structure to be less submerged and thus its weight to be less relieved.

The rolling wagons are not designed for the vertical reaction forces occurring at water levels lower than the minimum values at opening/closing of the gates listed in section 1.1 (e.g. in the event of dewatering the gate recess or even the entire lock chamber). In such cases the lower support wagons will be removed (by pulling them from underneath the floating gates) and subsequently the lock gates will be placed on their fixed bottom supports (see 3.3).
The table below shows the total vertical reaction forces on the support wagons at the lowest operating water level of the gates in normal service circumstances (symmetrical distribution of the total vertical reaction force over the wheels of the wagons). In the water retaining cases the listed vertical reactions are to be modified according to the friction forces acting at the lateral bearings.

Total vertical reaction forces in normal service circumstances

Gate PA1	Highest water level (water retaining = open/close)	Lowest water level (open/close)	Lowest water level (operations)
Upper wagon	600 kN	750 kN	800 kN
Lower wagon	600 kN	900 kN	1000 kN

Gate PA2-3	Highest water level (water retaining)	Lowest water level (open/close)
Upper wagon	600 kN	1000 kN
Lower wagon	600 kN	1400 kN

Gate PA4	Highest water level (water retaining)	Lowest water level (open/close)
Upper wagon	600 kN	1100 kN
Lower wagon	600 kN	1500 kN

The support wagons are designed taking in account that three watertight zones (of each two compartments of the air chamber) may be flooded accidentally at the same time, causing an additional possible vertical loading of the support wagons. This additional loading depends on the position of the flooded zone (to be chosen appropriately for each wagon) and the size of the compartment.

Characteristic values of the maximum vertical reactions (at lowest operating water levels) are listed in the table below. The total vertical reaction on the lower support wagon always exceeds the one on the upper support wagon. For all gates PA1, PA2-3 and PA4 the total vertical reaction on the lower support wagon amounts ca. 10% of the total weight of the corresponding gate structure.

Gate PA1	Side of flooded zone	Other side	Total vert. reaction
Upper wagon	1200 kN	500 kN	1700 kN
Lower wagon	1500 kN	900 kN	2400 kN

Gate PA2-3	Side of flooded zone	Other side	Total vert. reaction
Upper wagon	1800 kN	700 kN	2500 kN
Lower wagon	2400 kN	1400 kN	3800 kN

Gate PA4	Side of flooded zone	Other side	Total vert. reaction
Upper wagon	1900 kN	800 kN	2700 kN
Lower wagon	2500 kN	1500 kN	4000 kN

Maximum vertical reaction forces with flooded compartments

The maximum values found for gates PA1 are similar to the corresponding ones for gates of the Berendrecht lock. The values for gates PA2-3 and PA4 are similar to the values for the corresponding rolling wagons of the recently designed new rolling gates of the Van Cauwelaert lock (port of Antwerp). Note that for the proposed four-wheel rolling wagons (two wheels at each side of a rolling wagon), each wheel needs a bearing capacity not exceeding 1250 kN. Identical corresponding rolling wagons are proposed for gates PA2-3 and PA4. The listed total vertical reactions at the upper wagon are determinative for the design of the cantilevering support of each gate (see section 3.5).

5.3 HORIZONTAL FORCES AT THE SILL BEARING

Maximum horizontal reaction forces at the sill bearing occur during retaining of the (maximum) water level difference. They result directly from the 2D-beam grid model computations presented in appendix A after an optimization of the stiffness of the cantilevering bottom ends of the vertical frames. Doing so uplift from the sill bearing of the skin plating at the gate bottom edges is avoided.
To derive the maximum contact stress, the minimum spreading length (along the azobé beams of 500 mm width) is mentioned in the tables below.
.

	Reaction force at frame (3.15 m length)	Max. contact stress (min. 540 mm)
Gate PA1	7500 kN (ULS)	28 N/mm² (ULS)

	Reaction force at frame (3.18 m length)	Max. contact stress (min. 540 mm)
Gate PA2-3	11400 kN (ULS)	42 N/mm² (ULS)

	Reaction force at frame (3.18 m length)	Max. contact stress (min. 540 mm)
Gate PA4	10400 kN (ULS)	39 N/mm² (ULS)

5.4 HORIZONTAL FORCES AT THE LATERAL BEARINGS

Maximum horizontal reaction forces at the lateral bearings (on the lock walls) occur during retaining of the (maximum) water level difference. From the 2D-beam grid model computations presented in appendix A, the reaction forces at the horizontal frames are obtained (corresponding to the same optimized stiffness distribution as mentioned sub 5.3). Subsequently the part of the vertical frame structure at the contact with the lock walls is modeled as a continuously elastically supported beam, which is loaded by these reaction forces. The maximum contact stresses (along azobé beams of 500 mm width) are listed below.

Gate PA1	Max. contact stress (at R1)
	35 N/mm² (*)

Gate PA2-3 and PA4	Max. contact stress at R1	Max. contact stress at R3
	45 N/mm²	52 N/mm² (*)

(*) Based on our experience with 3D-modelling of the recently designed new rolling gates for the Van Cauwelaert lock (port of Antwerp) we expect that the contact stresses at R4 are overestimated at least by 10 N/mm² due to the underestimation of the beam stiffness at the air chamber. Therefore the contact stress at R1 should be considered as determinative, like in the case of Gate PA1.

5.5 CONCLUSION

The above mentioned computational results show that similar lay outs of the rolling support wagons and bearings of the rolling gates in operation at the large locks in the port of Antwerp (Belgium) are appropriate for use in the actual gates in the Panama case.
Moreover the pressure levels in the supporting and sealing beams require sufficient high strength materials, like azobé wood or high performance composite materials.

GATES OF WSB OF THE MAGDEBOURG (ROTHENSEE) LOCK SYSTEM

Update of Pacific Locks Conceptual Design and Harmonization of Atlantic Locks Conceptual design - Contract SAA-143351

PACIFIC LOCKS ACTUALIZATION

TASK P4e – CULVERT AND WSB CONDUIT GATES

Rev A

in association with

TABLE OF CONTENTS

Annexes

1. Abacus of gate weight versus gate parameter (W, h, H), (1 page)
2. Preliminary calculations of a WSB gate (Hs=50 m),
3. Estimate weights for culvert and WSB conduit gates, taking into account maximum static head,
4. Cross section of a gate wheel of Berendrecht lock,
5. Typical gate structure,
6. Upstream and downstream sealing (Music note J-shape type),
7. Side and bottom seals (typical example).
8. Pictures – Typical seals view (Zandvliet lock - Belgium)

1 SUITABILTY OF DIFFERENT TYPES OF GATES

1.1 GENERAL

Preliminary remark :
According to the normal wording practice, the term “valve” is only used in case of *butterfly valves* or of *cylindrical valves*. These types of valves have not been recommended neither for the culvert, nor for the Water Saving Basin conduit. Therefore, all other valves are called gates. As a consequence, the wording “culvert valves” and “conduit valves” used in previous reports have been replaced by *culvert gates* and *conduit gates*. The latter is also referred to as WSB gates (Water Saving Basins gates).

The analysis of the suitability of different types of gates is given in the report R4-E (Conceptual Design of Post Panamax locks – TASK 4 E - CULVERT AND CONDUIT VALVES), dated 15.11.2002.

In this report the different types of gates have been analyzed taking into account reliability, maintenance, manufacturing and construction costs, expected service life, design and construction, sensibility to cavitations and vibration.

In relation with the civil works, the overall size of the gates has also played a major role in determining the most suitable type of operating gate for filling and emptying the lock.

The types of gates/valves that have been examined are:

- Vertical-lift gates including:
  - fixed-wheel gates,
  - sliding gates
- Tainter gates including:
  - conventional tainter gates,
  - reverse tainter gates,
- Stoney gates,
- Butterfly valves,

- Cylindrical valves,

- Grid type gates.

To assess the most suitable type of gates/valves to be used for the Post Panamax locks, a comparative table has been elaborated. It is given in paragraph 1.2. below.

1.2 COMPARATIVE TABLE

The different types of lock gates/valves are listed in the table below. Several criteria are used to evaluate the gate/valve types. These criteria are linked with a weight factor, determined according to their importance.

The gates/valves are appraised on a 1 to 5 scale for each criterion. These scores are multiplied by the weight factor, resulting in a total quotation for each type of gate/valve.

The fixed wheel gate obtained the best overall quotation.

	weight factor	Fixed-wheel gate (FW)	Sliding Gate (Sl)	Grid Type Gate (GT)	Tainter Gate (Tt)	Butterfly Valve (Bt)	Cylindrical Valve (Cy)	Stoney Gate (St)
Reliability	0.20	4	4	2	4	4	3	3
Maintenance	0.20	4	4	2	3	3	3	2
Construction cost	0.15	5	4	3	3	3	3	3
Service life	0.15	4	3	2	4	4	3	2
Design and construction	0.15	4	3	2	4	3	3	3
Sensibility to vibration / cavitation	0.15	3	4	3	3	2	3	3
Total								
Total weight factors	1.00							
Total evaluation (max 5)		4.00	3.7	2.30	3.5	3.20	3.00	2.65
Total evaluation (%)		80	74	46	70	64	60	53

Note: the results of this comparative table remain valid for both flow direction through the gates/valves

1.3 CONCLUSIONS

The conclusions of the report R4E as referenced in §3 were as follows:

"Based on experience with Post Panamax locks and on engineering judgment there are only two types of gates that may realistically be used for the Post Panamax locks of the Panama Canal i.e. fixed wheel gates and sliding gates..

Nowadays vertical-lift gates are preferred for big locks because they are much cheaper to build and do not require the large space that is necessary (for example) for a tainter gate. Moreover, the hydraulic efforts are better distributed to the culvert walls and maintenance is easier .

Within this perspective the choice of fixed wheel gates seems obvious.

Another advantage of course is the actual know-how of ACP and the infrastructure for the maintenance of flat gates in use at the Panama Canal."

Moreover, the vertical lift gates have proven well for designs where sealing in both directions of water flow is required, such as between the lock chambers and the water saving basins.

2 DESCRIPTION AND DIMENSIONING

2.1 GENERAL

The analysis of the suitability of different types of gates has led to the conclusion that the most suitable type of gate is the fixed-wheel type.

For the 55 m lock chamber width (instead of 61 m previously), the dimensions of the lock culverts and water saving basins (WSB) conduits have been determined in the hydraulic study (report P4C)

The culvert dimensions are **9 (width) x 6 (height) m** (instead of 9 x 7.5 m previously).

The WSB conduit dimensions are **4.5 (width) x 6 (height) m** (instead of 5.7 x 7.5 previously)

Redundancy (two gates for each culvert) has to be foreseen for the culvert gates, therefore the size of the culvert gates shall be **4.5 x 6m, which is the same as the ones of the WSB conduits**.

On the Pacific side all culverts and WSB conduits are equipped with gates of the same size.

The height to width ratio is 1.33 and quite acceptable.

For the culvert gates, the basic principle adopted for operation reliability is to work with two gates in parallel so that any incident to any gate will not stop the operation of the locks. Furthermore, it also reduces the required gate size.

However the **risk of an asymmetrical operation** of the gates (if one gate fails to open or remains open in an intermediate position) shall have to be assessed (in the preliminary and/or final design). If required, interlocking devices shall have to be foreseen.

Each of the nine **WSB basins** is connected to the locks by four conduits. Two are connected on left hand (near to WSB) side of the corresponding lock chamber, two are connected to the right hand (far to WSB) side. **No** additional provision has been made for **redundancy** of the gates. In case of any trouble on a gate, one conduit will be out of order but the three remaining conduits of the concerned basin will be sufficient to operate almost normally.

However the **asymmetrical operation of the emptying and/or filling** of the corresponding lock chamber gates (if one gate fails to open or remains open in an intermediate position) shall have to be assessed (in the preliminary and/or final design). If required, interlocking devices shall have to be foreseen.

2.2 LAYOUT OF CULVERTS AND WSB CONDUITS

Each culvert and conduit gate is equipped upstream and downstream with bulkhead gates allowing access to the gate(s) after emptying by pumping (by movable pumps) of the space on both sides.

The basins conduits have been arranged two by two (in total four per WSB). The arrangement, with one conduit located on top of the other as foreseen in the initial conceptual design has been abandoned. It makes the WSB gates arrangement much easier and the operation much more reliable

2.2.1 CULVERTS AND CULVERT GATES

There are two culverts running along each side of the locks. Their sill is at the sill level of the lock chamber. However, the bottom of the rolling gates chambers prevents the culverts from remaining horizontal. Therefore, the culverts are diverted under the rolling gates and the culvert gates are implemented between the main rolling gates.

As mentioned here above, the culvert dimensions are W x H = 9m x 6m. The culverts are locally divided into two sections of W x H = 4.5m x 6m where the culvert gates are to be installed. At full opening of the gate, the total size and thus the mean water velocity remains unchanged.

The next figure shows a basic layout for a culvert gate with two isolating bulkheads. **There is only one flow direction from the left to the right.**

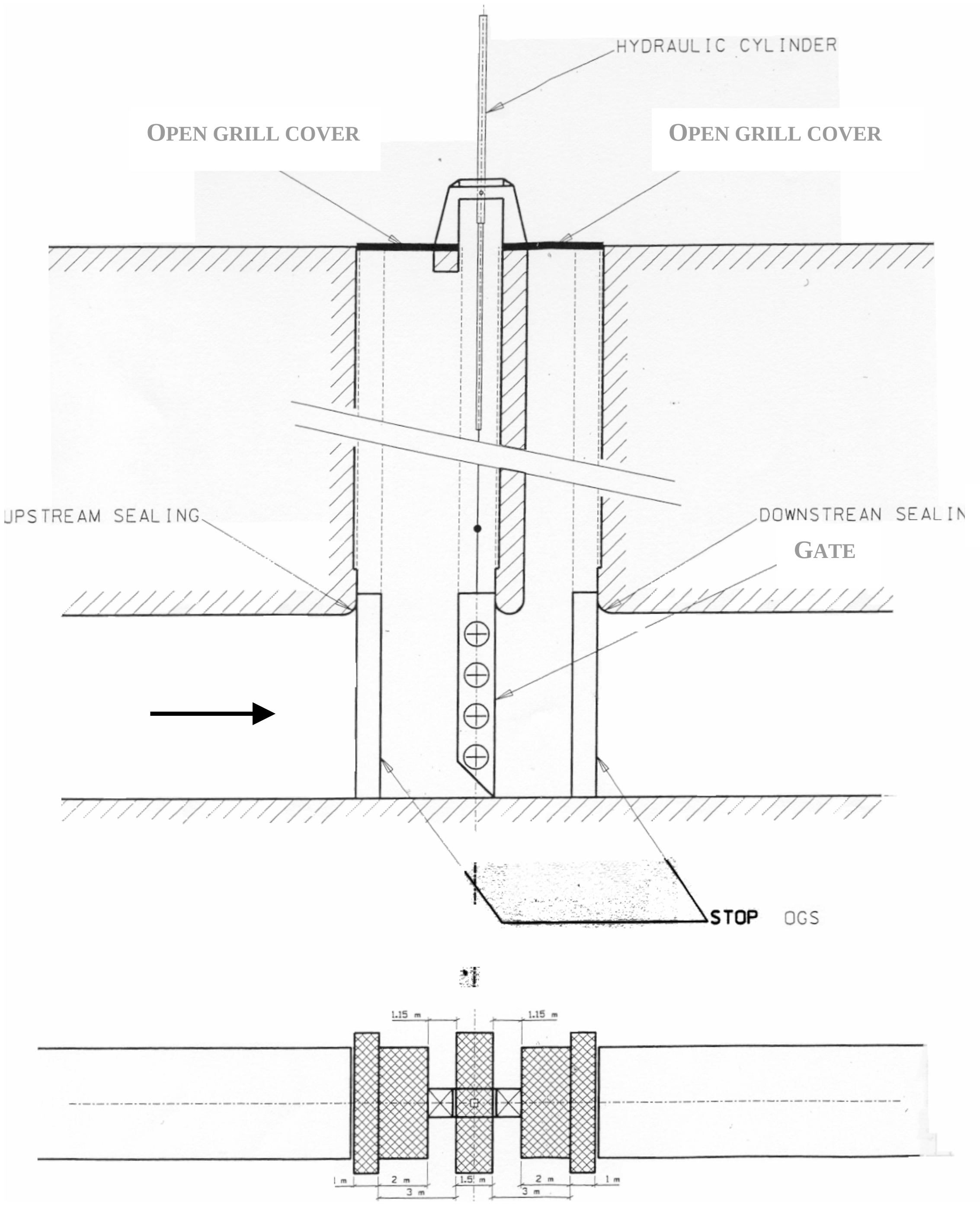

For emptying both sides of the culvert gate, the **sealing conditions** are to be as follows:

- the upstream bulkhead has to be tight on its upstream side,
- the downstream bulkhead has to be tight on its downstream side,
- the gate has to be **tight on its downstream side**.

That design has the advantage (regarding civil works) that only one vertical separation wall is required.

2.2.2 WSB CONDUITS AND CONDUIT GATES

The arrangement of the gates and bulkhead gates is shown on the civil works drawings (ref D4-A-103).

The **fixed-wheel gates** are designed with **upstream and downstream sealing.**

Their leaf structures (and therefore the corresponding slots) are dimensioned to support the maximum static pressure on both sides corresponding to following pressure conditions:

- maximum lock chamber level on one side and WSB completely empty on the other side,
- maximum WSB level on one side and lock chamber completely empty on the other side.

The hydraulic cylinders operating the gates have been pre dimensioned for two cases:

- for the normal operation with the locks and basins filled with water,
- for the maximum static head.

The power required for the gate operation in the most critical case, is the one taking into account maximum static head.

The bulkhead gate (WSB side) is of the sliding type in two or three elements and is designed with a double sealing system which allows to:

- empty the WSB while keeping the locks in operation,
- empty the space between the two bulkhead gates to give access to the conduit gate and slots for maintenance.

The bulkhead gate on the lock chamber side is also in two or three pieces and is designed with a sealing system which allows to:

- empty either the lock chamber or the WSB (for the emptying of the WSB it makes a redundancy while keeping the locks in operation),
- empty the space between the two bulkhead gates to give access to the conduit gate and slots for maintenance.

The basic data for designing the gates (dimensions and maximum static head) are the same as those of the bulkhead gates.

The bulkhead elements can be lowered or removed by means of a mobile gantry crane equipped with an automatic lifting beam.

The 36 conduit gates are also the same. They are dimensioned for the maximum head of 44.33m.

2.3 BASIC DATA FOR DESIGN

The values indicated below provide, for the culvert and WSB gates as well as for the bulkhead gates, the maximum static heads of water which have been taken into account for the estimation of the weight of the moving parts.

Maximum head on sill level of culvert gates:	39.24 m
Maximum head on sill level of WSB gates:	44.33 m

The values computed for the first conceptual design (61 m width lock chambers) were:

Maximum head on sill level of culvert gates:	40.03 m
Maximum head on sill level of WSB gates:	45.65 m

The weight of the gates has also been estimated taking into account the operating heads. The values indicated below provide the maximum operating heads of water which have been taking into account.

Maximum head on sill level of culvert gates:	25 m
Maximum head on sill level of WSB gates:	10 m

The operating heads used for the 61 m width lock chambers were:

Maximum head on sill level of culvert gates:	25 m
Maximum head on sill level of WSB gates (top):	30 m
Maximum head on sill level of WSB gates (top):	50 m

The same conditions are to be applied for the culvert and WSB conduit bulkheads.

2.4 ESTIMATED WEIGHTS

A reliable determination of the moving part of a fixed-wheel gate by a comprehensive study based on preliminary data and admissible stresses is a quite long and difficult exercise. To determine an approximate weight, it is common practice to make a comparison with existing gates, of course, of the same type.

Estimation of the weight is based on the main parameters, i.e.:

- the dimensions (width and height);
- water pressure on the sill.

It can be developed by a formula based on statistical data. The weight of the slot embedded fixed parts has then to be added.

This procedure gives an acceptable approach for conceptual design.

The formula used here (see Water Power and Dam Construction by P.C. Erbiste May 1984) is a function of W, h, and H where:

- W is the span,
- h is the gate height,
- H is the static head on the gate bottom seal.

The weight of the gate leaf is given by the formula (see abacus – annex 1):

Weight of a fixed-wheel gate: = 0.706 ($W^2.h.H)^{0.7}$

Given the static heads are the highest ones (compared to the operating heads), only them have been taken into account for the calculation of the weights.
Span width, height, static head on seal bottom and weight of gate or bulkhead leaf are given in annex 3.

The estimated weight of the culvert gate is 26.5 tons and the estimated weight of the WSB conduit gate is 28.9 tons. The weights of the culvert and WSB conduit gates are very close to each other. At this conceptual stage, it clearly appears that the same design should be used for both gates.

The incurred costs/benefits that will result are the following :

- From the standardization point of view : same drawings, same manufacturing processes, erection procedures, …
- From the operational and maintenance point of view : reduced amount of spare parts, better material knowledge of the maintenance people, …

It is reminded that to check the procedure, a preliminary calculation of a WSB fixed-wheel gate structure has been performed (see Annex 2). The calculation has confirmed the results of the above formula.

Moreover, the weight of **one meter** of embedded fixed parts is estimated to:

- Culvert fixed-wheel gates at the bottom of the slot:	800 kg (last 12m[1])
- Culvert fixed-wheel gates at the upper part of the slot (only for guiding):	200 kg
- Culvert sliding bulkhead at the bottom of the slot:	500 kg (last 9m[2])
- Culvert sliding bulkhead (only for guiding)	200 kg
- WSB fixed-wheel gates at the bottom of the slot:	1000 kg (last 12m)
- WSB fixed-wheel gates at the upper part of the slot:	200 kg
- WSB sliding bulkhead at the bottom of the slot:	500 kg (last 9m)
- WSB sliding bulkhead (only for guiding)	200 kg

Note: Lintel and sill embedded parts have been added separately. For the gates the weight of said parts is taken as 800 kg/m, for the bulkheads, it has been taken as 500 kg/m.

[1] *Two times the height of the gates (2x6=12m)*
[2] *One time first leaf plus two times second leaf (3+2x3=9m)*

2.5 CONSTRUCTION DETAILS

Hydraulic servomotor operated, the fixed wheel gates are equipped with wheels revolving on fixed axles cantilevered from the gate frame (see annex 4 for typical example of a sectional view of one wheel of the Berendrecht culvert gates). Wheels can be of the flat type (rolling on stainless steel tracks) or of the flanged type (rolling on rails). Tracks must withstand the bearing pressures and distribute them to the concrete structure behind. The **number of wheels** will be based on the steel characteristics. It shall **not be less than 6 wheels.**

A typical horizontal sectional view of a gate (or bulkhead) welded structure is shown in Annex 5. Horizontal plate girders or standard T or I-shape beams are the main force resisting members of the gate.

The distance between horizontal girders may vary according to the hydrostatic pressure. Diaphragm plates and intercostals are also used as reinforcement to distribute loads more uniformly.

WSB fixed-wheel gates have to resist to water pressure and **be tight in both directions** as for the locks submitted to tidal effects.

The access shaft for maintenance will be used as **surge chambers** during operation of the gates.

Tolerances must be adequate to assure watertight seals. That is the reason why it is recommended to use very rigid U-shape steel guiding for the gates to avoid any movement during embedding of the fixed parts.

The gate and wheels are permanently under water. Maintenance of these wheels and bearings is possible by lifting out of water the moving parts. Wear of these elements can be considerably reduced by using **self lubricating** material.

SEALING SYSTEM

Seals are usually made of rubber with or without a PTFE (Teflon) overlay (**PTFE overlay is preferred**). The seals are often of the music note shape or lip type.

For the WSB gates being tight for water flowing in both directions, the lip seals adopted for Berendrecht (see sectional view of the wheel) should be convenient.

Lintel seal and side seals: can be of the upstream or downstream type (see figure - Annex 6)

Bottom seal can be flat or also of the J-shape type.(see figure – Annexes 6 and 7)

MAINTENANCE OF THE GATES AND BULKHEADS

Maintenance work on gates and bulkheads (as wheels and relevant slots) consists mainly in the replacement of rubber seals and painting. Overhaul and/or replacement of wheels could also be foreseeable. Moreover, the maintenance works will have to include the replacement of the sacrificial anodes whenever necessary.

During normal operation, any trouble with one culvert or WSB gate (blocking or incident on the oil system) will not interfere on the ship transit except concerning the operation time. Every gate can be isolated and maintenance people can reach the upstream or downstream side of the gate by use of bulkheads after emptying of the space between them.

In case of planned replacement of seals or painting, the gate will be lifted out by use of a 100 tons gantry crane moving on rails. This crane will be provided by truck, assembled and installed on the railway located above the gate slot. After dismantling of the gate, the work will be carried out in good conditions in the maintenance building. Two mobile cranes will be necessary for the 52 gates and 14 bulkheads. Rails will be installed between and outside of all the rows of WSB and culvert slots.

For the culverts, 8 (4 x 2) bulkheads are foreseen. It enables to close completely one culvert using 2 x 2 bulkheads at each of the culvert extremities.
For the WSB conduit, 6 (2 x 3) bulkheads are foreseen. It enables to close completely one conduit.

Bulkheads gates can be stored outside or suspended into the slots (one piece of bulkhead gate per slot). To remove a bulkhead gate, the cranes will be equipped with an automatic lifting beam. Planned maintenance will also be done in the maintenance building.

3 REFERENCES

- Hydraulic gates and valves in free surface flow and submerged outlets by Jack Lewin
- Water Power and Dam Construction (review)
- Final report of the International commission for the study of locks (PIANC)
- Engineer manuals
- CCP (2002) “Diseño conceptual de las esclusas Post Panamax – Triple Lift Lock System, Task 4”

ANNEX 1

Abacus of gate weight versus gate parameter (W, h, H)

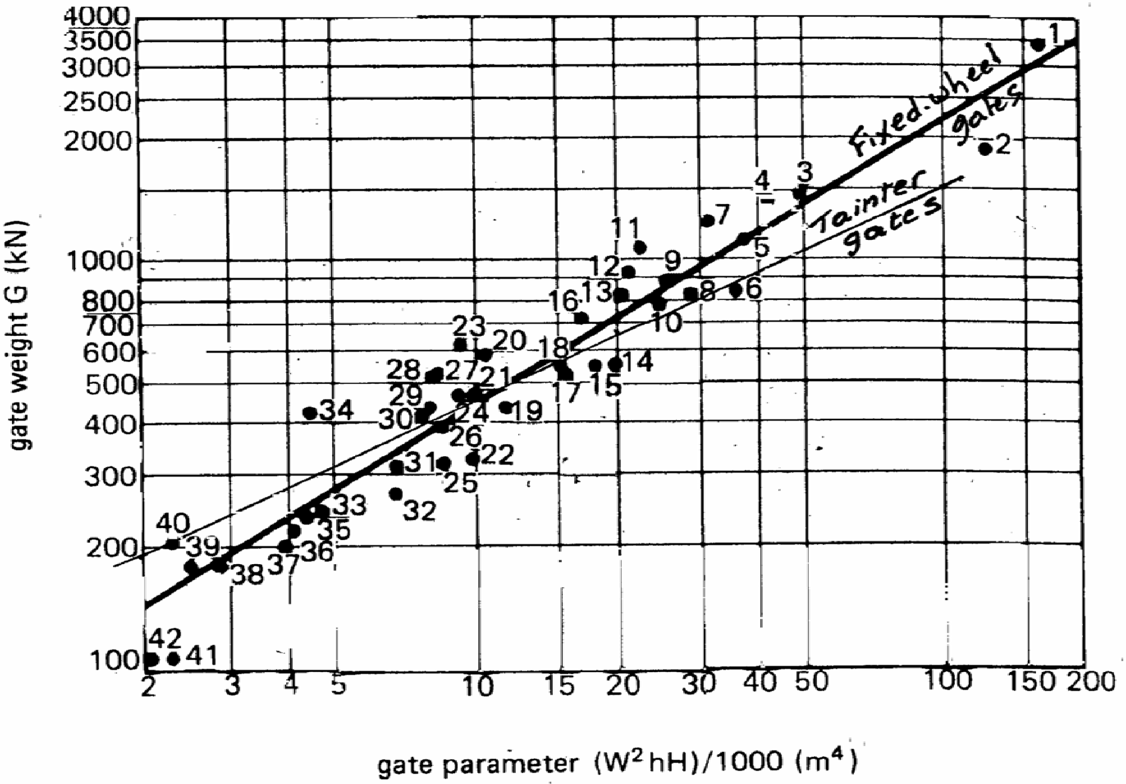

Weight of large fixed-wheel gates ($W^2hH > 2000\ m^4$).

ANNEX 2 (Remind of report R4-E date 15.11.2002)

TYPICAL CALCULATION OF A WSB GATE (Hs = 50m)

This calculation is the same as the one included in the report mentioned at the beginning of paragraph 1.1 of this report. The only goal of this calculation is to prove that the use of the general formula (see page 2-6) is relevant for weight calculation.

SKIN PLATE

The estimated skin plate thickness corresponds to a distance of 1.5m between the horizontal I beams and 1m between the vertical T shape intercostals is 4cm

STEEL PLATE		Mesh 1.00 x 1.50 m		LOAD : 50 t/m2	
		span maximum bending moment (tm) :			3.71333
		edges and corners maximum bending moment (tm) :			5.11170
thickness	I/v	relative displacement		maximum stresses	
		span	corner	span	corner
(m)	(m3)	(mm)	(mm)	(kg/mm2)	(kg/mm2)
0.040	0.0002667	0.880	1.540	12.55	19.17
0.035	0.0002042	1.314	2.300	16.39	25.04
0.030	0.0001500	2.087	3.653	22.30	34.08
0.025	0.0001042	3.605	6.312	32.12	49.07
0.020	0.0000667	7.042	12.328	50.18	76.68

choosen thickness: 4 cm

MAIN BEAMS

The horizontal main beams size depends on the span between them and load. According to the I/v required, alternatives were investigated i.e.:

- HE 1000 A
- W 1100 x 400 x 433

MAIN GIRDERS		length (m) :	5.7	distance (m):	1.5	load (t/m):	75	Moment (tm):	304.59375
		E (t/m2):	21000000						

DISPLACEMENT vs INERTIA		STRESS vs I/v	
I (m4)	f (m)	I/v (m3)	STRESS (t/m2)
0.0005	0.098177093	0.005	60918.75
0.0006	0.081814244	0.007	43513.392857
0.0007	0.070126495	0.009	33843.75
0.0008	0.061360683	0.011	27690.340909
0.0009	0.054542829	0.013	23430.288462
0.001	0.049088546	0.015	20306.25
0.0011	0.044625951	0.017	17917.279412
0.0012	0.040907122	0.019	16031.25
0.0013	0.03776042	0.021	14504.464286
0.0014	0.035063247	0.023	13243.206522
0.0015	0.032725698	0.025	12183.75
0.0016	0.030680341	0.027	11281.25
0.0017	0.028875615	0.029	10503.232759
0.0018	0.027271415	0.031	9825.6048387
0.0019	0.025836077	0.033	9230.1136364
0.002	0.024544273	0.035	8702.6785714
0.0021	0.023375498	0.037	8232.2635135
0.0022	0.022312976	0.039	7810.0961538
0.0023	0.021342846	0.041	7429.1158537
0.0024	0.020453561	0.043	7083.5755814
0.0025	0.019635419	0.045	6768.75
0.0026	0.01888021	0.047	6480.7180851
0.0027	0.018180943	0.049	6216.1989796
0.0028	0.017531624	0.051	5972.4264706
0.0029	0.016927085	0.053	5747.0518868
0.003	0.016362849	0.055	5538.0681818
0.0031	0.015835015	0.057	5343.75
0.0032	0.015340171	0.059	5162.6059322
0.0033	0.014875317	0.061	4993.3401639
0.0034	0.014437808	0.063	4834.8214286
0.0035	0.014025299	0.065	4686.0576923
0.0036	0.013635707	0.067	4546.1753731
0.0037	0.013267175	0.069	4414.4021739
0.0038	0.012918039	0.071	4290.0528169
0.0039	0.012586807	0.073	4172.5171233
0.004	0.012272137	0.075	4061.25
0.0041	0.011972816	0.077	3955.762987
0.0042	0.011687749	0.079	3855.6170886
0.0043	0.011415941	0.081	3760.4166667
0.0044	0.011156488	0.083	3669.8042169
0.0045	0.010908566	0.085	3583.4558824
0.0046	0.010671423	0.087	3501.0775862
0.0047	0.010444372	0.089	3422.4016854
0.0048	0.01022678	0.091	3347.1840659
0.0049	0.010018071	0.093	3275.2016129
0.005	0.009817709	0.095	3206.25
0.0051	0.009625205	0.097	3140.1417526
0.0052	0.009440105	0.099	3076.7045455
0.0053	0.00926199	0.101	3015.779703
0.0054	0.009090472	0.103	2957.2208738
0.0055	0.00892519	0.105	2900.8928571
0.0056	0.008765812	0.107	2846.6705607
0.0057	0.008612026	0.109	2794.4380734
0.0058	0.008463542	0.111	2744.0878378
0.0059	0.008320093	0.113	2695.5199115
0.006	0.008181424	0.115	2648.6413043
0.0061	0.008047303	0.117	2603.3653846
0.0062	0.007917507	0.119	2559.6113445
0.0063	0.007791833	0.121	2517.303719
0.0064	0.007670085	0.123	2476.3719512
0.0065	0.007552084	0.125	2436.75
0.0066	0.007437659	0.127	2398.3759843
0.0067	0.007326649	0.129	2361.1918605
0.0068	0.007218904	0.131	2325.1431298
0.0069	0.007114282	0.133	2290.1785714
0.007	0.007012649	0.135	2256.25
0.0071	0.00691388	0.137	2223.3120438
0.0072	0.006817854	0.139	2191.3219424
0.0073	0.006724458	0.141	2160.2393617
0.0074	0.006633587	0.143	2130.0262238
0.0075	0.00654514	0.145	2100.6465517
0.0076	0.006459019	0.147	2072.0663265
0.0077	0.006375136	0.149	2044.2533557
0.0078	0.006293403	0.151	2017.1771523
0.0079	0.00621374	0.153	1990.8088235
0.008	0.006136068	0.155	1965.1209677
0.0081	0.006060314	0.157	1940.0875796
0.0082	0.005986408	0.159	1915.6839623
0.0083	0.005914283	0.161	1891.886646
0.0084	0.005843875	0.163	1868.6733129
0.0085	0.005775123	0.165	1846.0227273
0.0086	0.005707971	0.167	1823.9146707
0.0087	0.005642362	0.169	1802.3298817
0.0088	0.005578244	0.171	1781.25
0.0089	0.005515567	0.173	1760.6575145
0.009	0.005454283	0.175	1740.5357143
0.0091	0.005394346	0.177	1720.8686441
0.0092	0.005335712	0.179	1701.6410615
0.0093	0.005278338	0.181	1682.8383978

for a deformation = span/1000 (.0057), I must be > 860000 cm4

To keep a stress < 15 kg/mm2, I/v must be > 20000 cm3

Best profile matching the 2 requirements (lower weight):

W 1100 x 400 x 433		433.24	kg/m'				
I =	1125573.94	cm4	deformation :	4.3612E-11	m		
I/v =	20317.22	cm3	stress:	14.991901	kg/mm2	ok with steel yield strength 24 kg/mm2	
With a HE1000B:		314.44	kg/m'				
I =	644748.07	cm4	deformation :	7.6136E-11	m		
I/v =	12894.96	cm3	stress:	23.6211473	kg/mm2	ok with steel yield strength 36 kg/mm2	

SECONDARY BEAMS

T beams coming from HE 600 A were considered

SECONDARY GIRDERS	length (m):	1.5	distance (m):	1	load (t/m):	50	M (tm):	9.375

DISPLACEMENT vs INERTIA		STRESS vs I/v	
I (m4)	f (m)	I/v (m3)	STRESS (t/m2)
1E-05	0.00313895	0.0002	46875
2E-05	0.00156948	0.00025	37500
3E-05	0.00104632	0.0003	31250
4E-05	0.00078474	0.00035	26785.71429
5E-05	0.00062779	0.0004	23437.5
6E-05	0.00052316	0.00045	20833.33333
7E-05	0.00044842	0.0005	18750
8E-05	0.00039237	0.00055	17045.45455
9E-05	0.00034877	0.0006	15625
0.0001	0.0003139	0.00065	14423.07692
0.00011	0.00028536	0.0007	13392.85714
0.00012	0.00026158	0.00075	12500

I/v should be > 600 cm3

HE600A 1/2

	b	h	S	y	S.y	bh3/12	d	S.d2
base	30	2.5	75	28.25	2118.75	39.0625	-18.0257	24369.573848
wall	1.3	27	35.1	13.5	473.85	2132.325	-3.27575	376.64181104
plate	30	4	120	-2	-240	160	12.22425	17931.875524
			230.1	10.22425033	2352.6	2331.3875		42678.091183

I =	45009.4787			
I/v1=	3164.27774	stress:	2.962761416	kg/mm2
I/v h =	2335.03129	stress:	4.014935487	kg/mm2
f (m)=	6.974E-05			

WEIGHTS:

Steel plate 40 x	7500 x 5700 mm	13.4235 t	
main girder W 1100 x 400 x 433 yield point 24 kg/mm2			
total length 5 x 5.7 m			12.34734
main girder HE1000B yield point 36 kg/mm2			8.96154
secondary girders 1/2 HE600A			
total length 5 x 7.5			4.6725
border plate	5 cm	10.362 t	
suspension		6 t	
axis, wheels		2.4 t	
variante 1	49.20534		
variante 2	45.81954		

CONCLUSION:

The estimated weight by 1st calculation is 46 or 49 tons according to the beam choice (HE 1000 A or W 1100 x 400 x 300 according to the ARBED catalogue (see extract hereunder). These values are to be compared with the 51 tons found by the above statistical formula.

Catalog
ProfilARBED - Beams selection program

PROFILARBED

page 1
02/09/02 15:25:37

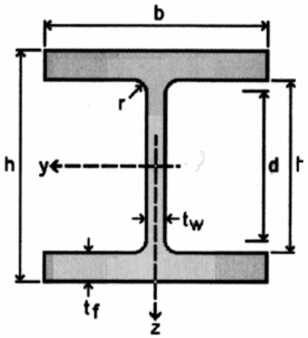

Listing with profiles according to the following rule:
I.y must be between 5000,00 cm4 and 3000000,00 cm4
W.y must be between 9000,00 cm3 and 71000,00 cm3
G ascending
Search in: IPE, IPN, HE, HL, HD, HP, HP(US), W, UB, UBP, UC, H

Profile						G [kg/m]	A [cm2] / A.vz [cm2]	I.y [cm4] / i.y [cm]	W.y [cm3] / W.y.pl [cm3]	I.z [cm4] / i.z [cm]	W.z [cm3] / W.z.pl [cm3]	.T [cm4]	i.T [cm] / I.omega [cm6]
W 1000 X 300 X 249	980,00	300,00	16,50	26,00	30,00	249,04	316,85	481 078,52	9 817,93	11 754,44	783,63	584,40	7,39
	928,00	868,00	103,65	3,08	12,37		180,74	38,97	11 346,88	6,09	1 244,71		26 620 893
HE 900 A	890,00	300,00	16,00	30,00	30,00	251,93	320,53	422 074,83	9 484,83	13 547,46	903,16	736,77	7,63
	830,00	770,00	111,15	2,90	11,51		163,33	36,29	10 811,04	6,50	1 414,48		24 961 500
UB 914 X 305 X 253	918,40	305,50	17,30	27,90	19,10	253,74	322,83	436 304,46	9 501,40	13 301,11	870,78	630,51	7,71
	862,60	824,40	95,48	2,99	11,80		167,85	36,76	10 942,00	6,42	1 370,54		26 284 181
W 920 X 310 X 253	919,00	306,00	17,30	27,90	19,00	254,02	323,18	437 456,16	9 520,26	13 366,25	873,61	630,91	7,72
	863,20	825,20	95,36	2,99	11,80		167,86	36,79	10 962,73	6,43	1 374,80		26 449 053
W 920 X 310 X 271	923,00	307,00	18,40	30,00	19,00	272,03	346,09	471 573,42	10 218,28	14 518,01	945,80	775,02	7,76
	863,00	825,00	100,66	3,00	11,06		178,81	36,91	11 782,87	6,48	1 490,95		28 842 178
W 1000 X 300 X 272	990,00	300,00	16,50	31,00	30,00	272,62	346,85	553 846,02	11 188,81	14 004,44	933,63	822,41	7,55
	928,00	868,00	113,65	3,10	11,37		184,56	39,96	12 824,38	6,35	1 469,71		32 073 875
HE 1000 A	990,00	300,00	16,50	31,00	30,00	272,62	346,85	553 846,02	11 188,81	14 004,44	933,63	822,41	7,55
	928,00	868,00	113,65	3,10	11,37		184,56	39,96	12 824,38	6,35	1 469,71		32 073 875
H 900 X 300 X 18 X 34	912,00	302,00	18,00	34,00	18,00	283,01	360,06	491 010,69	10 767,78	15 654,09	1 036,69	980,82	7,77
	844,00	808,00	107,09	2,97	10,49		173,06	36,93	12 337,07	6,59	1 622,45		30 079 980

ARBED GROUP

Catalog
ProfilARBED - Beams selection program

PROFILARBED

page 1
06/09/02 15:02:39

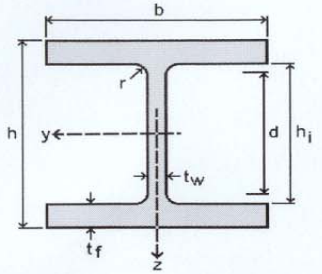

Listing with profiles according to the following rule:
I.y must be between 1125000,00 cm4 and 3000000,00 cm4
W.y must be between 10000,00 cm3 and 100000,00 cm3
G ascending
Search in: IPE, IPN, HE, HL, HD, HP, HP(US), W, UB, UBP, UC, H

Profile	h [mm] / h.i [mm]	b [mm] / d [mm]	t.w [mm] / S.s [mm]	t.f [mm] / A.L [m2/m]	r [mm] / A.G [m2/t]	G [kg/m]	A [cm2] / A.vz [cm2]	I.y [cm4] / i.y [cm]	W.y [cm3] / W.y.pl [cm3]	I.z [cm4] / i.z [cm]	W.z [cm3] / W.z.pl [cm3]	I.T [cm4]	i.T [cm] / I.omega [cm6]
W 1100 X 400 X 433	1 108,00	402,00	22,00	40,00	20,00	433,24	551,19	1 125 573,94	20 317,22	43 409,79	2 159,69	2 129,54	10,40
	1 028,00	988,00	125,43	3,75	8,66		254,39	45,19	23 160,71	8,87	3 361,78		123 500 699
HL 1100 M	1 108,00	402,00	22,00	40,00	20,00	433,24	551,19	1 125 573,94	20 317,22	43 409,79	2 159,69	2 129,54	10,40
	1 028,00	988,00	125,43	3,75	8,66		254,39	45,19	23 160,71	8,87	3 361,78		123 500 699
W 1100 X 400 X 499	1 118,00	405,00	26,00	45,00	20,00	499,28	635,21	1 294 059,56	23 149,54	49 984,12	2 468,35	3 134,95	10,45
	1 028,00	988,00	139,43	3,77	7,56		300,41	45,14	26 599,48	8,87	3 870,29		143 405 493
HL 1100 R	1 118,00	405,00	26,00	45,00	20,00	499,28	635,21	1 294 059,56	23 149,54	49 984,12	2 468,35	3 134,95	10,45
	1 028,00	988,00	139,43	3,77	7,56		300,41	45,14	26 599,48	8,87	3 870,29		143 405 493
W 1000 X 400 X 539	1 030,00	407,00	28,40	51,10	30,00	540,12	687,17	1 202 537,90	23 350,25	57 631,92	2 832,04	4 546,45	10,60
	927,80	867,80	165,75	3,58	6,64		316,39	41,83	26 823,86	9,16	4 435,56		137 552 834
HL 1000 X 554	1 032,00	408,00	29,50	52,00	30,00	554,76	705,81	1 232 371,55	23 883,17	59 098,19	2 896,97	4 859,98	10,61
	928,00	868,00	168,65	3,59	6,47		328,03	41,79	27 496,21	9,15	4 546,53		141 326 871
HE 1000 X 579	1 056,00	316,00	35,00	64,00	30,00	579,29	737,01	1 245 718,26	23 593,15	34 037,38	2 154,26	7 102,05	8,06
	928,00	868,00	198,15	3,25	5,63		393,33	41,11	27 950,86	6,80	3 498,29		82 804 383
W 1000 X 300 X 584	1 056,00	314,00	36,00	64,00	30,00	584,57	743,73	1 246 071,34	23 599,84	33 433,46	2 129,52	7 230,02	7,98
	928,00	868,00	199,15	3,24	5,56		403,25	40,93	28 039,18	6,70	3 474,83		81 242 078

ARBED GROUP

ANNEX 3

ESTIMATION OF WEIGHT FOR CULVERT AND CONDUIT GATES TAKING INTO ACCOUNT MAXIMUM STATIC HEADS
PACIFIC SIDE : TRIPLE LIFT (W = 55m) 3 x 3 WATER SAVING BASINS

			Width(m)	height(m)	Hmwc(m)	Hsécurité	Htot	T/m	L tot(m)	**Estimated weight (T)**	n	Total weight (T)
CULVERT GATES	Culvert gates		**4.5**	**6**	**39.24**					**26.5**	16	424
	Culvert gates slots	2*2gate height		12				0.8	24	19.2	16	
		2*[Htot-(2gate height)]		12	39.24	1.5	40.74	0.2	57.48	11.5	16	
		2*width	4.5					0.8	9	7.2	16	
		tot culvert gates slots										606
	Culvert bulkhead	equal to culvert gate - 3T								23.5	8	188
	Culvert bulkhead slots	2*2bulkhead height		12				0.5	24	12	16	
		2*[Htot-(2bulkhead height)]		12	39.24	1.5	40.74	0.2	57.48	11.5	16	
		2*width	4.5					0.5	9	4.5	16	
		tot culvert bulkhead slots										448
CONDUIT GATES	Conduit gates		**4.5**	**6**	**44.33**					**28.9**	36	1040
	Conduit gates slots	2*2gate height		12				1	24	24	36	
		2*[Htot-(2gate height)]		12	44.33	1.5	45.83	0.2	67.66	13.5	36	
		2*width	4.5					1	9	9.0	36	
		tot conduit gates slots										1675
	Conduit bulkhead	equal to conduit gate - 3T								25.9	8	207
	Conduit bulkhead slots	2*2bulkhead height		12				0.5	24	12	36	
		2*[Htot-(2bulkhead height)]		12	44.33	1.5	45.83	0.2	67.66	13.5	36	
		2*width	4.5					0.5	9	4.5	36	
		tot conduit bulkhead slots										1081

ANNEX 4 – CROSS SECTION OF A GATE WHEEL OF BERENDRECHT LOCK

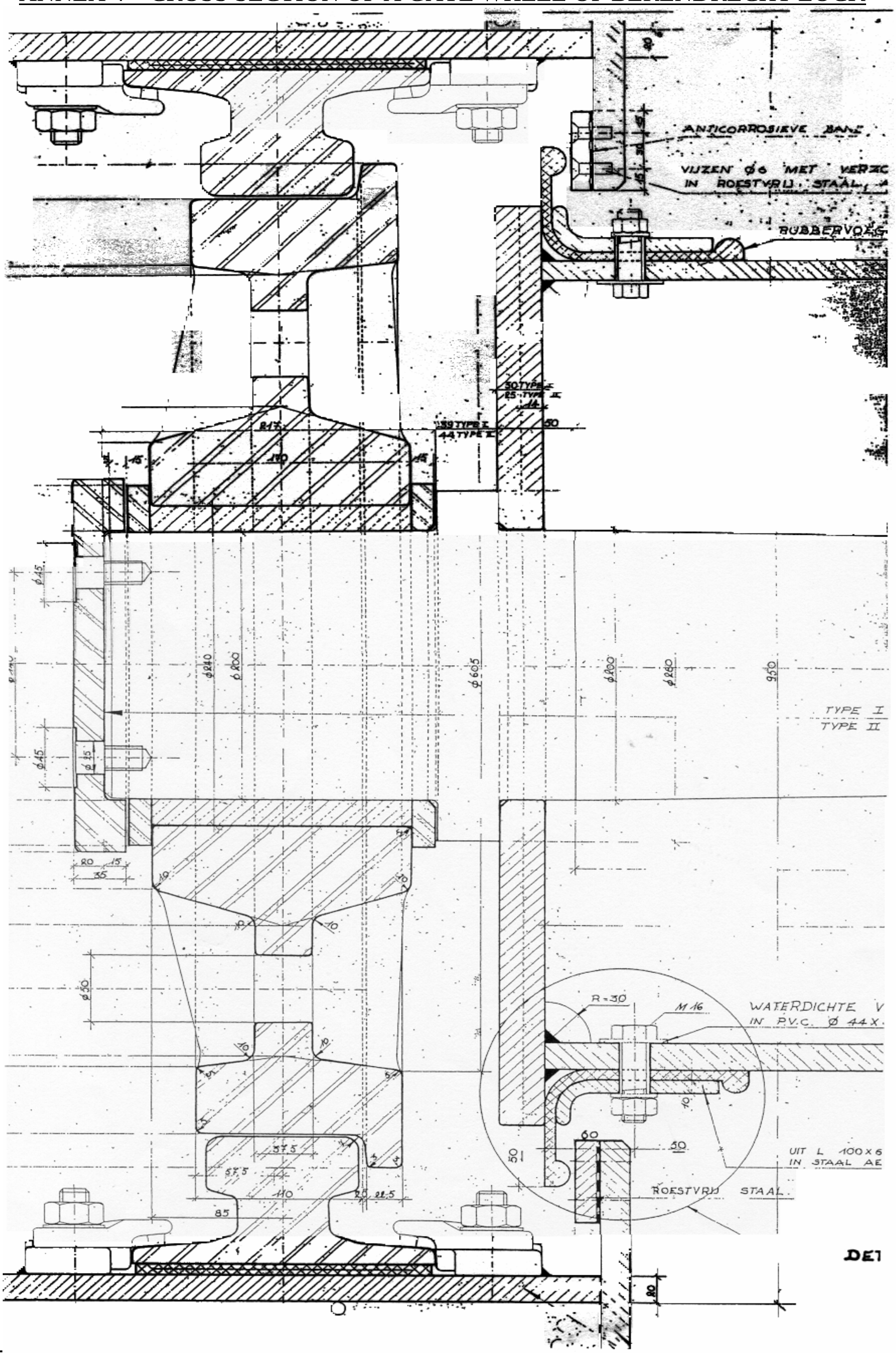

ANNEX 5

TYPICAL GATE STRUCTURE

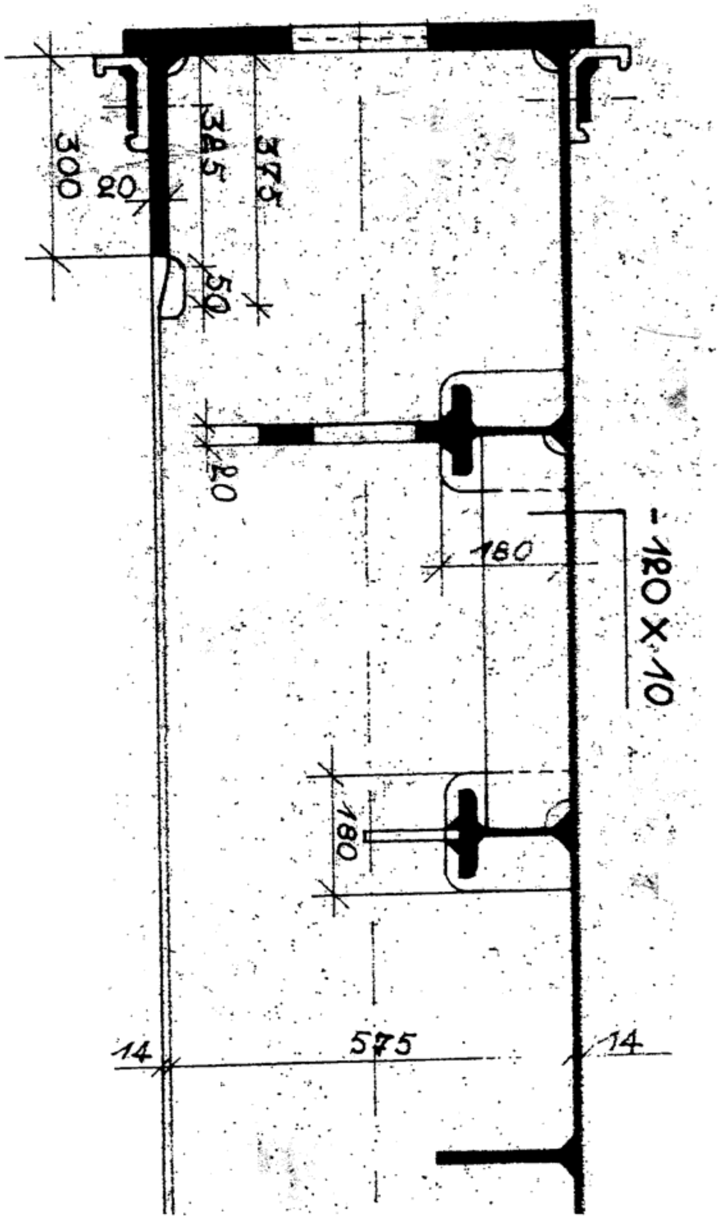

ANNEX 6

UPSTREAM AND DOWNSTREAM SEALING (Music not J-shape type)

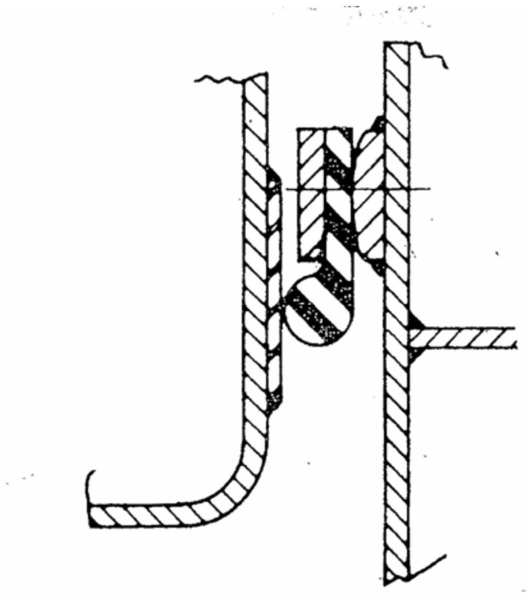

UPSTREAM SEALING

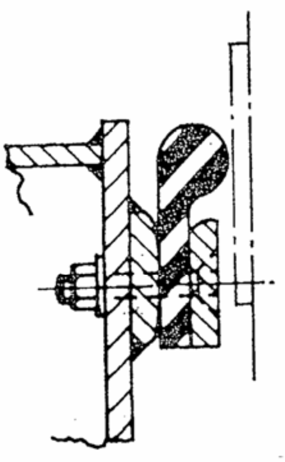

DOWNSTREAM SEALING

ANNEX 7

SIDE AND BOTTOM SEALS (BERENDRECHT)

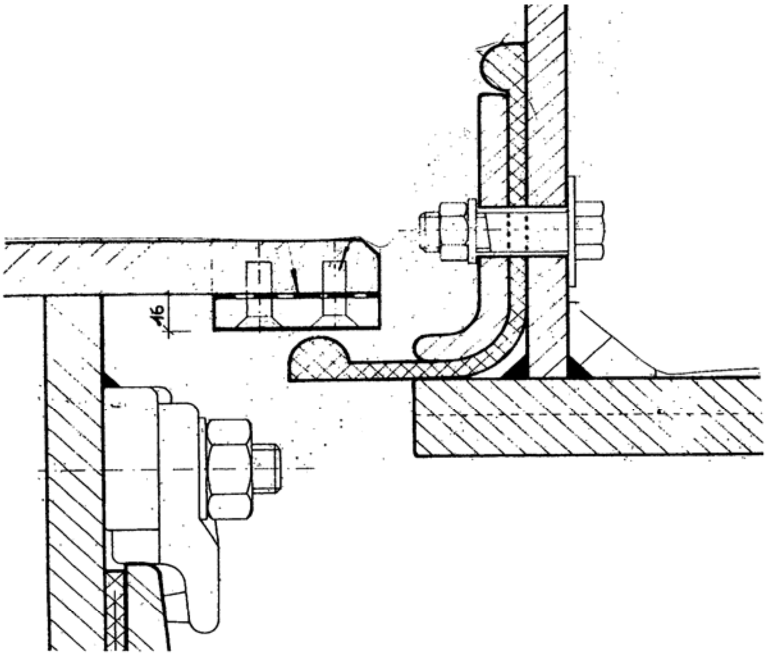

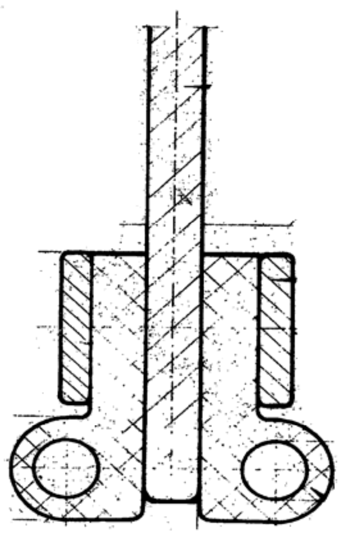

ANNEX 8 : Pictures – typical seals view (Zandvliet lock, Belgium)

Side seal left position (angular music note type)

Front seal (simple music note seal)

Side seal right position (angular music note type)

Bended music note seal – Pressing plate and protecting device

Double bottom seals

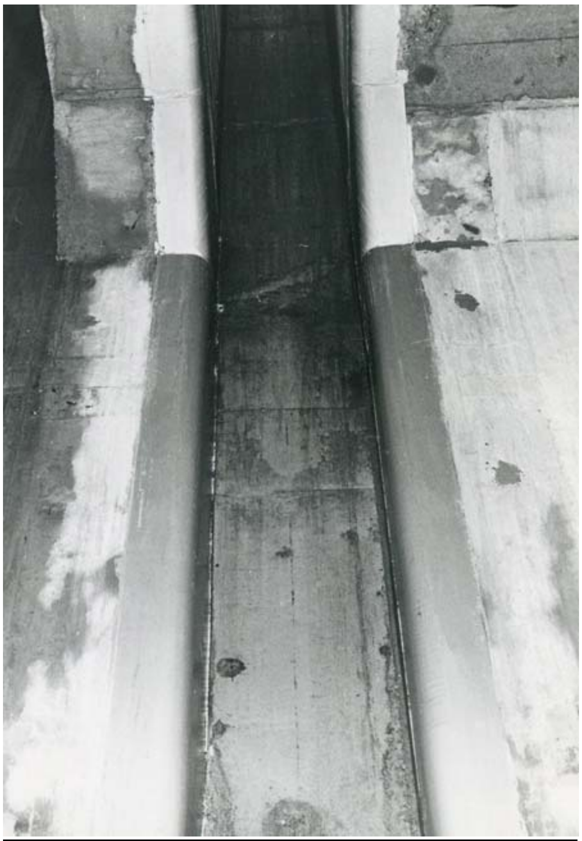

Detail of a gate slot

Handling device details

General view of culvert gate

Update of Pacific Locks Conceptual Design and Harmonization of Atlantic Locks Conceptual design - Contract SAA-143351

PACIFIC LOCKS ACTUALIZATION

TASK P4i – ENTRANCE WALLS

Rev A

in association with

1 General considerations

The entrance walls to the lock complex are the transitional part between the wider canal (trapezoidal section) and the lock (rectangular section). They are also required to guide the ship when entering the lock and, in case of emergency, for mooring of a ship.

The proposed layout of the entrance walls is shown on drawing D4-I-101. The entrance walls differ in layout and length according to their position to the east or the west of the lock entrance.

At the east side of the locks, it is strongly recommended to provide a quay wall, which can be used to moor vessels whenever there is a problem entering the locks. This can be caused by a failure of the lock gate operation, a problem with tug boat assistance, a vessel engine problem, unexpected weather conditions, etc… According to the design ship length, the quay length is approximately 400m and, has to be equipped with fenders, bollards and ladders.

The west side forms the future center wall between third and fourth lane, and has been kept shorter as it will only be a guiding wall for vessels entering the lock. If necessary, the access to the third locks complex can be separated from the fourth lane by means of heavy dolphins placed in the future center line of the two locks.

The entrance walls are counterfort retaining walls, the main difference with the lock walls being the fact that the wall height is smaller, and that there is no longitudinal culvert integrated in the structure.

2 Design criteria

Design criteria for the new lock structures have been given in the report of Task R2 – revA "Design Criteria". The main changes incorporated for the actualization of the Pacific locks conceptual design with respect to the previous conceptual design are as following:

- Use of vessel positioning by tugboat cancels locomotive loads on lock walls
- Updated design values for earthquake analysis
- Lock siting has been optimized in relation to new alignment
- Freeboard has been reduced to 1.5 m instead of 3 m

3 Technical description of entrance wall structure

The entrance walls are situated at the Lake Gatun side and at the Pacific side of the new locks. They are exposed to less severe loadings than the lock walls because the water levels are not so much fluctuating as in the lock chambers.
Another point of difference is the absence of culverts over most of their length.
The geotechnical conditions are almost the same as for the lock chambers and lock heads : part of them is in the "La Boca" formation, and another part is situated in firm Basalt rock.

As the lock walls are counterfort retaining wall due to merely geotechnical considerations, it is considered logical to retain the same wall type for the entrance walls.
From the practical point of view this is also considered as an advantage, as the contractor will be using the same techniques and methods as for the main construction work.

Below, a detailed description is given of the wall types adopted for the foundation in basalt rock and in the La Boca formation respectively. Reference is made to the following drawings:

- D4-B-101 Longitudinal view on the left bank lock wall
- D4-B-102 Longitudinal view on the right bank lock wall
- D4-B-103 Plan view lock chamber 1
- D4-B-105 Plan view lock chamber 3
- D4-I-101 Cross section of entrance walls

The structure is a reinforced concrete structure with reinforced concrete counterforts at regular distances.At the top surface of the wall, additional structural concrete is required to install a cable duct and other quay side equipment, including bollards, ladders and lighting recesses.

Due to the reduction in width of the top level structure, which was necessary to support the rail tracks in the original conceptual design - with the locomotive positioning system, the advantage of using RCC (roller compacted concrete) is no longer valid. To the contrary, the voluminous rock excavation enables re-use of material fragmented to the proper size, for backfilling purposes, which leads to economical benefit. Besides, the high frictional properties of the broken rock allow for reduction of the horizontal pressure, exerted by the fill on the vertical retaining wall, leading to structural optimization.
The width at the foundation level has been determined in function of required safety against overturning; sliding effects are negligible due to the embedment in solid rock.

The longest part of the entrance walls will be situated in the “La Boca” formation. Although the characteristics of this formation can be considered as fairly good corresponding to a rock mass type III – IV, with UCS-values ranging from 10-20 MPa, they are considerably lower than those of the basalt formation (RMT I-II, UCS-values 40-100 MPa).

Furthermore, it is also clear that the deformation behavior of the “La Boca” formation will be different than the one of the basalt formation under vertical loading.
(Deformation modules ranging from 2,5–6,6 GPa in La Boca, and from 8-12,5 GPa in basalt).

Due to the different geotechnical situation, it will be necessary to excavate with flatter sloping angles in the “La Boca” formation, thus increasing the excavation volumes. Under these circumstances with less favorable rock characteristics, the wall structure will be larger at the footing.

For conceptual design of the entrance walls, the safety against overturning and sliding is checked for the Pacific entrance (Type 1) and the Gatun Lake side entrance (Type 2). The conditions in the “La Boca” formation are predominant for design.

3.1 TYPE 1 – PACIFIC ENTRANCE

Pacific entrance: La Boca

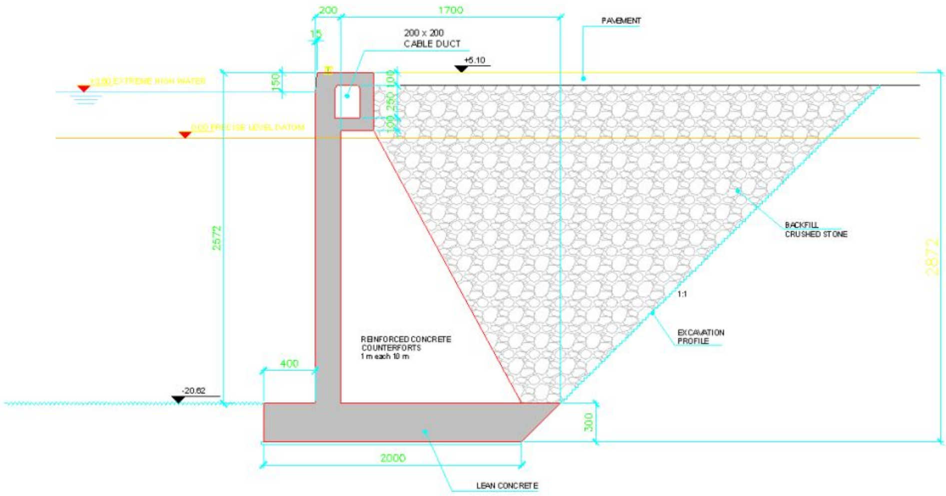

3.2 TYPE 2 – GATUN LAKE ENTRANCE

Gatun Lake side: La Boca

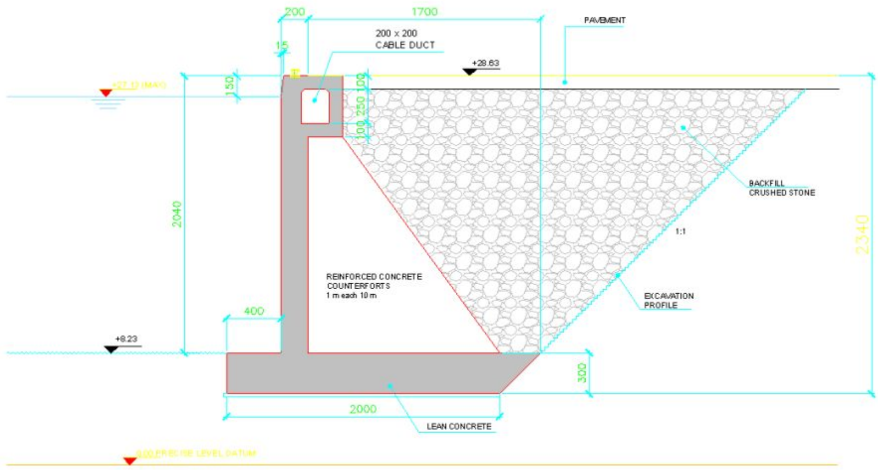

4 Analysis

4.1 LOADS

A. Self Weight (LC 1)

Concrete	γ= 25.0 kN/m³
Wet backfill	γ= 20.0 kN/m³
Dry backfill	γ= 18.0 kN/m³

B. Earth Pressure (LC 2)

As the counterfort retaining walls nears geometrically to a cantilever wall type, the active lateral pressures will be calculated for a Rankine situation:

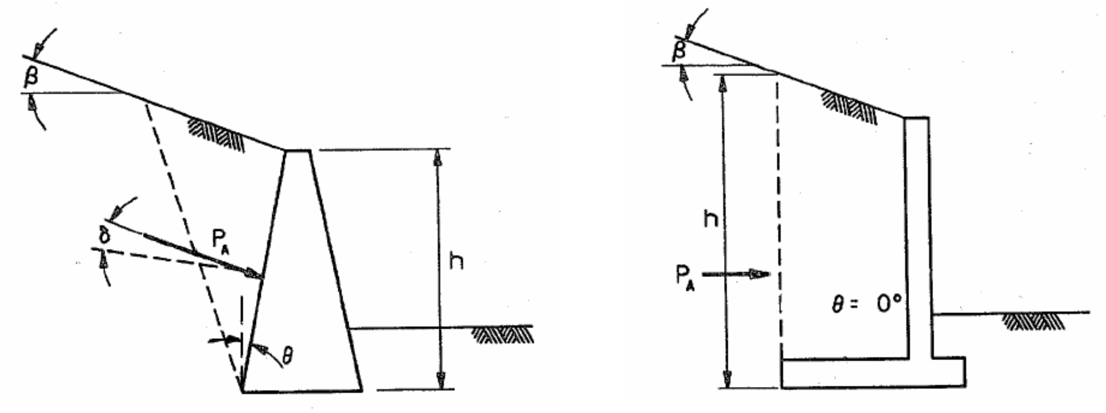

$$K_a = \frac{\cos^2(\varphi'-\theta)}{\cos^2\theta\cos(\theta+\delta)\left[1+\sqrt{\frac{\sin(\varphi'+\delta)\sin(\varphi'-\beta)}{\cos(\delta+\theta)\cos(\beta-\theta)}}\right]^2}$$

with $\delta = 0°$; $\beta = 0°$ and $\theta = 0°$

The angle of friction in the filling of crushed stone is 45°

C. Water Pressure (LC 3)

Inside the lock, the minimum water level will be applied.
At the backside of the wall the maximum water level of the lock chamber will be applied.

D. Vertical live load

On the surface a vertical live load p=10 kN/m² is applied, this load case is included in normal earth pressure load case (LC2). In seismic conditions, only half of the live load is taken into account (5 kN/m²) and is included in the seismic earth pressures load case (LC6).

E. Bollards (LC 4)

EAU1996 (Recommendations of the Committee for Waterfront Structures, Harbours & Waterways) gives recommendations for layout and loading of bollards for seagoing vessels (sections 5.12 – p. 143). Accordingly, bollards of 1500 kN working load have been retained with a spacing of 30 m. The wall is divided into segments of about 30m, so the total horizontal load applied to one meter of quay is 50 kN/m'.

F. Seismic Loads (LC 5, 6, 7 and 8)

F.1 Earthquake level

ACP stated in its Memerandum of 20 Jan 2005 on 'Seismic Design Criteria' that an earthquake with a return period of 5000 years should be considered as Maximum Credible Earthquake (= MCE) and taken equal to the Maximum Design Earthquake (= MDE).

F.2 Performance Grade

The highest performance grade (Grade S) is applicable for

- critical structures with potential for extensive loss of human life and property
- key structures that are required to be serviceable for recovery from earthquake disaster
- critical structures that, if disrupted, devastate economic and social activities

A catastrophic failure of the locks may cause flooding in the terminal cities of the canal.
This means that the level of damages is:

- Structural: minor or no damage
- Little or no loss of serviceability

for a MCE-event.

F.3 Analysis type

As this report concerns a conceptual design, a simplified analysis will be used considering equivalent static forces to apply the seismic loads on the structure.

F.4 Representative ground acceleration values

Based on the review of probabilistic seismic hazard analysis by Winter (2005), the following PGA-values can be taken as representative for the site at Miraflores:

Return period [years]	Representative PGA	Level	Load case
100	0.07		
500	0.16		
1000	**0.22**		
2500	0.32		
5000	**0.40**	MDE = MCE	LC6
10000	0.51		

The seismic coefficient k_e for use in retaining structures is defined as follows for Special Class Structures:

$$k_e = PGA/g \quad \text{for } PGA < 0.2\text{ g}$$

$$= \frac{1}{3}\left(\frac{PGA}{g}\right)^{\frac{1}{3}} \quad \text{for } PGA \geq 0.2\text{ g}$$

With according to eurocode design (CEN 1994)

$k_{h\text{ (horizontal)}} = k_e$
$k_{v\text{(vertical)}} = ½k_e$

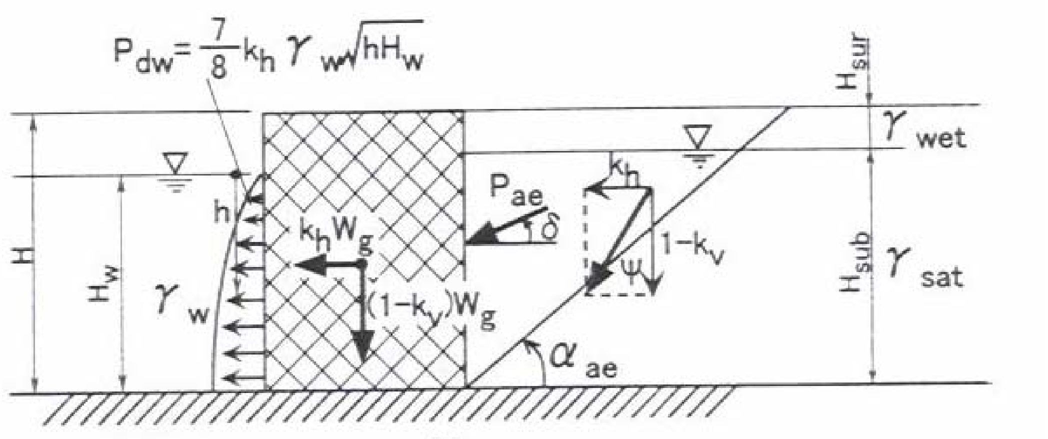

(a)

The seismic loads are calculated separately for earth pressure (LC 6), equivalent horizontal (LC 7) and vertical (LC 8) reaction forces on structural masses and water bodies (LC 5).

4.2 LOAD COMBINATIONS

According to ROSA 2000

A. Quasi Permanent Load Combination

QP1	1*LC1 + 1*LC2 + 1*LC3 + 1*LC4

B. Fundamental Load Combinations

F1	1.20*LC1 + 1.20*LC2 + 1*LC3 + 1.20*LC4
F2	0.90*LC1 + 1.20*LC2 + 1*LC3 + 1.20*LC4

C. Accidental Load Combination - MCE

MCE	1*LC1 + 1*LC3 + 0.25*LC5 + 1*LC6b + 0.25*LC7 + 0.12*LC8

4.3 CRITERIA

According to ROSA 2000

A. Sliding along the base

The factor of safety against sliding is given by the relation between the sum of the horizontal resisting forces and the sum of the horizontal driving forces:

$$FS_{(sliding)} = \frac{\sum F_{R'}}{\sum F_d} = \frac{\sum V \tan\delta + Q_{p,h}}{\sum H}$$

In which:
δ = the angle of friction between the soil and the base slab (=2/3φ')
Adhesion between the soil and the base slab is neglected

According to ROSA2000, the value of the safety factor the accidental load combination, MCE, is taken equal to 1.1. ΣV and ΣH are then given by:

$\Sigma V = (1-k_v)*G - P_{w,upl} - Q_{p,v}$

$\Sigma H = k_h*G + P_{w,h} + P_{w,sesm} + Q_{a,h}$

B. Turn over

Load Combination	Criterion
QP1	Compression zone A' > 90% A
F1 to F2	Compression zone A' > 10% A
MCE	Compression zone A' > 10% A

C. Load Bearing Capacity

$\gamma_d \,.\, q_{ref} < q_u$
γ_d . = 1.4 for load combination F1 to F2
γ_d . = 1.0 for load combination MCE

q_u = ultimate load bearing capacity
q_{ref} = reference pressure

D. Deformations

The deformations will be checked for frequent, rare and accidental load combinations QP1 and MCE.

E. Concrete Stresses

Fundamental load combinations: F1 tot F2: 1.125 x $\sigma_c < 0.85\ f_{ck}/1.5$
Accidental load combination: MCE: $\sigma_c < 0.85\ f_{ck}$

The factor 1.125 is a result of combination of the different factors in the load combinations between ROSA 2000 and Eurocode

F. Global Stability

Will be checked for the wall in La Boca formation only.

4.4 SOFTWARE

The calculations are made by means of “Esa-PrimaWin 3.60.381”, a finite element program. The gravity wall is modeled as a 2D WALL structure, allowing forces acting in its plane.

A non-linear analysis is performed to allow for compression only supports.

5 Type 1 – Pacific Entrance - Foundation in La Boca

5.1 INPUT DATA

5.1.1 GEOMETRY

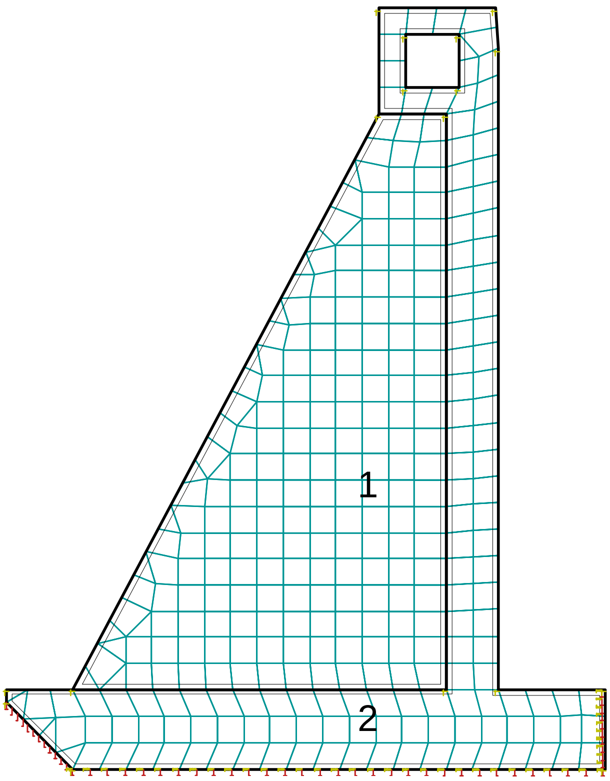

The FE model consists of the following three 2D macro structural elements:

No.	Element	Thickness
1	Reinforced concrete counterforts	0.1 m (each 10 m)
2	Retaining wall	1 m

5.1.2 MATERIALS

Name:		
C25/30-cracked		
	E modulus	20000.00 MPa
	Poisson coefficient.	0.20
	Density	2500.000 kg/m^3
	Expansion coefficient	0.01 mm/m.K

For the material corresponding to the reinforced concrete counterforts, the submerged weight of 15 kN/m^3 is taken into account, as the water pressure of LC3 are immediately applied to the main wall element.

5.1.3 SUPPORTS

The rock base is modeled by means of linear supports.

- Vertical to the base of the gravity wall and perpendicular to the boundary of the back toe, the bedding on the La Boca rock formation is characterized by a linear support of, K= 200 MN/m/m', working in compression only.
- Parallel to the base, sliding is restricted through a frictional resistance of 30% of the elasticity of the bedding.

5.1.4 LOADS

5.1.4.1 Self Weight (LC 1)

The total weight of the structure: 349 ton/m’.

5.1.4.2 Rock fill Pressure (LC 2)

from	5.1		3.6	
			λav =	λah =
λa =	0.1716		0.0000	0.1716
ϕ =	45	0.79	δ =	0
θ =	0	0.00		
γ =	18			
z	p		**pv**	**ph**
5.1	10		0.000	1.716
3.6	37		0.000	6.348

from	3.6	to	1.1	
			λav =	λah =
λa =	0.1716		0.0000	0.1716
ϕ =	45	0.79	δ =	0
θ =	0	0.00		
γ =	10			
z	p		**pv**	**ph**
3.6	37		0.000	6.348
1.1	62		0.000	10.638

from	1.1	to	-20.62	
			λav =	λah =
λa =	0.1716		0.0000	0.1716
ϕ =	45	0.79	δ =	0
θ =	0	0.00		
γ =	10			
z	p		**pv**	**ph**
1.1	62		0.000	10.638
–20.62	279.2		0.000	47.903

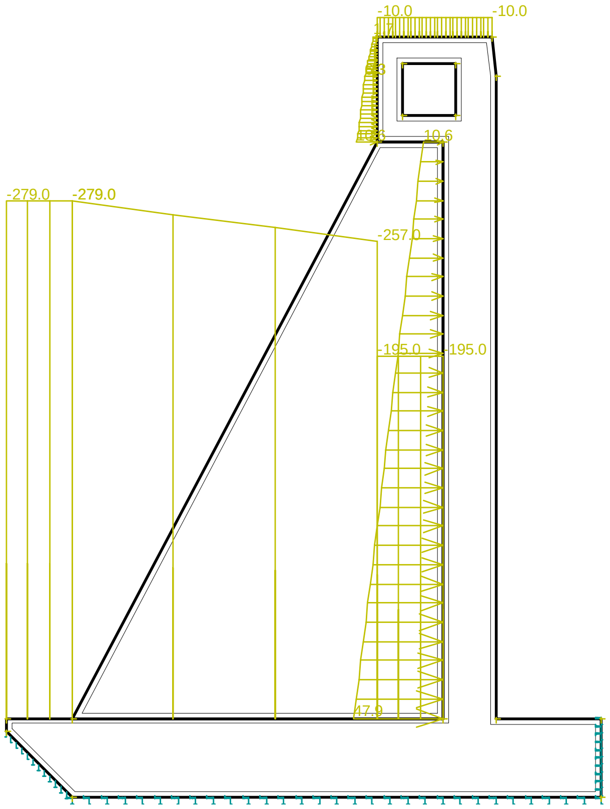

Soil weight on culvert block

X	**pv**
-4	279
0	279
11.5	257
11.5	195
14	195

5.1.4.3 Water Pressure (LC 3)

Water level inside the lock: -3.44m
Water level outside the lock: +3.60m

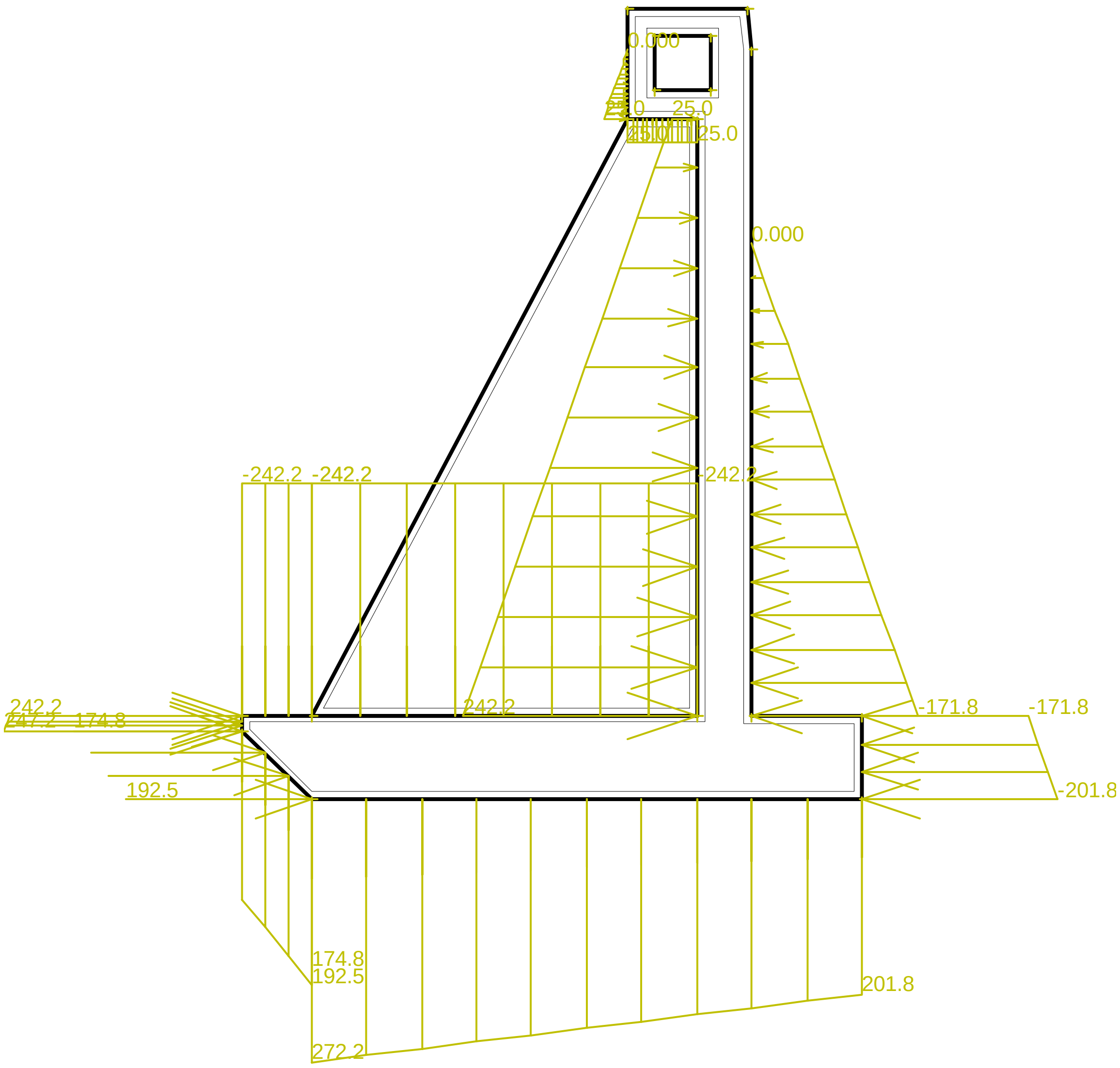

5.1.4.4 Bollard pull (LC 4)

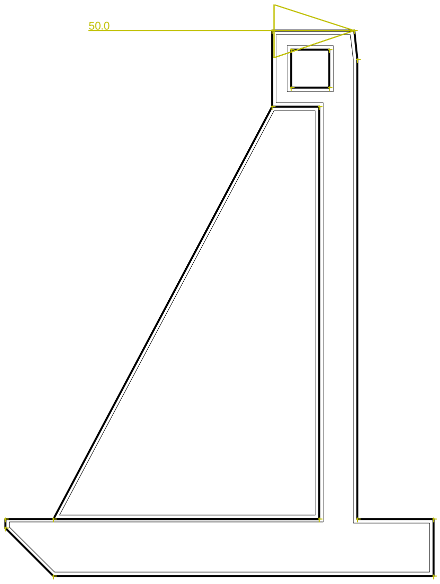

5.1.4.5 Water Pressure - Seismics (LC 5)

Water level inside the lock: -3.44 m
Water level outside the lock: +3.60 m

Water suction forces at the outside face of the wall according to Westergaard :

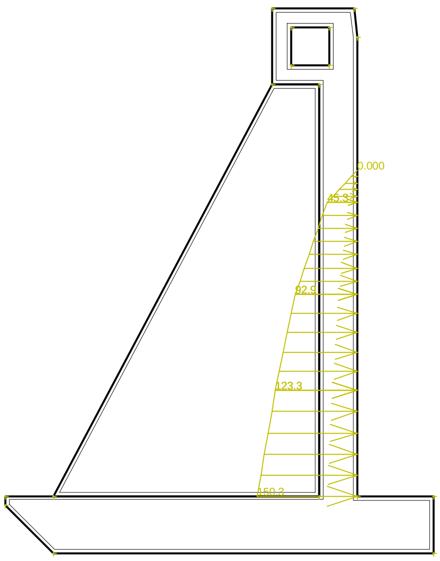

The seismic water pressure load case is valid for a unit value of k_e, and is multiplied by the respective k_e value in the corresponding load combinations.

5.1.4.6 Seismic Loads (LC 6, 7 and 8)

LC 6

The active lateral earth thrust under seismic conditions is calculated based on the Mononobe-Okabe (M-O) methodology. The M-O method is an extension of Coulomb's theory, wherein the M-O method takes into account the inertial forces acting on the soil mass during earthquake loading. It was developed to assess the stability of massive gravity walls, assuming that the retaining wall and the failure wedge act as rigid bodies.

The inertia forces are then accounted for by considering a seismic inertia angle, $\Psi = \text{atan}(k_h/(1-k_v))$, in which k_h represents the horizontal seismic coefficient or the modified horizontal seismic coefficient for dry and submerged layers respectively.

As the counterfort retaining wall under consideration is geometrically near to cantilever wall type, a Rankine situation is assumed for the calculation of the seismic active earth pressures on the vertical through the rear edge of structure. Consequently, the weight and inertia forces of the soil masses above the structure's rear base have to be taken into consideration.

Remark:

- The active lateral pressures and the horizontal inertia components of the soil masses are transferred to the front wall elements for ease of implementation.
- Half of the vertical live load is taken is accounted for in the seismic earth pressures.

LC 7 and 8

The inertia forces on the structural weight are calculated as follows:

$G_v = (1-k_v)\,G$

$G_h = k_h\,G$

With G the weight of the filling

G_v the vertical component of the weight in seismic conditions

G_h the horizontal component of weight in seismic conditions

PGA	0.4	g	k_e	0.246					CFR	0.1
k_h	0.246		k_v	0.123					Width	19

from	5.1		3.6		1.50				Width =	14.5
			λav =	λah =		k_h'	0.246		b =	4.5
λa =	0.3200		0.0000	0.3200						
φ =	45	0.79	δ =	0	0.00	ψ	15.6	0.27		
θ =	0	0.00								
γ =	18								**ph2**	64.102
z	p		**pv**	**ph1**		**Q1v**	**0.00**			**ph**
5.1	4.386		0.000	1.403		**Q1h**	**7.79**			65.506
3.6	28.070		0.000	8.982		**Q1**	**7.79**			73.084

from	3.6	to	1.1		2.50				Width =	14.5
			λav =	λah =		k_h'	0.491		b =	4.5
λa =	0.5638		0.0000	0.5638						
φ =	45	0.79	δ =	0	0.00	ψ	29.2	0.51		
θ =	0	0.00								
γ =	10								**ph2**	71.225
z	p		**pv**	**ph1**		**Q2v**	**0.00**			**ph**
3.6	28.070		0.000	15.826		**Q2h**	**55.02**			87.051
1.1	50.000		0.000	28.190		**Q2**	**55.02**			99.415

from	1.1	to	-20.62		21.72				Width =	17
			λav =	λah =		k_h'	0.491		b =	2
λa =	0.5638		0.0000	0.5638					b'=	16
φ =	45	0.79	δ =	0	0.00	ψ	29.2	0.51		
θ =	0	0.00								
γ =	10								**ph2**	
z	p		**pv**	**ph1**		**Q2v**	**0.00**			**ph**
1.1	50.000		0.000	28.190		**Q2h**	**1778.86**			100.643
−20.62	240.528		0.000	135.609		**Q2**	**1778.86**			202.413

1841.67

Soil weight on culvert block

X	**pv**
-3	241
0	241
11.5	221
11.5	171
14	171

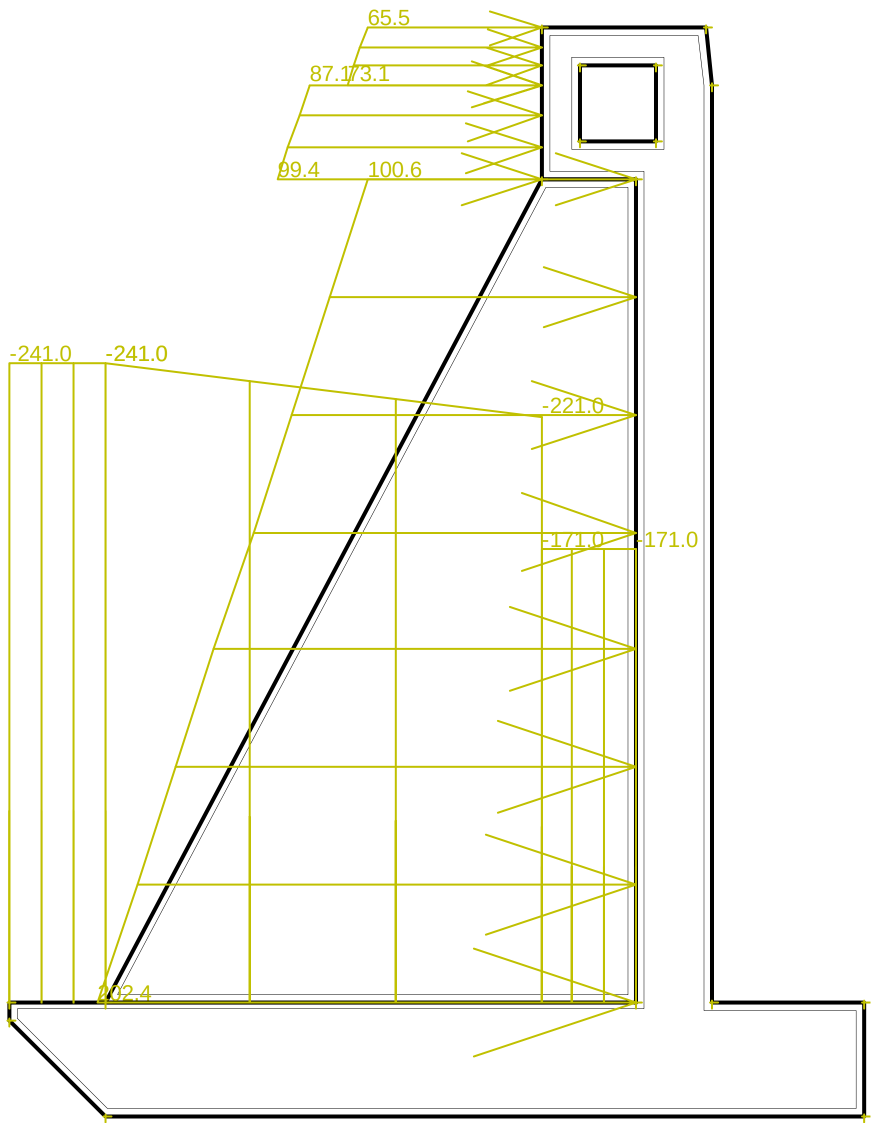

5.2 SLIDING

5.2.1 ACCIDENTAL LOAD COMBINATION – EARTH QUAKE MCE

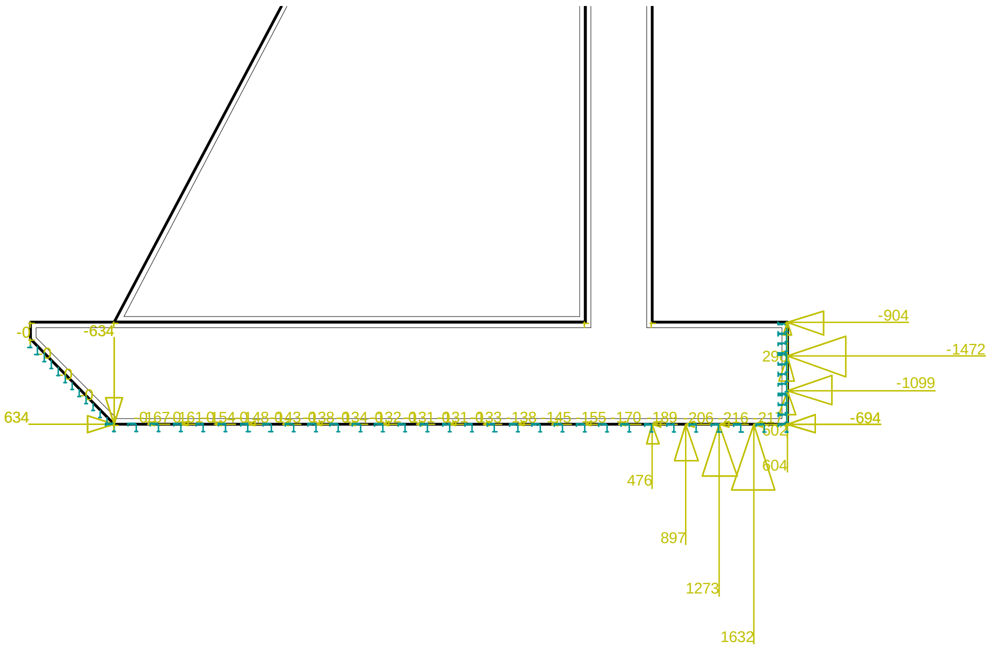

Analytically, it is found that :

$\Sigma V = 5613$ kN

$\Sigma H = 6805$ kN

To obtain the required safety ($\gamma_d = 1.1$) against sliding, a passive lateral pressure of 4245 kN has to be taken on the side face of the inner toe over a height of 3 m. This results in a pressure of 1.42 MPa, which is lower than the uni-axial compressive strength of the “La Boca” formation and concrete. The resistance to sliding is thus fulfilled.

Rock strength of La Boca:
Tensile Strength: 1.5 MPa
Uni-axial Compressive Strength: >12 MPa
It can be concluded that the sliding criterion is fulfilled.

5.3 TURN OVER

5.3.1 QUASI PERMANENT LOAD COMBINATION (QP1) – LOCK IN SERVICE

Criterion: Compression zone A'(= 100 %) > 90% A

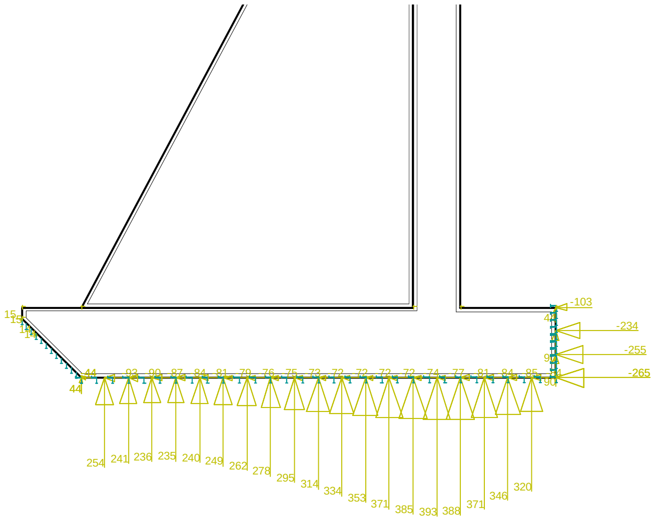

The magnitude of the vectors shown represent the support reaction in each node and not the soil pressure.

5.3.2 FUNDAMENTAL LOAD COMBINATIONS F1 TO F2

Criterion: Compression zone A' (= 100 %) > 10% A

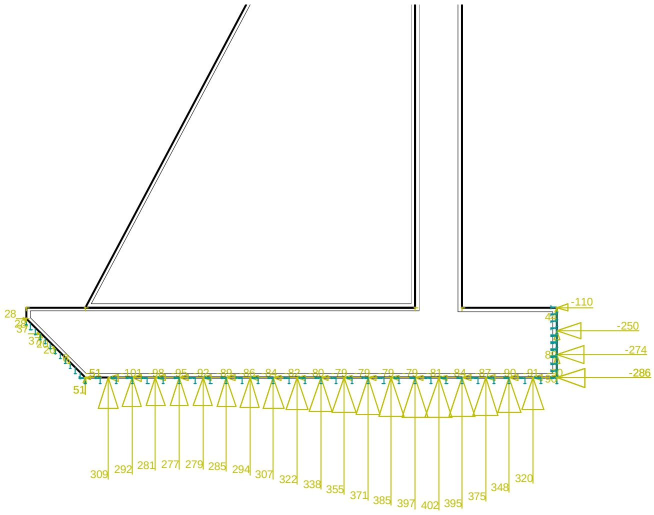

5.3.3 ACCIDENTAL LOAD COMBINATION – EARTH QUAKE MCE

Criterion: Compression zone A’ (= 25 %)> 10% A

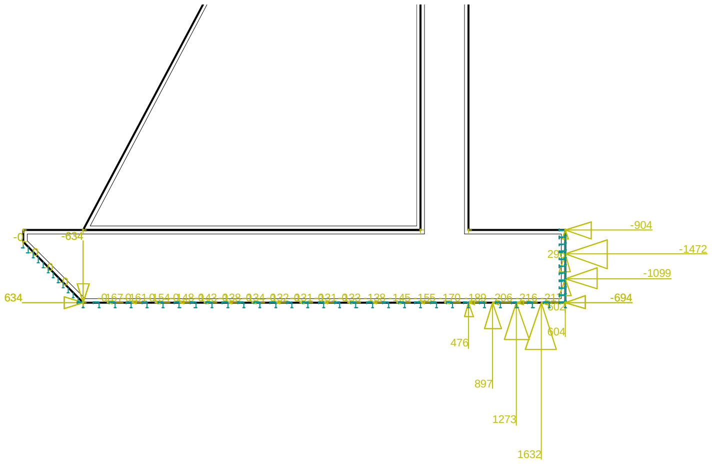

5.4 LOAD BEARING CAPACITY

5.4.1 FUNDAMENTAL LOAD COMBINATIONS F1 TO F2

Criterion: $\gamma_d \,.\, q_{ref} < q_u$
with $\gamma_d \,. = 1.4$

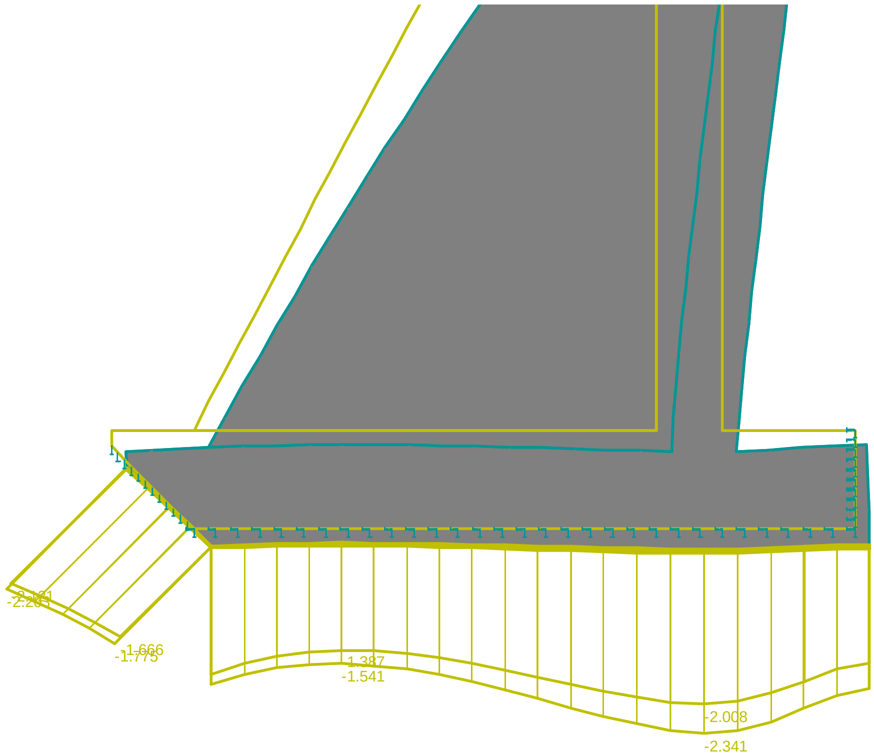

The maximum vertical displacement at the bottom of the wall is 2.341 mm, which is negligible.
This corresponds to a maximum vertical pressure of 0.0023 x 200000 kN/m² = 468 kN/m² = 0.47 Mpa.
Consequently:

$$\gamma_d \,.\, q_{ref} = 1.4*0.468 = 0.66 < q_u = 10MPa$$

(According to report R2-A the Uni-axial Compressive Strength of the La Boca rock varies from 10 to 20MPa).

5.4.2 ACCIDENTAL LOAD COMBINATION MCE

Criterion: $\gamma_d \cdot q_{ref} < q_u$
with γ_d . = 1.0 for accidental load combinations

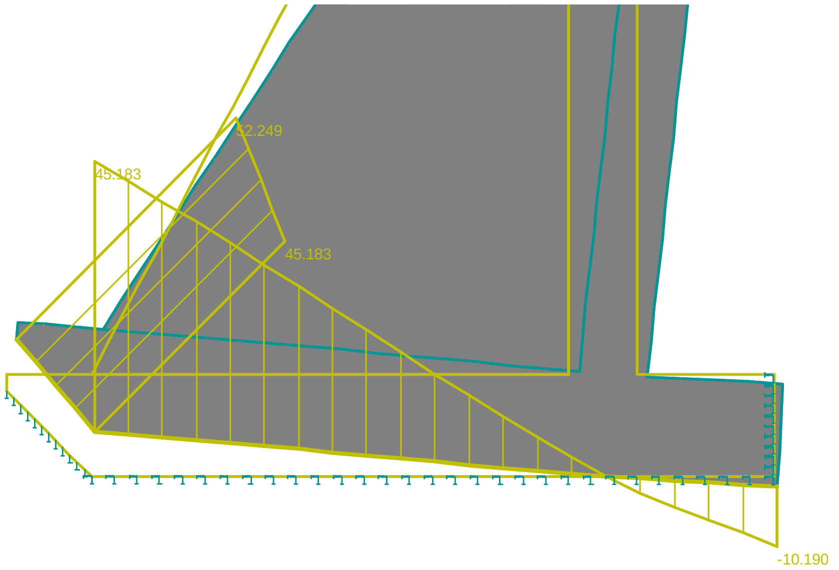

The maximal vertical displacement at the bottom of the wall is 10.19 mm
This means a vertical pressure of 0.0102 x 200000 kN/m² = 2038 kN/m² = 2.04 MPa

According report R2-A the Uni-axial Compressive Strength of the La Boca rock varies from 10 to 20MPa.

5.5 DEFORMATIONS

5.5.1 LOAD COMBINATION QP1 (LOCK IN SERVICE)

Maximal horizontal displacement, $u_{x,max}$ = 10.5 mm

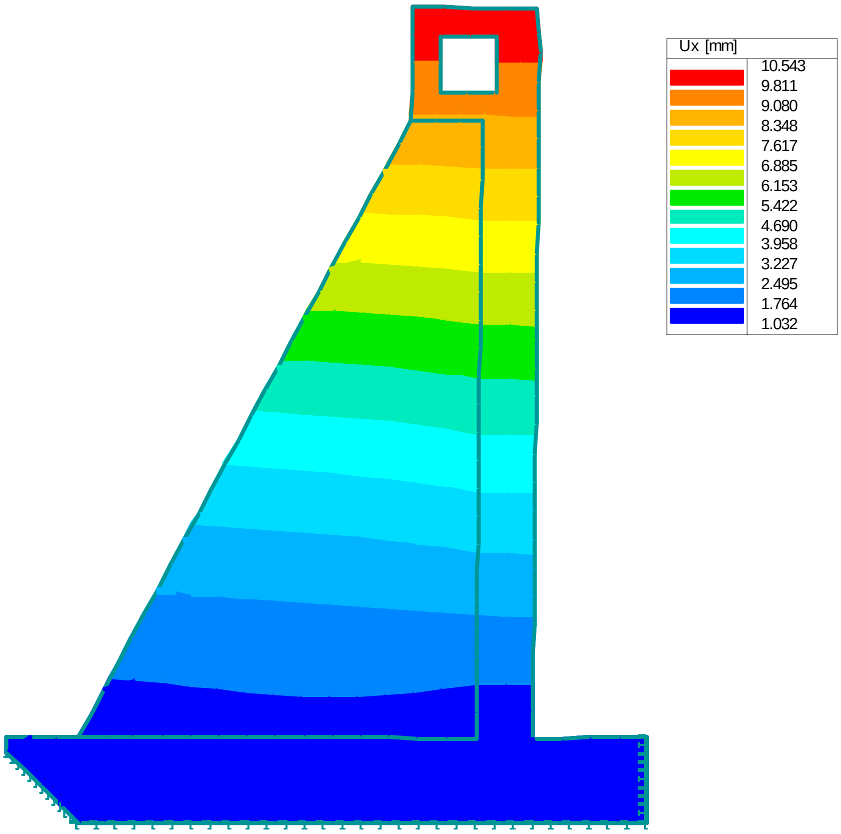

5.5.2 LOAD COMBINATION MCE (EARTH QUAKE)

Maximal horizontal displacement, $u_{x,max}$ = 109.6 mm

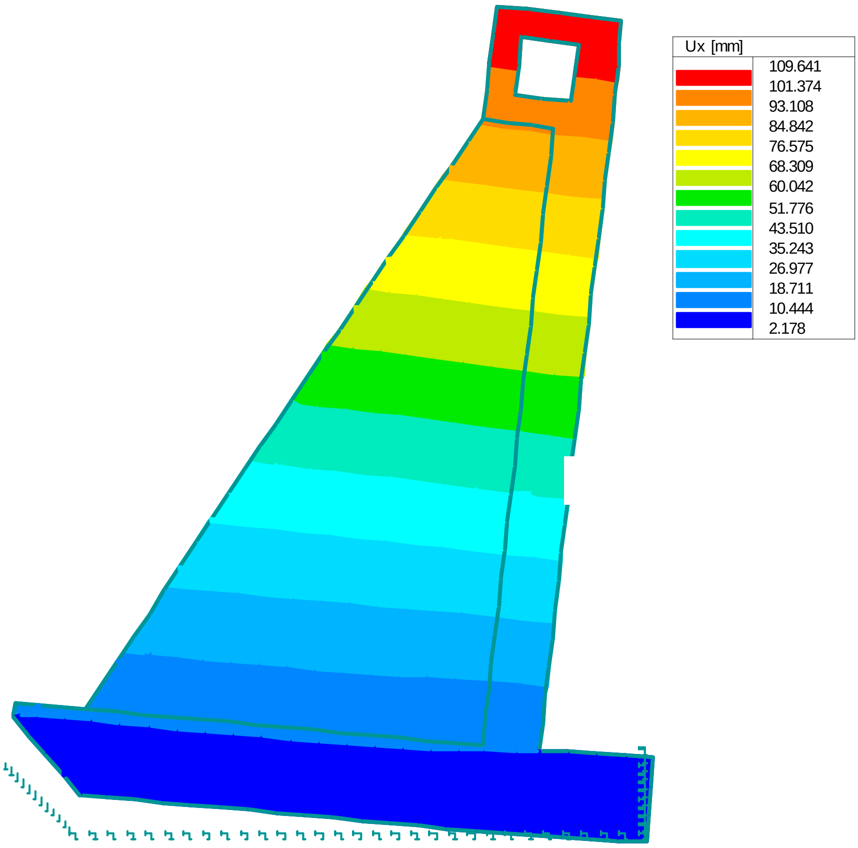

5.6 CONCRETE STRESSES

5.6.1 FUNDAMENTAL LOAD COMBINATIONS F1 TOT F2:

$1.125 \times \sigma_c < 0.85\ f_{ck}/1.5$
with $f_{ck} = 25 N/mm^2$:
$\sigma_c = 5.58\ N/mm^2 < 12.5\ N/mm^2$

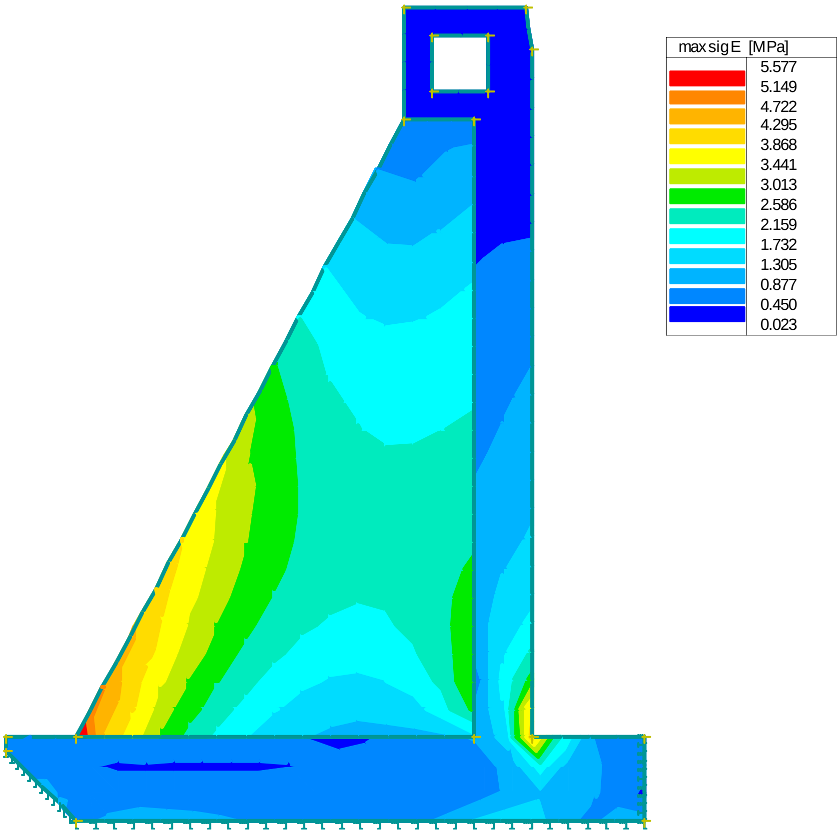

5.6.2 ACCIDENTAL LOAD COMBINATION MCE:

$\sigma_c < 0.85\ f_{ck}$
with $f_{ck} = 25\text{N/mm}^2$:
$\sigma_c = 12.94\ \text{N/mm}^2 < 21.25\ \text{N/mm}^2$

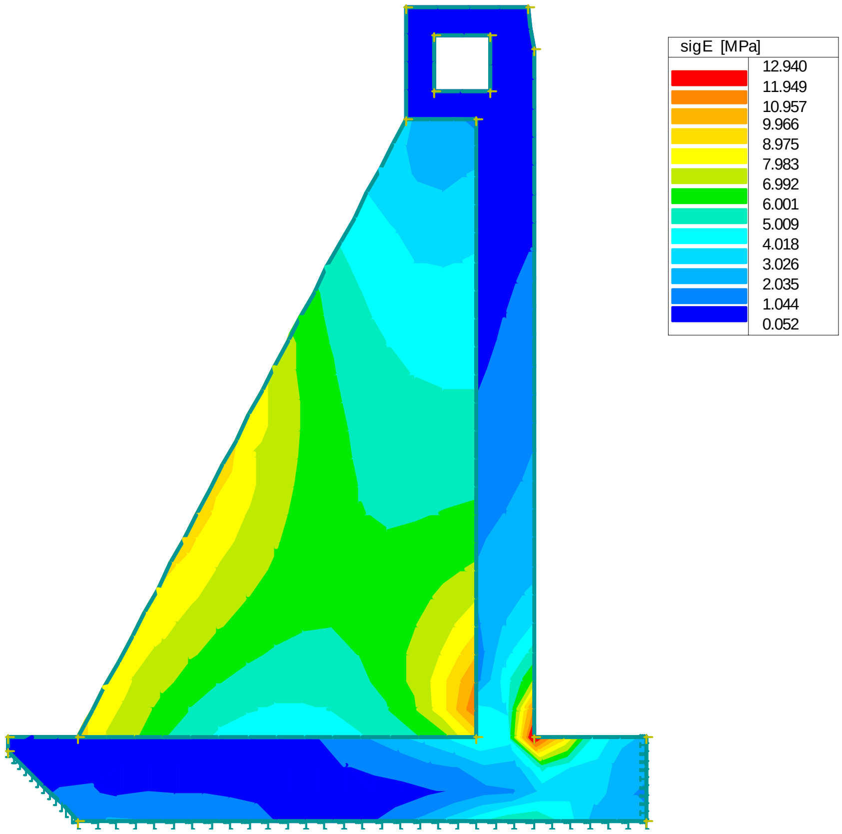

5.7 SUMMARY

Criterion	QP1 (Quasi Permanent Load Combination - Service)	F (Envelope of Fundamental Load Combinations)	MCE (Accidental Load Combination - MCE)
Compression zone A' > 90% A	100%	-	-
Compression zone A' > 75% A	-	-	
Compression zone A' > 10% A	-	100%	25%
Load Bearing Capacity			
1.4 $q_{ref} < q_u$ (MPa)	-	0.66	-
$q_{ref} < q_u$ (MPa)	-	-	2.04
Deformations			
maximal displacement (mm)	10.5	-	10.1
Concrete stresses			
1.125 x σc < 0.85 fck/1.5	-	45%	-
σc < 0.85 fck	-	-	61%
Deep Seeted Sliding			
	-	-	OK

6 Type 2 – Gatun Lake Entrance - Foundation in La Boca

6.1 INPUT DATA

6.1.1 GEOMETRY

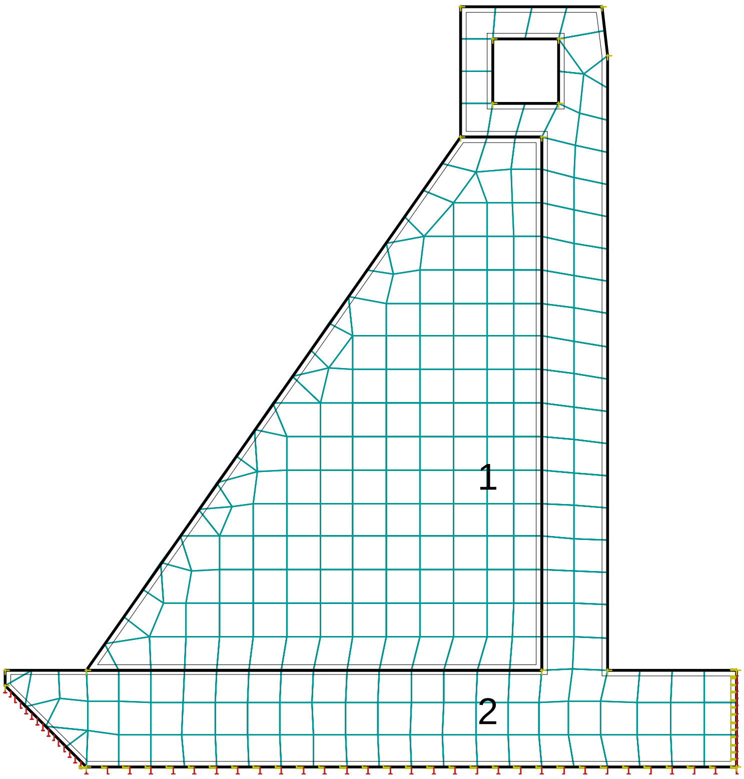

The FE model consists of the following three 2D macro structural elements:

No.	Element	Thickness
1	Reinforced concrete counterforts	0.1 m (each 10 m)
2	Retaining wall	1 m

6.1.2 MATERIALS

Name:		
C25/30-cracked		
	E modulus	20000.00 MPa
	Poisson coefficient.	0.20
	Density	2500.000 kg/m^3
	Expansion coefficient	0.01 mm/m.K

For the material corresponding to the reinforced concrete counterforts, the submerged weight of 15 kN/m^3 is taken into account, as the water pressure of LC3 are immediately applied to the main wall element.

6.1.3 SUPPORTS

The rock base is modeled by means of linear supports.

- Vertical to the base of the gravity wall and perpendicular to the boundary of the back toe, the bedding on the La Boca rock formation is characterized by a linear support of, K= 200 MN/m/m', working in compression only.
- Parallel to the base, sliding is restricted through a frictional resistance of 30% of the elasticity of the bedding.

6.1.4 Loads

6.1.4.1 Self Weight (LC 1)

The total weight of the structure: 311.5 ton/m'.

6.1.4.2 Rock fill Pressure (LC 2)

from	28.63		27.13	
			λav =	λah =
λa =	0.1716		0.0000	0.1716
ϕ =	45	0.79	δ =	0
θ =	0	0.00		
γ =	18			
z	p		**pv**	**ph**
28.63	10		0.000	1.716
27.13	37		0.000	6.348

from	27.13	to	24.63	
			λav =	λah =
λa =	0.1716		0.0000	0.1716
ϕ =	45	0.79	δ =	0
θ =	0	0.00		
γ =	10			
z	p		**pv**	**ph**
27.13	37		0.000	6.348
24.63	62		0.000	10.638

from	24.63	to	8.23	
			λav =	λah =
λa =	0.1716		0.0000	0.1716
ϕ =	45	0.79	δ =	0
θ =	0	0.00		
γ =	10			
z	p		**pv**	**ph**
24.63	62		0.000	10.638
8.23	226		0.000	38.775

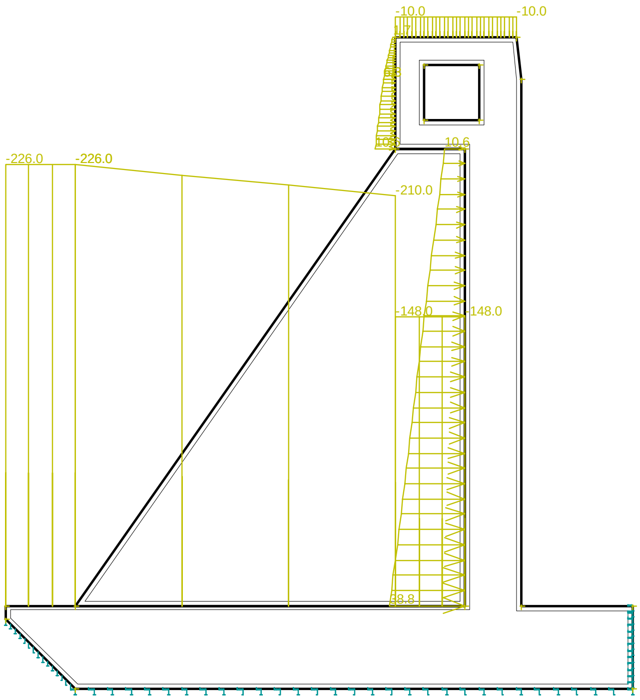

Soil weight on culvert block

X	**pv**
-3	226
0	226
11.5	210
11.5	148
14	148

6.1.4.3 Water Pressure (LC 3)

Water level inside the lock: +24.99 m
Water level outside the lock: +27.13 m

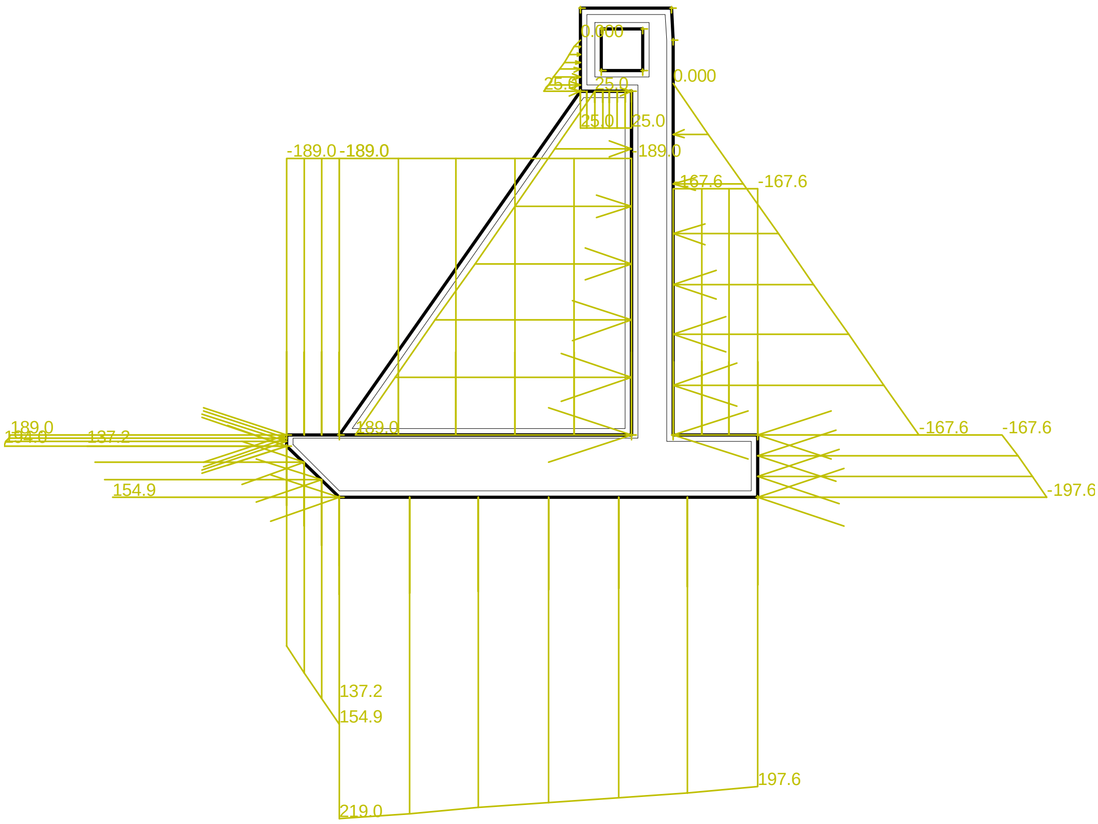

6.1.4.4 Bollard pull (LC 4)

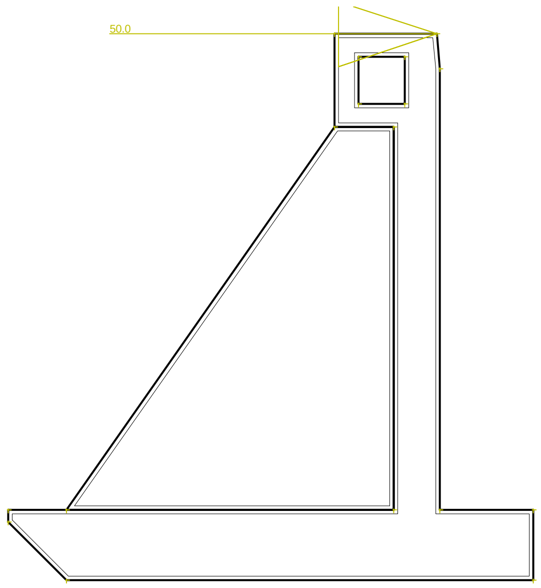

6.1.4.5 Water Pressure - Seismics (LC 5)

Water level inside the lock: +24.99 m
Water level outside the lock: +27.13 m

Water suction forces at the outside face of the wall according to Westergaard :

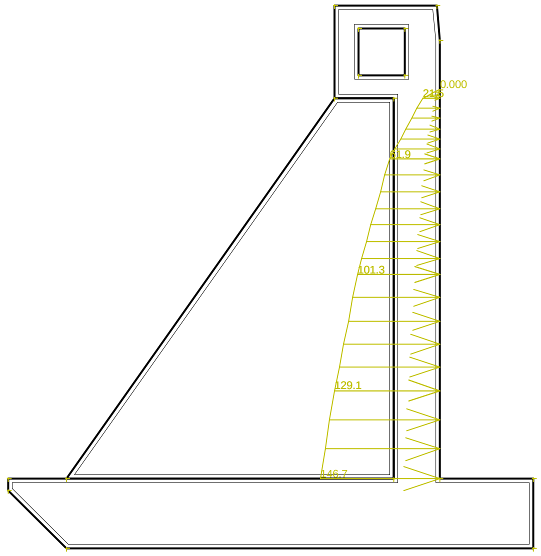

The seismic water pressure load case is valid for a unit value of k_e, and is multiplied by the respective k_e value in the corresponding load combinations.

6.1.4.6 Seismic Loads (LC 6, 7 and 8)

LC 6

The active lateral earth thrust under seismic conditions is calculated based on the Mononobe-Okabe (M-O) methodology. The M-O method is an extension of Coulomb's theory, wherein the M-O method takes into account the inertial forces acting on the soil mass during earthquake loading. It was developed to assess the stability of massive gravity walls, assuming that the retaining wall and the failure wedge act as rigid bodies.

The inertia forces are then accounted for by considering a seismic inertia angle, $\Psi = \text{atan}(k_h/(1-k_v))$, in which k_h represents the horizontal seismic coefficient or the modified horizontal seismic coefficient for dry and submerged layers respectively.

As the counterfort retaining wall under consideration is geometrically near to cantilever wall type, a Rankine situation is assumed for the calculation of the seismic active earth pressures on the vertical through the rear edge of structure. Consequently, the weight and inertia forces of the soil masses above the structure's rear base have to be taken into consideration.

Remark:

- The active lateral pressures and the horizontal inertia components of the soil masses are transferred to the front wall elements for ease of implementation.
- Half of the vertical live load is taken is accounted for in the seismic earth pressures.

LC 7 and 8

The inertia forces on the structural weight are calculated as follows:

$G_v = (1-k_v)\ G$

$G_h = k_h\ G$

With G the weight of the filling

G_v the vertical component of the weight in seismic conditions

G_h the horizontal component of weight in seismic conditions

PGA	0.4	g	k_e	0.246
k_h	0.246		k_v	0.123

CFR	0.1
Width	19

from	28.63		27.13		1.50				Width =	14.5
			λav =	λah =		k_h'	0.246		b =	4.5
λa =	0.3200		0.0000	0.3200						
ϕ =	45	0.79	δ =	0	0.00	ψ	15.6	0.27		
θ =	0	0.00								
γ =	18								ph2	64.102
z	p		pv	ph1		**Q1v**	**0.00**			ph
28.63	4.386		0.000	1.403		**Q1h**	**7.79**			65.506
27.13	28.070		0.000	8.982		**Q1**	**7.79**			73.084

from	27.13	to	24.63		2.50				Width =	14.5
			λav =	λah =		k_h'	0.491		b =	4.5
λa =	0.5638		0.0000	0.5638						
ϕ =	45	0.79	δ =	0	0.00	ψ	29.2	0.51		
θ =	0	0.00								
γ =	10								ph2	71.225
z	p		pv	ph1		**Q2v**	**0.00**			ph
27.13	28.070		0.000	15.826		**Q2h**	**55.02**			87.051
24.63	50.000		0.000	28.190		**Q2**	**55.02**			99.415

from	24.63	to	8.23		16.40				Width =	17
			λav =	λah =		k_h'	0.491		b =	2
λa =	0.5638		0.0000	0.5638					b'=	16
ϕ =	45	0.79	δ =	0	0.00	ψ	29.2	0.51		
θ =	0	0.00								
γ =	10								ph2	
z	p		pv	ph1		**Q2v**	**0.00**			ph
24.63	50.000		0.000	28.190		**Q2h**	**1127.41**			100.643
8.23	193.861		0.000	109.299		**Q2**	**1127.41**			176.102

1190.22

Soil weight on culvert block

X	pv
-3	194
0	194
11.5	179
11.5	129
14	129

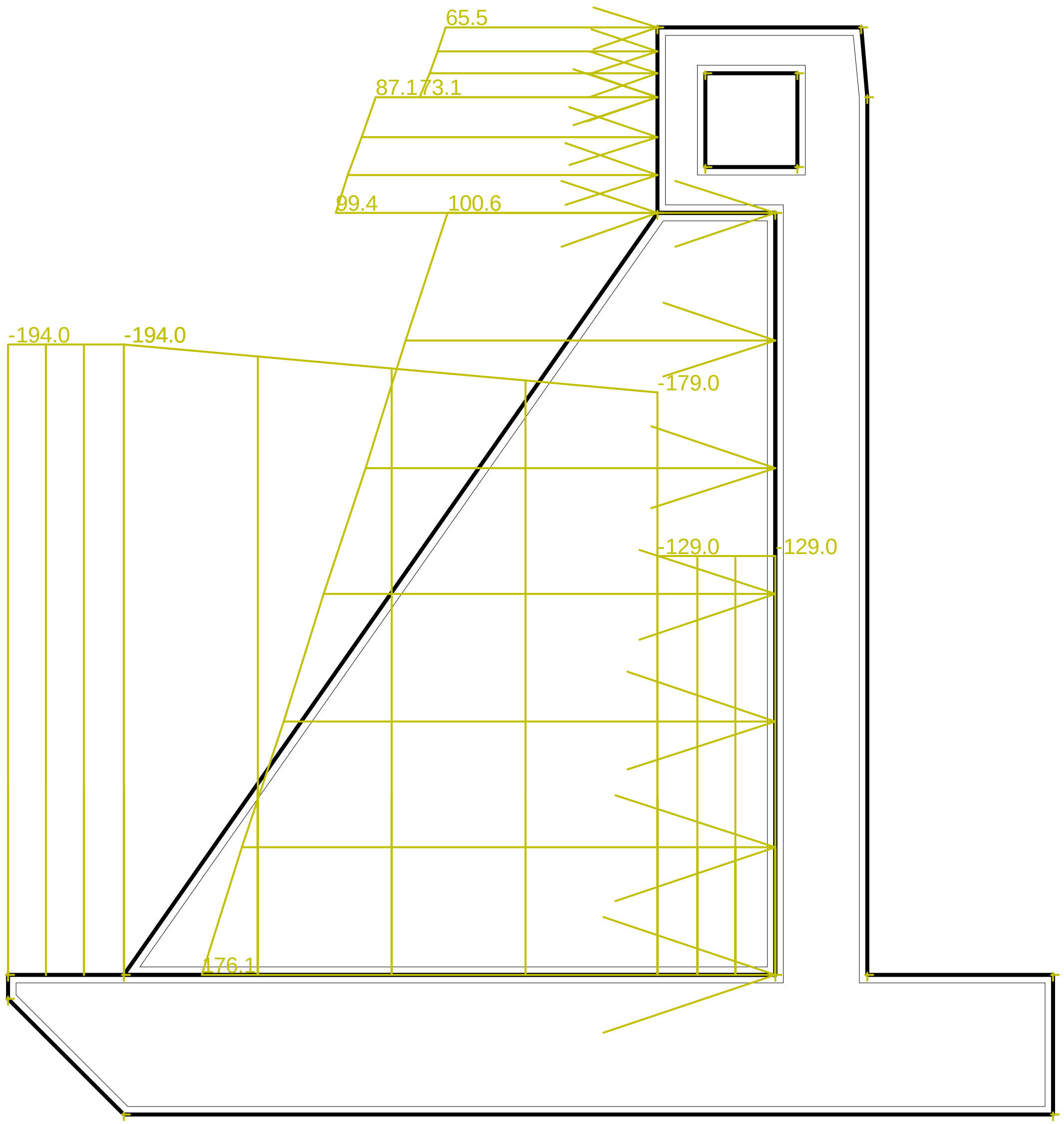

6.2 SLIDING

6.2.1 ACCIDENTAL LOAD COMBINATION – EARTH QUAKE MCE

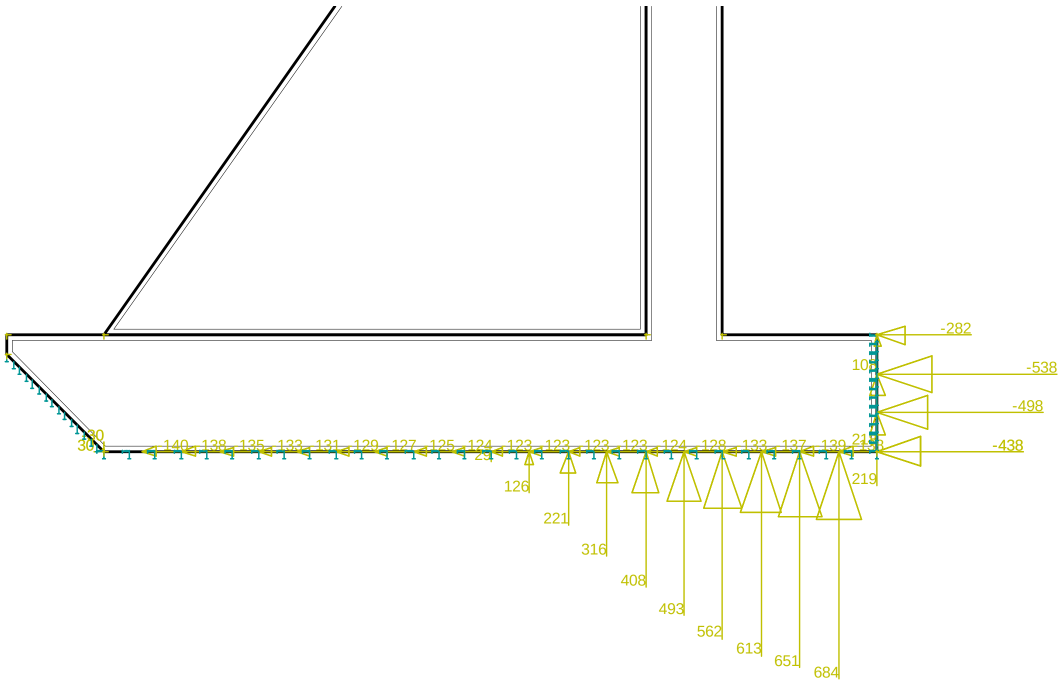

Analytically, it is found that :

$\Sigma V = 4825$ kN

$\Sigma H = 4389$ kN

To obtain the required safety ($\gamma_d = 1.1$) against sliding, a passive lateral pressure of 2042 kN has to be taken on the side face of the inner toe over a height of 3 m. This results in a pressure of 0.68 MPa, which is lower than the uni-axial compressive strength of the “La Boca” formation and concrete. The resistance to sliding is thus fulfilled.

Rock strength of La Boca:
Tensile Strength: 1.5 MPa
Uni-axial Compressive Strength: >12 MPa
It can be concluded that the sliding criterion is fulfilled.

6.3 TURN OVER

6.3.1 QUASI PERMANENT LOAD COMBINATION (QP1) – LOCK IN SERVICE

Criterion: Compression zone A'(= 100 %) > 90% A

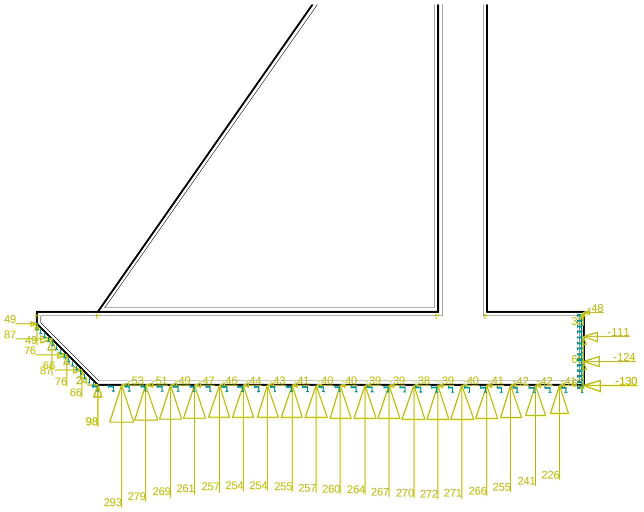

The magnitude of the vectors shown represent the support reaction in each node and not the soil pressure.

6.3.2 FUNDAMENTAL LOAD COMBINATIONS F1 TO F2

Criterion: Compression zone A' (= 100 %) > 10% A

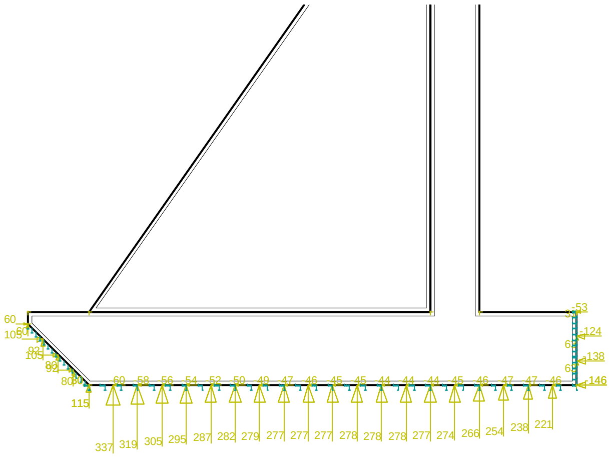

6.3.3 ACCIDENTAL LOAD COMBINATION – EARTH QUAKE MCE

Criterion: Compression zone A' (= 45 %)> 10% A

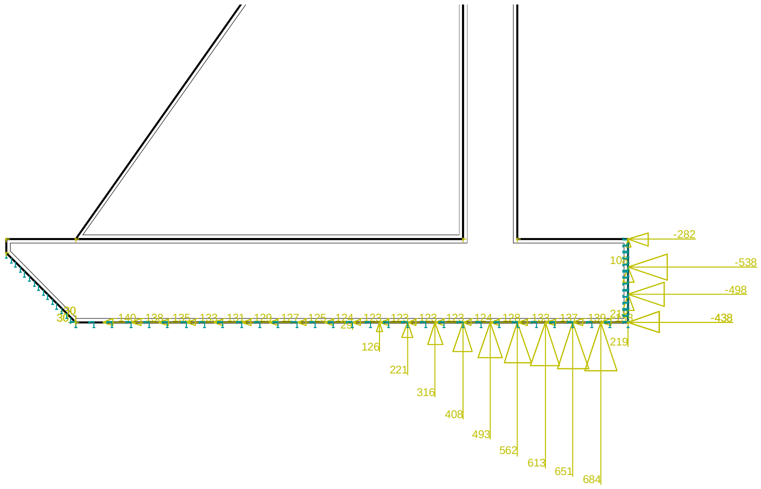

6.4 LOAD BEARING CAPACITY

6.4.1 FUNDAMENTAL LOAD COMBINATIONS F1 TO F2

Criterion: $\gamma_d \,.\, q_{ref} < q_u$
with $\gamma_d \,. = 1.4$

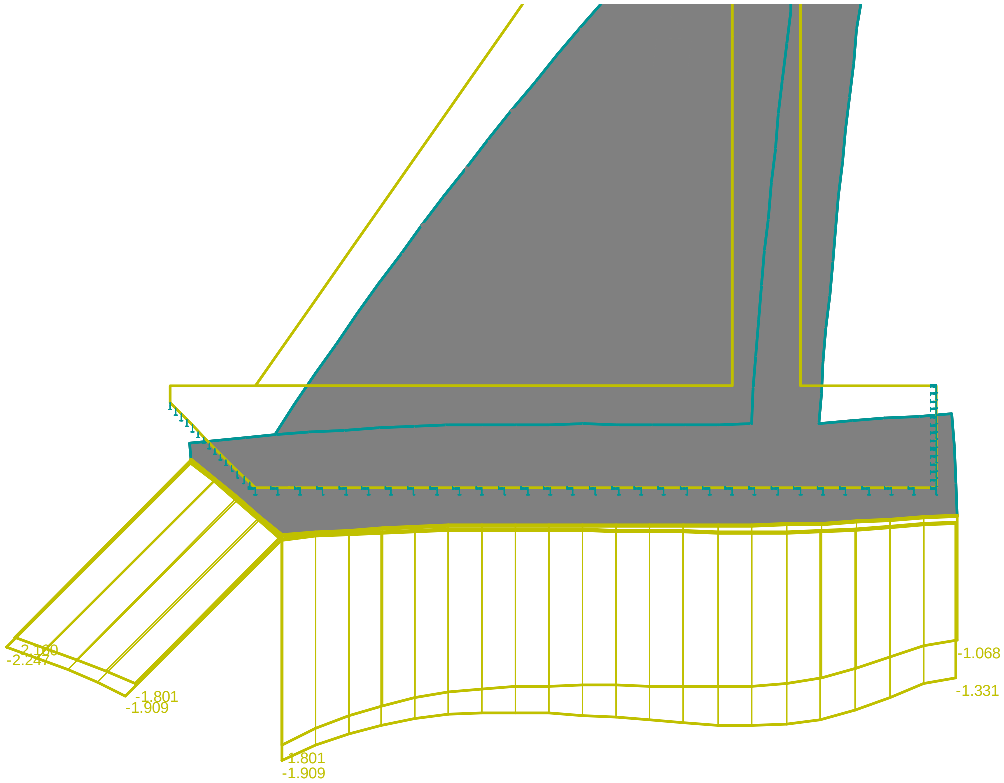

The maximum vertical displacement at the bottom of the wall is 1.909 mm, which is negligible.
This corresponds to a maximum vertical pressure of 0.0019 x 200000 kN/m² = 382 kN/m² = 0.38 Mpa.
Consequently:

$$\gamma_d \,.\, q_{ref} = 1.4*0.382 = 0.535 < q_u = 10\text{MPa}$$

(According to report R2-A the Uni-axial Compressive Strength of the La Boca rock varies from 10 to 20MPa).

6.4.2 ACCIDENTAL LOAD COMBINATION MCE

Criterion: $\gamma_d \cdot q_{ref} < q_u$
with γ_d . = 1.0 for accidental load combinations

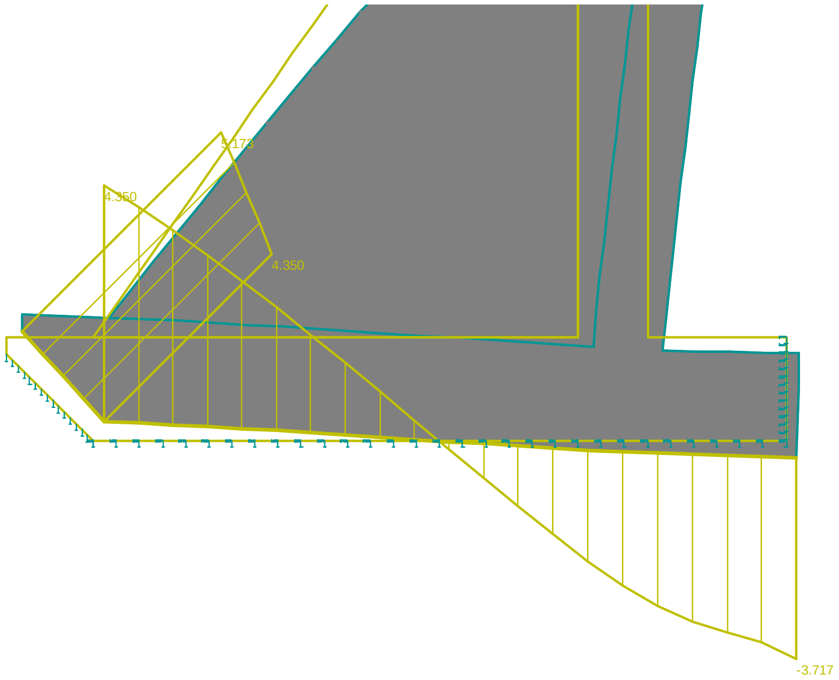

The maximal vertical displacement at the bottom of the wall is 3.717 mm
This means a vertical pressure of 0.0037 x 200000 kN/m² = 743 kN/m² = 0.74 MPa

According report R2-A the Uni-axial Compressive Strength of the La Boca rock varies from 10 to 20MPa.

6.5 DEFORMATIONS

6.5.1 LOAD COMBINATION QP1 (LOCK IN SERVICE)

Maximal horizontal displacement, $u_{x,max}$ = 3.1 mm

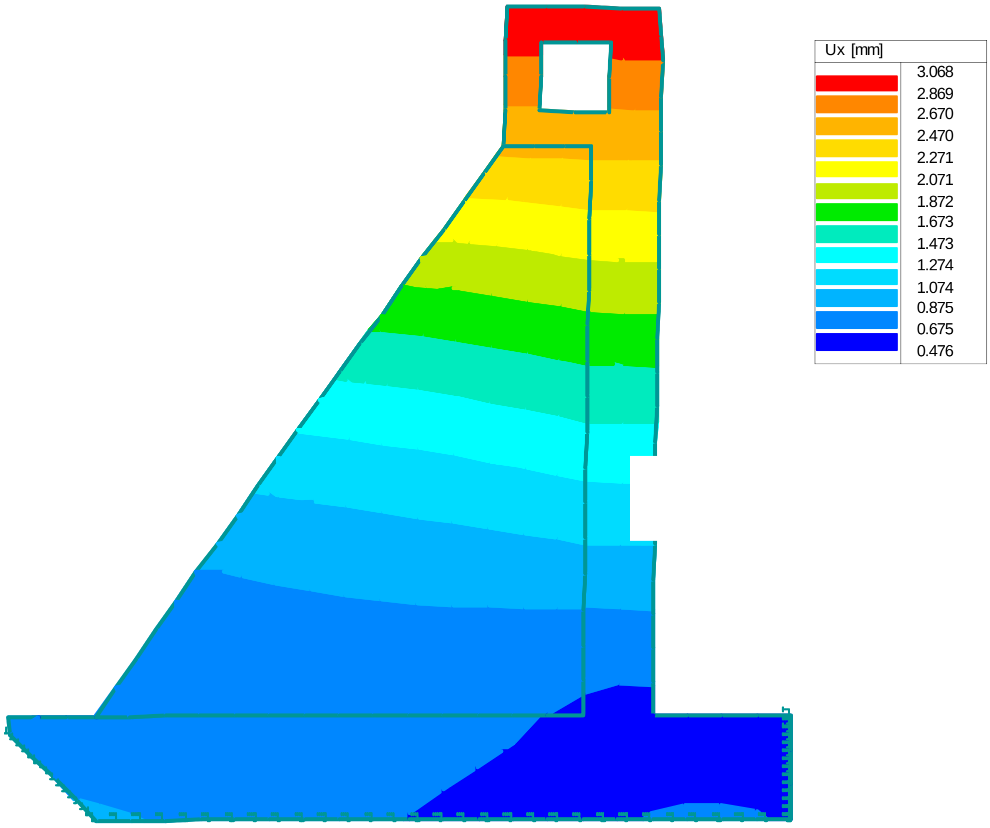

6.5.2 LOAD COMBINATION MCE (EARTH QUAKE)

Maximal horizontal displacement, $u_{x,max}$ = 22.2 mm

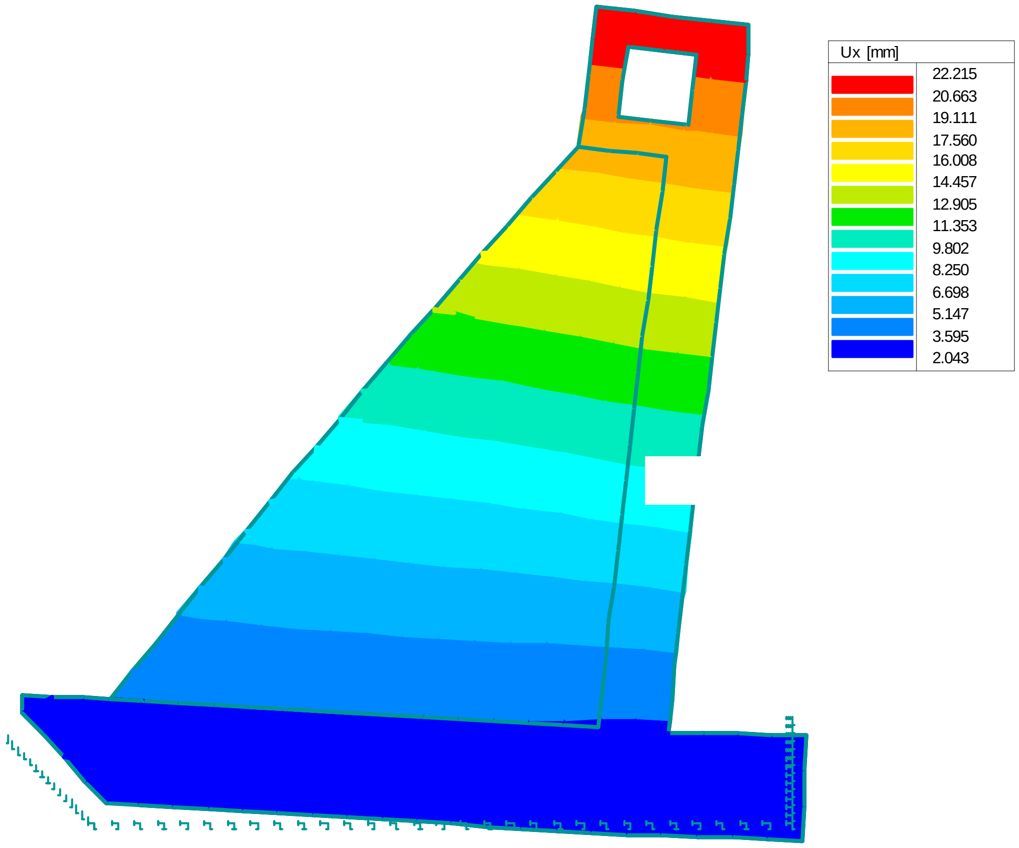

6.6 CONCRETE STRESSES

6.6.1 FUNDAMENTAL LOAD COMBINATIONS F1 TOT F2:

$1.125 \times \sigma_c < 0.85\ f_{ck}/1.5$
with $f_{ck} = 25 N/mm^2$:
$\sigma_c = 1.88\ N/mm^2 < 12.5\ N/mm^2$

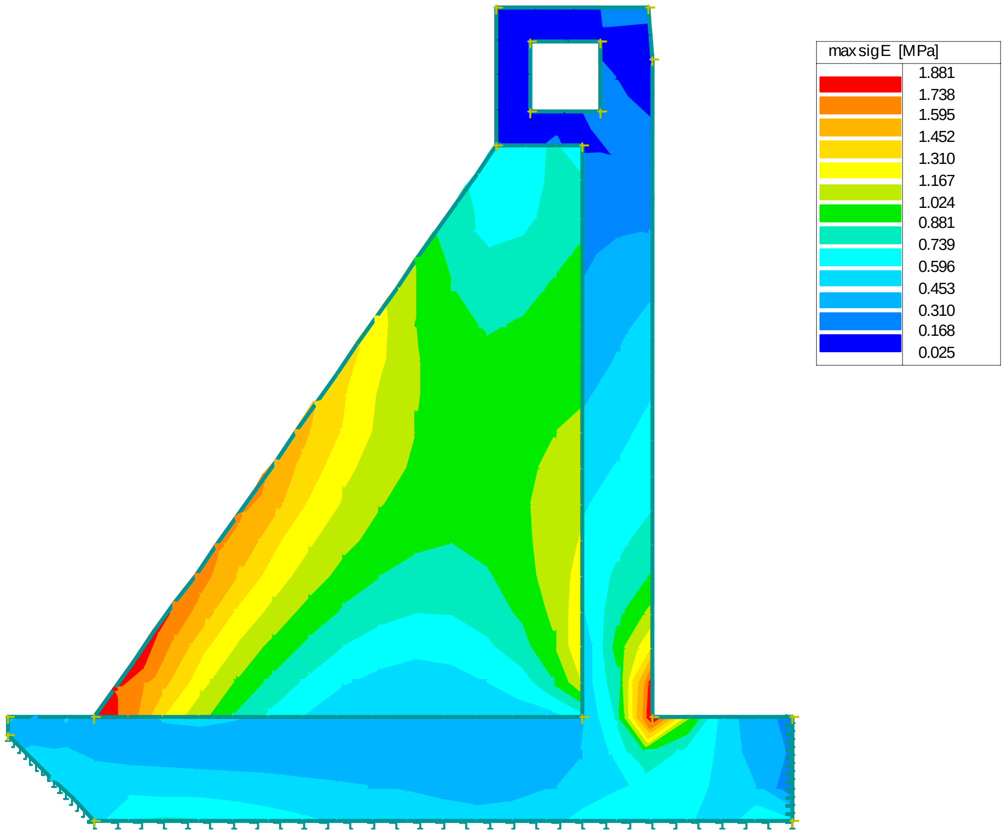

6.6.2 ACCIDENTAL LOAD COMBINATION MCE:

$\sigma_c < 0.85\ f_{ck}$
with $f_{ck} = 25 N/mm^2$:
$\sigma_c = 5.65\ N/mm^2 < 21.25\ N/mm^2$

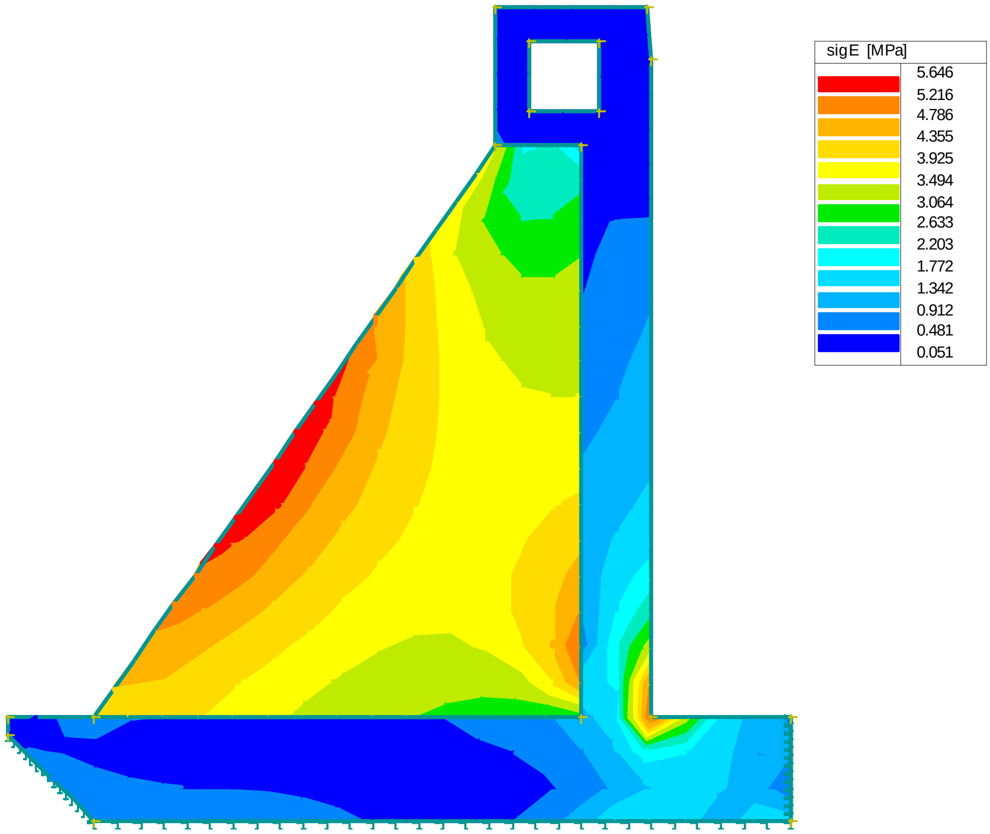

6.7 SUMMARY

Criterion	QP1 (Quasi Permanent Load Combination - Service)	F (Envelope of Fundamental Load Combinations)	MCE (Accidental Load Combination - MCE)
Compression zone A' > 90% A	100%	-	-
Compression zone A' > 75% A	-	-	
Compression zone A' > 10% A	-	100%	45%
Load Bearing Capacity			
1.4 $q_{ref} < q_u$ (MPa)	-	0.535	-
$q_{ref} < q_u$ (MPa)	-	-	0.743
Deformations			
maximal displacement (mm)	3.1	-	22.2
Concrete stresses			
1.125 x σc < 0.85 fck/1.5	-	15%	-
σc < 0.85 fck	-	-	31%
Deep Seeted Sliding			
	-	-	OK

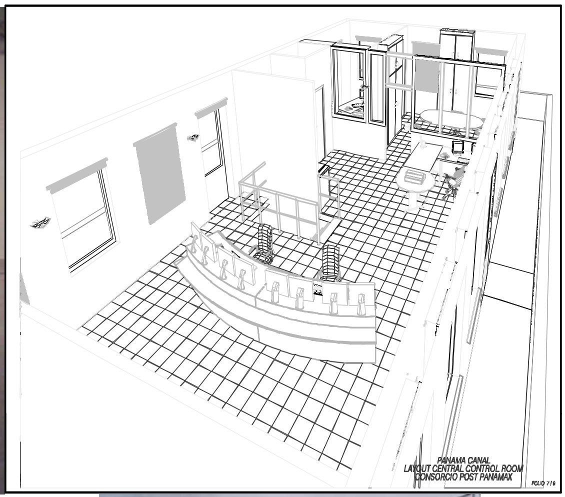

Update of Pacific Locks Conceptual Design and Harmonization of Atlantic Locks Conceptual design - Contract SAA-143351

PACIFIC LOCKS ACTUALIZATION

Task P4f – OPERATING MACHINERY
Task P4g – LIGHTING
Task P4h – ELECTRICAL AND POWER REQUIREMENTS
Task P4j – OPERATING STRUCTURES
Rev A

Tractebel Development Engineering · TECHNUM · COYNE ET BELLIER · Compagnie Nationale du Rhône

in association with

SBE · PORT OF ANTWERP · FITA AOSO

TABLE OF CONTENTS

Annexes

1. Estimation of gate engine power for culvert and conduit gates taking into account operating heads
2. Estimation of gate engine power for culvert and conduit gates taking into account maximum static heads

1 INTRODUCTION

The present document gives the impact of the actualization on the following subjects:

- the gates and valves operating machinery (Task 4 F). This corresponds to the operating machinery of the main lock gates and of the culvert and conduit gates,
- the control system architecture (including SCADA[1]), which includes the monitoring of the whole lock system. The control system architecture is also included in Task 4 F,
- the lighting system (Task 4 G),
- the electrical and power requirements (Task 4 H),
- the operating structures (Task 4 J), which deals with the arrangement of the various technical buildings[2].

The **original conceptual design (CCP 2002)** has been made for a **triple lift lock with a width of 61 m** and **locomotive tracks** for the positioning of the ships inside the lock chambers.

For the actualization studies, the width of the lock chambers has been reduced by 6 m. Hence, the **actual lock width is 55 m**. Furthermore, the use of vessel positioning by tugboat assistance cancels the locomotives on the lock walls.

[1] ***SCADA = System Control And Data Acquisition***
[2] ***Electrical rooms, Maintenance building, Rolling gates technical rooms, WSB technical building, Culvert technical building, Emergency Diesel Room and (Main) Control room***

2 Impact of actualization on operating machinery (Task P4f)

2.1 MACHINERY OF THE (MAIN) ROLLING GATES

The characteristics of the operating machinery for the 61m width lock has been determined taking into account the information available from the Berendrecht lock (Belgium) which has main gates of similar size of the one foreseen for the 61 m Post Panamax locks. The power output of the main motor was foreseen to be 330 kW.

For the 55 m width lock chamber, the power output of the motor should be slightly less than 330 kW. The power output of the gate moving system (drums and gear boxes) should also be slightly less than that of the Berendrecht lock.
The impact on the costs is not significant.

In CCP 2002 it was recommended to define the final value of the main motor. CPP recommends to proceed with physical model tests of the gates and to fix the various parameters (nominal speed, gate geometry, presence of mud, etc.).

The opening and closing times will be optimised based on model tests results.

2.2 MACHINERY OF THE CULVERT AND WSB CONDUIT GATES

The calculation of the rated output of the motor of the main oil pumps mounted on the hydraulic power pack is enclosed in Annexes 1 and 2, respectively for operating and maximum static heads. This calculation takes into account the actual dimensions of the culvert and WSB conduit gates (see P4c).

A summary of the output for different options is given hereafter:

61 m, (operating heads)	culvert gates:	75 kW,
	WSB conduit gates:	41 kW.

61 m, (maximum static heads)	culvert gates:	116 kW,
	WSB conduit gates:	166kW.
55 m (operating heads)	culvert gates:	53kW,
	WSB conduit gates:	23kW.

(see annex 1 – Estimate of the gate engine power taking into account operating heads)

55 m (maximum static heads)	culvert gates:	81kW,
	WSB conduit gates:	91kW.

(see annex 2 – Estimate of the gate engine power taking into account maximum static heads)

Regarding the two last values, standardization of the servomotors is possible if we consider the operation under maximum static heads.
But another alternative could be envisaged in the next step of the studies:

Regarding the design of the motors (two per gate) :

- for the operating heads, one motor will operate the gate, one will remain on stand-by (one redundancy degree).
- operation under maximum static heads should be with the two motors in operation (no redundancy).

Of course the power output of the motors will have to be slightly adapted to fit the above operation procedures.

2.3 CONTROL SYSTEM ARCHITECTURE

The control system architecture doesn't change at all. Nothing was foreseen for the operation, the control and the signalisation (I&C) of the locomotive tracks. Consequently there is no impact on the control system. Reference is made to CCP 2002 and its corresponding drawings.

3 Impact of actualization on lighting (Task P4g)

3.1 OUTSIDE LIGHTING

3.1.1 LOCK CHAMBER WALLS

The dimensioning criterion is the height of the chamber and not the width. The lighting of the walls is essential (and not the water surface).
Reference is made to the CCP 2002.

Vertical recess in the lock walls are equipped on the top of a turned-down lighting system fixed under a hinged plate with easy access from the working platform.
The inclined section at the top of the lock chamber wall is not important for the recess. There is no significant change to do to the system.

The impact on the price is negligible.

3.1.2 LIGHTING POLES

The location of the lighting poles is slightly easier without the locomotive tracks.
The philosophy of the lighting is to have a lighting level along the lock chamber (both side) and decreasing lighting level after the fictive line running along the dead end of the main rolling gates recesses.

Although the length of the entrance walls has been modified, the number of lighting poles is the same.

Side WSB – Gatun lake entrance :
- 8 lighting poles.
- 60 m between two LP
- 6 floodlights of 1000 W

Side WSB – Chamber locks :
- 3 x 5 lighting poles.
- 93m between two LP
- 12 floodlights of 1000 W

Side WSB – Pacific Entrance :

- 8 lighting poles.
- 60 m between two LP
- 6 floodlights of 1000 W

Other side :

- 30 lighting poles
- 59 m between two LP
- 6 floodlights of 1000 W

The number of floodlights has decreased. But there is no major impact on the price of the whole lighting because the most important part of the price is the mast.

Therefore no significant changes are to be taken into account for the actualization. As a consequence, no financial impacts have been considered. Reference is made to CCP 2002 and its corresponding drawings.

3.2 INTERNAL LIGHTING

Reference is made to CCP 2002. No change is required.

4 Impact of actualization on electrical and power requirements (Task P4h)

Reference is made to CCP 2002.

A few changes in the electrical substation from HV1 through HV8 are to be foreseen (drawing D4-H-107).

As a reminder, it was foreseen to feed the locomotive from transformers exclusively dedicated to this purpose. Eight 630 kV transformers (one per substation) are to be removed as well as eight MV cubicles linked to the transformers. The removed transformers and linked cubicles incur a cost saving of around $700.000. It is just around 0.35% of the budgetary prices of the equipment and 0.08 % of the total costs of the works.

5 Impact of actualization on operating structures (Task P4j)

More space is available in the HV1 through HV8 electrical rooms due to the removal of the transformers and associated MV cubicles, originally foreseen for vessel positioning with locomotives.

The size of the HV buildings has been kept equal to the size foreseen in the first conceptual design.

Reference is made to report CCP 2002 and its corresponding drawings.

6 References

- CCP (2002). Diseño conceptual de las Esclusas Post Panamax. Triple Lift Lock System, task 4.

ESTIMATION OF THE GATE ENGINE POWER
PACIFIC SIDE : TRIPLE LIFT (W=55m) 3 X 3 WATER SAVING BASINS
TAKING INTO ACCOUNT OPERATING HEADS

	LOCK CULVERT GATE	WSB CONDUIT GATE
Maximum effort (T)	96	41
Oil pressure (bar)	200	200
Stroke (m)	6,00	6,00
Opening time (min)	2,00	2,00
Cylinder section (m²)	0,048	0,021
Cylinder oil volume (m³)	0,288	0,123
Oil flow (m³/min)	0,144	0,062
mechanical efficiency	0,9	0,9
POWER (kW)	**53**	**23**

Calculus of the forces on the gate

	LOCK CULVERT GATE	WSB CONDUIT GATE
Gate width (m)	4,5	4,5
length of horizontal seal (m)	4,9	4,9
Gate heigth (m)	6	6
length of vertical seal (m)	6,3	6,3
width of seal (cm)	3	3

OPENING

		LOCK CULVERT GATE	WSB CONDUIT GATE
Sealing friction forces Fs			
Fs = f x 1,5 x p x A	f (friction coefficient)	0,15	0,15
	p (hydraulic pressure on the gate) (bar)	2,5	1,0
	A (Area of sealing contact) (m²)	0,525	0,525
	Fs (kg)	2953	1181
Wheel friction Fw			
Fw = Q x (fd x d + fr) / D	Q (max load on the gate) (kg)	771750	308700
	fd (friction coeff of the wheel bushings)	0,12	0,12
	fr (friction coeff of wheels rolling on slot rails)	0,2	0,2
	d (diameter of wheel shaft) (cm)	20	20
	D (wheel diameter) (cm)	80	80
	Fw (kg)	25082	10033
Hydraulic load F1 on the top seal of the gate			
F1 = p x l x ls	p (hydraulic pressure on the gate) (bar)	2,5	1,0
	l (width of the seal) (m)	0,08	0,08
	ls (length of the seal) (m)	4,9	4,9
	F1 (kg)	9800	3920
Hydraulic load F2 on the top of the gate			
F2 = p x gt x ls	p (hydraulic pressure on the gate) (bar)	2,5	1,0
	gt (gate thickness) (m)	1	1
	ls (length of the seal) (m)	4,9	4,9
	F2 (kg)	122500	49000
Hydraulic load F3 under the gate			
F3 = F2 x dlc	F2 (kg)	122500	49000
	dlc (dynamic load coefficient)	0,8	0,8
	F3 (kg)	98000	39200
Weight W (under water)			
W = rw x 6.85/7.85 x 1.05	rw (real weight) (kg)	19345	10186
	W (weight under water) (kg)	17725	9333
Maximum opening load			
F = Fs + Fw + F1 + F2 - F3 + W	**F (T)**	**80**	**34**

CLOSING

		LOCK CULVERT GATE	WSB CONDUIT GATE
Sealing friction forces F's			
F's = 0.1 x p x A	p (hydraulic pressure on the gate) (bar)	2,5	1,0
	A (Area of sealing contact) (m²)	0,525	0,525
	Fs (kg)	1313	525
Wheel friction F'w			
F'w = Q x (f'd x d + f'r) / D	Q (max load on the gate) (kg)	771750	308700
	f'd (friction coeff of the wheel bushings)	0,08	0,08
	f'r (friction coeff of wheels rolling on slot rails)	0,1	0,1
	d (diameter of wheel shaft) (cm)	20	20
	D (wheel diameter) (cm)	80	80
	F'w (kg)	16400	6560
Hydraulic load F'1 on the top seal of the gate			
F'1 = 0.5 x F1	F1 (kg)	9800	3920
	F'1 (kg)	4900	1960
Hydraulic load F'2 on the top of the gate			
F'2 = 0.9 x F2	F2 (kg)	122500	49000
	F'2 (kg)	110250	44100
Hydraulic load F'3 under the gate			
F'3 = 0.5 x F3	F3 (kg)	98000	39200
	F'3 (kg)	49000	19600
Weight W'			
real weight of the gate	W' (kg)	19345	10186
Maximum braking force			
B = W' + F'1 + F'2 - F'3 - F'w - F's	**B (T)**	**68**	**30**

ESTIMATION OF THE GATE ENGINE POWER
PACIFIC SIDE : TRIPLE LIFT (W=55m) 3 X 3 WATER SAVING BASINS
TAKING INTO ACCOUNT MAXIMUM STATIC HEADS

	LOCK CULVERT GATE	WSB CONDUIT GATE
Maximum effort (T)	147	164
Oil pressure (bar)	200	200
Stroke (m)	6,00	6,00
Opening time (min)	2,00	2,00
Cylinder section (m²)	0,073	0,082
Cylinder oil volume (m³)	0,440	0,493
Oil flow (m³/min)	0,220	0,247
mechanical efficiency	0,9	0,9
POWER (kW)	**81**	**91**

Calculus of the forces on the gate

	LOCK CULVERT GATE	WSB CONDUIT GATE
Gate width (m)	4,5	4,5
length of horizontal seal (m)	4,9	4,9
Gate heigth (m)	6	6
length of vertical seal (m)	6,3	6,3
width of seal (cm)	3	3

OPENING

Force	Parameter	LOCK CULVERT GATE	WSB CONDUIT GATE
Sealing friction forces Fs			
Fs = f x 1,5 x p x A	f (friction coefficient)	0,15	0,15
	p (hydraulic pressure on the gate) (bar)	3,9	4,4
	A (Area of sealing contact) (m²)	0,525	0,525
	Fs (kg)	4635	5236
Wheel friction Fw			
Fw = Q x (fd x d + fr) / D	Q (max load on the gate) (kg)	1211339	1368467
	fd (friction coeff of the wheel bushings)	0,12	0,12
	fr (friction coeff of wheels rolling on slot rails)	0,2	0,2
	d (diameter of wheel shaft) (cm)	20	20
	D (wheel diameter) (cm)	80	80
	Fw (kg)	39369	44475
Hydraulic load F1 on the top seal of the gate			
F1 = p x l x ls	p (hydraulic pressure on the gate) (bar)	3,9	4,4
	l (width of the seal) (m)	0,08	0,08
	ls (length of the seal) (m)	4,9	4,9
	F1 (kg)	15382	17377,36
Hydraulic load F2 on the top of the gate			
F2 = p x gt x ls	p (hydraulic pressure on the gate) (bar)	3,9	4,4
	gt (gate thickness) (m)	1	1
	ls (length of the seal) (m)	4,9	4,9
	F2 (kg)	192276	217217
Hydraulic load F3 under the gate			
F3 = F2 x dlc	F2 (kg)	192276	217217
	dlc (dynamic load coefficient)	0,8	0,8
	F3 (kg)	153821	173773,6
Weight W (under water)			
W = rw x 6.85/7.85 x 1.05	rw (real weight) (kg)	26523	28887
	W (weight under water) (kg)	24301	26467
Maximum opening load			
F = Fs + Fw + F1 + F2 - F3 + W	**F (T)**	**122**	**137**

CLOSING

Force	Parameter	LOCK CULVERT GATE	WSB CONDUIT GATE
Sealing friction forces F's			
F's = 0.1 x p x A	p (hydraulic pressure on the gate) (bar)	3,9	4,4
	A (Area of sealing contact) (m²)	0,525	0,525
	Fs (kg)	2060	2327
Wheel friction F'w			
F'w = Q x (f'd x d + f'r) / D	Q (max load on the gate) (kg)	1211339	1368467,1
	f'd (friction coeff of the wheel bushings)	0,08	0,08
	f'r (friction coeff of wheels rolling on slot rails)	0,1	0,1
	d (diameter of wheel shaft) (cm)	20	20
	D (wheel diameter) (cm)	80	80
	F'w (kg)	25741	29080
Hydraulic load F'1 on the top seal of the gate			
F'1 = 0.5 x F1	F1 (kg)	15382	17377,36
	F'1 (kg)	7691	8688,68
Hydraulic load F'2 on the top of the gate			
F'2 = 0.9 x F2	F2 (kg)	192276	217217
	F'2 (kg)	173048	195495,3
Hydraulic load F'3 under the gate			
F'3 = 0.5 x F3	F3 (kg)	153821	173773,6
	F'3 (kg)	76910	86886,8
Weight W'			
real weight of the gate	W' (kg)	26523	28887
Maximum braking force			
B = W' + F'1 + F'2 - F'3 - F'w - F's	**B (T)**	**103**	**115**

CPP Consorcio Post-Panamax

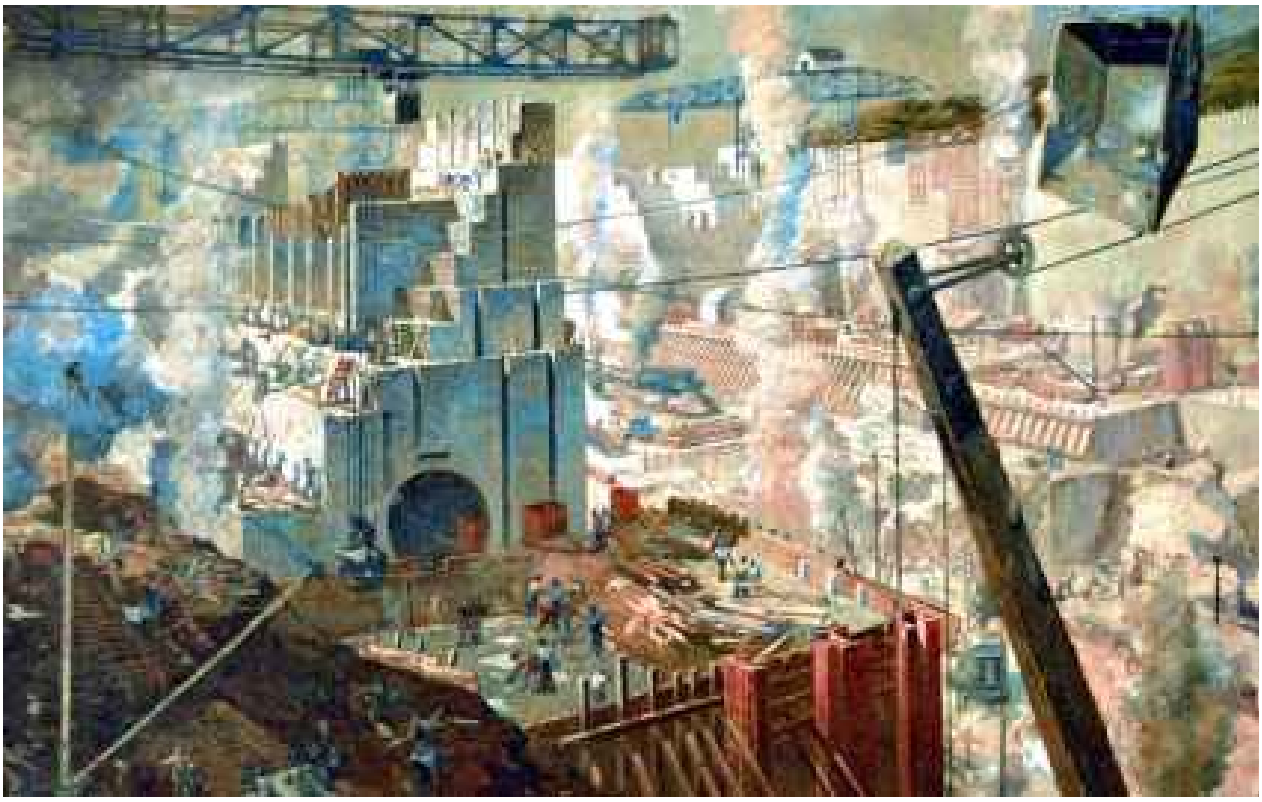

Update of Pacific Locks Conceptual Design and Harmonization of Atlantic Locks Conceptual Design – Contract SAA - 143351

PACIFIC LOCKS ACTUALIZATION

TASK P4L – Construction Plan and Schedule

Tractebel Development Engineering · TECHNUM · COYNE ET BELLIER · Compagnie Nationale du Rhône

in association with

SBE · PORT OF ANTWERP · FITA AOSO

SUMMARY

1 Introduction

This Chapter aims to detail how the actualized (2005) Pacific Post Panamax Locks will be constructed and put into operation. The purpose of this document is to show a feasible construction plan and schedule, compatible with today's modern construction techniques.
The following paragraphs will therefore describe the Construction Plan together with a general organization of the Works, distribution of main construction features within the project area, and the corresponding Construction Schedule of the actualized (2005) Pacific Locks.
The Construction Works analyzed in the present chapter are limited on the North by the extremity of the side-approach-wall from Gatun Lake , and on the South by the extremity of the Pacific side-approach-wall. Furthermore, works related to the excess excavation material transport and deposit are not considered here.

2 Construction Plan

2.1 General

Construction planning is an essential activity during the design of the Project. Therefore, we have developed a Construction Plan foreseeing the use of the most effective construction techniques. Access space as well as availability of resources has been taken into account in the selection of procedures and equipment.

The Construction Plan does the following:

- Defines the work tasks.
- Describes the technology and resources required to perform the work and the manner in which these must be handled to ensure their availability in a timely manner.
- Identifies any interactions among the different work tasks.

2.2 DESCRIPTION OF WORK TO BE PERFORMED

2.2.1 ACTIVITIES

Land Clearing
- Equipment
- Disposal

Excavation
- Rock
  - Drilling
  - Blasting
  - Use for fill
  - Pile for use in aggregate production
  - Haul away to deposit site
  - Stabilization
- Soil
  - Use for fill
  - Haul away to deposit site
  - Stabilization

Tunnels and Trenches

Drainage Ditching and Dewatering

Fill and Compaction
- Rock
  - Transportation and Depositing
  - Compaction
- Soil
  - Transportation and Depositing
  - Compaction

Access Roads and Structures
- Permanent
- Temporary
- Bridges and Culverts

Forms
- Production
  - Wood
  - Steel
- Transportation
- Storage
- Placement

Concrete Production
- Cement handling and storage
- Aggregate production and stockpiling
- Additives
- Batching plant
- Temperature control

Aggregates
Ice
Transportation
Placement
Transit mixers and transportation vehicles
Pumping
Pipelines and conduits
Pumps

Shotcrete

Cement handling and storage
Aggregate production and stockpiling
Additives
Transportation
Equipment storage and maintenance facility

Utilities

Power supply and distribution system
Water supply and distribution system
Sewerage and waste disposal
Communications
Lighting

Offices

Project management and engineering

Shops

Machine
Electrical
Vehicle
Welding
Pipe
Carpentry

Warehousing and Storage

Materials
Parts
Explosives
Fuel and lubricants

Personnel Facilities

Dressing rooms
Sanitary Facilities
Dining Facilities
Security

Construction Equipment

Storage
Servicing and repair

Firefighting facilities

2.2.2 FACILITIES

1. Concrete

It is foreseen that the bulk of the concrete will be transported by conveyor belt, although other alternatives may also be used for transporting concrete to special areas. A decision whether to pump or to transport concrete in buckets will directly affect the cost and duration of tasks involved in building construction. A decision between these two alternatives should consider the relative costs, reliability, and availability of equipment for the two transport methods. Unfortunately, the exact implications of different methods depend upon numerous considerations for which information may be sketchy during the planning phase. These are:

Quality Control laboratory
Cement storage silos
Loading and conveying equipment
Water storage tanks
Aggregate handling and stockpiling facilities
Batching Plant
Concrete transportation equipment
Transportation equipment cleaning facilities
Concrete temperature control equipment and facilities

2. Aggregate Processing Plant

Rock crushing and classification equipment, including crushers, screens, conveyors, waterpumps, fuel storage tanks, hoppers and stockpiles
Crushers, screens, washers and their feeding and discharge mechanisms
Loading, moving and hauling equipment
Emission Control Equipment

3. Metal and Reinforcing Steel Shop

Deliveries of structural and reinforcing steel will be scheduled in accordance with the execution of the work in order to reduce on-site storage to a minimum. Fabrication of rebar will be performed at this location whenever feasible and transported for placement at the worksite when required. Pre-assembly of structural steel sections will also be done here and transported to the location when required.

Unloading, classification and storage of steel sections and reinforcement bars
Welding area
Fabricating area
Transportation and handling equipment
Bridge crane

4. Concrete Form Shop

Unloading, classification and storage of metal and wood materials
Fabrication facility
Repair facility
Form storage and assembly area
Handling, loading, and transportation equipment

5. Shotcrete Facilities

Equipment storage and repair facility
Cement storage and transportation equipment
Aggregate stockpiling, loading and transportation equipment

6. Drilling and Blasting Facility

Drill and bit storage and repair shop

7. Powder Magazine (located and managed in coordination with Canal Protection and Safety Department).

Equipment storage warehouse
Loading, handling and transportation equipment

8. Pipe Shop

Receiving and storage facilities
Handling equipment
Shop equipment

9. Fuel and Lubricants Facilities

Storage tanks and warehouses
Service stations
Lubricant disposal

10. Compressed Air

Compressors
Storage
Distribution

The work production capacity for the different activities required to build the actualized (2005) Post Panamax Locks Project can be established using information obtained from similar projects, as shown in the following Table:

REQUIRED WORK PRODUCTION CAPACITY

Type of Activity	Production Adopted for the Locks m^3/month	Factor	Production Capacity Required m^3-month
Rock Excavation	200,000	2	400,000
Soil Excavation	500,000	2	1,000,000
Fill	200,000	1.5	300,000
Conventional Concrete	40,000	1.5	60,000
Roller Compacted	80,000	1.5	120,000

3 Construction Schedule

3.1 GENERAL

In order to establish realistic Schedules based on feasible work production capacities, an analysis of large construction Projects carried out in different countries has been carried out. The analysis is presented below.

The excavation activity and, especially, the production rate does not take into consideration the huge excavation works to be done in connection with linking the canal to Gatun Lake.

3.2 WORK PRODUCTION CAPACITY

The Table 3.1, presented on the next page, sums up the information gathered from various large Construction Projects undertaken during the last ten years.

The different Projects are presented in columns. The top line summarizes the main characteristics and dimensions of each Project
The left column lists the different types of work considered. Each project column details the corresponding total quantity of work, the monthly peak and mean production capacities (highlighting with a red circle the relevant specific work of each project), and the extreme right column gives the selected production capacity for the actualized (2005) Post Panamax Locks.
The following comments can be made:

- The ACP Cut-Widening Project shows a mean production for rock excavation in the range of 100.000 m3/month. It has been verified (source: ACP) that the Contractors involved in those works were not working at full capacity. The Consultant considers that double that production capacity is a perfectly achievable target, for the works entailed. This production capacity can easily be increased if the Project Works are considered in their entirety i.e. together with the Gatun channel link.

WORKS PRODUCTION CAPACITY

References in large Construction Projects
and recommendation for the Post Panamax Locks project

PROJECT		**Garafiri**	**Al Wahda**	**Birecik**	**Katze**	**Tha Dan**	**ACP Cut Widening**	**ACP Cut Widening**	**Other Sources**	**Production adopted for the LOCKS**
Description Type		Earth dam	Earth dam	Composite dam Earth & concrete	Arch dam	RCC gravity dam	Cartagena Soil Excavations	Gold Hill Rock excavations	Boskalis dredging	**m3/month**
Height		75m	90m	62m	185m	95m				
Length		725m	2700m	2507m	710m	2600m				
Year of construction		1994-1998	1992-1996	1997-1999	1991-1997	1996-1998	1999-2001	1997-1999		
Country		Guinea	Morocco	Turkey	Lesotho	Thailand	Panama	Panama		
Excavation	**Unit**									
Rock										
Total Volume	m3				975,300			1,485,000		**Exc. Rock**
Monthly Mean Production	m3/month				80,000			**100,000**		**200,000**
Monthly Peak Production	m3/month							170,000		
Soil										
Total Volume	m3	4,805,132		11,000,000	278,000		2,250,000			**Exc. Soil**
Monthly Mean Production	m3/month	190,000		**500,000**			125,000			**500,000**
Monthly Peak Production	m3/month	400,000								
Dredging										
Total Volume	m3									**Dredging**
Monthly Mean Production	m3/month								**380,000**	**400,000**
Monthly Peak Production	m3/month									
Fill										
Total Volume	m3	5,275,757	27,000,000	9,000,000						**Fill**
Monthly Mean Production	m3/month	290,000	**482,000**	**500,000**						**200,000**
Monthly Peak Production	m3/month	575,000	1,500,000	750,000						
Concrete										
Conventional Concrete										**Conventional**
Total Volume	m3	108,528	600,000	1,660,000	2,360,000					**Concrete**
Monthly Mean Production	m3/month	4,930	13,000	**70,000**	**75,000**					**40,000**
Monthly Peak Production	m3/month	9,000	28,000	104,000	115,000					
Roller Compacted Concrete										
Total Volume	m3					5,000,000				**RCC**
Monthly Mean Production	m3/month					**130,000**				**80,000**
Monthly Peak Production	m3/month					170,000				
Source of information		*Coyne et Bellier*					*ACP*		*Boskalis*	

- The concrete placement capacity of the Birecik and Katze projects, reaching roughly 70.000 m3/month, are quite high because of the project type involving mainly large mass concrete structures without any significant reinforcement constraints. For the actualized (2005) Post Panamax Locks, it is considered that the geometry is to some extent more complicated than for a gravity dam, which justifies the chosen monthly mean production capacity for concrete placement of 40.000 m3/month

- The same comment made above applies for RCC placement. As a matter of fact, the working area of Tha Dan dam is wide and long and, above all, the RCC placement is continuous; whereas, for the actualized (2005) Post Panamax Locks the areas where RCC is required are of smaller dimensions, and the rhythm of placement is governed by the conventional concrete construction progress. An RCC monthly mean capacity placement of 80.000 m3/month seems more appropriate at this stage for the actualized (2005) Post Panamax Locks.

3.3 DESCRIPTION OF THE CONSTRUCTION SCHEDULE

3.3.1 QUANTITIES

The quantities given in the construction schedule are the quantities, as computed from the drawings, without any mark-up for contingencies.

3.3.2 CONSTRUCTION HYPOTHESIS

The construction schedule presented below is based on a certain construction sequence. The sequence of work adopted supposes that:

- The work starts from Lockhead 1 located on the Gatun Lake side, and progresses southward, except for the Gatun side-approach-wall which progresses northward.

- Only a single Lockhead can be built at a time.

- The concreting of one Chamber can start only if all the excavation is completed in the area, including the corresponding WSB´s culverts excavation close to the Lockwall or below the Chamber itself. It is assumed that one third of the culvert excavation has to be done together with the chamber excavations.

- The rest of the WSB´s culvert excavation and the proper WSB´s excavation will be done after chamber and lockwall excavations are completed. As a matter of fact, the WSB´s excavations may even be completed when the Lock structure is filled with water.

- The filling of the lock from the Pacific side can only start when all the civil works and electromechanical equipment erection of the Lock is completed Of course the valves of the WSB shall also be erected, tested and dry commissioned because, at that time, the WSB construction will still be going on and must be isolated from the Locks.

- Once the Locks are opened on the Pacific side, and filled up to the Pacific level, all the rolling gates erected in a shipyard will be transported by flotation up to the locks and stored in Chamber 3 (Pacific side).

- The two downstream rolling gates are then shifted and suspended into the Lockhead 4 recesses. The same will be sealed with bulkhead gates and pumped out. The rolling gate will be fitted with wooden seals, wagons, etc. (finishing operations). Once ready for operation, the gates will be shifted into the Lock.. The same procedure can then be repeated for the Lockhead 3, 2, and 1

3.3.3 KEY DATES

The Construction Schedule details the following Key Dates:

- Completion of the Civil Work of each Lockhead
- Connection of the locks to the Pacific and filling the Chambers 3 and 2 up to the Pacific level
- Connection of the Locks to the Gatun lake
- Locks and WSB starting date for commercial operation

3.3.4 CRITICAL PATH

The excavation works during the three first years are on this Critical Path. Of course if the excavation production rate is increased to a much higher level as required for the works of the connection Canal to the Gatun lake, then the critical path would certainly be shifted into the concreting activities.
The concreting activities have been scheduled assuming a mean rate of concrete placement of 40,000 m3 per month. Some float has been left for instance between the end of excavation of task Chamber 3-Lockhead 4 and the concreting of Lockhead 4. This results directly from the limitation in the concrete placement rate.

4 Conclusion

The Construction Schedule shows that the total construction time for the Locks and associated WSB is coming to five years. It is certainly possible to compact a little bit more the Construction Schedule, however the Consultant considers that at the present Conceptual Design Stage it is recommended to leave some float in the critical path.
The Construction Schedule assumes that the works progress from North to South. A reverse progression could have been analyzed considering that the flooding of the Locks starts from the Pacific side. Some construction time may be saved assuming that the flooding takes place when the Gatun side of the Lock remains under construction finishing. However the corresponding saving will be limited to about two months (time needed for the rolling gate finishing works in the Lockhead 4) as the main longitudinal culverts and the Gatun water intakes will rapidly be needed to fill the lock chamber 3 and raise the water level in order to float and install the rolling gates in the next Lockhead 3.

CONSTRUCTION SCHEDULE

ACTUALIZATION (2005) PACIFIC POST PANAMAX LOCKS (W = 55M / 3 WSB)

Tractebel Development Engineering — TECHNUM — CNR PROJETS — COYNE ET BELLIER

Excavations
Backfill
Concreting
Rolling Gate
Electromechanical equipment
RCC

Item No	ITEMS	Qty	Unit
1	**CIVIL WORKS FOR LOCKS**		
1.1	Mobilization		
1.2	Contractor installation		
1.3	Access roads		
1.4	Excavation for Locks		
1.4.1	Lockhead 1 (basalt)	387,500	m3
1.4.2	Chamber 1 and lockhead 2 (La Boca predominant)	1,322,000	m3
1.4.3	Chamber 2 and lockhead 3 (Basalt predominant)	1,224,200	m3
1.4.4	Chamber 3 and lockhead 4 (basalt)	2,133,600	m3
1.4.5	Gatun approach walls (basalt)	93,150	m3
1.4.6	Pacific approach wall (La Boca)	483,300	m3
1.5	Excavation for WSB		
1.5.1	WSB Chamber 1	186,500	m3
1.5.2	WSB Chamber 2	261,300	m3
1.5.3	WSB Chamber 3	560,000	m3
1.5.4	Culvert 11 and 12	424,000	m3
1.5.5	Culvert 21 and 22	424,000	m3
1.5.6	Culvert 31 and 32	424,000	m3
1.6	Fill for WSB		
1.6.1	WSB Chamber 1	802,500	m3
1.6.2	WSB Chamber 2	363,000	m3
1.6.3	WSB Chamber 3	15,750	m3
1.7	Backfilling for Lockwalls		
1.7.1	Gatun approach walls	275,700	m3
1.7.2	Lockhead 1 and Chamber1	330,000	m3
1.7.3	Lockhead 2 and Chamber 2	354,300	m3
1.7.4	Lockhead 3 and Chamber 3	747,200	m3
1.7.5	Lockhead 4 and Pacific approach wall	601,600	m3
1.8	Concreting Locks		
1.8.1	Lockhead 1 and U/S transition segments	117,300	m3
1.8.2	Chamber 1 bottom culvert	8,500	m3
1.8.3	Chamber 1 Lockwall East and West	175,200	m3
1.8.4	Chamber 1 Bottom Concrete Slabs/filling	15,900	m3
1.8.5	Lockhead 2	138,800	m3
1.8.6	Chamber 2 bottom culvert	8,500	m3
1.8.7	Chamber 2 Lockwall East and West	173,300	m3
1.8.8	Chamber 2 Bottom Concrete Slabs/filling	15,800	m3
1.8.9	Lockhead 3	140,400	m3
1.8.10	Chamber 3 bottom culvert	8,500	m3
1.8.11	Chamber 3 Lockwall East and West	210,100	m3
1.8.12	Chamber 3 Bottom concrete filling	26,400	m3
1.8.13	Lockhead 4 and D/S transition segments	172,400	m3
1.8.14	Gatun approach walls	78,100	m3
1.8.15	Pacific approach wall	88,900	m3

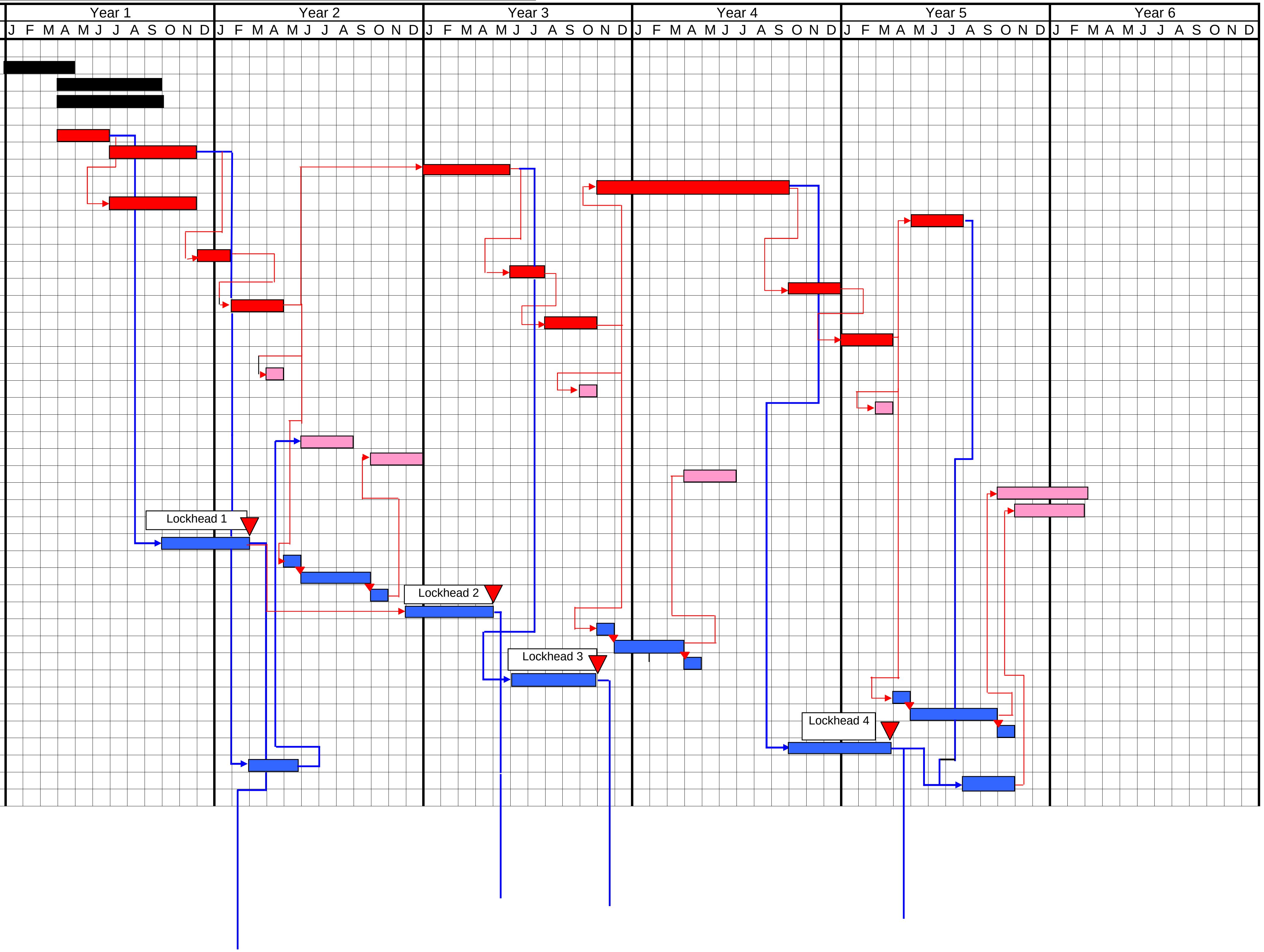

CONSTRUCTION SCHEDULE

ACTUALIZATION (2005) PACIFIC POST PANAMAX LOCKS (W = 55M / 3 WSB)

Tractebel Development Engineering — TECHNUM — CNR PROJETS — COYNE ET BELLIER

Excavations
Backfill
Concreting
Rolling Gate
Electromechanical equipment
RCC

Item No	ITEMS	Qty	Unit
2	**LOCKS ROLLING GATES**		
2.1	Detailed design		
2.2	Construction		
2.2.1	Lock gates 11 and 12	3,460	t
2.2.2	Lock gates 21 and 22	5,670	t
2.2.3	Lock gates 31 and 32	5,670	t
2.2.4	Lock gates 41 and 42	5,870	t
2.3	Transport		
2.3.1	Lock gates 11 and 12		
2.3.2	Lock gates 21 and 22		
2.3.3	Lock gates 31 and 32		
2.3.4	Lock gates 41 and 42		
2.4	Erection		
2.4.1	Lock gates 11 and 12		
2.4.2	Lock gates 21 and 22		
2.4.3	Lock gates 31 and 32		
2.4.4	Lock gates 41 and 42		
2.5	Testing and comissioning		
2.5.1	Lock gates 11 and 12		
2.5.2	Lock gates 21 and 22		
2.5.3	Lock gates 31 and 32		
2.5.4	Lock gates 41 and 42		
3	**ELECTROMECHANICAL EQUIPMENT FOR LOCKS**		
3.1	Detail design		
3.2	Valve construction	1,160	t
3.3	Transport		
3.4	Erection		
3.5	Comissioning		
4	**WATER SAVING BASINS**		
4.1	Lining WSB 1	100,000	m2
4.2	Concreting		
4.2.1	Culverts, Intakes and valve block WSB 11	50,860	m3
4.2.2	Culverts, Intakes and valve block WSB 12	50,860	m3
4.2.3	Culverts, Intakes and valve block WSB 21	50,860	m3
4.2.4	Culverts, Intakes and valve block WSB 22	50,860	m3
4.2.5	Culverts, Intakes and valve block WSB 31	50,860	m3
4.2.6	Culverts, Intakes and valve block WSB 32	50,860	m3
4.2.7	Walls WSB 1	30,430	m3
4.2.8	Walls WSB 2	30,430	m3
4.2.9	Walls WSB 3	30,430	m3
4.3	RCC culvert fill	222,400	m3
4.4	Electomechanical for WSB		
4.4.1	Valve and Stoplog Gate Detail Design		
4.4.2	Valve and gate Construction	4,100	t
4.4.3	Transport		
4.4.4	Erection		
4.4.5	Tests and comissioning		

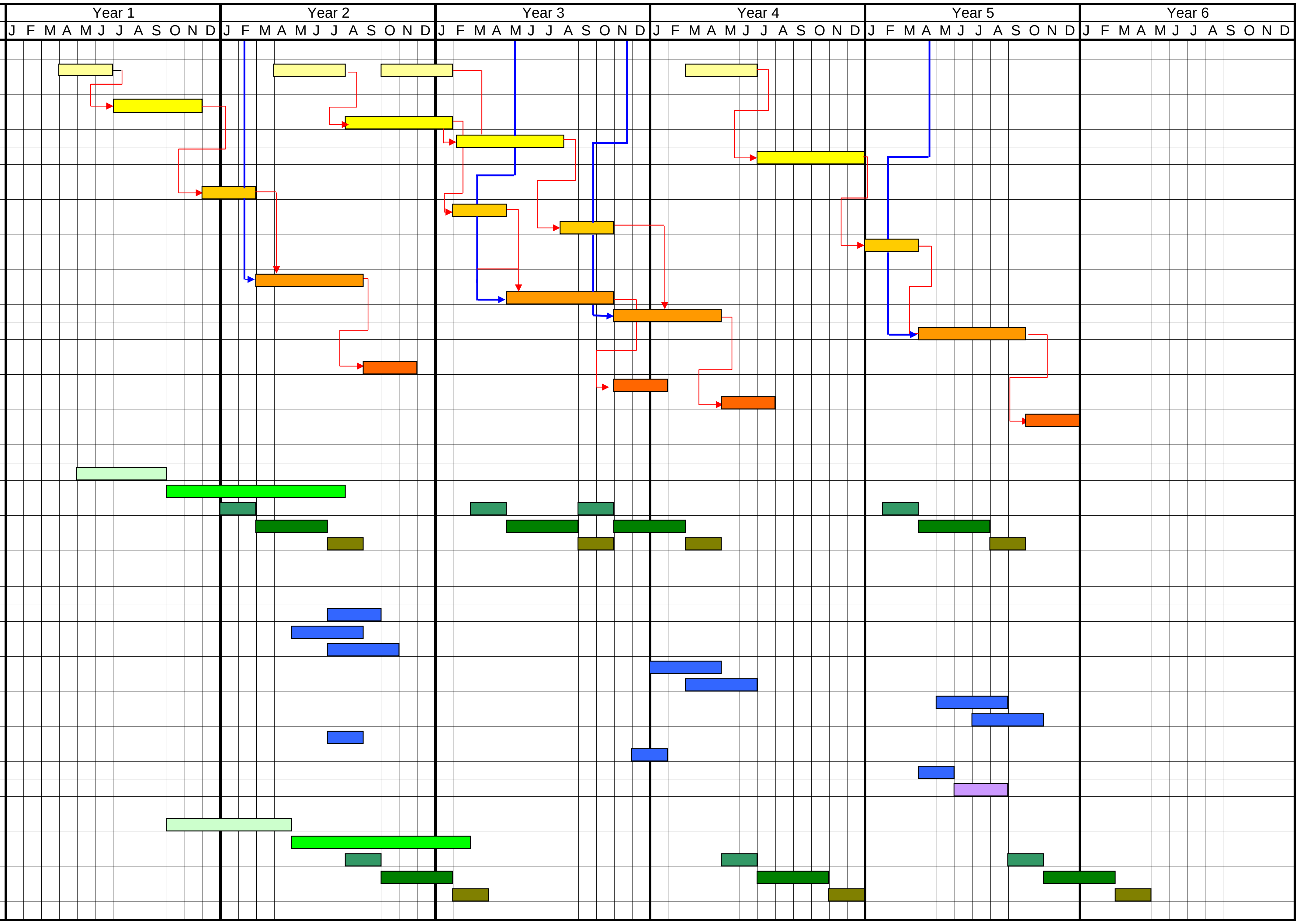

Appendix A : 2D-beam grid model: Gate PA1 - 7 m 19 frames

Table of contents

Basic data
Type of structure : General XYZ

Number of nodes:	133
Number of members:	222
Number of 1D macros:	25
Number of bound. lines:	270
Number of 2D macros:	1
Number of profiles :	14
Number of cases:	5
Number of m aterials:	2

Material

Name:		
S 355		
	Ultimate strength Yield design	510.000 MPa 355.000 MPa
	E modulus	210000.00 MPa
	Poisson coeff.	0.30

Name:		
	Density	7850.000 kg/m^3
	Extensibility	0.012 mm/m.K
S 355LG		
	Ultimate strength	510.000 MPa
	Yield design	355.000 MPa
	E modulus	210000.00 MPa
	Poisson coeff.	0.30
	Density	7.850 kg/m^3
	Extensibility	0.012 mm/m.K

List of material
Group of members :
1/222

no.	Name:	quality	unit weight kg/m	length m	weight kg
1	R1 Top (Numerical)	S 355	1251.29	57.24	71623.84
2	R3 (Numerical)	S 355	1590.41	57.24	91035.07
3	R4 top ac (Numerical)	S 355	2724.73	57.24	155963.83
4	R5 Bottom ac (Numerical)	S 355	2825.21	57.24	161715.31
5	R6 (Numerical)	S 355	1791.37	57.24	102538.02
6	R7 Bottom (Numerical)	S 355	1628.87	57.24	93236.80
7	VF R1-R3 (700.0,0.3,318.0,1.6)	S 355	962.91	54.23	52218.74
8	VF R3-R4 (700.0,0.3,318.0,1.6)	S 355	962.91	54.23	52218.74
9	VF ac (700.0,1.6,318.0,1.6)	S 355	1674.00	93.50	156518.71
10	VF R5-R6 (700.0,0.3,318.0,1.6)	S 355	962.91	60.69	58439.16
11	VF R6-R7 (700.0,0.3,318.0,1.6)	S 355	962.91	60.86	58602.85
12	Bottom cantilever (130.0,4.0,65.0,4.0)	S 355	791.28	24.13	19093.59
13	Urand lijf11 (700.0,1.1,184.0,1.6,159.0)	S 355	1063.89	27.06	28788.99
14	Urand lijf 25 (700.0,2.5,184.0,1.6,159.0)	S 355	1829.68	11.00	20126.46

List of material - Macro2D
Group of members :
1/223

no.	Name:	quality	unit volume weight kgm^3	volume m^3	weight kg
300	S 355LG	S 355LG	7.85	58.10	456.07

The total weight of the structure: 1122576.19 kg
Surface for painting: 9590.07 m^2

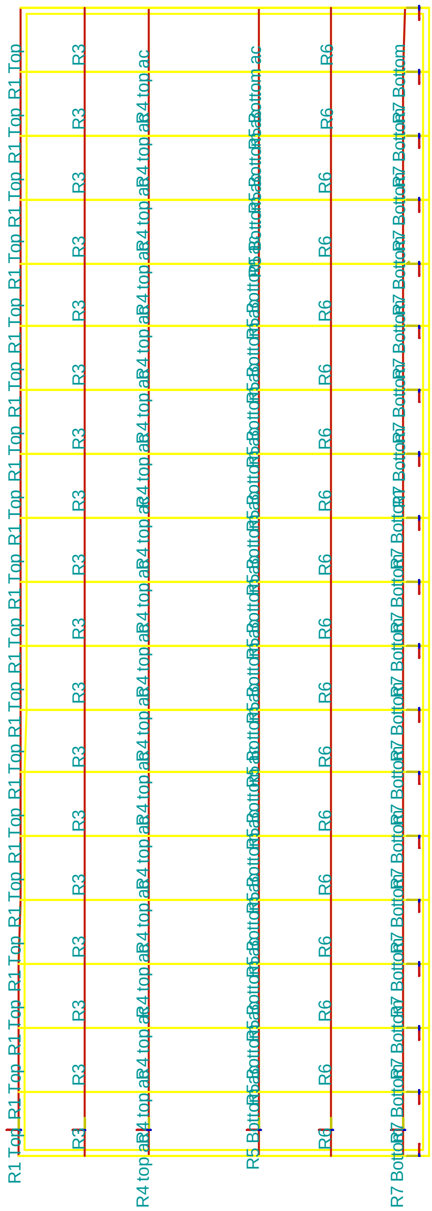

Horizontal frames

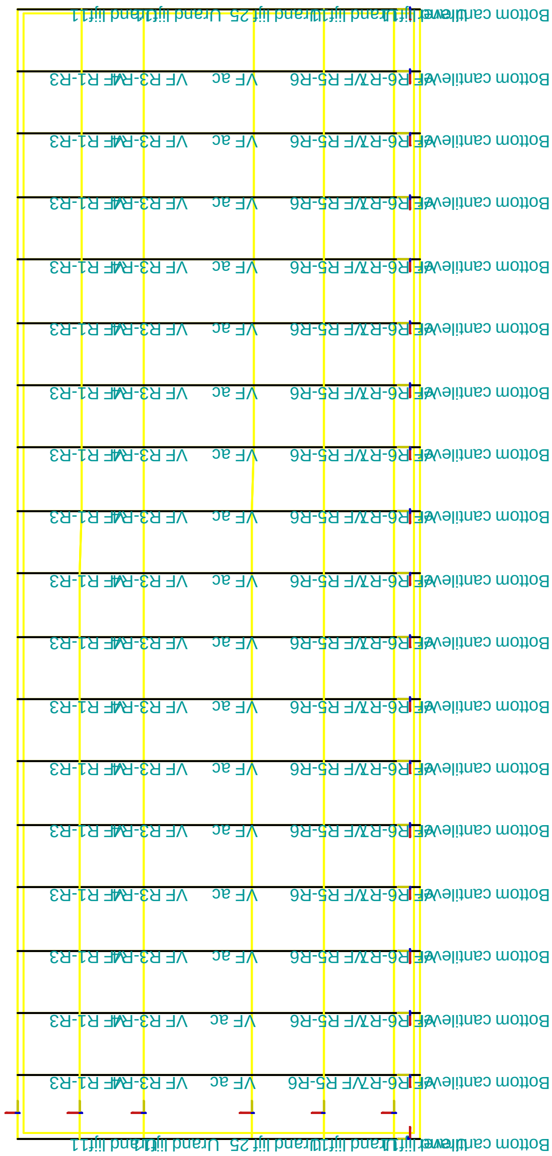

Vertical frames

Supports

support	node	type	flexibility kN/mm-kNmm/rad	Size m
1	1	Y		0.20
2	11	X		0.20
3	19	Y		0.20
4	20	Y		0.20
5	30	X		0.20
6	38	Y		0.20
7	39	Y		0.20
8	49	X		0.20
9	57	Y		0.20
10	58	Y		0.20
11	68	X		0.20
12	76	Y		0.20
13	87	X		0.20
14	96	Z		0.20
15	97	YZ	ky =510.00	0.20
16	98	YZ	ky =510.00	0.20
17	99	YZ	ky =510.00	0.20
18	100	YZ	ky =510.00	0.20
19	101	YZ	ky =510.00	0.20
20	102	YZ	ky =510.00	0.20
21	103	YZ	ky =510.00	0.20
22	104	YZ	ky =510.00	0.20
23	105	YZ	ky =510.00	0.20
24	106	XYZ	ky =510.00	0.20
25	107	YZ	ky =510.00	0.20
26	108	YZ	ky =510.00	0.20
27	109	YZ	ky =510.00	0.20
28	110	YZ	ky =510.00	0.20
29	111	YZ	ky =510.00	0.20
30	112	YZ	ky =510.00	0.20
31	113	YZ	ky =510.00	0.20
32	114	Z		0.20
33	122	X		0.20
34	132	Y		0.20
35	133	Y		0.20

Loadcases

Case	Name:	Description
1	WR normal + 27.13 +16.51 PLD	Variable - LC Water Excl.
2	WR ultimate +28.13 +16.51 PLD	Variable - LC Water Excl.
3	DWC +28.13 +7.58 PLD	Variable - LC Water Excl.
4	Self Weight	Self weight. Direction -Z
5	EQ : Westergaard MCE	Variable - Earth quake

Loadcase no. 1 - Free loads

Rectangles

Index	Distribution	x m	y m	qx kN/m^2	qy kN/m^2	qz kN/m^2	System	Validity	Location
1	Dir Y	0.00	16.51	0.00	-106.20	0.00	Global	All	Length
1		57.24	27.13	0.00	0.00	0.00			
2	Uniform	0.00	7.83	0.00	-106.20	0.00	Global	All	Length
2		57.24	16.51						

Loadcase no. 2 - Free loads

Rectangles

Index	Distribution	x m	y m	qx kN/m^2	qy kN/m^2	qz kN/m^2	System	Validity	Location
1	Dir Y	0.00	16.51	0.00	-116.20	0.00	Global	All	Length
1		57.24	28.13	0.00	0.00	0.00			
2	Uniform	0.00	7.83	0.00	-116.20	0.00	Global	All	Length
2		57.24	16.51						

Loadcase no. 3 - Free loads

Rectangles

Index	Distribution	x m	y m	qx kN/m^2	qy kN/m^2	qz kN/m^2	System	Validity	Location
1	Dir Y	0.00	7.83	0.00	-203.00	0.00	Global	All	Length
1		57.24	28.13	0.00	0.00	0.00			

Loadcase no. 5 - Free loads

Rectangles

Index	Distribution	x m	y m	qx kN/m^2	qy kN/m^2	qz kN/m^2	System	Validity	Location
1	Dir Y	0.00	27.04	0.00	-16.20	0.00	Global	All	Length
1		57.24	27.58	0.00	-11.40	0.00			

Index	Distribution	x m	y m	qx kN/m^2	qy kN/m^2	qz kN/m^2	System	Validity	Location
2	Dir Y	0.00	25.95	0.00	-22.90	0.00	Global	All	Length
2		57.24	27.04	0.00	-16.20	0.00			
3	Dir Y	0.00	24.86	0.00	-28.00	0.00	Global	All	Length
3		57.24	25.95	0.00	-22.90	0.00			
4	Dir Y	0.00	7.83	0.00	-72.00	0.00	Global	All	Length
4		57.24	19.05	0.00	-46.60	0.00			
5	Dir Y	0.00	19.05	0.00	-46.60	0.00	Global	All	Length
5		57.24	23.76	0.00	-32.30	0.00			
6	Dir Y	0.00	23.76	0.00	-32.20	0.00	Global	All	Length
6		57.24	24.86	0.00	-28.00	0.00			
7	Dir Y	57.24	27.58	0.00	-11.40	0.00	Global	All	Length
7		0.00	27.91	0.00	-7.20	0.00			
8	Dir Y	0.00	27.91	0.00	-7.20	0.00	Global	All	Length
8		57.24	28.13	0.00	0.00	0.00			

Combinations

Combi	Norm	Case	coeff
1.Water	User-ultimate	1 WR normal + 27.13 +16.51 PLD	1.35
1.Water	User-ultimate	2 WR ultimate +28.13 +16.51 PLD	1.20
1.Water	User-ultimate	3 DWC +28.13 +7.58 PLD	1.00
1.Water	User-ultimate	4 Self Weight	1.35
2.Water +EQ	User-ultimate	1 WR normal + 27.13 +16.51 PLD	1.00
2.Water +EQ	User-ultimate	2 WR ultimate +28.13 +16.51 PLD	1.00
2.Water +EQ	User-ultimate	3 DWC +28.13 +7.58 PLD	1.00
2.Water +EQ	User-ultimate	4 Self Weight	1.00
2.Water +EQ	User-ultimate	5 EQ : Westergaard MCE	1.00
3.	User-serviceability	1 WR normal + 27.13 +16.51 PLD	1.00
3.	User-serviceability	2 WR ultimate +28.13 +16.51 PLD	1.00
3.	User-serviceability	3 DWC +28.13 +7.58 PLD	1.00
3.	User-serviceability	4 Self Weight	1.00
3.	User-serviceability	5 EQ : Westergaard MCE	1.00

Basic rules for generation of ultimate load combinations:
1 : 1.35*LC1 / 1.20*LC2 / 1.00*LC3 / 1.35*LC4
2 : 1.00*LC1 / 1.00*LC2 / 1.00*LC3 / 1.00*LC4 / 1.00*LC5

Basic rules for generation of serviceability load combinations:
1 : 1.00*LC1 / 1.00*LC2 / 1.00*LC3 / 1.00*LC4 / 1.00*LC5

List of extreme ultimate load combinations
1/ 2 : +1.00*LC4
2/ 1 : +1.35*LC4
3/ 2 : +1.00*LC3+1.00*LC4
4/ 2 : +1.00*LC4+1.00*LC5
5/ 1 : +1.00*LC3+1.35*LC4
6/ 1 : +1.20*LC2+1.35*LC4
7/ 1 : +1.35*LC1+1.35*LC4
8/ 2 : +1.00*LC2+1.00*LC4+1.00*LC5
9/ 2 : +1.00*LC3+1.00*LC4+1.00*LC5

List of extreme serviceability load combinations
1/ 1 : +1.00*LC4
2/ 1 : +1.00*LC1+1.00*LC4
3/ 1 : +1.00*LC3+1.00*LC4
4/ 1 : +1.00*LC4+1.00*LC5
5/ 1 : +1.00*LC1+1.00*LC4+1.00*LC5
6/ 1 : +1.00*LC2+1.00*LC4+1.00*LC5
7/ 1 : +1.00*LC3+1.00*LC4+1.00*LC5

Calculation protocol.

Linear calculation

Number of 2D elements	7344
Number of 1D elements	1833
Number of mesh nodes	7540
Number of equations	45240
Loadcases	LC 1 WR normal + 27.13 +16.51 PLD
	LC 2 WR ultimate +28.13 +16.51 PLD LC 3 DWC +28.13 +7.58 PLD
	LC 4 Self Weight
	LC 5 EQ : Westergaard MCE
Bending theory	Mindlin
Start of calculation	09.03.2005 15:35
End of calculation	09.03.2005 15:35

Sum of loads and reactions.

		X	Y	Z
loadcase 1	loads	0.0	-85042.2	0.0
	reactions	-0.0	85042.2	-0.0
	contact	0.0	0.0	0.0
loadcase 2	loads	0.0	-96387.0	0.0
	reactions	-0.0	96387.0	-0.0
	contact	0.0	0.0	0.0
loadcase 3	loads	0.0	-117940.2	0.0
	reactions	-0.0	117940.2	-0.0
	contact	0.0	0.0	0.0
loadcase 4	loads	-0.0	-0.0	-11225.8
	reactions	-0.0	0.0	11225.8
	contact	0.0	0.0	0.0
loadcase 5	loads	0.0	-54102.4	0.0
	reactions	-0.0	54102.4	-0.0
	contact	0.0	0.0	0.0

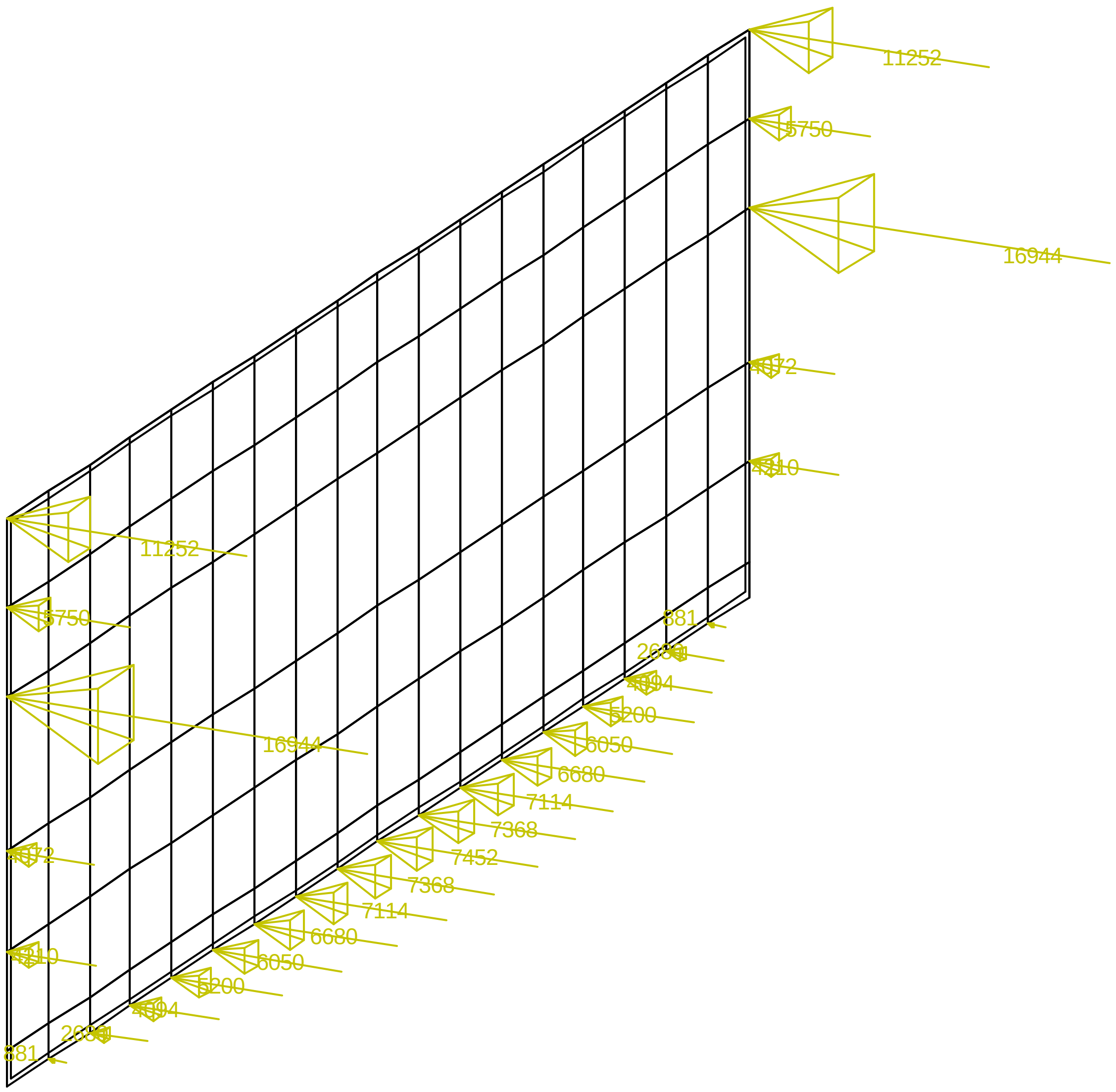

Reaction forces - ULS (SW+DWC+EQ)

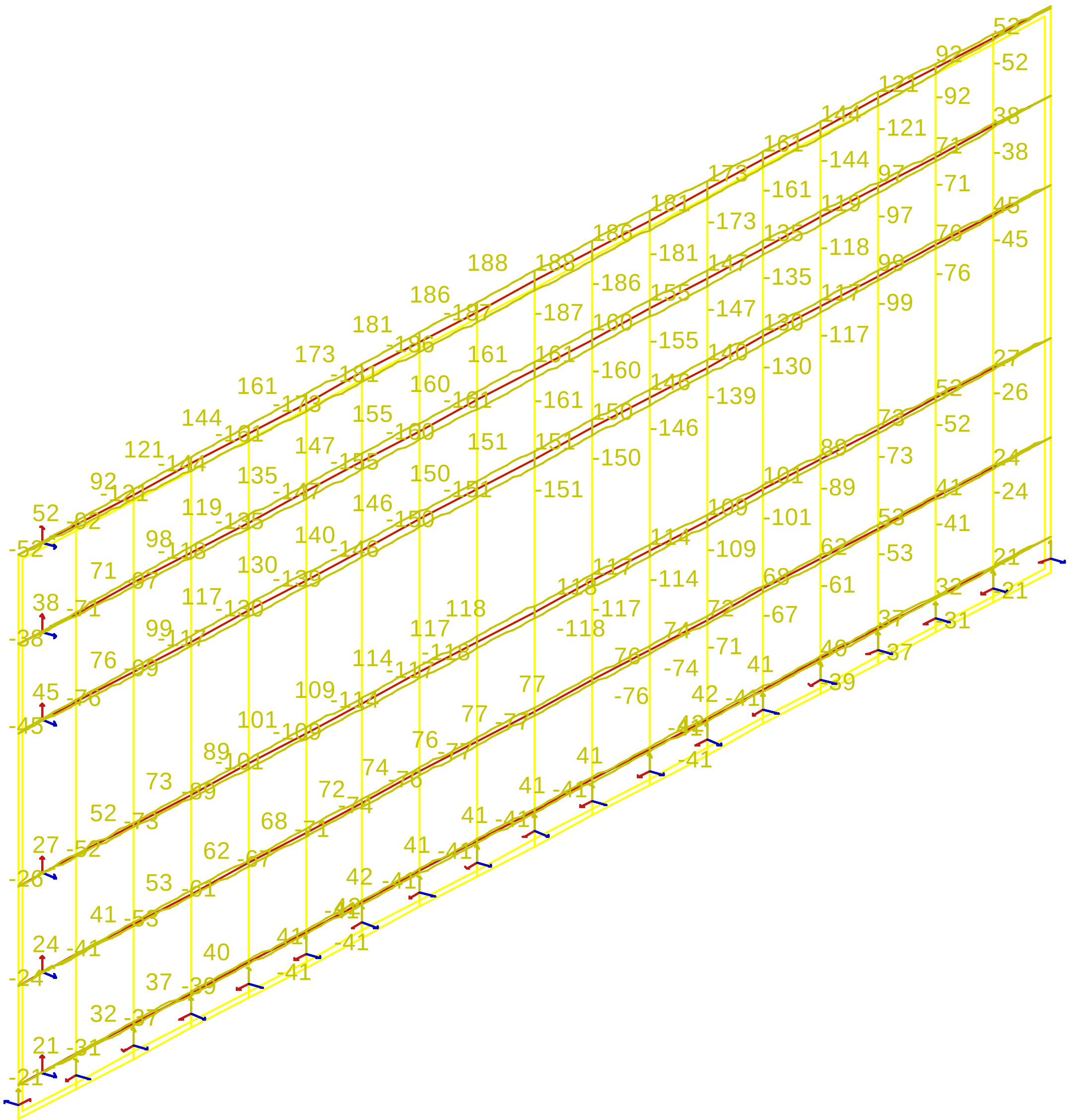

Normal stresses in horizontal frames : ULS

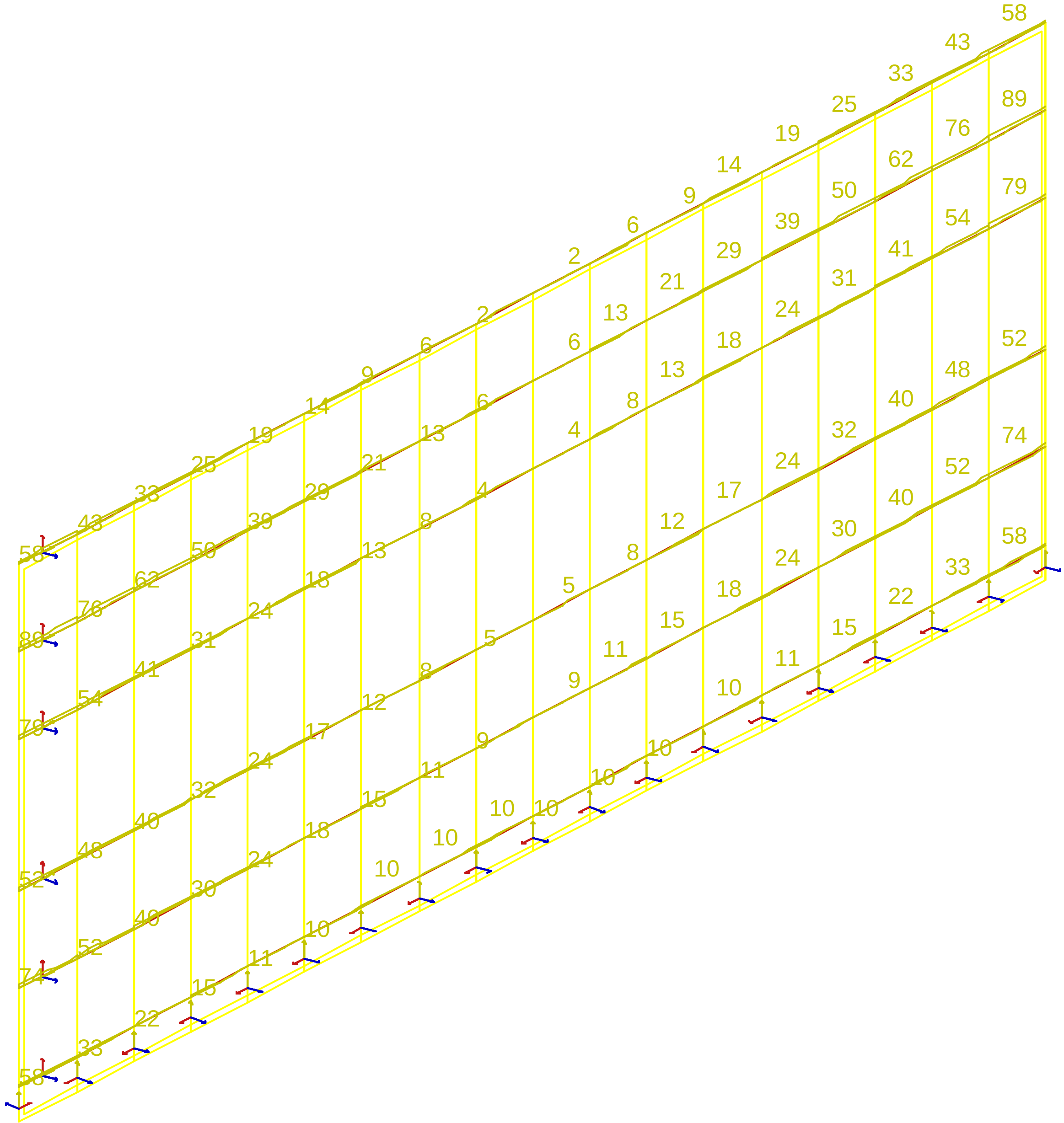

Shear stresses in horizontal frames : ULS

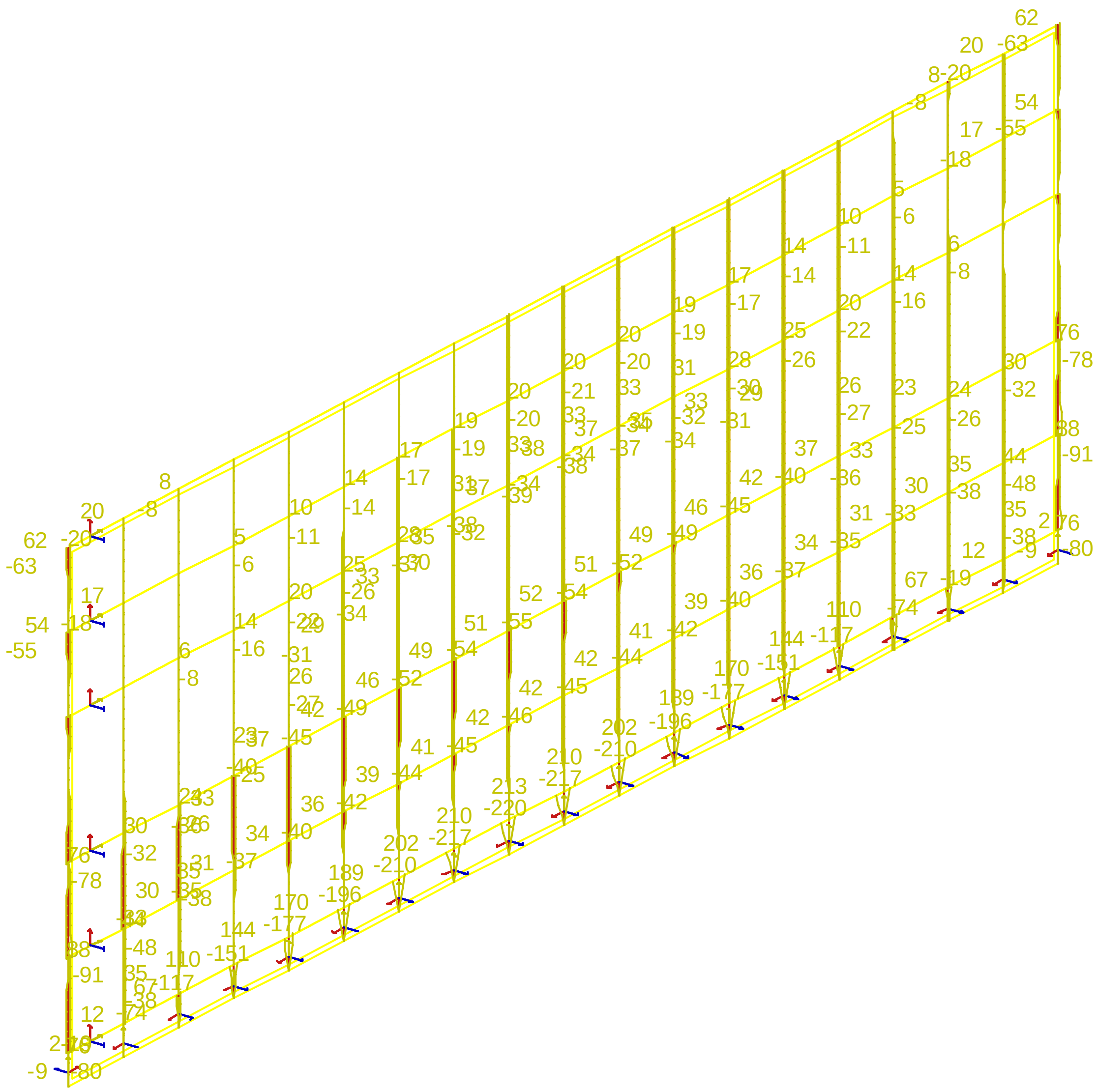

Normal stresses in vertical frames : ULS

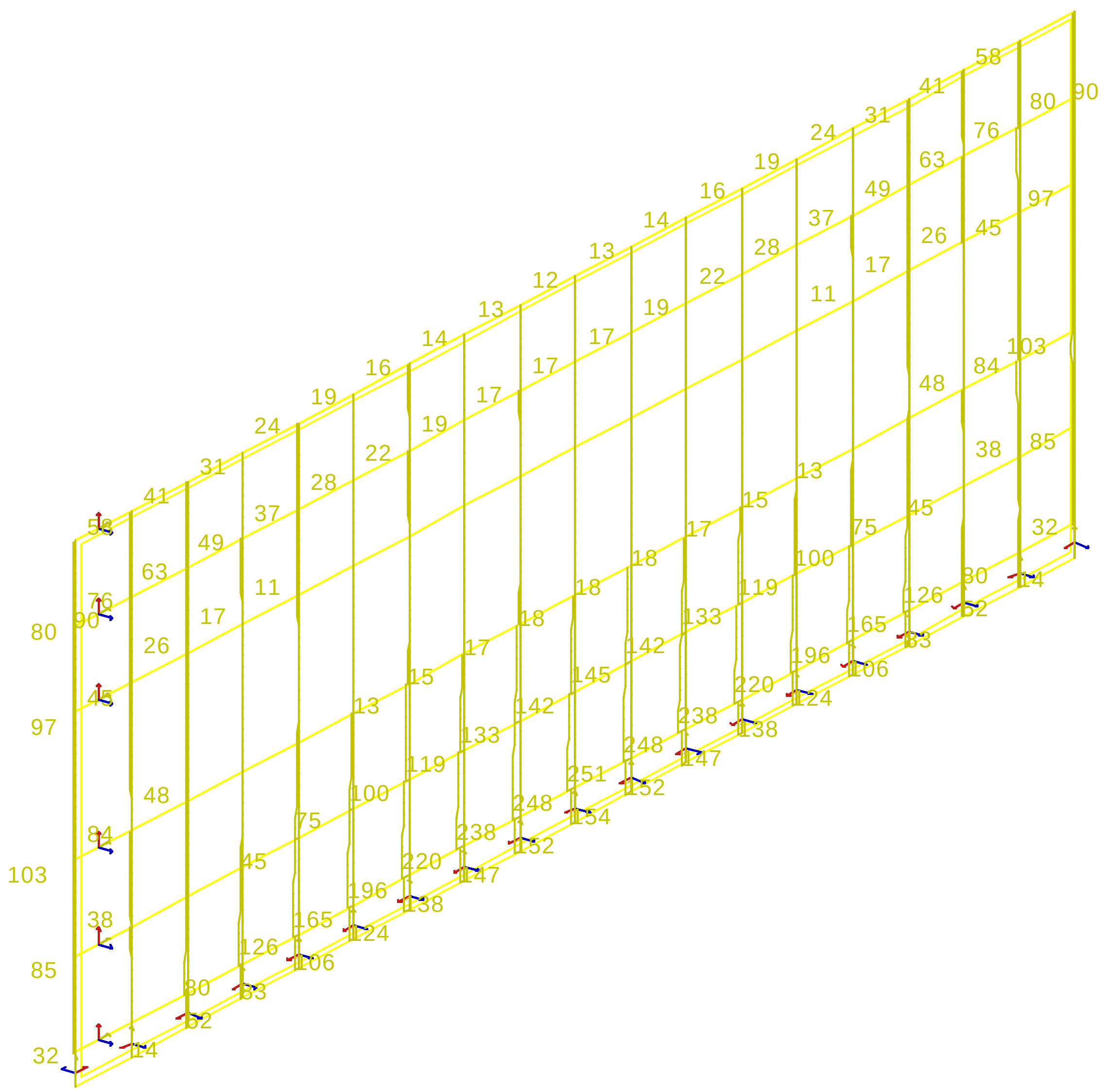

Shear stresses in vertical frames : ULS

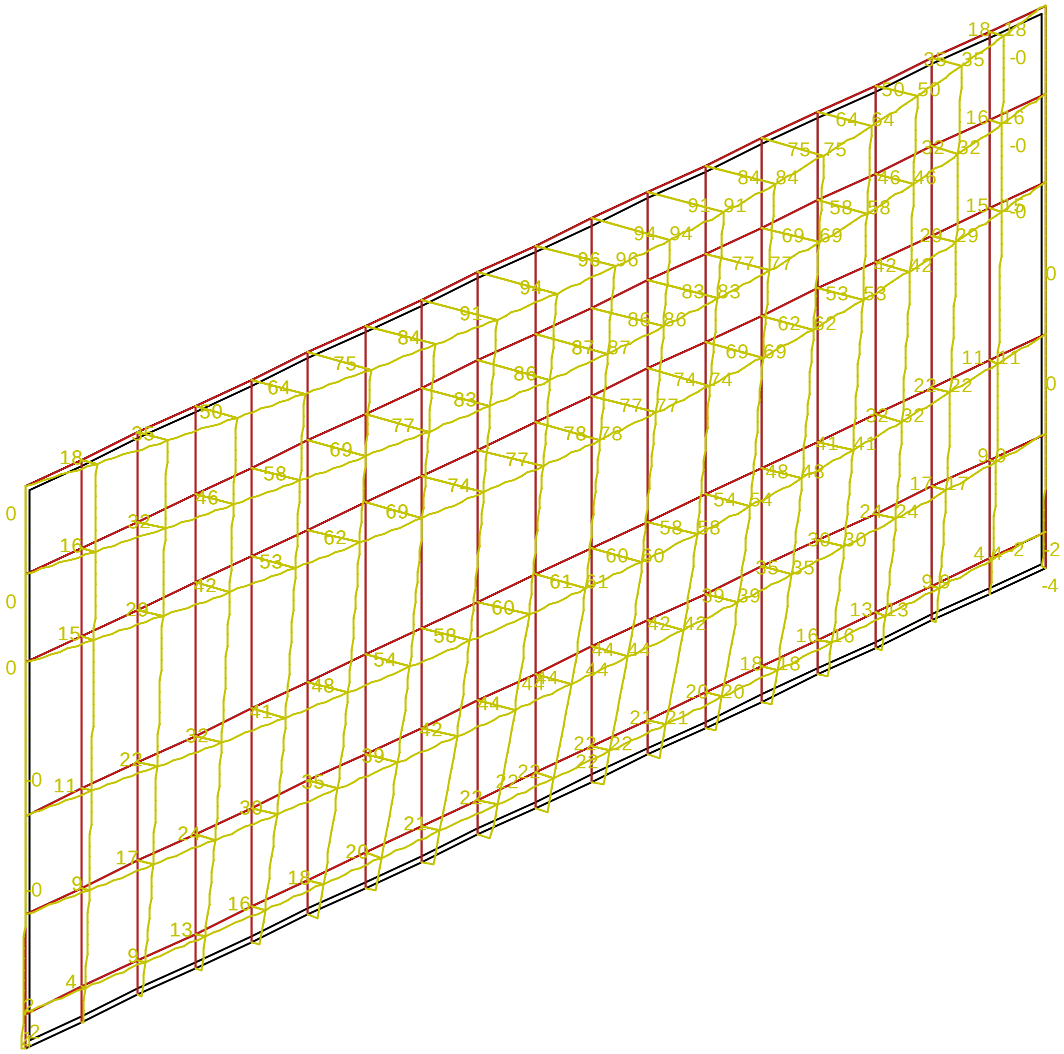

Deformations - uz in beams : SLS

Appendix B : 3D-FEM calculation half gate : Gate PA1 - 7 m 19 frames

Table of contents

Basic data
Type of structure : General XYZ

Number of nodes:	1076
Number of members:	1128
Number of 1D macros:	1118
Number of bound. lines:	1271
Number of 2D macros:	189
Number of profiles :	77
Number of cases:	6
Number of materials:	2

Material

Name:		
S 355		
	Ultimate strength	510.000 MPa
	Yield design	355.000 MPa
	E modulus	210000.00 MPa
	Poisson coeff.	0.30
	Density	7850.000 kg/m^3
	Extensibility	0.012 mm/m.K

Loadcases

Case	Name:	Description
1	WR normal +27.13 +16.51 PLD	Variable - LC Water Excl.
2	WR ultimate +28.13 +16.51 PLD	Variable - LC Water Excl.
3	DWC +28.13 +7.58 PLD	Variable - LC Water Excl.
4	Self Weight	Self weight. Direction -Z
5	EQ : Westergaard	Variable - Earth quake
6	Blow out (200 kN/m^2)	Variable - Maintenance

Variable loads group

Name:		Description
LC Water	Excl.	EC1 - load type Cat A
Earth quake		EC1 - load type Cat A
Maintenance		EC1 - load type Cat A

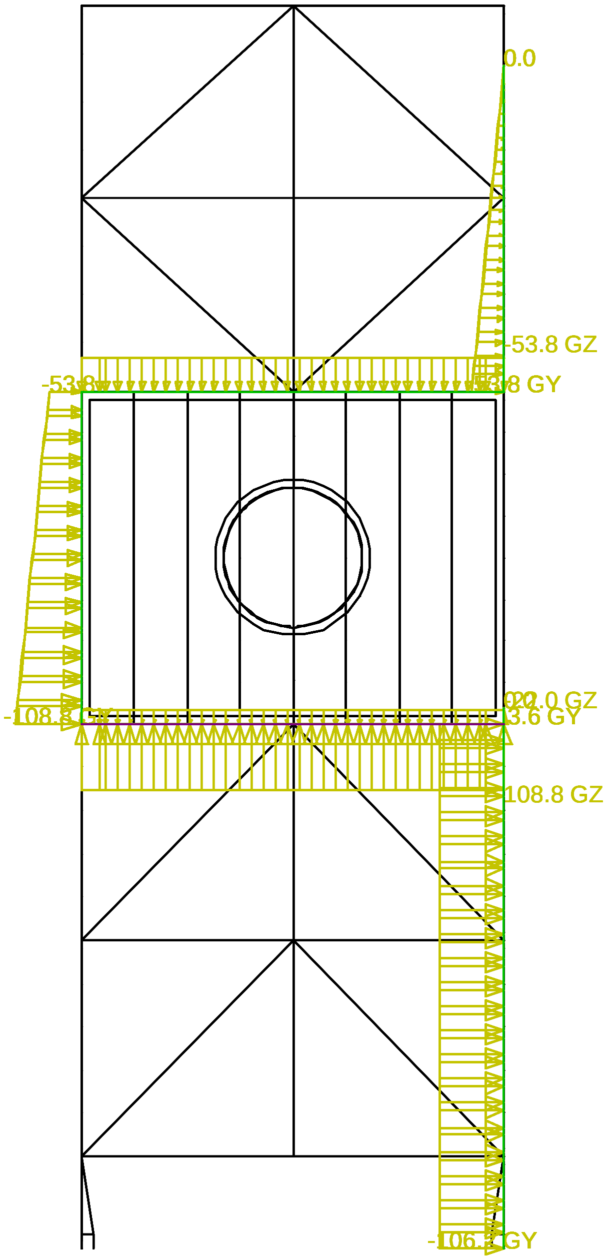

LC WRN (+27.13 +16.51 PLD)

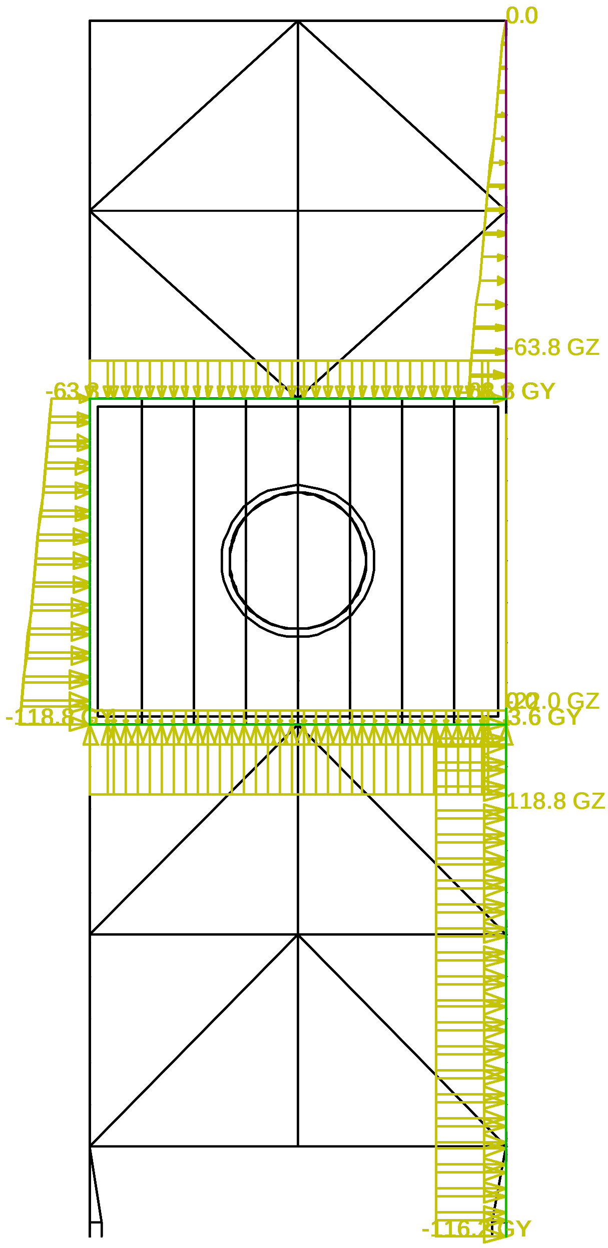

LC WRU (+28.13 +16.51 PLD)

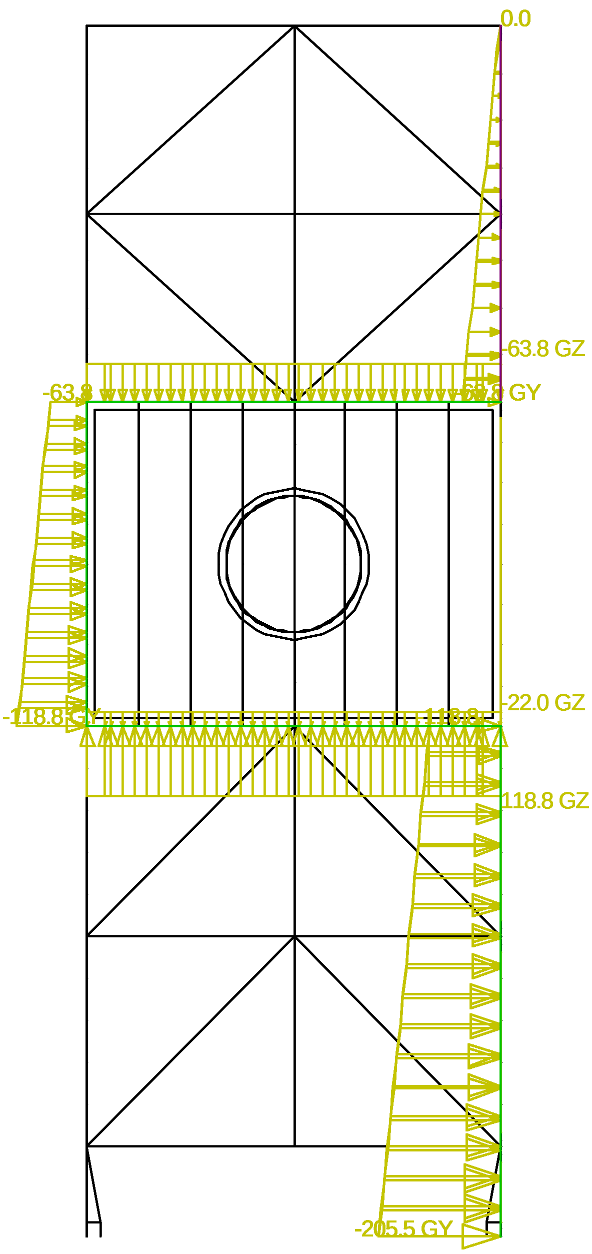

LC DWC (+28.13 +7.58 PLD)

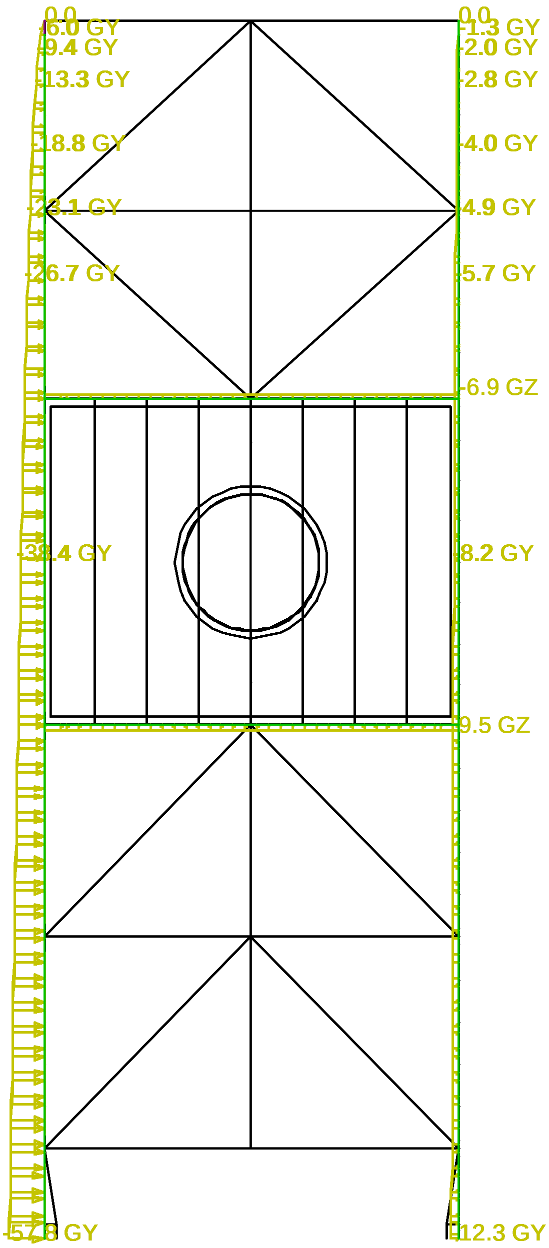

LC EQ : Westergaard MCE

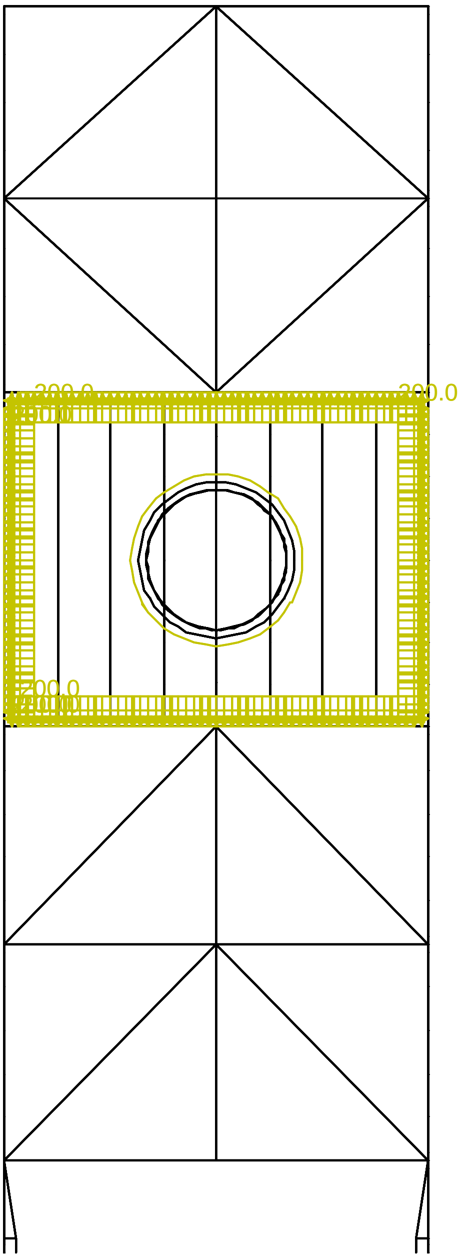

LC Blow out (200 kN/m^2)

Combinations

Combi	Norm	Case	coeff
1.Water	User-ultimate	1 WR normal +27.13 +16.51 PLD	1.35
1.Water	User-ultimate	2 WR ultimate +28.13 +16.51 PLD	1.20
1.Water	User-ultimate	3 DWC +28.13 +7.58 PLD	1.00
1.Water	User-ultimate	4 Self Weight	1.35
2.Water+EQ	User-ultimate	1 WR normal +27.13 +16.51 PLD	1.00
2.Water+EQ	User-ultimate	2 WR ultimate +28.13 +16.51 PLD	1.00
2.Water+EQ	User-ultimate	3 DWC +28.13 +7.58 PLD	1.00
2.Water+EQ	User-ultimate	4 Self Weight	1.00
2.Water+EQ	User-ultimate	5 EQ : Westergaard	1.00
3.	User-serviceability	1 WR normal +27.13 +16.51 PLD	1.00
3.	User-serviceability	2 WR ultimate +28.13 +16.51 PLD	1.00
3.	User-serviceability	3 DWC +28.13 +7.58 PLD	1.00
3.	User-serviceability	4 Self Weight	1.00
3.	User-serviceability	5 EQ : Westergaard	1.00

Basic rules for generation of ultimate load combinations:
1 : 1.35*LC1 / 1.20*LC2 / 1.00*LC3 / 1.35*LC4
2 : 1.00*LC1 / 1.00*LC2 / 1.00*LC3 / 1.00*LC4 / 1.00*LC5

Basic rules for generation of serviceability load combinations:
1 : 1.00*LC1 / 1.00*LC2 / 1.00*LC3 / 1.00*LC4 / 1.00*LC5

List of extreme ultimate load combinations
1/ 2 : +1.00*LC4
2/ 1 : +1.35*LC4
3/ 2 : +1.00*LC1+1.00*LC4
4/ 2 : +1.00*LC2+1.00*LC4
5/ 2 : +1.00*LC3+1.00*LC4
6/ 2 : +1.00*LC4+1.00*LC5
7/ 1 : +1.00*LC3+1.35*LC4
8/ 1 : +1.20*LC2+1.35*LC4
9/ 1 : +1.35*LC1+1.35*LC4
10/ 2 : +1.00*LC1+1.00*LC4+1.00*LC5
11/ 2 : +1.00*LC2+1.00*LC4+1.00*LC5
12/ 2 : +1.00*LC3+1.00*LC4+1.00*LC5

List of extreme serviceability load combinations
1/ 1 : +1.00*LC4
2/ 1 : +1.00*LC1+1.00*LC4
3/ 1 : +1.00*LC2+1.00*LC4
4/ 1 : +1.00*LC3+1.00*LC4
5/ 1 : +1.00*LC4+1.00*LC5
6/ 1 : +1.00*LC1+1.00*LC4+1.00*LC5
7/ 1 : +1.00*LC2+1.00*LC4+1.00*LC5
8/ 1 : +1.00*LC3+1.00*LC4+1.00*LC5

Calculation protocol.

Linear calculation

Number of 2D elements Number of 1D elements Number of mesh nodes Number of equations	28592 10543 27452 164712
Loadcases	LC 1 WR normal +27.13 +16.51 PLD
	LC 2 WR ultimate +28.13 +16.51 PLD
	LC 3 DWC +28.13 +7.58 PLD
	LC 4 Self Weight
	LC 5 EQ : Westergaard
	LC 6 Blow out (200 kN/m^2)
Bending theory	Mindlin
Start of calculation	09.03.2005 19:05
End of calculation	09.03.2005 19:11

Sum of loads and reactions.

		X	Y	Z
loadcase 1	loads	0.0	-43280.5	6611.2
	reactions	0.0	43280.5	-6611.2
	contact	0.0	0.0	0.0
loadcase 2	loads	0.0	-49020.6	6611.2
	reactions	0.0	49020.6	-6611.2
	contact	0.0	0.0	0.0
loadcase 3	loads	0.0	-60431.5	6611.2
	reactions	0.0	60431.5	-6611.2
	contact	0.0	0.0	0.0
loadcase 4	loads	0.0	0.0	-6759.0
	reactions	0.0	-0.0	6759.0
	contact	0.0	0.0	0.0
loadcase 5	loads	0.0	-27157.2	520.9
	reactions	-0.0	27157.2	-520.9
	contact	0.0	0.0	0.0
loadcase 6	loads	0.0	-0.0	-0.0
	reactions	-0.0	-0.0	-0.0
	contact	0.0	0.0	0.0

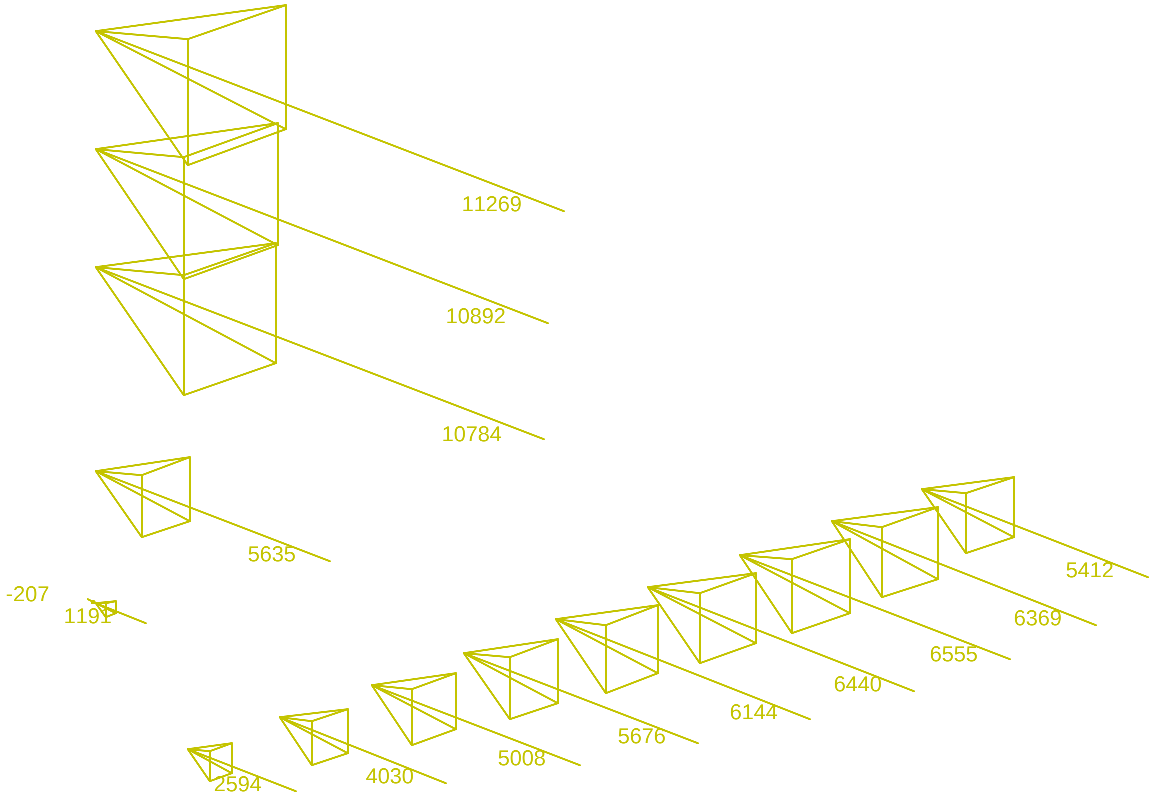

Reaction forces - ULS (SW+DWC+EQ)

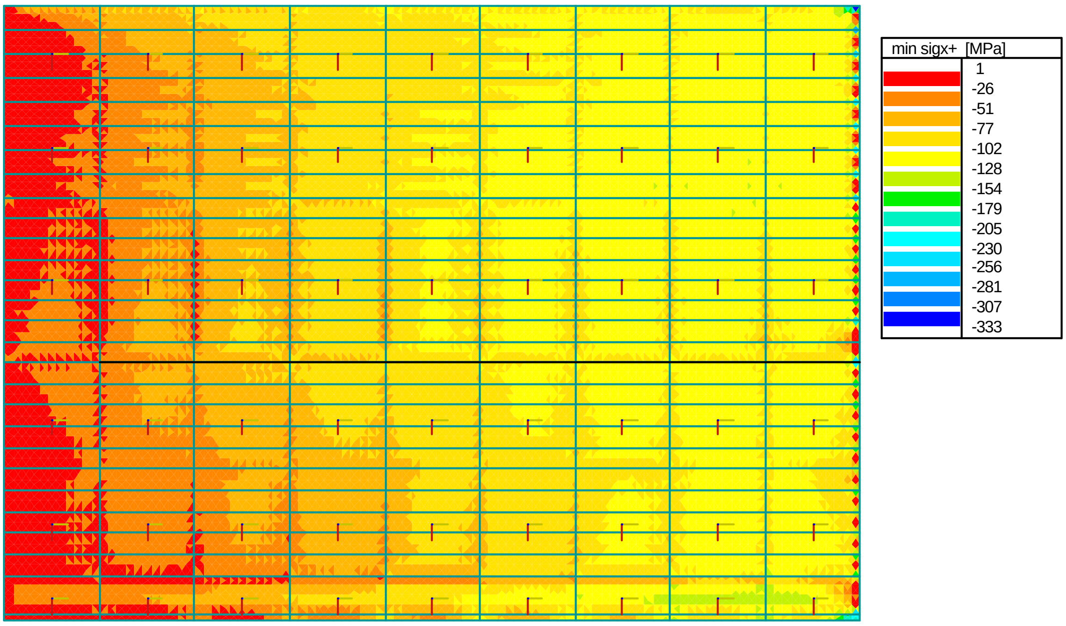

Upstream plating : normal stresses - min sigx+ - ULS

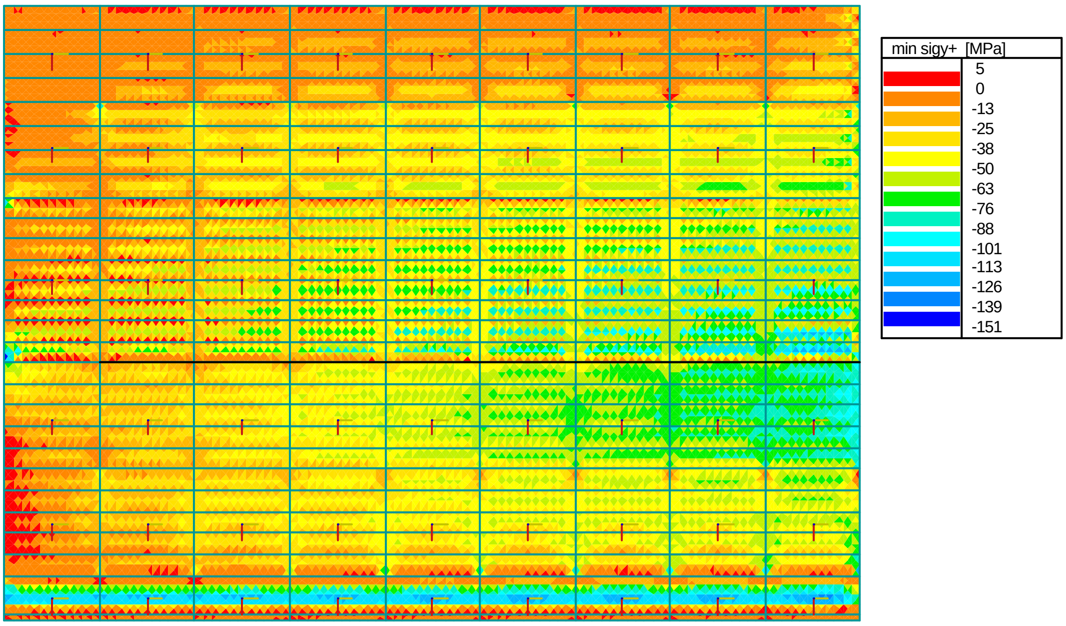

Upstream plating : normal stresses - min sigy+ - ULS

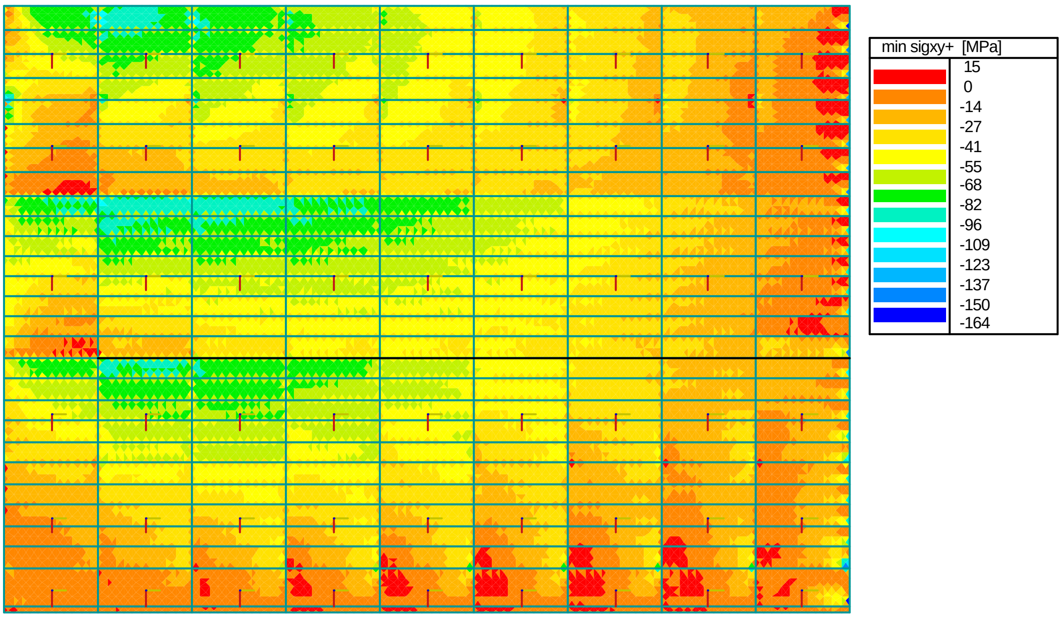

Upstream plating : shear stresses - min sigxy+ - ULS

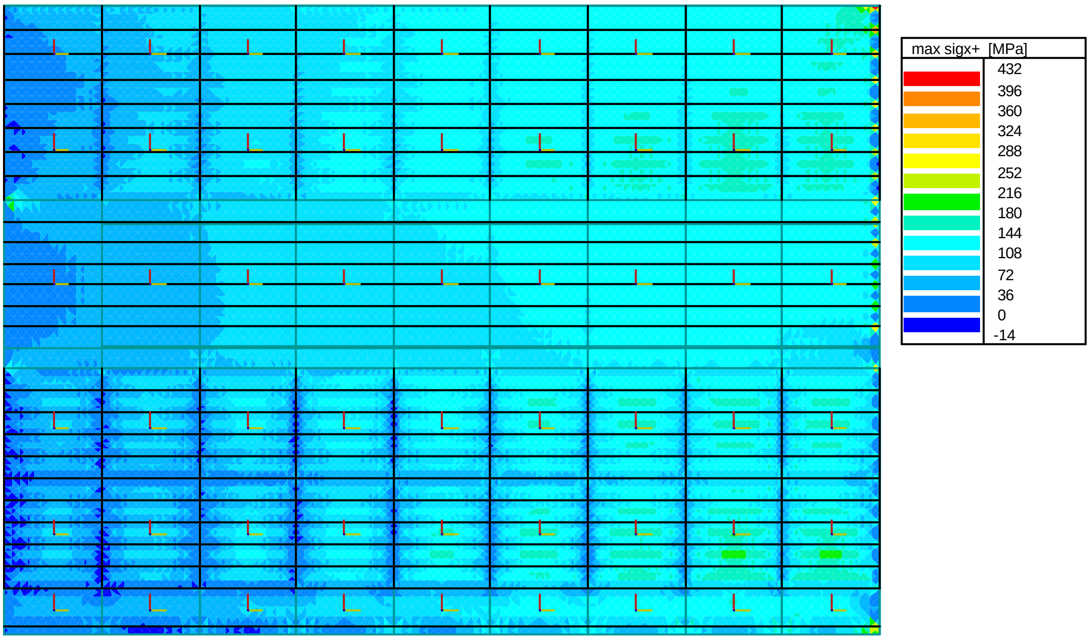

Downstream plating : normal stresses - max sigx+ - ULS

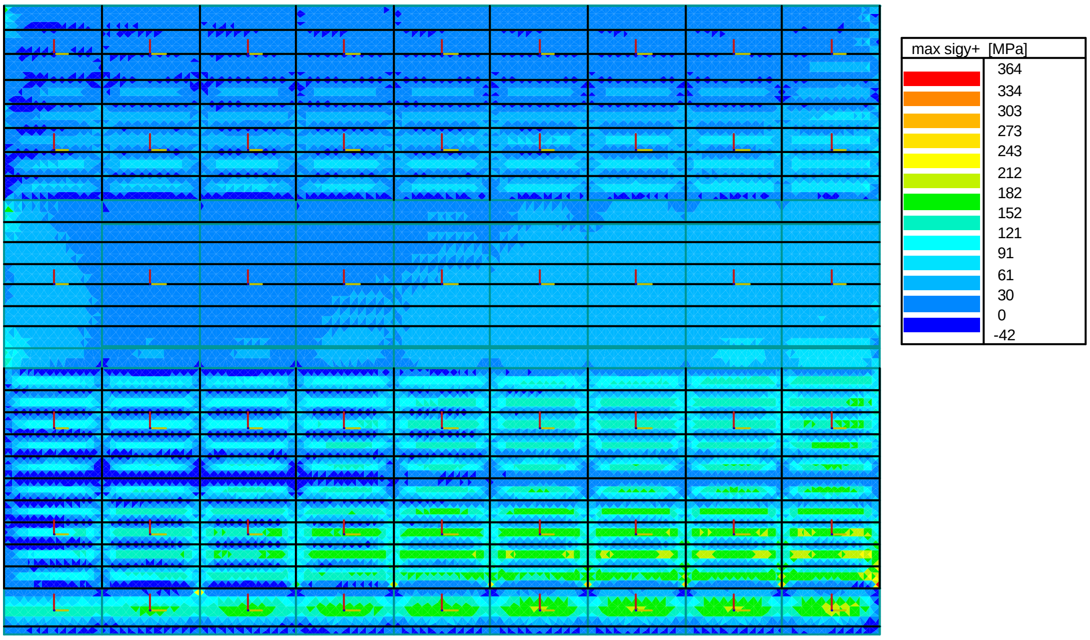

Downstream plating : normal stresses - max sigy+ - ULS

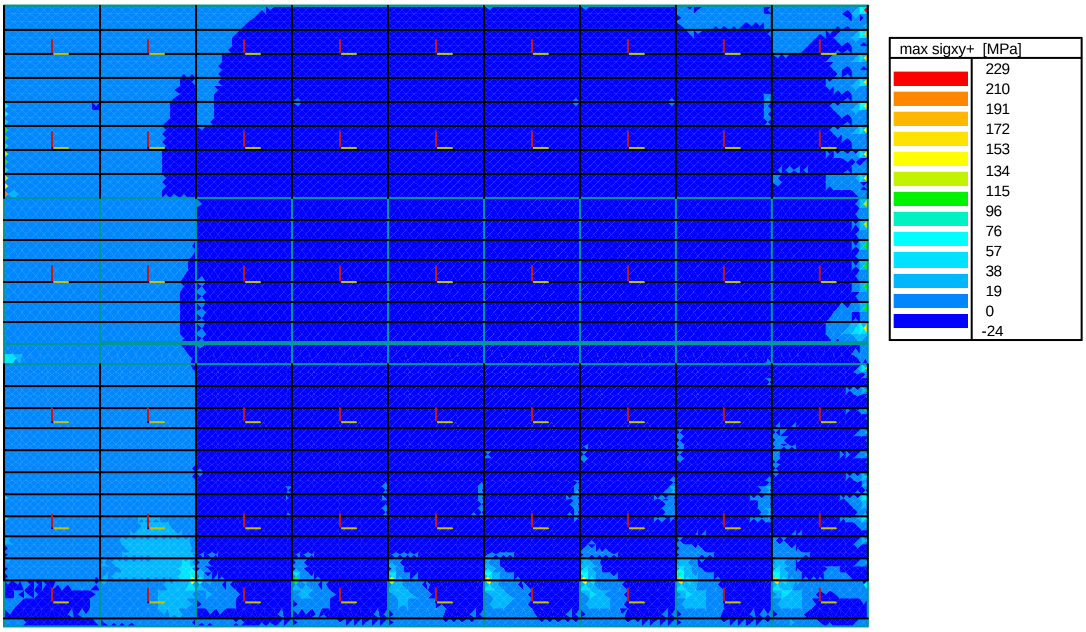

Downstream plating : shear stresses - max sigxy+ - ULS

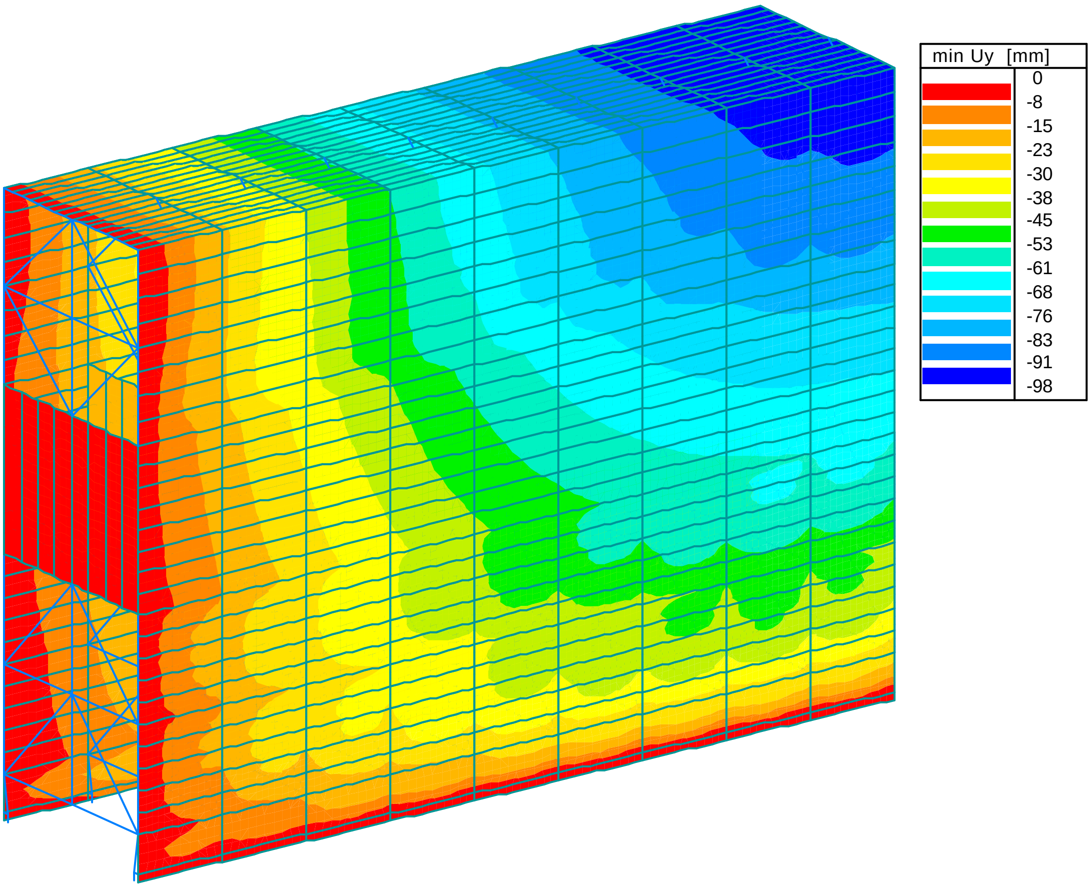

Deformations - min Uy - SLS